

61st HIGHWAY GEOLOGY SYMPOSIUM

www.HighwayGeologySymposium.org

Oklahoma City, Oklahoma

August 23rd - 26th, 2010

PROCEEDINGS



Hosted By

The Oklahoma Department of Transportation

The Oklahoma Geological Survey

Table of Contents

61 st HGS Organizing Committee Members	2
Steering Committee Officers	3
Steering Committee Members	4
History, Organization, and Function	7
Emeritus Members	11
Medallion Award Winners	12
Future Symposium Schedule	13
Sponsors	14
Exhibitors	18
61 st Highway Geology Symposium Agenda	23
Skirvin Hotel Layout	28
TRB Session – “Asset Management in a World of Dirt”	30
HGS Proceedings – Paper Abstracts & Notes	44

61st ANNUAL HIGHWAY GEOLOGY SYMPOSIUM

Oklahoma City, Oklahoma
August 23rd - 26th, 2010

Local Organizing Committee

Tanya Ham	Oklahoma Department of Transportation
Brenda Morris	Oklahoma Department of Transportation
Kevin Lowe	Oklahoma Department of Transportation
Chuck Howard	Oklahoma Department of Transportation
Gary Webber	Oklahoma Department of Transportation
Jeff Dean	Oklahoma Department of Transportation
Butch Reidenbach	Oklahoma Department of Transportation

Ken Luza	Oklahoma Geological Survey
Stan Krukowski	Oklahoma Geological Survey

Jim Nevels, Jr.	Geotechnical Consultant
-----------------	-------------------------

Special Thanks to

Tim Tegeler	Oklahoma Department of Transportation
Keith Stout	Oklahoma Department of Transportation
David Saulsberry	Oklahoma Department of Transportation
Ken Phillips	Oklahoma Department of Transportation
Carl Eldridge	Oklahoma Department of Transportation
Michele Anderson	Oklahoma Department of Transportation
Joshua Jones	Oklahoma Department of Transportation
Nick Betz	Oklahoma Department of Transportation
Bart Vleugals	Oklahoma Department of Transportation
Scott Cosby	Oklahoma Department of Transportation

Extra Special Thanks to

Mary Dell Dean

HIGHWAY GEOLOGY SYMPOSIUM

NATIONAL STEERING COMMITTEE OFFICERS 2010

**Michael Vierling -
(CHAIRMAN)**

Term: 9/2006 until 2010
(YAA) Engineering Geologist
Canal Design Bureau
New York State Thruway Authority
200 Southern Blvd
Albany, NY 12209
E-Mail: michael_vierling@thruway.state.ny.us
Phone: 518-471-4378
Fax: 518-436-3060



**Jeff Dean -
(VICE-CHAIRMAN)**

Term: 9/2006 until 2010
Oklahoma DOT
200 NE 21st St.
Oklahoma City, OK 73105
Ph: (405)521-2677 or (405)522-0988
Fax: (405)522-4519
Email: jidean@odot.org



**Vanessa Bateman -
(SECRETARY)**

Term: 9/2006 until 2010
Tennessee Department of Transportation
Geotechnical Engineering Section
Address: 6601 Centennial Blvd.
Nashville, TN 37243-0360
Phone: (615) 350-4137
Fax: (615) 350-4128
Email: vanessa.bateman@state.tn.us



**Russell Glass -
(TREASURER)**

(Publications & Proceedings)
Retired NCDOT
100 Wolf Cove
Asheville, NC 28804
Ph: (828) 252-2260
Email: frgeol@aol.com



HIGHWAY GEOLOGY SYMPOSIUM 2010

NATIONAL STEERING COMMITTEE MEMBERS

Ken Ashton (Membership)
West VA Geological Survey
P.O. Box 879
Morgantown, WV 26507-0879

Ph: (304)594-2331
Fax: (304)594-2575
ashton@geosrv.wvnet.edu

Vanessa Bateman (Secretary)
Tennessee Department of Transportation
Geotechnical Engineering Section
Address: 6601 Centennial Blvd.
Nashville, TN 37243-0360

Phone: (615) 350-4133
Fax: (615) 350-4128
vanessa.bateman@state.tn.usTransportation

Richard Cross
Golder Associates
RD 1 Box 183A
Solansville, NY 12160

Ph: (518)868-4820
Cell: (603)867-4191
dick_Cross@juno.com

John D. Duffy
California Dept. of Transportation
50 Higuera St.
San Luis Obispo, CA 93401

Ph: (805)527-2275
Fax: (805)549-3297
John_D_Duffy@dot.ca.gov

Jeff Dean (Vice-Chairman)
Oklahoma Dept of Transportation
200 NE 21st St.
Oklahoma City, OK 73105

Ph: (405)522-0988
Fax: (405)522-4519
idean@odot.org

Tom Eliassen
Transportation Geologist
State of Vermont, Agency of Transportation
Materials & Research Section
National Life Building, Drawer 33
Montpelier, VT 05633

Ph: 802-828-2516
fax: 802-828-2792
tom.eliassen@state.vt.us

Marc Fish
Engineering Geologist
WSDOT Geotechnical Division
Environmental & Engineering Programs
Materials Laboratory
PO Box 47365
Olympia, WA 98504-7365

360-709-5498 (office)
360-485-5825 (cell)
fishm@wsdot.wa.gov

Russell Glass (Treasurer)
(Publications & Proceedings)
NCDOT (Retired)
100 Wolf Cove
Asheville, NC 28804

Ph: (828) 252-2260
frgeol@aol.com

Bob Henthorne
Chief Geologist
Kansas Dept. of Transportation
Materials and Research Center
2300 Van Buren
Topeka, KS 66611-1195

Phone 785-291-3860
Fax 785-296-2526
roberth@ksdot.org

HIGHWAY GEOLOGY SYMPOSIUM 2010

NATIONAL STEERING COMMITTEE MEMBERS

Peter Ingraham

Golder Associates
540 North Commercial Street, Suite 250
Manchester, New Hampshire 03101-1146

Ph: (603)668-0880
Fax: (603)668-1199
pingraham@golder.com

Daniel Journeaux

Janod Inc.
34 Beeman Way
P.O. Box 2487
Champlain, NY 12919

Phone: (518) 298-5226
Fax: (450) 424-2614
info@janod.biz

Richard Lane

NHDOT, Bureau of Materials & Research
5 Hazen Drive, Concord
New Hampshire 03301

Phone: (603) 271-3151
Fax: (603) 271-8700
dlane@dot.state.nh.us

Henry Mathis - (By-Laws)

H.C. Nutting A/ Terracon Co.
561 Marblerock Way
Lexington, KY 40503 Office: (859)296-5664

Cell: 859-361-8362
Office: 859-455-8530
Fax: 859-455-8630
hmathis@iglou.com

Harry Moore - (Historian, Appt.)

Tenn. DOT (retired)
Golder Associates
Senior Consultant
3730 Chamblee Tucker Rd.,
Atlanta, GA 30341

Atlanta Office phone: 770-496-1893
HLMoore@golder.com

John Pilipchuk

NCDOT Geotechnical Engineering Unit
5253 Z-Max Blvd
Harrisburg, NC 28075

Ph: 704-455-8902
Fax: 704-455-8912
jpilipchuk@dot.state.nc.us

Nick Priznar

Sr. Eng. Geologist
Arizona D.O.T.
121 N. 21st Ave. 068R
Phoenix AZ, 85009

Ph: (602)712-8089
Fax: (602)712-8138
npriznar@azdot.gov

Erik Rorem

Geobrugg North America, LLC
551 W. Cordova Road, PMB 730
Santa Fe, NM 87505

Phone: 505-438-6161
Fax: 505-438-6166
erik.rorem@geobrugg.com

Christopher A. Ruppen (YAA)

Michael Baker Jr., Inc.
4301 Dutch Ridge Rd.
Beaver, PA 15009-9600

Ph: (724)495-4079
Fax: (724)495-4017
Cell: (412)848-2305
cruppen@mbakercorp.com

HIGHWAY GEOLOGY SYMPOSIUM 2010

NATIONAL STEERING COMMITTEE MEMBERS

Stephen Senior

Ministry of Transportation, Ontario
Soils and Aggregates Section
1201 Wilson Ave.
Rm 220, Building C
Downsview, ON M3M 1J6 Canada

Ph: (416)235-3743
Fax: (416)235-4101
stephen.senior@mto.gov.on.ca

Michael P. Schulte, P.G.

WYDOT Geology Program
5300 Bishop Blvd.
Cheyenne, WY 82009-3340

Office: (307) 777-4222
Cell: (307) 287-2979
Fax: (307) 777-3994
Mike.Schulte@dot.state.wy.us

Jim Stroud (Appt)

Vulcan Materials Company
Manager of Geological Services
4401 Patterson Ave.
PO Box 4239 Winston-Salem, NC 27105

Office 336-744-2940
Fax 336-744-2018
336-416-3656 (M)
stroudj@vmcmail.com

Steven Sweeney

NYS Canal Corporation

Phone: (518) 334-2511
Email: ssweeney2@nycap.rr.com

John F. Szturo R.G.

HNTB Corporation
KC Office
715 Kirk Drive
Kansas City, MO 64105

Direct Line 816 527-2275
Fax 816 472-5013
Cell 913 530-2579
jszturo@hntb.co

Robert Thommen

Rotec International, LLC
P.O.Box 31536
Sante Fe, NM 87594-1536

Ph: 505-989-3353
Fax: 505-984-8868
thommen@www.rotecinternational-usa.com

Michael P. Vierling (Chairman)

Engineering Geologist
Canal Design Bureau
New York State Thruway Authority
200 Southern Blvd
Albany, NY 12209

Phone: 518-471-4378
Fax: 518-436-3060
michael_vierling@thruway.state.ny.us

Terry West (Medallion, Emetrius)

Earth and Atmospheric Science Dept.
Purdue University West Lafayette, IN

47907-1297 Ph: (765)494-3296
Fax: (765)496-1210
trwest@cas.purdue.edu

HIGHWAY GEOLOGY SYMPOSIUM

HISTORY, ORGANIZATION, AND FUNCTION

Established to foster a better understanding and closer cooperation between geologists and civil engineers in the highway industry, the Highway Geology Symposium (HGS) was organized and held its first meeting on March 14, 1950, in Richmond Virginia. Attending the inaugural meeting were representatives from state highway departments (as referred to at that time) from Georgia, South Carolina, North Carolina, Virginia, Kentucky, West Virginia, Maryland, and Pennsylvania. In addition, a number of federal agencies and universities were represented. A total of nine technical papers were presented.

W.T. Parrott, an engineering geologist with the Virginia Department of Highways, chaired the first meeting. It was Mr. Parrott who originated the Highway Geology Symposium.

It was at the 1956 meeting that future HGS leader, A.C. Dodson, began his active role in participating in the Symposium. Mr. Dodson was the Chief Geologist for the North Carolina State Highway and Public Works Commission, which sponsored the 7th HGS meeting.

Since the initial meeting, 61 consecutive annual meetings have been held in 32 different states. Between 1950 and 1962, the meetings were east of the Mississippi River, with Virginia, West Virginia, Ohio, Maryland, North Carolina, Pennsylvania, Georgia, Florida,, and Tennessee serving as host state.

In 1962, the symposium moved west for the first time to Phoenix, Arizona where the 13th annual HGS meeting was held. Since then it has alternated, for the most part, back and forth from the east to the west. The Annual Symposium has moved to different location as follows:

List of Highway Geology Symposium Meetings

<u>No.</u>	<u>Year</u>	<u>HGS Location</u>	<u>No.</u>	<u>Year</u>	<u>HGS Location</u>
1 st	1950	Richmond, VA	2 nd	1951	Richmond, VA
3 rd	1952	Lexington, VA	4 th	1953	Charleston, WV
5 th	1954	Columbus, OH	6 th	1955	Baltimore, MD
7 th	1956	Raleigh, NC	8 th	1957	State College, PA
9 th	1958	Charlottesville, VA	10 th	1959	Atlanta, GA
11 th	1960	Tallahassee, FL	12 th	1961	Knoxville, TN
13 th	1962	Phoenix, AZ	14 th	1963	College Station, TX
15 th	1964	Rolla, MO	16 th	1965	Lexington, KY
17 th	1966	Ames, IA	18 th	1967	Lafayette, IN
19 th	1968	Morgantown, WV	20 th	1969	Urbana, IL
21 st	1970	Lawrence, KS	22 nd	1971	Norman, OK

23 rd	1972	Old Point Comfort, VA	24 th	1973	Sheridan, WY
25 th	1974	Raleigh, NC	26 th	1975	Coeur d'Alene, ID
27 th	1976	Orlando, FL	28 th	1977	Rapid City, SD
29 th	1978	Annapolis, MD	30 th	1979	Portland, OR
31 st	1980	Austin, TX	32 nd	1981	Gatlinburg, TN
33 rd	1982	Vail, CO	34 th	1983	Stone Mountain, GA
35 th	1984	San Jose, CA	36 th	1985	Clarksville, TN
37 th	1986	Helena, MT	38 th	1987	Pittsburg, PA
39 th	1988	Park City, UT	40 th	1989	Birmingham, AL
41 st	1990	Albuquerque, NM	41 st	1991	Albany, NY
43 rd	1992	Fayetteville AR	44 rd	1993	Tampa, FL
45 th	1994	Portland, OR	46 th	1995	Charleston, WV
47 th	1996	Cody, WY	48 th	1997	Knoxville, TN
49 th	1998	Prescott, AZ	50 th	1999	Roanoke, VA
51 st	2000	Seattle, WA	52 nd	2001	Cumberland, MD
53 rd	2002	San Luis Obispo, CA	54 th	2003	Burlington, VT
55 th	2004	Kansas City, MO	56 th	2005	Wilmington, NC
57 th	2006	Breckinridge, CO	58 th	2007	Pocono Manor, PA
59 th	2008	Santa Fe, NM	60 th	2009	Buffalo, NY
61 st	2010	Oklahoma City, OK			

Unlike most groups and organizations that meet on a regular basis, the Highway Geology Symposium has no central headquarters, no annual dues and no formal membership requirements. The governing body of the Symposium is a steering committee composed of approximately 20 - 25 engineering geologist and geotechnical engineers from state and federal agencies, colleges and universities, as well as private service companies and consulting firms throughout the country. Steering committee members are elected for three-year terms, with their elections and re-elections being determined principally by their interests and participation in and contribution to the Symposium. The officers include a chairman, vice chairman, secretary, and treasurer. all of whom are elected for a two-year term. Officers, except for the treasurer, may only succeed themselves for one additional term.

A number of three-member standing committees conduct the affairs of the organization. The lack of rigid requirements, routing and relatively relaxed overall functioning of the organization is what attracts many participants.

Meeting sites are chosen two to four years in advance and are selected by the Steering Committee following presentations made by representatives of potential host states. These presentations are usually made at the steering committee meeting, which is held during the Annual Symposium. Upon selection, the state representative becomes the state chairman and a member pro-tem of the Steering Committee.

The symposia are generally scheduled for two and one-half days, with a day-and-a-half for technical papers plus a full day for the field trip. The Symposium usually begins on Wednesday morning. The field trip is usually Thursday, followed by the annual banquet

that evening. The final technical session generally ends by noon on Friday. In recent years this schedule has been modified to better accommodate climate conditions and tourism benefits.

The field trip is the focus of the meeting. In most cases, the trips cover approximately 150 to 200 miles, provide for six to eight scheduled stops, and require about eight hours. Occasionally, cultural stops are scheduled around geological and geotechnical points of interests. To cite a few examples: in Wyoming (1973), the group viewed landslides in the Big Horn Mountains; Florida's trip (1976) included a tour of Cape Canaveral and the NASA space installation; the Idaho and South Dakota trips dealt principally with mining activities; North Carolina provided stops at a quarry site, a dam construction site, and a nuclear generation site; in Maryland, the group visited the Chesapeake Bay hydraulic model and the Goddard Space Center. The Oregon trip included visits to the Columbia River Gorge and Mount Hood; the Central mine region was visited in Texas; and the Tennessee meeting in 1981 provided stops at several repaired landslide in Appalachia regions of East Tennessee.

In Utah (1988) the field trip visited sites in Provo Canyon and stopped at the famous Thistle Landslide, while in New Mexico, in 1990, the emphasis was on rockfall treatments in the Rio Grande River canyon and included a stop at the Brugg Wire Rope headquarters in Santa Fe.

Mount St. Helens was visited by the field trip in 1994 when the meeting was in Portland, Oregon, while in 1995 the West Virginia meeting took us to the New River Gorge Bridge that has a deck elevation of 876 feet above the water.

In Cody, Wyoming the 1996 field trip visited the Chief Joseph Scenic Highway and the Beartooth Uplift in northwest Wyoming. In 1997 the meeting in Tennessee visited the newly constructed future I-26 highway in the Blue Ridge of East Tennessee. The Arizona meeting in 1998 visited the Oak Creek Canyon near Sedona and a mining ghost town at Jerome, Arizona. The Virginia meeting in 1999 visited the "Smart Road" Project that was under construction. This was a joint research project of the Virginia Department of Transportation and Virginia Tech University. The Seattle Washington meeting in 2000 visited the Mount Rainier area. A stop during the Maryland meeting in 2001 was the Sideling Hill road cut for I-68 which displayed a tightly folded syncline in the Allegheny Mountains.

The California field trip in 2002 provided a field demonstration of the effectiveness of rock netting against rock falls along the Pacific Coast Highway. The Kansas City meeting in 2004 visited the Hunt Subtropolis which is said to be the "world's largest underground business complex". It was created through the mining of limestone by way of the room and pillar method. The Rocky Point Quarry provided an opportunity to search for fossils at the North Carolina meeting in 2005. The group also visited the US-17 Wilmington Bypass Bridge which was under construction. Among the stops at the Pennsylvania

meeting were the Hickory Run Boulder Field, the No.9 Mine and Wash Shanty Museum, and the Lehigh Tunnel.

The New Mexico field trip in 2008 included stops at a soil nailed wall along US-285/84 north of Santa Fe and a road cut through the Bandelier Tuff on highway 502 near Los Alamos where rockfall mesh was used to protect against rockfalls. The New York field trip in 2009 visited the Niagara Falls Gorge and the Devil's Hole Trail.

At the technical sessions, case histories and state-of-the-art papers are most common; with highly theoretical papers the exception. The papers presented at the technical sessions are published in the annual proceedings. Some of the more recent papers may be obtained from the Treasurer of the Symposium.

Banquet speakers are also a highlight and have been varied through the years.

A Medallion Award was initiated in 1970 to honor those persons who have made significant contributions to the Highway Geology Symposium. The selection was and is currently made from the members of the national steering committee of the HGS.

A number of past members of the national steering committee have been granted Emeritus status. These individuals, usually retired, resigned from the HGS Steering Committee, or are deceased, have made significant contributions to the Highway Geology Symposium. A total of 30 persons have been granted Emeritus status. Ten are now deceased.

Several Proceedings volumes have been dedicated to past HGS Steering Committee members who have passed away. The 36th HGS Proceedings were dedicated to David L. Royster (1931 - 1985, Tennessee) at the Clarksville, Indiana Meeting in 1985. In 1991 the Proceedings of the 42nd HGS held in Albany, New York were dedicated to Burrell S. Whitlow (1929 - 1990, Virginia).

HIGHWAY GEOLOGY SYMPOSIUM

EMERITUS MEMBERS OF THE STEERING COMMITTEE

Emeritus Status is granted by the Steering Committee

R.F. Baker*
John Baldwin
David Bingham
Virgil E. Burgat*
Robert G. Charboneau*
Hugh Chase*
A.C. Dodson*
Walter F. Fredericksen
Brandy Gilmore
Robert Goddard
Joseph Gutierrez
Richard Humphries
Charles T. Janik
John Lemish
Bill Lovell
George S. Meadors, Jr.*
Willard McCasland
David Mitchell
W.T. Parrot*
Paul Price*
David L. Royster*
Bill Sherman
Willard L. Sitz
Mitchell Smith
Steve Sweeney
Sam Thornton
Berke Thompson*
Burrell Whitlow*
W.A. "Bill" Wisner
Earl Wright
Ed J. Zeigler
(* Deceased)

HIGHWAY GEOLOGY SYMPOSIUM

Medallion Award Winners

The Medallion Award is presented to individuals who have made significant contributions to the Highway Geology Symposium over many years. The award, instituted in 1969, is a 3.5 inch medallion mounted on a walnut shield and appropriately inscribed. The award is presented during the banquet at the annual Symposium.

Hugh Chase*	1970
Tom Parrott*	1970
Paul Price*	1970
K.B. Woods*	1971
R.J. Edmondson*	1972
C.S. Mullin*	1974
A.C. Dodson*	1975
Burrell Whitlow*	1978
Bill Sherman	1980
Virgil Burgat*	1981
Henry Mathis	1982
David Royster*	1982
Terry West	1983
Dave Bingham	1984
Vernon Bump	1986
C.W. "Bill" Lovell	1989
Joseph A. Gutierrez	1990
Willard McCasland	1990
W.A. "Bill" Wisner	1991
David Mitchell	1993
Harry Moore	1996
Earl Wright	1997
Russell Glass	1998
Harry Ludowise*	2000
Sam Thornton	2000
Bob Henthorne	2004
Mike Hager	2005
Joseph A. Fischer	2007
Ken Ashton	2008
A. David Martin	2008
Michael Vierling	2009
Richard Cross	2009

(*Deceased)

HIGHWAY GEOLOGY SYMPOSIUM

FUTURE SYMPOSIUM SCHEDULE AND CONTACT LIST

2011	Kentucky	Henry Mathis	859-455-8530	hmathis@iglou.com
2012	California	Bill Webster	916-227-1041	Bill Webster@dot.ca.gov
2013	OPEN	Mike Vierling Chairman HGS	518-436-3197	Michael Vierling@thruway.state.ny.us



61st HIGHWAY GEOLOGY SYMPOSIUM SPONSORS

The following companies have graciously contributed toward the sponsorship of the Symposium. The HGS relies on sponsor contributions for refreshment breaks, field trip lunches and other activities. We gratefully appreciate the contributions made by these sponsors.



Baker

Michael Baker Jr., Inc.
4301 Dutch Ridge Road
Beaver, PA 15009
Phone: (724) 495-4079 Fax: (724)
495-4112
www.mbakercorp.com

Michael Baker Corporation has evolved into one of the leading engineering and energy management firms by consistently solving complex problems for its clients. We view challenges as invitations to innovate. **Baker** has been providing geotechnical services since the mid-1950's. Professional geotechnical engineers and geologists are supported by a staff of highly trained assistants. Expertise covers most major facets of geotechnical investigation and design, including geologic reconnaissance, subsurface investigations, geotechnical analysis and design, and geotechnical construction phase services.

Geobrugg North America, LLC.
551 W. Cordova Road, PMB 730
Santa Fe, New Mexico 87505
Phone: (505)438-6161
Fax: (505) 438-6166
www.geobrugg.com



Geobrugg helps protect people and infrastructures from the forces of nature. These technologically mature protection systems are manufactured in Santa Fe, New Mexico; but are installed world-wide. With its basic component, the high-strength steel wire, our natural hazard mitigation systems offer proven protection against rockfalls, avalanches, mudflows, debris flows, and slope failures. With a bedrock belief in total customer satisfaction, **Geobrugg** strives to provide exceptional assistance to our customers in mitigating against natural hazard problems.



Golder Associates, Inc.
670 N. Commercial Street, Suite 103
Manchester, NH 03101
Phone: (603) 668-0880 Fax: (603) 668-
1199
www.golder.com

Golder Associates is an international group of science and engineering companies. The employee-owned group of companies provides comprehensive consulting services in support of environmental, industrial, and natural resources and civil engineering projects. Founded in 1960, **Golder Associates** now has nearly 6,000 employees in over 150 offices worldwide and has completed projects in more than 140 countries.



Hi-Tech Rockfall Construction, Inc.
PO Box 674
Forest Grove, Oregon 97116
Phone: (503) 357-6508
Fax: (503) 357-7323
www.hitechrockfall.com

HI-TECH Rockfall Construction Inc. specializes in rockfall safety problems on highways, railroads, dams, construction sites and many other locations. The principals of **HI-TECH** have over 50 years of combined experience in the rockfall industry. Our highly skilled employees have extensive experience in all types of rockfall drapery systems, rockfall barriers, debris flow barriers, rock scaling, rock bolting, and shotcrete. Commendations for safety excellence from the Associated General Contractors of America and SAIF Corporation indicates the level of attention that **HI-TECH** imparts to all of our employees in this very specialized field

Janod, Inc.
34 Beeman Way,
Champlain, NY 12919
Phone: (518)298-5226
Fax: (450) 424-2614
www.janod.biz



Janod has specialized in rock stabilization and rock remediation since 1968

Janod was founded in 1968 by Douglas Journeaux, and at that time, soft earth tunneling was the principle part of our operations. In 1970 **Janod** was introduced to rock slope stabilization when called in by Quebec Cartier Mining Looking towards the future of rock stabilization to perform some emergency work along the railway. **Janod** has since become a specialist in rock stabilization, and employs a combination of innovative mechanized equipment and highly trained rock remediation technicians who have an intimate knowledge of geology and influence of climatic conditions unexposed rock structures. **Janod** takes pride in having successfully met many different challenges at numerous and varied worksites throughout North America.

MACCAFERRI

Maccaferri, Inc.
10303 Governor Lane
Boulevard
Williamsport, Maryland 21795
Phone: (301) 223-6910
Fax: (301) 223 4590
www.maccaferri-usa.com

Maccaferri is a world leader in engineered environmental solutions. Our expertise includes solutions in retaining wall systems (gabion, geogrid), steep slopes, embankments, drainage systems, rockfall protection and erosion protection. Part of a worldwide industrial group, **Maccaferri** has more than 125 years of experience in soil stabilization. Traditionally known for its double twist Gabions and Reno mattresses, **Maccaferri** has extended its product range significantly over the last decade, enabling us to offer an unrivalled range of wire, geosynthetic and natural fiber products to the construction industry.

**Mountain Management /
IGOR Paramassi**
1135 Terminal Way
Suite 106 Financial Plaza
Building
Reno, NV 89502
Phone: (866) 466-7223
Fax: (450) 455-8762
www.mountainmanagement.biz



Mountain Management is a new North American distributor and manufacturer of rock fall barrier, erosion control and avalanche systems. Our suppliers have more than 20 years experience in mitigation systems. Our systems are guaranteed and have proven over the years to assemble and install with more ease and less time required. We have the latest in design and technology. Many of our products are patent protected and field tested. Mountain Management Rock Fall protection systems are capable of handling energies ranging from 50to 5000 Kilojoules. Submitted to testing, our systems are the outcome of more than 20 years of combined field experience and Rock Fall Simulation Studies.



**Oklahoma Aggregates
Association**
3500 North Lincoln Blvd.
Oklahoma City, OK 73105
Phone: (405) 524-7680
Fax: (405) 524-7677
www.okaa.org

OKAA is an organization of business leaders, in the Oklahoma aggregate industry, working together to promote the use of aggregate products, provide unequalled membership services, and develop a true working relationship between aggregate producers and allied industries within the State of Oklahoma and beyond.

61st HIGHWAY GEOLOGY SYMPOSIUM EXHIBITORS

Thanks to all participating exhibitors. The exhibit booths are in the Centennial and Grand Ballrooms



AIS Construction, Inc.
6420 Via Real, Suite 6
Carpinteria, CA 93013
Phone: (805)-684-4344 Fax: (805) 566-6534
www.aisconstruction.com



Michael Baker Jr., Inc.
4301 Dutch Ridge Road
Beaver, PA 15009
Phone: (724) 495-4079 Fax: (724) 495-4112
www.mbakercorp.com



BURGESS ENGINEERING AND TESTING, INC.

Burgess Engineering and Testing, Inc.
809 N.W. 34th St.
Moore, OK 73160
Phone: (405) 790-0488 Fax: (504) 790-0788
www.burgessengineer.com



Central Mine Equipment Company
4215 Rider Trail North,
Earth City, MO 63045
Phone: (800) 325-8827 Fax: (314) 291-4880
www.cmeco.com



Contech Construction Products, Inc.
820 Cincinnati Ave.
Tulsa, Oklahoma 74119
Phone: (918) 504-7630 Fax: (866) 671-6267
www.contech-cpi.com



Dataforensics
3280 Pointe Parkway, Suite 2000
Norcross, GA 30097
Phone: (678) 406-0106 Fax: (678) 367-0870
www.dataforensics.net



Gannett Fleming

**ISO 9001:2008
CERTIFIED**

Gannett Fleming
601 Holiday Drive, Suite 200, Foster Plaza III
Pittsburg, PA 15220
Phone: (412) 922-5575 Fax: (412) 922-3717
www.gannettfleming.com



Geobrugg North America, LLC.
551 W. Cordova Road, PMB 730
Santa Fe, New Mexico 87505
Phone: (505)438-6161 Fax: (505) 438-6166
www.goebrugg.com



Geokon, Inc.
48 Spencer Street
Lebanon, NH 03766
Phone: (603) 448-1562 Fax: (603) 448-3216
www.geokon.com



Golder Associates, Inc.
670 N. Commercial Street, Suite 103
Manchester, NH 03101
Phone: (603) 668-0880 Fax: (603) 668-1199
www.golder.com



Hi-Tech Rockfall Construction, Inc.
PO Box 674
Forest Grove, Oregon 97116
Phone: (503) 357-6508 Fax: (503) 357-7323
www.hitechrockfall.com



Horn and Associates, Inc.
216 North Main Street
Winchester, KY 40391
Phone: (859) 744-2232 Fax: (859) 744-5892
www.hornandassociates.com



Janod, Inc.
34 Beeman Way,
Champlain, NY 12919
Phone: (518)298-5226 Fax: (450) 424-2614
www.janod.biz



KANE Geotech, Inc.
7400 Shoreline Drive, Suite 6
Stockton, CA 95219
Phone: (209) 472-1822 Fax: (209)0802
www.kanageotech.com



Maccaferri, Inc.
10303 Governor Lane Boulevard
Williamsport, Maryland 21795
Phone: (301) 223-6910 Fax: (301) 223 4590
www.maccaferri-usa.com



Monotube Pile Corp.
1825 16th St. N.E., P.O. Box 7339
Canton, Ohio 44705
Phone: (330)454 6111 Fax: (330) 454-1572
www.monotube.com



**Mountain Management /
IGOR Paramassi**
1135 Terminal Way
Suite 106 Financial Plaza Building
Reno, NV 89502
Phone: (866) 466-7223 Fax: (450) 455-8762
www.mountainmanagement.biz



Oklahoma Aggregates Association
3500 North Lincoln Blvd.
Oklahoma City, OK 73105
Phone: (405) 524-7680 Fax: (405) 524-7677
www.okaa.org



Oklahoma Geological Survey
The University of Oklahoma
100 E. Boyd, Room N-131
Norman, OK 73019
Phone: (405) 325-3031 Fax: (405) 325-7069
www.ogs.ou.edu



Professional Service Industries, Inc.
801 S.E. 59th St.
Oklahoma City, OK 73129
Phone: (405) 632-8800 Fax: (405) 631-2180
www.psiusa.com



Roadbond Service Company
6413 Hill City Highway
Tolar, TX 76476
Phone: (817) 613-7095 Fax: (254) 835-5297
www.RoadbondSoil.com



INTERNATIONAL, LLC

Rotec International, LLC
7 Camino Don Patron
Santa Fe, New Mexico 87506
Phone: (505) 989-3353 Fax: (505) 984-8868
www.rotecinternational-usa.com



SIMCO Drilling Equipment, Inc.
802 Furnas Drive
Osceola, IA 50213
Phone: (800) 338-9925 Fax: (641) 342-6764
www.simcodrill.com



Soil Nail Launcher, Inc.
2841 North Avenue
Grand Junction, CO 81501
Phone: (970) 210-6170 Fax: (970) 245-7737
www.soilnaillauncher.com



Standard Testing and Engineering Co.
3400 North Lincoln
Oklahoma City, OK 73105
Phone: (405) 528-0541 Fax: (405) 528-0559
www.stantest.com



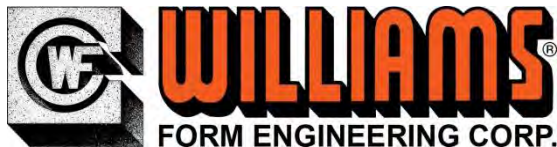
TenCate Geosynthetics, N.A.
14064 S. Hagen St.
Olathe, KS 66062
Phone: (913) 909-7150 Fax: (831) 665-5970
www.tencate.com



Tensar International Corporation
21622 Redcrested Glen Ct.
Spring, Texas 77388
Phone: (281) 217-9616 Fax: (281) 966-1513
www.tensar.com



Terracon Consultants, Inc.
5301 Beverly Drive
Oklahoma City, OK 73105
Phone: (405) 525-0453 Fax: (405) 557-0549
www.terracon.com



Williams Form Engineering, Corp.
251 Rooney Road
Golden, CO 80401
Phone: (303) 216-9300 Fax: (303) 216-9400
Williamsform.com



Zonge Geosciences, Inc.
7711 W. 6th Ave. Suite G
Lakewood, Co 80214
Phone: (720) 962-4444 Fax: (720) 962-0417
1800geophysics.com

61st Highway Geology Symposium Agenda

Monday, August 23rd

11:00 AM to 5:30 PM

HGS Registration is open

12:00 PM - 5:00 PM

TRB Session - Asset Management in a World of Dirt

Location: Continental Room - 14th Floor

6:30 PM to 8:30 PM

Welcome Reception/ Ice Breaker Social

Location: Exhibition Areas in Centennial & Grand Ballrooms

Sponsored by: **Oklahoma Aggregates Association**

Tuesday, August 24th

6:30 AM to 8:00 AM

Breakfast Buffet

Location: Venetian Room - 14th Floor

Sponsored by: **Janod**

7:00 AM to 12:00 PM

HGS Registration is open

8:30 AM to 4:30 PM

Guest Field Trip

Location: Meet at Registration table

8:00 AM to 8:10 AM

Welcome, Opening remarks

Location: Grand Ballroom

8:10 AM - 8:40 AM

Geology and Mineral Resources of Oklahoma, Luza, Krukowski

Technical Session I - Geophysical and Imaging Applications / Site Investigation Techniques

8:40 AM to 9:00 AM

Mapping Soft-Soil Zones and Top-of-Bedrock Beneath High-Traffic Areas of Honolulu, Sirles, Batchko

9:00 AM to 9:20 AM

**Continuous Subsurface Profiling of Roads Using MASW
(Multi-Channel Analysis of Surface Waves) - Lee**

9:20 AM to 9:40 AM

**Subsurface Geotechnical Exploration Enhancement Through the Use of
Refraction Microtremor (ReMi) Geophysical Survey Techniques - Satterfield,
Roth, Hundley, Bryant, Miller**

9:40 AM to 10:00 AM

**Karst Features in Limestone Evaluated Utilizing an Accoustic Televiewer,
New I-70 Mississippi River Bridge, St. Louis, Missouri - Keller**

10:00 AM to 10:20 AM - Break

Location: Exhibition Areas in Centennial & Grand Ballrooms
Sponsored by: **HI-Tech Rockfall Construction**

**Technical Session II - Geophysical and Imaging Applications /
Site Investigation Techniques**

10:20 AM to 10:40 AM

**Determination of In-Situ Density of Planned Roadway Cuts in Cemented
and Coarse-Grained Soils Using Geophysical Methods to Estimate
Earthwork Factors - Frechette**

10:40 AM to 11:00 AM

**Geophysical Methods Mapping Subsurface Evaporite Features Aid
Roadway Geometric Design - Homan, Sirles**

11:00 AM to 11:20 AM

**Site Characterization and Remediation in Karst Terrain - Fisher, McWhorter,
Fisher**

11:20 AM to 11:40 AM

**Geotechnical Investigation to Support Design of an ADA Compliant Access
Ramp on the South Rim of the Grand Canyon at Mather Point Overlook,
Grand Canyon National Park, Arizona - Mitchell**

11:40 AM to 12:00 PM

**Case Study Using Geotechnical Instrumentation to Monitor
Fill Foundation Stability, Buche, Kane**

12:00PM to 1:20PM - Buffet Lunch

Location: Venetian Room - 14th Floor
Sponsored by: **Management / IGOR Paramasssi**

Technical Session III - Case Histories

1:20 PM to 1:40 PM

Construction of the Amelia Earhart Bridge - Henthorne

1:40 PM to 2:00 PM

Bridge Over Snake River: Geotechnical Engineering on Unstable ground
Hood, Norrish, Martens

2:00 PM to 2:20 PM

Road and Housing Construction on Reclaimed Coal Mine Spoil Undergoes Settlement Damage in Southwest Indiana - West, Johansen

2:20 PM to 2:40 PM

Emergency Rock Remediation I-40 - Journeaux

2:40 PM to 3:00 PM

Emergency Rock Slope Stabilization in the Ocoee Gorge, US Route 64, Polk County, Tennessee - Bateman, Smerkanicz, Sneyd

3:00 PM to 3:20 PM - Break

Location: Exhibition Areas in Centennial & Grand Ballrooms
Sponsored by: **Michael Baker Jr., Inc.**

Technical Session IV - Geotechnical Applications

3:20 PM to 3:40 PM

Geotechnical Engineering for a Super-load Delivery over Pennsylvanian Highways, Ruppen, Gaffney, Saylor

3:40 PM to 4:00 PM

Subsurface Stabilization of Problematic Soil Areas, President George Bush Turnpike - Gregory

4:00 PM to 4:20 PM

Safe and Sound, Missouri Department of Transportation, Design - Build Program of Replacing 554 Bridges - Szturo

4:20 PM to 4:40 PM

Using TDA (lightweight Tire Derive Aggregate) as a Green Alternative for Reconstruction of a Landslide Road Failure, McCormick

4:40 PM to 5:00 PM

Using LiDAR Laser Scanning for Geotechnical Characterizations in Rock
Priznar

5:00 PM to 5:10 PM

Field Trip Overview

5:10 PM

ADJOURN FOR THE DAY

5:20 PM to 6:30 PM

Steering Committee Meeting

Location: Hilton Honors Lounge

Wednesday, August 25th

6:30 AM **Boxed Breakfast** provided (to take on bus)

Location: First Floor near

Sponsored by: **Mountain Management / IGOR Paramasssi**

7:00 AM to 5:30 PM

Highway Geology Field Trip

Lunch sponsored by **Geobruigg**

Drinks sponsored by **Golder**

6:00 PM to 7:00 PM **Social Hour**

Location: Grand Ballroom

Social Hour sponsored by: **Maccaferri, Inc.**

7:00 PM to 10:00 PM

HGS Annual Banquet

Location: Grand Ballroom

Thursday, August 26

6:30 AM to 8:00 AM Breakfast Buffet

Location: Venetian Room - 14th Floor

Sponsored by: **Janod**

Technical Session V - Slope Stabilization and Mitigation

8:00 AM to 8:20 AM

Assessment of the Garvin Landslides - Clarke, Nevels

8:20 AM to 8:40 AM

Rockfall Mitigation Field Techniques and Design - Wagner, Kane

8:40 AM to 9:00 AM

Flexible Facing Analysis for Soil Nailing - Brunet, Lovekin, Bertolo

9:00 AM to 9:20 AM

Use of Dimensional Modeling for Sizing Flexible Barriers Installations that Mitigate Debris Flow Natural Hazards - Amend

9:20 AM to 9:40 AM

The Latest in Testing Procedures and Technological & Installation Developments in Rockfall Protection Barriers - Kalejta

9:40 AM to 10:00 AM

North Slope Landslide Investigation, US-62 Chickasha, Oklahoma - Nevels

10:00 AM to 10:20 AM – Break

Location: Exhibition Areas in Centennial & Grand Ballrooms

Sponsored by: **Geobrugg**

Technical Session VI - Soil Mechanics Related Studies

10:20 AM to 10:40 AM

Influence of Various Cementitious Additives on the Durability of Stabilized Subgrades - Solanki, Zaman

10:40 AM to 11:00 AM

Understanding the Behavior of Integral Abutment Bridges Through Field Instrumentation - Muraleetharan, Miller, Hanlon

11:00 AM to 11:20 AM

Importance of Soils Suction in Pavement Foundations - Bulut

11:20 AM to 11:40 AM

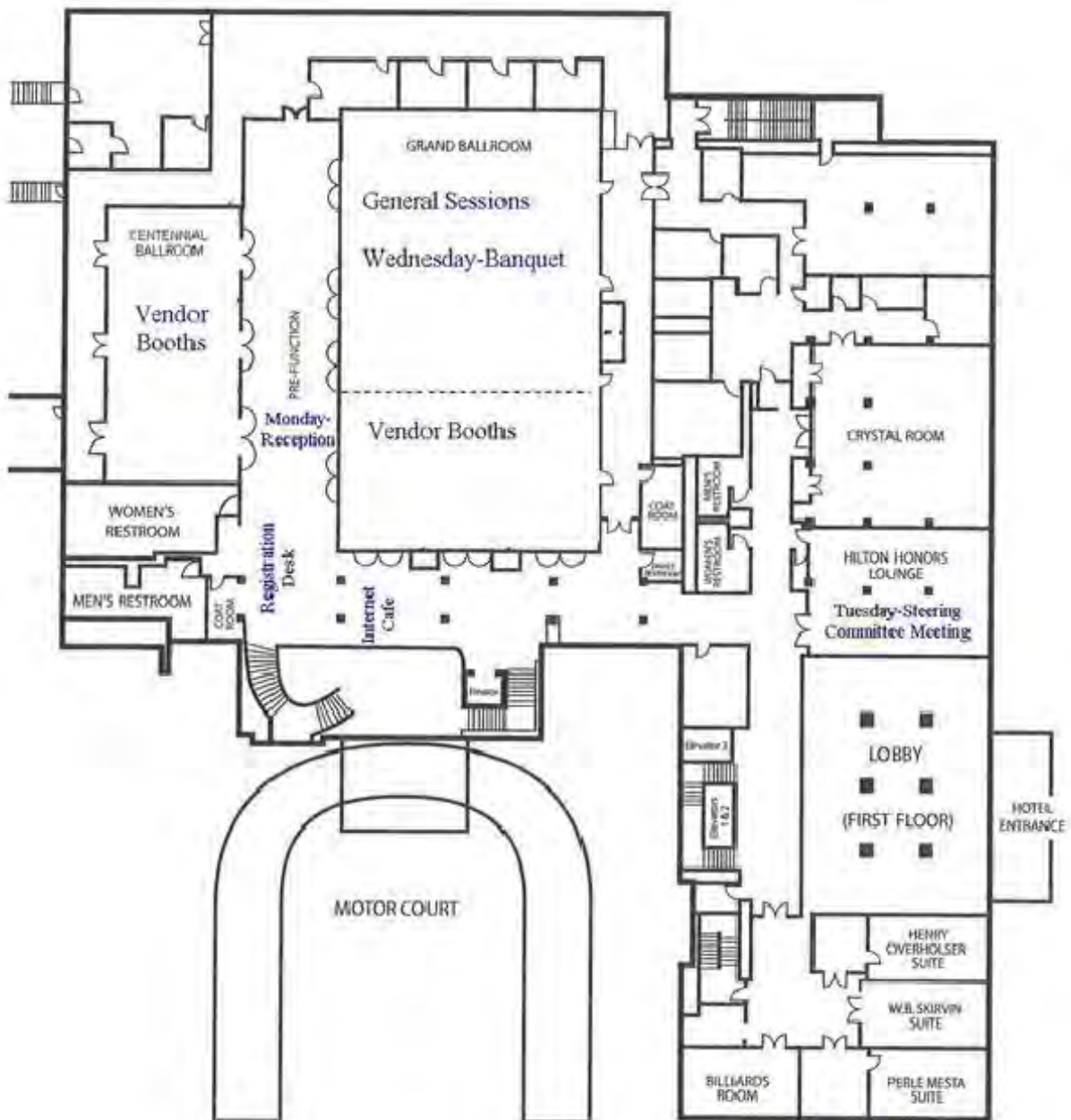
Influence of Moisture Content on the Pullout Capacity of Geotextile Reinforcement in Marginal Soils - Hatamie, Miller

11:40 AM to 12:00 PM

Effects of Sample Preparation Method on Aggregate Shape Characteristics
Singh, Zaman, Commuri

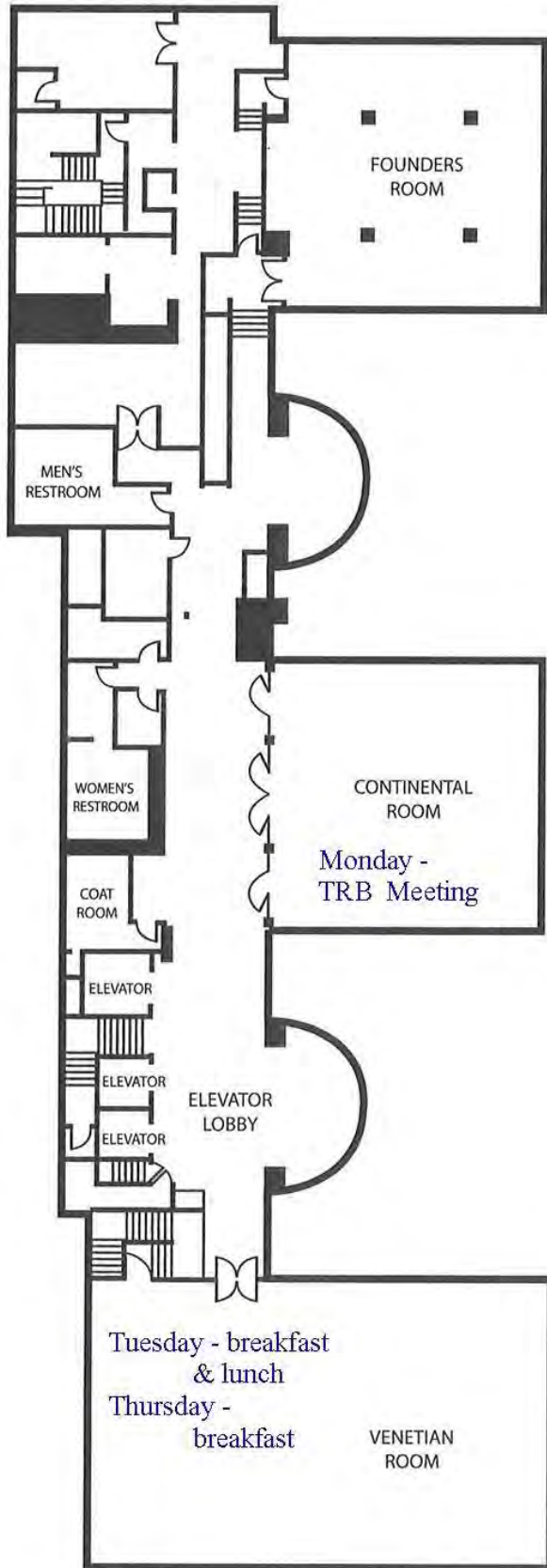
12:00 PM CLOSING REMARKS-ADJOURN

Skirvin Hilton
2nd Floor



(FIRST FLOOR)
doors to load buses for
Wednesday field trip
*pick up for return
transportation to airport

Skirvin Hilton
14th Floor



Geotechnical Asset Management Symposium

“Asset Management in a World of Dirt”

Sponsored by:

TRB Committee AFP10 – Engineering Geology

**TRB Committee AFP20 – Exploration and Classification of
Earth Materials**

August 23, 2010 Oklahoma City, OK

**GAM Symposium at HGS:
“Asset Management in a World of Dirt”
August 23 - Oklahoma City, OK**

Agenda

- 12:00 Opening/Introduction – Larry Pierson/Vanessa Bateman/Dave Stanley
- 12:15 Keynote Speaker: J. Erik Loehr (University of Missouri) – Overview of Geotechnical Asset Management
- 12:45 Blaise Hansen (WYDOT) – “Database Development for GAM”
- 1:15 Kirk Beach/Robert Liang (Ohio DOT/University of Akron) – “Enterprise Database for GAM”
- 1:45 Chris Power (Mott MacDonald) – “GAM for United Kingdom Highways”
- 2:15 Break
- 2:30 Matt DeMarco (FHWA) – “National Park Service Retaining Wall Inventory”
- 3:00 Darren Beckstrand (Landslide Technology) – “Alaska’s Unstable Slope Management Program – Field Data Collection and Management”
- 3:30 John Thornley (HDL Anchorage) – “Geotechnical Asset Management of Buried Structural Components”
- 4:00 Discussion
- 5:00 Closing

The Geology Program's Contribution to the Wyoming Department of Transportation Asset Management Program

By Blaise Hansen, GIT, EIT, and Mike Schulte, PG

ABSTRACT

The Wyoming Department of Transportation (WYDOT) recognizes that implementing Transportation Asset Management (TAM) programs is an essential component to improve cost effectiveness and project scheduling. The Geology Program contributes to this process by managing over 15,000 records of data pertaining to geotechnical engineering. Working with the Information Technology (IT) program, the Oracle Application Express 3.2.1.00.10 software was utilized to develop and design databases for Library, Geologic Maps, Aggregate Sources, and Projects. Establishing a central storage location is indispensable to accessing, searching, and the sharing of information. This has resulted in the ability to establish trends to enhance design recommendations and to organize the increasing amount of geotechnical information obtained with further investigations. The status of integration is almost 100% complete, with future applications to include the ability to display information geographically and combining data with other agencies for project development.

Enterprise Database System for Effective Geotechnical Asset Management at Ohio DOT

Kirk Beach
Geology Program Manager
Office of Geotechnical Engineering
Ohio Department of Transportation
Columbus, Ohio 43223

Robert Y. Liang
Professor
Department of Civil Engineering
University of Akron
Akron, Ohio 44325-3905

Asset management has been recognized as an important agency function in performing strategic and systematic evaluation of cost-benefits of various built infrastructures so that maintenance, repair, or rehabilitation decisions can be made with well-defined objectives, known conditions, constraints, and desired outcomes. Priority setting and resource allocation, based on various scenario investigations, would ultimately help preserve values of the built infrastructure, and extend their service life with optimum repair and maintenance strategies. In short, asset management is about agency's operating, maintaining, and preserving the built infrastructure system in the most cost-effective manner to achieve desired service objectives. To facilitate effective asset management, there is a need for developing an enterprise level tool that is built on GIS based database platform with internet connectivity. Ohio DOT has spent a considerable amount of effort in developing a general tool for building their enterprise level geological hazard management system. The developed tool can be easily adapted for their geotechnical asset management as well. In this presentation, the makeup of the system in a GIS based database platform will be briefly described with emphasis on analogies between the database for geotechnical asset management and geological hazard management. The four components of the system include: (a) an inventory module containing relevant information such as traffic count, physical attributes of the inventory site, and maintenance record, (b) heuristic condition rating matrices for each physical site, (c) a repair and maintenance cost estimation module, and (c) a project tracking module. The functionalities of each component will also be described in detail, again with particular attention to its applications in asset management. More interestingly, the special tools (Tablet PC with blue tooth connections with various site reconnaissance devices) for field work in collecting physical conditions of the site, such as spatial coordinates, images of features, wireless connections with different physical measurement devices and internet connections, etc. As an illustrative example, ODOT current practice on collecting mechanically stabilized wall (MSEW) performance data will be used to demonstrate the usefulness of such an enterprise level Asset Management System. The challenges and benefits in developing such an enterprise based geotechnical asset management system will be discussed at the end of this presentation.

Making Informed Decisions: Geotechnical Asset Management for the UK Highways Agency

David Patterson (UK Highways Agency)

Christopher Power (Mott MacDonald)

Mark Rudrum (Arup)

David Wright (Atkins)

Abstract

The UK Highways Agency has responsibility for the maintenance and upkeep of a network of over 7,000 km (4350 miles) of Motorway and major trunk roads in England. As with any major road authority, this stewardship role includes management of a diverse range of assets (pavements, structures, drainage, technology etc.) all of which are supported by the crucially important Geotechnical Asset. The UK Highways Agency is no different from any US federal, state or local transportation agency in that key budgetary decisions have to be made across all assets that are balanced to provide a selected level of service provision for a minimum optimum Whole Life Cost.

The Highways Agency has an established Geotechnical Asset Management (GAM) process in place that is now underpinning the development of increasingly sophisticated Decision Support Tools (DSTs). These DSTs are not yet fully integrated into the HA business, but are now beginning to be recognised as a major part of the wider Agency Integrated Asset Management (IAM) strategy.

This paper will describe the GAM processes of the UK HA. It will describe the collection of Geotechnical Asset inventory and condition information (that underpins the entire process), the storage of core data in a Geotechnical Data Management System (HA GDMS), the importance of data quality and currency and the development of Decision Support Tools to assist in long-term asset investment planning. It will describe current research and development projects that are being undertaken to support the developing strategy of the HA and will outline the vision of the Agency for a future integrated asset management strategy. The paper will hopefully enable UK and US geotechnical practitioners to recognise that despite major differences in scale and geographical location, we are all seeking to overcome the same challenges, and that an exchange of experience can be extremely beneficial to future developments.

The National Park Service Retaining Wall Inventory and Assessment Program (WIP): 3,500 Walls Later

Matthew J. DeMarco
Geotechnical Group Lead FHWA
Central Federal Lands Highway Division
Lakewood, CO
Matthew.DeMarco@fhwa.dot.gov

Abstract

Beginning in 2004, the FHWA Federal Lands Highway Division (FLH) teamed with the National Park Service (NPS) to develop and implement a retaining wall inventory and condition assessment program supporting roadway asset management efforts underway throughout U.S. Parks. The vast majority of Park earth retaining structures were built prior to 1960, with many built circa 1935, making the assessment of this aging asset a high priority within the NPS. The NPS Retaining Wall Inventory and Assessment Program (WIP) assesses wall performance and develops preliminary repair/replace work orders by measuring, describing, and/or evaluating nearly 60 wall parameters within five main categories: Location, Function, Geometrics, Condition, and Required Action. Beyond the basic inventory aspects of the WIP, the condition assessment considers 25 numerically rated wall elements along with apparent design criteria, failure consequence, and cultural concerns to determine recommended actions and costs to monitor, maintain, repair or replace a given wall. To date, approximately 3,500 walls have been assessed in 33 National Parks, including 20+ wall types within a wide range of geographic settings. Findings indicate the overall health of the 4 million square feet of inspected retaining wall assets within the NPS is good, with approximately a third of the walls requiring minor maintenance or repair and less than 3% of the total asset requiring substantial element repair or complete wall replacement despite the relative old age of the inventory. This presentation describes key development and implementation aspects of the WIP and overviews the condition assessment and wall performance findings for the various wall types encountered. In addition, remedial actions by wall type are discussed, identifying common wall element distresses and deficiencies and recommended repair strategies. The soon-to-be-published comprehensive WIP Procedures Manual will be made available to meeting participants at the time of the presentation.

Alaska's Unstable Slope Management Program

Field Data Collection and Management

Darren Beckstrand, C.E.G.
Landslide Technology
10250 SW Greenburg Road, Suite 111
Portland, Oregon

Thomas Westover
Landslide Technology
10250 SW Greenburg Road, Suite 111
Portland, Oregon

Lawrence Pierson, C.E.G.
Landslide Technology
10250 SW Greenburg Road, Suite 111
Portland, Oregon

David Stanley, C.P.G.
Alaska Department of Transportation and Public Facilities
5750 E. Tudor Road
Anchorage, Alaska

Landslide Technology in partnership with the Alaska Department of Transportation and Public Facilities (AKDOT&PF) have begun a multi-year project to implement an unstable slope asset management program (USMP). Unstable embankments, and soil and rock slopes will be inventoried and rated according to hazard and risk criteria initially developed by University of Alaska Fairbanks and subsequently finalized by Landslide Technology and AKDOT&PF geotechnical and maintenance personnel.

For such efforts in the past, it had been common practice to collect field data on paper forms and then to transcribe the information into an electronic database. In order to automate this process and avoid common data entry and transcription errors, an electronic database was prepared with data entry forms that matched the rating system that accepted all field rating information, digital photographs, and GPS positions. This concept is not new. Electronic field data has been used to collect similar field information with a number of methods that require various hardware and software packages that range from handheld GPS computers with custom database software to laptop computers with spreadsheets. For the USMP, a ruggedized convertible tablet Windows-based computer with built-in GPS was selected as the primary piece of hardware. This provided the benefits of a laptop computer, such as familiar operations, large screen size, and ease of use with the added capabilities of a built-in GPS and pen-based data entry. The tablet PC also allows the annotation of photographs in the field with notes and conceptual mitigation measures. Other supporting hardware includes digital cameras with built-in GPS and geotagging capabilities, and laser rangefinders.

The field data collection database was built using Microsoft Access as the database software. The database was coded with the interoperability with Google Earth, enabling simplified visualization and accessibility of rating data and site photographs. For more detailed geographic analysis and mapping, the database functions well with ArcGIS software. Using this common software package will enable the Department to easily augment the database in the future to add standard of service and life-cycle information as the asset management efforts are completed and the ultimate goal of completing a Geotechnical Asset Management system for unstable slopes is realized. This database will serve as the basis for the gathering system wide information and managing data for this asset management program.

MSE WALL CORROSION IN NEVADA – A CASE STUDY IN GEOTECHNICAL ASSET MANAGEMENT

John D. Thornley, A.M. ASCE, P.E.¹
Raj V. Siddharthan, M. ASCE, Ph.D., P.E.²
David A. Stanley, J.D., C.P.G., L.G., L.E.G.³

ABSTRACT

Transportation system geotechnical assets such as earth retaining structures may be difficult to manage due in part to a shortfall in knowledge about their performance, service lives and life cycle costs. One area of concern for geotechnical structures is the lack of understanding about the potential for corrosion-related failure of buried reinforcements used in mechanically stabilized earth (MSE) walls. Recently, the Nevada Department of Transportation discovered high levels of corrosion at two wall locations in Las Vegas. The resulting investigations of these walls produced direct measurements of metal losses and electrochemical properties of the MSE reinforced fill. One MSE wall was replaced with a cast-in-place concrete tie-back wall at great expense.

It is shown in this paper that the original MSE reinforced fill approval electrochemical test results at the two wall locations are significantly different from those measured in post-construction investigations. The internal stability analyses (using AASHTO 2007 LRFD) of two un-repaired MSE walls were also performed and determined that the estimated remaining service lives are significantly less than the design life of 75 years.

Asset management alternatives evaluation contrasts the cost framework of wall failure, wall replacement, and proactive initiatives such as corrosion monitoring and management. Although monitoring programs for MSE walls are recommended (FHWA, March 2001), few owners of MSE walls use monitoring as a routine management technique. This case study offers evidence that corrosion monitoring of buried geotechnical components can be an effective tool in the toolbox of transportation agencies across the United States.

By following asset management principles, transportation agencies can understand what assets they have through inventorying processes, can understand the condition of the assets through condition surveys, can set service lives and performance standards and use life-cycle cost tools to compare alternatives for mitigation, rehabilitation or repair of the assets in order to meet the agency minimum performance standards. Case studies such as this demonstrate that the essential link between technical analysis and management principles can yield a more efficient and fiscally responsible transportation system that can focus on preservation of assets while maintaining the agency required level of service

¹ Geotechnical Engineer, Hattenburg Dilley & Linnell, LLC, 3335 Arctic Boulevard, Suite 100, Anchorage, AK 99503; PH (907) 564-2139; FAX (907) 564-2122; email: jthornley@hdlalaska.com

² Professor, Department of Civil and Environmental Engineering, University of Nevada, Reno, Mailstop 258, Reno, NV 89557-0258; PH (775) 784- 1411; FAX (775) 784-1390; email: siddhart@unr.edu

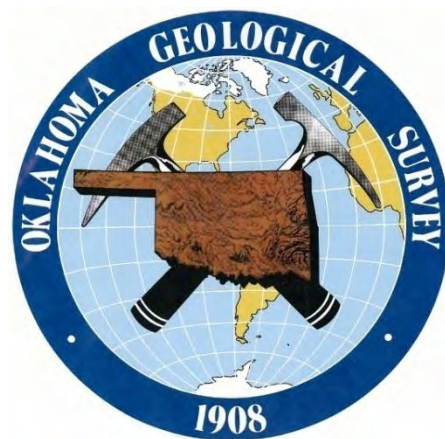
³ Chief Engineering Geologist, Alaska Department of Transportation and Public Facilities, 5800 E. Tudor Rd. Anchorage, Alaska 99507; PH (907) 269-6236; Fax (907) 269-6231; email: dave.stanley@alaska.gov

61st HIGHWAY GEOLOGY SYMPOSIUM

Oklahoma City, Oklahoma

August 23rd - 26th, 2010

Hosted By



The Oklahoma Department of Transportation
The Oklahoma Geological Survey

Proceedings Paper Abstracts & Notes

1. Geology and Mineral Resources of Oklahoma.....	48
Luza, Krukowski	
2. Mapping Soft-Soil Zones and Top-of-Bedrock Beneath High-Traffic Areas of Honolulu	50
Sirles, Batchko	
3. Continuous Subsurface Profiling of Roads Using MASW (Multi-Channel Analysis of Surface Waves)	52
Lee	
4. Subsurface Geotechnical Exploration Enhancement Through the Use of Refraction Microtremor (ReMi) Geophysical Survey Techniques	54
Satterfield, Roth, Hundley, Bryant, Miller	
5. Karst Features in Limestone Evaluated Utilizing an Acoustic Televiwer, New I-70 Mississippi River Bridge, St. Louis, Missouri	56
Keller	
6. Determination of In-Situ Density of Planned Roadway Cuts in Cemented and Coarse-Grained Soils Using Geophysical Methods to Estimate Earthwork Factors	58
Frechette	
7. Geophysical Methods Mapping Subsurface Evaporite Features Aid Roadway Geometric Design	60
Homan, Sirles	
8. Site Characterization and Remediation in Karst Terrain	62
Fisher, McWhorter, Fisher	
9. Geotechnical Investigation to Support Design of an ADA Compliant Access Ramp on the South Rim of the Grand Canyon at Mather Point Overlook, Grand Canyon National Park, Arizona	64
Mitchell	
10. Case Study Using Geotechnical Instrumentation to Monitor Fill Foundation Stability	66
Buche, Kane	
11. Construction of the Amelia Earhart Bridge	68
Henthorne	

12. Bridge Over Snake River: Geotechnical Engineering on Unstable ground	70
Hood, Norrish, Martens	
13. Road and Housing Construction on Reclaimed Coal Mine Spoil Undergoes Settlement Damage in Southwest Indiana	72
West, Johansen	
14. Emergency Rock Remediation I-40	74
Journeaux	
15. Emergency Rock Slope Stabilization in the Ocoee Gorge, US Route 64, Polk County, Tennessee	76
Bateman, Smerkanicz, Sneyd	
16. Geotechnical Engineering for a Super-load Delivery over Pennsylvanian Highways	78
Ruppen, Gaffney, Saylor	
17. Subsurface Stabilization of Problematic Soil Areas, President George Bush Turnpike	80
Gregory	
18. Safe and Sound, Missouri Department of Transportation, Design – Build Program of Replacing 554 Bridges	82
Szturo	
19. Using TDA (lightweight Tire Derive Aggregate) as a Green Alternative for Reconstruction of a Landslide Road Failure	84
McCormick	
20. Using LiDAR Laser Scanning for Geotechnical Characterizations in Rock	86
Priznar, Coxon	
21. Assessment of the Garvin Landslides	88
Clarke, Nevels	
22. Rockfall Mitigation Field Techniques and Design	90
Wagner, Kane	
23. Flexible Facing Analysis for Soil Nailing	92
Brunet, Lovekin, Bertolo	
24. Use of Dimensional Modeling for Sizing Flexible Barriers Installations that Mitigate Debris Flow Natural Hazards	94
Amend	

25. The Latest in Testing Procedures and Technological & Installation Developments in Rockfall Protection Barriers	96
Kalejta	
26. North Slope Landslide Investigation, US-62 Chickasha, Oklahoma	98
Nevels	
27. Influence of various Cementitious Additives on the Durability of Stabilized Subgrades	100
Solanki, Zaman	
28. Understanding the Behavior of Integral Abutment Bridges Through Field Instrumentation	102
Muraleetharan, Miller, Hanlon	
29. Importance of Soils Suction in Pavement Foundations	104
Bulut	
30. Influence of Moisture Content on the Pullout Capacity of Geotextile Reinforcement in Marginal Soils	106
Hatamie, Miller	
31. Effects of Sample Preparation Method on Aggregate Shape Characteristics	108
Singh, Zaman, Commuri	

Geology and Mineral Resources Of Oklahoma

LUZA, K. V., Oklahoma Geological Survey, Norman, OK 73019, kluza@ou.edu,
KRUKOWSKI, S. T., Oklahoma Geological Survey, Norman, OK 73019, skrukowski@ou.edu,
JOHNSON, K. S., Oklahoma Geological Survey, Norman, OK 73019, ksjohnson@ou.edu

ABSTRACT

Oklahoma is a region of complex geology with several mountain ranges, uplifts, and sedimentary basins. The principal mountain belts, the Ouachita, Arbuckle, and Wichita occur in the southern third of Oklahoma. These were sites of folding, faulting, and uplifting during the Pennsylvanian Period. Principal sites of sedimentation were elongated basins that subsided more rapidly than adjacent areas and received 10,000–40,000 ft of sediment. Major basins were confined to the southern half of Oklahoma and included Anadarko, Arkoma, Marietta, Hollis, and Ouachita. Rocks in Oklahoma, mostly sedimentary, are from every geologic period. Permian (about 46%) and Pennsylvanian (about 25%) units comprise the majority of outcrops.

Oklahoma energy resources, particularly oil and natural gas, and coal, had a value of \$14.6 billion in 2006. Major nonfuel mineral production is widespread, but concentrated in major mountain belts in the south and in the Ozark uplift in the northeast. Oklahoma raw nonfuel minerals had a value of \$684 million in 2006, ranking first in the nation in gypsum and iodine production; second in tripoli; fourth in feldspar; seventh in industrial sand and gravel; tenth in masonry cement; and eleventh in common clays. Other industrial minerals of significant value included crushed stone (limestone, dolomite, gypsum, sandstone, rhyolite, and granite), portland cement, and construction sand and gravel. Significant production also includes helium, salt, building stone, and volcanic ash. Almost all Oklahoma mines are open pit except for salt and iodine produced from brine wells; helium from natural gas wells; and one underground limestone mine.

Mapping Soft-Soil Zones and Top-of-Bedrock Beneath High-Traffic Areas in Honolulu

Phil Sirles¹, Zoran Batchko²

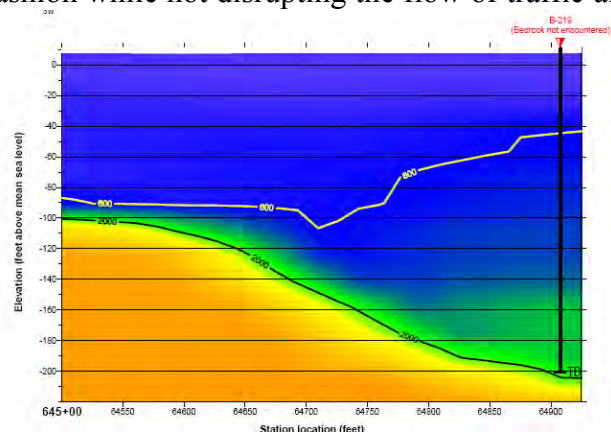
ABSTRACT

Two-dimensional passive surface-wave data were acquired, processed and interpreted for the Honolulu High-Capacity Transit Corridor Project - Waipahu to Aiea - Ewa, Oahu, Hawaii. The project consisted of two distinct geophysical objectives to meet geotechnical engineering needs: first, to determine the lateral and vertical extent of soft-soil conditions; and second, to map the depth-to-bedrock. The Refraction Microtremor (ReMi) method was used along both the Farrington and the [King] Kamehameha Highways. Initially, *blind tests* were conducted to determine the viability of the passive-surface wave seismic technique to meet project objectives. Results were extremely correlative with known geologic conditions, based geotechnical boring data, and the program progressed for the eastern portion of the HHCTCP.

Approximately 2.66-line miles of two-dimensional (2D) ReMi seismic data were acquired along 12 separate lines. Line locations were selected based on a variety of geologic settings and the need for subsurface information between, below and beyond geotechnical borings. Results indicate the seismic and geologic/geotechnical data could be integrated to yield valuable information beneath the areas investigated. An example seismic section is shown below (taken from Line 3). The seismic survey results provided good subsurface information regarding the presence of-, lateral variation of-, and extent of- soft soils which would cause distinct problems for design of deep foundations along the HHCTCP. Additionally the 2D seismic survey revealed that basaltic bedrock can be encountered as shallow as 5 feet, to depths greater than 230 feet beneath the existing highways. The method was extremely effective for meeting project objectives in a timely, safe and economical fashion while not disrupting the flow of traffic along two very busy highway corridors.

Example Seismic Section

(portion of Line 3)



¹ Zonge Geosciences, Inc., 1990 S. Garrison St. #2, Lakewood, Colorado, 80227. P: 720-962-4444, F: 720-962-0417, phils@zonge.us

² PB Americas , 444 Flower St., Ste 3700, Los Angeles, CA, 90071 P: 213-362-9470, F: 213-362-9480

batchko@pbworld.com

Continuous Subsurface Profiling of Roads Using

MASW (multi-channel analysis of surface waves)

Richard Lee, P.G., R.GP.

Quantum Geophysics

29 Richard Lee Lane, Phoenixville, PA 19460

ABSTRACT

Roads are especially challenging environments for doing geophysics. Traffic-induced ground vibrations make it difficult to acquire good seismic refraction and microgravity data. Impervious surfaces and crushed-stone covered shoulders make for poor SP (self-potential) coupling, and buried piping and utilities often found in right-of-ways can impact electrical resistivity measurements. GPR (ground penetrating radar) is a high-resolution profiling method but radar depth of investigation is severely impeded by silty and clayey soils, a condition often found in carbonate terrain. Also, GPR does not work on reinforced concrete roads because the lower antennae frequencies required to look deeper cannot penetrate through the mat of reinforcement steel.

MASW (multi-channel analysis of surface waves) is a relatively new seismic method that is gaining acceptance in the geotechnical community. MASW identifies the vertical distribution of shear wave velocities based upon the dispersion of surface waves (Rayleigh Wave). Since shear wave velocities are a measure of material stiffness, the MASW method can map top of rock, karst, zones of enhanced weathering, low strength materials, and fracture zones. MASW is non-invasive, is not impacted by buried piping or other utilities in the right-of-way, and it is not influenced by reinforcement steel. Upwards of 1,000 +/- feet of road can be surveyed at night when interference from vehicle traffic is minimal.

We will show how MASW was used on a major interstate in Pennsylvania to identify the root cause of sinkhole activity to depths of 80' directly beneath the reinforced roadway, and to identify a paleo-collapse feature in the carbonate rocks of Florida.

Subsurface Geotechnical Exploration Enhancement through the use of Refraction

Microtremor (ReMi) Geophysical Survey Techniques.

Matthew Satterfield, EI, Project Engineer, PSI, Thornton, CO 303-424-5578

Nicholas Roth, PE, Senior Engineer, PSI, St. Louis, MO 314-432-8073

Paul Hundley, PE, Regional Engineer, Columbus, OH 614-876-8000

Steve Bryant, PE, Vice President, PSI, Portland, OR 503-279-1778

Kevin C. Miller, PE, Chief Engineer, PSI, St. Louis, MO 314-432-8073

ABSTRACT

Refraction Microtremor (ReMi) geophysical survey techniques have been growing in use over the past few years. This technique records ambient ground noise on simple seismic refraction equipment. Then, wavefield analysis of the noise allows picking of Rayleigh-wave phase velocities. The data reduction is typically accomplished with proprietary analytical software. Typically, a 1-dimensional shear wave velocity profile is obtained in the data reduction processes. Certain software packages allow for the optimization of first-arrival time picks for the development of 2-dimensional profile models based on P-wave velocities. These P-wave velocity sections have proved effective in geotechnical applications, including the prediction of rock rippability for excavation purposes, mapping lateral velocity variations across faults and discontinuities, and in the search for voids resulting from underground mining and karst activities. No subsurface exploration technique is perfect, but when various techniques are used in conjunction on a geotechnical exploration, the results are often enhanced. This paper will summarize the ReMi technique, but will concentrate on presenting a series of projects where the ReMi technique was actually used in conjunction with other geotechnical exploration techniques that resulted in enhanced understanding of the subsurface physical characteristics. The following projects will be incorporated into the paper as examples of geotechnical exploration enhancement with the ReMi survey techniques.

- Wyoming Wind Farm Rock Quality and Seismic Site Class
- Arizona Road Drainage Rippability
- Texas Karst Topography Study
- Illinois Retail Development Underground Mining Study
- Ohio Commercial Development Rock Surface Profile and Rippability

KARST FEATURES IN LIMESTONE EVALUATED UTILIZING AN ACOUSTIC TELEVIEWER, NEW I-70 MISSISSIPPI RIVER BRIDGE, ST. LOUIS, MISSOURI

Adrian Keller, HNTB, Kansas City, MO, USA

ABSTRACT

Borehole televiewers are downhole inspection devices that can be utilized to view in-situ rock conditions and should be considered by geotechnical engineers and geologists as a supplemental means of investigating rock. The optical televiewer (OTV) produces a digital optical image and the acoustic televiewer (ATV) utilizes reflected acoustic waves to produce images of the borehole walls. Soft or fractured zones, solution features, open joints or other voids often unobservable during traditional rock coring techniques can be detected and measured utilizing this technology. The devices can be used to measure the strike and dip of joints, bedding planes, shear surfaces, or other structural features, eliminating the need for expensive oriented cores or downhole logging.

An acoustic televiewer was utilized in the fall of 2008 during the investigation phase for the New I-70 Mississippi River Bridge in St. Louis, Missouri. An ATV was utilized in each of ten river borings to produce images of the rock mass in the borehole and allow further investigation of the voids identified during rock coring. Voids interpreted as karst features were readily identified in the ATV logs in multiple borings and at similar elevations, suggesting connectivity.

Measurements of the void's width, location in the borehole and orientation allowed a more thorough understanding of the potential impact the karst features may have on the planned deep foundations. An extensive grouting program was eliminated based on the results of the ATV.

Determination of In-Situ Density of Planned Roadway Cuts in Cemented and Coarse-Grained Soils Using Seismic Geophysical Methods to Estimate Earthwork Factors

Daniel N. Fréchette, Ph.D., P.E.³

ABSTRACT

Earthwork factors can be a challenging parameter to determine on roadway projects and can have a huge impact on the cost of a project if not done correctly. Estimates that are wrong result in additional costs associated with the need to obtain additional borrow material or dispose of surplus material. The difficulty in estimating earthwork factors increases when working in cemented and coarse-grained soils. These soils are typically hard or very dense, which make in-place density data difficult to obtain. The majority of open-end drive samples obtained in these soils are disturbed due to the presence of cohesionless soils or the large number of SPT hammer blows required to advance the sampler. To overcome the limitations of obtaining in-situ samples and subsequently in-place densities using traditional methods, seismic geophysical methods consisting of seismic refraction and surface wave refraction microtremor (ReMi) can be utilized. AMEC used these seismic geophysical methods to determine in-place density on a recent roadway project in Arizona. The results obtained from the seismic geophysical methods were checked against values obtained from soil core samples, sand cone and nuclear test methods. The soil core samples were obtained in the deep roadway cut sections and the sand cone and nuclear test methods were obtained in the shallow roadway cut sections. The seismic geophysical methods provided reasonable estimates for in-place density when compared to the more traditional methods in the cemented and coarse-grained soils tested. These methods should be considered as an additional tool to obtain in-place densities for the development of earthwork factors.

³ AMEC Earth & Environmental, Inc., 1405 West Auto Drive, Tempe, Arizona 85284, 480-940-2320, 480-785-0970 (fax), daniel.frechette@amec.com

Geophysical Methods to Map Subsurface Evaporite Features to Aid Roadway Geometric Design

Mike Homan, P.E.
Terracon Consultants, Inc.
10930 East 56th Street
Tulsa, OK 74146
(918)-250-0461
mhhoman@terracon.com

Phil Sirles
Zonge Geosciences, Inc.
1978 South Garrison Street, Suite
3
Lakewood, Colorado 80227
(720) 962-4444
phils@zonge.us

Justin Rittgers
Zonge Geosciences, Inc.
1978 South Garrison Street, Suite
3
Lakewood, Colorado 80227
(720) 962-4444
justinr@zonge.us

ABSTRACT

Surface sinks, distressed highway sections, voids and evaporite bedrock with variable weathering have complicated highway design for the Oklahoma Department of Transportation (ODOT) in western Oklahoma. ODOT contracted with Terracon Consultants and Zonge Geosciences to collect approximately 45,000 linear feet of Direct Current Electrical Resistivity Imaging (ERI) data along Highway US-412 in Major County near Woodward, Oklahoma. The data was collected, using the Dipole-Dipole technique, to aid the design and construction efforts by identifying and discriminating between sections of highway underlain by solid gypsum or gypsum containing voids (resistivity > 1000 ohm-meters) and sections containing combinations of claystone and weathered gypsum (resistivity <100 ohm-meters).

Initial geophysical results were used to locate 18 confirming borings and identify the need and locations of additional geophysical testing. Borehole data correlated with the resistivity models and allowed for the assignment of resistivity ranges to specific lithologies which became the basis of all data interpretation for the geophysical survey.

The results presented here show that ERI offers an accurate and cost-effective approach to mapping lateral and vertical variations in material properties that can be directly associated with lithology. This can help alleviate common issues confronted when making geologic interpretations based on limited data from widely spaced borings. Two useful generalizations can be drawn about this specific project: 1) the highest values of resistivity more often correlate with gypsum hosting numerous smaller (0.5-1.5 feet diameter) voids than with large voids, and 2) large sections of the surveyed area (several 1,000s of feet) along US-412 are underlain by clay, weathered gypsum and gypsum-clay as confirmed by the borings, and will not likely pose many issues with regards to required mitigation efforts.

In summary, the ERI geophysical technique, as confirmed by the borings, successfully separated the sections of highway into distinct areas underlain by claystone and weathered gypsum and sections with gypsum dissolution features requiring different mitigation tactics. Success of the geophysical program can be related to a well integrated geologic, geotechnical and engineering program where ODOT, Terracon and Zonge personnel worked closely together to assess the subsurface data.

The results of the geophysical survey and boring program are being used in the final roadway design process to minimize the potential of sinkholes or caverns and the resultant impact on the new roadway construction. With the ERI and boring results delineating between those areas having gypsum rock and those areas not having gypsum rock, the design team has been able to focus attention on those portions of the alignment with existing or potential solution cavities. Thus, the design challenge is now on horizontal and vertical alignment of the highway and minimizing cut depths into the subsurface profiles that have gypsum rock and minimizing water seepage into the ground in those same areas.

SITE CHARACTERIZATION AND REMEDIATION IN KARST TERRANE

Joseph A. Fischer, James G. McWhorter & Joseph J. Fischer⁴

ABSTRACT

Conventional geotechnical investigative tools and analyses in karst are often unsatisfactory. Younger karsts of, for example Florida, require a much different understanding and approach than the flat or folded older karsts within the continental U.S. Support solutions vary from large mats, H-piles, drilled shafts and pin piles to jet grouting, high-mobility and low-mobility grouting, sometimes with non-cementitious grouts.

Whatever the project, any investigations should start with a geologic understanding of the particular karst terrane below the site/area of interest. In most locales, information is available from state and federal sources as well as, perhaps, local universities.

Generally, conventional soil mechanics investigations, whether or not combined with geophysics, are inadequate to define the vagaries of a subsurface consisting of cavernous bedrock with weathered and open seams, and soft and/or weak soils below apparently competent materials. The often-solutioned nature of the subsurface can also provide an opportunity for undiluted contaminants to reach domestic ground water supplies, particularly during construction.

Potential solutions are many, but generally represent a significant increase in cost over conventional structural/pavement support. However, defining the support solution usually results in increased costs and time overruns, as well as creating a need for increased funds to provide a suitable foundation while protecting domestic groundwater supplies. In addition, the provision of qualified construction inspection at karst sites is vital as the amount of geotechnical investigation required to adequately define all hazards is either impossible or cost prohibitive.

⁴ Geoscience Services, 3 Morristown Rd., Bernardsville, NJ 07924 - Phone: 908-221-9332 – Fax 908-221-0406 – E-mail: geoserv@hotmail.com (all authors).

**Geotechnical Investigation to Support Design of an ADA Compliant Access Ramp on the
South Rim of the Grand Canyon at Mather Point Overlook,
Grand Canyon National Park, Arizona**

Gregg S. Mitchell
HDR Engineering, Inc.
3200 East Camelback Road, Suite 350
Phoenix, AZ 85018
(602) 952-5760
gregg.mitchell@hdrinc.com

Michael L. Rucker
AMEC Earth & Environmental, Inc.
1405 West Auto Drive
Tempe, AZ 85284
(480) 940-2320
michael.rucker@amec.com

ABSTRACT

A geotechnical investigation was performed to support design of improvements to the Mather Point at Grand Canyon National Park, including a new Americans with Disabilities Act (ADA) compliant ramp to be located within an existing approximately 1H:1V natural slope along the edge of the South Rim. The slope, extending about 60 feet from the existing Rim Trail to an approximately 1,000-foot vertical drop below, consists of a thin veneer of soil and talus intermingled with loose, dislodged boulders and large rock blocks overlying dolomitic limestone of the Kaibab Formation.

The original geotechnical investigation scope included geologic mapping, geophysical surveys, and test borings along the ramp alignment. However, worker safety considerations required that the investigation be performed remotely, behind existing safety railings. Geologic mapping focused on the Mather Point rock outcrop with visual assessment of the actual ramp alignment. Geophysical surveys and core borings were performed along the existing trail and other accessible areas.

Mapping at exposed rock surfaces indicated a complex geology including three highly-persistent joint sets extending vertically through 8- to 12-foot thick layers of dolomitic limestone exhibiting alternating relative hardness and competence. Geophysical and coring results confirmed apparent rock conditions.

The investigation indicated variable rock conditions both laterally and vertically across the site, such that rock anchoring and over-excavation would likely be necessary and a field-fit approach to construction would be required. Inspection and approval of the stabilized cut slope prior to ramp construction are stipulated in the construction specifications.

Geologic mapping, geophysical surveys, and traditional boring methods each provided unique data and were effectively combined to characterize the geologically complex site, considering that direct site access by investigators was not possible. The project demonstrated that these investigative methods can all be important components of a geotechnical investigation and can be effectively used together on geologically complex sites.

Case Study Using Geotechnical Instrumentation to Monitor Fill

Foundation Stability

BUCHE, Matthew,

KANE GeoTech, Inc., 7400 Shoreline Dr. Suite 6,

Stockton, CA 95219,

matt.buche@kanegeotech.com

KANE, William F.,

KANE GeoTech, Inc., 7400 Shoreline Dr. Suite 6,

Stockton, CA 95219,

william.kane@kanegeotech.com

ABSTRACT

Highway reconstruction projects may involve time and/or economic constraints requiring accelerated work schedules. Such projects commonly include fill placement and MSE walls to construct new abutments. Accelerated work schedules can result in rapid loading increments, a cause for concern when placed upon underlying soft soil foundations. When subjected to rapid loading, foundations can experience increased lateral deformation, a catalyst for failure. To avoid embankment failure, geotechnical instrumentation has been used to assess soil foundation performance during construction. Methods of analysis and determination of loading thresholds based on lateral and vertical displacements of foundation soil are outlined by Saye and Ladd (2004). The application of the method was used in 2009 for monitoring purposes at a site in the Western United States. Geotechnical instruments were installed to observe soil foundation settlement and horizontal displacement to analyze its performance during construction. The technique allowed project managers to monitor embankment stability, identify a potential problem, and avoid a catastrophic failure by temporarily removing fill.

Construction of the Amelia Earhart Memorial Bridge.

Bob Henthorne,

Chief Geologist, Kansas Dept. of Transportation,

2300 Van Buren, Topeka, KS 66611

ABSTRACT

The replacement of the Amelia Earhart Memorial Bridge has been ongoing for several years. The contract to construct the new Tied Arch Structure was let in 2009, with the winning bid going to Archer Western INC. The construction of the bridge has required a host of geotechnical monitoring tools from Pile Driving Analyzers, Cross-hole Sonic Logging, and under water cameras. The construction will entail pile bent, and drilled shaft foundations as well as retaining walls placed on stabilized soil.

This paper will discuss the construction sequence for the bridge including several major successes as well as one catastrophic failure!

Bridge over Snake River: Geotechnical Engineering on Unstable Ground

Kirk Hood
Wyoming Department of
Transportation
5300 Bishop Blvd.
Cheyenne, WY 82009
(307) 777-4418
Kirk.Hood@dot.state.wy.us

Norman Norrish
Wyllie & Norrish Rock
Engineers Inc.
17918 NE 27th St
Redmond, WA 98052
(425) 861-7327
nnorrish@msn.com

Jamie Martens
HNTB Corporation
715 Kirk Drive
Kansas City, MO 64105
(816) 527-2348
jamartens@hntb.com

ABSTRACT

The Wyoming Department of Transportation intends to improve US Highways 26/89 south of Jackson in Teton County, Wyoming beginning at milepost (MP) 140.69 and extending northerly through Hoback Junction terminating at MP 142.50. The route is located in mountainous terrain adjacent to the confluence of the Snake and Hoback Rivers and crosses Federal, State, County, and privately owned properties. The corridor is heavily traveled by commuters, commercial vehicles, and seasonal recreational traffic. Landslides have significantly impacted the transportation infrastructure within the project limits. An active landslide is located near the west abutment of the existing bridge over the Snake River, and construction of the existing bridge in 1950 re-activated a portion of the slide mass. Since construction, the abutment has experienced periodic movement as evidenced by inclinometer readings and settlement of the abutment. Subsurface conditions consist of colluvium/landslide and alluvial terrace deposits overlying sandstone, siltstone, and shale of the Cretaceous-aged Aspen Formation. Key components of the project include installation of three rows of ground anchors in the vicinity of the west abutment for landslide mitigation, construction of a new, two-hinged arch span bridge over the Snake River, and construction of an approximately 1,000 linear foot long anchored soldier pile and lagging retaining wall to accommodate roadway realignment. Design challenges included definition of the “active slide”; development of stability models consistent with inferred stratigraphy, current topography and documented displacement history; and integration of reinforcement anchors with bridge foundation elements to avoid conflicts. Construction sequencing is vital to install and commission as many of the ground anchors as possible prior to the excavations required for the bridge foundation elements.

Road and Housing Construction on Reclaimed Coal Mine Spoil Undergoes Settlement Damage in Southwest Indiana

Terry R. West and Nils I Johansen, P.E., Dept of Earth & Atmospheric Sciences, Purdue University, W. Lafayette, IN and University of Southern Indiana, Evansville, IN, respectively (trwest@purdue.edu)

ABSTRACT

Coal mining in Pennsylvanian-aged rocks of southwestern Indiana has occurred for over 100 years. Seventeen counties from Terre Haute to Evansville have experienced both surface and underground coal mining. Since coal measures in Indiana dip southwest toward the Illinois Basin, geologic units show increased overburden thickness as they extend westward. Shallow strip mines prevailed in the early history of mining, but increased stripping capacity occurring in later years allowed for deeper extraction. Underground room and pillar mining was conducted on the deeper coal seams beyond the limits of strip mining at the time of extraction.

Early in mining history, reclamation of surface strip mines was virtually non-existent.

Abandoned mine lands consisting of cast-over strip piles prevailed long the eastern boundary of the coal-bearing strata. In recent years, however, Federal mining laws have required that strip mines be properly reclaimed with the land surface restored to that which was present before mining. With this history in mind, we find that for recent strip mine areas, the overburden thickness is typically about 100 feet and the mined areas are carefully reclaimed to mimic their original contours. A primary consideration for reclamation is to allow the surface material to support vegetation, including row crops, pasture and forestation. Consequently, the surface material is left in a loose condition so as not to discourage plant growth.

Currently some reclaimed land is being sold by mining companies for development as housing tracts. Roads and house lots are then developed on the reclaimed land. In southern Warrick County, north of Evansville and near Interstate 164, problems have developed in a housing area on the reclaimed mine spoil. Foundation settlement leading to interior damage in homes has occurred. Streets have also undergone major settlement. In the paper these settlement problems are discussed and mitigation procedures are addressed.

**Interstate 40, Emergency Rock Remediation,
Haywood County, North Carolina**

**Daniel Journeaux,
President**
Janod Contractors
Inc.
34 Beeman Way
Champlain, NY 12919
(518) 298-5226
daniel@janod.biz

Jody C. Kuhne, LG, PE
North Carolina DOT
Geotechnical Engineering
Asheville Area Office
PO Box 3279
Asheville, NC 28802
(828) 298-3228
jkuhne@dot.state.nc.us

Noel Philippon
Janod Contractors Inc.
34 Beeman Way
Champlain, NY 12919
(518) 298-5226
daniel@janod.biz

Peter C. Ingraham, P.E.
Golder Associates Inc.
670 North Commercial
St., Ste. 103
Manchester, NH, 03101
(603) 668-0880
pingraham@golder.com

ABSTRACT

On Saturday morning, October 24, 2009 at 02:30 there was a massive rock slide on Interstate 40 in North Carolina at Mile Marker 3.4 just by the border of Tennessee. The volume of material was in the range of 80,000 cubic yards and some of the blocks were the size of city busses. Phillips and Jordan out of Knoxville Tennessee were called in as the emergency contractor to remove the material from the slide and find a subcontractor for the rock remediation in the slope. Noel Philippon of Janod arrived on site Monday October 26th and there was a scaling crew on site to begin the initial scaling on October 28th. Since the slide was still active every precaution was being taken to monitor the slope for movement while the scaling and material removal operations were taking place.

Jody Khune the State Geotechnical Engineer mapped out the slope and concluded that the slope consisted of several potential wedge failures and the initial consensus was that it was very likely that there could be further rockfalls from the same failure plane. The initial plan was to drill and blast up to where the failure plane daylighted 900 feet further up the slope. When that proved to be too expensive NCDOT short listed contractors to bid on installing 50,000lnft of rock anchors in 60 days to stabilize the structure. The team of Phillips and Jordan and Janod were the successful bidders on the project and the contract work started on December 28, 2009. There were several challenges on the project that became exponentially more complicated due to the fact that the work was to be performed during the worst weather of the year for that area and in one of the most severe winters in the last 30 years. Due to the time restraints in designing such a complicated project there were several changes to the design that were proposed by Janod. The presentation will discuss in detail the design and construction challenges that were not only met but exceeded most predictions.

EMERGENCY ROCK SLOPE STABILIZATION IN THE OCOEE GORGE, U.S. ROUTE 64, POLK COUNTY, TENNESSEE

Vanessa Bateman, P.G., P.E.⁵, Jay R. Smerekanicz, P.G.⁶, and Deana Sneyd, P.G.⁷

On November 10, 2009, a large rockslide struck U.S. Route 64 in the Ocoee Gorge in Polk County, Tennessee, following an intense rainfall event associated with tropical storm Ida. The slide damaged the roadway and a sidewalk, blocked access to a boat ramp, and impacted area access as well as the local economy. Approximately 15,000 cubic yards of falling rock, soil and forest vegetation buried the roadway to a height of nearly 25 feet. An adjacent historic concrete faced timber crib dam operated by the Tennessee Valley Authority (TVA) was not impacted by the slide. An initial smaller slide occurred early in the morning closing the roadway and mobilizing maintenance, repair and TV crews to site. Observation of the slope during the initial cleanup indicated a larger slide mass was failing and provided sufficient warning to evacuate workers clearing the initial rock debris before the main slide fell, avoiding potential loss of life. Television news crews on site to cover the initial smaller slide obtained rare video footage of a major rockslide occurring.

Originally called the Copper Road because it was constructed to haul ore west along the Ocoee River valley to Cleveland, Tennessee, U.S. Route 64 is a vital east-west two-lane highway providing the only principal access between extreme southeast Tennessee and adjacent North Carolina. The roadway follows the winding Ocoee River, the site of the whitewater events of the 1996 Summer Olympic Games. The river and roadway traverse the Cherokee National Forrest, providing access to outdoor enthusiasts. The roadway also serves as the primary route for emergency and commercial vehicles serving the towns, tourist camps and whitewater rafting outfits in the area. In the 1960's, the roadway was realigned and widened as part of the regional roadway improvements; the widening design included removal of the toe of planar beds steeply dipping towards the roadway. The rock slope, like many within the Ocoee Gorge, has been monitored closely the Tennessee Department of Transportation (TDOT) under their rockfall hazard monitoring program, and had been scheduled for repairs/maintenance.

The rocks in the Ocoee Gorge consist of late Precambrian, complexly folded, thin to medium bedded, low-grade metasediments, including slates, phyllites and metagraywackes. Differential weathering of thin beds of slate and phyllite bounded by more competent metagraywacke can lead to planar and wedge failure of steeply dipping beds, intersecting joints and cleavage planes. Exposure of these weak beds in the toe of the slope, in conjunction with over 5 inches of rain over a 24-hour period, led to planar sliding failure of a portion of the rock slope. Remediation included scaling of loose rock and soil; trim blasting of remaining beds on the slope to remove the potential for further rockfall; installation of pattern rock bolts throughout the slope; and installation of drains at the toe of the slope. Due to the proximity of the TVA dam, blasting vibrations had to be monitored. Limited access along the two-lane highway hampered rock slope mitigation construction.

Author e-mail addresses and phone numbers:

Vanessa Bateman (Vanessa.Bateman@tn.gov) ph. 615/350-4133

Deana Sneyd (deana_sneyd@golder.com) ph. 770/496-1893

Jay Smerekanicz (jay_smerekanicz@golder.com) ph. 603/668-0880

⁵ State of Tennessee, Department of Transportation, 6601 Centennial Boulevard, Nashville, TN 37243

⁶ Golder Associates Inc., 670 North Commercial St., Ste. 103, Manchester, NH, 03101

⁷ Golder Associates Inc., 3730 Chamblee Tucker Road, Atlanta, GA 30341

Geotechnical Engineering For A Super-Load Delivery Over Pennsylvania Highways

Chris Ruppen, Don Gaffney & Dave Saylor; Michael Baker Jr., Inc.

ABSTRACT

This fast-track project required delivery of two new steam generators in September 2009 to support Three Mile Island's license renewal to continue operations through 2034. The delivery was managed by AREVA NP, Inc., with Baker providing route planning and engineering support. The route to TMI from their off-loading point in Maryland was characterized by its 75-mile length, hilly terrain, narrow rural roadways, and many water crossings. The steam generators on their transporter units; coming in at 825 tons, 153-feet long, 18-feet wide and 24-feet high each; were the largest loads ever transported on Pennsylvania and Maryland highways.

The geotechnical challenges included foundation support or temporary bypasses at several bridges, stability of sections of roadway, and consideration of pavement structure. One section of the route originated as an Indian hillside trail along a stream in the 1600's had hadn't progressed much past black-topping in the centuries since: it was in very poor shape with the entire roadway showing signs of creeping toward the adjacent river. Additional portions of the overall route required detailed pavement analyses, subgrade settlement, and design of temporary roadways to bypass bridges lacking the capacity to support the load. Temporary bypasses were designed with various gradations of aggregate with geotextile and geogrid reinforcement for additional aggregate stability.

Baker's geotechnical team uniquely combined existing techniques and theory to model the transporters. Embankments were analyzed for local and global stability which found the existing roadways theoretically capable of satisfactorily supporting the transporters. Flexible pavement design methods are based on repetitive vehicle loads, but our model viewed each transporter as a temporary structural load and analyzed the structural response from a pavement-and-subgrade strength position. This required analysis of how the wheels of the transporter interacted with each other and how the stress from the combined wheels distributed through the pavement to the subgrade soils.

The true test came as the transporters passed. Any failure of the roads during the move would have been devastating to the project as it would have meant a complete stoppage in traffic while the road could be made safe to pass the transporters or the transporters could be rerouted. Success is measured in performance in line with analyses. Baker's geotechnical team's analyses permitted the transport of the generators without extraordinary and expensive stabilization construction or extended disruption of private land owners and traffic along the route.

Subsurface Stabilization of Problematic Soil Areas

President George Bush Turnpike

Dallas County, Texas

Garry H. Gregory¹, Ph.D., P. E., D.GE

¹ Principal Consultant, Gregory Geotechnical,

2001 West 44th Avenue, Stillwater, OK 74074

405-714-3689 ggregory@gregeo.com

Adjunct Professor of Civil Engineering – Oklahoma State University

ABSTRACT

When the North Texas Tollway Authority (NTTA) planned to construct the \$400 million President George Bush Turnpike (PGBT) in Dallas, County, Texas, one of the challenging engineering aspects was subsurface stabilization of problematic soil areas along the proposed route. These problematic soil areas consisted of two closed landfills, a system of water treatment plant backwash lagoons, a deep rubble fill area, a steep slope area adjacent to an active landfill, and roadway embankments constructed of high plasticity clays. The PGBT design required a variety of improvements in the problematic soil areas including earthfill embankments to approximately 10 m (33 ft) in height, MSE Walls to approximately 8 m (26 ft) in height, and excavation cuts to approximately 7 m (23 ft) deep in one of the closed landfill areas. These areas were stabilized with a variety of subsurface techniques including, dynamic compaction, lime-fly ash slurry injection, compaction grouting, deep soil mixing, vibro-concrete columns, geogrid reinforcement, and fiber-reinforced soil (FRS). Geotechnical instrumentation was installed to monitor vertical and lateral deformations in the stabilized areas to verify performance prior to construction of pavements. The geotechnical design was completed in late 2001 and construction was completed in early 2005. To date the project has performed as expected in the stabilized areas.

Safe and Sound, Missouri Department of Transportation, Design - Build Program of Replacing 554 Bridges

John F. Szturo R.G.,
Senior Geologist, HNTB Corporation,
715 Kirk Drive, Kansas City, MO 64105
Ph 816.527.2275, jszturo@hntb.com

ABSTRACT

The Missouri Department of Transportation plans to replace 802 of Missouri's most worn out bridges in five years – by Oct 31st, 2014. The 802 bridges are divided into two groups. 248 have been identified for rehabilitation by multiple design bid build processes and 554 will be completely replaced by a single design build contract.

The Missouri Highways and Transportation Commission selected KTU Constructors to replace 554 bridges in a single design-build contract. Some key provisions of KTU's proposal: Quoted price of \$487 million. Committed to finish by Dec. 31, 2013, – 10 months earlier than required. Average bridge closure for 493 bridges will be 45 days – nearly half of what a normal MoDOT bridge project would take. Overall, the schedule will demand one bridge be turned over every two and a half days during the project duration.

The schedule will necessitate completing the subsurface investigations and foundation recommendations for all 554 bridges within the first 18 months of the project, or about two every three days.

Many creative and innovative methods were used to form the logistics necessary to perform the geotechnical engineering for 554 bridges for the 18 month schedule. The logistics dealt with scheduling borings, drilling, sampling, testing, reporting, recommendations and plan production.

Using TDA (light weight Tire Derived Aggregate) as a green alternative for reconstruction of a landslide road failure

William V. McCormick, CEG,
Kleinfelder Inc.,
2240 Northpoint Parkway,
Santa Rosa, California, 95407 USA
(707) 571-1883, bmccormick@kleinfelder.com

ABSTRACT

A 300-foot-long stretch of road in California has been plagued with re-occurring landsliding and a previously failed retaining wall, making it unusable. Available funds prevented a more robust retaining wall mitigation that would have required multiple rows of tiebacks. Previous failures have resulted in loss of (clayey) earth materials needed for slope reconstruction and stability analysis indicated that a stable slope could not be constructed due to environmental setback restrictions from an adjacent wetland and creek. An alternative design was developed using light weight (50 pcf) Tire Derived Aggregate (TDA, shredded waste tire fill) which is available free of charge for civic projects in California. The light weight TDA significantly reduced the driving force for future sliding. The ultimate design consisted of a geo-grid reinforced engineered soil buttress at the base of the slope, continuous blanket drain to address spring activity and alternating layers of TDA and soil in the upper portion of the road prism. Over 330,000 tires were removed from waste dumps and utilized as permanent fill on this road and made the project feasible by reducing costs up to 36%.

Using LiDAR Laser Scanning for Geotechnical Characterization in Rock

Nick Priznar, Engineering Geologist, ADOT, Geotechnical Design Section

Virgil Coxon, ADOT, Survey Section

ABSTRACT

For several year's two sections of ADOT have collaborated on the use of laser scanning for acquiring very accurate three dimensional data in previously inaccessible terrain for geotechnical assessments. The application LiDAR appears to hold promise to reduced field investigation costs, increase the amount of usable data collected, and greatly reduce the level of exposure to field personnel while performing rock mass characterization studies.

LiDAR was used to supplement and analyze rock mass discontinuity orientations on high cut slopes on I-8, MP 20, Telegraph Pass, In Yuma County, Arizona in 2008. Due to the limited and potentially hazardous access to the rock cut face ADOT and its collaborators extracted orientation data from an existing LiDAR point cloud that was originally generated to create a digital terrain model for the highway corridor. Three dimensional data sets of discontinuity surfaces with similar orientation properties were grouped together and displayed on the point cloud image. The average orientation of these groups was downloaded into a standard rock slope stability programs and used to augment the analysis of proposed mitigation for the site.

Laser scanning was also utilized to study the geometry and behavior of an unlined, historic rock tunnel on SR 191. The structural support elements and rock reinforcement in the crown and side walls have shown distress and degradation. Interior laser scans of the tunnel were conducted on 50-ft centers and then interpreted in conjunction with panoramic photographic techniques to locate and inventory a steel rib canopy and some 2,443 rock bolts supporting the tunnel. The scan data were invaluable in designating which elements were candidates for replacement or repair. The scans were also used to locate and project discontinuities which were assessed for rock fall inside the tunnel and at the approach portals.

Assessment of the Garvin Landslides

Christopher R. Clarke, P.E.
Geotechnical Lab Supervisor
Oklahoma Department of Transportation,
Materials Division
200 N.E. 21st Street, Oklahoma City, OK 73105-
3204
(405) 522-4994
cclarke@odot.org

James B. Nevels, Jr., P.E., Ph.D
Geotechnical Consultant
605 Mimosa Dr., Norman, OK 73019
(405) 818-2897
jnevels1@cox.net

ABSTRACT.

A shallow landslide failure in a highway cut-section slope occurred on January 13, 2005 in high plasticity residual clay soils creating a costly maintenance problem. The site location was approximately 3.1 miles east of Garvin in McCurtain County, Oklahoma along the westbound lanes of US 70 highway. The north facing cut-section slope failure designated as slide A was investigated in 2005, and repairs were recommended and completed in the summer of 2006. The repair solution applied was a counterfort trench drain system. Two additional slides have recently occurred designated as slide B and slide C in February 2010 and March 2010, respectively. Each of these two new landslides are relatively the same size as slide A and are spoon shaped. The standard Oklahoma Department of Transportation (ODOT) Roadway Design slope design of 3:1 was applied to the north facing cut-section slope in the original construction.

This paper continues with the enhancement of the mechanisms of stability degradation discovered with slide A, addresses more detail in the site investigation and geologic description, and further assesses the back calculated shear strength. Also investigated is the question of why slide A survived when slides B and C failed. Upon further review the mobilized shear strength at the time of these recent as well as the original slope failure was more likely the fully softened shear strength rather than the assumed residual shear strength.

Unique to the investigation of slides B and C is the application of moisture diffusion and matric suction associated with the mechanisms of stability degradation, and a detailed back analysis is made to estimate the slip surface utilizing dynamic cone soundings (DCP) supplemented with borings and closely spaced moisture content sampling are made. Critical to the study is the evaluation of the fully softened shear strength reasoned to be the operating shear strength of these first time slides. The factor of safety for a 3-dimensional analysis is estimated from the investigated 2-dimensional analysis. The GSTABL7 as well as the Geotase computer programs look into alternate stabilization methods that were not considered in the repair of slide A.

ROCKFALL MITIGATION FIELD TECHNIQUES AND DESIGN

WAGNER, Dane A., KANE GeoTech, Inc., 7400 Shoreline Drive Suite 6, Stockton, CA 95219,
dane.wagner@kanegeotech.com

KANE, William F., KANE GeoTech, Inc., 7400 Shoreline Drive Suite 6, Stockton, CA 95219,
william.kane@kanegeotech.com

ABSTRACT

Rockfall is a geologic hazard that results in the catastrophic loss of life and substantial property damage to roadways, railways, and infrastructure. Over the past fifty years, rockfall mitigation practice has seen rapid advancement, with the greatest technological strides occurring in the last ten years. During this time, the design methodology has also matured from empirical field methods to a system of quantitative analysis producing design loads and forces. The design of mitigation systems must take into account a variety of factors and physical characteristics to properly provide safety. Current design practices today focus on both the safety and economic costs of mitigating hazardous slopes by involving a qualified geotechnical investigation and analysis with a consideration on practicality. Analysis methods such as the Rockfall Hazard Rating System (RHRS) and the Colorado Rockfall Simulation Program (CRSP) have allowed for the determination of site specific mitigation options. Choosing the proper mitigation approach must incorporate analyses with crucial information from the field and may involve active, passive, or a combination of mitigation solutions. After the proper mitigation system has been selected for the specific site, system design incorporates the quantitative data from the analyses to engineer for the variety of loads subjected upon the system; including those on the system, the foundation, and the anchors and/or bolts. This paper reviews the state of current rockfall mitigation practice and provides a comprehensive approach to analysis and design for use by geologists and engineers.

Flexible Facing Analysis for Soil Nailing

Ghislain Brunet
Maccaferri, Inc
10303 Governor Lane Blvd.,
Williamsport, MD 21795-3116
Ph: 301-223-6910
gbrunet@maccaferri-usa.com

Jonathan Lovekin
Maccaferri, Inc
10303 Governor Lane Blvd.,
Williamsport, MD 21795-3116
Ph: 301-223-6910
jlovekin@maccaferri-usa.com

Paola Bertolo
OFFICINE MACCAFERRI
S.p.A.
Via Kennedy 10
40069 Zola Predosa
Paola.Bertolo@maccaferri.com

ABSTRACT

Soil nailing is a technique in which [soil](#) slopes, [excavations](#) or [retaining walls](#) are reinforced by the insertion of relatively slender elements - normally steel reinforcing bars. The bars are usually installed into a pre-drilled hole and then [grouted](#) into place or drilled and grouted simultaneously. A rigid or flexible facing system is used to stabilize the soil between the anchors.

Flexible facing systems have been used for many years to maintain and improve stability between the anchor system. Despite this long use, the design methods usually take into account only the anchor design to reach the expected safety factor. No calculation method exists to help the designer choose the correct facing type and evaluate the facing behavior against the load of the unstable material layer. The geomechanical properties and the load can change with time (e.g. by softening and weathering phenomena).

To solve this lack of knowledge Maccaferri has developed the BIOS System (Best Improvement Of Slopes). With this new approach it is easy for the designer to verify the effectiveness of the selected facing system, checking the work both for Ultimate and Serviceability Limit State.

The Ultimate limit state check is necessary to avoid total collapse of the entire system. The Serviceability limit state check is necessary to avoid having the system be under designed with respect to the potential deformation of the mesh. This check takes into account the long term behavior of the slope material. Large debris displacement over time can produce unacceptable deformation of the system between the nails. This can lead to interference with the protected structure or deeper stability problems in the slope.

Use of Dimensional Modeling for Sizing Flexible Barriers Installations That Mitigate Debris Flow Natural Hazards

Frank Amend,

Geobrugg North America,

PO Box 7453, Rocky Mount, NC 27804-0453

(T) 252-937-2552, E-mail: frank.amend@geobrugg.com

ABSTRACT

The previous large-scale fires in California and the resultant mudflow disasters that were produced have demonstrated that some kind of properly designed flexible barrier could be useful in handling the complex forces present in a fluid/slurry torrent and could be a tool to effectively stop debris flows and/or mitigating such hazards. Intensive research has been conducted which identified flow volumes, velocity, and density resulting in pressure as the primary design parameters and have acknowledged specific engineering criteria necessary for use in debris flow applications. Such research has included 1:1 laboratory testing with small-scale, artificially generated debris flows, real-scale 1:1 field-testing as well as computer simulations modeling the behavior of barriers during such events.

A design model for debris flow barriers (based on a finite element software program, but not included in the paper) has been calibrated and verified by real-scale field-testing and is the only known valid model for tested barrier type ((GB) ring-net barriers) in debris flow applications. During the model's development, it became clear that each application site where a debris flow barrier would be considered requires specific dimensioning to be completed for each barrier as no "one-size-fits-all" criteria exists for a properly designed solution. Furthermore, the loading associated with debris flows vastly differs from that of rockfall, thereby necessitating different barrier design criteria.

This research has led to an initial dimensioning model for flexible barriers to be used for debris flow mitigation, which is currently being applied in numerous cases. These barriers have been installed and impacted by actual debris flows. The subsequent observations have provided invaluable information regarding performance, design assumptions, and maintenance requirements including cleanout.

**The Latest in Testing Procedures and Technological & Installation Developments in
Rockfall Protection Barriers**

John Kalejta Jr.

Geobrugg North America, LLC

Geobrugg Protection Systems

551 Cordova Rd., PMB 730

Santa Fe, NM 87505

Tel: 505-220-1404

E-mail: john.kalejta@geobrugg.com

www.geobrugg.com

ABSTRACT

The latest rockfall protection barriers are tested under the most rigorous vertical drop conditions according to the Swiss Federal Institute for Forest, Snow and Landscape Research (WSL). More recently, rockfall barriers have been tested and certified under the ETAG 27 guideline of the European Organization of Technical Approvals (EOTA). The EOTA test certification is comprised of two so-called Service Energy Level (SEL) tests: the barriers are loaded with two hits of 33% of the nominal energy without intermediary maintenance. The Maximum Energy Level (MEL) test is then performed with 100% of the nominal energy.

Geobrugg's newest rockfall barriers, the GBE series, have verified a residual useful height corresponding to the highest category, A, of the ETAG 27. In other words, after the MEL test, a residual height of at least 50% of the nominal barrier height was attained in the impact field. The GBE rockfall barriers, with full European Technical Approval certificates, protect against impact energies up to 1,000 kJ with over 50% residual height in the impact field, require no secondary mesh and have simple anchorages due to lower force transmission. Higher energy versions of the GBE barrier, up to 3,000 kJ, are under development.

The time spent installing rockfall protection barriers is a large factor in project cost calculations. These new technological breakthroughs were developed to facilitate rapid installation by contractors through modular design, the use of lightweight components and partial factory pre-assembly. A recent installation case in New Mexico will be presented. The ultimate goal of any project is the most economical solution to rockfall and safety problems without compromise of the technical solution.

North Slope Landslide Investigation, US 62

Chickasha, Oklahoma

James B. Nevels, Jr., Ph.D., P.E.¹

ABSTRACT.

Shallow landslide failures in highway embankments constructed in medium to high plasticity create costly maintenance problems. The site location of the embankment landslides recently and currently under investigation are in Grady County, Oklahoma within the Chickasha city limits along the west approach embankment over the old St. Louis & San Francisco Railroad line on US 62 highway. The south slope embankment slope failures were investigated in 2005 were deep seated slides and were repaired at a contract cost of \$400,000 plus in 2008. The north embankment slopes are now under study, but they are noticeably shallow seated.

This paper investigates the mechanisms of stability degradation that leads to these shallow slope failures. The basic reason for these slope failures is because of right of way restrictions the side slopes were built steeper than the standard Oklahoma Department of Transportation (ODOT) side slopes set at 3:1 in order to accommodate a four lane widening. Unique to this investigation is the application of moisture diffusion and matric suction associated with the mechanisms of stability degradation. Further in the investigation a detailed back analysis is made to estimate the slip surface, and in doing so the use of dynamic cone soundings (DCP) supplemented with borings and closely spaced moisture content sampling are made. Critical to the study is the evaluation of the fully softened shear strength reasoned to be the operating shear strength of this first time slide. Finally the study looks into the use of 2-dimensional slope stability analysis to estimate a 3-dimensional slope failure. The GSTABL7 and the newer Geostase computer programs are utilized. These computer solutions look into alternate stabilization methods that were requested.

1. James B. Nevels, Jr., P.E., Ph.D., LLC, Consulting Geotechnical Engineer, 605 Mimosa Dr., Norman, OK 73069-8622.

Influence of Various Cementitious Additives on the Durability of Stabilized Subgrades

Solanki, Pranshoo, Doctoral Candidate, School of Civil Engineering and Environmental Science,
University of Oklahoma, 202 West Boyd Street, Room 334, Norman, Ok, 73019-1024,
Ph: 405) 325-4236 Fax: (405) 325-4217 E-mail: pranshoo@ou.edu

Zaman, Musharraf M. , David Ross Boyd Professor and Aaron Alexander Professor, Associate Dean for
Research and Graduate Education, College of Engineering, University of Oklahoma ,
202 West Boyd Street, Room 107, Norman, OK, 73019,
Ph: (405) 325-2626 (Office) or (405) 325-4536 (Secretary) Fax: (405) 325-7508 E-mail: zaman@ou.edu

Dean, Jeff , Oklahoma Department of Transportation, Pavement Engineer, Oklahoma Department of
Transportation, 200 N.E. 21st Street, OKC, OK 73105,
Ph: (405) 503-1463 E-Mail: jdean@odot.org

ABSTRACT

Durability of pavement materials induced by changes in climatic conditions namely, freeze-thaw and wet-dry (W-D), have been recognized by pavement engineers as a major factor in poor pavement performance. The repeated action of F-T and W-D deteriorates the integrity of the pavement structure through changes in the engineering properties of pavement material such as resilient modulus and unconfined compressive strength. To this end, durability of stabilized soil specimens was evaluated by conducting F-T cycling, W-D cycling, vacuum saturation and tube suction tests.

The soils used in this study are three commonly encountered subgrade soils in Oklahoma. These soils belong to Port series (CL-ML), Kingfisher series (CL), and Caranasaw series (CH). Three different cementitious additives, namely, 6% lime, 10% class C fly ash (CFA) and 10% cement kiln dust (CKD) are used. Specimens are compacted at near optimum moisture content with a target density between 95% and 100% of the maximum dry density. After compaction, specimens are cured for 7 days and tested for durability against F-T and W-D cycles in accordance with ASTM D 560 and 559 test methods, respectively. Also, specimens are tested for durability using two time-efficient procedures, namely, vacuum saturation in accordance with ASTM C 593 test method and tube suction test. Preliminary results indicate that F-T and W-D durability of stabilized subgrade soils is influenced by characteristics of both soil and additive. Also, durability evaluated using vacuum saturation test produced good correlations with residual strength of specimens subjected to F-T and W-D cycles indicating that vacuum saturation could be used as a time-efficient and inexpensive method for evaluating durability of stabilized soils

Understanding the Behavior Of Integral Abutment Bridges Through Field Instrumentation

K. K. "Muralee" Muraleetharan 1, Gerald A. Miller 2, and Bryce Hanlon 3

1 School of Civil Engineering and Environmental Science, The University of Oklahoma,
202 W. Boyd, Room 334,

Norman, OK 73019, Phone: 405-325-4247, Email: muralee@ou.edu

2 School of Civil Engineering and Environmental Science, The University of Oklahoma,
202 W. Boyd, Room 334,

Norman, OK 73019, Phone: 405-325-4253, Email: gamiller@ou.edu

3 EST, Inc., 3201 South Berry Road,

Norman, OK 73072, Phone: 405-307-8378,

Email: bryce.hanlon@estinc.net

ABSTRACT

Integral Abutment Bridges (IAB) or jointless bridges are bridges without any joints within the bridge deck or between the superstructure (decks and girders) and the abutments. An IAB provides many advantages during construction and maintenance of a bridge. The behavior of abutments in an IAB is, however, poorly understood. Soil-structure interactions occurring during heating and cooling of the bridge at the abutments are complex, especially in skewed and long span IABs. This paper describes a field instrumentation effort to understand these soil-structure interactions.

The North bound I-44 Bridge over the Medicine Bluff Creek in Comanche County near Lawton, Oklahoma was instrumented for this project. This is a 210 feet long, three span IAB with a 100 skew. Three abutment piles were instrumented with strain gages, earth pressure cells and tilt meters were placed on abutment walls, crack meters were placed between the bridge deck and the pavement, and thermistors were placed on the bridge deck, and the girders. The data collection began in June 2009. This paper will discuss the results from these instruments during heating and cooling of the bridge and will provide insight into the soil-structure interaction between the abutment and the piles supporting them and the surrounding soil.

Importance of Soil Suction in Pavement Foundations

Rifat Bulut ,

Oklahoma State University

School of Civil and Environmental Engineering

207 Engineering South

Stillwater, Oklahoma 74078

Phone: 405-744-7436

Fax: 405-744-7554

E-mail: rifat.bulut@okstate.edu

ABSTRACT

This paper reports on several soil suction measurement methods, and use of soil suction in pavement foundations. These techniques have been widely used in engineering practice and in research laboratories. Each of these techniques has its own limitations and capabilities, and active research into improving these techniques and their use in engineering practice is ongoing in universities, research laboratories, and private sector. This paper outlines working principles, calibration, measurement, and application areas of the filter paper method, tensiometers, thermocouple psychrometers, transistor psychrometer, chilled-mirror psychrometer, thermal conductivity sensors, and electrical conductivity sensors.

Influence of Moisture Content on the Pullout Capacity of Geotextile Reinforcement in Marginal Soils

Kianoosh Hatami, Lina Garcia and Gerald A. Miller

School of Civil Engineering and Environmental Science (CEES), University of Oklahoma,
Norman, OK, USA

ABSTRACT

Departments of transportation across the U.S. are invariably faced with a persistent problem of landslides and slope failures along highways. Repairs and maintenance work associated with these failures cost these agencies millions of dollars annually. An ideal solution for the construction or repair of slopes and embankments is to reinforce them using geosynthetics and large quantities of coarse-grained, free-draining soils to stabilize these structures. However, such coarse-grained soils are not readily available in Oklahoma and many other parts of the U.S. Consequently, the production and transportation costs for these materials can be prohibitive amounting to millions of dollars annually. A possible solution to this problem would be to use locally available soils that are of marginal quality (e.g. soils with more than 15% fines content) but are significantly less expensive.

One main concern in internal stability of reinforced soil slopes constructed with marginal soils is the pullout capacity of reinforcement when the soil moisture content increases significantly. Current design guidelines and test protocols for reinforced soil slopes in North America do not include specific procedures to account for the reduction in interface strength due to increased moisture content.

In this study, a moisture reduction factor (MRF) was introduced to account for the influence of moisture content on the soil-geotextile reinforcement interface strength in reinforced soil structures constructed with marginal soils. The MRF values were determined through large-scale and small-scale pullout tests on an Oklahoma marginal soil at different moisture content values. The variation of the MRF value with the soil moisture content is presented and discussed. It is found that the pullout capacity of geotextile reinforcement in a marginal soil can especially be affected on the wet side of the soil optimum moisture content.

Effects of Sample Preparation Method on Aggregate Shape Characteristics

Dharamveer Singh¹, Musharraf Zaman² F.ASCE, and Sesh Commuri³

¹Doctoral Candidate, School of Civil Engineering and Environmental Science, University of Oklahoma, 202 W. Boyd Street, Room 211, Norman, Oklahoma, USA, 73019, email: dvsingh@ou.edu

²David Ross Boyd Professor and Aaron Alexander Professor, Associate Dean for Research, College of Engineering, University of Oklahoma, Norman, Oklahoma, USA, 73019, email: zaman@ou.edu

³Associate Professor, School of Electrical and Computer Engineering, University of Oklahoma, Norman, Oklahoma, USA, 73019, email: scommuri@ou.edu

ABSTRACT

Hot Mix Asphalt (HMA) is a mixture of aggregates and asphalt binder, aggregates contributing to approximately 96 % of the total weight of the HMA mixture. The performance of HMA greatly depends upon the aggregate shape characteristics such as angularity, 2D form, texture and sphericity. These aggregate shape parameters may change while they go through different process of HMA production and sample preparation. Hence, it becomes vital to quantify these aggregate parameters in predicting the performance of HMA mixes.

A laboratory study was undertaken to evaluate the effects of sample preparation method on the aggregate shape characteristics. The loose HMA mix was collected from the Haskell Lemon plant in Norman. A Superpave Gyratory Compactor (SGC) was used to prepare 6" diameter x 6.7" height samples at four different target air voids (5 %, 7%, 9% and 12%). These samples were cut and cored to get final samples of size 4" diameter and 6" height. The sample size 4" diameter x 6" height is recommended by the American Association of State Highway and Transportation Officials (AASHTO) for conducting performance testing (dynamic modulus, flow number and flow time) of HMA mixes. Aggregates were retrieved from these samples after burning in a National Center for Asphalt Technology (NCAT) oven. In addition, original aggregate and loose HMA mix aggregate samples were used to compare them with other aggregates retrieved from SGC compacted samples. A total of six different types of aggregate were used in this study: original aggregates, plant burnt aggregate, 5% air voids aggregates (AVA), 7% AVA, 9% AVA, and 12% AVA. Each aggregate type was divided in coarse aggregates (retained 1/2" and #4) and fine aggregates (retained #8 and #16). A total of 36 aggregate samples were used to measure aggregate shape characteristics using an Aggregate Imaging System (AIMS).

A statistical method, called Analysis of Variance (ANOVA), was used to compare six types of aggregate shape parameters. It was found that coarse aggregates exhibit more sensitivity to changing their shape parameters compared to fine aggregates. The texture and 2D form of coarse aggregate particles changes while they go through different process of sample preparation and HMA production. On the other hand, fine aggregate particles do not show any significant change in their shape characteristics. No significant change was observed in angularity and sphericity for both types of aggregates. These results are expected to develop a better understanding of HMA mixture behavior in light of aggregate properties pertaining to aggregate shape.

GEOLOGY AND MINERAL RESOURCES OF OKLAHOMA

LUZA, K. V., Oklahoma Geological Survey, Norman, OK 73019, kluza@ou.edu,
KRUKOWSKI, S. T., Oklahoma Geological Survey, Norman, OK 73019, skrukowski@ou.edu,
JOHNSON, K. S., Oklahoma Geological Survey, Norman, OK 73019, ksjohnson@ou.edu

Oklahoma is a region of complex geology with several mountain ranges, uplifts, and sedimentary basins. The principal mountain belts, the Ouachita, Arbuckle, and Wichita occur in the southern third of Oklahoma. These were sites of folding, faulting, and uplifting during the Pennsylvanian Period. Principal sites of sedimentation were elongated basins that subsided more rapidly than adjacent areas and received 10,000–40,000 ft of sediment. Major basins were confined to the southern half of Oklahoma and included Anadarko, Arkoma, Marietta, Hollis, and Ouachita. Rocks in Oklahoma, mostly sedimentary, are from every geologic period. Permian (about 46%) and Pennsylvanian (about 25%) units comprise the majority of outcrops.

Oklahoma energy resources, particularly oil and natural gas, and coal, had a value of \$14.6 billion in 2006. Major nonfuel mineral production is widespread, but concentrated in major mountain belts in the south and in the Ozark uplift in the northeast. Oklahoma raw nonfuel minerals had a value of \$684 million in 2006, ranking first in the nation in gypsum and iodine production; second in tripoli; fourth in feldspar; seventh in industrial sand and gravel; tenth in masonry cement; and eleventh in common clays. Other industrial minerals of significant value included crushed stone (limestone, dolomite, gypsum, sandstone, rhyolite, and granite), portland cement, and construction sand and gravel. Significant production also includes helium, salt, building stone, and volcanic ash. Almost all Oklahoma mines are open pit except for salt and iodine produced from brine wells; helium from natural gas wells; and one underground limestone mine.

INTRODUCTION

The soils, topography, and vegetation of Oklahoma depend on its local geology and climate. The highest elevation (4,973 ft) in Oklahoma is on Black Mesa in the northwest corner of the Panhandle; the lowest elevation (287 ft) is in the southeast corner of the State. Mean annual precipitation varies from less than 20 in. in the Panhandle to over 55 in. in the Ouachita Mountains. The distribution of vegetation in Oklahoma is very diverse. Piñon Pine–Juniper is found in the northwest; central Oklahoma is a mosaic of forest, woodland, and grassland vegetation; and cypress bottoms occur in sloughs and back swamps in southeast Oklahoma.

Oklahoma is a region of complex geology where several major sedimentary basins are set near mountain ranges and uplifts (Fig. 1). About 99% of all outcrops are sedimentary. Remaining outcrops are (1) igneous rocks, mainly in the Wichita and Arbuckle Mountains; (2) metamorphic rocks in the eastern Arbuckles; and (3) mildly metamorphosed rocks in the core of the Ouachita Mountains. Rocks formed during every geologic period occur in Oklahoma. About 46% of Oklahoma has Permian rocks

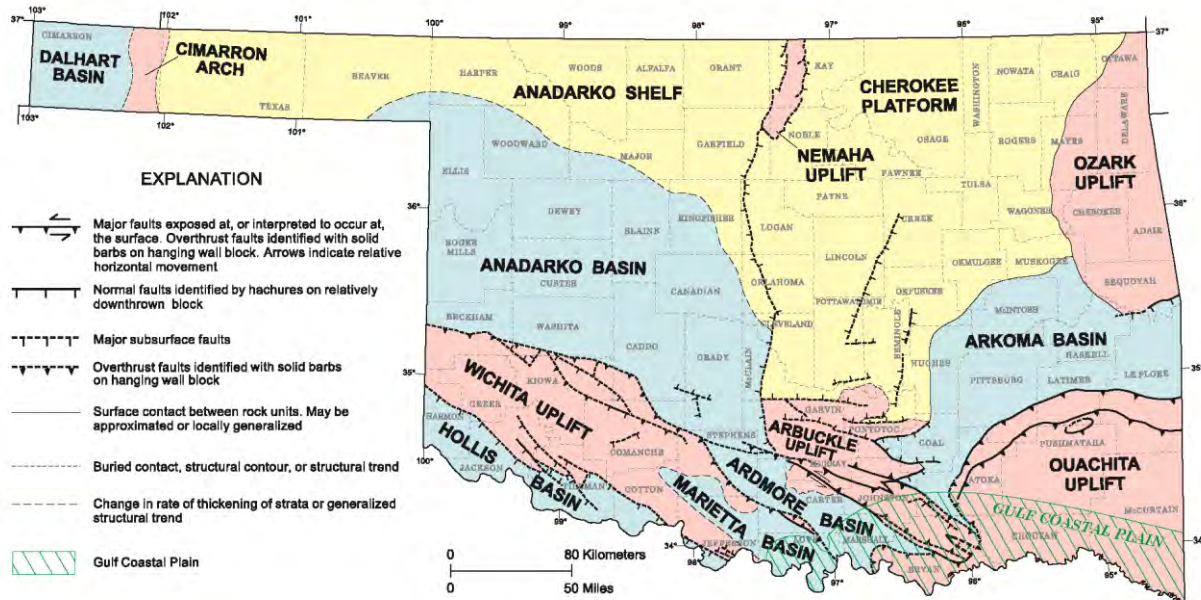


Fig. 1. Major geologic provinces of Oklahoma (modified from Northcutt and Campbell, 1995) resulted from tectonic uplift and downwarping mainly during the Pennsylvanian Period.

exposed at the surface. Other extensive outcrops are Pennsylvanian (about 25%), Tertiary (11%), Cretaceous (7%), Mississippian (6%), Ordovician (1%), and Cambrian (1%); Precambrian, Silurian, Devonian, Triassic, and Jurassic rocks each are exposed in less than 1% of Oklahoma (Fig. 2).

GEOLOGY

Upper Cambrian through Mississippian rocks in Oklahoma are represented by marine sediments deposited in a broad epicontinental seas. This basin, which extended across almost all parts of the southern Midcontinent, was a shelf-like area that received thick and extensive sediments of marine carbonates interbedded with thinner marine shales and sandstones. The sedimentary units thicken into protobasins such as the Anadarko, Ardmore, Arkoma, and other basins. Sediments were deposited later upon and across the present-day major uplifts. Strata subsequently were stripped away during Pennsylvanian uplift and erosion.

Orogenic activity during the Pennsylvanian Period sharply uplifted crustal blocks, subdividing the broad, shallow-marine protobasins into a series of well-defined basins. Orogenic activity was limited to folding, faulting, and uplift. Pennsylvanian orogenic pulses caused (or contributed to): (1) folding and thrusting of the Ouachita fold belt; (2) raising of the Wichita, Criner, Arbuckle, and Nemaha uplifts; and (3) pronounced down-warping of the Anadarko, Ardmore, Arkoma, and Marietta basins (Fig. 1).

Pennsylvanian strata in Oklahoma consist of sequences of marine and nonmarine shale, sandstone, conglomerate, and limestone that thicken markedly into rapidly subsiding basins.

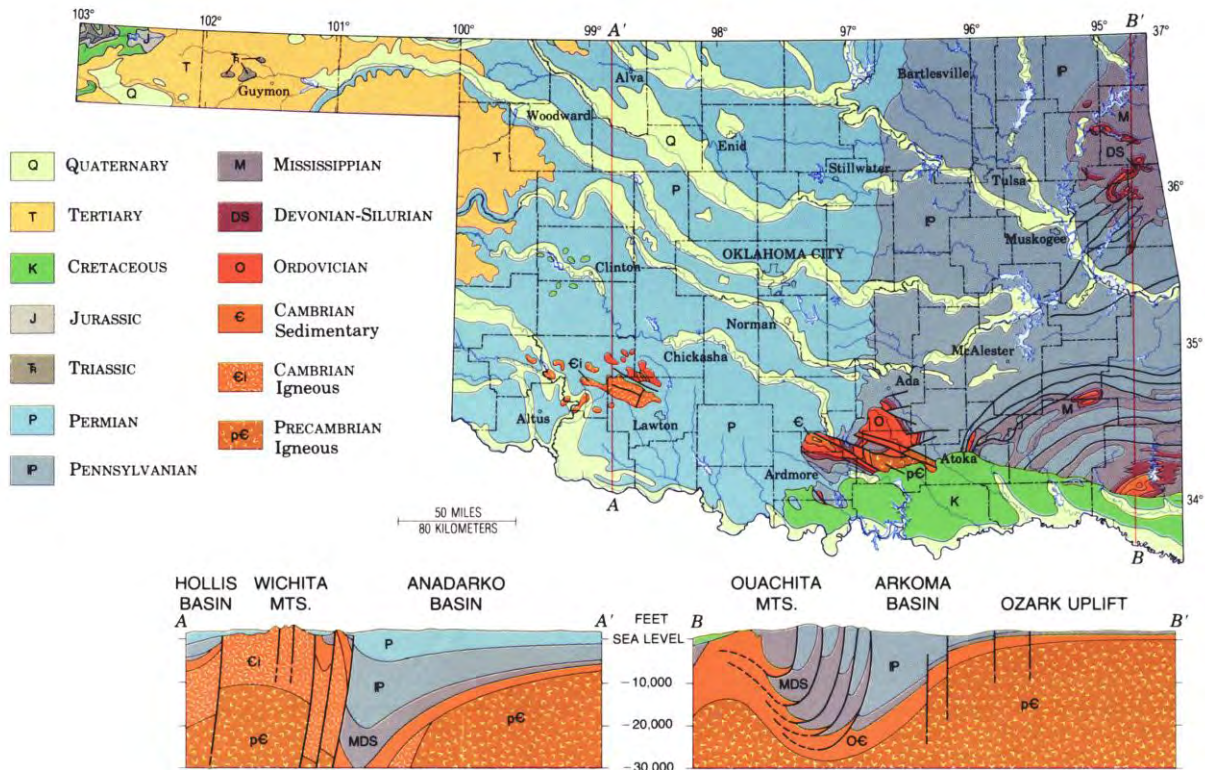


Fig. 2. Generalized geologic map and cross sections that show the subsurface configuration of rock units in Oklahoma.

Thick wedges of terrigenous clastic sediments were shed from nearby uplifts, and thinner carbonate sequences were deposited on shallow-water shelf areas distal to the uplifts. Successively younger Pennsylvanian units commonly overlap older units at the margins of the basins and across some uplifts. Thin coal beds are abundant in Desmoinesian strata, mainly in the Arkoma basin and the Cherokee platform. Total thickness of Pennsylvanian strata in various basins is 10,000–15,000 ft in the Anadarko, Ardmore, Arkoma, and Marietta basins, and about 4,000 ft in the Hollis basin. In most shelf or platform areas, Pennsylvanian strata typically are 1,500–4,000 ft thick.

Permian strata are limited to the western half of Oklahoma. Clastics were eroded from the Ouachitas on the east, the ancestral Rocky Mountains on the west, and the Wichita Mountains in southwest Oklahoma. Sediments accumulated mainly in the Anadarko basin, Hollis basin, and the Panhandle. Early Permian carbonates and shales, both gray and redbeds, are overlain by a major evaporate and redbed sequence in Middle and Late Permian. Evaporites, salt and gypsum/anhydrite, thicken into basins that continued to subside faster than adjacent uplifts and arches. Permian strata are as much as 7,000 ft thick in the Anadarko basin, 4,000 ft thick in the Hollis basin, and 1,000–3,000 ft thick in nearby shelf or platform areas.

The major outcrop of Mesozoic rocks is in the Gulf Coastal Plain of southeast Oklahoma. Cretaceous strata occur in an eastward-trending belt about 175 mi long and as much as 40 mi

wide. Beds mostly consist of nonmarine sandstone and clay units at the base. The sequence passes upward into marine limestone and shale beds and terminates with nonmarine sandstone beds. A second area of Mesozoic rocks, Triassic and Jurassic, is in the northwest corner of the Oklahoma Panhandle. Especially prominent is the Morrison Formation, a nonmarine deposit that contains uranium in the western United States.

Tertiary sediments are confined to the High Plains of western Oklahoma and the Panhandle. The principal unit, the Ogallala Formation, consists of Pliocene sand and clay derived by stream outwash from the Rocky Mountains and caliche units. Some volcanic ash and lacustrine deposits also occur.

Three major mountain regions, Ouachita, Arbuckle, and Wichita, occur in the southern part of Oklahoma (Figs. 1 and 2). The Ouachita Mountains in southeast Oklahoma is an arcuate fold belt that consists mostly of Mississippian and Early Pennsylvanian sandstone and shale units (Stanley, Jackfork, Johns Valley, and Atoka formations). Locally, sediments about 30,000 ft-thick, were deposited in a great trough through Morrowan and Atokan time. The depocenter shifted northward in Atokan time to the southern part of the Arkoma basin. The trough was destroyed during the Ouachita orogeny (Desmoinesian), with northward thrusting and complex folding of Ouachita-facies rocks to form the present-day Ouachita Mountains. Resistant units of steeply dipping sandstone form long, sinuous mountain ridges and hogbacks that tower 1,000–1,500 ft above intervening shale valleys.

The Arbuckle Mountains in south-central Oklahoma make up an area of low to moderate hills containing 15,000 ft of folded and faulted sediments ranging in age from Cambrian to Pennsylvanian (Ham, 1969). About 89% of these sedimentary rocks are limestone and dolomite units; the remainder are shale and sandstone units. Rocks in this part of southern Oklahoma were thrust upward and folded and faulted during several mountain-building episodes in the Pennsylvanian Period. The sedimentary cover was eroded from the underlying Precambrian granites in a 150-square-mile area in the southeast part of the Arbuckle Mountains, making this the largest exposure of Precambrian rocks in the State.

In the Wichita Mountains of southwest Oklahoma, granite, rhyolite, and gabbro are the dominant rocks. These are Middle and possibly Early Cambrian in age and are flanked by scattered outcrops of Cambrian and Ordovician limestone and dolomite units like those of the Arbuckle Mountains. The Wichita fault blocks were thrust upward and slightly northward during several Pennsylvanian uplifts, at which time the cover of pre-Pennsylvanian sediments were eroded. The igneous rocks form mountains that rise 500–1,000 ft above the surrounding plain of Permian red beds.

A portion of the Ozark uplift occurs in northeast Oklahoma. This deeply dissected plateau formed in gently dipping Mississippian limestone and chert beds. Caves, solution cavities, and other karst features are more prevalent here than in any other part of Oklahoma.

Much of the geologic discussion was taken from Johnson and Mankin (1971), Johnson and others (2001), and Johnson (2008a-c). General discussions of Oklahoma geology are presented by Ham and Wilson (1967), Ham (1969), and Johnson and others (1988).

MINERAL RESOURCES

Because of its geologic history, Oklahoma has abundant mineral resources that include petroleum (crude oil and natural gas), coal, non-fuel minerals (e.g., lead, zinc, gypsum, limestone, sand and gravel), and water. The value of petroleum, coal, and non-fuel minerals was about \$14.6 billion in 2006, making the minerals industry the greatest source of revenue in the state in recent years. Industrial minerals production value was about \$684 million in 2006.

Although Oklahoma has an important history mining metals, none are mined today. Underground mining in the Miami-Picher field of northeast Oklahoma yielded about 1.3 million tons of lead and about 5.2 million tons of zinc from 1891 to 1970. Oklahoma led the nation in zinc production almost every year from 1918 through 1945. About 1.9 million tons of copper-shale ore were mined southwest of Altus, Oklahoma, between 1964 and 1975. Principal metallogenic provinces of Oklahoma are in the northeast (Ozark uplift) and in the Ouachita, Arbuckle, and Wichita mountains.

Industrial minerals are nonfuel, nonmetallic minerals with economic potential. They are mined for local, national, and international markets. Industrial mineral industries are active in all Oklahoma counties. Some of the most important regions producing industrial minerals are the Wichita, Arbuckle, and Ouachita Mountains, and the Ozark uplift.

Crushed-stone and building stone resources include limestone, dolomite, granite, and rhyolite; other major construction resources are cement (made from limestone and shale) and sand and gravel deposits along modern and ancient rivers. Industrial sand (high-purity silica sand) is used for glassmaking, foundry sands, ceramics, and abrasives. Enormous resources of gypsum in western Oklahoma provide raw materials for wallboard, plaster, portland cement (as a retarder), and soil conditioners (Fig. 3). Thick layers of rock salt underlie most of western Oklahoma, and natural springs emit high-salinity brine to several salt plains. Oklahoma iodine, produced from deep brines in the northwest, is the nation's sole domestic supply. Other important industrial minerals in Oklahoma include clays and shales (to make brick and tile), tripoli, and volcanic ash (abrasives and/or absorbent materials).

The total estimated value of \$684 million for industrial mineral production in 2006 ranked Oklahoma 32nd of 50 states. Leading nonfuel commodities during 2006 were crushed stone (\$253 million), sand and gravel (\$91.9 million), industrial sand (\$40.4 million), iodine (withheld), and gypsum (\$27.4 million). Construction materials accounted for a large majority of Oklahoma's mineral value, (55%) in 2006: crushed stone, construction sand and gravel, and gypsum (cement was withheld as company proprietary data; United States Geological Survey, 2006).

Raw materials for portland and masonry cements are limestone (for calcium) and clay or shale (for alumina and silica). Oklahoma has these in abundance; they are discussed separately below. Historically, local demand, along with cheap, readily available energy, was responsible for the beginning of the cement industry in Oklahoma. Three plants currently manufacture cement in Mayes, Pontotoc, and Rogers Counties. In the recent past, cement manufacture accounted for nearly one third the value of Oklahoma industrial minerals production.

Much of the data herein are based upon Johnson, 1969, 1977, 1999), Morris (1982), and the Oklahoma Department of Mines (ODOM) (2006–2007); the reader is referred to these and others cited herein for additional commodity information.

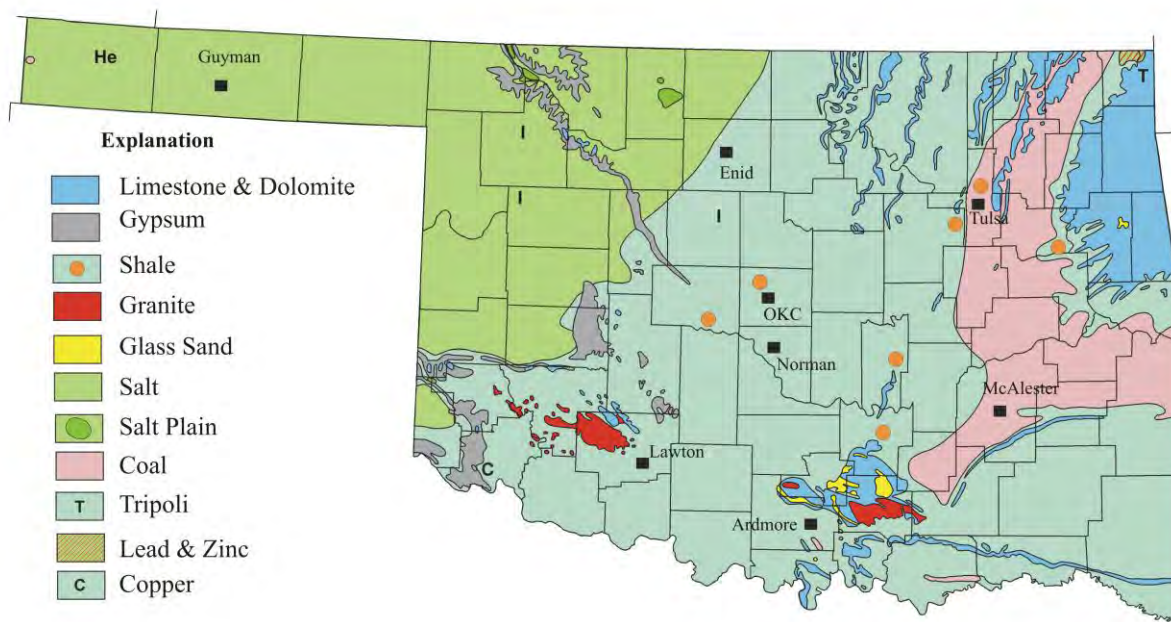


Fig. 3. Major mineral resources (exclusive of oil and gas) in Oklahoma. Helium (He) and iodine (I) not shown in explanation.

ENERGY (FUEL) MINERALS

Petroleum Resources: prehistoric Americans utilized oil and tar from petroleum seeps for medicinal purposes and adhesives; early settlers used oil for lubricating and lamp oil. The first recorded production was 30 bbls of oil in 1891, but the first profitable oil well was completed in 1897 at Bartlesville. Petroleum production has occurred in 74 of 77 Oklahoma counties.

Discoveries between 1905 and 1928 established Oklahoma as an oil state with many oil fields, e.g., Glennpool, Cushing, and Oklahoma City. Continuous exploration has found additional major oil and gas fields (Fig. 4A-C). Oklahoma led the nation in petroleum production from 1907 through 1923; presently it is the fifth leading producer of oil, behind Texas, Alaska, Louisiana, and California. Behind Texas, Oklahoma typically shares second or third place with New Mexico in producing natural gas.

Over 500,000 wells have been drilled in Oklahoma looking for petroleum; about 120,000 still produce. Cumulative production through 2008 was about 14.9 billion bbls of oil and 99.1 trillion cu ft of natural gas. Oklahoma produced 1.7 trillion cu ft of natural gas and 65 million bbls of oil in 2008 (Oklahoma Corporation Commission, 2009).

Coal Resources: vast resources of bituminous coal occur in eastern Oklahoma. Over 200 million tons were produced since coal mining began in 1873. Since the 1950s almost all Oklahoma coal has been mined by surface methods: it is safer, recovers more coal, and costs less (Fig. 5). Surface mining is restricted to mining depths of 50–100 ft, so only a portion of coal resources are recoverable. Coal beds are typically 0.8–10.0 ft thick, have 0.4%–6.5% sulfur, and contain 11,500–14,500 Btu per pound. Production peaked at about 57 million tons in 1981; with about



A



C



B

Fig. 4. (A) Loffland Brothers Rig 32 used to drill Lone Star Producing Company's deepest producing gas well in North America; (B) deep producing oil well at the University of Oklahoma's north base campus; and (C) shallow producing oil well near Chelsea, Oklahoma.



Fig. 5. Coal mining in northeast Oklahoma.

1.5 million tons mined in 2008 (Oklahoma Geological Survey, 2009). Most Oklahoma coal generates electricity or is made into coke for steelmaking.

INDUSTRIAL MINERALS

Nonmetallic minerals are distributed widely in Oklahoma (Fig. 3), and are mined primarily for local, regional, and national markets. Crushed stone and dimension stone resources include limestone, dolomite, and granite deposits; other construction resources are limestone and shale for cement, and sand and gravel deposits along modern and ancient rivers. Industrial sand (high-purity silica sand) in the Arbuckle Mountains is used in glassmaking, foundry sands, ceramics, and abrasives. Enormous reserves of gypsum in western Oklahoma are mined for wallboard, plaster, portland cement (a retarder), and soil amendments. Thick layers of rock salt underlie western Oklahoma at depths of 30–3,000 ft; natural salt-water springs emit brine to several salt plains in the region. In northwest Oklahoma, three companies produce iodine from deep oil-field brines (7,000–10,000 ft deep). Oklahoma is the sole domestic producer of iodine. Other important nonmetallic minerals from Oklahoma are clays and shales (brick and tile), and tripoli and volcanic ash (abrasives, pigments, and absorbents).

Iodine: iodine is a grayish-black, nonmetallic element, solid at ordinary temperatures. In northwest Oklahoma, it is dissolved in iodine-rich natural brines (100–1,560 ppm iodine; 300–350 ppm in most producing wells) 6,000–10,000 ft below the surface (Fig. 6). Oklahoma iodine brines are the richest in the world (Krukowski and Johnson, 2006). Major production comes from near Woodward and Vici, in Morrowan (basal Pennsylvanian) sandstones in a south-trending paleo-valley called the “Woodward trench.” Production is also a byproduct of oil and gas drilling into other Paleozoic rocks (sandstones, limestones, and dolomites) with iodine-rich brines. After brines are treated chemically, iodine crystals are precipitated. Effluent brine is treated and re-injected downstream into the producing formation (Cotton, 1978).



Fig. 6. Iochem Corporation's iodine plant near Vici, Oklahoma.

Iodine production in Oklahoma began in 1977. Three plants in Oklahoma are the sole domestic source of iodine; they yielded about 4.8% of global output in 2006 (Lyday, 2007). The last reported production was 1,570 metric tpa in 2005 valued at \$16.79 per kg (Lyday, 2007). The U.S. Geological Survey (USGS) reported iodine at \$21.10 for 2009 (Angula, 2010). Major uses include catalysts, stabilizers, radiopaques, human and livestock nutrition, biocides and disinfectants, pharmaceuticals, photography, and colorants.

Gypsum: enormous resources of high-purity gypsum occur in western Oklahoma. Blaine and Cloud Chief Formations (both Permian) gypsums are 5–30 ft thick and 95%–99% pure, and 25–100 ft and 92%–97% pure, respectively (Fig. 7). Total gypsum resources are estimated at 48 billion short tons. Gypsum beds typically form hills in the semiarid climate, and gypsum layers are nearly flat lying, so the gypsum is best mined in open pits (Johnson, 1978).

Oklahoma ranked fourth in U.S. gypsum production in 2009 (Angulo, 2010), down from first place in 2008 (Angulo, 2009). The latest figure reported by the ODOM was 4,969,157 short tons produced in 2007 (Oklahoma Department of Mines, 2006–2007); about 1,000,000 short tons less were mined in 2009. Uses include plaster for interior walls and wallboard, special plasters for medical and other uses, retarders in portland cement, fillers, road metal, and soil conditioner.

Tripoli: tripoli is a white to cream-colored, microcrystalline, high-purity silica. It is porous, lightweight, and friable. It is derived from a partly siliceous, parent sedimentary rock from which soluble carbonate minerals were leached (Quirk and Bates, 1978). Important tripoli deposits occur in northeast Oklahoma; first mined in the Missouri-Oklahoma tripoli district in 1869.



Fig. 7. Texas Gypsum Company's Cloud Chief gypsum quarry near Fletcher, Oklahoma.

Deposits typically are 2–20 ft thick and occur in Mississippian cherty limestones beneath only 2–10 ft of overburden.

Excavated tripoli is dried, crushed, and screened to various sizes. Ground tripoli is used mainly as a paint additive, as a mild abrasive, or in buffing and polishing compounds. It is prized for its abrasiveness, resistance, porosity, permeability, absorption, and low specific gravity. One company operates several pits in Ottawa County. The USGS reported the average value of tripoli at \$129 per metric ton as an extender and filler in 2008, mostly in paints (93% of production); and \$208 per ton as an abrasive (5% of production; Dolley, 2009). The ODOM (2006–2007) reported production at 44,793 short tons in 2007.

Industrial Sand: two operators in the Arbuckle Mountains (Fig. 8) mine high-purity silica sand (Ordovician Simpson Group); plant-run sand contains 99.8% silica and normally only 0.01%–0.03% iron oxide (Ham, 1945). Ordovician sand also occurs in northeast Oklahoma; outcrops of Cretaceous sands of 98.5%–99.5% silica occur south and east of the Arbuckles. Alluvium from the Arkansas River near Muskogee produces feldspar sand for glassmaking: processed sand includes about 75% quartz (silica), about 25% feldspar, and < 0.04% iron oxide. Oklahoma produced 1.64 million metric tons of industrial sand in 2006 valued at \$40.4 million (excluding feldspar). In 2009 Oklahoma ranked fourth in U.S. industrial sand production (Dolley, 2010); and fourth in feldspar (Fig. 9A-C) production based solely on the Arkansas River feldspar sand operation (Cordier, 2010).

Glass manufacturing plants in Oklahoma and adjacent states use the industrial sands to produce container glass, flat glass, tumblers, tableware, and Pyrex[®]. Other uses include foundry sand, ceramics, sodium silicate, and silica flour (for ceramics, abrasives, and inert filler).

Clay and Shale: clay and shale for making red brick and tile occur in almost every county. Some areas have light-firing clay, low-grade refractory clay, and clay for stoneware and pottery. Clay for lightweight aggregate is common in eastern Oklahoma.



Fig. 8. Hydraulic mining of high-purity silica sand of the Oil Creek Formation in U.S. Silica Company's Mill Creek quarry.

Specialty clays also occur in Oklahoma, such as bentonite associated with, and altered from, volcanic ash. A company in Dewey County mines bentonite for absorbents. High oil prices and a corresponding increase in petroleum exploration drilling provide the recent impetus to find bentonite in Oklahoma. Oil service companies need raw materials for drilling fluids proximal to actual oil field drilling. Helpful reports on clay and shale in Oklahoma are Bellis (1972) and Johnson and others (1980).

Shale has been important to the construction industry in Oklahoma, even before statehood. Over 120 brick plants have operated since 1888, mostly in central Oklahoma (Morris, 1982). An excellent history of brick making in Oklahoma is Robison (1980). Five brick plants in Oklahoma can manufacture 450 million bricks per year. Shale is also a major ingredient for cement manufacture as a source of silica and alumina. In 2007 Oklahoma produced 1,304,528 million short tons of clay and shale (Oklahoma Department of Mines, 2006–2007). The USGS reported Oklahoma as seventh in U.S. production of common clay; 1.05 million metric tons valued at \$4.06 million (Virta, 2007).

Helium: a colorless, odorless, and nonpoisonous gas, helium is the second lightest element. A plant near Keyes in the Panhandle extracts helium from natural gas in the Hugoton and Keyes



A

B



C



Fig. 9. Some dredge operations in Oklahoma: (A) Arkhola Sand & Gravel Co. feldspar sand operation in the Arkansas River; (B) Dolese Bros. Co. sand and gravel operation near Newcastle; and (C) Dolese Bros. Co. sand and gravel operation near Mustang (note producing oil well below upper right hand corner).

gas fields. Once managed by the U.S. Bureau of Land Management, helium plants were privatized over the last two decades. Major uses of helium include cryogenics, pressurizing and purging, welding cover gas, controlled atmospheres, leak detection, breathing mixtures, and others.

Helium was a strategic mineral during the Cold War; purging rockets and jet engines was crucial to the U.S. Department of Defense. The U.S. Government, therefore, controlled its production and sale. When the Cold War ended, helium lost its strategic significance, and its production and sale was privatized. Only Oklahoma, Texas, and Kansas produce Grade A helium in the U.S.

Limestone (Figs. 10-11): limestone is abundant in northeast Oklahoma, in the Wichita and Arbuckle mountains, and in southeast Oklahoma (Rowland, 1972). Its main use is for concrete aggregate in highway and other construction, railroad ballast, cement manufacture, glassmaking, and making chemical-grade lime. Other uses include dimension stone and pulverized limestone or ground calcium carbonate (GCC), the latter used in construction materials such as roofing shingles and asphalt paving; animal feed additives; in soil conditioners; in flue gas desulphurization; and in dust control in coal mines. In western and Panhandle areas, caliche substitutes for some purposes.

Arbuckle and Wichita mountains limestones are several hundred to several thousand feet thick; their outcrops cover large areas. These are an almost unlimited resource. Principal markets for crushed limestone are Oklahoma City and Dallas-Fort Worth metropolitan areas. Usable limestones supplying local markets in southeast, northeast, and north-central Oklahoma commonly are 10–50 ft thick. In 2007, 93 companies reported mining 48,094,063 tons of limestone in 36 of 77 counties, accounting for 57% of all tonnage mined in Oklahoma (Oklahoma Department of Mines, 2006–2007).



Fig. 10. Martin Marietta Materials limestone (West Spring Creek Formation) quarry near Troy, Oklahoma. Primary crusher near center of photograph.



Fig. 11. The Goodland Limestone, 65 ft thick, is mined near Idabel, Oklahoma.

Sandstone: sandstone deposits in eastern Oklahoma are mostly hard; are gray, brown, or buff; and some are suitable for dimension stone or aggregate. Most sandstone in western Oklahoma is soft or friable; is reddish-brown; is suitable only locally for building material. Several operators in east-central Oklahoma quarry sandstone for dimension stone. In eastern Oklahoma, several quarries mine sandstone for riprap and aggregate.

Granite: granite and similar igneous rocks of the Wichita and Arbuckle mountains in southern Oklahoma produce dimension stone for monuments and building trades (Fig. 12A-B); crushed granite and rhyolite mostly for railroad ballast; and intermittently for aggregate and rip-rap. A brick company tested Wichita-Mountains granite in 2006, for use as grog in brick manufacture. Granitic rock in Oklahoma is Precambrian and Cambrian in age. Colors are red, pink, gray, and black; textures range from finely to coarsely crystalline.

Quarries in Greer, Kiowa, Johnston, and Murray counties regularly produce granite and rhyolite. In 2007 Oklahoma produced about 4,570,242 short tons of granite and rhyolite (Oklahoma Department of Mines, 2006–2007).

Sand and Gravel: sand and gravel deposits are widespread and accessible throughout Oklahoma. Principal deposits occur along major rivers, in terrace remnants of Pleistocene riverbeds, and in Tertiary deposits in the northwest (Figs. 9A–C). Gravels are common in western Oklahoma; Wichita and Arbuckle mountains vicinities; and Cretaceous rocks south of the Arbuckle and Ouachita mountains.

Sand and gravel are used in construction chiefly as aggregate. The paving industry uses vast amounts in both asphalt and portland-cement concretes. The ODOM (2006–2007) reported that 272 companies produced 23,339,108 short tons of sand and gravel in 59 of 77 counties in Oklahoma in 2007. These figures included industrial sand and some fill-dirt production.

Chat: Chat is crushed limestone, dolomite, and chert generated as a waste byproduct from mining and milling lead/zinc ores in the Tri-State district of northeast Oklahoma. It exists in large stockpiles in Ottawa County. Historically used for railroad ballast, today the majority is aggregate for asphalt mixes. A single hauler produced 252,081 short tons in 2007 (Oklahoma Department of Mines, 2006–2007).



A

B



Fig. 12. (A) Granite dimension stone quarry near Troy, Oklahoma, and (B) polishing granite at Willis Granite Products near Granite, Oklahoma.

Dimension Stone: This is stone finished to a specified dimension and/or shape (Fig.12A) It typically is quarried in rectangular blocks, sawed into slabs for finishing (usually a smooth surface or high luster polish), and used in buildings, monuments (Fig. 12B), furniture, industrial applications, and other uses. Fieldstone, flagging, and rubble, are sold in their natural state, or broken into diverse shapes and sizes for building, paving, decorating, or other purposes (Mead and Austin, 2006).

Oklahoma sandstones, limestones, dolomites, and granites are suitable for building and ornamental purposes. Commercial and home construction use of native stone is extensive in Oklahoma in recent years. The ODOM (2006–2007) reported 137 companies produced 741,674 short tons of dimension stone in nine counties in 2007.

Salt: thick Permian salts underlie western Oklahoma at depths of 30–3,000 ft and more (Jordan and Vosburg, 1963). Individual beds are 5–25 ft thick and interbedded with thin shale and anhydrite layers. Salt beds are suitable for underground or solution mining, but only the latter has taken place in Oklahoma.

Brines formed by dissolution of salt in the shallow subsurface discharge as salt springs at the surface; emissions range from 150 to 3,000 tpd of salt per site (Fig. 13). The springs produced salt commercially since the earliest twentieth century, and even earlier by prehistoric people. Small operators tapped the salt plains in the north- and southwest, each producing about 2,000–10,000 tpa of solar salt in iron drying pens. Native Americans precipitated salt from brines onto feathers or small branches for barter. Cargill Incorporated produced 127,990 short tons of solar salt from the Big Salt Plain in Woods County in 2007 (Oklahoma Department of Mines, 2006–2007) for use in water softeners, stockfeed, and road de-icing.



Fig. 13. Cargill, Incorporated’s operation at Big Salt Plain, Woods County, Oklahoma.

Miscellaneous Minerals: asphaltite formed when crude oil migrated to or near the surface: lighter hydrocarbons evaporated; thicker, heavier residues impregnated rocks or filled voids. Sources of asphaltite are sedimentary rocks in and around the Arbuckle and Ouachita mountains (Jordan, 1964). Smaller deposits occur similarly in the Wichita Mountains and northeast Oklahoma. Sulphur and Dougherty districts in the Arbuckles produced about 3 million tons of asphaltite between 1891 and 1960. The Ouachitas produced asphaltite between 1890 and 1916. Asphaltite used for road-surfacing and also for roofing pitch, paints, varnishes, rubber substitutes, and electrical-wire insulation. High oil prices recently renewed interest and exploration for asphaltite.

High-purity dolomite occurs in the Arbuckle Mountains (Ham, 1949); it is quarried for its high-purity at one site and for crushed stone at two others. The high-purity Royer Dolomite is about 500 ft thick; other dolomites are 400–500 ft thick. Smaller lower grade deposits, are in northeast and western Oklahoma. Uses of dolomite include dimension stone, glassmaking flux, animal feed, and soil amendments.

Lime is manufactured in Sequoyah County from high-calcium, Silurian St. Clair Limestone mined by surface and underground methods. Other high-calcium limestone deposits occur in northeast, south-central, and southeast Oklahoma. Uses include steelmaking, flue gas desulphurization, soil stabilization, paper manufacturing, sanitation and water treatment, and production of stuccos, plasters, and mortars.

Volcanic ash occur in western and east-central Oklahoma (Burwell and Ham, 1949), the result of airborne ash and dust accumulating from Tertiary and Pleistocene volcanic eruptions primarily in New Mexico and Wyoming. It is used as an abrasive in polishing powders, scouring soaps, and cleansing powders; in pozzolan cement; and in insulating compounds.

SUMMARY

Oklahoma geology is complex with several sedimentary basins set near mountain ranges and uplifts. The state contains many classic areas where fundamental concepts of geology, petroleum exploration, and minerals production were formulated through the years. Oklahoma has abundant mineral resources that include crude oil, natural gas, coal, and non-fuel minerals. Nonmetallic minerals are mined primarily for local, regional, and national markets. Crushed stone and dimension stone resources include limestone, dolomite, and granite deposits. Other construction resources are limestone and shale for cement and high-purity silica sand for glassmaking, foundry sands, ceramics, and abrasives. Gypsum is mined for wallboard, plaster, portland cement, and soil amendments. Oklahoma is the sole domestic producer of iodine. Other important nonmetallic minerals from Oklahoma are clays and shales, tripoli, salt, and volcanic ash.

REFERENCES CITED

- Angulo, M.A., 2009, Iodine, *in* Unites States Geological Survey, mineral commodities summary, January, 2009: Washington, DC, United States Geological Survey, p. 72–73.
- Angulo, M.A., 2010, Iodine, *in* Unites States Geological Survey, mineral commodities summary, January, 2010: Washington, DC, United States Geological Survey, p. 76–77.
- Bellis, W.H., 1972, Clay products in Oklahoma: Oklahoma Geology Notes, v. 32, p. 157–168.
- Burwell, A.L.; and Ham, W.E., 1949, Cellular products from Oklahoma volcanic ash, with a section on geology and petrology: Oklahoma Geological Survey Circular 27, 89 p.
- Cordier, D.J., 2010, Feldspar, *in* Unites States Geological Survey, 2010 Minerals Yearbook: Washington, DC, United States Geological Survey, p. 54–55.
- Cotton, H.M., 1978, Iodine in northwestern Oklahoma, *in* Johnson, K.S., and Russell, J.A., eds., Thirteenth annual forum on the geology of industrial minerals: Oklahoma Geological Survey Circular 79, p. 89–94.
- Dolley, T.P., 2009, Silica [advanced release], *in* Unites States Geological Survey, 2008 Minerals Yearbook: Washington, DC, United States Geological Survey, p. 66.1–66.16.
- Dolley, T.P., 2010, Sand and gravel (industrial), *in* Unites States Geological Survey, 2010 Minerals Yearbook: Washington, DC, United States Geological Survey, p. 138–139.
- Ham, W.E., 1945, Geology and glass sand resources, central Arbuckle Mountains, Oklahoma: Oklahoma Geological Survey Bulletin 65, 103 p.
- Ham, W.E., 1949, Geology and dolomite resources, Mill Creek–Ravia area, Johnston County, Oklahoma: Oklahoma Geological Survey Circular 26, 104 p.
- Ham, W. E., 1969, Regional geology of the Arbuckle Mountains, Oklahoma: Oklahoma Geological Survey Guidebook 17, 52 p.
- Ham, W. E.; and Wilson, J. L., 1967, Paleozoic epirogeny and orogeny in the central United States: American Journal of Science, v. 265, p. 332–407.
- Johnson, K.S., 1969, Mineral map of Oklahoma (exclusive of oil and gas fields): Oklahoma Geological Survey Map GM-15, scale 1:175,000.
- Johnson, K.S., 1977, Minerals, minerals industries, and reclamation in Oklahoma, *in* Morris, J.W., ed., Geography of Oklahoma: Oklahoma Historical Society, The Oklahoma Series, v. 6, p. 93–111.
- Johnson, K.S., 1978, Major gypsum districts of western Oklahoma, *in* Johnson, K.S., and Russell, J.A., eds., Thirteenth annual forum on the geology of industrial minerals: Oklahoma Geological Survey Circular 79, p. 6–14.
- Johnson, K.S., 1999, Geology and industrial-mineral resources of Oklahoma, *in* Johnson, K.S., ed., Proceedings of the 34th Forum on the Geology of Industrial Minerals, 1998: Oklahoma Geological Survey Circular 102, p. 1–12.
- Johnson, K. S., 2008a, Geologic history of Oklahoma, *in* Johnson, K. S. and Luza, K. V. (eds.), Earth Sciences and mineral resources of Oklahoma: Oklahoma Geological Survey Education Publication 9, p. 3–5.
- Johnson, K. S., 2008b, Geologic map of Oklahoma, *in* Johnson, K. S. and Luza, K. V. (eds.), Earth Sciences and mineral resources of Oklahoma: Oklahoma Geological Survey Education Publication 9, p. 6.

- Johnson, K. S., 2008c, Geologic cross sections of Oklahoma, *in* Johnson, K. S. and Luza, K. V. (eds.), *Earth Sciences and mineral resources of Oklahoma: Oklahoma Geological Survey Education Publication 9*, p. 7.
- Johnson, K. S.; Amsden, T. W.; Dennison, R. E.; Dutton, S. P.; Goldstein, A. G.; Rascoe, B., Jr.; Sutherland, P. K.; and Thompson, C. M., 1988, Southern Midcontinent region, *in* Sloss, L. L. (ed.), *Sedimentary cover—North American craton*, U.S. Geological Society of America, *The Geology of North America*, v. D-2, p. 307–359.
- Johnson, K.S.; Luza, K.V.; and Roberts, J.F., Jr., 1980, Disposal of industrial wastes in Oklahoma: Oklahoma Geological Survey Circular 80, 82 p.
- Johnson, K. S.; and Mankin, C. J., 1971, Geology of Oklahoma—a summary, *in* Proceedings of the 22nd annual highway geology symposium, p. 1–7.
- Johnson, K. S.; Northcutt, R. A.; Hinshaw, G. C.; and Hines, K. E., 2001, Geology and petroleum reservoirs in Pennsylvanian and Permian rocks of Oklahoma, *in* Johnson, K. S. (ed.), *Pennsylvanian and Permian geology and petroleum in the southern midcontinent*, 1998 symposium: Oklahoma Geological Survey Circular 104, p. 1–19.
- Jordan, L., 1964, Petroleum-impregnated rocks and asphaltite deposits of Oklahoma: Oklahoma Geological Survey Map GM-8, 16-page text.
- Jordan, L.; and Vosburg, D.L., 1963, Permian salt and associated evaporites in the Anadarko basin of western Oklahoma—Texas Panhandle region: Oklahoma Geological Survey Bulletin 102, 76 p.
- Krukowski, S.T.; and Johnson, K.S., 2006, Iodine, *in* Kogel, J.E., Trivedi, N.C., Barker, J.M., and Krukowski, S.T., eds., *Industrial minerals & rocks, commodities, markets, and uses*, seventh edition: Society for Mining, Metallurgy, and Exploration, Inc. Littleton, CO., p. 541–551.
- Lyday, P.A., 2007, Iodine, *in* United States Geological Survey, mineral commodities summary, January, 2007: Washington, DC, United States Geological Survey, p. 80–81.
- Mead, L.; and Austin, G.S., 2006, Dimension stone, *in* Kogel, J.E., Trivedi, N.C., Barker, J.M., and Krukowski, S.T., eds., *Industrial minerals & rocks, commodities, markets, and uses*, seventh edition: Littleton, CO., Society for Mining, Metallurgy, and Exploration, Inc., p. 907–923.
- Morris, J.W., 1982, Nonmetallic resources, *in* Morris, J.W., ed., *Drill bits, picks, and shovels, a history of mineral resources in Oklahoma: Oklahoma Historical Society, The Oklahoma Series*, v. 17, p. 162–178.
- Northcutt, R. A.; and Campbell, J. A., 1995, Geologic provinces of Oklahoma: Oklahoma Geological Survey Open File Report 5-95, 1 sheet, scale 1:750,000, 6-page explanation and bibliography.
- Oklahoma Corporation Commission, 2009, 2008 report on oil and gas activity within the State of Oklahoma: Oklahoma Corporation Commission, 149 p.
- Oklahoma Department of Mines, 2006–2007, Annual report, Ninety-second annual report calendar years 2006 and 2007: Oklahoma Department of Mines, 56 p.
- Oklahoma Geological Survey, 2009, [Coal] Production Data (Documentation) From 1873 to present. <http://www.ogs.ou.edu/level3-databases.php> accessed February 11, 2010.

- Quirk, W.F.; and Bates, A.K., 1978, Tripoli deposits of southwest Missouri and northeast Oklahoma, *in* Johnson, K.S., and Russell, J.A., eds., Thirteenth annual forum on the geology of industrial minerals: Oklahoma Geological Survey Circular 79, p. 47–50.
- Robison, L., 1980, Made out-a mud: Oklahoma City, OK, privately published, 232 p.
- Rowland, T.L., 1972, General survey of carbonate mineral deposits in Oklahoma: Oklahoma Geology Notes, v. 32, p. 73–89.
- Virta, R.L., 2007, Clay and shale [advanced release], *in* United States Geological Survey, mineral commodities summary, January, 2007: Washington, DC, United States Geological Survey, p. 18.1–18.24.
- United States Geological Survey, 2006, Oklahoma, *in* Minerals yearbook, area reports, domestic 2006: Washington, DC, United States Geological Survey, p.38.1–38.6.

**Mapping Soft Soil Zones and Top-Of-Bedrock
Beneath High-Traffic Areas in Honolulu**

Phil Sirles

Zonge Geosciences, Inc.
7711 West 6th Avenue, Suite G
Lakewood, CO, 80214
(720)-962-4444
phils@zonge.us

Zoran Batchko

PB Americas
444 Flower Street, Suite 3700
Los Angeles, CA 90071
(213)-362-9470
Batchko@pbworld.com

Prepared for the 61st Highway Geology Symposium, August, 2010

Acknowledgements

The authors would like to thank Dr. Robin Lim and his staff at Geolabs for their assistance while in the field collecting these data, and also for integration of geologic and geotechnical information during preparation of this paper. Zonge also appreciates the input received from the PB Americas geotechnical design team.

Disclaimer

Statements and views presented in this paper are strictly those of the authors, and do not necessarily reflect positions held by their affiliations, the Highway Geology Symposium (HGS), or others acknowledged above. The mention of trade names for commercial products does not imply the approval or endorsement by HGS.

Copyright Notice

Copyright © 2010 Highway Geology Symposium (HGS)

All Rights Reserved. Printed in the United States of America. No part of this publication may be reproduced or copied in any form or by any means – graphic, electronic, or mechanical, including photocopying, taping, or information storage and retrieval systems – without prior written permission of the HGS. This excludes the original author(s).

ABSTRACT

Two-dimensional passive surface-wave data were acquired, processed and interpreted for the Honolulu High-Capacity Transit Corridor Project - Waipahu to Aiea - Ewa, Oahu, Hawaii. The project consisted of two distinct geophysical objectives to meet geotechnical engineering needs: first, to determine the lateral and vertical extent of soft-soil conditions; and second, to map the depth-to-bedrock. The Refraction Microtremor (ReMi) method was used along both the Farrington and the Kamehameha Highways. Initially, *blind tests* were conducted to determine the viability of the passive-surface wave seismic technique to meet project objectives. Results were extremely correlative with known geologic conditions, based geotechnical boring data, and the program progressed for the eastern portion of the HHCTCP.

Approximately 2.66-line miles of two-dimensional (2D) ReMi seismic data were acquired along 12 separate lines. Line locations were selected based on a variety of geologic settings and the need for subsurface information between, below and beyond geotechnical borings. Results indicate the seismic and geologic/geotechnical data could be integrated to yield valuable information beneath the areas investigated. An example seismic section is shown below (taken from Line 3). The seismic survey results provided good subsurface information regarding the presence of-, lateral variation of-, and extent of- soft soils which would cause distinct problems for design of deep foundations along the HHCTCP.

Results indicate that thick soft-soil conditions exist; and, that the basalt bedrock has considerable relief. The bedrock can be encountered as shallow as 1.5 m (5 ft), to as deep as 70 m (230 ft) in this area beneath the existing highways. An innovative application of 2D seismic testing successfully mapped the lateral and vertical variability of the soft-soils beneath areas with very high traffic volume, without interrupting vehicle flow. The method was extremely effective for meeting project objectives in a timely, safe and economical fashion while not disrupting the flow of traffic along two very busy highway corridors.

INTRODUCTION

In August 2008, Zonge Geosciences, Inc. (Zonge) conducted an innovative seismic survey west of Honolulu, Hawaii. Figure 1 outlines the project area, which generally lies between Waipahu and Aiea. Objectives of the seismic investigation were two-fold: 1) Determine the thickness and lateral variability of soft-soil deposits; and, 2) Determine the depth-to-bedrock.

To meet the objectives a 2D ReMi survey was performed. The surveys were conducted in areas of very high traffic volume along segments of the Farrington and [King] Kamehameha highways. The project follows the proposed alignment for the Honolulu High-Capacity Transit Corridor Project (HHTCP). The seismic data were acquired in (coned-off) traffic lanes, medians, and along sidewalks. Line locations were selected depending on crew safety, day of the week, and lane closure/accessibility. Geologic and geotechnical data were provided, in the form of boring logs and shear-wave velocity data, to aid the seismic interpretation.

In general terms, the geologic setting does not vary considerably over the 8.05 km (5-mile) survey area; that is, there are overburden soils overlying bedrock. However, for engineering design purposes the stiffness of the overburden and the depth to the bedrock are critical parameters. These design data are most commonly obtained with geotechnical drill holes, sampling and lab testing. Beneath most of the Honolulu area, the overburden materials are described as a complex series of soils that range from coarse-grained, loose- to very-dense sands and gravels (with cobbles) to fine-grained, very soft to very stiff clays. In addition to these coarse- and fine-grained soils, interbedded layers of coralline, mudflow or clinker deposits are also present within the overburden. Across this project area bedrock is defined as basalt. Outcrops and boring logs indicate that the bedrock has significant variability in the degree of weathering, fracture density, and other lithologic characteristics (i.e., vuggy, pillows, etc.). Depth to bedrock was anticipated to vary significantly beneath this portion of the HHTCP project site, with no consistent or regional dip. Similarly, the stiffness of the (undifferentiated) overburden was expected to vary considerably.



Figure 1: Project location map showing the area of investigation (red box).

Topographic relief on the bedrock surface is generally attributed to erosional features such as paleo-channels or relief caused at the time the basalt flow was deposited. As a result, the subsurface soil/bedrock interface is complex. The water table is typically shallow due to the proximity to the coast. Numerous borehole logs identifying soil classification, bedrock lithology, and associated geotechnical properties of the subsurface materials encountered were made available for correlation with the seismic data.

SCOPE AND METHOD

The primary focus of the seismic survey was to define the thickness and lateral variability of the overburden soil deposits; and, to a lesser extent the soil / bedrock interface. The combination of a need for subsurface imaging, the complex geologic setting, and the field conditions of an urban, noisy, heavy traffic project area created a unique opportunity to apply a relatively new seismic method. The ReMi method was selected because it is not affected by saturated soil conditions, since it produces shear-wave velocity profiles.

The ReMi field method was selected because it satisfies all the conditions and survey needs described above. ReMi is relatively new, but it is becoming a standard and robust geophysical method for use in urban settings to derive the IBC site classification (Louis, 2001). ReMi is a one-dimensional (1D) ‘*seismic sounding*’ technique that measures passive-surface wave dispersion to model the shear-wave (S-wave) velocity distribution with depth. The S-wave velocity sounding is obtained below a surface array of standard refraction-type geophones and recording equipment. The 2D approach has been utilized to image the soil / bedrock interface beneath rivers and in urban settings where noisy site conditions prohibit use of refraction, reflection, or active surface-wave (MASW) seismic techniques.

Line lengths were adjusted *on-the-fly* based on access, as dictated by local traffic control, as well as based the need for access to commercial businesses. Twelve locations were selected for seismic testing; however the actual line position was not finalized until the field conditions were assessed daily. Approximately 5.121 line km (16,800 feet) of data were acquired.

Independent line maps were generated using Google Earth images which are reasonably accurate; an example is shown on Figure 2 (*next page*). They indicate the general line location and nearby intersections and the geotechnical boring locations. Note that some of the line segments represent a continuous profile. For example, Lines 2, 3, 4 and 5 combine for over 1.68 line km (5,500 feet) of continuous 2D profile. An average of approximately 457 to 487 line m (1,500 to 1,600 feet) was acquired daily.

INSTRUMENTATION AND APPROACH

Seismic ReMi data were acquired along the proposed HHCTCP site using a 24-channel Seismic Source DAQ LinkII seismograph. Analog signals from vertically-oriented geophones are collected in the DAQ seismograph where it is anti-alias filtered, converted to a digital signal, transmitted to the laptop. DAQ LinkII units have 24 channels; however, 48 receivers were placed on the ground along the survey line at 10 foot intervals to move along more rapidly in traffic. The receivers were 4.5-Hz low-frequency geophones, mounted on plates for the asphalt and

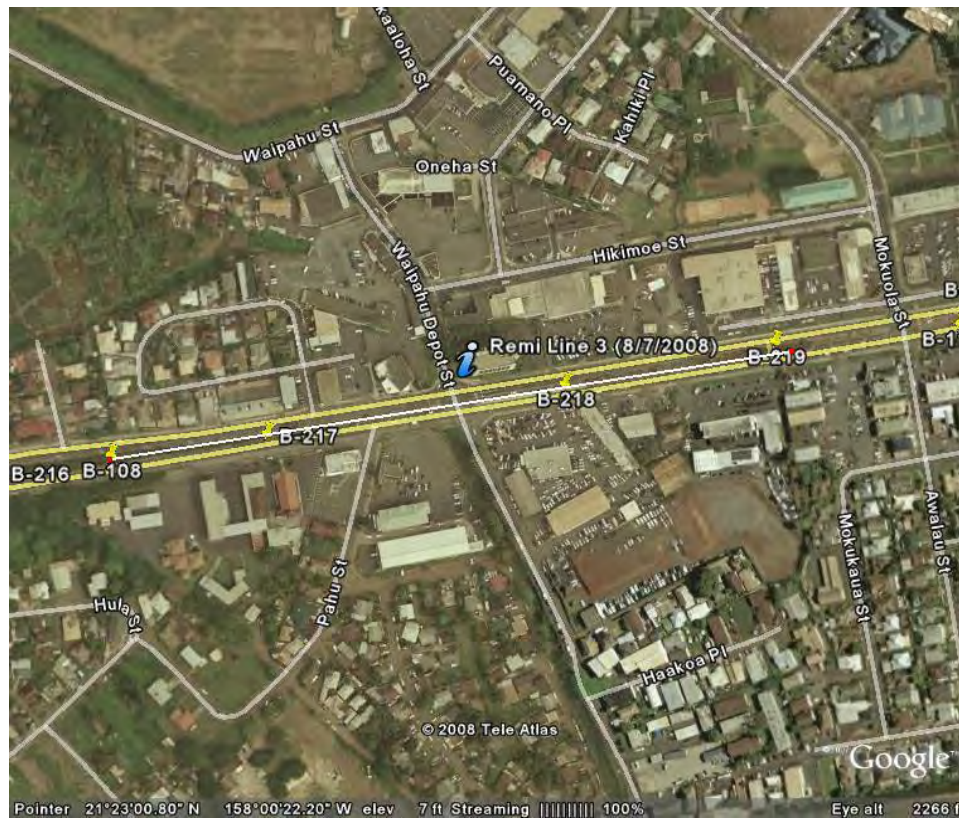


Figure 2: General 2D ReMi line location map - seismic line is white [showing date acquired] and geotechnical boreholes (e.g., B-217) shown with yellow markers [Google Earth background image]. Results from Line 3 are presented in Figures 3a and 3b.

concrete surface. Using a roll box, the 24 geophone array would increment by 4 receivers for each recording. Thus a 1D sounding was produced every 12.2 m (40 ft) along the line.

Although ReMi is a passive surface-wave technique, an uncorrelated active source was used to augment the ambient energy. A rubber-tired backhoe was typically placed 30 to 60 m (100 to 200 ft) off the end of the line. The un-timed source was placed off the end of the line to decrease the affect of side-swipe and apparent phase velocity measurements caused by energy propagating into the side of the receiver array from the heavy traffic. No timing was required for the backhoe source which thumped and drove around to create additional high-amplitude surface waves that would propagate in a more classic cylindrical wave front ‘*down-the-line*’.

DATA PROCESSING

ReMi is a surface-wave survey technique. Inversion of the Rayleigh wave dispersion produces a one-dimensional shear-wave velocity profile through an empirical relationship. That is, to model S-wave velocity the ReMi method uses ambient noise, or vibrational energy that exists at a site without the use of correlated input energy from hammers or explosives with triggering mechanisms (like those used on refraction and reflection surveys). Ambient or vibrational energy can be anything from traffic to construction activities, tidal energy and

microtremor earthquakes. The HHCTCP site was rich with all of these noise sources, and the energy from a backhoe added extra ‘in-line’ seismic energy to produce quality results.

For nearly all the sounding locations along the project corridor at least ten, unfiltered, 30-second ambient energy records were recorded using a 2 msec sample rate. In order to get through busy intersections quickly, only five 30-second records were acquired. For quality analysis purposes, records were collected with and without the backhoe source. It was found the backhoe source greatly increased the frequency content (i.e., amplitude and spectrum) of the recordings.

According to Louis, 2001 (1), noise records which included the hits from the backhoe were processed using the SeisOpt® ReMi™ software, © Optim Inc. Four processing steps were used to derive a 2D ReMi Vs profile:

Step 1: Generate a velocity spectrum from the (10) time series. This is a Fourier frequency analysis which plots slowness (p) versus frequency (f) curve (i.e., a p - f curve). The distinctive shape and slope of dispersive surface waves is an advantage of the p - f analysis because body waves and airwaves do not have dispersive (i.e., frequency dependent) velocity.

Step 2: Pick the Rayleigh-wave dispersion curve. The picks are made along the lowest edge of the p - f ‘envelope’ which bounds the dispersive-wave energy. Using the procedure outlined by Pullammanappallil and others, 1993 and 1994, (2 and 3) because higher-mode Rayleigh waves have phase velocities above those of the fundamental mode, the ReMi approach preferentially yields the fundamental-mode surface wave phase velocities

Step 3: Model a shear wave velocity sounding. The ReMi method interactively forward-models the normal-mode dispersion data with a code adapted from Saito, 1979 and 1988 (4 and 5). The modeling iterates on phase velocity at each period (frequency). The analysis approach and the propagation properties of surface waves allow velocity reversals (e.g., a low Vs layer beneath a high Vs layer) to be successfully modeled.

Step 4: Generate 2D shear wave profiles. After a series of 1D soundings have been modeled, the data are entered into a smoothing algorithm that produces a 2D smooth-model of a series of 1D models.

The 2D profiles generated in Step 4 produced cross-sections of the subsurface with soundings spaced at 12.2 m (40 ft). Although independent data from geologic drilling and geotechnical tests (e.g., lithologies and blow counts) were integrated with the results, they were not used to fix or constrain the model inversion in Step 4. The geologic data are interpreted with the shear-wave results. Soil stiffness and rock competency (e.g., from RQD), and the depth bedrock was encountered are important parameters for understanding and analyzing the 1D models from Step 3, and then generating interpretations from the 2D profiles.

RESULTS

As might be expected for a data set that covers over 5 km (16,000 ft) of proposed HHTCP alignment, only a small sample of results can be presented in this paper. Lines 3 and 4 provided some of the most dramatic and significant results from the project. Their results are included and discussed below.

ReMi profiles for data acquired along Line 3 are presented on Figures 3a and 3b. A portion of Line 4 is presented on Figures 4. The figures were created to allow comparison from line to line; that is, each figure uses the same color scale (i.e., Vs velocity), and horizontal to vertical exaggeration. Each figure presents only 231.6 m (760 feet) of 2D ReMi data. This length was determined by the geotechnical design team to be most useful for integration with plans and profiles. Stationing along the ‘distance’ axis is project stationing, and elevations were taken from profile drawings.

Geotechnical borings locations have been posted on the figures for interpretation of material property data with the S-wave velocity results. A few of the boring locations are approximate as they had not yet been drilled when the seismic survey was performed. Two velocity contour values have been identified on each cross-section: 1) a 183 meters per second (m/s) (600 feet per second - ft/s), a contour that represents the interpreted transition from undifferentiated *soft or loose* soil deposits to *stiff or dense* soil deposits; and, 2) a 610 m/s (2,000 ft/s) contour that best depicts the top-of-bedrock. Respectively, the contour lines shown were selected based on: the IBC classification for *soft soils* (i.e., Vs < 600 ft/s); and, an average S-wave velocity for the *depth-to-bedrock* as determined from boreholes. Analysis of all the data indicated the average Vs of about 610 m/s (2000 ft/s) best represents the *velocity interface* between undifferentiated overburden / stiff soils and basalt at this site. The soil/bedrock interface, as described on the geologic logs of each borehole, shows a wide variation in the degree of weathering (e.g., *slightly- to highly-weathered*), as well as a significant difference in the fracture density (e.g., *moderately- to intensely-fractured*).

By closely inspecting each boring log along each ReMi profile an actual bedrock Vs velocity *at that location* could be determined. Using the available borings, depths to bedrock and velocities obtained at that depth (as determined by 2D ReMi) yield a range between about 550 to 730 m/s (1,800 and 2,400 ft/s). The correlation between the degree of weathering and fracture density and an increase or decreases of seismic-wave velocity in rock formations is well documented (i.e., Caterpillar Performance Handbook, Edition 35, 2004, *charts for rippability*). Similarly, a variation was observed at independent boring locations. For this project, an ‘average’ or ‘apparent’ velocity interface of 610 m/s (2000 ft/s) is used to distinguish the soil/bedrock contact.

As previously described, ReMi is a seismic technique that averages the subsurface bulk properties beneath the receiver line (i.e., a 70 m or 230-feet,). Each sounding represents that bulk or average shear-wave velocity (processing Step 3). Using data acquired beneath over 350 soundings the smooth models shown on Figures 4 and 5 are the best representation of the depth to- and geometry of- the basalt contact between, below and beyond geotechnical drill hole control. As anticipated at this site, the ReMi data indicate significant variation and relief on the bedrock surface; additionally, there is considerable correlation between boring logs and bedrock depths as interpreted by 2D ReMi profiling.

As shown on Figures 3a and 3b, east of boring B-218 along the profile there is a definite deepening of the bedrock surface to greater than about 60 m (200 feet) beneath Station 64900 on Line 3. This trend is confirmed further east along Line 4 (Figure 4) at approximate station 65050

near boring B-110. Note boring B-110 terminated at 54 m (~177 feet) bgs without encountering bedrock, which confirms the deep bedrock contact. Along this east end of Line 4 (Figure 4) the depth to bedrock determined by 2D ReMi imaging is the deepest within the survey area (approximately 70 m or 230 ft).

It should be noted that the 70 m (230 foot) depth is the absolute maximum resolvable depth with the field set-up and instrumentation used for this investigation. The true depth to bedrock may not be resolvable in this area, compared with other places along the line(s), because of the depth-to-bedrock and the wavelengths that could be measured using a 70.1m (230-foot) line length. However, the shape, size and approximate depth of this anomalously deep bedrock are substantiated by the data. As this long continuous profile continues east toward Line 5 (not included here), bedrock slowly rises to less than about 30 m (100 feet) and continues to rise to within 3 m (10 feet) of the ground surface. Also shown on Figure 4 is a stretch beneath Line 4 where a very thick layer of *soft soil* (<183 m/s or 600 ft/s) was detected. The lateral variability and thickness of the soft soils was not anticipated at this site.

CONCLUSIONS

Acquisition of 2D seismic data along the HHCTCP project detected the presence of thick and laterally variable *soft soils*, as defined by the IBC standard, and also yielded good imaging of the soil/bedrock contact. The ReMi method was selected because of its ability to acquire seismic data in *very* noisy – high-traffic environments and to distinguish between saturated soils and basaltic bedrock based on their shear-wave velocity. Correlation with geologic logs with low SPT blow counts in soft soil intervals and for depth-to-bedrock was good. The seismic and geologic data show a relatively narrow range of S-wave velocities that could be appropriately interpreted as the soil/basalt contact. The ReMi data clearly identify areas of thick soft soil deposits, in excess of 18.3 m (60 ft) thick using the S-wave velocity IBC classification between soft and stiff soils (<183 m/s or <600 ft/s). Boring logs and ReMi data collectively indicate that the basalt interface may be identified by velocities ranging from about 550 m/s (1,800 ft/s) if intensely weathered and highly fractured, to greater than 730 m/s (2,400 ft/s) in areas with lesser fracture density or little weathering at the soil/bedrock interface. Overall, the geometry of the bedrock surface, its relief and depth, is illustrated by using a velocity contour of 610 ms/ (2,000 ft/s). Bedrock was well defined over long segments of the proposed HHCTCP site, and correlation with shallow downhole shear-wave velocity measurements (made by another contractor) correlate with the 2D ReMi results.

The method proved that it can be used when basaltic bedrock is shallow (e.g., 3 m bgs or 10 feet), and when it is quite deep (60+ m bgs or 200+ ft bgs) with a 24-channel seismic set-up using a 70.1 m (230-foot) long spread. Additional uncorrelated surface-wave energy (generated by a backhoe) significantly added to the quality of the *p-f* curves and thus the ability to pick the surface-wave dispersion data. Quality of the ReMi data ranged from good to very good, which is directly attributed to the use of the backhoe and the tidal (low-frequency) energy present near the coast. Although the basaltic bedrock velocity clearly varies across the site, additional analysis of geotechnical data regarding degree of weathering and fracture density would likely narrow the velocity range used to define depth-to-bedrock.

REFERENCES

1. Louie, J. N., Faster, Better: Shear-wave velocity to 100 meters depth from refraction microtremor arrays: *Bulletin of the Seismological Society of America*, v. 91, 2001, p. 347.
2. Pullammanappallil, S.K., and Louie, J.N., Inversion of seismic reflection travel times using a nonlinear optimization scheme: *Geophysics*, v. 58, 1993, p. 1607-1620.
3. Pullammanappallil, S.K., and Louie, J.N., A generalized simulated-annealing optimization for inversion of first arrival times: *Bulletin of the Seismological Society of America*, v. 84, 1994, p. 1397-1409.
4. Saito, M., Computations of reflectivity and surface wave dispersion curves for layered media; I, Sound wave and SH wave: *Butsuri-Tanko*, v. 32, no. 5, 1979, p. 15-26.
5. Saito, M., Compound matrix method for the calculation of spheroidal oscillation of the Earth: *Seismological. Research Letters*, v. 59, 1988, p. 29.

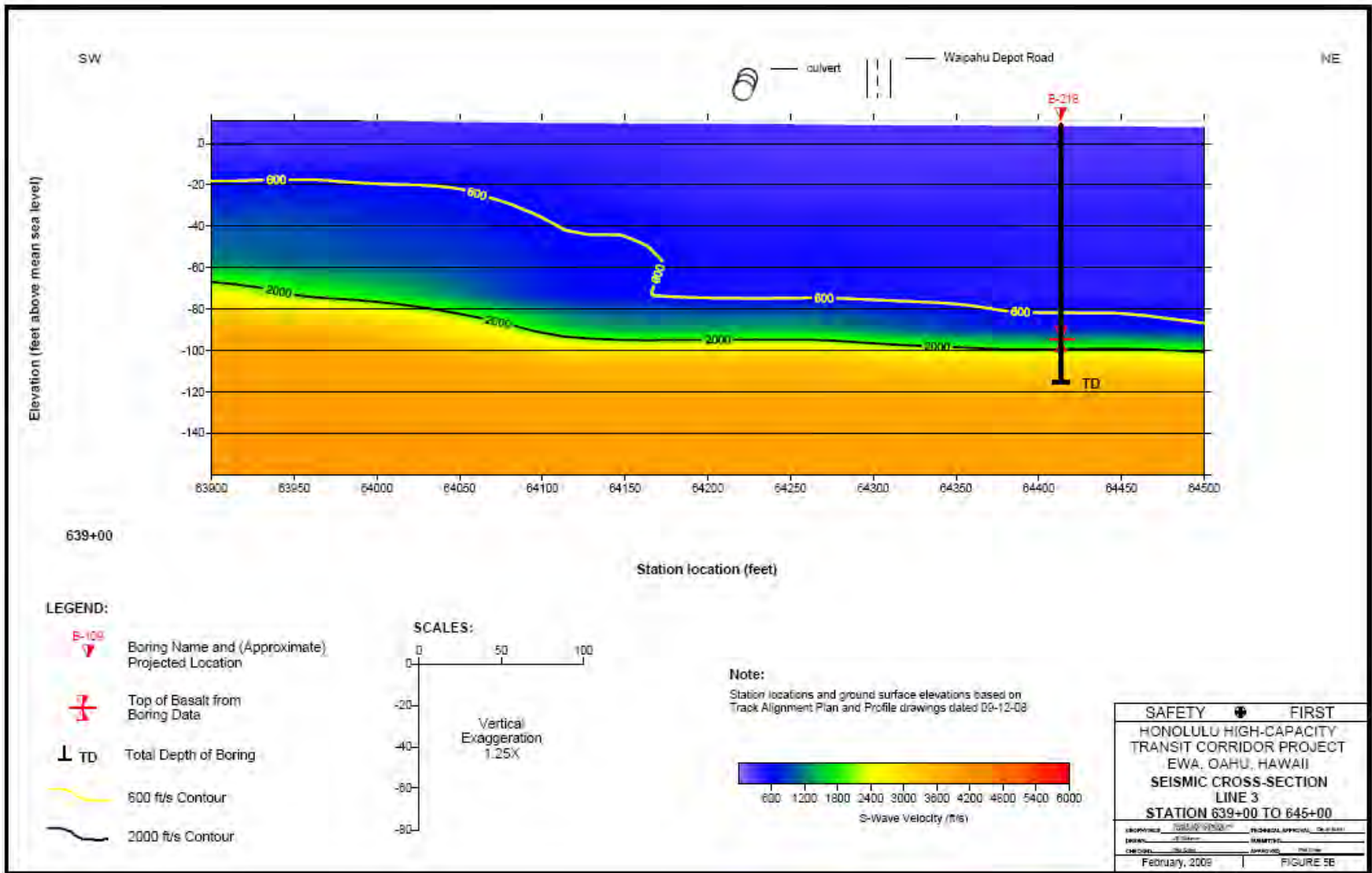


Figure 3a. 2D ReMi results from Line 3 (continued on Figure 3b).

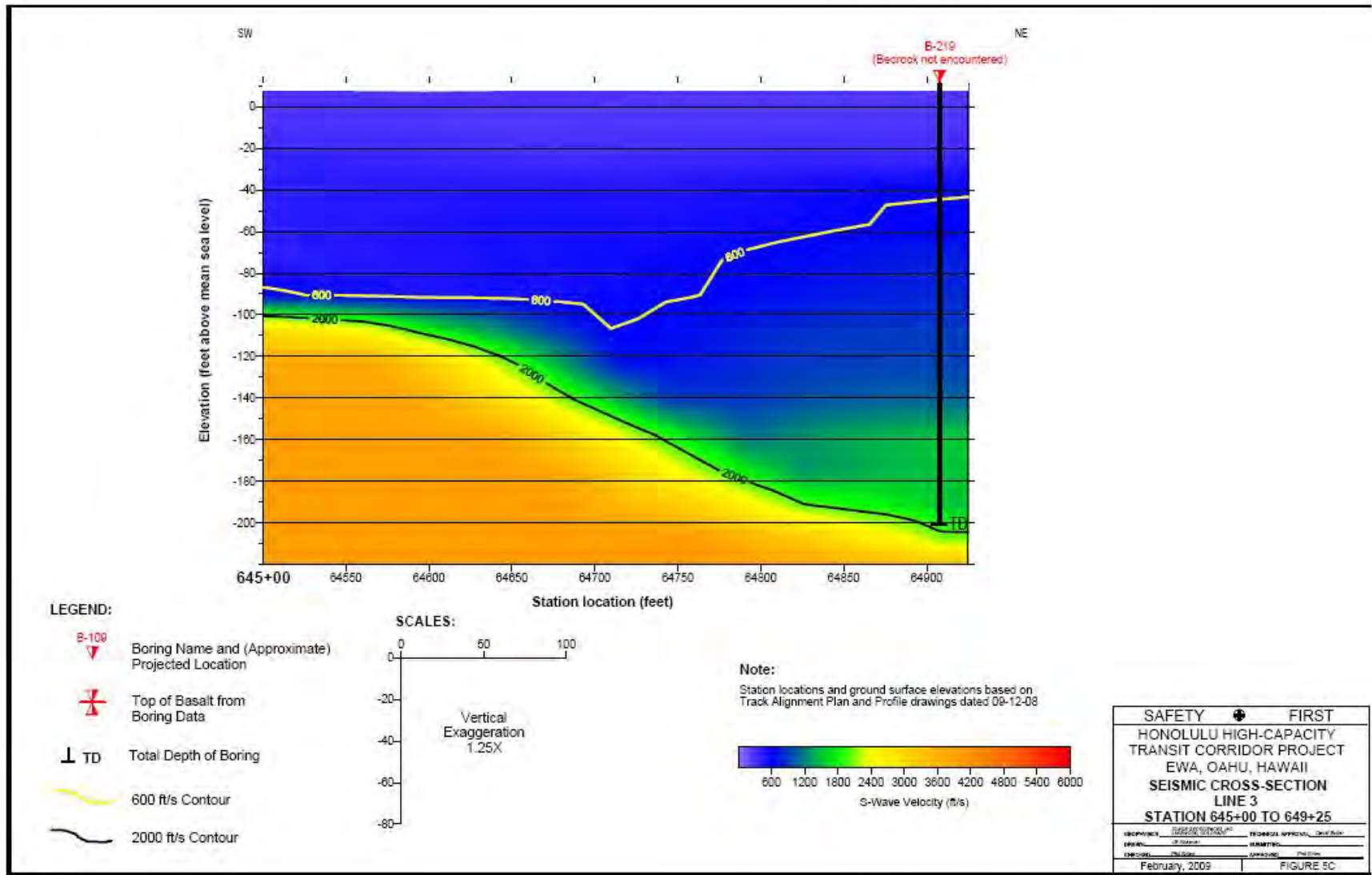


Figure 3b. 2D ReMi results from Line 3 (continuation from Figure 3a).

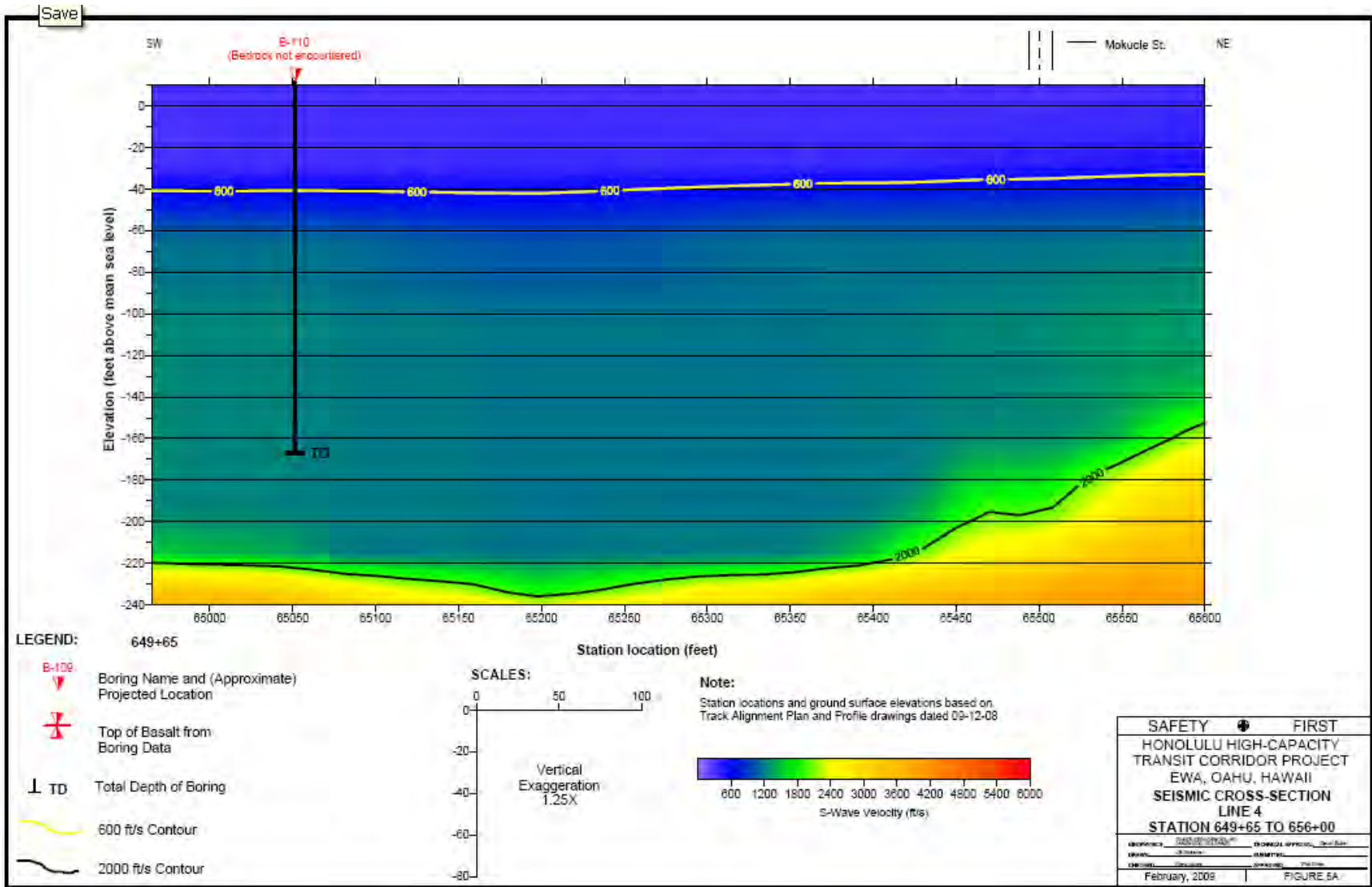


Figure 4. 2D ReMi results from a portion of Line 4 (small portion of Line 4 only).

Continuous Subsurface Profiling of Roads Using MASW
(multi-channel analysis of surface waves)

Richard Lee, P.G., R.GP.

Quantum Geophysics

29 Richard Lee Lane

Phoenixville, PA 19460

(610) 917-9100

rich@quantumgeophysics.com

Prepared for the Highway Geology Symposium, August, 2010

Disclaimer

Statements and views presented in this paper are strictly those of the author, and do not necessarily reflect positions held by their affiliations, The Highway Geology Symposium (HGS), or others acknowledged above. The mention of trade names for commercial products does not imply the approval or endorsement by HGS.

Copyright Notice

Copyright © 2010 Highway Geology Symposium (HGS)

All Rights Reserved. Printed in the United States of America. No part of this publication may be reproduced or copied in any form or by any means – graphic, electronic, or mechanical, including photocopying, taping, or information storage and retrieval systems – without prior written permission of the HGS. This excludes the original author.

ABSTRACT

Roads are especially challenging environments for doing geophysics. Traffic-induced ground vibrations make it difficult to acquire good seismic refraction and microgravity data. Impervious surfaces and crushed-stone covered shoulders make for poor SP (self-potential) coupling, and buried piping and utilities often found in right-of-ways can impact electrical resistivity measurements. GPR (ground penetrating radar) depth of investigation is severely impeded by silty and clayey soils, a condition often found in carbonate terrain. Also, GPR does not work on reinforced concrete roads because the lower antennae frequencies required to look deeper cannot penetrate through the mat of reinforcement steel.

MASW (multi-channel analysis of surface waves) is a relatively new seismic method that is gaining acceptance in the geotechnical community. MASW identifies the vertical distribution of shear wave velocities based upon the dispersion of surface waves (Rayleigh Wave). Since shear wave velocities are a measure of material stiffness, the MASW method can map top of rock, pinnacles, voids, zones of enhanced weathering, and fracture zones. MASW is non-invasive, is not impacted by buried piping or other utilities in the right-of-way, insensitive to 60 cycle (Hz) noise from nearby electrical lines, and it is not influenced by reinforcement steel. Upwards of 1,000 +/- feet of road can be surveyed at night when interference from vehicle traffic is minimal.

MASW is a continuous profiling method which is key because the causes of sink activity tend to be small, localized and highly unpredictable (this is why drilling tends to be ineffective for evaluating karst terrain).

We will show how MASW was used on a major interstate in Pennsylvania to identify the root cause of sinkhole activity to depths of 80' directly beneath the reinforced roadway, and to identify a paleo-collapse feature in the carbonate rocks of Florida.

INTRODUCTION

Roads present challenging conditions with respect to acquiring good geophysical data. Traffic-induced ground vibrations interfere with seismic surveys (mask first arrivals) and gravity surveys (cause unstable readings). Paved surfaces make it difficult to implant electrical resistivity electrodes. Buried utilities and piping often found in the ROW (right-of-way) impact electrical resistivity measurements by attracting the electrical current. Paved surfaces make for poor SP (self potential) coupling. GPR (ground penetrating radar) can penetrate through reinforced concrete as long as antenna frequencies are about 400 to 500 MHz or greater. Lower frequencies observe a mat of reinforcement steel as a sheet of metal (a virtual metal deck) through which there is no further penetration (metal is a perfect reflector). Once through the reinforced concrete, however, GPR penetration depths can be severely impeded by fine-grained soils. Clays and silts tend to hold onto water (moisture) which tends to absorb and attenuate radar signals, thereby limiting penetration depths to no more than about 3' to 4' below ground surface (bgs).

As with most technology-based sciences, geophysics has evolved through advancements in hardware and software. In the last 2 decades, these advancements have included: 1) the ERI (electrical resistivity imaging) method, which makes it much more cost-effective to do electrical resistivity surveys than using the traditional 4-pin method; 2) the landstreamer, which makes it easier to do seismic surveys over paved surfaces without having to implant geophones; 3) accelerated weight drops, which puts more energy into the earth than the traditional 12-lb sledge hammer, and 4) surface wave seismic methods which look at the stiffness of materials by determining shear wave velocities (V_s).

A surface wave method that is gaining increasing popularity amongst the geotechnical community is MASW (multi-channel analysis of surface waves). First described in 1999 by the Kansas Geological Survey (KGS) for engineering applications (*1*), MASW is a profiling method that determines the vertical distribution of shear wave velocities. Shear wave velocities (V_s) are a measure of material stiffness (density) much like N-values from standard penetration test (SPT) borings and shear strength from laboratory analysis. Rocks are characterized by much higher V_s than soil. Saprolitic (weathered) rocks are generally characterized by V_s that are intermediate between soil and rock. MASW can identify conditions pre-disposed to sink activity which include zones of enhanced weathering, fractured rocks, pinnacles, voids, and abrupt changes in bedrock topography. Air-filled voids are observed as localized low V_s anomalies because air has no resistance to shear.

THE MASW METHOD

MASW determines the vertical distribution of shear wave velocities based upon the dispersion of surface waves (Rayleigh Wave). Surface waves are dispersive in that they comprise a continuous spectrum of different frequency waves that travel at different propagation velocities, known as phase velocity. By examining dispersion curves (phase velocity vs. frequency), subsurface s-wave (V_s) profiles can be interpreted as a function of depth, and material properties can be estimated or qualitatively assessed.

The method utilizes standard commercially-available instrumentation to collect shot records (seismograms) in a manner much like seismic refraction. Just as in refraction, MASW utilizes seismic waves generated by striking the ground (or a metal plate coupled to the ground) with a 12-lbs. or 16-lbs. sledge hammer (or other means of creating a seismic wave). The major difference is that MASW utilizes geophones on the order of 4.5 Hz whereas refraction utilizes higher frequency geophones typically between 14 and 40 Hz. The manner in how data are acquired is also slightly different. Figure 1 is a schematic of the MASW data acquisition procedure.

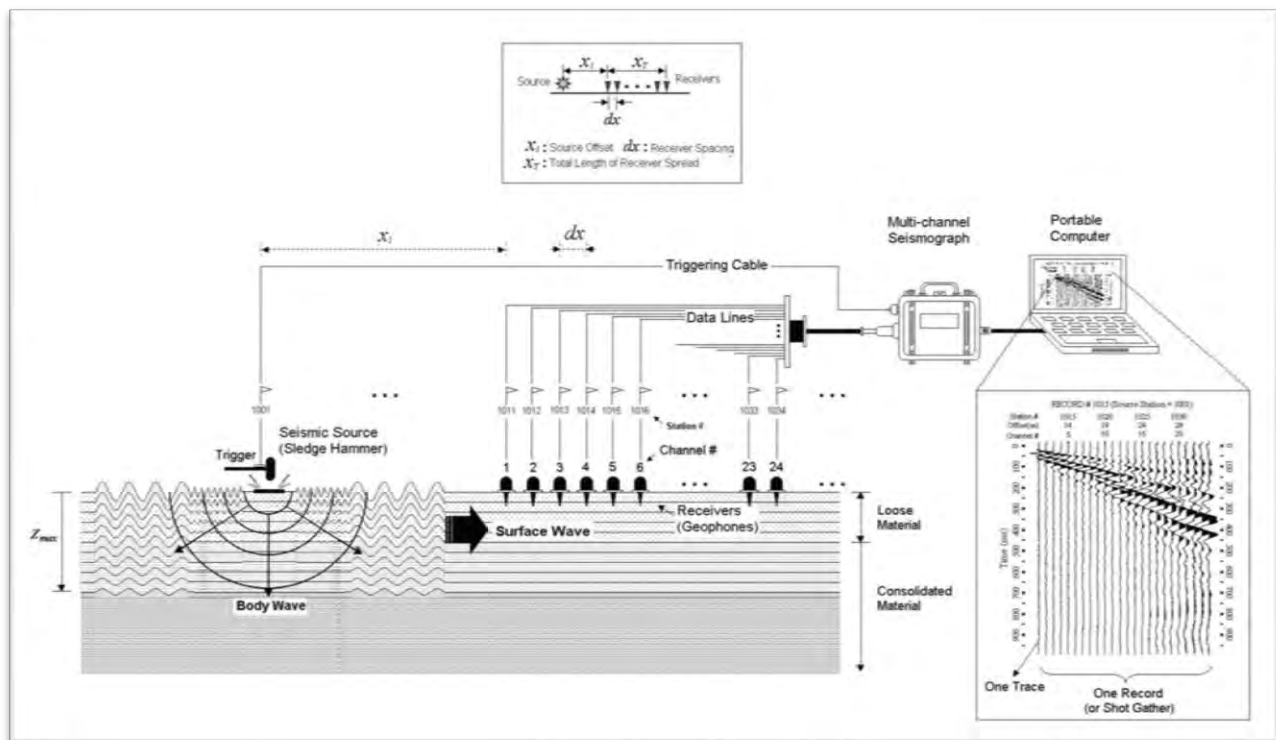


Figure 1 – A schematic illustrating a typical field configuration with an MASW survey. Reprinted by permission from Kansas Geological Survey Open-file Report 2004-30, MASW to Map Shear Wave Velocity of Soil.

Shot records are made at a pre-determined interval along a survey line in a mode known as “roll-along” - the shot and receiver spread geometry stays fixed while being moved along a line. Each record is then processed and inverted into a 1-D profile of shear wave velocities. The 1-D s-wave profile is analogous to a boring log. A 2-D s-wave profile is created by interpolating between the 1-D profiles from multiple shot records. This process is illustrated in Figure 2.

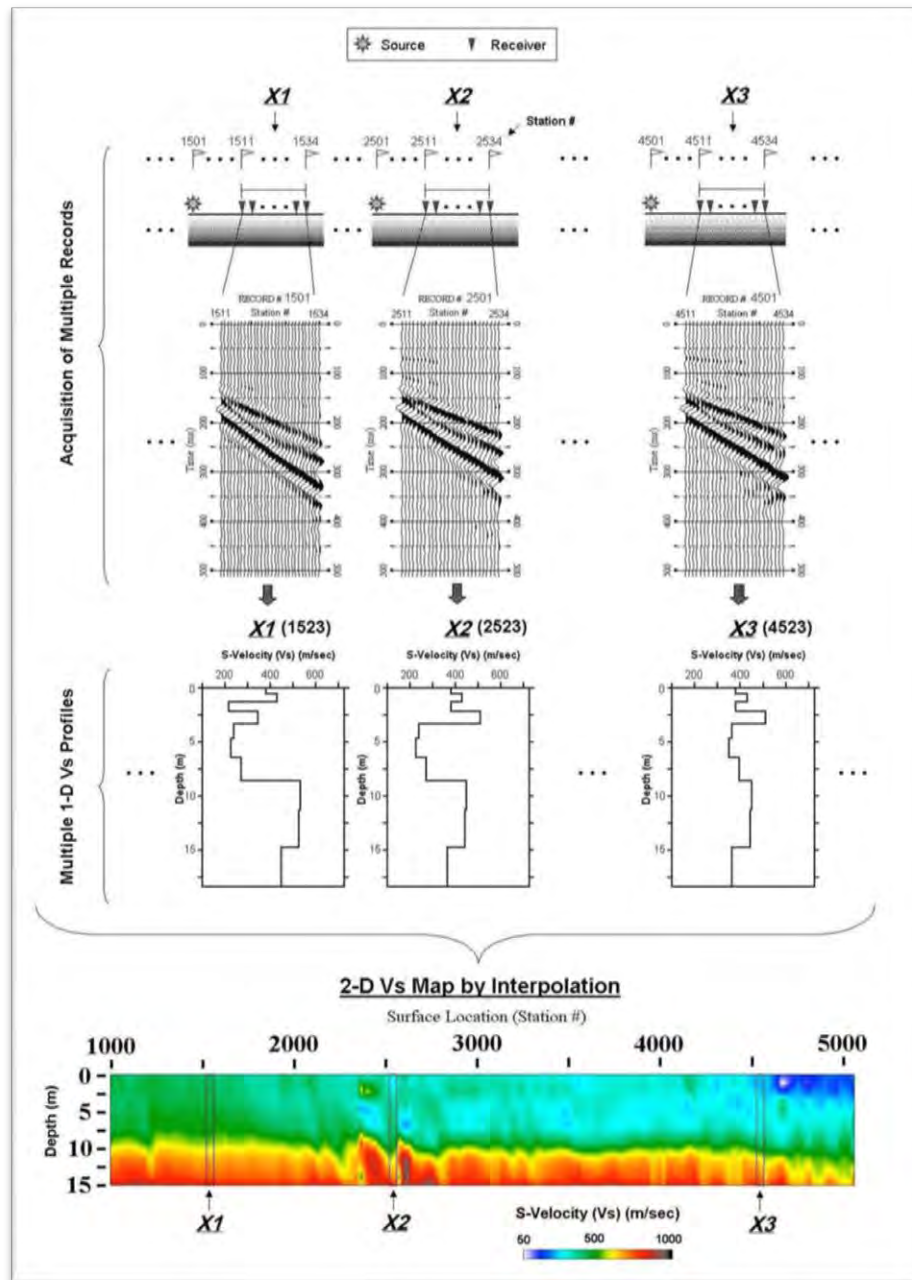


Figure 2 – Illustration of the procedure to generate a 2-D Vs profile from a roll-along mode MASW survey. Reprinted by permission from Kansas Geological Survey Open-file Report 2004-30, MASW to Map Shear Wave Velocity of Soil.

The 1-D Vs profile best represents conditions in the middle of the receiver spread. Therefore, if working with 24 geophones spaced 3 feet apart, a 15-foot shot offset, and the shot is located at station 0, the 1-D Vs profile from the 1st shot record is plotted at station 49.5 feet (1/2 the receiver spread length + shot offset distance). If shot records are being made every 3 feet along a survey line, the next 1-D Vs profile is plotted at station 52.5 feet, and every 3' thereafter.

MASW can explore to depths upwards of about 85' bgs, depending on site conditions, seismic source, and length of receiver spread. Wider geophones spacings result in deeper depths of exploration because the resulting receiver spread is primed to detect lower frequency waves which travel much deeper than higher frequency waves.

MASW ALONG AN INTERSTATE (PENNSYLVANIA)

A section of I-476 (Blue Route) in Montgomery County, PA is underlain by carbonate rocks prone to sinkhole activity. Sinkholes have occurred in the shoulders and right-of-way (ROW), in the median, and beneath the reinforced concrete roadway. Phase I drilling in support of planned reconstruction showed that top of rock (TOR) varied between < 5 feet to over 30 feet below ground surface (bgs). The drilling, however, proved ineffective in identifying the causes of sinkhole activity. Consequently, engineers turned to using geophysics as an exploratory tool.

Site conditions and scope dictates the choice of the appropriate geophysical method. Stormwater pipes and other buried utilities in the ROW precluded the use of the ERI method. Microgravity could have been conducted at night when ground vibrations from vehicle traffic is minimal but it was deemed cost-prohibitive given the 3,300 linear feet of roadway that needed to be evaluated. GPR would not have been able to penetrate more than just a few feet into the silty/clayey soils underlying the roadway. MASW was deemed the best method for the desired objective.

The MASW survey of I-476 occurred over the course of 3 nights, working between 10:00 PM and 5:30 AM. Vehicle traffic is minimal during this time of the day and good quality data can be acquired with little to no risk of "road noise contamination". Appropriate signage was set and the inside southbound lane was closed-off with a tapered alignment of traffic cones. A crash attenuator truck, positioned between the MASW survey vehicle and oncoming traffic in the adjacent lanes, shadowed the survey vehicle at a distance of 200 to 300 feet.

The MASW survey incorporated a Geometrics StrataVisor 24-channel seismograph and 24 4.5 Hz geophones mounted on a landstreamer tethered to a van (survey vehicle). A landstreamer comprises a kevlar strip with adjustable plates. Geophones are screwed into the plates which couples the geophones to the ground surface; thereby eliminating the need to

implant geophones.

Data were acquired with a geophone spacing of 3' and a shot offset of 12'. Shot records were made every 3' of traverse, stacking 3 shots per location to increase the signal-to-noise ratio. Seismic waves were generated by using a Peg-40kg accelerated weight drop or by striking the road surface with a 12-lbs. sledge hammer. The seismograph was positioned between the 2 front seats so that the driver can monitor for oncoming traffic before firing the Peg-40kg and then review the data prior to moving onto the next shot location. The data acquisition process is documented in a 5-minute video (oral presentation).

MASW data were processed using the software program Surfseis by the Kansas Geological Survey (KGS).

The MASW survey linked 44 of 52 reported sinkholes to the following subsurface conditions: 1) the transition from shallow competent rock to enhanced weathered rock, 2) a potential fracture zone or fault, 3) pinnacled rock, and 4) potential voids. These observations were later confirmed by another round of drilling (Phase II). Figure 3 shows a representative MASW-derived Vs profile that was acquired in 1 night of work. The profile is 800 feet long and is constructed from a total of 267 1-D Vs profiles spaced 3 feet apart.

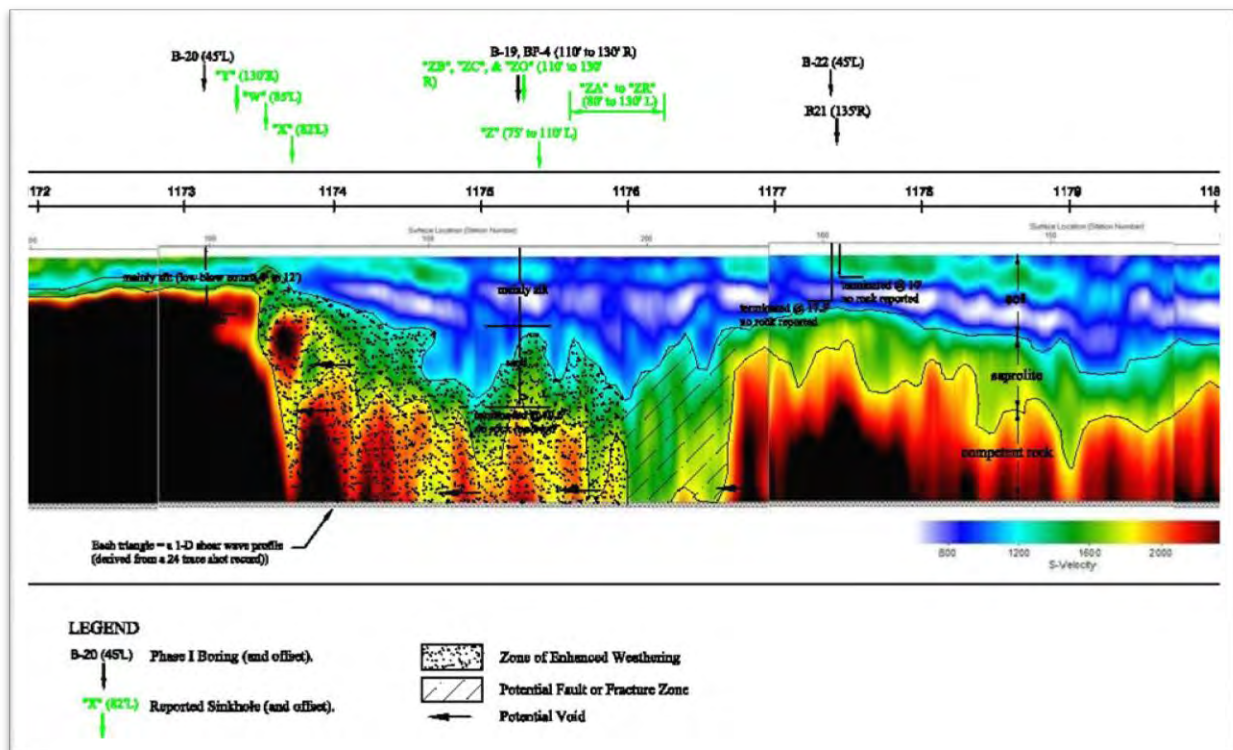


Figure 3 – Vs profile showing reported sinkholes associated with the transition between shallow, competent rock and enhanced weathered rock, and a potential fault or fracture zone. Reported sinkholes are projected into profile. Borings (Phase I) preceded the MASW survey.

The profile in Figure 3 shows 2 groups of sinkholes. One group coincides with the transition between shallow, competent rock and enhanced weathered rock. Competent rock is relatively impermeable, basically a barrier to infiltration. During a storm event, storm water ponds onto and spreads along the shallow bedrock surface. When it comes into contact with enhanced weathered rocks, the storm water triggers sink activity by carrying away loose materials and continues the weathering process via dissolution. The other group of sinkholes is associated with an apparent fracture zone or fault.

MASW SURVEY ALONG A PROPOSED MSE WALL (FLORIDA)

A mechanically stabilized earth (MSE) wall will be constructed as a result of expanding the capacity of a 1-lane road in western Florida. Both 2-D ERI and MASW were run to determine whether the wall alignment may be underlain by subsurface conditions pre-disposed to sink activity. ERI proved ineffective because of extremely high contact resistance associated with “sugar-powder” dry sands. High ground contact resistance lead to poor ERI data quality. Adding salt-water to the base of the electrodes, hydrating bentonite pellets to create a clay conductive plug at each electrode location, and even using aluminum foil to increase the “electrical footprint” did not improve (lower) the ground contact resistance measurements.

Again, where site conditions precluded the use of ERI, MASW was very effective in identifying subsurface conditions associated with sink activity. Figure 4 is a 460-foot long MASW-derived Vs profile that shows a paleo-collapse feature and a low velocity anomaly suggestive of a void. Standard penetration test borings of the paleo-collapse feature confirmed that it is a relic sinkhole.

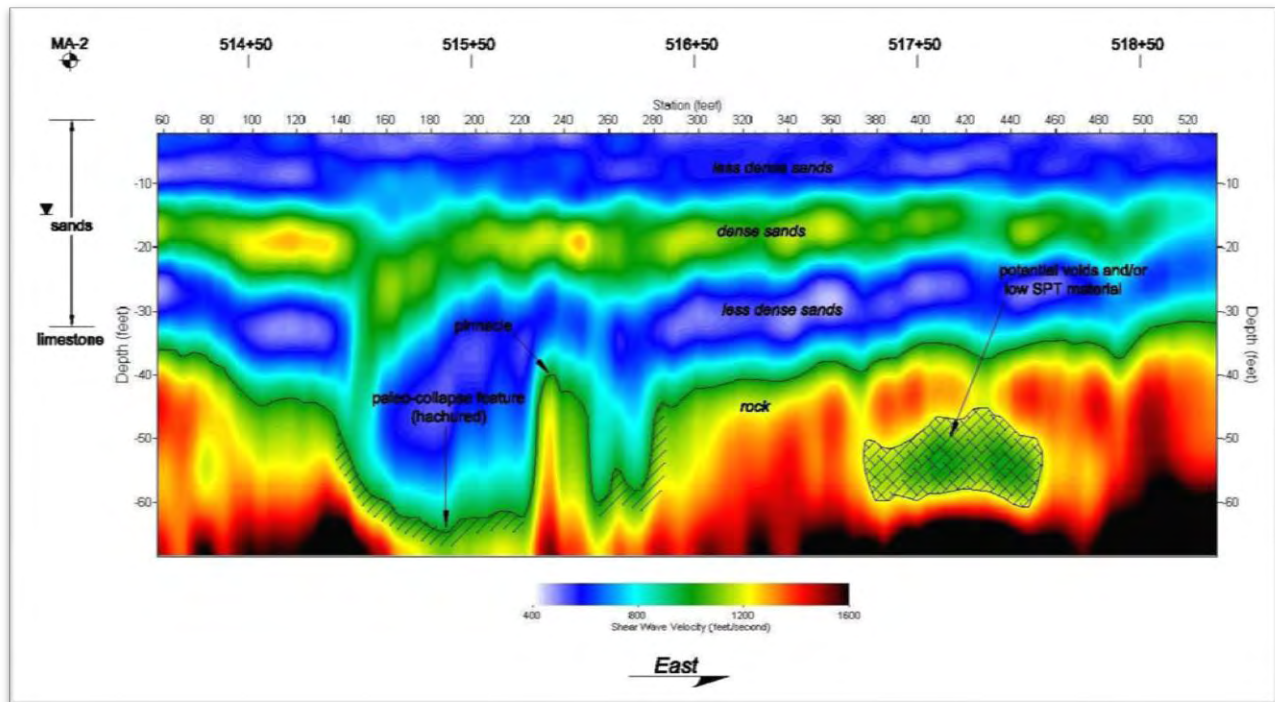


Figure 4 – Vs profile of a paleo-collapse feature (relic sinkhole), a pinnacle, and a low velocity anomaly indicating a potential void or low SPT material. Boring preceded the MASW survey.

REFERENCES

- Journal
 1. Park, C.B., Miller, R.D., Xia, J., 1999, Multichannel analysis of surface waves: Geophysics, v. 64, n. 3, pp. 800-808.

SUBSURFACE GEOTECHNICAL EXPLORATION ENHANCEMENT THROUGH THE USE OF REFRACTION MICROTRMOR (ReMi)

Matthew Satterfield, P.E. - Project Engineer, PSI Thornton, CO

Nicholas J. Roth, P.E. - Senior Engineer, PSI Saint Louis, MO

Kevin C. Miller, P.E. - Chief Engineer, PSI Midwest Region

Steve Bryant, P.E. - Vice President, PSI Portland, OR

Paul Hundley, P.E. - Regional Engineer, PSI Columbus, OH

One of the main limitations of subsurface exploration today involves the limited amount of insitu measurement that can economically be performed. For example, borings which performed standard penetration testing on a 100 foot square grid produces a typical 1 ½ inch diameter sample that is roughly a 1 in 815,000 sample representation at any given depth. Therefore, techniques that enhance our knowledge of the subsurface materials and their properties between exploration points improved our ability to assess the performance of the subsurface material to respond to construction needs. One such technique involves the use of geophysical equipment to evaluate the change in various waveform velocities below the ground surface. The changes and relative magnitude of these velocities in combination with borehole data improves our understanding of the extents and properties of the subsurface materials. One of these techniques is Refraction Microtremor (ReMi) geophysical analysis.

Refraction Microtremor (ReMi) is a cost effective method of evaluating the subsurface strata at near surface depths using non-destructive surface performed techniques. ReMi is a form of Multi-Channel Analysis of Surface Waves (MASW) which uses standard P-wave recording

equipment and ambient noise to produce average one-dimensional shear-wave profiles down to depth of approximately 100 meters. The ReMi method is described in Louie, 2001 (Louie, J, N., 2001, Faster, Better: Shear-wave velocity to 100 meters depth from refraction microtremor arrays: Bulletin of the Seismological Society of America, v. 91, p. 347-364).

In general, the ReMi method records ambient or generated Rayleigh waves with a 12, 24 or 36 channel digital refraction gear with 4.5 to 14 hertz vertical geophones and recording cable. Typical data acquisition includes 5 to 10 records, usually 15 to 30 seconds in length. Within each record, a sampling interval of 1 to 5 milliseconds is used to acquire readings depending on the anticipated materials and spacing of the geophones.

Once the records are obtained, each individual record is preprocessed to reduce anomalies in the raw data. These data are then processed to produce a velocity spectrum. This process involves computing a surface wave, phase velocity dispersion spectral ratio image by p-tau and Fourier transforms across the array. The resulting spectrum is in the slowness-frequency (p-f) domain. The p-f transformation helps segregate the Rayleigh Wave arrivals from other surface waves, body waves, sound waves, etc. The p-f image is generated for each record, and a final p-f image for each test is generated by combining some or all of the individual images.

The fundamental mode dispersion curve on the final p-f image can be seen as a distinct trend from the aliasing and wave-field transformation truncation artifact trends in the spectra. Once the fundamental mode dispersion curve is visually interpreted, data points along this curve are picked. Using the picked data points, an interactive forward-modeling process is used to model a shear wave velocity profile with a resulting dispersion curve that approximately matches the

selected data points. The process and resulting velocity profiles are able to identify the various velocity layers in the subsurface, including velocity inversion within the profile.

To create two-dimensional profiles, a one-dimensional profile is created for a predetermined set of geophones with the following set overlapping the previous and preceding set. Each one-dimensional profile is then combined to create a two dimensional profile.

The ReMi equipment used in the following case studies included a Seismic Source DAQLink II 24-Bit acquisition system and STC-85 – SM-4 10 hertz geophones developed by Source Technology. Field acquisition incorporated a 24 channel digital refraction cable. SeisOpt ReMi Version 4.0 (VSpect and Disper modules) software developed by Optim LLC was used to process the collected data and create shear wave velocity profiles.

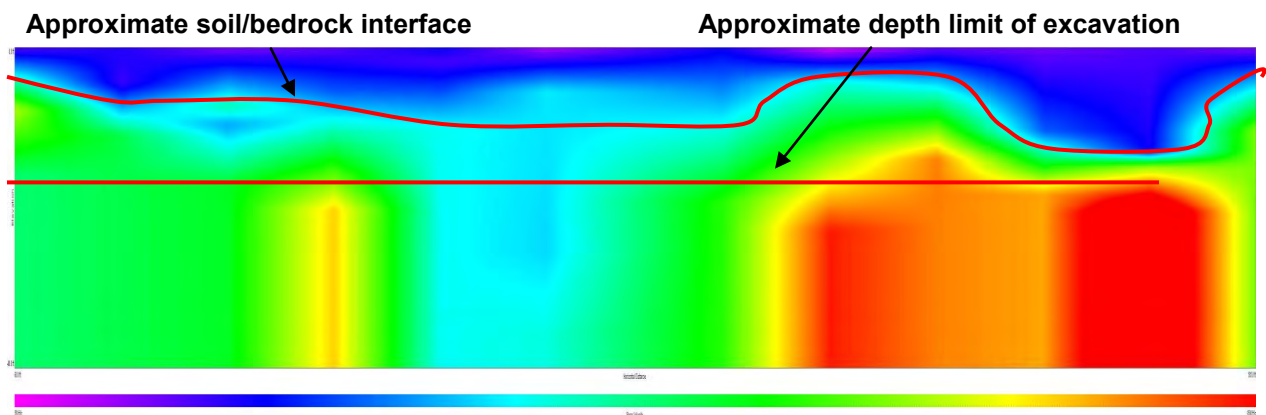
Using this technique we can create a waveform subsurface image that represent a trapezoidal area that, at depth, is roughly 60% to 70% of the surface trace of the instrumentation. Therefore, we have included the following case studies of how this technique has been used in various parts of the USA.

Rippability Study – Phoenix, Arizona

PSI was asked by a client to provide an analysis of the rippability of the subsurface materials they might encounter during the construction of a sanitary sewer line under a roadway in Phoenix, Arizona. The rippability of rock is the ability to loosen rock during excavation using steel tynes attached to various sizes of bulldozers. This rippability can be estimated by determining the shear wave velocity of the rock. Due to the nondestructive nature of the ReMi

testing, PSI proposed to perform overlapping ReMi profiles lines to determine the shear wave velocity of the soils and bedrock to a depth of 20 feet (the approximate depth limit of the utility line). The lines used a geophone spacing of 15 feet and overlapped the previous line by 4 geophones. Due to the busy intersection, 2 profiles were performed on either side of the intersection, creating profiles that were 585 feet in length.

The fairly busy roadway's alignment consisted of 3 lanes, one each in both directions and one turning lane and had an adjacent school located on the block. This allowed PSI to perform our testing in the middle turn lane and provided a considerable amount of roll-along vibrations from the passing school buses. Data was recorded in 20 second sample intervals with a 2 millisecond sampling rate per channel. Once collected, the data were checked for their fidelity. To assure that a robust profile was being made, both individual recordings and multiple summed (stacked) recordings were evaluated. Two dimensional profiles were then generated for each set of combined profile lines.



The results of the ReMi testing shows soils and bedrock with shear wave velocities ranges of 3,000 to 5,000 feet per second (ft/s) with a few isolated areas of higher shear wave velocity. PSI interpreted this as bedrock with lenses of denser material or possible lenses of caliche. The

upper 5 to 10 feet shows relatively lower shear wave velocity material (1,500 to 2,500 feet/s) which was interpreted as overburden soils. A high shear wave velocity also interpreted as bedrock, was also shown on the east side of the profile starting at approximately 400 feet east of the starting point and continuing to the maximum depths compiled, 40 feet.

Rippability is a function of the equipment selected including its weight and cutting teeth and not a function of a backhoe bucket. The data shown in the profile indicated that the material to the depth of the possible excavation for the utility trench exhibit high shear wave velocities. Based upon the data and published information in the Caterpillar Performance Handbook, PSI believes that a D9 Caterpillar Dozer or backhoe with associated rock bucket would be sufficient for excavation of the trench for utility placement.

PSI performed this study to reduce the guesswork associated with opening an excavation and having the incorrect equipment needed to excavate the soils and bedrock to the desired depth. This allowed for a reduction in the amount of time that the roadway would be inaccessible and also help in reducing the construction costs of the project.

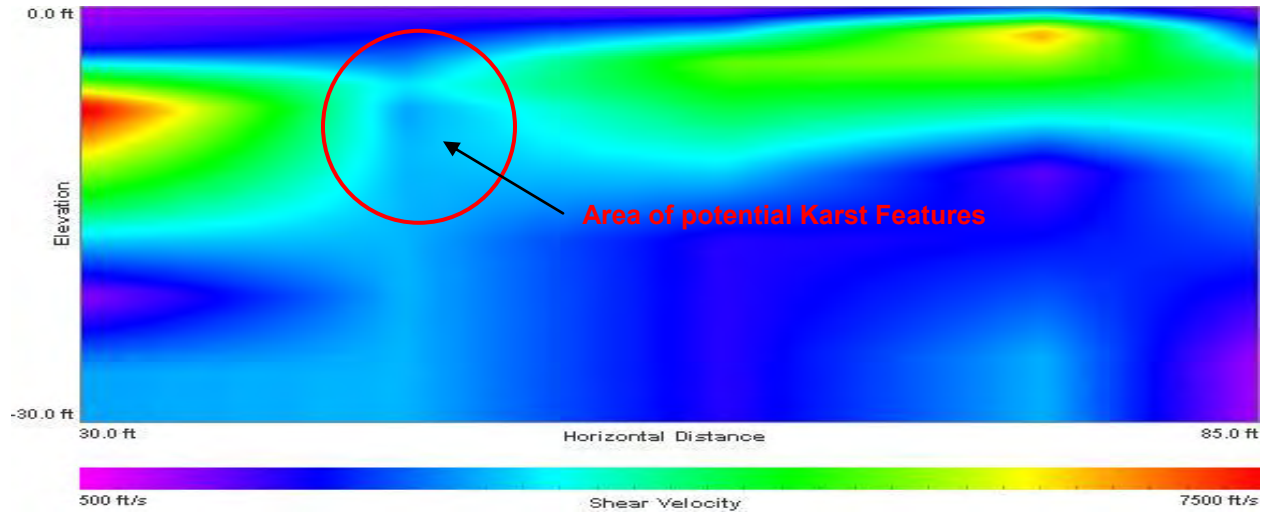
Karst Topography Study - San Antonio, Texas

PSI was asked to determine the shear wave velocities of the subsurface soils/limestone materials to assist in identifying the potential existence of karst features within the footprint of a proposed 4 story university building in San Antonio, Texas. Published data showed that karst features are present within the bedrock underlying portions of the campus. Karst topography is the dissolution of layers of soluble bedrock, usually carbonate rock such as limestone or dolomite. Many karst topography areas contain distinct surface features such as sinkholes and caves. However, in many areas, the dissolution of the bedrock has not propagated to the surface and may not be seen from surface elevations.

Therefore, PSI performed a limited geotechnical investigation consisting of soil borings for the proposed development and found limestone bedrock within the upper 5 feet across the site. PSI was subsequently asked to perform a ReMi investigation to identify areas of possible karst activity for further investigation. PSI performed a series of 6 ReMi lines across the site to identify areas of low shear wave velocity materials. Geophone spacing was varied from 5 to 15 feet depending on the amount of linear feet available and to better define results at varying depths.

The ReMi profiles revealed approximately 5 to 10 feet of overburden soils that were identified by low to very low shear wave velocity (500 ft/s to 1,000 ft/s) material. The overburden material overlaid moderate shear wave velocity (2,000 ft/s to 5,000ft/s) to high shear wave velocity (5,000 ft/sec and greater) material which is identified as limestone. The profiles indicated that the limestone was poorly to well cemented in parts and appears to be weathered in the upper five feet. Lower shear wave velocity materials were noted below and between

moderate to high shear wave velocity materials. These zones of lower shear wave velocity material may be an indication of karst limestone features, clay and/or gravel seams within the limestone.



To better achieve accurate results of the ReMi profiling, PSI also performed Resistivity profiling within the building footprint. Resistivity profiles were performed parallel to and bisecting to the ReMi lines. Large areas of low shear wave velocity material within the bedrock elevation as well as areas showing a combination of low shear wave velocity and low resistance material were identified as areas of further interest.

PSI identified 5 areas of elevated potential for further investigation as karst features. Further investigation alternatives provided included additional borings or test pits and/or downhole geophysical testing to further characterize the anomalies identified during our evaluation. PSI performed this study to limit the subsurface exploration for a karst topography investigation. ReMi profiling allowed the subsurface exploration to focus on areas that may have a higher likelihood of exhibiting karst features.

Wind Farm Foundation Design - Laramie, Wyoming

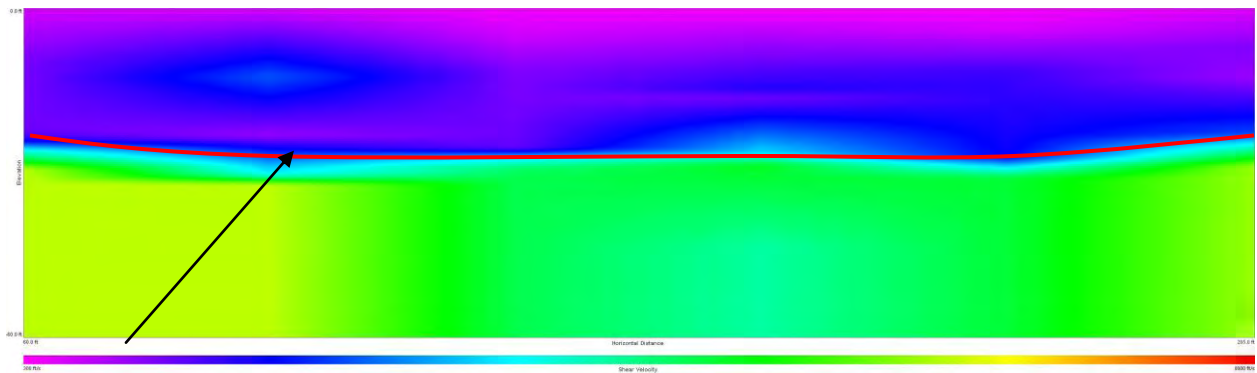
PSI was asked to perform ReMi testing to aid in the preliminary design of a large wind farm near Laramie, Wyoming. The proposed site included approximately 25 acres of wind turbines. Due to the scale of the project site area in combination with the minimal amount of subsurface investigation requested, ReMi was performed at different locations dependent on what was encountered during drilling operations. The primary objective in this study was to determine shear wave velocities for potential foundation design of the wind turbines. Due to the changing subsurface strata of the project site, several ReMi lines were performed to characterize the different shear wave velocities for different rock formations. PSI performed a series of 6 ReMi lines across the site with geophone spacing of 15 feet.

As expected, the ReMi profiles varied at each location, dependent on the materials encountered during drilling. Two profile are reviewed below.

The ReMi profile 1 (seen below) revealed approximately 30 to 40 feet of overburden soils that were identified by low to very low shear wave velocity (500 ft/s to 1,000 ft/s) material. The overburden material overlaid moderate shear wave velocity (2,000 ft/s to 5,000) material which was identified as granite bedrock which was indentified by drilling operations. \

The drilling operations encountered granite bedrock at 34 feet and cores samples indicated that the granite bedrock was fairly to highly fractured in parts. Compressive strengths performed on the bedrock indicated strength of approximately 1,000 psi.

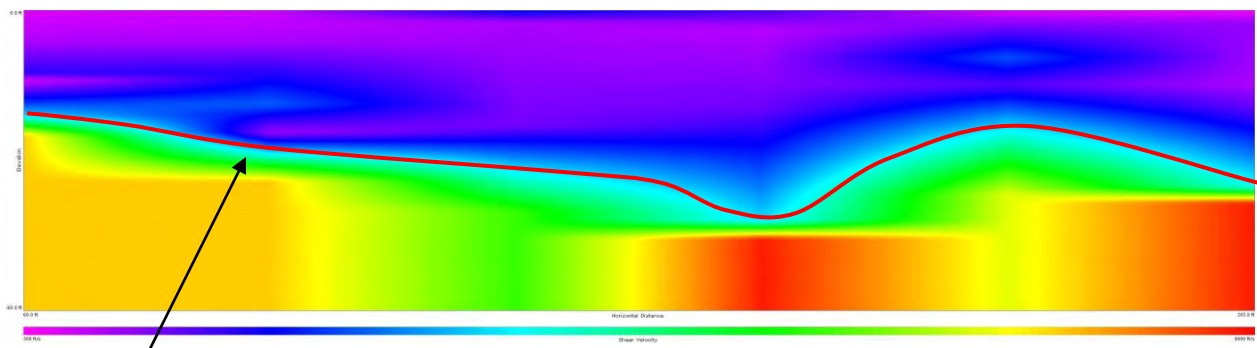
Profile 1



Approximate Bedrock Elevation

In contrast, the ReMi Profile 2 (seen below) revealed approximately 40 to 60 feet of overburden soils that were identified by low to very low shear wave velocity (500 ft/s to 1,000 ft/s) material. The overburden material overlaid moderate shear wave velocity (2,000 ft/s to 5,000) to very high (5,000 ft/sec and greater) material which was identified as granite bedrock during drilling operations. The ReMi profile indicates that granite bedrock dips steeply. The drilling operations encountered granite bedrock at approximately 30 feet and cores samples indicated that the granite bedrock fairly intact with vary little fracturing. Compressive strengths performed on the bedrock indicated strength of approximately 2,500 psi.

Profile Line 2



Approximate depth of bedrock

PSI performed this study to aid in the design of the foundations for the proposed wind turbines. Due to the large scale of the proposed wind farm, several different bedrock formations appear to underlie the site. By further characterizing separate formations, foundation design can be designed to match varying material types as opposed to the more limited delineation shown on the geologic maps.

Underground Coal Mines - Madison County, Illinois

Southern Illinois has a long history of underground coal mining activity. There are four coal seams that generally underlay Southern Illinois and have been commercially developed. These seams include the: Danville, Herrin, Springfield, and Colchester coal seams. In Madison County, Illinois, located to the northeast of Saint Louis, Missouri, the general geology consists of 40 to 50 feet of overburden soil underlain by bedrock consisting of various layers of shale and limestone. The shallowest commercially viable coal seam, usually the Danville Coal Seam, has been reported to be as shallow as 100 feet below the ground surface. Based on the depth of the coal, the mining techniques of the era and the geology, damage to surface structures resulting from mine subsidence is possible. The coal seams in this area can have fairly thick under clays, therefore, mine subsidence in this area can be caused by the pillars pushing through the under clays in the mine floor as well as the roof rock failures.

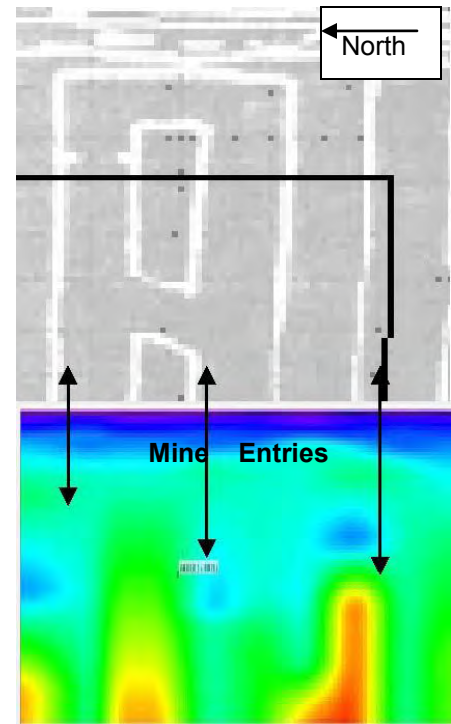
One of the greater challenges in evaluating the risk of mine subsidence associated with a structure, is the age of the mine and the reliability of the mining maps. The Illinois State Geological Survey (ISGS) warrants that their mine area maps are only accurate to within 500

feet. In addition, due to the age of some of the mines, ISGS also does not always have detailed maps available for review, which also could have an impact on evaluating the risk of subsidence. PSI was asked to investigate an approximately 90,000 ft², single-story commercial structure located in Madison County, Illinois that was constructed in 1995. In 2008, the structure was reported to have visible distress to the structure. The distress included cracking of the floor slab, particularly at column lines, running parallel to the short side of the building (east-west). Cracking was also observed at the corners of the structure near the south end of the building. In 2008, a survey of the building's floor slab was performed and showed that the south end of the building had experienced approximately 7 inches of differential settlement compared to the north end of the building. Based on the survey, the building experienced an increasing amount of differential movement towards the southern end of the building.

A review of a coal mine map of the area, published by the ISGS, indicated the site had historical underground activity which operated from 1920 to 1940. According to the information provided, the mine is approximately 200 to 210 feet below the existing ground surface in the Herrin Coal seam with an average thickness of 5 to 6 feet and a maximum thickness of 8 feet. The coal was reportedly mined using the room-and-pillar panel (RPP) method of excavation, which indicates that the mine was excavated in a manner consisting of thin pillars with thicker panels between the chambers.

To approximate the location of the mine entries, a 2D profile of the site was developed using ReMi. ISGS provided a record map of the mine and the mine entries were able to be identified and compared with the surface features including the existing structure. Based on the ReMi evaluation, two of the mine entries were located approximately 180 feet to 220 feet below the

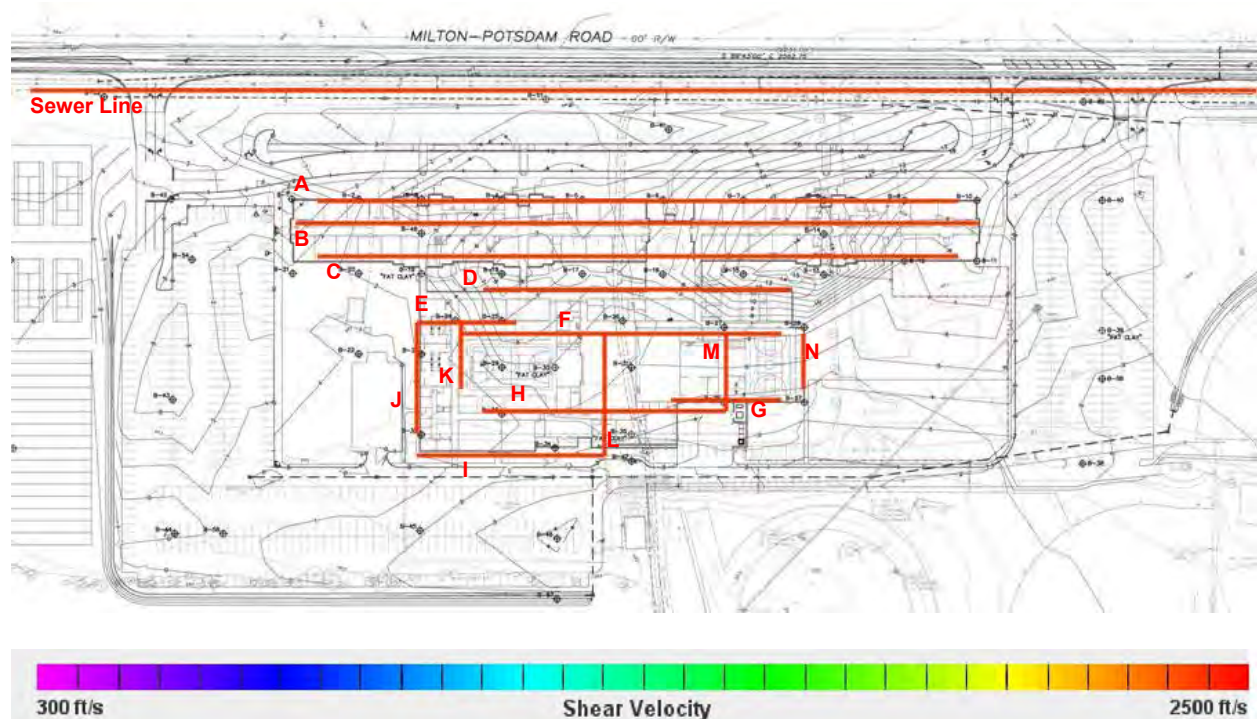
ground surface, which is consistent with coal in the Herrin seam reportedly mined at this location. The third entry was located at an approximate depth of between 120 feet and 150 feet below the ground surface, about 50 feet higher than the other two entries. The depth of opening is consistent with the overlaying Danville coal seam, but no records show that that seam was mined. This reduction in the roof rock thickness typically results in more subsidence since the overlying stresses cannot “bridge” and be supported by the surrounding material.



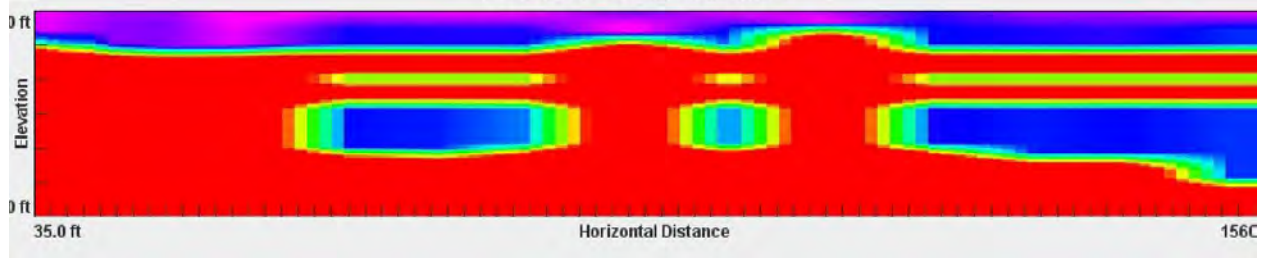
The results from the ReMi profile indicated that the roof rock above the two deeper mine openings under the northern portion of the building had a higher shear wave velocity (~4,000 ft/s). However, under the southern portion of the structure, the roof rock above the detected mine openings had a lower shear wave velocity (~2,500 ft/s). The lower shear wave velocity in the roof rock is indicative of mine subsidence propagation upward through the roof rock due to the collapse and alternation of the bedrock. It is unknown as to why the mine opening is 50 feet higher at the southern end of the building than at the northern end; however, this shallower mine was likely the cause of the mine subsidence. Without the use of a geophysical survey, such as ReMi, the subsurface conditions would not have been known and an appropriate engineering solution for the structure could not have been prepared.

Rock Profiling and Rippability – West Milton, Ohio

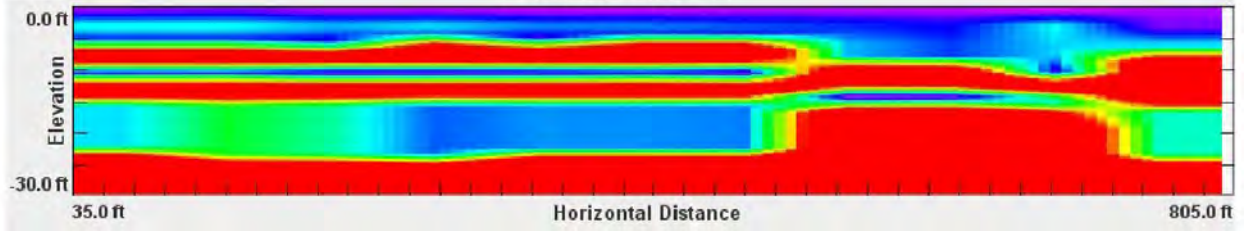
Western Ohio, particularly in West Milton, is underlain by relatively shallow limestone that can be highly variable in terms of weathering. For a proposed academic building located off Milton-Potsdam Road in Miami County, ReMi was used to evaluate subsurface conditions estimate the rippability of the shallow rock for installation of a sewer line as well as construction of the proposed foundations. A total of 94 arrays were used in evaluating the subsurface conditions at the site. Seventy-eight arrays were located within the proposed building footprint area and sixteen arrays were located along the alignment of the sanitary sewer line. The arrays used to record ambient seismic noise at the site varied from 69 to 115 feet long and consisted of 24 geophones spread along a line at 3-foot to 5-foot spacings. Data was recorded in 20-second sample intervals, with a 1-millisecond sampling rate per channel. Nearby vehicle traffic from Milton-Potsdam Road and the on-going subsurface exploratory drilling operations performed at the site provided the ambient noise for the evaluation. The following is a layout of the various ReMi line and the 16 two-dimensional shear wave velocity profiles for the site.



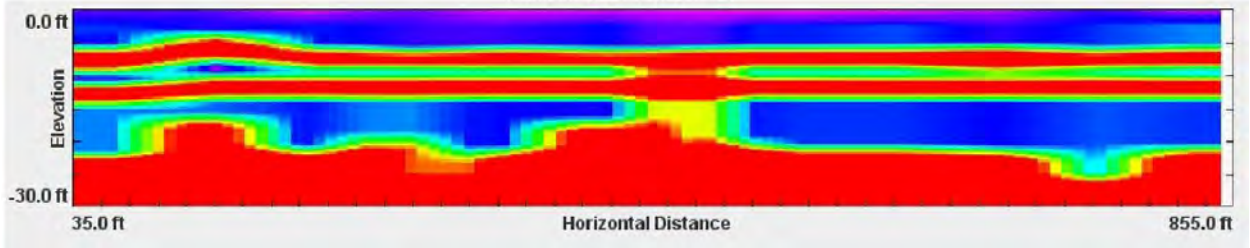
PROFILE SEWER LINE



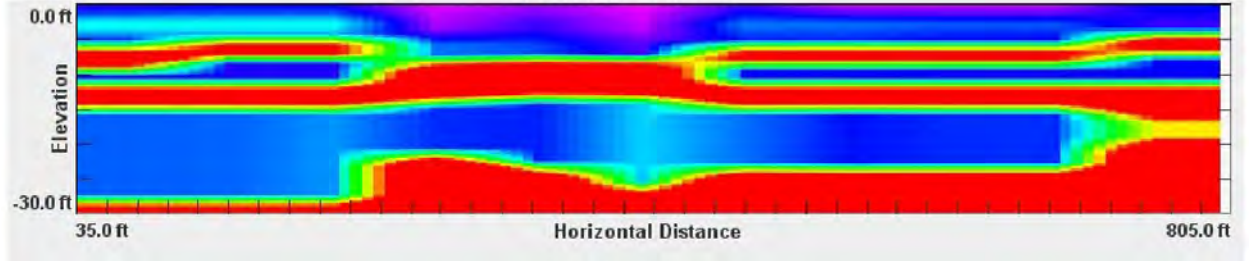
PROFILE LINE "A"



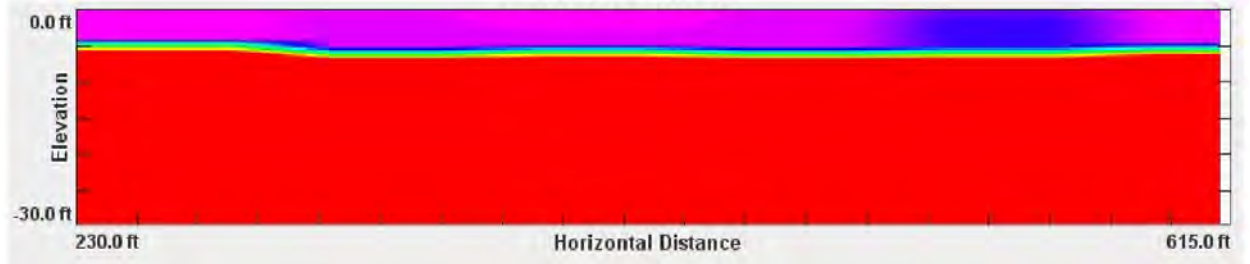
PROFILE LINE "B"



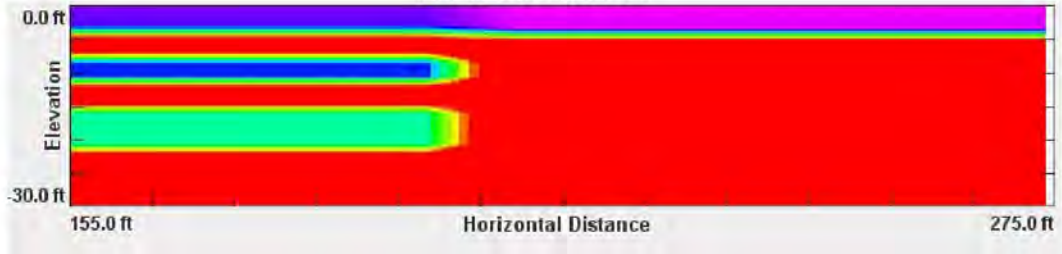
PROFILE LINE "C"



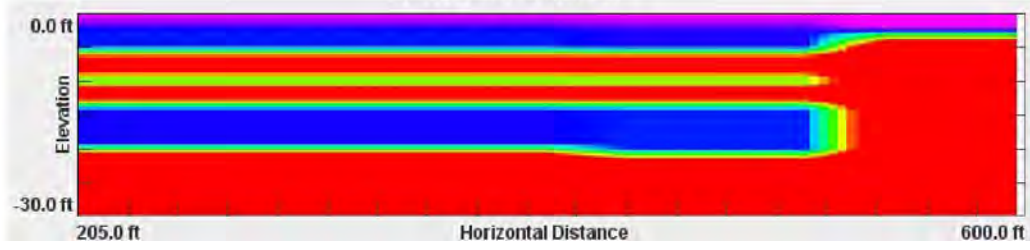
PROFILE LINE "D"



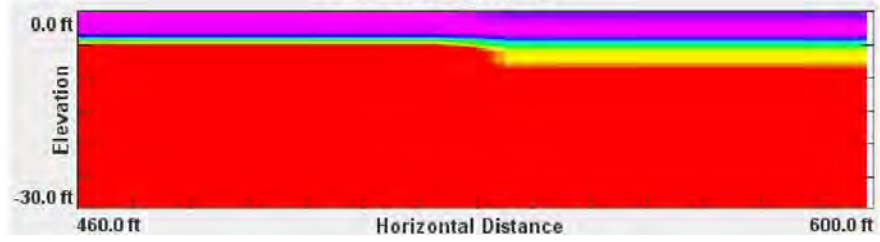
PROFILE LINE "E"



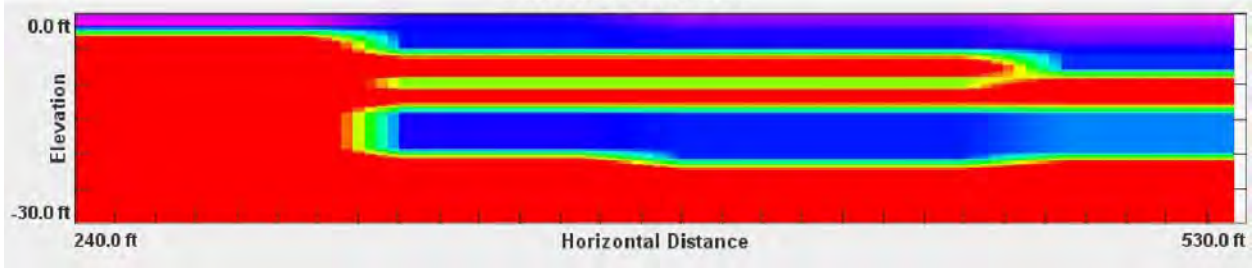
PROFILE LINE "F"



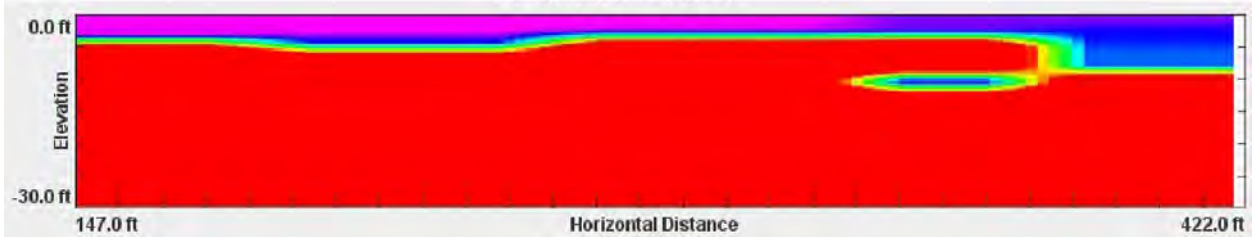
PROFILE LINE "G"



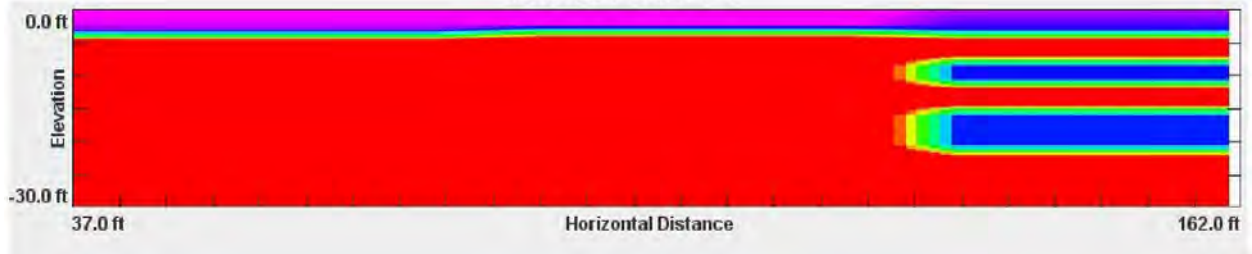
PROFILE LINE "H"



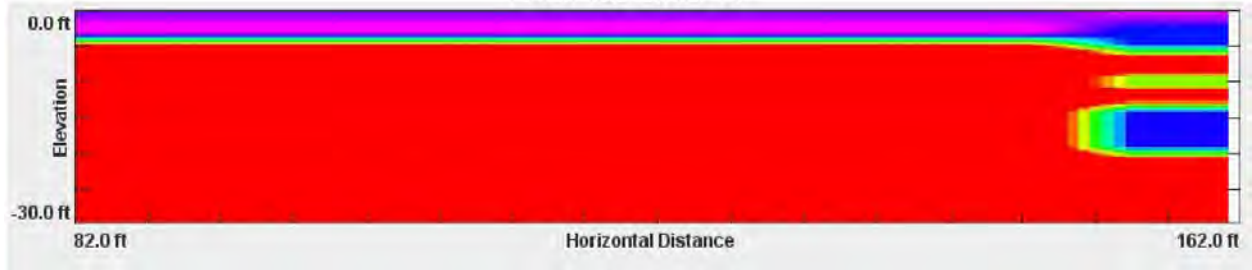
PROFILE LINE "I"



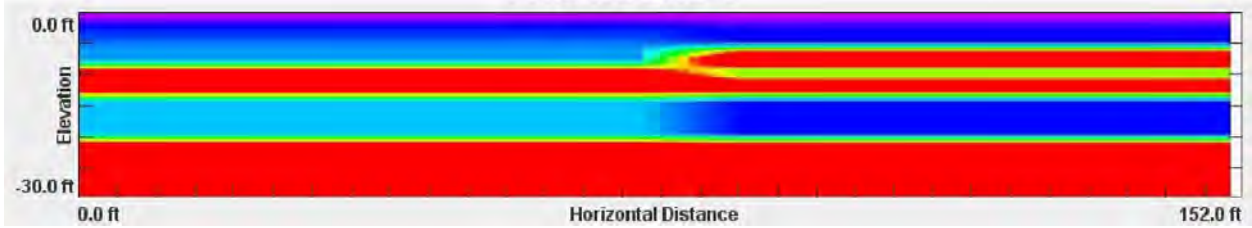
PROFILE LINE "J"



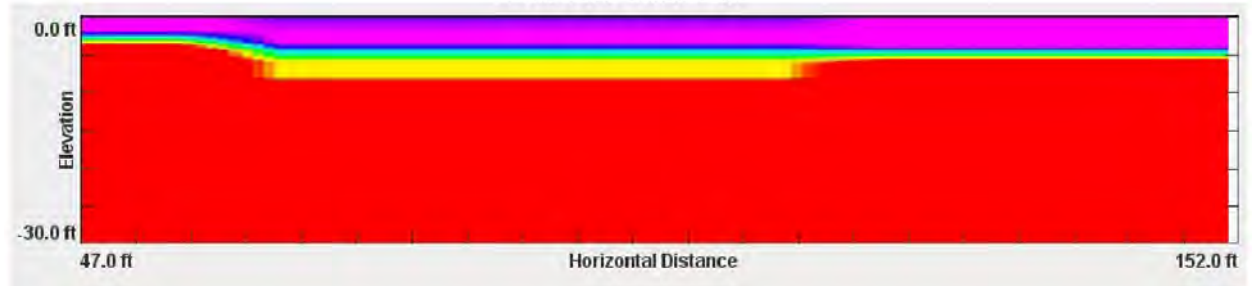
PROFILE LINE "K"



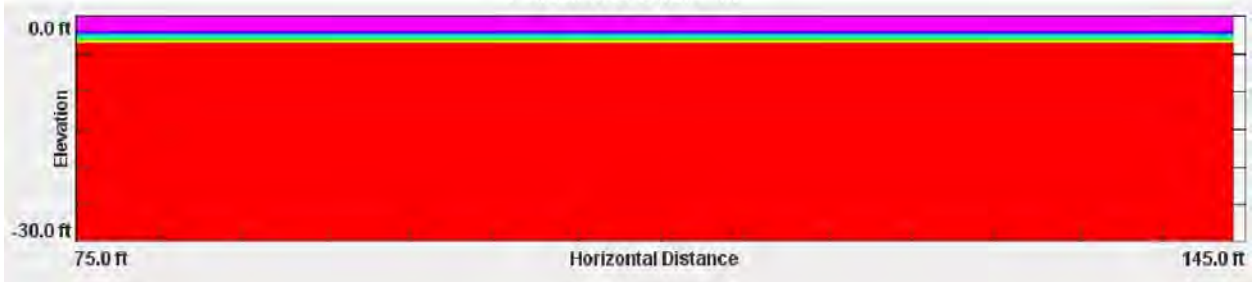
PROFILE LINE "L"



PROFILE LINE "M"



PROFILE LINE "N"



Based on a review of the two-dimensional profiles developed for this project and the subsurface information obtained from the geotechnical exploration, the upper 2 to 8 feet consisted of soil with shear wave velocities ranging from 200 ft/s to 1,200 ft/s underlain by an intact limestone that contains areas of weathering with depth. The rippability of a soil or rock is generally evaluated based on the seismic wave or compression wave velocity which is generally on the order of $1\frac{3}{4}$ times the calculated shear wave velocity. Based on the ripper performance charts provided in the Caterpillar Performance Handbook (32nd Edition), the upper 8 feet of material could be excavated with conventional excavation equipment; however, the limestone at depth with compressive wave velocity over 6,000 ft/s would require additional effort such as blasting.

Summary

ReMi is a relatively useful geophysical method for evaluating major changes over a large area and improving our understanding of what happens between boring and below the surface. Though the ReMi technique is often not the only means of acquiring valuable geotechnical data, it is an excellent means to extrapolate information between borings and provide useful information at depth without the expense of deep borings. Often times, a client will request a 1-D profile for seismic site classification. The same amount of field work is performed to generate the 1-D seismic profile as to provide a 2-D profile. It typically, is of engineering and economical benefit to spend the additional computational time to prepare a 2-D profile to enhance the subsurface information collected from site borings.

**Karst Features in Limestone Evaluated Utilizing an Acoustic Televiewer,
I-70 Mississippi River Bridge, St. Louis, Missouri**

Adrian Keller, P.E., R.G.
HNTB Corporation
715 Kirk Street
Kansas City, MO 64105
(816)-472-1201
adkeller@hntb.com

Prepared for the 61st Highway Geology Symposium, August, 2010

Acknowledgements

The author would like to thank the following individuals for photographs that were utilized in this paper:

Peter Ingraham – Golder Associates, Inc.
Tom Eliassen – Vermont Agency of Transportation

Disclaimer

Statements and views presented in this paper are strictly those of the author(s), and do not necessarily reflect positions held by their affiliations, the Highway Geology Symposium (HGS), or others acknowledged above. The mention of trade names for commercial products does not imply the approval or endorsement by HGS.

Copyright Notice

Copyright © 2010 Highway Geology Symposium (HGS)

All Rights Reserved. Printed in the United States of America. No part of this publication may be reproduced or copied in any form or by any means – graphic, electronic, or mechanical, including photocopying, taping, or information storage and retrieval systems – without prior written permission of the HGS. This excludes the original author(s).

ABSTRACT

Borehole viewers are downhole inspection devices that can be utilized to view in-situ rock conditions and should be considered by geotechnical engineers and geologists as a supplemental means of investigating rock. The optical viewer (OTV) produces a digital optical image and the acoustic viewer (ATV) utilizes reflected acoustic waves to produce images of the borehole walls. Soft or fractured zones, solution features, open joints or other voids often unobservable during traditional rock coring techniques can be detected and measured utilizing this technology. The devices can be used to measure the strike and dip of joints, bedding planes, shear surfaces, or other structural features, eliminating the need for expensive oriented cores or downhole logging.

An acoustic viewer was utilized in the fall of 2008 during the investigation phase for the New I-70 Mississippi River Bridge in St. Louis, Missouri. An ATV was utilized in each of ten river borings to produce images of the rock mass in the borehole and allow further investigation of voids identified during rock coring. Voids interpreted as karst features were identified in the ATV logs in multiple borings and at similar elevations, suggesting connectivity. Measurements of the void's width, location in the borehole and orientation allowed a more thorough understanding of the potential impact the karst features may have on the planned deep foundations. An extensive grouting program was eliminated based on the results of the ATV.

INTRODUCTION

Optimizing the design of deep foundations requires a thorough understanding of the bearing strata. Developing design parameters for deep foundations founded on or in bedrock involves characterizing the bedrock mass. In addition to determining intact rock strength parameters, proper rock mass characterization requires knowledge of joint spacing, joint quality, orientation of the joints and orientation of bedding planes or rock foliation. In areas of the country where bedrock is not exposed in outcrops at the surface, this information is obtained from subsurface exploration with drilled borings and rock coring. Expensive oriented coring methods have traditionally been used to obtain information regarding orientation of joints, bedding planes or rock foliation. Poor recovery or quality of rock core can often lead to a lack of understanding of the rock conditions and result in a poorly optimized foundation design.

Borehole viewers can be utilized to image rock conditions in the borehole walls and view in-situ rock properties missed from traditional rock coring techniques. Borehole viewers have been utilized in the geotechnical engineering field to evaluate bedrock conditions for tunneling, rock cut slopes or dam abutments where the characterization of the rock mass is paramount. This technology is a proven and highly cost-effective way to evaluate rock mass conditions in-situ and should be considered by geotechnical engineers when designing deep foundations in rock.

Borehole viewers come in two types, optical and acoustic viewers. Optical viewers (OTV) produce images of the borehole walls utilizing a digital optical image. Acoustic viewers (ATV) produce images of the borehole walls by transmitting and receiving ultrasonic acoustic waves. The resulting images are high resolution images that can be used to determine strike and dip of bedding planes, joints, foliation, or other discontinuities important to the geotechnical engineer or geologist.

An acoustic viewer was utilized as part of the subsurface investigation in the Fall 2008 for the proposed New Mississippi River Bridge in St. Louis, Missouri (Figure 1). The new bridge will span the Mississippi River and carry Interstate 70 from St. Louis, Missouri to St. Clair County, Illinois.

Prior investigators reported voids in the bedrock during rock coring in the area of the main tower foundations. An extensive grouting program was recommended by the prior consultants to fill the voids and reduce the potential for vertical deformation of the bridge foundations.

The acoustic viewer was utilized in the 2008 investigation to assess the quality of the limestone bedrock and the condition of the voids as part of evaluating deep foundation options to support the main towers of the bridge. The two deep foundation options considered for the bridge were dredged caissons founded on the bedrock surface or drilled shafts and rock sockets founded within the bedrock.



Figure 1. Rendering of the I-70 Mississippi River Bridge looking southwest.

Ten borings were drilled from a barge in the river at the two main tower pier locations. An acoustic televiewer was utilized in each of the ten borings to produce images of the rock mass in the borehole and allow further investigation of the voids. Voids in the rock were not detected during drilling but were readily identified on the ATV logs. The voids were interpreted as solution features in the limestone and were correlated to the recovered rock core during supplemental logging in the laboratory. The presence of the solution features at similar elevations also suggested connectivity.

Measurements of the void's width, location in the borehole and orientation allowed a more thorough understanding of the potential impact the solution features may have on the planned deep foundations. The acoustic televiewer logs were key pieces of information necessary to properly characterize the rock mass and were the primary impetus for eliminating the bedrock grouting program.

BOREHOLE TELEVIEWERS

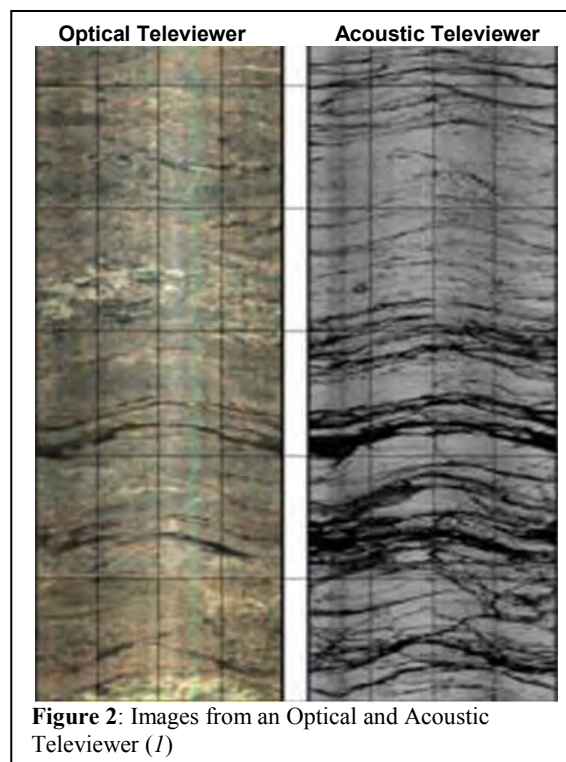
Borehole televiewers were developed and have been in use in the oil industry since the 1960's (1,2). Advancements in technology and computer data processing capabilities have made borehole televiewers more accessible to the geotechnical community; however the use in deep foundation design has been limited.

Borehole televewers are primarily utilized to create images of the borehole walls following rock coring. In-situ rock conditions can be viewed when evaluating the rock mass for joint locations, joint spacing and condition of the joints.

Often in geotechnical engineering, information from the zones of poor core recovery or zones of highly fractured rock becomes the areas of highest concern. The borehole televewers allow the practitioner to view the borehole walls in areas of poor rock core recovery or in zones of weak and/or fractured rock. The borehole televewers allow proper repositioning of the recovered core pieces or core sections where recovery was low and intervals have been lost. Essentially, the televewer log provides the ability to view 100 percent of the corehole record by viewing the walls of the borehole.

The use of optical and acoustic televewer equipment is gaining popularity over oriented core collection because it is generally less expensive, less labor intensive and is particularly useful where access or ability to drill inclined holes is limited or where local drilling capabilities lack the equipment necessary to collect oriented cores (*1*).

Two types of borehole televewers are available. An optical televewer generates a continuous color image of the borehole wall using an optical imaging system (Figure 2). The acoustic televewer creates images by transmitting and receiving an ultrasonic acoustic pulse reflected from the walls of the borehole.



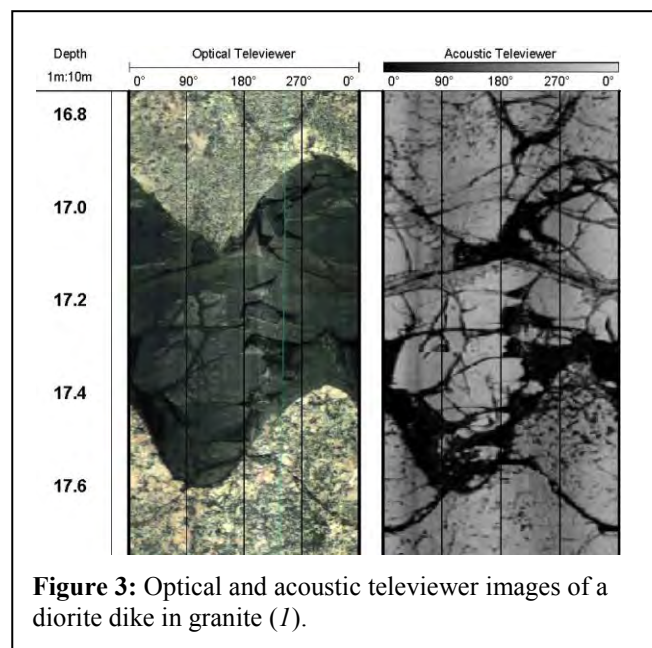
The OTV generates a high resolution digital color image and is capable of resolving fractures as narrow as 0.1 mm with a radial resolution of 1 degree (*1*).

With the ATV, the amplitude and travel time of the acoustic wave is recorded continuously in the borehole. The travel time of the reflected acoustic wave is recorded to generate continuous caliper data of the borehole diameter. The amplitude of the reflected acoustic pulse represents the elastic properties of the bedrock formation. Light colored features are generated from the higher amplitude waves and represent a sound and smooth borehole. Reflected energy that is lost in voids, fractures and discontinuities produces dark bands on the amplitude logs.

Because the OTV is an optical image the borehole must be air-filled or filled with clear fluid. The ATV requires the borehole to be filled with fluid but can be performed in murky conditions or holes filled with drilling slurry.

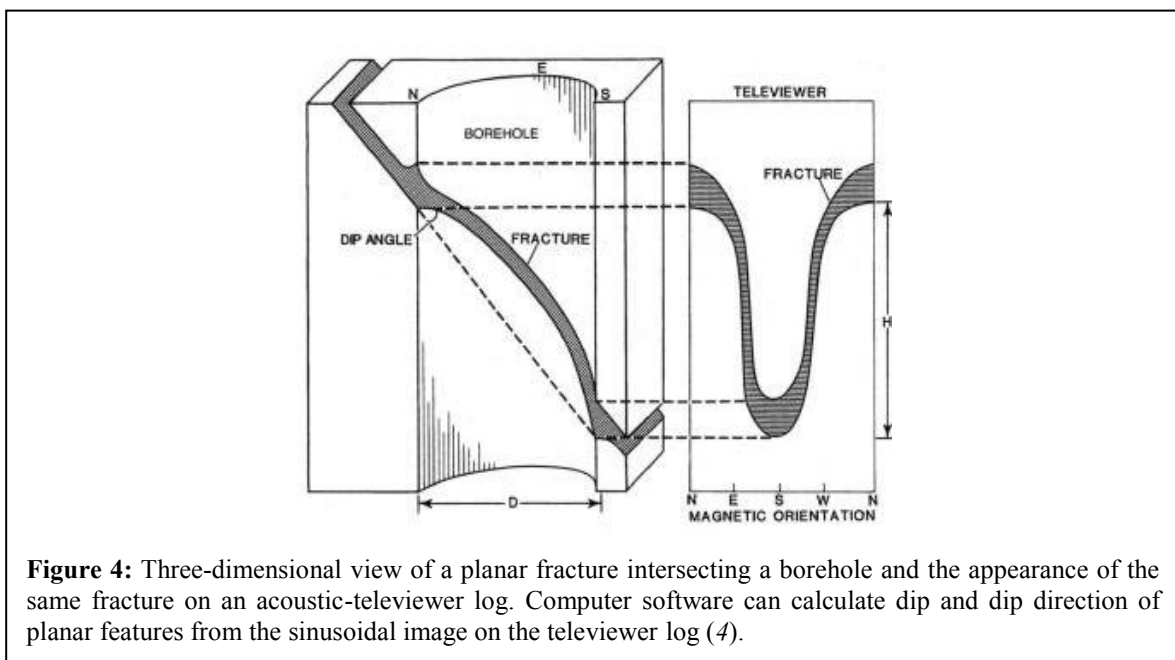
Image quality is sensitive to borehole shape and the position of the televiewer probe. Smooth, cylindrical boreholes with a well-centered tool return the maximum acoustic energy because of the resulting high incidence angle and low scattering of the acoustic beam (*3*). Changes in the acoustic wave reflectivity can be associated with borehole roughness, changes in rock density and other energy absorption features of the rock such as fractures, voids, bedding planes, or foliation.

The optical and acoustic televiewers can be complimentary tools if used in tandem. The optical color images from an OTV can provide lithology data often unobservable with an ATV. The acoustic televiewer is better at creating images of the fractures, joints, bedding planes and other structural features of the bedrock formation. Figure 3 illustrates this concept.



Both types of televiwers orient their images utilizing a three-axis magnetometer and three-component accelerometer allowing accurate orientation recording of the images from inclined or vertical boreholes.

The three dimensional image of the borehole wall is displayed in 2 dimensions by “unwrapping” the image along a common point, typically the north side of a vertical borehole or the high-side of an inclined borehole. Planar features such as bedding planes, joints or fractures that intersect the borehole will appear as sinusoidal waves in the televiwer image. The dip direction of the feature can be determined by the orientation of the low side of the sinusoidal wave. In Figure 4, the planar feature dips to the south. The dip angle can be calculated knowing the height or amplitude of the sinusoidal wave (H) and the diameter of the borehole from the caliper log (D).



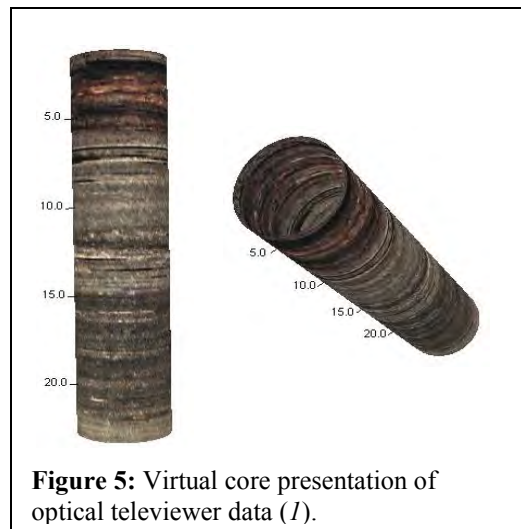
Both the optical and the acoustic televiwer probes are less than 2 inches in diameter and can be utilized to image boreholes with diameters between 2 and approximately 18 inches depending on borehole conditions.

During logging, the probe is lowered or raised slowly in the borehole and the data is recorded directly to a computer acquisition device. Logging rates generally are between 4 and 6 feet per minute. The probes are centered in the borehole with three centralizing bands in two locations along the probe. As the probe proceeds up or down the borehole, the optical images or the acoustic reflection parameters can be viewed in real-time.

Computer software is available to facilitate post-processing and quickly generate the televiwer logs and other statistical summaries. Structural features are picked manually from the televiwer logs searching for the sinusoidal forms. Each feature detected is rated based on apparent aperture and its orientation is depicted on the log by displaying a matching sinusoid.

Structural data is collected quicker than with oriented core methods and statistical plots can be generated to present structural data with stereonet or rose diagrams.

Another common display option for the data is the projection of the image onto a virtual core. The virtual core is created by taking the negative image of the borehole wall and wrapping the image into a cylinder which can be rotated and viewed from any orientation. Figure 5 illustrates the virtual core. The image of the virtual core is more easily interpreted by the viewer since it more closely resembles the recovered core from the borehole.



I-70 MISSISSIPPI RIVER BRIDGE

The I-70 Mississippi River Bridge (MRB) is a cable-stayed structure that spans the Mississippi River from St. Louis, Missouri to St. Clair County, Illinois.

The new bridge has a total span length of 6,460 feet with the cable-stayed unit approximately 2,770 feet (Figure 6). The open span between the two main towers is 1500 feet. The two main tower Piers will be located within the river. The side spans from the main towers to the anchor piers are approximately 635 feet each.

Investigative borings were performed in the Fall of 2008 to assess subsurface soil and rock conditions. Five borings were drilled at each of the two main tower locations from barges in the river. The depth of water was approximately 40 feet at the time of drilling. Subsurface conditions generally consisted of 40 to 70 feet of loose to medium dense alluvial sands and gravels overlying limestone bedrock. Rock coring was extended approximately 100 feet into the underlying limestone bedrock.

Two foundation options for the main tower piers were designed in the baseline plan set for contractor bidding. The main tower piers could be supported on drilled shafts with rock sockets bearing in the underlying limestone or dredged well caissons supported on the surface of the bedrock.

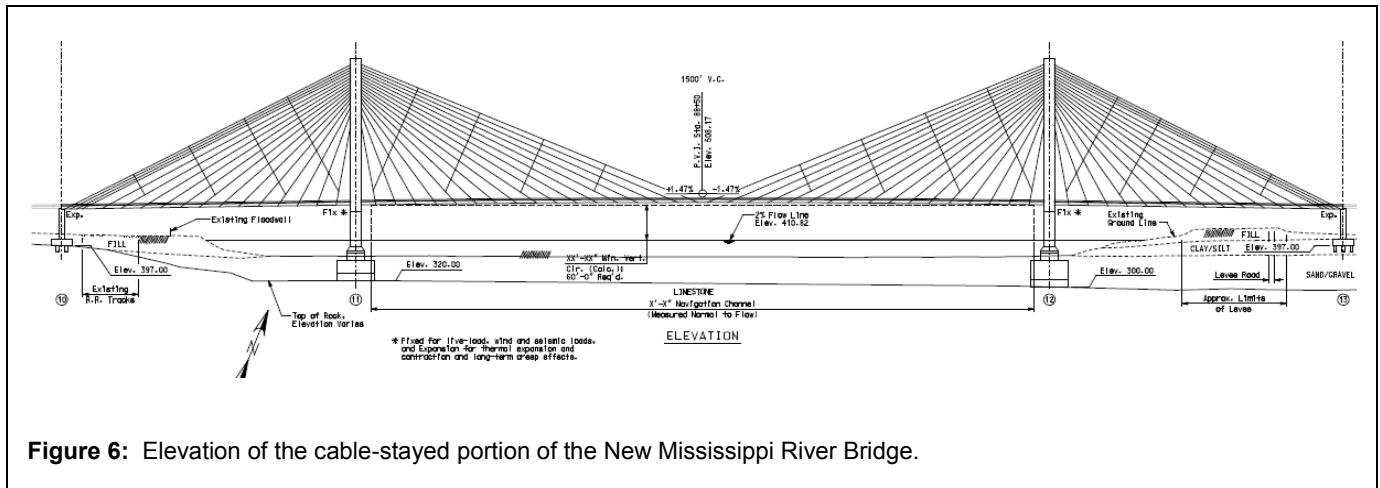


Figure 6: Elevation of the cable-stayed portion of the New Mississippi River Bridge.

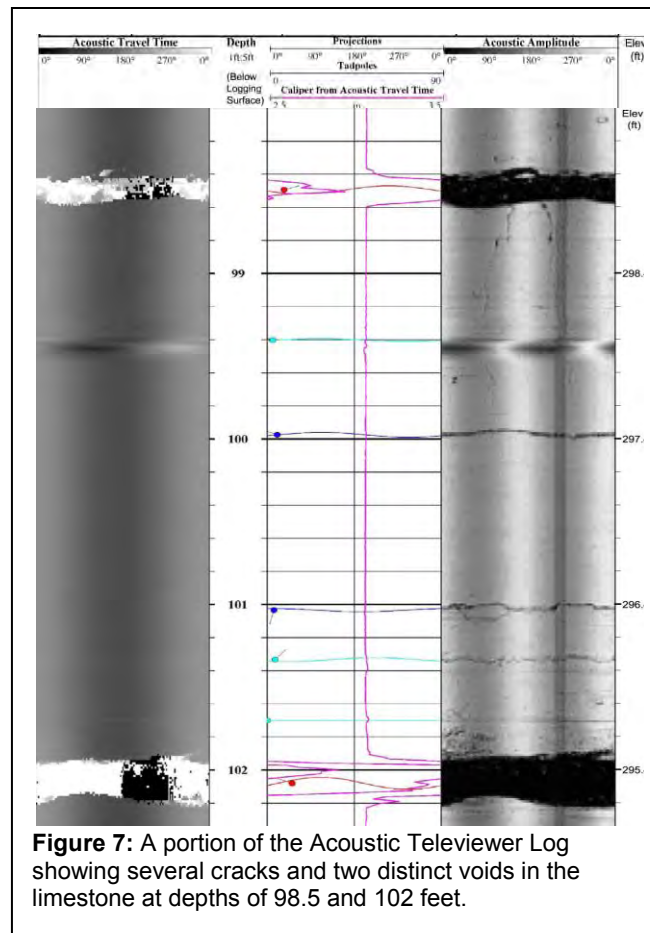
Investigation by a previous consultant was performed in 2001-2003. Thin voids and fracture zones were described to a depth of 30 to 40 feet into the bedrock. The conclusion was that the voids were a result of solutioning in the limestone, also known as karst. Geophysical testing including borehole ground penetrating radar and seismic tomography were utilized during the prior investigation in an attempt to characterize the void/fracture zones. Packer testing was also performed in the fractured rock zones. The resulting high flow rates during packer testing were interpreted as the voids being interconnected. The consultant recommended an extensive grouting program in the bedrock prior to foundation construction.

During review of the previous reports, the location of the void/fracture zones identified in boring logs did not correlate well with the location and configuration of fracture zones identified on the ground penetrating radar logs or the images generated by the seismic tomography. The orientation of the void/fracture zones was also not consistent between the two geophysical testing methods.

HNTB recognized that having a thorough understanding of the void/fracture zones was critical in evaluating the two deep foundation options for the main tower piers.

During the exploration program in the Fall of 2008, the acoustic televiewer was utilized in the 10 borings at the main tower piers. The intent of the ATV was to confirm the presence and gain an understanding of the voids and fracture zones described by the previous consultant.

While the borings and subsequent laboratory testing suggested that the limestone rock was good to very good quality, the rock did contain fractures, discontinuities and voids. These features were readily identified in the ATV logs. The voids, $\frac{1}{4}$ inch to approximately 3 inches wide, were identified as deep as 50 feet below the rock surface. A sample of the ATV logs is included as Figure 7. The voids were also visible in the video record from the downhole television camera.

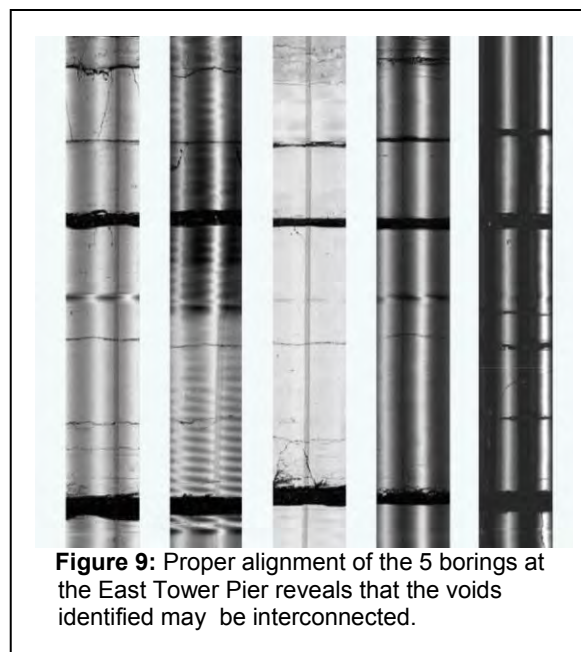


The orientation of the fractures and voids were generally measured parallel to bedding and are flat lying. Two to three prominent voids were observed in the upper 10 to 12 feet of the bedrock at the tower locations. The acoustic travel time caliper measurements suggested that the diameter of the borehole at the location of the voids was 4 to 5 inches suggesting that the voids locally may have been in-filled with soil. Subsequent logging of the core in the laboratory appeared to confirm the presence of the voids.

The texture of the core above and below the voids was weathered and the surface showed signs of solutioning. Mineralization and staining was present on the surfaces, which also suggested the void may have been widened by flowing water (Figure 8).

The solution features in the upper 10 to 12 feet of the east tower boreholes were identified at similar elevations, as shown in Figure 9, suggesting possible interconnection. Similarly, possible interconnection was identified from dissolution seams in the west tower borings.

A concern for the bridge performance was the presence of the voids in the rock beneath the main tower foundations. The ATV logs provided a more thorough understanding of the bedrock to assess the impact of the voids on the performance of the deep foundations.



It was determined that the drilled shaft foundation option would be less affected by the thin voids in the limestone rock provided the voids are not located within close proximity to the bottom of the drilled shaft. The concern regarding the voids below the bottom of the rock socket could be reduced by limiting the design of the rock socket to the resistance resulting from side friction only and relying on zero capacity from end bearing.

In order to include end bearing resistance in the foundation capacity, we recommended drilling investigative core holes at each drilled shaft location, consistent with Missouri DOT requirements, and recommended acoustic televiewer logs be generated to a minimum depth of 10 feet below the bottom of the rock socket.

Performance of the dredge well caisson was a potential concern due to the presence of the 2 to 3 prominent voids within the upper 10 to 12 feet of the rock. The dredged well caisson was designed to bear on the surface of the bedrock below the alluvial soils. Since the footprint of the

caisson was 83 feet by 123 feet, the voids were certainly within the influence zone of the foundation bearing pressures. Based on the loads provide by the structural engineer and calculated bearing pressures, HNTB determined that sufficient thickness of intact rock existed above the voids to resist the potential for shearing of the intact rock and collapsing the void space.

Based on the additional information that the bridge towers could accommodate vertical deformation in excess of the cumulative thickness of the void space observed in the acoustic televiewer logs, we were able to eliminate the need for bedrock grouting.

The acoustic televiewer logs allowed a more thorough understanding of the bedrock conditions beneath the tower foundations and provided the ability to maximize the foundation design.

SHORTCOMINGS OF BOREHOLE TELEVIEWERS

Since the orientation of the borehole televiewer is based on a magnetometer located within the probe, ferromagnetic minerals present in the rock may not allow proper orientation of the images. Similarly, steel borehole casing may also affect image orientation. This can be overcome by orienting the image to the high side (top of the borehole) in inclined holes using the inclinometer data collected by the televiewer. Alternatively, a gyroscopic tool, which is unaffected by magnetic materials, can be run separately to collect borehole orientation data and later used to rotate the televiewer image during post processing (*I*). The orientation systems should be carefully checked for proper functioning prior to use.

Properly centralizing the acoustic televiewer probe is also important for quality acoustic televiewer logs. Boreholes which are out of round or where the probe is not properly centralized will produce dark vertical bands in the televiewer log. These bands can conceal fracture information. This can be seen in the logs on the right side of Figure 9.

Rock type can also affect the image quality and interpretation of the televiewer logs. Softer rock will more likely be affected by drilling stresses, fracture widening and washout from fluid circulation during coring. Fractures can appear wider on the televiewer logs than may actually be observed in the core sample. This can be more pronounced where steeply dipping fractures or bedding planes intersect the borehole wall. The rock edges at the high and low sides of the borehole will be more likely to experience damage from drilling stresses, be widened during water circulation or mechanical breakage from drilling operations. This concept is illustrated in Figure 3, where the thickness of the crack is wider at the top and bottom of the sinusoid.

Due to this widening in different rock types, a bias can occur where fracture identification is more visible in certain rock. Cracks can appear wider than may actually exist beyond the borehole walls. Cracks which appear open in the televiewer logs may actually be healed or closed cracks in the recovered rock core.

Since the post-processing, fracture identification and feature rating is often done in the office and in the absence of the rock core, subsequent correlation must be done with the recovered rock core to confirm the presence of features identified on the borehole televiewer logs.

As previously mentioned the optical televiewer can be utilized in an air-filled borehole or in a borehole filled with clear fluid. The acoustic televiewer must have a fluid filled hole, however, it can operate in murky fluid or in borings drilled with drilling slurry.

CONCLUSIONS

Optimizing the design of deep foundations requires a thorough understanding of the bearing strata. Developing design parameters for deep foundations founded on bedrock involves characterizing the bedrock mass. Poor recovery or quality of rock core can often lead to a lack of understanding of the rock conditions and result in a poorly optimized foundation design.

Borehole viewers can be utilized to view in-situ rock conditions within the borehole walls following coring. Borehole viewers are an alternative to expensive oriented coring methods used to obtain information regarding the condition and orientation of joints, bedding planes or rock foliation.

The application of this technology at the I-70 New Mississippi River Bridge resulted in a more thorough understanding of the rock conditions beneath the bridge site and eliminated the need for an extensive grouting program. Borehole viewers are gaining popularity within the geotechnical engineering community and should be considered by other geotechnical practitioners when designing deep foundations in rock.

REFERENCES

1. Eliassen, T., Richter, D., Crow, H., Ingraham, P., and Carter, T. Use of Optical Televiewer and Acoustical Televiewer Logging Methods in Lieu of Oriented Coring Methods. *Transportation Research Board Workshop on Geotechnical Methods Revisited*, Preprint, Kansas City, Missouri, 2005, 16 p.
2. Zemanek, J., Glenn, E.E., Norton, L.J., and Caldwell, R.L., Rempe, D.M. and Davisson, M.T. Formation Evaluation by Inspection with the Borehole Televiewer. *Geophysics*, vol. 35, 1970, pp. 254-269.
3. Davatzes, N. C. and Hickman, S. Comparison of Acoustic and Electrical Image Logs from the Coso Geothermal Field, CA. *Proceedings of the Thirtieth Workshop on Geothermal Reservoir Engineering*, Stanford University, Stanford, California, SGP-TR-176, 2005, 11 p.
4. Keys, W.S. Borehole Geophysics Applied to Ground-Water Investigations. *Techniques of Water-Resources Investigations of the USGS*, Book 2, Chapter E2, 1990, 150 p.

Determination of In-Situ Density of Planned Roadway Cuts in Cemented and Coarse-Grained Soils Using Seismic Geophysical Methods to Estimate Earthwork Factors

Daniel N. Fréchet, PhD, PE
AMEC Earth & Environmental, Inc.
1405 West Auto Drive
Tempe, AZ 85284
(480)-940-2320
daniel.frechette@amec.com

Prepared for the 61st Highway Geology Symposium, August, 2010

Acknowledgements

The author would like to thank the individuals for their contributions in the work described:

Michael Rucker, PE – AMEC Earth & Environmental

Disclaimer

Statements and views presented in this paper are strictly those of the author(s), and do not necessarily reflect positions held by their affiliations, the Highway Geology Symposium (HGS), or others acknowledged above. The mention of trade names for commercial products does not imply the approval or endorsement by HGS.

Copyright Notice

Copyright © 2010 Highway Geology Symposium (HGS)

All Rights Reserved. Printed in the United States of America. No part of this publication may be reproduced or copied in any form or by any means – graphic, electronic, or mechanical, including photocopying, taping, or information storage and retrieval systems – without prior written permission of the HGS. This excludes the original author(s).

ABSTRACT

Earthwork factors can be a challenging parameter to determine on roadway projects, yet can have a huge impact on the cost of a project if not done correctly. Estimates that are incorrect result in additional costs associated with the need to obtain additional borrow material or dispose of surplus material. The difficulty in estimating earthwork factors increases when working in cemented and coarse-grained soils. These soils are typically hard or very dense, and commonly include gravel and cobble-sized particles which make in-place density data difficult to obtain. The majority of open-end drive samples obtained in these soils are disturbed due to the presence of cohesionless soils or the large number of SPT hammer blows required to advance the sampler. To overcome the limitations of obtaining in-situ samples and subsequently in-place densities using traditional methods, seismic geophysical methods consisting of seismic refraction and surface wave refraction microtremor (ReMi) can be utilized. AMEC used these seismic geophysical methods to determine in-place density on a recent roadway project in Arizona. The results obtained from the seismic geophysical methods were checked against values obtained from soil core samples, sand cone and nuclear test methods. The soil core samples were obtained in the deep roadway cut sections and the sand cone and nuclear test methods were obtained in the shallow roadway cut sections. The seismic geophysical methods provided reasonable estimates for in-place density when compared to the more traditional methods in the cemented and coarse-grained soils tested. These methods should be considered as an additional tool to obtain in-place densities for the development of earthwork factors.

INTRODUCTION

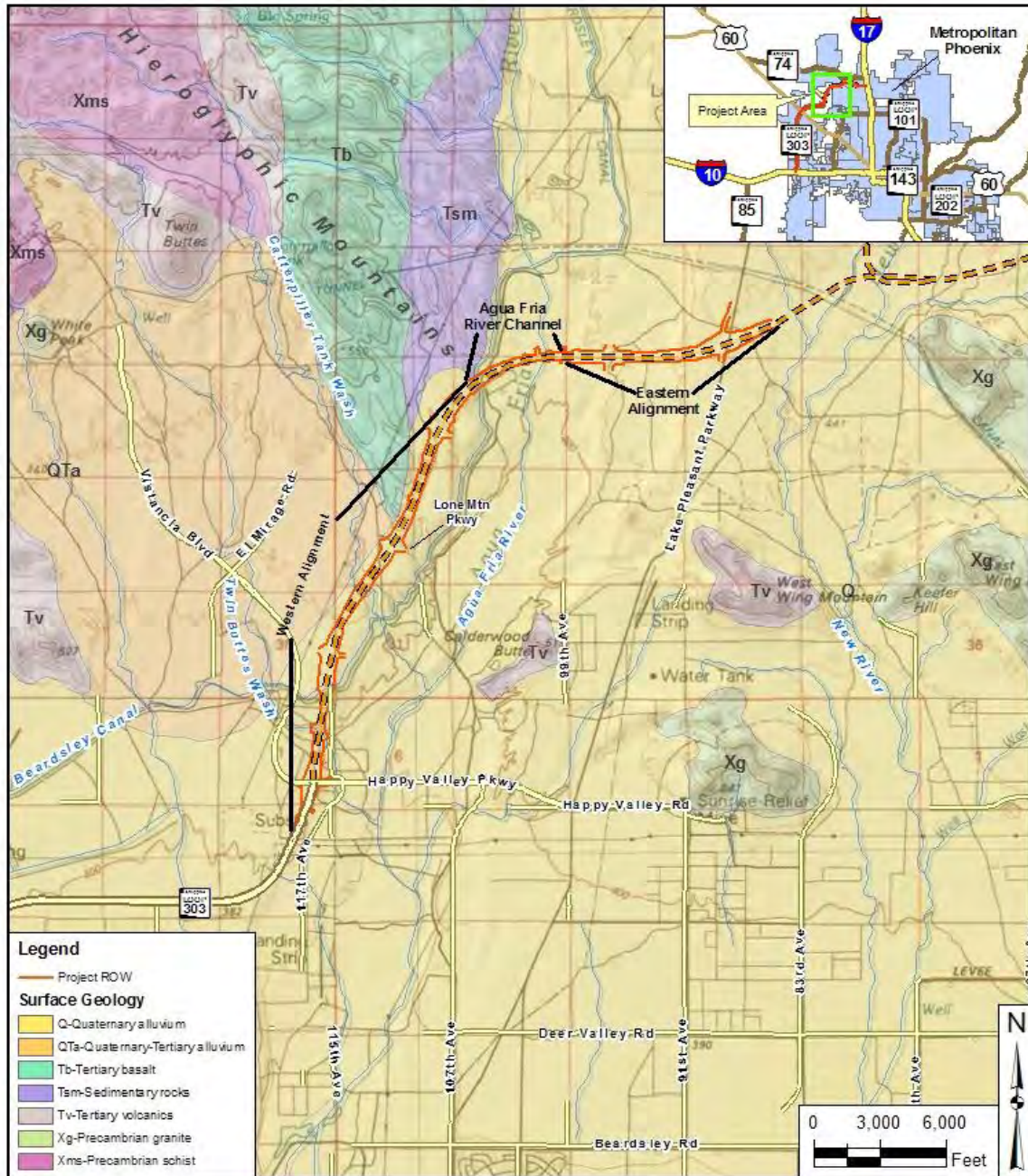
The Arizona Department of Transportation (ADOT) in association with the Maricopa Association of Governments is in the process of designing and constructing the State Route (SR) 303 Loop (approximately 39 miles) that connects Interstate 10 and Interstate 17 around the western and northern edges of metropolitan Phoenix (see the vicinity map on Figure 1). Portions of the SR 303L currently exist as two-lane roadways with the remaining segments being designed or constructed. ADOT plans to improve the SR 303L to an interim roadway generally consisting of four general purpose lanes, two in each direction of travel. AMEC Earth & Environmental was part of the design team for the Happy Valley Parkway to Lake Pleasant Parkway segment. The segment has a length of approximately seven miles beginning at the existing SR 303L, extending north-northeast for approximately four and a quarter ($4 \frac{1}{4}$) miles to the Beardsley Canal and then continuing east for approximately two and three-quarter ($2 \frac{3}{4}$) miles, crossing the Agua Fria River and Lake Pleasant Parkway. The site is predominately undeveloped native desert with sparse vegetation. The existing natural terrain slopes gently to the south by southwest and is divided by the Agua Fria River channel.

The SR 303L profile consists of elevated portions with a maximum fill embankment height of 40 feet and cut sections as deep as 55 feet (see Figure 2). The estimated amount of excavation for the project is 4.3 million cubic yards, and the estimated amount of embankment fill required is 2.6 million cubic yards. The excess 1.7 million cubic yards of material will be used during construction of a continuation segment of the SR 303L to the west. The large excavation and embankment fill volumes for the project necessitated a detailed investigation into the earthwork factors for the site soils. Local geologic material conditions across the project site dictated the feasible investigation techniques that could be used to adequately characterize the in-situ density of the site soils so an accurate estimate of earthwork factors could be obtained.

GEOLOGIC SETTING AND GEOTECHNICAL PROFILE

Regional Geologic Setting

The SR 303L from Happy Valley Parkway to Lake Pleasant Parkway is located in the northern portion of the Phoenix metropolitan area and lies within the Basin and Range physiographic province. This province typically is characterized by a series of structurally uplifted mountain blocks composed of Tertiary to Precambrian bedrock separated by intervening down dropped basins or valleys which commonly have been filled with thick sequences of Tertiary to Quaternary volcanic and sedimentary materials. The terrain in northern Phoenix consists of several uplifted mountain ranges which are separated by alluvial valleys. These mountain ranges typically trend to the NW, dip to the NE, and are composed of eroded Proterozoic and Cenozoic age rocks. The alluvial valleys are more commonly composed of Cenozoic age sedimentary rocks and surficial deposits. The project site is located southeast of the Hieroglyphic Mountains. The Agua Fria River, an active river channel, flows roughly south through the center of the project corridor. The geologic units, in relation to regional geographic features and the project area, are shown on Figure 1 (1), (2), (3).



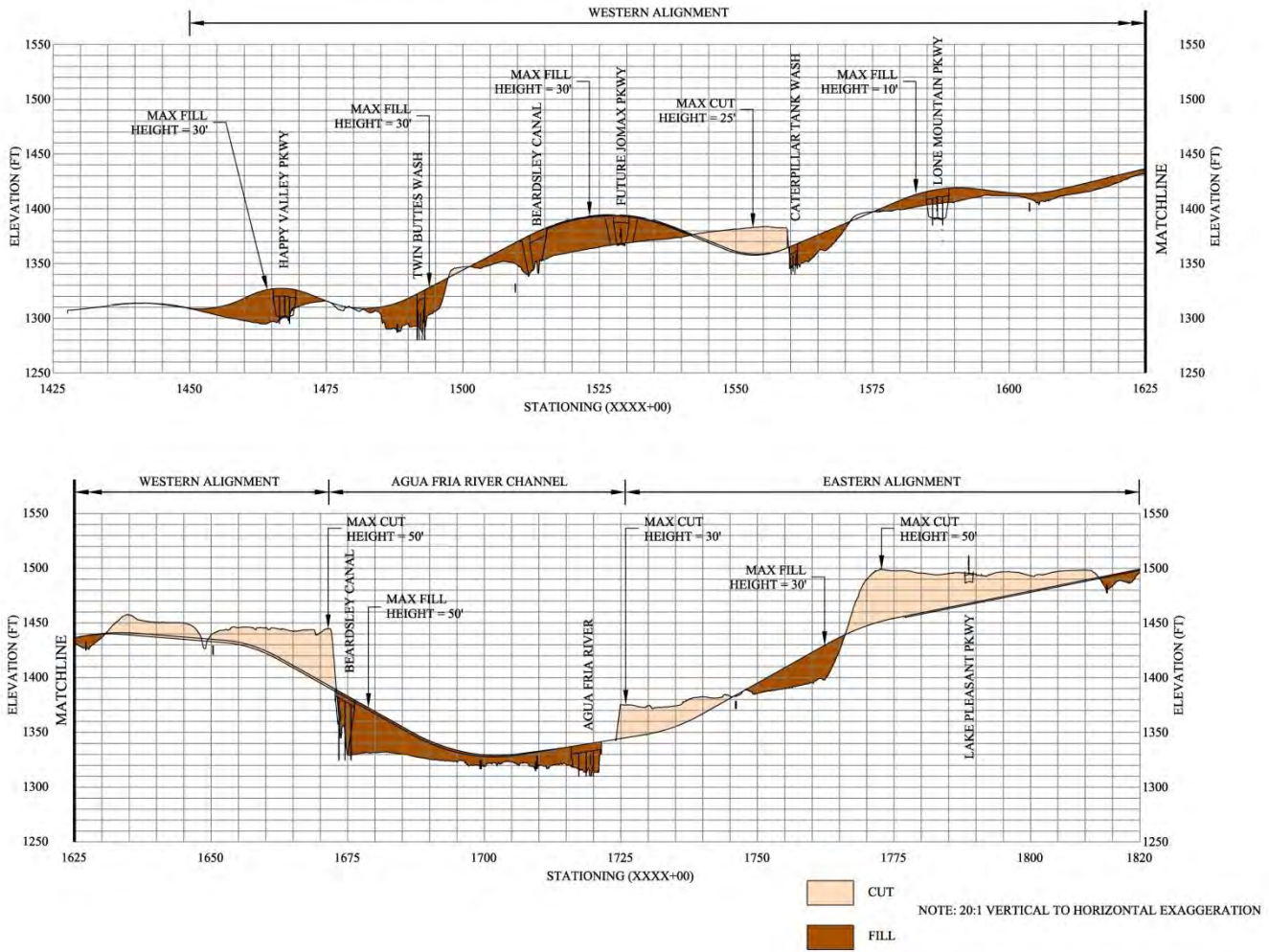


Figure 2 – Roadway Profile Showing Cut and Fill Sections

Geologic units exposed within the Hieroglyphic Mountains include Precambrian metamorphic schist (Xms) and plutonic porphyritic granite (Xg) that are overlain by Tertiary volcanic (Tv) and sedimentary units (Tsm). Volcanic rocks near the project site are dark gray, vesicular basaltic lava flows. Overlying the volcanic unit is a Tertiary sedimentary fanglomerate and sandstone unit. This sedimentary unit is exposed along the western bank of the Agua Fria River and consists primarily of consolidated to partly-consolidated, clast- and matrix-supported conglomerate with subangular clasts up to 1.5 inches in diameter. There is also a Quaternary-Tertiary alluvium (QTa) unit that flanks the bedrock units of the southern Hieroglyphic Mountains. This older alluvium unit consists of partly consolidated silt, sand, gravels, and cobbles.

The Quaternary alluvium (Q) unit in the project area consists of alluvial fan deposits and river terrace deposits of the Agua Fria River. The alluvial fan deposits are predominantly located to the northeast along the edge of the mountains and exposed in some of the larger tributaries of the Agua Fria River. They consist of stratified sand, gravel, cobbles, and boulders, with significant soil development, desert pavement, and cementation present on the oldest alluvial fan surfaces. The Agua Fria River is flanked by several stream terraces, which formed by floodplain aggradation and subsequent river incision. The terraces are generally moderately-graded, bedded gravels, cobbles, and boulders, with increasing soil development and cementation on the older terraces, each progressively more distal to and higher than the modern channel. The youngest Quaternary deposits are located within the Agua Fria River channel. These river deposits predominantly consist of sand with considerable subrounded to well-rounded gravel- to cobble-sized clasts.

Local Geologic Setting

The local geologic setting varies across the project and is broken into three areas: Western Alignment, Agua Fria River Channel and Eastern Alignment (see Figure 1).

Western Alignment

The Western Alignment area is approximately 4 ¼ miles long. It is bounded on the south by the existing SR 303L and extends north-northwest to the northern Beardsley Canal crossing. The local geologic setting of the Western Alignment is a combination of river terrace deposits from the Agua Fria River Channel and alluvial fan development from the Hieroglyphic Mountains. Portions of the project north of Lone Mountain Parkway encounter rock outcrops consisting of basalt.

Agua Fria River Channel

The Agua Fria River Channel area is defined by the historical meandering of the Agua Fria River. The historic channel is approximately one mile wide with the edges defined by steep slopes approximately 60 feet lower in elevation than the Western and Eastern Alignment sections on either side (see Figure 3). Flows in the river are intermittent and controlled by a dam less than five miles upstream. When the river does flow it flows along the eastern edge of the channel area.



Figure 3 – Steep Slope along the West Bank of the Agua Fria River Channel Area

Eastern Alignment

The Eastern Alignment area is approximately 1 ³/₄ miles long. It begins immediately west of the Agua Fria River Channel and extends to the project limits east of Lake Pleasant Parkway. This segment consists of an upper terrace located on the eastern half of the segment, and a lower terrace located on the western half.

Geotechnical Profile

The geotechnical profile varies across the projects three local geologic areas. Each of these geologic areas contain unique soil characteristics and soil strata, however, for the purpose of general discussion the soil profile is divided into three strata. Table 1 provides approximate depths for the various strata in each local geologic area.

Table 1 – Depth of Soil Strata for Local Geologic Units			
	Depth of Soil Strata (feet)		
Stratum	Western Alignment	Agua Fria River Channel	Eastern Alignment
A	0 – 3 to 10	0 – 25 (when present)	0 – 3 to 8 feet
B	> 3 to 10	< 85 to 100	> 3 to 8 feet
C	---	> 85 to 100	---

Stratum A

Stratum A consists primarily of low to medium and medium plasticity clay, clayey sand and silty sand with occasional non plastic zones. This layer is typically characterized by soils with silt/clay content over 30 percent with a silt/clay content of 55 to 90 percent in the Agua Fria River Channel section. A moderately to strongly cemented layer is observed at varying depths within Stratum A. Depending on the thickness, the cemented layer occasionally extends into Stratum B. The cemented layer is identified in isolated areas at the ground surface and to depths of 20 feet. These soils within the Agua Fria River Channel section are uncemented. Within the Western Alignment the moderately to strongly cemented soils are primarily within the upper terrace. Figure 4 shows a near surface zone of strongly cemented material with clasts of cobbles and occasional boulders.



Figure 4 – Near Surface Strongly Cemented Soil in Stratum A

Stratum B

Stratum B consists of coarse-grained soils classified predominately as sand and gravel with silt or clay; poorly graded gravel with sand; sand, gravel and cobbles; silty sand and gravel; and clayey sand and gravel with occasional boulders throughout. The soils typically have a combined percent sand and gravel content greater than 80 percent with the majority of soils having a higher gravel content. These soils are characterized as having a percent silt/clay content below 12 percent. The plasticity of these soils varies from non plastic to medium plasticity with liquid limits predominately between 20 and 50 with isolated values up to 60. These soils are predominately uncemented to weakly cemented with isolated 1 to 5-foot thick zones of

moderately to strongly cemented zones. These soils are generally characterized as hard or very dense with refusal SPT blowcounts. The Stratum B soils within the Agua Fria River Channel section are typically coarser and contain more cobbles and boulders.

Stratum C

Stratum C, only identified within the Agua Fria River Channel area, consists of predominately sand and gravel in fine-grained matrix with significant moderately to strongly cemented layers. These layers are thicker than Stratum B with some of the strongly cemented zones behaving similar to a weak rock. These weak rock zones displayed characteristics similar to a conglomerate consisting of 3- to 10-inch cobble clasts and fine-grained gravel embedded in a strongly cemented matrix (see Figure 5). Stratum C continuously produces refusal blowcounts.



Figure 5 – Weak Rock (Conglomerate) Typical of Stratum C Soils

DETERMINATION OF EARTHWORK FACTORS

Equation 1 shows the general formula for calculating earthwork factors.

$$\% \text{ Shrink} = \left[1 - \frac{\gamma_{\text{ex}}}{\gamma_{\text{emb}}} \right] 100 \quad (\text{Equation 1})$$

where:

γ_{ex} = in-situ dry density of material to be excavated

γ_{emb} = dry density of compacted embankment material

ADOT Materials Group policy determines γ_{emb} by using 95 percent of the maximum dry density obtained from the Standard Proctor test (ASTM D698).

The two variables in Equation 1, γ_{ex} , γ_{emb} , are obtained during the subsurface investigation and through laboratory testing of samples obtained during the subsurface

investigation. Of these two variables the most difficult one to calculate is γ_{ex} . The subsurface investigation must be tailored to be able to measure γ_{ex} .

SUBSURFACE INVESTIGATION

The typical subsurface investigation performed to characterize the site soils, specifically in-situ density for ADOT urban freeway projects, includes obtaining relatively undisturbed samples using open-end drive sampling (2.42-inch diameter brass rings) during drilling and measuring the in-situ density in the laboratory and/or excavating a test pit to the cut depth and performing in-situ density tests as the excavation is advanced. The test pit is excavated with safe side slopes to allow field personnel to enter the excavation and perform in-situ density tests using the nuclear method (ASTM D2922) and the sand cone (ASTM D1556) method.

The hard/very dense cemented and coarse-grained site soils are not suited to these methods. Intact open-end drive samples are difficult to obtain. The majority of these samples are disturbed due to the presence of cohesionless soils or the large number of SPT hammer blows required to advance the sampler. Test pits were not suitable for most of the project due to planned cut depths (up to 55 feet); the hardness of some of the materials (blasting was required for portions of the strongly cemented material); restricted environmental clearance due to many protected species of plants including saguaros and barrel cactus; and restrictions on ground disturbance due to the presence of culturally significant areas within the project boundaries.

To overcome the limitations of obtaining in-situ samples and subsequently in-place densities using typical investigative methods, seismic geophysical methods consisting of seismic refraction and surface wave refraction microtremor (ReMi) were utilized. AMEC has experience using these seismic geophysical methods to determine in-place density in rock environments (4, 5). The application of these methods to determine in-situ densities of soils is limited. Additional investigative methods consisting of soil cores and test pits were conducted to supplement, calibrate and increase the confidence in the seismic geophysical methods.

Additional Investigative Methods

Drilling – Soil Cores

Soil core samples were obtained from approximately every third roadway boring in the cut sections using a track-mounted Burley 2500 using a HQ size, wireline, diamond bit, rock coring system. The HQ core system produces 2.50-inch diameter core and a 3.78-inch diameter borehole. In general, the soil cores remained intact in the fine-grained cohesive and cemented soils, but not in the coarse-grained cohesionless soils (see Figure 6). Laboratory density tests were performed on the intact core samples. Therefore, it was difficult to obtain the in-situ density of the uncemented coarse-grained cohesionless soils using this method.

PROJECT		State Route 303 Loop		Happy Valley Parkway to Lake Pleasant Parkway	
JOB NO.		7-117-001016	DATE	1-9-08	
RIG TYPE		Burley 2500 Track-mounted			
METHOD		HQ Wireline Coring			
OPERATOR		CRUX			
LOGGED BY		SVH			
LOCATION		Sta. 1546+52, 58' L			
		State Route 303L			
ELEVATION		1383'			
DATUM		Aztec Basemap			
INCLINATION		Vertical			

Boring Operation and Drill Rate (min/feet)	Depth in Feet	Sample Type	Unconfined Compression or Point Load Index Test (psi)	% Core Recovery	% Drilling Fluid Rec.	Rock Quality Designation (RQD)	DISCONTINUITIES										Condition	Bedding and/or Fabric	Weathering or USCS (Soils)	Rock Type & Remarks
							Spacing					Orientation								
							1	2	3	4	5	H	45	V						
1/9 HQ4.0	0	HQ		90	100	N/A										N/A	N/A	SC	CLAYEY SAND, trace of fine grained, subangular to subrounded gravel, predominantly fine to medium grained, subangular to subrounded sand, weakly to moderately cemented, low to medium plasticity, white, light brown to gray	
4.1		HQ		95													SM			
	5																	GP	SILTY SAND WITH GRAVEL, some fine grained, subangular to subrounded gravel, predominantly fine to medium grained, subangular to subrounded sand, strongly cemented, low plasticity to nonplastic, white & gray note: 4" diameter cobbles below 3.5'	
	3.3	S		N/A																
	7.7	HQ		75														note: predominantly medium to coarse grained, subangular to subrounded sand below 5.5' note: uncemented below 6.0'		
	3.0	HQ		95																
	10																	GRAVEL WITH SAND, trace of 3.5" diameter cobbles, predominantly fine grained, subangular to subrounded gravel, predominantly medium to coarse grained, subangular to subrounded, nonplastic to low plasticity, gray & brown note: SPT blow count of 50/5" at 5.3' note: weakly cemented below 10.0' note: silty to clayey sand zones from 10.0' to 20.0' note: SPT blow counts of: 50/3" at 10.3', 50/1" at 15.3' note: SPT blow counts of: 50/3" at 20.3'		
	5.0	S		N/A																
	4.0	HQ		0																
	15																			
	3.3	HQ		50																
	4.1	S		N/A																
	3.3	HQ		30																
	20	HQ		95																
		S		N/A																



GROUNDWATER		
DEPTH (ft)	HOUR	DATE
	none	

BORING OPERATION
 B - BDBGM 2" O.D. Wireline Rock Coring
 BWC - B-size casing
 HQ - 3.78" O.D. Wireline Rock Coring
 NQ - 2.8" O.D. Wireline Rock Coring
 S - 2" O.D./1.38" I.D. Tube Sample
 D - Disturbed Bulk Sample

LOG OF TEST BORING NO. B-030

Figure 6 – Typical Core Log with Photographs of Soil Cores

Test Pits

Test pits were excavated using a CAT 345C in the planned Jomax Road retention basin to approximately 20 feet. In-situ density tests were performed as previously described and representative bulk samples were taken at various depths from these test pits. The test pit log, including a photo of the test pit, is shown in Figure 7.

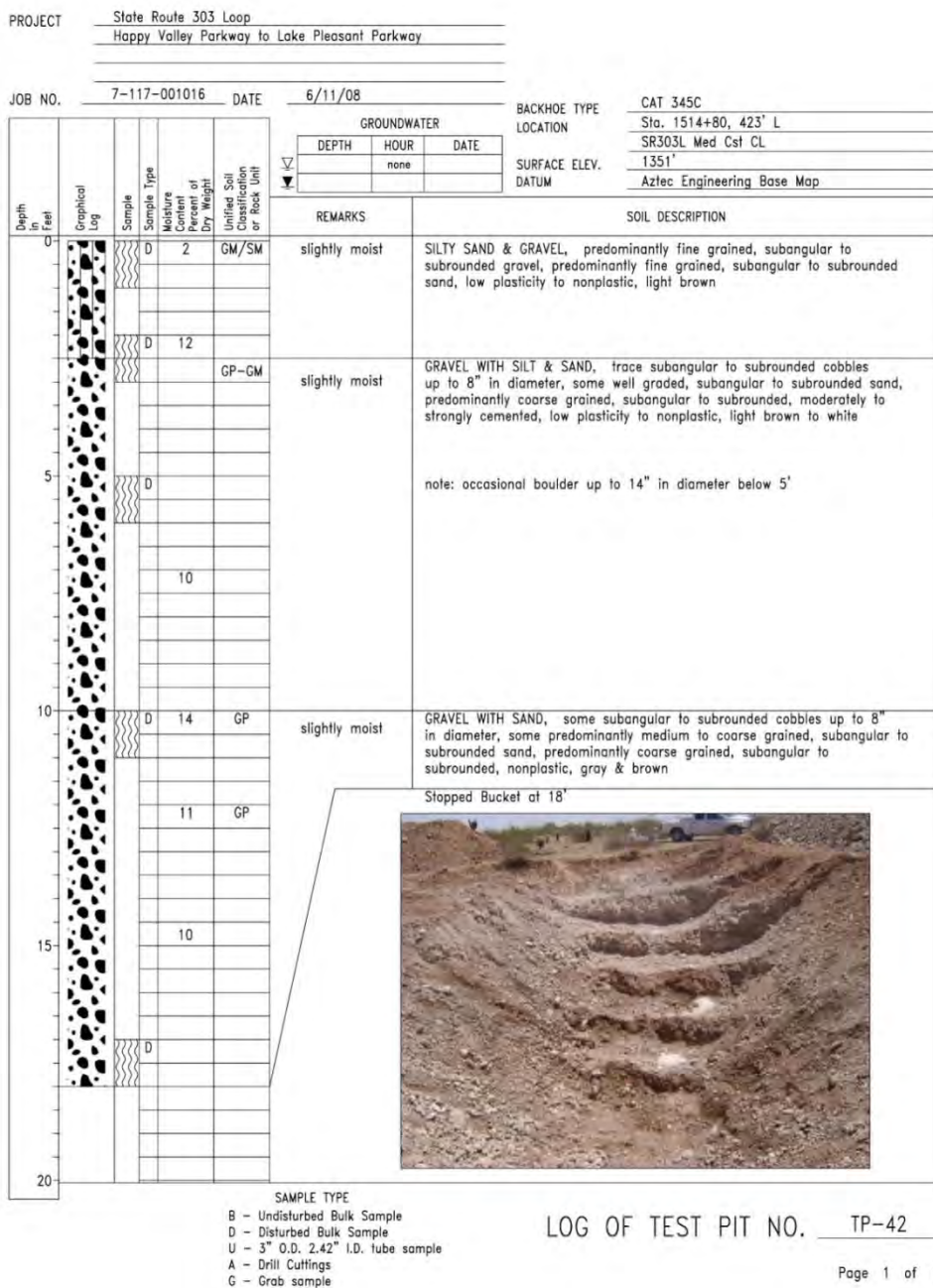


Figure 7 – Test Pit Log and Photograph of Large Test Pit Excavation with Benches

Surface Seismic Investigations

Surface geophysical methods, consisting of seismic refraction and surface wave refraction microtremor (ReMi) were used to obtain compression wave (p-wave) and shear wave (s-wave) results, respectively. Refraction seismic surveys were completed using a Smartseis SE-12 12-channel signal enhancement seismograph and a 12-geophone array with 10-foot spacing between geophones. A sledgehammer energy source was used to collect compression wave (p-wave) data and jumping beyond the end geophone array was performed to generate surface wave energy for shear wave (s-wave) data.

DETERMINATION OF IN-SITU DENSITY OF EXCAVATED SOIL

The determination the in-situ density for the cemented and coarse-grained soils from soil cores and test pits was previously described. The determination of in-situ density from the surface seismic investigation is more complex and an in-depth discussion of this procedure is beyond the scope of this paper. A brief overview of the process is as follows: The surface seismic investigation measures the velocity of compression and shear waves as they pass through the soil. The elastic modulus of the soil is obtained using established calculations between seismic velocity and soil elastic modulus. The elastic soil modulus is related to soil density through the soil porosity based on percolation theory. Figure 8 shows the relationship between seismic velocity (p-wave and s-wave) and dry density (6). Figure 8 presents two curves one for chemical gels and one for physical gels. Cohesionless granular materials and fractured material masses behave as physical gels while unfractured cemented, cohesive or welded soils behave as chemical gels. A complete discussion of the procedure for developing the relationship between seismic velocities and dry density, and percolation theory is published elsewhere (6).

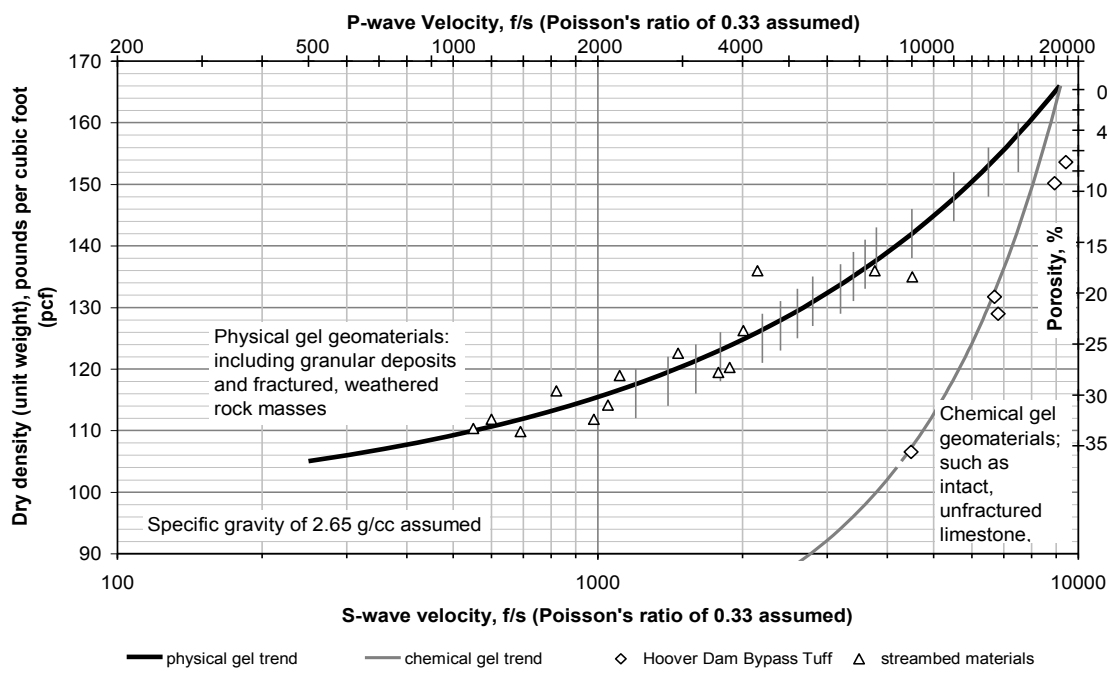


Figure 8 – Relationship between Seismic Velocity and Dry Density (6)

COMPARISON OF THE VARIOUS METHODS TO MEASURE IN-SITU DENSITY

Sand Cone and Nuclear Test Methods versus Seismic Geophysical Methods

A test pit was excavated within the footprint of the planned Jomax Retention Basin located west of Jomax Ramp A within the Western Alignment area. In-place densities were obtained using sand cone and nuclear test methods. Sand cone density test results were rock-corrected in accordance with procedures presented in ASTM D1556. Prior to excavating the test pit compression and shear wave velocities were measured while conducting a refraction seismic line across the planned test pit. In-situ densities were obtained from the seismic velocities using the correlation previously discussed.

Depth	USCS Soil Classification ¹	Degree of Cementation	Dry Density (pcf ²)		
			Sand Cone Method	Nuclear Method	Seismic Methods
0	GM/SM	Uncemented	104.2	103.5	108.9
2.5	GP-GM	Uncemented	93.0	96.4	108.9
5	GP-GM	Moderately to Strongly	---	101.1	128.0
7.5	GP-GM	Moderately to Strongly	81.5	127.5	128.0
10	GP	Weakly to Moderately	102.4	111.1	128.0
12.5	GP	Uncemented	102.3	116.1	117.8
15	GP	Uncemented	111.8	112.2	117.8
17.5	GP	Uncemented	---	113.8	117.8

Notes: ¹Unified Soil Classification System classification

²pounds per cubic foot

The soils encountered in the test pit were coarse-grained with cementation varying from uncemented to strongly cemented. The test data indicates that the presence of cementation results in a decrease in the in-situ densities measured using the sand cone and nuclear methods. The cemented soils make it difficult to advance the probe for the nuclear gauge or advance the hole for the sand cone resulting in disturbing the surrounding soil, which results in loosening of the soils and/or creating a void around the nuclear gauge and subsequently decreases the measured in-situ density. In-situ densities measured using the nuclear method compared favorably to the results of the seismic methods.

The sand cone method varied greatly in the coarse-grained soils. This result was expected based on ASTM D1556, which indicates that the sand cone test may not be suitable for soils containing appreciable amounts of coarse material larger than 1.5 inches. The material encountered in large test pit had a significant percentage of gravel, with the majority of the soils having greater than 35 percent. Furthermore, the maximum particle sizes exceed 3 inches. These conditions made sand cone testing unreliable below 3 feet.

Soil Cores versus Seismic Geophysical Methods

Sixty-one in-situ density tests were completed on soil cores obtained from 13 different borings. Seismic geophysical methods were conducted at each boring location. The measured in-situ densities were averaged based on the soil classification the results are presented in Table 3.

USCS Soil Classification ¹	Average Dry Density (pcf ²)		Difference in Average Dry Density (pcf)
	Soil Cores	Seismic Methods	
GC	117.0	109.5	7.4
GM	116.2	113.0	3.2
GP	134.8	125.7	9.1
GP/SP	130.2	124.0	6.2
GP-GC	139.8	117.5	22.3
GP-GM/SP-SM	122.6	120.7	1.9
ML/SM	107.2	102.8	4.4
SM/SP-SM	102.2	103.8	-1.6
		Average Difference³	4.4

Notes: ¹Unified Soil Classification System classification

²pounds per cubic foot

³Average difference did not include value for GP-GC soil due to the large variance

The average difference in dry density of 4.4 pcf presented in Table 3 indicates close agreement between the soil cores and the seismic methods for both cemented and coarse-grained soils. The in-situ densities obtained from the soil cores were, on average, 4.4 pcf greater than values obtained from seismic methods. A reasonable explanation for this is that soil core densities could only be completed on intact samples, which one would expect to have higher values. The seismic geophysical methods take into account the entire mass and would be expected to trend lower.

DETERMINATION OF DENSITY OF COMPACTED EMBANKMENT MATERIAL

The density of compacted embankment material can be determined using the maximum dry density of the soil obtained from the Standard Proctor laboratory test. This method is viable when a representative sample can be obtained. The investigation in the deep roadway excavation areas used percussion hammer drilling techniques, which are typically used in cemented and coarse-grained soils, coring and seismic geophysical methods. Soil samples obtained using the percussion hammer method could not be used because the drill bit pulverizes the soil breaking it down into very small pieces that are no longer representative of the soils to be excavated. The seismic geophysical methods do not obtain any samples for testing. Therefore, the only soil samples available for this project were from the soil cores. The density of the compacted embankment fill for all methods was based on the results from the soil cores. Therefore, the variations in earthwork factors determined for each method are similar to the variation in measurements of in-situ density.

An alternative to the laboratory test method is measurement of the in-situ density of existing roadway embankment fills using seismic geophysical methods. This is commonly done on projects where existing roadways are being improved. Unfortunately, this method was not viable for the current project due to the relatively undisturbed native desert environment that didn't have any existing roadway embankments.

CONCLUSION

In-situ density data obtained using the seismic geophysical methods were checked against values obtained from soil core samples, sand cone and nuclear test methods. In-situ densities measured using seismic geophysical methods compared favorably to in-situ densities measured from soil cores on both cemented and coarse-grained soils. Comparison of the seismic geophysical methods to sand cone and nuclear methods was difficult due to the large amount of data from the sand cone and nuclear methods that was deemed invalid. However, the data obtained from the sand cone and nuclear methods that were reasonable compared favorably to the seismic geophysical methods.

The true test for suitability of predicted earthwork factors comes during construction. The contractor for the SR 303L project has completed the majority of the earthwork activities and there have been no disagreements on earthwork quantities. In fact, the contractor was complimentary on the level of detail provided in the geotechnical report and on the depth of study on earthwork factors provided in the report. Based on the close correlation between the various methods and the successful project construction seismic geophysical methods should be considered as an additional tool to obtain in-situ densities in cemented and coarse-grained soils for the development of earthwork factors.

REFERENCES:

- 1 Huckleberry, G., 1995,** Geology of the Lower Agua Fria River, Lake Pleasant to Sun City, Maricopa County, Arizona, Arizona Geological Survey Open File Report 95-5, 32 p., 2 sheets, scale 1:24,000.
- 2 Reynolds, S. J., and Grubensky, M. J.,** Geologic Map of the Phoenix North 30' x 60' Quadrangle, Central Arizona, Arizona Geological Survey Open File Report 93-17, scale 1:100,000, 1993.
- 3 Wahl, S.J., Reynolds, S.J., Capps, R.C., Kortemeier, C.P., Grubensky, M.J., Scott, E.A., and Stimac, J.A.,** Geologic Map of the Southern Hieroglyphic Mountains, Central Arizona, Arizona Geological Survey Open File Report 88-1, 6 p., 1 sheets, scale 1:24,000, 1998.
- 4 Rucker, M. L. Percolation Theory Approach to Estimating Earthwork Factors in Weathered Granites. In *49th Highway Geology Symposium Proceedings*, Prescott, Arizona. 1998, pp. 421-430.
- 5 Rucker, M.L. Estimating Earthwork Factors for Roadcuts using Surface Geophysics. *Proceedings of the Fourth North American Rock Mechanics Symposium Narms 2000*. A.A. Balkema/Rotterdam/Broofield, 2000, pp. 709-714.
- 6 Rucker, M.L., Estimating In-situ Geo-material Mass Density, Modulus and Unconfined Compressive Strength from Field Seismic Velocity Measurements, In *Highway Geophysics-Nondestructive Evaluation Conference*, Charlotte, NC, Dec. 1-4, 2008.

Geophysical Methods to Map Subsurface Evaporite Features to Aid Roadway Geometric Design

Mike Homan, P.E.

Terracon Consultants, Inc.
10930 East 56th Street
Tulsa, OK 74146
(918)-250-0461
mhhoman@terracon.com

Phil Sirles

Zonge Geosciences, Inc.
1978 South Garrison Street, Suite 3
Lakewood, Colorado 80227
(720) 962-4444
phils@zonge.us

Justin Rittgers

Zonge Geosciences, Inc.
1978 South Garrison Street, Suite 3
Lakewood, Colorado 80227
(720) 962-4444
justinr@zonge.us

Disclaimer

Statements and views presented in this paper are strictly those of the author(s), and do not necessarily reflect positions held by their affiliations, the Highway Geology Symposium (HGS), or others acknowledged above. The mention of trade names for commercial products does not imply the approval or endorsement by HGS.

Copyright Notice

Copyright © 2010 Highway Geology Symposium (HGS)

All Rights Reserved. Printed in the United States of America. No part of this publication may be reproduced or copied in any form or by any means – graphic, electronic, or mechanical, including photocopying, taping, or information storage and retrieval systems – without prior written permission of the HGS. This excludes the original author(s).

ABSTRACT

Surface sinks, distressed highway sections, voids and evaporite bedrock with variable weathering have complicated highway design for the Oklahoma Department of Transportation (ODOT) in western Oklahoma. ODOT contracted with Terracon Consultants and Zonge Geosciences to collect approximately 45,000 linear feet of Direct Current Electrical Resistivity Imaging (ERI) data along Highway US-412 in Major County near Woodward, Oklahoma. The data was collected, using the Dipole-Dipole technique, to aid the design and construction efforts by identifying and discriminating between sections of highway underlain by solid gypsum or gypsum containing voids (resistivity > 1000 ohm-meters) and sections containing combinations of claystone and weathered gypsum (resistivity <100 ohm-meters).

Initial geophysical results were used to locate 18 confirming borings and identify the need and locations of additional geophysical testing. Borehole data correlated with the resistivity models and allowed for the assignment of resistivity ranges to specific lithologies which became the basis of all data interpretation for the geophysical survey.

The results presented here show that ERI offers an accurate and cost-effective approach to mapping lateral and vertical variations in material properties that can be directly associated with lithology. This can help alleviate common issues confronted when making geologic interpretations based on limited data from widely spaced borings. Two useful generalizations can be drawn about this specific project: 1) the highest values of resistivity more often correlate with gypsum hosting numerous smaller (0.5-1.5 feet diameter) voids than with large voids, and 2) large sections of the surveyed area (several 1,000s of feet) along US-412 are underlain by clay, weathered gypsum and gypsum-clay as confirmed by the borings, and will not likely pose many issues with regards to required mitigation efforts.

In summary, the ERI geophysical technique, as confirmed by the borings, successfully separated the sections of highway into distinct areas underlain by claystone and weathered gypsum and sections with gypsum dissolution features requiring different mitigation tactics. Success of the geophysical program can be related to a well integrated geologic, geotechnical and engineering program where ODOT, Terracon and Zonge personnel worked closely together to assess the subsurface data.

The results of the geophysical survey and boring program are being used in the final roadway design process to minimize the potential of sinkholes or caverns and the resultant impact on the new roadway construction. With the ERI and boring results delineating between those areas having gypsum rock and those areas not having gypsum rock, the design team has been able to focus attention on those portions of the alignment with existing or potential solution cavities. Thus, the design challenge is now on horizontal and vertical alignment of the highway and minimizing cut depths into the subsurface profiles that have gypsum rock and minimizing water seepage into the ground in those same areas.

INTRODUCTION

ODOT wants to modify both the vertical and horizontal alignment of two portions of US-412 in Major County, Oklahoma. The highway alignment areas include a section which extends from the Major/Woodward County Line eastward approximately 10,110 feet and a second section which extends from approximately 2,325 feet east of the US-412 and US-281 Junction, eastward approximately 9,000 feet (Figure 1).

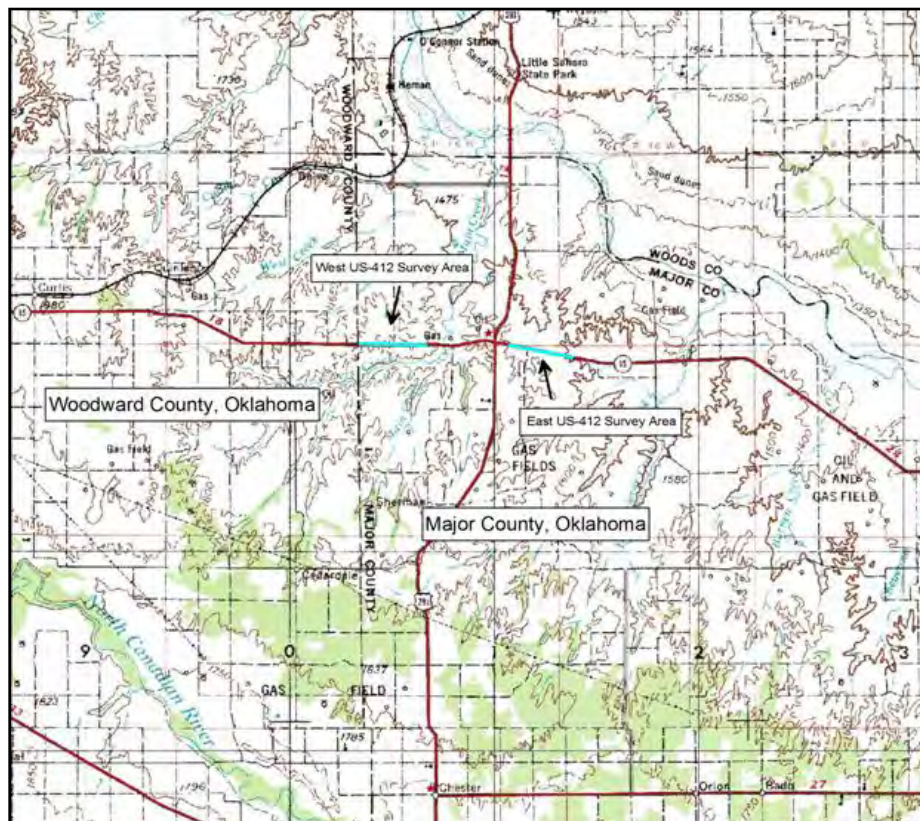


Figure 1, US-412 Study Areas

Initially, the goal was to increase capacity by changing the highway from two-lanes to four-lanes. Along the western section of the study area, the two new lanes were to be offset to the north of the existing lanes. The eastern section of highway alignment was planned to include two new lanes south of the existing highway. Sight distance requirements required the design of deep cuts and fills.

This part of western Oklahoma is characterized by surface sinks, distressed highway sections, voids and exposed evaporate bedrock with variable weathering, which, historically, have been shown to impact the long-term performance of highway projects. Large systems of caverns are known to exist in this part of Oklahoma, with at least one known cave extending beneath US-412. As rainwater and groundwater run through fractures in the rock and between rock layers, dissolution of gypsum results in widening fractures, weakened sections of highly weathered material, large caverns and sinkholes due to the removal of materials that previously supported overlying rock and soils.

A geophysical survey program was designed for this project with the intent to map the lateral and vertical extents of the gypsum units associated with the dissolution features to help ODOT mitigate possible adverse impacts on the planned highway expansion projects. Terracon Consultants, Inc. (Terracon) teamed with Zonge Geosciences, Inc. (Zonge) for electrical resistivity (ER) geophysical surveying. In addition to the geophysical surveying, 18 borings were drilled to calibrate, or “ground-truth”, the geophysical results to physical subsurface conditions and to provide geotechnical information for design and construction of both cuts and fills along the highway alignment.

ER surveying is a geophysical technique which measures the electrical resistivity of the subsurface which is then correlated to subsurface geology and structure as determined with geotechnical borings. ER surveying employs two electrode pairs, one pair providing the electrical source (current electrodes) while the second pair measures the electric potential between the electrodes (measurement electrodes). Once measurements are obtained, they are processed to account for the array geometry (electrode arrangement) and other factors associated with data acquisition (e.g., topography, culture, etc.). Finally, mathematical inversion of an entire data set is performed, and the result is a two-dimensional (2D) earth model of the subsurface electrical resistivity structure; or, an electrical cross-section. Information obtained from boreholes is then used to correlate resistivity structure to lithologies and geologic structure.

Work for this project included:

- Field reconnaissance
- ER geophysical surveying along two lines at both US-412 projects
- Evaluation of preliminary geophysical results
- Consultation with ODOT to select additional ER survey and geotechnical confirmation boring locations
- Additional ER surveying
- Drill confirmation borings
- Synthesize ER and boring information into comprehensive geological interpretation

SITE GEOLOGY

Based on information published in the ODOT manual, “Engineering Classification of Geologic Materials, Division Six”, the project sites are underlain by two geologic units.

The Flowerpot Unit consists predominantly of reddish-brown, blocky, silty clay shale with a few thin sandstone, siltstone, and dolomite beds. Topographically, the Flowerpot Unit generally forms broad flats and gently rolling hills. The upper portion forms the steep slopes of scarps and buttes capped by gypsums of the overlying Blaine Unit.

The Blaine Unit consists of three prominent gypsum beds separated by red-brown shales which are locally gypsiferous. Topographically, the Blaine Unit forms the most pronounced

escarpments in western Oklahoma. The thick gypsum beds form ledges that extend the entire length of the outcrop of the Blaine Unit.

Underlying the resistant gypsums of the Blaine Unit are the weakly resistant shales of the Flowerpot Unit. The shales erode much faster than the gypsums, thus leaving an escarpment that is several feet higher than the near level terrain of the Flowerpot Unit. Isolated buttes and highly dissected canyons are common along the outcrop contact of the two units.

Of particular concern to the design and construction of the upgrades to US-412 is the excavatability of the Blaine Unit and the fact that the gypsum is prone to formation of dissolution cavities when exposed to flowing water.

GEOPHYSICAL SURVEYS

Knowledge of the subsurface material properties is critical to the engineering and construction phases of any highway project. The gypsum formations and dissolution caverns that extend beneath the highway in this part of the State extenuates the need for a more detailed, or continuous, analysis of the subsurface stratigraphy along the highway alignment.

Field Reconnaissance

The field reconnaissance included visual observation of the geophysical survey areas via vehicle and foot. Using direct observation, geologic maps, topographic maps, and aerial photos, areas that could potentially contain subsurface voids, such as those shown in Figure 2, were identified. Additionally, land access, potential worker safety, and general project logistics/coordination concerns were identified and addressed.



Figure 2, Small Surface Void in Cut Section of HW-412

Electrical Resistivity Survey

The ER geophysical survey design for the US-412 projects (West Section and East Section) included initially acquiring ER data along two lines, one located along the approximate new road alignment, and one located adjacent to the existing roadway (Rittger, et. al, 2008). For the US-412 West Section, ER data was collected along the existing roadway and approximately 150 feet north along the planned new roadway alignment. For the US-412 East Section, ER data was collected along the existing roadway and approximately 150 South along the planned road alignment.

The geophysical technique utilized for this project's ER survey is referred to as the Double-dipole, or more commonly, the dipole-dipole technique (Telford et. al., 1976). As shown in Figure 3, in the dipole-dipole electrode configuration, a controlled electrical signal is transmitted into the ground via a grounded dipole consisting of two current electrodes (A and B). At varying distances from the midpoint of the current dipole, the electrical potential drop is measured and recorded at a different grounded dipole, called a receiver or potential dipole (M and N). This potential difference measured by the receiver dipole is due to the electric field created by the source current dipole. For this survey, an axial (or polar) dipole configuration was used, where the receiver dipole is in-line with the transmitter dipole (Al'pin, 1966).

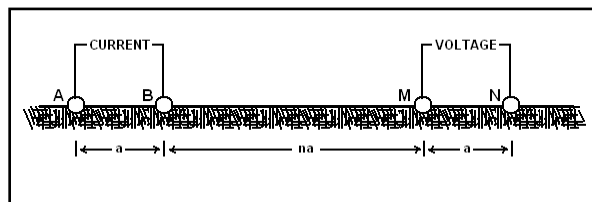


Figure 3, electrode configuration for the dipole-dipole DC resistivity technique

Both the current and potential dipoles have two electrodes with constant spacing, referred to as the “a” spacing, and the distance between the transmitting and receiving dipoles is varied by multiples of “a”. Here, “n” is normally an integer value between 1 and 6. For this survey, an a-spacing of 20 feet was used.

The main material property of earth materials measured by electrical methods is resistivity (ρ), which is the reciprocal of conductivity (σ). Electrical resistivity is a quantitative measure of how difficult it is to send current through a material.

Variations in subsurface porosity, fluid content, fluid chemistry, permeability and soil or rock type all affect resistivity measurements. Cultural features (i.e., man-made items) such as fencing, power lines, and pipelines can also significantly affect resistivity measurements if not properly insulated from the ground or adequately avoided.

Ohm's Law states that the ratio of the measured potential drop across the receiver dipole (M and N) to the measured output current across the transmitter dipole (A and B) yields the apparent resistivity (ohm-meters) at a certain point below the array.

Apparent resistivity is an average value for the non-homogeneous volume sampled by each measurement, and does not necessarily represent the true resistivity of earth materials at a certain lateral location or depth (Abraham, et al., 2004). This is the raw data to be modeled in order to obtain a true resistivity model of the earth below the dipoles.

As depicted in Figure 4, each measured and calculated apparent resistivity value is plotted at the center-point (or station) between the two dipoles and at a depth equal to the “n” value to create a pseudo-section. The pseudo-section is a generalized way to plot data coverage and quickly detect major anomalous readings prior to processing.

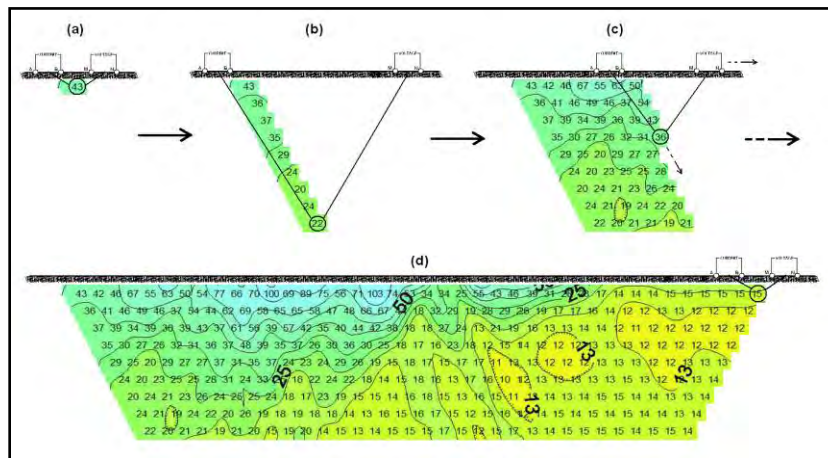


Figure 4, Sequence of data collection in a dipole-dipole ER survey

The instrumentation used to perform this geophysical survey was the Zonge Electrical Tomography Acquisition (ZETA) system produced by Zonge Engineering and Research Organization, Inc.

The first order of business in developing the field program was to optimize the data quality by testing various station spacing, electrode setup, currents, and filters. The optimization process resulted in an ER station spacing of 10 feet. There is an inherent balance between station spacing, depth of investigation, and lateral resolution. Larger station spacing would result in deeper depth of investigation but at a loss of lateral resolution. Preliminary field testing indicated that 10 feet spacing would provide a nominal depth of investigation of 60 feet or greater while maintaining good resolution of expected anomalies.

Production mode ER data collection was conducted immediately after parameter optimization. Initially, ER data was collected along 38,220 feet of test alignment. Relative elevations were recorded at every station (electrode) using a hand level and stadia-rod, and these elevations were converted to absolute elevations via tying to survey marks.

After preliminary processing and interpretation, Terracon and Zonge met with ODOT to review the results, identify areas for additional ER data collection, and identify confirmation borehole locations. Fifteen locations were identified as areas requiring additional ER geophysical surveying. These areas were typically selected because potential horizontal highway

alignment reconfiguration would bring the new alignment outside the boundaries of the initial survey or to further track a potential karst feature that was identified in the initial survey.

Additional ER geophysical surveying was conducted, resulting in collection of an additional 6,580 feet of ER data. The more focused additional ER surveying was conducted along approximately 34% of the 19,110 feet of highway alignment.

During ZETA data acquisition, multiple waveforms are stacked and averaged to reduce random noise in the data blocks. All data blocks are repeated at least twice to establish data repeatability. All individual blocks are recorded and saved digitally, along with standard error of the mean (SEM) values. The receiver operator monitors data quality in the field, and contact resistance issues are resolved and data acquisition is repeated if necessary. Data quality for this project ranged from fair to excellent with respect to SEM and block repeatability for ZETA.

Processing for ER data acquired using the ZETA system was performed using proprietary software developed by Zonge.

Smooth-model inversion mathematically back-calculates (or inverts) from the measured data to determine a likely distribution of true resistivity values. Comparison of the observed field data and the calculated pseudo-section plots is a useful method for evaluating how well the mathematical model fits the observed data. The results of the smooth-model inversion are intentionally gradational, rather than showing abrupt, blocky changes in the subsurface. The inversion results should not be considered a unique solution, and some ambiguity remains in any mathematical representation of the data. Confidence in any interpretation increases with corroborating information.

Confirmation Borings

Preliminary ER results were reviewed by Zonge, Terracon, and ODOT to determine boring locations to assist in the interpretation of the geophysical data. The objective of the geotechnical boring program was to provide geophysical ground-truthing and to provide preliminary geotechnical information for the planned road construction. The geophysical ground-truthing involves correlating lithology and geotechnical information obtained from the boreholes to the ER results. The geotechnical information includes standard penetration value (N) for soils and percent recovery (REC) and rock quality designation (RQD), compressive strength, and elastic modulus (E) values for rock cores.

The boreholes were advanced using rotary wash methods with both truck-mounted and all-terrain drilling vehicles. Representative soil samples were obtained by the split barrel sampling procedure in accordance with the appropriate ASTM designation. Rock cores were obtained with a standard diamond-bit, double-barrel, core-barrel.

The soil and rock core samples obtained were logged for lithology (and/or lack of lithology if voids were encountered). Table 1 shows the locations and results of the geotechnical borings.

Confirmation/Geotechnical Borehole Locations ODOT Major/Woods County Geophysical Survey				
No.	Location	Purpose	Completion Depth (feet)	Comment
WEST AREA				
B-1	54+500 (150' North)	Geotech	40	
B-2	54+810 (150' North)	Void and Geotech	25	Void Detected 11 to 13', then small voids to 14' bgs
B-3	55+017 (150' North)	Void and Geotech	38	Voids Detected between 22-24, 25-26 and 28-35' bgs
B-5	55+210 (85' North)	Void and Geotech	40	Small Voids between 15-22' bgs, water loss @ bgs
B-6	55+290 (20' North)	Void and Geotech	40	Small Voids @ about 22.5' bgs, water loss @ 9.5' bgs
B-7	55+450 (146' North)	Void and Geotech	44	
B-8	55+720 (150' North)	Void and Geotech	36	Small Void @ 9.5' bgs, water loss @ 9.5' bgs
B-10	55+850 (75' North)	Void and Geotech	30	Water loss @ 14' bgs
B-9	56+035 (150' North)	Void and Geotech	42	Water loss @ 4.5'
B-11	56+520 (85' North)	Void and Geotech	35	Voids from 32-33.5' bgs
B-12	56+680 (150' North)	Void and Geotech	50	
EAST AREA				
B-13	2046+050 (150' South)	Void and Geotech	36	Water loss @ 12.7' bgs
B-14	2047+000 (85' South)	Void and Geotech	34	Small Voids 19-21' bgs, water loss @ 21' bgs
B-15	2050+047 (150')	Void and Geotech	13.5	Abandoned Due to Void @ about 13.5' bgs
B-15A	2050+050 (150')	Void and Geotech	64	
B-16	2070+050 (150')	Void and Geotech	45	
B-17	2079+000 (150')	Void and Geotech	55	Small Voids from about 42' bgs

Table 1, Geotechnical Boring Locations and Findings

Geological Interpretation

After the 18 borings were completed, correlations were made between lithology as determined from the geotechnical borings and calculated resistivity values in the final models. This allowed for the assignment of a range of resistivity values expected for a given lithology. The three main materials encountered in the 18 borings were: 1) clay and clay/weathered-gypsum mixtures, 2) gypsum, and 3) large voids and highly fractured gypsum with many small voids.

Once ground-truthing of the models was complete, the ranges of resistivities within a given material were plotted, and are presented on Figure 5.

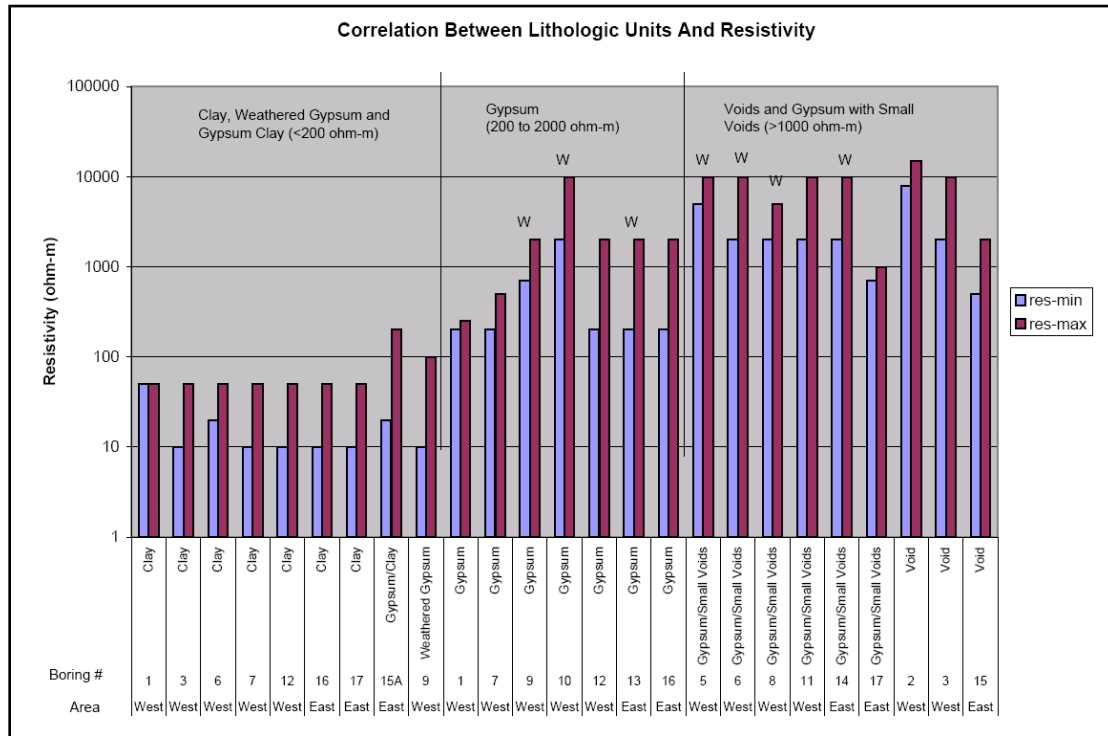


Figure 5, Correlation Between Lithologic Units and Resistivity

Each of these three material types correspond to a range of resistivities, and a unique color was assigned for each range on the color scale shown in Figure 6. This color scale was used for all final models, and it became the foundation of all interpretations for this project. The letters “C” and “G” and “V” were annotated on the color scales of all final models to indicate the interpreted lithologies.

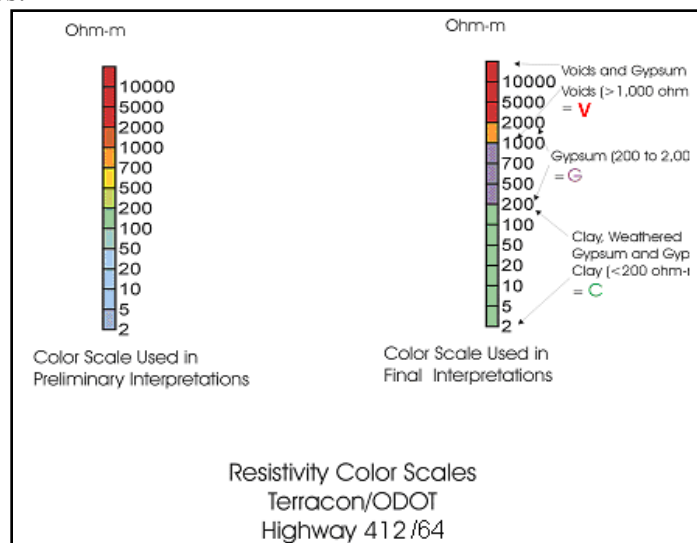


Figure 6, Resistivity Color Scales

The final interpretation of the geophysical data and geotechnical borings were presented in 2D figures (electrical cross-sections), such as shown on Figure 7. These figures offer a pictorial representation of the boundaries of materials with potential karst features and those of clay and weathered shale.

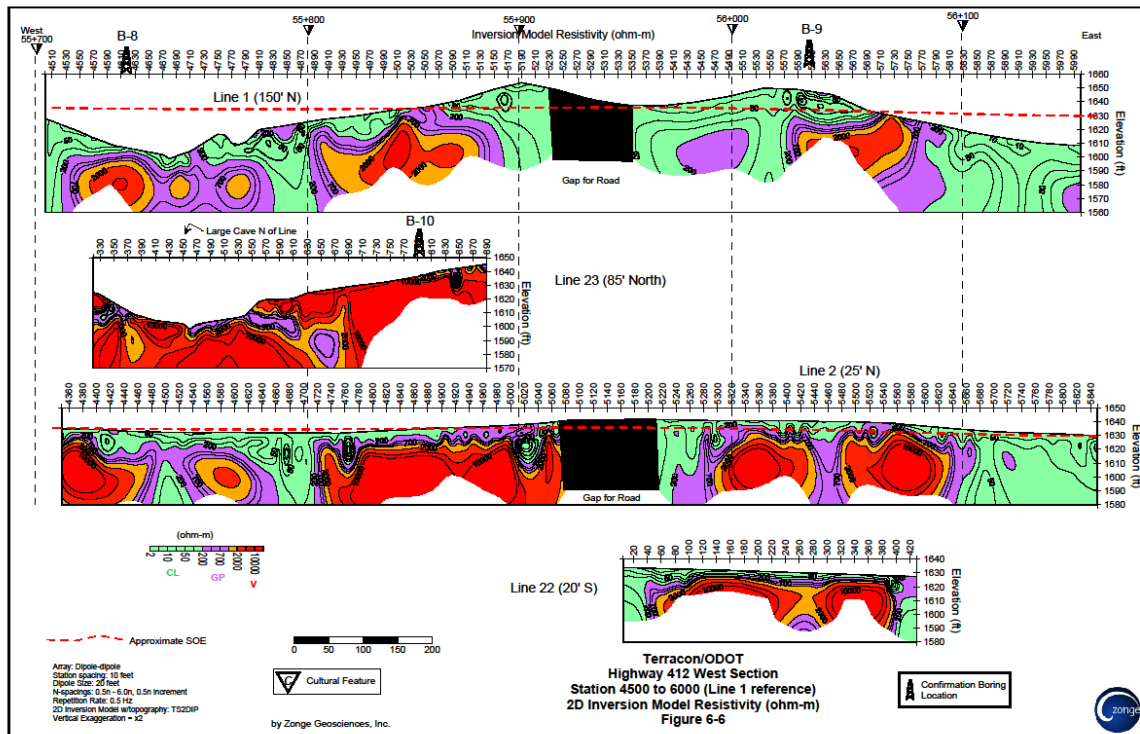


Figure 7, Example 2D Earth Models from ERI surveys

DESIGN RECOMMENDATIONS

A total of approximately 45,000 feet of ER geophysical surveying was conducted and 2D models of the subsurface ER structure were prepared. Based on the ER results, the geophysical design team reached the following conclusions.

First, there are two areas of particular concern for encountering void features in the western section of US-412. One section is about 1,000 feet in length, and the second area is about 1,300 feet in length. Three other shorter sections of lesser concern were also encountered. One of these was encountered in the western section. That area is about 300 feet long. The other two lesser areas are in the east section. One is 800 feet long and the second is 500 feet long.

Second, depths to potential voids in the two areas of particular concern range from immediately below the ground surface to approximately 20 feet below ground surface. The background electrical resistivities in these areas are suggestive of weathered rock, implying that in these areas, the mechanical competency should be addressed for highway construction.

One significant observation is that many of the confirmation boreholes were specifically located to encounter open voids and only one boring encountered a significant (greater than 3 feet) open void. Thus, in the final design phase a much greater number of boreholes will be

drilled for statistically meaningful results. Based on the data gathered, it appears that most of the voids in the project areas are rubble filled. Although the geophysical methods successfully identified voids, in this area the difference in geophysical signature between rubble filled and an open void is small. If surface runoff water can be routed around areas with rubble filled voids, the risk of damage to the highway after construction is lowered.

Roadway construction in known karst formation areas requires that roadway embankments and cut sections be designed so that the impact of the karst formations on the roadway will be lessened or eliminated. Avoidance measures and some combination of drainage and/or bridging methods are usually the best steps to take in a proactive approach (Moore, 2006).

Subsurface void development in known karst formations is generally due to dissolution of materials from surface storm water runoff and/or groundwater flow, both during and after construction. Increased stormwater runoff can result in development of new void features or exacerbate existing conditions. Thus, surface storm water runoff must be routed away from areas identified as having voids, potential voids, or rubble filled voids. Studies (Moore, 1987, 2003) show that the majority of collapse-type karst problems occur in unlined ditches. Unlined ditches are typically sodded at best, and have gradients of less than 3 percent, and often, less than 1 percent. Ditch liners can include Portland cement concrete, asphalt pavement, or 60 mil PVC or geomembrane material. In addition, the final design must consider curbs for embankment sections to channel deep water from running off the edge of the pavement surface. Lined ditches should be strategically utilized to minimize ponding of rainwater and minimize the potential of rainwater to erode soil cover, exposing potentially erodible gypsum rock.

Those areas identified as having sinkholes or subsidence can be remediated for roadway use by bridging over the affected area to provide adequate stability to the roadway. Various approaches to bridging have included conventional bridge spans supported on foundation elements founded on solid bedrock, rip-rap backfill, rock pads, grouting of the void or subsided area, concrete slabs, and geogrids (Moore, 2006).

Rock pads can be constructed at the base of embankment fill to bridge depressions and sinkholes. Typically, the rock pads include large native non-degradable stone (rip-rap) and or broken concrete. Such open graded mixtures of rock and/or broken concrete provide stability and drainage to the roadway fill (Moore, 2006).

Both horizontal and vertical alignment changes can minimize the impact of the new roadway to known karst formation areas. For example consideration can be given to the use of a passing lane through the steeper hills containing karst formations, instead of a wider 4-lane divided section. Such an alignment will minimize the amount of cut into the gypsum rock identified in the geophysical survey and confirmed with the soil borings. Similarly, the vertical grade through the hills with gypsum rock can be held to as high an elevation as economically feasible to minimize cuts into the gypsum rock. To reduce the potential for long-term formation of dissolution cavities from rainwater runoff, the design must minimize the amount of exposed rock in the cut sections after construction.

As the design of the new alignments progresses, additional geotechnical borings should be performed to confirm the competency of subsurface materials immediately beneath the proposed highway alignment.

SUMMARY

In summary, electrical resistivity geophysical surveying along approximately 19,000 feet of US-412, identified approximately 2,300 feet as areas most likely to cause difficulty during and after construction due to the presence of subsurface voids. The design team must minimize the impact of the new roadway to the identified karst formation areas. The design should consider lined ditches to channel stormwater away from the karst formation areas, minimize cuts into known karst formations, and maximize fills and consider rock rip-rap fill at the base of the fills to bridge sinkholes or depressions. Strong consideration should also be given to modifying the horizontal alignment, if possible, to minimize the depth of cut into the gypsum formations.

REFERENCES:

- Telford, W.M., Geldart, L.P. Sheriff, R.E., Keys, D.A., 1976, *Applied Geophysics*, Cambridge University Press, p. 632-662.
- Al'pin, L.M., Berdichevskii, M.N., Vedrintsev, G.A., Zagarmistr, A.M., 1966, *Dipole Methods for Measuring Earth Conductivity, Selected and translated from the Russian* by George V. Keller, Colorado School of Mines, Golden, CO, p. vii-4.
- Abraham, J.D., Lucius, J.E., 2004, *Direct Current Resistivity Profiling to Study Distribution of Water in the Unsaturated Zone Neat the Amargosa Desert Research Site, Nevada*, United States Geological Survey, Denver, CO, available on the web at <http://pubs.usgs.gov/of/2004/1319>.
- Rittgers, J., Butler, D., Sirles, P., 2008, *Subsurface Void Detection in Oklahoma Evaporite Deposits Using Geophysical Methods*, In *Proceedings of the 59th Annual Highway Geology Symposium*: Santa Fe, NM, May 6-9, pp. 445-468.
- Moore, H. L., 2006, *A Proactive Approach to Planning and Designing Highways in East Tennessee Karst*, The Geological Society of America, *Environmental & Engineering Geoscience*, Vol. XII, No. 2, pp. 147-160.
- Moore, H. L., 1987, Sinkhole development along “untreated” highway ditchlines in East Tennessee. In Beck, B. (Editor), *Karst Hydrogeology: Engineering and Environmental applications, Proceedings of the 2nd Multidisciplinary Conference on Sinkholes*: Orlando, FL, A. A. Balkema, Rotterdam, The Netherlands, pp. 115-119.
- Moore, H. L., 2006, *Recent sinkhole occurrences along highways in East Tennessee, a historical perspective*, In *Proceedings of the 54th Annual Highway Geology Symposium*: Burlington, VT, September 24-26, pp. 46-55.

Site Characterization And Remediation In Karst Terrane

Joseph A. Fischer
James G. McWhorter
Joseph J. Fischer
Geoscience Services
3 Morristown Rd.
Bernardsville, NJ 07924
Phone: 908-221-9332
Fax 908-221-0406
E-mail: geoserv@hotmail.com

Prepared for the 61st Highway Geology Symposium, August 2010

Disclaimer

Statement and views presented in this paper are strictly those of the authors and do not necessarily reflect positions held by their affiliation, the Highway Geology Symposium (HGS) or others acknowledged above. The mention of trade names for commercial products does not imply approval or endorsement by HGS.

Copyright

Copyright © 2010 Highway Geology Symposium (HGS)

All Rights reserved. Printed in the United States of America. No part of this publication may be reproduced or copied in any form or by any means – graphic, electronic, or mechanical, including telecopying, taping, or information storage and retrieval systems – without prior written permission of the HGS. This excludes the original authors.

ABSTRACT

Conventional geotechnical investigative tools and analyses in karst are often unsatisfactory. Younger karsts of, for example Florida, require a much different understanding and approach than the flat or folded older karsts within the continental U.S. Support solutions have varied from large mats, H-piles, drilled shafts and pin piles to jet grouting, high-mobility and low-mobility grouting, sometimes with chemical grouts.

Whatever the project, any investigations should start with a geologic understanding of the particular karst terrane below the site/area of interest. In most locales, information is available from state and federal sources as well as, perhaps, local universities.

Generally, conventional soil mechanics investigations, whether or not combined with geophysics, are inadequate to define the vagaries of a subsurface consisting of cavernous bedrock with weathered and open seams, and soft and/or weak soils below apparently competent materials. The often-solutioned nature of the subsurface can also provide an opportunity for undiluted contaminants to reach domestic ground water supplies, particularly during construction.

Potential solutions are many, but generally represent a significant increase in cost over conventional structural/pavement support. Defining an appropriate support solution usually results in increased costs and time overruns, as well as creating a need for increased funds to provide a suitable foundation while protecting domestic groundwater supplies. In addition, the provision of qualified construction inspection at karst sites is vital as the amount of geotechnical investigation required to adequately define all hazards is either impossible or cost prohibitive.

INTRODUCTION

The results of solutioning in carbonate rocks should be of interest to those exploring and/or remediating the route, location, design and installation of highway facilities. Solutioned carbonates are found in various guises throughout the U.S.A and Caribbean Islands. We have ancient, folded and faulted, Proterozoic marble and Paleozoic (limestone, dolomite and skarn) carbonates in the eastern and western U.S.A. There are also the flat-lying, less-stressed carbonates of the central U.S.A.; the recent, soft, coralline carbonates of Florida and the “near-shore” islands of Bermuda, the Bahamas and their Caribbean cousins; as well as the even more confusing Cretaceous and Tertiary carbonates of the central graben of St. Croix in the U.S. Virgin Islands.

Hence, subsurface performance and any required remediation can vary by age, compactness, grain size, tectonic history and climate history. Their physical characteristics range from soft, coralline “limerock” to firm clayey soils to extremely hard dolomites and marbles.

When working in a particular karst environment, an investigation directed by those with experience in another karst environment must recognize the significance of these differences and their impact on the results.

GEOTECHNICAL CONCERNS

The title of this section is simplistic, but is intended to be all encompassing and includes: engineering geology, rock mechanics, soil mechanics, hydrogeology/geohydrology and geophysics. In addition to the need to evaluate the subsurface constraints, an investigation must be aware of what stage the planning or development of the project is currently in as well as the overall nature of the project in order to plan and conduct an appropriate investigation. Is it a preliminary route assessment, a site study for final design, or perhaps a remedial effort during construction or a failure while in operation? Is it to be undertaken during a due diligence phase? Does the lead organization recognize the possible problems of a site or alignment underlain in all or part by carbonates (i.e., what additional funding is available for “geotechnical investigation”, construction and remediation)?

Ground water contamination is another concern. Roadway stormwater runoff or spills can quickly reach the ground water table with little or no filtering through sinkholes formed near the roadway or in stormwater utilities.

ENGINEERING GEOLOGY

Typical types of sinkhole possibilities in karst terrane are presented on Figure 1. However, one must also recognize the different impacts on landscapes, subsurface material types and likely, the degree of weathering/solutioning present that can lead to different sets of difficulties to design, construction and potential remediation. In most cases, practitioners can take advantage of one or more of the following sources; USGS, State geologic surveys, local universities, local investigations; or they can work with another practitioner experienced within the locale. Some states even have county-by-county statistics and locations of sinkhole occurrences.

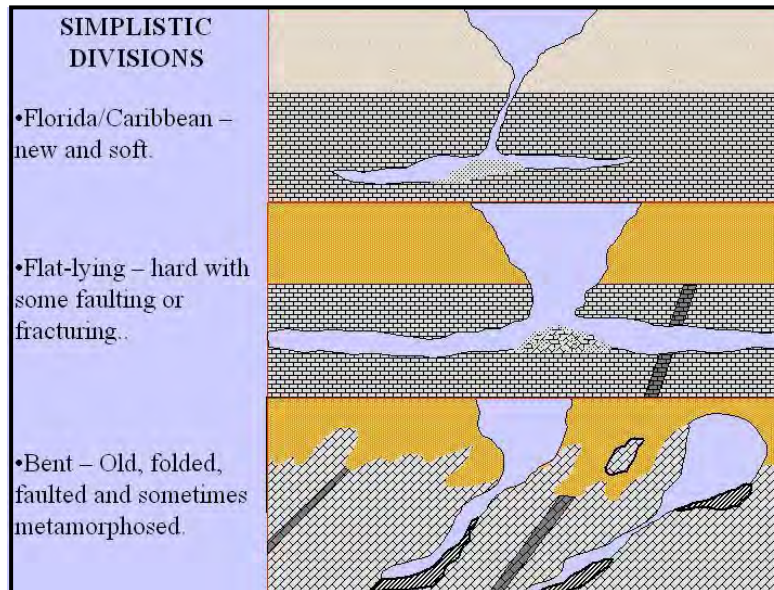


Figure 1 – Typical Karst Sections

Any investigation must recognize that bedrock weathering, erosion and glacial impacts in the northern U.S.A. can result in highly variable near-surface cover above an erratic bedrock surface. Hence, the impacts of a variety of environmental effects need to be considered in any site or route evaluation.

Before planning an investigation, obtain as much generally available subsurface information about the area of interest as possible. Figures 2 and 3 provide examples of geotechnical information currently available for one portion of recent roadway reconstruction near Clinton, NJ. All of the rock and surficial materials information was either on a computer or files in our office, or readily available on the internet. Although generally not of high resolution, archival aerial photography is available on the internet. Figure 4A and 4B compares an internet printout of a photo versus a scan of a contact print that is commercially available. Satellite imagery can be useful for some sites. A series of aerial photographs over extended time periods can be useful in assessing the changes over time as well as their possible causes. Is that group of trees growing within an unfarmed sinkhole? Why did the farmer leave a portion of his land fallow or not planted? Are the observed changes in vegetation type and color significant? Hence, an initial evaluation for a route or site can be conducted with generally available information, which is then ground-truthed with a site reconnaissance.

There is generally a great deal of engineering geologic data available. However, interpretation does require an understanding of local subsurface conditions and the mechanism(s) of solutioning to put that information into the proper context. Without this understanding, establishing the extent and nature of the possible geotechnical concerns will be woefully lacking because it is generally ridiculously uneconomical to attempt to completely define the complexities of karst with any detail.

Figure 3 – USDA Web Soils Survey Results For AASHTO Group Classification

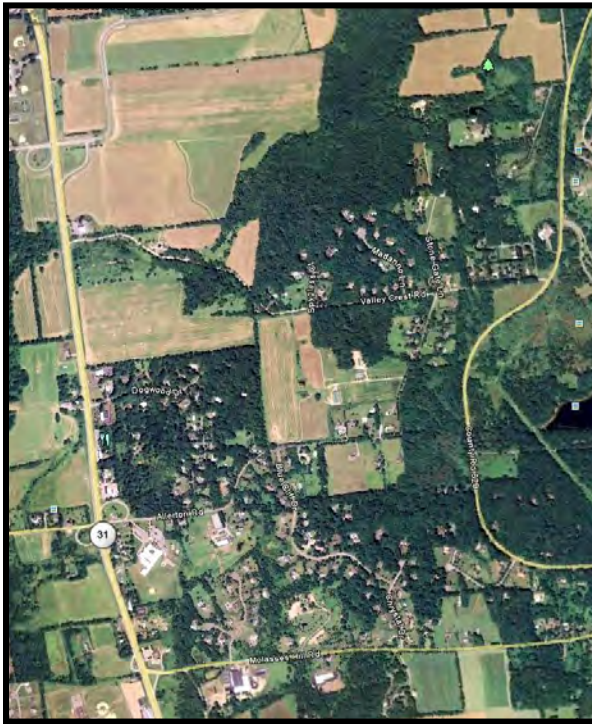


Figure 4A – Example of a recently taken aerial photo download from the internet.



Figure 4B – Scan of a historical (1959) contact print from original aerial photo.

ADDITIONAL INVESTIGATION

Under the assumption that a review of the available data has not frightened the owner/designer away from the karst area, it becomes necessary to perform a field investigation specific to the area of interest and the planned construction.

It is probably easiest to consider two types of investigation – direct and indirect. Direct investigation generally means drilling or digging a hole. Indirect usually implies some form of geophysical investigation.

Test pits can be excavated with conventional equipment and usually provide the most return for the money, but are generally limited in depth. A great deal of information can be obtained from a test pit operation conducted under the technical inspection of a geotechnical engineer/engineering geologist who can identify geologic origin as well as soil and rock type. Where encountered, rock type, depth, fracturing and its variability, as well as extent and type of weathering are worthwhile recording. Overburden soils can be examined for the extent of decomposition and long-term moisture movements through zones of weakness where minute channels have appeared and/or if deposition or alteration of minerals has occurred.

The next most definitive means of obtaining subsurface information is from test borings. We believe test borings in karst terrane should be drilled utilizing rotary wash boring equipment in the overburden soils, weathered rock (saprolite) and the underlying, less weathered, materials. Water losses should be monitored and double- or triple-tube,

split barrel coring operations should be performed under the technical inspection of qualified professionals and by competent, experienced drillers willing to share the information they can sense from the performance of the drill rig. Finally, tremie grouting the holes with a low viscosity grout and recording the depths of grout take and quantities of grout accepted at each level as the tremie pipe is withdrawn can be very diagnostic of the subsurface conditions.

The use of a split inner barrel in a double- or triple-tube core barrel really should be mandatory in any area whose bedrock has been previously subjected to tectonism. The hard, but brittle, indurated carbonates of the eastern and western U.S. would be expected to come out of a single tube core barrel in pieces when subjected to the normal “hammering” extraction process. The core run should be measured and examined in the split barrel. A good driller and a properly-maintained and set-up split barrel yields a far better understanding of the angle of inclination of fractures, soil-filled or weathered, and even sometimes fill materials within previously solutioned zones. Oriented core can also aid in defining bedding and fracture dips and orientation. Unless the investigation expects the core to come out of the barrel easily in one or two pieces, a split barrel should be used.

Air- or hydro-track drilled probes also provide some level of direct information. An experienced operator knows the consistency and competence of the material he is drilling through and the experienced observer can often work with the driller to assess the subsurface conditions, i.e. soft or firm soils, competent rock, open voids or soft soil-filled cavities can be interpreted to some degree. Of course, more subsurface information can be gleaned from an air-track than from the rapid penetration and power of a hydro-track. Newer drilling equipment that records down pressure and drilling rate can also be quite useful although such equipment is not always readily available.

Many geophysical tools have been advanced as suitable for use in karst areas, without, however, defining the type of “karst” being investigated and the nature of the resolution necessary to define the anomalies of significance to the designers. In addition, one must also consider the existence of potential cultural anomalies along a route or in the area to be developed by highway structures. Overhead power lines, buried pipes, traffic noise and available space can influence the type of geophysical procedures used

If an engineer or geologist wishes to consider the use of geophysics on a project, the investigation should be planned in conjunction with an experienced geophysicist who understands the nature of the target (*1*). We believe that in no case should a survey be a “stand alone” investigation. Interpretation of the results should be accomplished in conjunction with hard data from borings, probes and/or test pits, not just from a computer-interpreted set of the data, even with the sophisticated interpretation programs presently available. One should also remember that any test boring, test pit, probe or geophysical result must be interpreted in light of the available geologic information.

As an example of the problems inherent in using geophysics, even in conjunction with test borings, a recent HGS meeting presentation provides a quick summary of the problems encountered even when using a local firm with geophysical personnel and a local District geotechnical engineer while attempting to delineate an area of “highly variable top of rock with pinnacles, voids and boulders” (*2*), i.e., an Appalachian karst site. The subsurface investigation consisted of (in chronological order):

- A. Test borings with measured grout quantities, except where large quantities of grout were placed when operations were discontinued;
- B. 2-D electrical resistivity (the author's indicated that some difficulty was experienced in interpreting the results);
- C. Difficulty in locating "the exact area of the problem" (i.e., a problem with resolution in relation to the size and depth of the anomalies).
- D. Most of the survey line down the median of the roadway picked up the stormwater drainage piping (seismic was ruled out because of traffic noise);
- E. MASW (Multi-channel Analysis of Surface Waves), which was "more revealing of subsurface conditions related to top of rock and soil density" was the second technique tried;
- F. Eventually, "confirmation borings" were drilled at selected locations.

Finally, perhaps in despair, the authors of that paper separated the areas into three categories for remediation.

1. "Sinkhole-prone areas with shallow rock".
2. "Slightly sinkhole-prone areas with deep bedrock".
3. "Highly sinkhole-prone areas with deep bedrock".

The author's of that paper state "Construction recommendations were broken down based on geology and sinkhole history", not geophysics.

Apparently, the geophysics field program was only able to differentiate between "shallow" and "deep" rock in the local karst. "Sinkhole-prone" conditions were likely determined by the number of encountered sinkholes per roadway length.

While the older and folded rock present a resolution problem to a geophysical survey, the younger carbonate of the southern U.S. are generally more amenable to Ground Penetrating Radar and seismic surveys, including the latest in surface wave studies, low cost MASW. Again, it is necessary to work with a geophysicist who understands the geology of an area and does not "over-process" the data to make intersecting lines match at the point of crossing and perhaps influencing more realistic data at greater distances from the area of interest.

Possibly even more complicated is the evaluation of ground water concerns. The writers have seen wells 25 feet apart with yields varying in hundreds of gallons per minute. Certainly knowing the locations of geologic structure, dips of strata and general information on solutioning helps, but siting wells in karst is at best an educated guess and conventional aquifer modeling formulas are generally inapplicable.

Other geohydrologically-related concerns are problematic. Solutioned carbonates are not isotropic, anisotropic or slab-fissured models. A finite element model would work only if one had enough input parameters to define the subsurface in detail. Conduit flow is often assumed, but may not always be appropriate. In truly cavernous carbonates, dye tracing may be the only way to define rates and paths of water movement as well as the influence of precipitation rates on ground water levels and paths.

GEOTECHNICAL SOLUTIONS

If the nature of the karst below an area of interest has been reasonably well assessed, generally conventional foundation support procedures are available.

The first step in any site preparation is to eliminate or at least reduce the effects of near-surface water accumulation. Some typical concepts are:

- Appropriate drainage.
- Designing impermeable linings for drainage swales and water courses.
- Using full depth asphalt designs for pavement boxes, or in some instances reinforced concrete.
- If conventional, flexible or rigid pavement designs are used, lining the subgrade/subbase interface and the sides of the pavement box with an impermeable material in conjunction with subbase drainage discharging into catch basins to reduce water infiltration below the road surface.
- Using gasketed joints on storm sewers and drainage pipe.
- Not bedding utility pipes, storm sewers or culverts with crushed stone or other permeable material. The use of indigenous materials or a low-permeability quarry process material while adjusting the structural requirements accordingly.
- Placing the discharge locations of storm sewers away from the roadway or structures.

When rock is shallow, achieving some form of support directly atop sound or remediated rock is preferable. Procedures that can be economically used include:

1. Excavating to rock and filling observed cavities and open joints with some form of cementitious grout.
2. Grout can also be placed from the surface using either a low or high mobility grout. Generally a high mobility grout should be used within the bedrock itself. High mobility grout is generally less costly as fewer grout holes, hence less setup, is needed and the PVC tremie pipe is easier to install and remove than the steel pipe generally used in compaction (low mobility) grouting operations. Low mobility grouting is generally most suitable in loose, sandy materials, particular if one wants to compact the overburden granular soils. However, consideration must be given to pore pressure effects in cohesive soils.
3. Dynamic compaction has proven useful, i.e., dropping a substantial weight (some 15 to 20 tons) from heights of some 40 to 100 feet. Surprisingly, the vibration effects on nearby structures are less than one might expect, but must still be considered. The ground surface after dynamic compaction operations are completed can look like a World War I battlefield and will require substantial grading and/or filling.
4. Standard sinkhole remediation often consists of excavation to a sound base and placing a variety of backfill materials such as a graded rock (including boulders) to construct a filter or “dental” grouting. One should not start such excavations unless some idea of the depth to rock is known.
5. A common solution is to install piles or caissons to sound rock. H piles have been a problem in areas of pinnacled bedrock as a result of their flexibility. Cases have been recorded where H piles were redirected by the side of a pinnacle with the pile tip eventually returning to the surface.
6. Pin piles, as a result of their installation procedures, have been used successfully. However, pin piles are generally quite slender and consideration must be given to their lateral support in areas of soft, wet soils often found directly atop the bedrock in some karst regimes.
7. Mathematical geomechanical models (3, 4, 5, 6) have been advanced for estimating the load bearing capacity of the materials above a cavity, but all require a good

knowledge of the subsurface dimensions of the cavity and roof, as well as the strength properties of the overlying soils and rock.

SUMMARY AND CONCLUSION

Working in a karst environment is difficult and requires engineering judgment and a geologic understanding of the vagaries that likely exist. The variety of karst regimes within the U.S.A makes it difficult to carry experience from one region to the next. Even within a locale, each project seems different than the last. Increased costs should be expected in planning, investigation and design over what one might expect at a geologically conventional site.

REFERENCES

- Conference Proceedings
 1. Fischer, J.A., D.L. Jagel, J.J. Fischer and R.S. Ottoson. The Expectation and Realities of Geophysical Investigation in Karst. In *Proceedings: 55th Highway Geology Symposium*, Kansas City, MO, 2004, pp. 94-102.
 2. Shelley, B and S. McInnes. Getting it Right the Third Time: Reconstruction of Interstate 476 over Unstable Karst in Plymouth Meeting, PA. In *Proceedings: 60th Highway Geology Symposium*, Buffalo, NY, 2009, pp. 169-178.
 6. Tharp, T.M. Cover-Collapse Sinkhole Formation and Piezometric Surface Drawdown. In *Geotechnical and Environmental Applications of Karst Geology and Hydrology, Proceedings of 8th Multidisciplinary Conference n Sinkholes and the Engineering and Environmental Impacts of Karst*, Louisville, KY, pp. 53-58.
- Journals
 3. Kulhawy, F.H. Geomechanical Model for Rock Foundation. 104(2), *J. Geo. Eng.* (ASCE), 1978.
 4. Badie, A. and M.C. Wang. Stability of Footings Above Voids in Clay. 110(11), *J. Geo. Eng.* (ASCE), 1984.
 5. Wang, M.C. and C.W. Hseih. Collapse Load of Strip Footing Above Circular Void, 113(5).1, *J. Geo. Eng.*, 1987.

**Geotechnical Investigation and Design of an Americans With Disabilities Act
(ADA) Compliant Ramp Along the South Rim of the Grand Canyon at
Mather Point, Grand Canyon National Park, Arizona**

Gregg S. Mitchell

HDR Engineering, Inc.
3200 East Camelback Road, Suite 350
Phoenix, AZ 85018
(602) 952-5760
gregg.mitchell@hdrinc.com

Michael L. Rucker

AMEC Earth & Environmental, Inc.
1405 West Auto Drive
Tempe, AZ 85284
(480) 940-2320
michael.rucker@amec.com

Prepared for the 61st Highway Geology Symposium, August, 2010

Acknowledgements

The authors would like to thank the Federal Highway Administration, Central Federal Lands Highway Division and the United States Department of Interior, National Park Service for awarding this project to HDR and for allowing HDR to present this project at the Highway Geology Symposium. Special thanks go to the following individuals, Tom Puto - FHWA Project Manager, Nathan Allen - FHWA Designer Engineer, Haramy Khamis - FHWA Geotechnical Engineer, Dan Onisko - FHWA Construction Engineer, Victoria Stinson - NPS Project Manager, and Don Singer – NPS Safety Manager.

Disclaimer

Statements and views presented in this paper are strictly those of the author(s), and do not necessarily reflect positions held by their affiliations, the Highway Geology Symposium (HGS), or others acknowledged above. The mention of trade names for commercial products does not imply the approval or endorsement by HGS.

Copyright Notice

Copyright © 2010 Highway Geology Symposium (HGS)

All Rights Reserved. Printed in the United States of America. No part of this publication may be reproduced or copied in any form or by any means – graphic, electronic, or mechanical, including photocopying, taping, or information storage and retrieval systems – without prior written permission of the HGS. This excludes the original author(s).

ABSTRACT

Geotechnical investigation was performed to support design of improvements to Mather Point at Grand Canyon National Park, including a new Americans with Disabilities Act (ADA) compliant ramp to be cut into an approximately 1H:1V natural slope along the edge of the South Rim of the Grand Canyon. The slope, extending about 60 feet from the existing Rim Trail to an approximate 800-foot vertical drop, consisted of a thin veneer of soil and talus with loose and dislodged boulders and rock blocks overlying dolomitic limestone.

The geotechnical investigation, as initially proposed, included geologic mapping, geophysical surveys, and test borings along the ramp alignment. However, site conditions and access, and worker safety considerations required that the investigation be performed on adjacent areas located behind existing safety rails. Geologic mapping focused on the Mather Point East Overlook rock outcrop with limited distant visual assessment of the actual ramp alignment. Seismic surveys and test cores were performed along the existing trail system. Mapping indicated a complex geology including three highly persistent joint sets extending vertically through numerous 8- to 12-foot thick layers of dolomitic limestone with alternating relative hardness and competence. Geophysical survey and rock coring results confirmed the observed rock conditions.

The investigation indicated that widely variable rock conditions were expected both laterally and vertically, rock anchoring and over-excavation along the cut slope might be necessary, and a field-fit approach to construction would be required. Inspection and approval of the cut slope prior to ramp construction was stipulated in the project specifications. This project demonstrated that geologic mapping, geophysical surveys, and traditional test boring methods are all important components of a geotechnical investigation that can be effectively used together on geologically complex sites, especially where direct site access is not possible.

INTRODUCTION

Under contract to the Federal Highway Administration, Central Federal Lands Highway Division, HDR Engineering Inc. (HDR) completed a geotechnical investigation (HDR, 2009) to support the design of a new Americans with Disabilities Act (ADA) compliant pedestrian path (herein referred to as the ADA Route) and ADA compliant grading of the East Overlook at Mather Point for the National Park Service, Grand Canyon National Park (GCNP), Visitor Center & Mather Point Improvements Project (the project) located at Mather Point in the GCNP, Grand Canyon, Arizona. The purpose of the geotechnical investigation was to evaluate subsurface soil and rock conditions and engineering properties and provide recommendations and criteria in support of design of the ADA Route.

Project Location & Scope

The project is located along the south rim of the Grand Canyon within the GCNP. The site investigated comprises a scenic overlook area known as the East Overlook at Mather Point. The proposed new ADA Route is to begin from the west side of the East Overlook, extending west about 190 feet to connect to the existing south rim trail at a maximum 4.75-percent grade. The proposed alignment traversed relatively rugged, steeply sloped terrain immediately adjacent to and below the existing South Rim Trail, and immediately adjacent to and above the canyon rim. To maintain a gently-sloping, near-flat profile, both cuts and fills are required. Soil retaining systems utilized along the ADA Route were anticipated to consist of anchored retaining stones or short retaining walls. At the East Overlook, excavation, or trimming of existing rock exposures to accommodate a near-flat ADA compliant area was planned.

The originally proposed scope included design and implementation of OSHA compliant fall protection to allow direct investigation of the proposed ADA Route alignment near the edge of the canyon where near-vertical to vertical to undercut rock conditions extend for about vertical 800 feet. However, design and implementation of such fall protection was determined to be cost-prohibitive and outside of the design schedule time constraints. The investigation was therefore moved to areas as close to the proposed alignment as practical while remaining behind existing safety railings between the west side of the East Overlook and the existing Rim Trail. Because the actual ADA Route alignment could not be directly accessed, detailed field mapping of accessible rock exposures became an integral component of the geotechnical investigation and a field-fit approach to final design and construction of the ADA Route was deemed necessary.

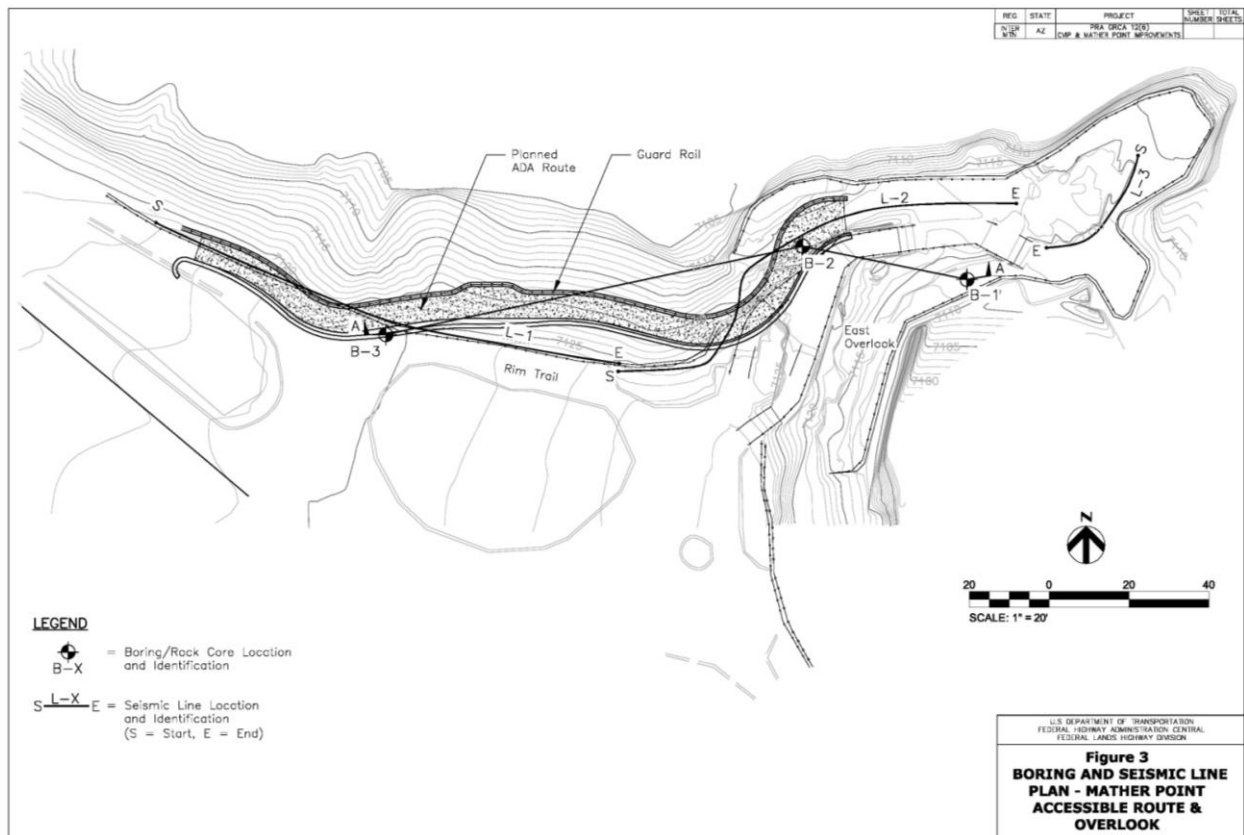
INVESTIGATION

The geotechnical investigation included review of existing data, site reconnaissance and geologic mapping, subsurface investigation including exploratory drilling, soil and rock sampling and seismic refraction and refraction microtremor (ReMi) surveys, and laboratory testing. The site configuration and locations investigated are illustrated on Figure 1.

Review of Existing Data

The available data that was collected and reviewed consisted primarily of published geologic maps and reports. Previous geotechnical reports or as-built drawings specifically covering Mather Point at the East Overlook or the immediate vicinity were not available. A geotechnical

report prepared by AGRA Earth & Environmental, Inc. (AEE, 1997) for the Visitor Center/Transit Facility (located around 600 to 800 feet to the south of the project site) was



reviewed and utilized to compare relevant soil and rock data, to supplement the investigation.

Figure 1: Site Plan

Site Reconnaissance and Geologic Mapping

A site reconnaissance was performed during the geotechnical field investigations. During the reconnaissance, observations of exposed geotechnical and geologic conditions at and in the immediate vicinity of the project elements were made and documented.

Geotechnical Investigation

Exploratory drilling included three (3) test borings, identified as Borings B-1, B-2, and B-3. Drilling was completed using rock coring methods to depths ranging from approximately 8.5 to 10 feet below the existing ground surface (bgs). All cores were advanced utilizing a portable electrical-powered concrete core drill utilizing a 36-inch long, 2.75-inch inside diameter, 3.0-inch outside diameter core barrel. Hand sampling included collecting four surface/near-surface composite bulk soil samples and one surface rock sample. Depth to rock at hand sampled areas

was estimated by pushing a soil probe into the soil surface until refusal. Encountered materials were visually classified in the field and logged by an HDR field geologist. Soil materials were logged in accordance with ASTM D2487 (Unified Soil Classification System {USCS}) and rock materials were logged in accordance with standard practice, including International Society of Rock Mechanics guidance, and U.S. Department of the Interior, Bureau of Reclamation Engineering Geology Field Manual (Second Edition) practices (DOI BOR, 2001).

A series of three combined seismic refraction and refraction microtremor (ReMi) surveys was performed to supplement information collected from the rock cores and geologic mapping. Two 120-foot long lines with 24 geophone arrays at 5-foot geophone spacing (Survey Lines L-1 and L-2) and one 36-foot long line with 12 geophone array at 3-foot geophone spacing (Survey Line L-3) were completed. The seismic surveys were performed by Michael Rucker, P.E., of AMEC Earth & Environmental, Inc. (AMEC), under direction of HDR. The surveys included collection of compression wave (p-wave) and surface wave data (for estimation of shear wave [s-wave] profiles), which were interpreted for depths and seismic velocities to estimate subsurface geometries and relative strength of the subsurface materials. Interpreted depths of investigation for the p-wave seismic refraction results ranged from about 9 to 30 feet; velocity reversals from softer rock horizons underlying harder rock horizons limited the p-wave depths of investigation. S-wave profiles interpreted from the ReMi results were not limited by velocity reversals, and had depths of investigation ranging from about 36 to 110 feet below site grades.

Laboratory Testing

Laboratory tests on soil included sieve analysis, plasticity index, pH, resistivity, chloride content, and soluble sulfate content. Laboratory tests on rock included point load index (diametral) and unconfined compressive strength.

GENERAL CONDITIONS & GEOLOGIC SETTING

General Conditions

Site area topography ranges from relatively flat to undulating adjacent to and away from (to the south of) the canyon rim, where the ground surface slopes gently downward to the southwest at a gradient of about 160 feet per mile (0.03 ft/ft). Topography is steep to near vertical along the canyon rim with some undercut and overhanging areas. Site elevations range from approximately 7,129 feet at the top (southwest end) of the East Overlook to 7,112 feet at the lowermost horizontal surfaces of the East Overlook (along its east and west sides).

Geologic Setting

Regional Geology

The project site is located on the north edge of the 5,000-square mile Coconino Plateau within the Colorado Plateau Physiographic Province, most of which extends above 5,000 feet in elevation with steep drops in elevation resulting from geologic structure, erosion, or both at all of its margins. The northern roughly two-thirds of the plateau, including the site region, is a Cenozoic upland composed of nearly flat-lying Paleozoic and younger bedrock ranging in thickness from around 5,000 feet at the northern end of the plateau to around 8,000 feet at the

southern end. Erosion of the stratigraphy on the plateau has created a land surface characterized by low-relief hills and mesas, broad mature valleys, and several internal drainage areas with no free-flowing streams. Structurally the plateau is characterized by large erosional escarpments and regional folds, faults, and other fractures that help to define its boundaries and geologic framework. The sedimentary rocks generally are flat lying to gently dipping with regional dips of about two degrees to the southwest over the majority of the plateau. The uppermost geologic materials on the plateau consist of unconsolidated alluvial, colluvial, and landslide deposits of Quaternary age which occur as a veneer or as thicker discontinuous deposits. The alluvium consists of variable thickness deposits of silt, clay, and fine sand. The colluvium is coarse-grained material confined to steep slopes of canyons and mountainsides. The youngest rocks are Paleozoic and consist of (from youngest to oldest) the Kaibab Formation, Toroweap Formation, Coconino Sandstone, Schnebly Hill Formation, Hermit Formation, Supai Group, Redwall Limestone, Temple Butte/Martin Formation, Muav Limestone, Bright Angel Shale, and Tapeats Sandstone. The oldest rocks are Precambrian in age. In the Grand Canyon area, the Precambrian rocks consist of metamorphic rocks, igneous rocks, and the Grand Canyon Supergroup (Bills et al., 2007) overlain unconformably by the Paleozoic-Aged materials.

Site Geology

Geologic materials at and in the vicinity of the site include mixtures of Quaternary alluvium and colluvium and Late Permian limestone bedrock of the Kaibab Formation. Alluvial sediments consist of clay, silt, and fine sand derived from weathering of the underlying and nearby limestone bedrock. Colluvial deposits consist of coarse-grained (gravel-, cobble-, and boulder-size) particles of limestone. Typically a mixture of both types, these sediments exist as a veneer, or as thicker discontinuous deposits, with the colluvium mostly confined to slopes along the canyon walls. Bedrock at and in the vicinity of the site is Late Permian Kaibab limestone consisting of thin to thickly bedded calcareous sandstone and magnesian limestone. The sandstone units (not encountered in the borings for this investigation) are described as composed of very fine to medium grained quartz ranging in color from yellowish-gray to pale orange. The limestone units are described as thinly to thickly bedded, silty, very sandy, yellow-gray to grayish-yellow, and dolomitic. The upper portion of the Kaibab limestone is described as interbedded light-red to grey limestone, siltstone, sandstone, and gypsum (Bills et al., 2007). Thickness of the Kaibab limestone near the site is about 300 feet (Metzger, 1961).

SITE AND SUBSURFACE CONDITIONS

Observed/Mapped Site Conditions

General - Dolomitic limestone of the Kaibab Formation comprises rock exposures at and in the vicinity of the site. In general, horizontally-bedded exposures consist of moderately-soft to moderately-hard, unweathered (except joints) to moderately weathered rock. Vertical and steeply-sloped exposures include slightly- to highly-weathered, loose, dislodged, and/or toppled blocks of rock with widely-spaced, wide to very wide, open and nearly-vertical joints.

Vertical exposures clearly exhibit alternating horizons of relatively harder more competent rock and relatively-softer, less competent rock. In general, the softer rock horizons undercut the harder rock horizons to varying degrees ranging from several inches to more than one foot. For

clarity of discussion, the rock layers are identified as Rock Horizons H1 through H7, inclusive (Photo 1).



Photo 1 – Rock Horizons Exposed Along the West Side of the East Overlook and East End of the ADA Route

Odd numbered rock horizons consist of relatively harder more competent rock, and even numbered horizons consist of relatively softer less competent rock. Only Rock Horizons H1, H2, and H3 are anticipated to be encountered during construction of the proposed project improvements and will comprise the rock on which the improvements will be supported.

Horizontal rock exposures were generally limited to the East Overlook and consisted of relatively flat-lying, generally-competent rock that dips gently to the southwest with very steep to nearly-vertical joints in three distinct sets. These were identified as Joint Sets A, B, and C. Discontinuities within each identified joint set exhibit consistent orientation (strikes) and dip with strong to very strong persistence. Joint spacing ranges from close to very wide with generally tight to very tight apertures. Joint set apparent dip (in degrees from horizontal) and orientation (in degrees clockwise from north) are summarized as follows: Joint Set A – 60/011 to 65/011, Joint Set B - 85/046, and Joint Set C - 78/311 to 83/311. These joint sets appeared generally continuous through the various rock horizons as observed in horizontal and vertical exposures. Joint Sets A, B, and C, as mapped in the field for the East Overlook, are shown on Figure 2.

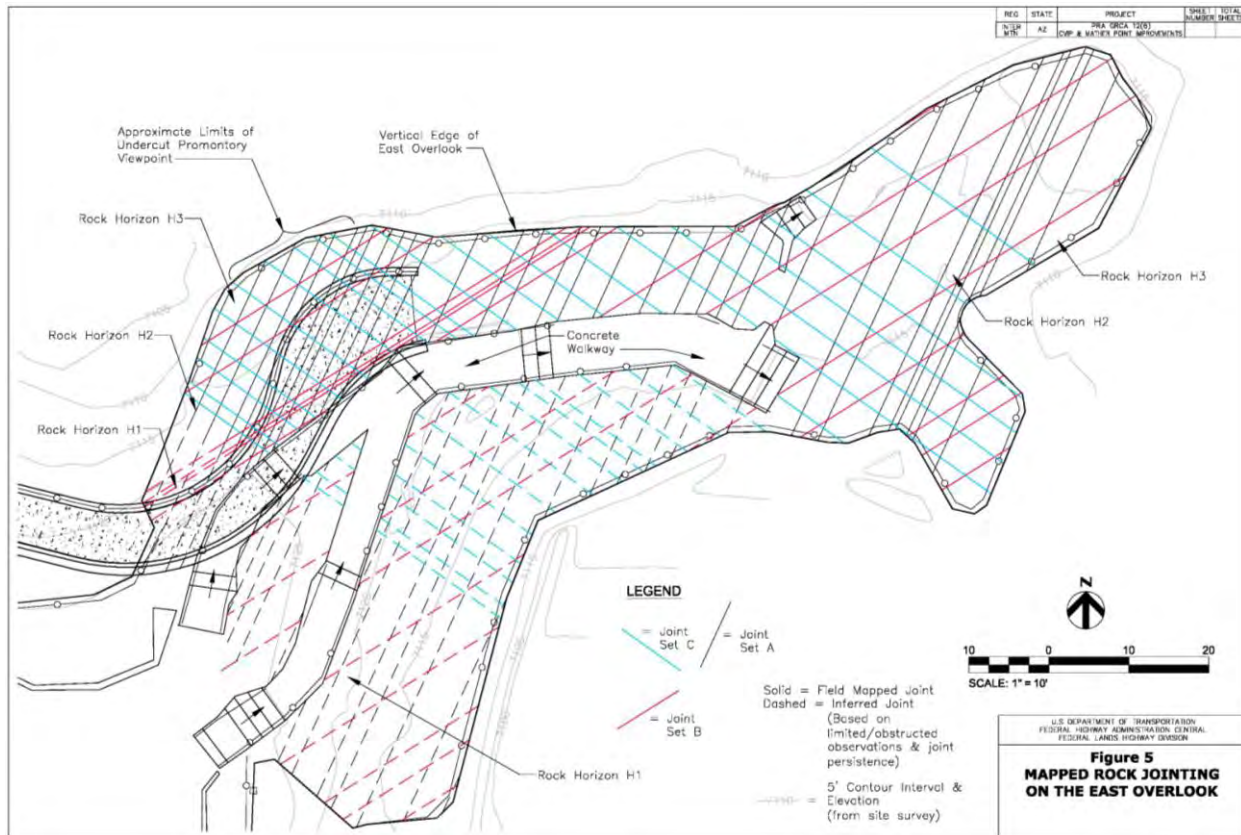


Figure 2: Mapped Rock Jointing

Across the rock horizons, bedding ranges from thinly laminated to thickly bedded, with discontinuities of varying degree. Discontinuities range from open and clean, to closed and tight, to faint bedding plane traces. In general, Horizons H1 and H3 exhibit medium to thick bedding and Horizons H2 and H4 exhibit thinly laminated to thin bedding. Open, clean discontinuities were observed primarily at vertical exposures. Closed and tight discontinuities and faint bedding plane traces were observed mainly in the core samples and to a lesser extent in vertical and horizontal exposures.

ADA Route - The proposed new ADA Route alignment traverses alluvial and colluvial sediments interspersed with slightly- to highly-weathered intact rock and loose, dislodged or rotated, and/or toppled blocks of rock (Photo 2).



**Photo 2 – ADA Route Alignment
(line rods denote approximate alignment; note dislodged, rotated, or toppled rock blocks on slope)**

Topography along the proposed alignment is typically at an approximate 1H:1V (horizontal: vertical) slope and varies from less steep to near vertical. Below the ADA Route alignment, the slope terminates at a six- to eight-foot thick layer of vertical rock face (Horizon H3, Photo 1) with widely-spaced, wide to very wide, open and nearly-vertical joints with evidence of dislodging by translation and/or rotation. This layer of rock is underlain by a softer, less competent rock unit (Horizon H4, Photo 1) that has undercut the layer above from less than one foot to as much several feet, but typically in the range of about one to 1-½ feet. Undercutting appears to be more pronounced in areas of relatively close joint spacing as appears to be the case in the vicinity of the east ADA Route tie-in to the East Overlook (Photo 3).



Photo 3 – West side of East Overlook (Horizon H3 and Undercutting Horizon H4)

East Overlook (ADA Overlook) - The majority of the East Overlook consists of generally competent rock with relatively-flat, horizontal exposures and nearly-vertical slope face exposures, the layering and characteristics of which are a continuation of those forming the canyon rim. Soils are absent over the vast majority of the East Overlook. Exposed horizontal surfaces clearly exhibit steeply-dipping to nearly-vertical joints in three distinct sets, each exhibiting consistent orientation and dip and strong to very strong persistence. Joint spacing ranges from close to very wide with generally tight to very tight apertures (Photos 4 and 5).

Along the west side of the overlook where the eastern end of the ADA Route will tie-in to the overlook, joint spacing within and between the three joint sets decreases. Horizontal discontinuities observed in rock exposures comprising the overlook consist of thinly laminated to medium bedding planes, ranging from clean and open to very tight or intact with faint bedding plane traces. The overlook rock exposed along the proposed ADA accessible areas (areas to be locally ground and leveled to achieve ADA compliance) consists of moderately-soft to moderately-hard, unweathered (except joints) to moderately-weathered rock. The rock exposed at the location of the ADA Route tie-in consists of soft to very soft, slightly- to highly-weathered rock with very-closely to closely-spaced joints (Photo 6).

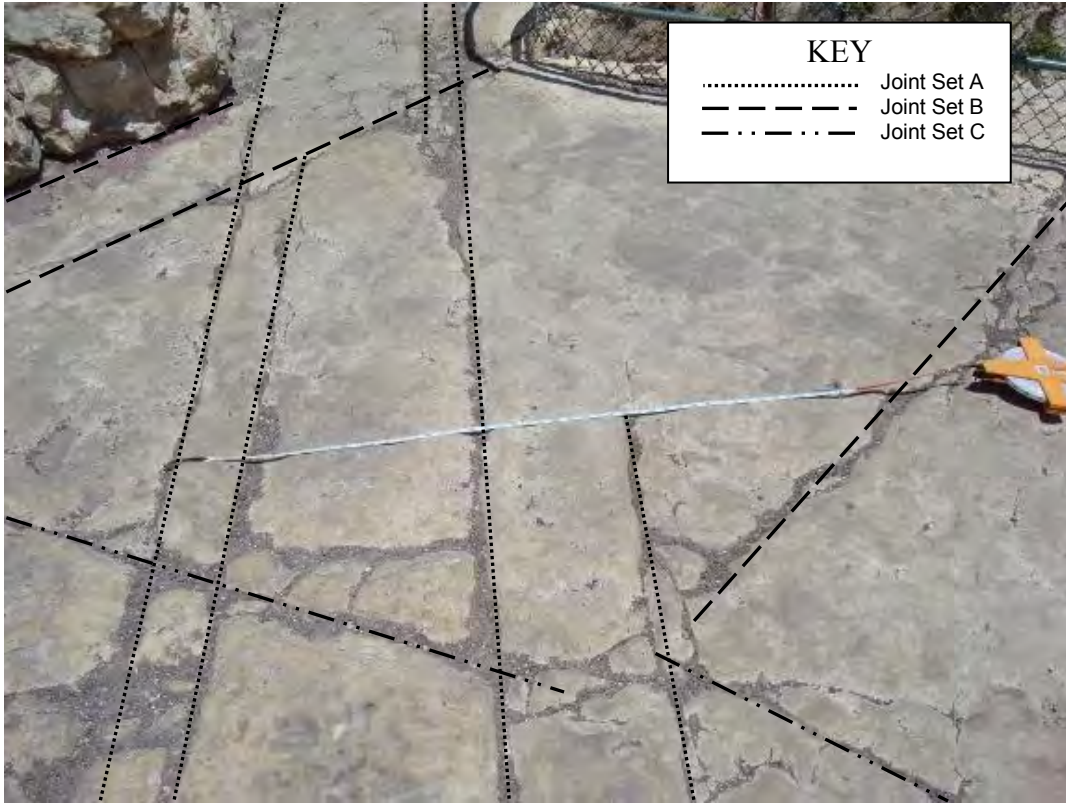


Photo 4 – East-Central Portion of East Overlook Showing Three Joint Sets

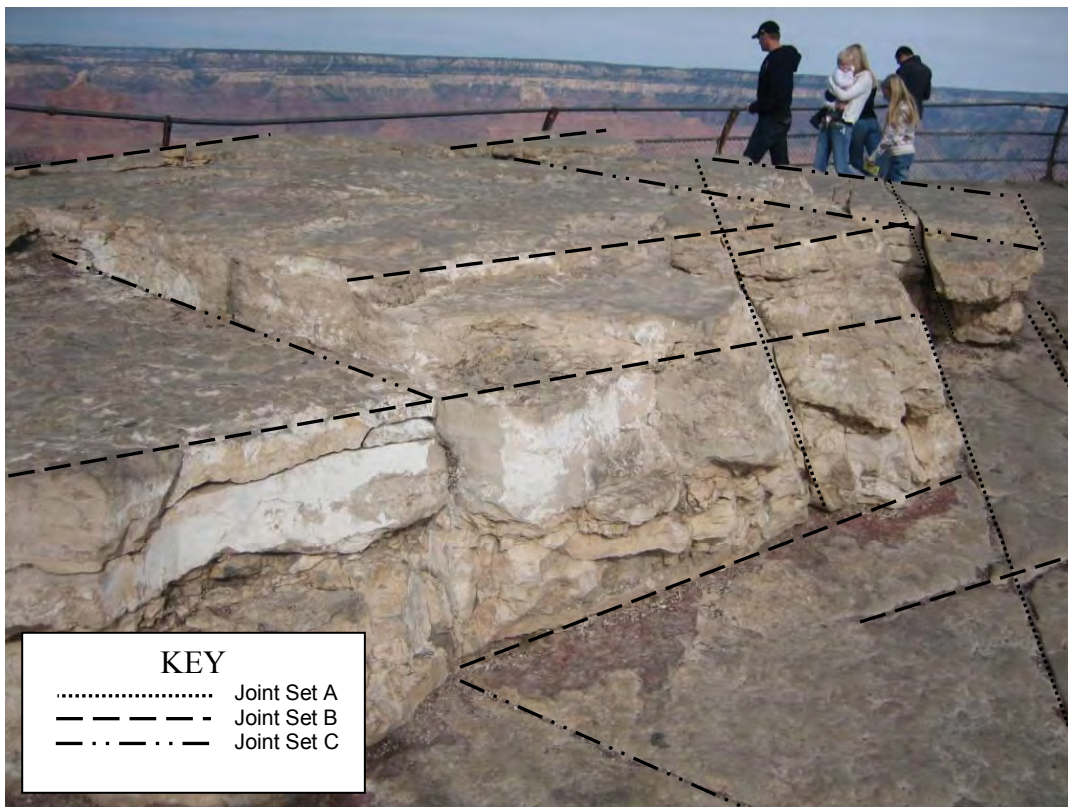


Photo 5 – East Overlook Showing Continuous Jointing Through Horizons H2 and H3



Photo 6 – ADA Route Tie-In Location Showing Horizon H2 and Part of Overlying Horizon H1

Subsurface Conditions

Seismic Surveys - Based on the seismic survey results, an uppermost approximately 7- to 9-foot thick rock layer identified as Rock Horizon H1 underlies the site including the existing Rim Trail west of the East Overlook, and comprises the west tie-in and western portions of the proposed ADA Route. Proceeding from the ground surface downward through Horizon H1, p-wave velocities in the range of 800 to 1,000 feet/second (f/s) were interpreted in the upper few feet, whereas p-wave velocities of 3,500 to 4,100 f/s, including isolated zones of 8,000 to 12,600 f/s, were interpreted for the lower five to seven feet. Corresponding s-wave velocities were 560 f/s in the upper few feet and 2,400 to 2,600 f/s in the lower five to seven feet. The lower-velocity values obtained for the upper few feet of Horizon H1 are consistent with alluvial/colluvial soils, and the underlying higher but variable velocities are consistent with variably weathered fractured dolomitic limestone.

Horizon H2 is an approximately 7- to 9-foot thick layer of relatively weaker rock which comprises the central and eastern portions of the ADA Route and the east tie-in to the overlook. For Horizon H2, interpreted p-wave velocity was about 2,700 to 4,000 f/s, and interpreted s-wave velocity was about 1,400 to 1,500 f/s.

Horizon H3 is an approximately 8- to 12-foot thick layer of relatively stronger rock encountered at (and comprising) the East Overlook view point areas. For Horizon H3, interpreted p-wave velocities were 7,500 to 11,100 f/s and s-wave velocities were 3,500 to 5,100 f/s, except for a narrow (8- to 9-foot wide) band of rock crossing the East Overlook from east to west, where a p-wave velocity of about 4,200 to 4,600 f/s was interpreted.

Horizon H4 is a relatively weaker, approximately 9- to 11-foot thick layer of rock with interpreted s-wave velocity in the range of 1,000 to 2,200 f/s. The next lower layer, Horizon H5, is an approximately 12-foot thick layer of relatively stronger rock with interpreted s-wave velocity in the range of 2,700 to 5,100 f/s. The next lower layer, Horizon H6, is a relatively weaker approximately 12-foot thick layer of rock with an interpreted s-wave velocity of 2,200 f/s. The deepest layer interpreted, Horizon H7, is a relatively stronger rock layer with interpreted s-wave velocity of 3,300 to 5,600 f/s.

Rock Horizons H1, H2, and H3 constitute the bedrock on which proposed project improvements will be founded and constructed. Underlying rock layers are not anticipated to be encountered during construction. Interpreted seismic velocities for Horizons H1 through H4, inclusive, are plotted on Figure 3.

Borings - Horizons H1 through H4, inclusive, were encountered in the borings. Competent rock was encountered in, and core samples successfully recovered from all three borings completed for the investigation. The investigation target depth of 10 feet bgs was reached at Borings B-1 and B-2. At Boring B-3 the core drill could not be advanced beyond 8-½ feet bgs due to machine wobble and binding of the core barrel while trying to drill below this depth. These drilling conditions are believed attributable to poor quality, broken, and/or very soft rock at the top of Horizon H2. In general, the core barrel advanced with relative ease, requiring only the weight of the drill or light hand pressure. Drill rates ranged from 1.0 to 6.4 minutes/foot, with an average rate of 3.1 minutes/foot.

Sandy dolomitic limestone was encountered at all three borings. Color ranged from light tan, to light grayish tan, to mottled in red, grey, tan, white, and purple. Bedding ranged from laminated to medium and planar to undulating planar, and was typically expressed as faint bedding plane traces. With few exceptions, bedding planes did not represent discontinuities. Most breaks in the recovered rock cores appeared to be machine breaks. Hardness ranged from very soft to moderately soft. Overall, core recoveries varied from 47 to 100 percent with the poorest recoveries associated with core runs obtained from Rock Horizons H2 (Boring B-2, depths of zero to about 4.0 feet and B-3, depths of 8.0 to 8.5 feet) and H4 (Boring B-1, depths of 9.25 to 10.0 feet). In general, relatively high rock quality designation (RQD) cores were obtained from the stronger H1 and H3 Horizons and relatively low RQD cores were obtained from the weaker H2 and H4 Horizons.

The unconsolidated alluvial soils consist of silty to clayey sand deposits ranging in thickness from zero to about one foot, which classify as non-plastic silty sand (USCS Classification SM). These sands were predominately fine-grained with fines content ranging from 18 to 41 percent by weight. The colluvium consists of fine gravel- to large boulder-size particles of dolomitic limestone and occurs with the alluvium mainly on steep slopes along and below the existing Rim Trail and proposed ADA Route alignment.

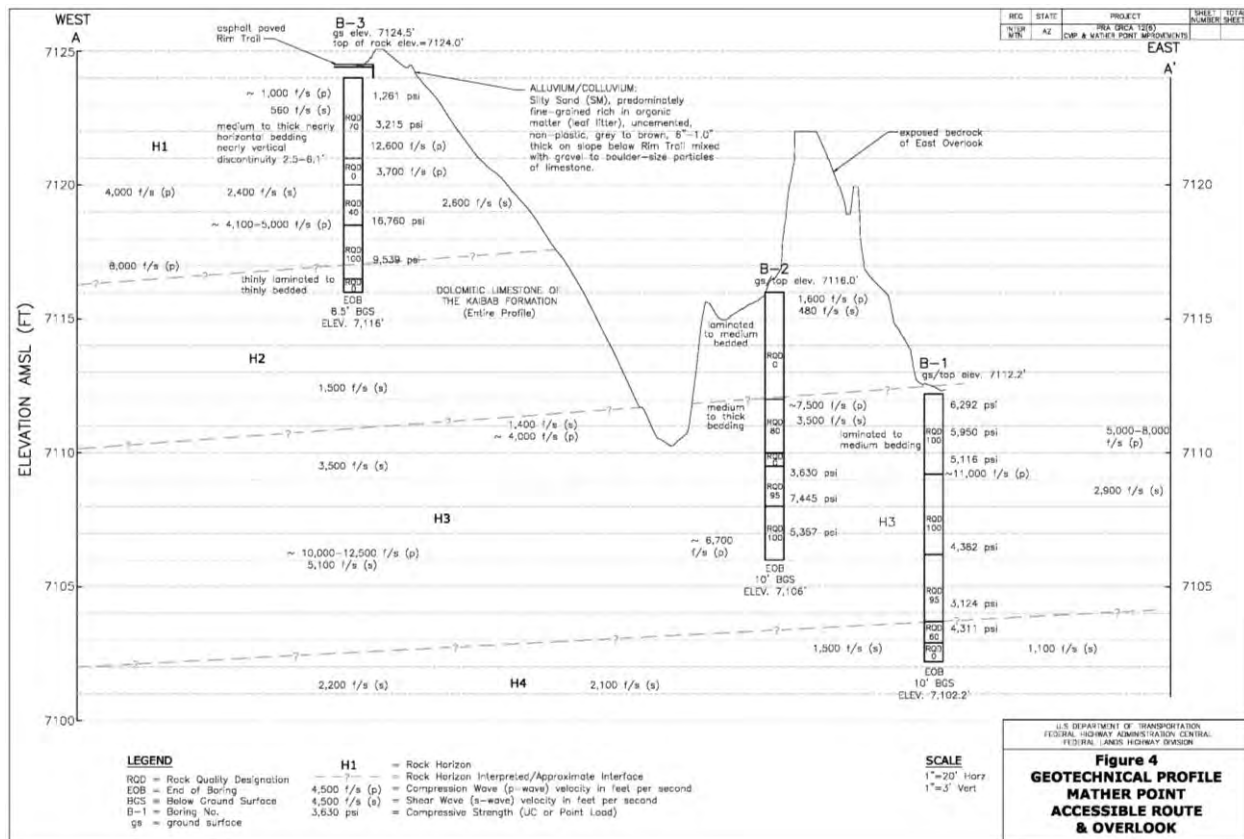


Figure 3: Geotechnical Profile

Summary - Bedrock conditions for Horizons H1 through H4, based on seismic refraction surveys, boring and core data, and strength tests, are summarized in Table 1.

Table 1 - Rock Properties & Interpreted Conditions Summary					
Rock Horizon	Approximate Thickness (feet) (based on seismic surveys)	Core Recovery	Rock Quality Designation (RQD)	Seismic Survey Compression Wave (p-wave) and Shear Wave (s-wave) Velocities	Point Load Index and Unconfined Compressive Strength Values for Core Samples
H1	7 to 9	65 to 100% Average = 84%	zero to 100 Average = 50	Near canyon rim/Mather Point: p-wave = 3,500 to 5,000 f/s (isolated zones of 8,000 to 12,600 f/s). s-wave = 2,400 to 2,600 f/s Near Visitor Center: p-wave = 4,200 to 6,600 f/s (isolated zones of 7,100 to 11,000 f/s)	Near canyon rim/Mather Point: 1,261 to 16,760 psi, average = 5,876 psi Near Visitor Center: 725 to 21,844 psi, average = 4,592 psi

Table 1 - Rock Properties & Interpreted Conditions Summary					
Rock Horizon	Approximate Thickness (feet) (based on seismic surveys)	Core Recovery	Rock Quality Designation (RQD)	Seismic Survey Compression Wave (p-wave) and Shear Wave (s-wave) Velocities	Point Load Index and Unconfined Compressive Strength Values for Core Samples
H2	7 to 9	50 to 92% Average = 71%	zero	p-wave = 2,700 to 4,000 f/s s-wave = 1,400 to 1,500 f/s	No core samples with sufficient L:D ratio obtained from H2 Horizon. Zero RQD values obtained for cored H2 rock
H3	8 to 12	50 to 100% Average = 84%	zero to 100 Average = 80	p-wave = 7,500 to 11,100 f/s s-wave = 3,500 to 5,100 f/s	3,124 to 7,445 psi, average = 5,067 psi
H4	9 to 11	47% (one core run only)	zero	s-wave = 1,000 to 2,200 f/s	No core samples with sufficient L:D ratio obtained from H2 Horizon; H2 Horizon penetrated only about 1 to 1 ½ feet

Where test borings coincided with depths/lithologies investigated by the seismic surveys, data obtained from each investigative method correlated well as shown on Figure 3.

Groundwater and Soil Moisture Conditions

Groundwater was not encountered in any of the three borings, all of which were advanced into rock to relatively shallow depths (8.5 to 10 feet bgs). Water was used during coring to cool and lubricate the core drill. This introduced free water to the porous limestone. As such, evaluation of natural moisture conditions of the rock underlying the locations investigated could not be made. Based on information obtained, depth to groundwater beneath the subject site is at an approximate depth of about 1,000 feet to 3,000 feet bgs (Metzger 1961).

Geologic & Geotechnical Considerations

Geologic and geotechnical conditions which could result in impacts to the proposed site improvements and facilities, consideration of which should be incorporated into final design, were identified and evaluated as follows.

Earthquakes and Active Faults - The project site is located within a moderate earthquake hazard zone with seven moderate earthquakes (magnitude 5.0 to 7.0) recorded over the last 150 years and having epicenters located between 30 and 60 miles from the project site (Fellows, 2000). The USGS Earthquake Hazards Program, Quaternary Fault and Fold Database of the United States (USGS, 2003) identified four fault zones or systems for which geologic evidence suggests Quaternary-age (past 1.6 million years) deformation located within 20 miles of the project site. These faults are described as having possible Quaternary activity and assigned slip rates of less than 0.2 millimeters per year (Pearthree, P.A., 1997a, b, c, d). The potential for strong ground accelerations in the immediate vicinity of the project is considered low to moderate. Based on site conditions identified by this investigation, any ground shaking could result in movement of

rock blocks and result in slope failures along the canyon rim including the areas of the ADA Route and East Overlook.

Site Seismicity - Probabilistic earthquake ground motion values were obtained from the USGS National Seismic Hazard Mapping Project, Earthquake Hazards Program (USGS, 2002) and seismic acceleration contour and fault maps for the State of Arizona which are based on research, field investigations, and seismic analyses (Euge, Schell and Lam 1992). Peak ground acceleration values in rock for a 10-percent probability of exceedance in 50 years derived from these two sources were 0.11g (USGS) and 0.15g (Euge, 1992.).

Volcanic Activity - No active volcanoes are known to exist in the region of the project site, including Arizona and Utah. The geologic map covering the site does not indicate volcanic rocks within the vicinity (Grand Canyon Association, 1996). The potential for volcanic activity at the project site or in the region is considered very low.

Erosion - The land surface along the South Rim at and in the vicinity of the site slopes gently to the southwest and away from the rim edge. As such, surface flows from storm events are directed away from the rim and erosion from these flows is minimal. No indications of major active erosion including rills or gullies were observed in soils along this slope, including the ADA Route alignment. The major erosion forces impacting soil and rock at the site (and the South Rim in general) include freeze-thaw action and gravity, and to a lesser extent wind and water that come in direct contact with exposed surfaces. Based on observed conditions, the various limestone layers that comprise the site area weather and erode back at different rates. As relatively weaker layers undercut relatively stronger layers, the stronger layers lose support from below, become loose and dislodged along bedding planes and joints, and eventually topple into the canyon. The rate at which this process occurs is not known. However, as presented by AMEC, a rough estimate of lateral erosion rate at the site using the distance from the Colorado River (about 13,000 feet at Mather Point) and a best guess of the time of the Grand Canyon's forming (about five to six million years ago) leads to a rough approximation of about 2 to 3 feet per thousand years, or about one-quarter to one-third of an inch per decade.

Rockfall and Slope Failure - Rockfall and slope failure is considered a potential hazard for two portions of the project site. These include the relatively steep slope which forms the ADA Route alignment and adjacent areas, and the nearly vertical to undercut cliff face that forms the edges of the East Overlook (ADA Overlook). Along these portions of the site, and along the canyon rim as a whole, slope failure is an ongoing process that forms and shapes the exposed geology, including the three rock horizons that constitute the surface on which the ADA Route and Overlook will be constructed (Horizons H1 through H3, inclusive). The primary failure mechanism of the more competent Rock Horizons H1 and H3 appears to be by separation of rock blocks along discontinuities (joint sets as previously described) which then dislodge, rotate, and/or topple. Separation along discontinuities is typically affected by chemical and physical weathering, and in the case of Horizons H1 and H3, is primarily caused by loss of support as the weaker underlying rock layers (Horizons H2 and H4) weather and erode more quickly. Dislodging, rotation, and toppling of rock blocks are prevalent along the exposed edge of Horizons H1 and H3 and appear more prevalent at locations of relatively more extensive undercutting. Any ground shaking could result in movement of rock blocks and result in slope

failures. The potential for rockfall and/or slope failure affecting the proposed improvements was evaluated to be moderate.

DISCUSSION & RECOMMENDATIONS

General

Depending upon in which rock horizon construction occurs, there is the potential for mass rock slope failure. It was recommended that all improvements for the ADA Route and East Overlook be founded on competent, intact rock. Loose, closely-jointed rock and detached or partially detached and unstable rock blocks or zones, which may already be in translation or toppling, or prone to same, were recommended for removal when practicable, such that competent intact rock is exposed. Alternatively, restraint of detached or partially detached blocks or masses of rock with rock anchors in lieu of removal was recommended. Where competent intact rock cannot be exposed, foundations or anchorages which extend vertically and/or laterally into competent intact rock were recommended. Pathway structures supported on cantilevered elements which extend laterally and upward from and are sufficiently embedded in a layer of suitably intact and competent rock, supported by rock anchors were also recommended.

Rock Slope Stability

Detailed evaluation of rock slope stability was not performed as part of the investigation. However, general statements regarding apparent site conditions can be made based on visual observations and geologic mapping.

Three joint sets control the configuration of the proposed ADA Route alignment and East Overlook. Horizontal rock exposures of the East Overlook generally exhibit close to very wide joint spacing with healed/cemented, closed (tight to very tight) apertures that, in the vertical plane, appear continuous through the various horizons. In the more competent, stronger rock horizons (Horizons H1 and H3), joint sets generally form blocky geometries ranging in size from small (10 to 30 joints per square meter) or medium (3 to 10 joints per square meter) to very large (< one joint per square meter) and may be relatively competent and stable in exposures. In the relatively less competent weaker rock horizons (Horizons H2 and H4), joint sets generally form crushed, tabular, and blocky geometries ranging in size from crushed (>60 joints per square meter) to medium (3 to 10 joints per square meter) and may be relatively less competent and less stable in exposures.

In the majority of the mapped horizons, block size and shape appears controlled more so by bedding thickness than joint spacing, except where two or more joint sets with relatively close joint spacing converge. The area below the ADA Route and the East Overlook (Rock Horizon H3) is undercut by Rock Horizon H4 to varying degree, ranging from less than one foot up to several feet, but typically in the range of about one to 1-½ feet. Undercutting appeared more pronounced where multiple joint sets of relatively close spacing converge. The primary failure mechanism of the more competent Horizon H3 rock at and nearby the project site appears to be by separation along discontinuities (joint sets as described above) forming blocks which then dislodge, rotate, and topple.

Based on the predominant conditions observed, the undercutting of Horizon H3 by Horizon H4 did not appear to be of an extent sufficient to cause instability of rock blocks comprising perimeter viewing areas (the edges) of the East Overlook.

Site Grading and Subgrade Preparation

Removal of all vegetation and debris in areas designated for slope cuts and fills was recommended with exposed surfaces to receive fill or pavements cleaned of residual soils to expose sufficiently competent rock. Loose or dislodged rock fragments were recommended to be removed prior to placement of fills.

Maintenance of positive site drainage was recommended both during and subsequent to construction of cut and fill slopes. Ponding of water along embankments or retaining walls was identified as having the potential to result in degradation (softening or loosening) of the limestone rock or fills that could promote subgrade settlement or movement. Maintenance of positive site drainage was identified as essential for the long-term performance of project elements.

Excavatability

Excavatability of the alluvial/colluvial soil deposits and Rock Horizons H1 and H2 was based on data obtained through seismic surveys and criteria from the Caterpillar Performance Handbook (Caterpillar 2008). The alluvial/colluvial soils were not expected to require the use of heavy or specialized equipment for trench or mass excavation. However, large boulders or blocks of detached rock were expected to be interspersed within these materials, and where encountered special handling for removal was recommended. In most cases, Rock Horizon H1 was predicted to be rippable to marginally rippable using a Cat D7G (200 horse power, or hp) bulldozer and rippable for a Cat D8L (335 hp) bulldozer or equivalent. Isolated zones of Rock Horizon H1 were predicted to range from marginally rippable to unrippable using a Cat D8L. Rock Horizon H2 was predicted to be excavatable using a trackhoe or bulldozer of greater than about 200 hp. Smaller equipment with greater than about 150 HP was anticipated to be effective through at least some of the Horizon H2 material.

Areas requiring significant excavation include the ADA Route and east tie-in to the East Overlook, where use of heavy equipment most likely will not be possible due to the existing narrow and steep slopes and relatively small size of the proposed improvement areas. Therefore, alternative rock excavation methods such as boom-mounted impact hammers and non-explosive or soundless chemical demolition agents (chemical expansive agents) were proposed for consideration.

Rock Anchors and Tiedowns

Allowable loads for rock anchors and tiedowns were determined for the upper three rock horizons (Horizons H1, H2, and H3). As the encountered rock horizons and their respective elevations along the ADA Route vary, evaluation in the field during construction was recommended. The anchor type evaluated consisted of one-inch nominal diameter Grade 75 deformed bar (Dywidag or equivalent) gravity- or pressure-grouted in three-inch diameter anchor holes into existing bedrock. Allowable anchor loads were determined utilizing methods

recommended by Adams and Radhakrishna (1977), FHWA (1999), Hoek and Brown (1980), and Littlejohn and Bruce (1977). Values for UCS, as presented in Table 2, were based on conservative lower-bound values obtained for laboratory tested rock cores (Horizons H1 and H3) or estimated (average) UCS based on seismic refraction surveys where UCS test data on core samples were not available (Horizon H2). UCS was assumed to be constant with depth for the effective depth of penetration of the anchors (along the bond zone), specified to be a minimum of 5 feet below the referenced bedrock horizon contact. A factor of safety (FOS) of 2.0 was applied to determine allowable (working) loads. Side resistance and overburden stress of thin soil deposits and planned fills above the rock contact were neglected.

Table 2 – Rock Anchor Allowable Load Design Parameters

Rock Horizon	Unconfined Compressive Strength (UCS) (psi)	Rock Quality Designation (RQD) (%)	Allowable Load		
			Bar-to-Grout Bond	Grout-to-Rock Bond	Rock-to-Rock Shear
H1	1,261 ⁽¹⁾	Min = 0 Max = 100 Avg = 53 Stdev = 43	12 kips/ft. bond zone 60 kips/5-ft. bond zone	37 kips/ft. bond zone 185 kips/5-ft. bond zone	44 kips/5-ft. bond zone
H2	650 ⁽²⁾	0	12 kips/ft. bond zone 60 kips/5-ft. bond zone	19 kips/ft. bond zone 95 kips/5-ft. bond zone	18 kips/5-ft. bond zone
H3	Min = 3,124 ⁽³⁾	Min = 0 Max = 100 Avg = 79 Stdev = 35	12 kips/ft. bond zone 60 kips/5-ft. bond zone	88 kips/ft. bond zone 440 kips/5-ft. bond zone	75 kips/5-ft. bond zone

Notes: (1) Minimum UCS value obtained for Rock Horizon H1 core samples, used for allowable load calculations.

(2) Average estimated UCS based on range of p-wave velocities obtained for Horizon H2 (AMEC, 2009/Rucker, 2008)

(3) Minimum UCS value obtained for Rock Horizon H3 core samples, used for allowable load calculations.

Based on the analysis, the controlling failure mode (failure mode with the lower-bound allowable load) for anchor design was determined to be rock-to-rock shear for Horizons H1 and H2, and bar-to-grout bond for Horizon H3. Recommendations for testing to verify anchor performance as designed included both verification tests and proof tests.

CONCLUSIONS

When planning a geotechnical investigation to support design of structural improvements (such as building foundations, roadway elements, or bridge piers and abutments), engineers and engineering geologists focus subsurface investigation (test borings, soil and rock sampling, and laboratory testing) at the specific locations where improvements are to be constructed. Sometimes physical constraints or safety limitations and considerations make this impossible and the subsurface investigation must be performed as close as practical to, but away from the actual planned location of the structural improvement. In such cases, geotechnical evaluation and recommendations need to be made assuming that conditions encountered will be the same or substantially similar to those encountered during construction and greater emphasis is often placed on non-invasive investigative techniques to fill in the data gaps and supplement information obtained through invasive investigation.

For this project, detailed geologic mapping and geophysical investigation (seismic refraction and ReMi surveys) were combined with traditional test boring, soil and rock sampling, and laboratory testing to investigate the subsurface and gain the greatest level of confidence possible given the physical and safety limitation imposed by the project location. Results obtained from each of these investigative approaches correlated very well and a good level of confidence in the individual results was realized. Results indicated that widely variable rock conditions could be expected during construction. Because of the variable rock conditions anticipated, geotechnical recommendations also included options for design and construction depending on the actual conditions encountered. This included a field-fit approach to final design and construction of the ADA Ramp and its tie-in with the East Overlook with specified field inspection and approval by the project geotechnical engineer or engineering geologist.

The geotechnical report and design recommendations presented therein received high praise from the Owner's representatives and the project manager. The overall result was a design and bid package for which both the design team and Owner were comfortable, even though some site conditions remained unknown.

In conclusion, traditional boring methods, geophysical surveys, and geologic mapping each provided unique data and were effectively combined to characterize the geologically complex site, considering that direct site access by investigators was not possible. The project demonstrated that these investigative methods can all be important components of a geotechnical investigation and can be effectively used together on geologically complex sites where direct access to the planned locations is not possible during geotechnical investigation.

REFERENCES

- Adams, J.I. and Radhakrishna, H.S., 1977, *Uplift Capacity of Footings and Anchors for Transmission Towers*, Ontario Hydro Research Quarterly, first quarter.
- AGRA Earth & Environmental, Inc, (AEE), 1979, *Final Geotechnical Investigation Report, Mather Point Orientation/Transit Facility, Grand Canyon National Park, Grand Canyon, Arizona*, December 29.
- AMEC Earth & Environmental, Inc. (AMEC), 2009, *Seismic Refraction Evaluation, Mather Point East Overlook, Grand Canyon, Arizona*, July 13.
- Arizona Department of Transportation (ADOT), 1989, *Materials Preliminary Engineering and Design Manual*, March.
- Bills, D. J., Flynn, M. E., and Monroe, S. A., 2007, *Hydrogeology of the Coconino Plateau and Adjacent Areas, Coconino and Yavapai Counties, Arizona*, USGS Scientific Investigations Report 2005-5222.
- Caterpillar Tractor Company, (CAT) 2008, *Caterpillar Performance Handbook, Edition 38*, Peoria, Illinois, October.
- Euge, K.M., Schell, B.A. and Lam, I.P., 1992, *Development of Seismic Acceleration Contour Maps for Arizona, Final Report, Report No. FHWA-AZ92-344*, prepared for the Arizona Department of Transportation, Phoenix, AZ, September
- Fellows, Larry D., 2000, *Volcanism in Arizona*, Arizona Geology, Vol. 30, No.4, Published by Arizona Geological Survey, Winter.
- FHWA, 1999, *Ground Anchors and Anchored Systems*, Geotechnical Engineering Circular No. 4, U.S. Department of Transportation, Federal Highway Administration, Office of Bridge Technology, Washington, D.C., FHWA-IF-99-015, June.
- Grand Canyon Association, 1996, *Geologic Map of the Eastern Part of the Grand Canyon National Park*.
- HDR Engineering Inc., (HDR) 2009, *Grand Canyon National Park Mather Point Improvements, Grand Canyon, Arizona, Geotechnical Investigation Report*, October.
- Hoek, E. and Brown, E.T., 1980, *Underground Excavations in Rock*, Institution of Mining and Metallurgy, London, England.
- Littlejohn, G.S. and Bruce, D.A., 1977, *Rock anchors - State of the Art*, Foundation Publications Ltd., Brentwood (Essex), England.
- Metzger, D.G., 1961, *Geology in Relation to Availability of Water Along the South Rim, Grand Canyon National Park*, Arizona, Geological Survey Water-Supply Paper 1475-C.

National Climatic Data Center (NCDC), 2005, Air Freezing Index – USA Method (Base 32 Degrees Fahrenheit), <<http://www.ncdc.noaa.gov/oa/fpsf/fpsfpublications.html>>, last updated July 15, 2005, accessed July 2009.

Pearthree, P.A., compiler, 1997a, Fault number 991, Bright Angel fault zone, in Quaternary fault and fold database of the United States: U.S. Geological Survey website, <http://earthquakes.usgs.gov/regional/qfaults>, accessed July 15, 2009.

Pearthree, P.A., compiler, 1997b, Fault number 992, Eminence fault zone, in Quaternary fault and fold database of the United States: U.S. Geological Survey website, <http://earthquakes.usgs.gov/regional/qfaults>, accessed July 15, 2009.

Pearthree, P.A., compiler, 1997c, Fault number 993, Central Kaibab fault system, in Quaternary fault and fold database of the United States: U.S. Geological Survey website, <http://earthquakes.usgs.gov/regional/qfaults>, accessed July 15, 2009.

Pearthree, P.A., compiler, 1997d, Fault number 994, West Kaibab fault system, in Quaternary fault and fold database of the United States: U.S. Geological Survey website, <http://earthquakes.usgs.gov/regional/qfaults>, accessed 07 July 15, 2009.

Rucker, M.L., 2008, *Estimating In-Situ Geo-Material Mass Density, Modulus and Unconfined Compressive Strength from Field Seismic Velocity Measurements*, Highway Geophysics-Nondestructive Evaluation Conference, Charlotte, NC, Dec. 1-4.

United States Department of the Interior (DOI), Bureau of Reclamation (BOR), 2001, *Engineering Geology Field Manual, Second Edition*.

United States Department of the Interior (DOI), National Park Service (NPS), 2002, *Environmental Assessment, Mather Campground Rehabilitation*.

United States Geological Survey (USGS), 2003, Quaternary Fault and Fold Database of the United States, Version 1.0, USGS Open-file Report 03-417, <<http://earthquake.usgs.gov/regional/qfaults/>>, accessed July 2009.

Case Study Using Geotechnical Instrumentation to Monitor Fill Foundation Stability

Matthew V. Buche
KANE GeoTech, Inc.
7400 Shoreline Dr., Suite 6
Stockton, CA 95219
(209)-472-1822
matt.buche@kanegeotech.com

William F. Kane
KANE GeoTech, Inc.
7400 Shoreline Dr., Suite 6
Stockton, CA 95219
(209)-472-1822
william.kane@kanegeotech.com

Prepared for the 61st Highway Geology Symposium, August, 2010

Acknowledgments

The authors would like to thank the individuals for their contributions in the work described:

Mathew Fielding– Terracon Consultants, Inc.
Chris Weaver – Advanced Shoring & Underpinning, Inc.
Brian Garrett – PDA Engineering, Inc.

Disclaimer

Statements and views presented in this paper are strictly those of the authors, and do not necessarily reflect positions held by their affiliations, the Highway Geology Symposium (HGS), or others acknowledged above. The mention of trade names for commercial products does not imply the approval or endorsement by HGS.

Copyright Notice

Copyright © 2010 Highway Geology Symposium (HGS)

All Rights Reserved. Printed in the United States of America. No part of this publication may be reproduced or copied in any form or by any means – graphic, electronic, or mechanical, including photocopying, taping, or information storage and retrieval systems – without prior written permission of the HGS. This excludes the original authors.

ABSTRACT

Highway reconstruction projects may involve time and/or economic constraints requiring accelerated work schedules. Such projects commonly include fill placement and MSE walls to construct new abutments. Accelerated work schedules can result in rapid loading increments, a cause for concern when placed on underlying soft soil foundations. When subjected to rapid loading, foundations can experience increased lateral deformation and failure. To avoid embankment failure, geotechnical instrumentation can be used to assess soil foundation performance during construction. Methods of analysis and determination of loading thresholds based on lateral and vertical displacements of foundation soil are outlined by Saye and Ladd (2004). The application of the method was used in 2009 for monitoring purposes at a site in the western United States. Geotechnical instruments were installed to observe soil foundation settlement and horizontal displacement to analyze its performance during construction. The technique allowed project managers to monitor embankment stability, identify a potential problem, and avoid a catastrophic failure by temporarily removing fill.

INTRODUCTION

Embankments constructed on soft ground often require geotechnical instrumentation to monitor the progress of consolidation and determine stability during fill placement (1). When subjected to rapid loading, these soft soil foundations can experience increased lateral deformation, a catalyst for bearing capacity failure. Monitoring programs provide data used to interpret foundation performance during construction, forewarn conditions of increasing instability and potential failure, and allow modifications to be made to construction schedules to remediate developing adverse conditions. Monitoring is often done using manually read instrumentation such as stand-pipe piezometers, probe inclinometers, and manually read settlement gages such as those described by the California Department of Transportation (2).

Analytical methods for performance monitoring were discussed by Saye and Ladd (3) and Bartlett et al. (4) during foundation performance monitoring of MSE walls and embankments constructed for the I-15 highway widening project near Salt Lake City, Utah. The monitoring program was implemented to control construction processes and improve geotechnical design (4). In addition to controlling the rate and placement of fill to prevent failure, other goals were to determine the effectiveness of prefabricated vertical wick drains for accelerating the time of consolidation and quantifying the amount of settlement affecting urban structures and subsurface utilities along the project.

Recently, a highway reconstruction project was begun in the western region of the United States with similar project goals and geologic subsurface materials as the I-15 project. It involved the construction of several mechanically stabilized earth (MSE) Hilfiker-type walls retaining embankment fill for bridge approaches. Geotechnical instrumentation was implemented for foundation performance monitoring during construction similar to methods used at the I-15 highway reconstruction project. As with most monitoring programs of embankments on soft ground, horizontal displacements provided the most direct instability data (1). Reliable instrumentation and monitoring was crucial during construction because the use of ramp loading fill techniques resulted in increased rates of fill placement and potential destabilization.

This paper presents the data from one of the several MSE walls monitored, discusses the instrumentation and methodology used to monitor foundation performance during construction, compares the results with methods used at the I-15 reconstruction project in Salt Lake City, and presents how the technique aided the decision by engineers and project managers to use remedial measures to avoid a potential failure.

SUBSURFACE CONDITIONS

Most of the geologic features of the region were created by volcanic events and tectonic extension resulting in linear fault block mountain ranges delineated by normal faults occurring from the Miocene to present (5). Quaternary incision and backfilling by rivers and streams was

followed by aeolian loess deposits and basalt flows of the Late Pleistocene. The general geological subsurface materials encountered during exploratory drilling can be described with depth as: about 25-ft of fill, 40-ft to 50-ft of native soils and regolith, and 10-ft to 15-ft thick gravel deposits above 20-ft to 30-ft of basalt bed rock. A typical profile is shown in Figure 1. The fill material was from the pre-existing bridge and highway. Beneath the fill the native soil and regolith materials consisted of interbedded, poorly sorted layers and lenses of fluvial sand, silt, and clay deposits.

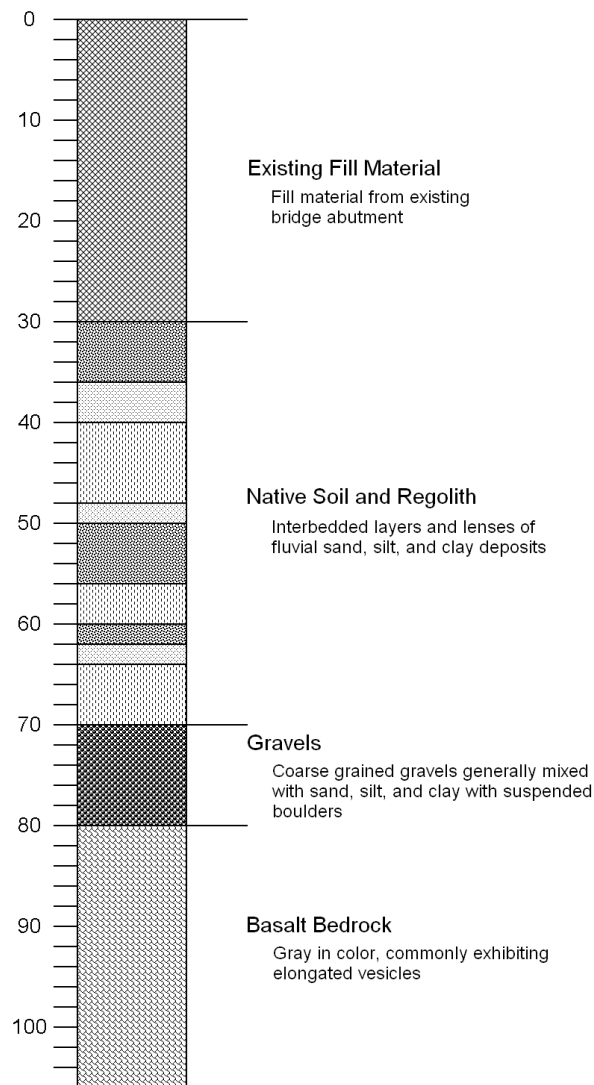


Figure 1 – Idealized and Generalized Geologic Profile Typical of the Project Location

Above the basalt bedrock, sections of coarse-grained gravels generally mixed with sand, silt, and clay with intermittent, suspended boulders were encountered. The basalt bedrock was gray in color and commonly exhibited elongated vesicles. Before construction, project design plans involved ground modification techniques such as the use of stone columns to improve the bearing capacity of the soft subsurface materials.

GEOTECHNICAL INSTRUMENTATION

The purpose of the geotechnical instrumentation was to collect geotechnical data to allow project engineers to monitor embankment and MSE retaining wall settlement and stability. This information was used to control the fill placement schedules and rates. Measured values included horizontal ground deformation, vertical ground deformation, and pore water pressure. These values were collected manually by field technicians from field surveys of inclinometer installations using an inclinometer probe, and remotely from vibrating wire settlement cells and piezometers. All vibrating wire sensors were integrated to an Automated Data Acquisition System (ADAS) composed of a programmed Campbell Scientific CR1000 datalogger with measurement and communication peripherals (Figures 2 and 3). Remote communication was established through the use of a Sierra Wireless RavenXTV CDMA cellular modem utilizing the Verizon Wireless broadband data service. All instrumentation was powered using a solar panel and protected in a steel enclosure, Figures 2 and 3.

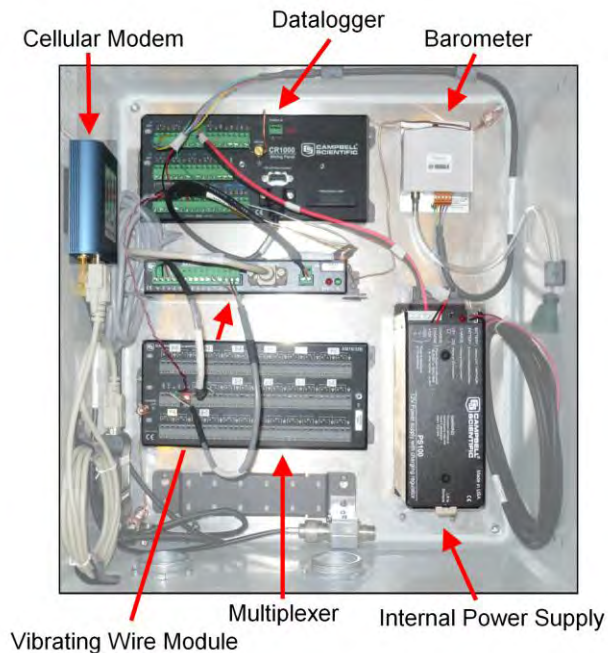


Figure 2 –Instrumentation Inside of the Automated Data Acquisition System Enclosure



Figure 3 – Typical ADAS Enclosure

Instrument Arrays

The typical instrument array for embankment and MSE retaining wall performance monitoring consisted of one or more instrument groups. In general, an instrument group included an inclinometer, settlement cell, and two piezometers at staggered depths (Figure 4). Inclinometer installations were located outside of the embankment or MSE wall dimensions perpendicular to the centerline of the structure (perpendicular to highway). The settlement cell and piezometers were located “inside” of the inclinometer installation with settlement cells generally 3 to 4-ft below pre-construction grade. Piezometers were offset 5-ft from or along the centerline adjacent to the group settlement cell and installed at variable depths below the survey surface as determined by project engineers and subsurface conditions. Reflective monuments were used to provide additional vertical deformation data. The surveying data was not included in developing this paper.

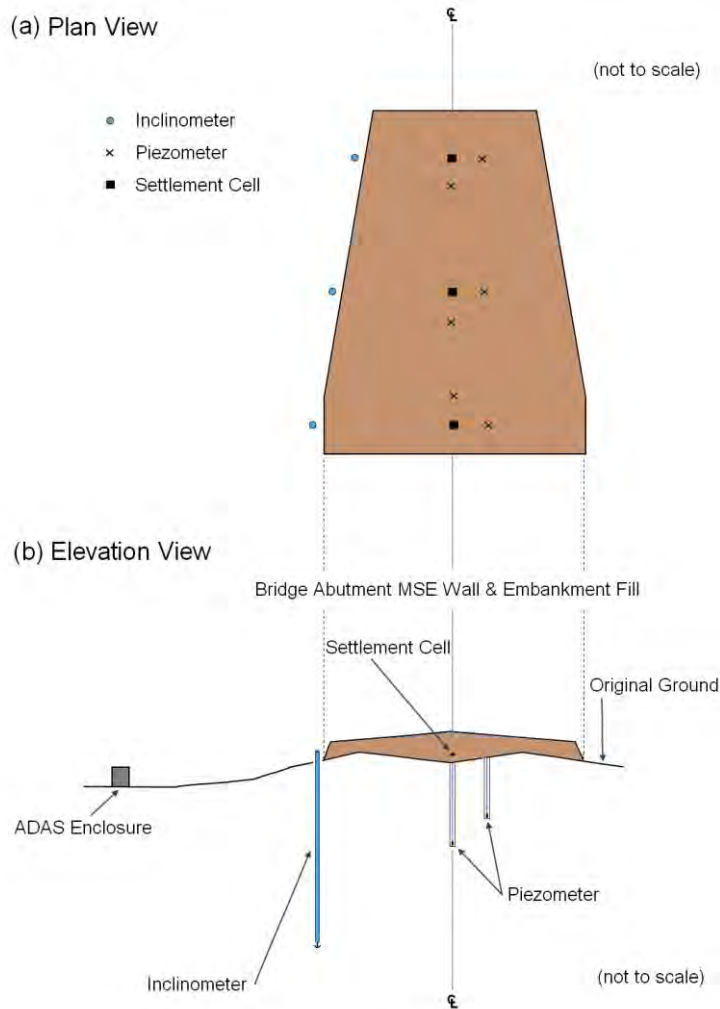


Figure 4 - Soil foundation abutment with typical instrumentation array in plan view (a) and elevation view (b)

Inclinometers

The maximum length of the inclinometer systems installed was approximately 85-ft. Each consisted of 10-ft sections of Slope Indicator 2.75-in outside diameter QC casing (Figure 5), a Digitilt Inclinometer Probe, and a Digitilt Datamate II logger to take measurements. Slope Indicator DMM and DigiPro software programs were used to produce profiles at 2-ft increments. Project specifications required the use of a Slope Indicator casing anchor at each installation (Figure 5). Total drilling depth was required to be within 15-ft of either dense gravel or bedrock. The annular space was backfilled with a cement/bentonite grout mix. Above grade, a steel, cylindrical monument was placed around the casing stick-up for protection. However, a few

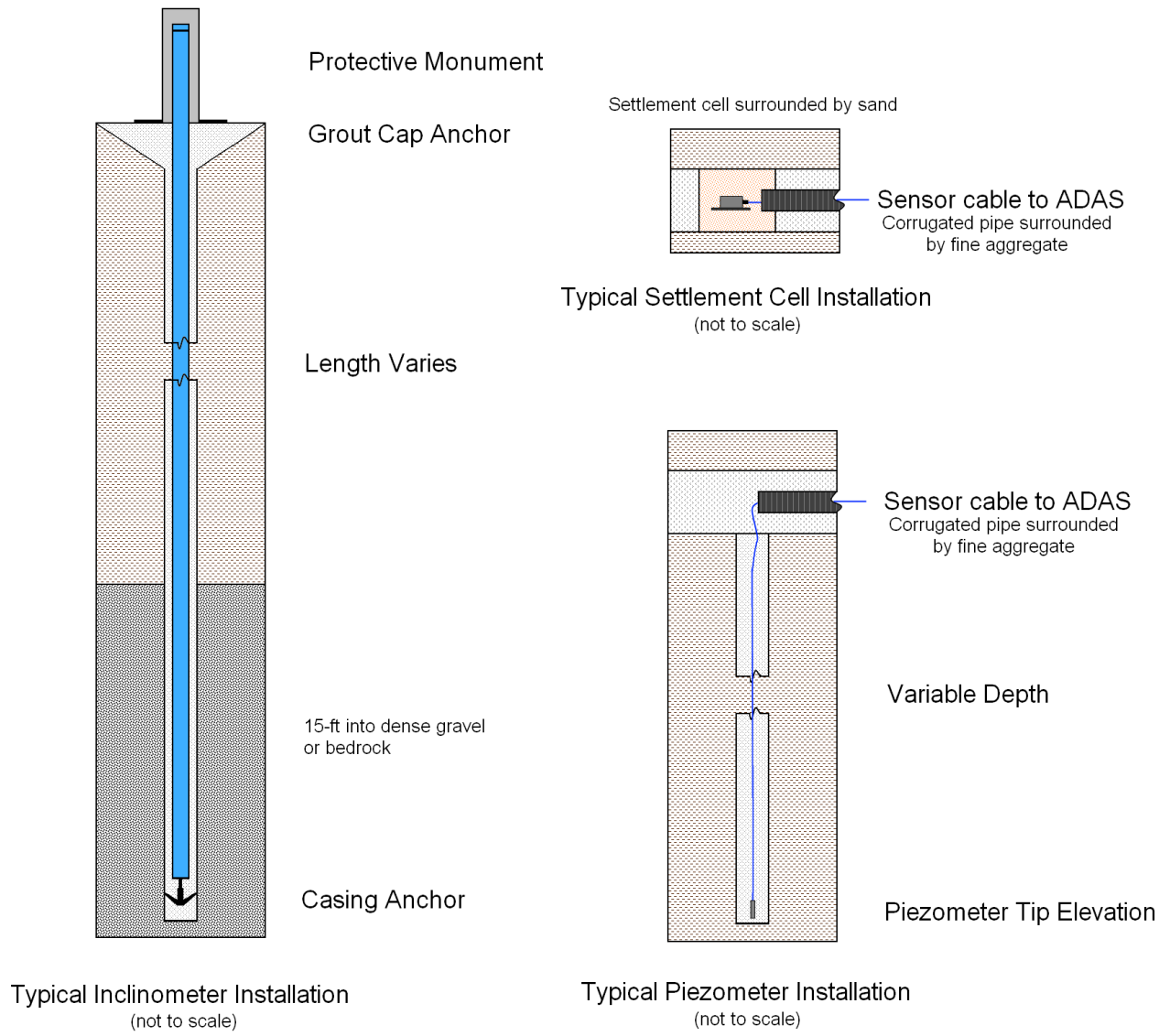


Figure 5 - Typical Instrument Installations

installations were located close to the MSE wall to get a better representation of deformation near the wall's face. As construction commenced and the height of the embankment fill increased, they were fitted with extenders and casing couplings to allow continued surveys as the project progressed.

Piezometers

Geokon Model 4500 Drive Point vibrating wire piezometers were selected to measure increases in soil foundation pore water pressures beneath the bridge abutment MSE walls and the embankment fills (Figure 4 and 5). Vibrating wire sensors utilize a sensitive stainless steel diaphragm to which a steel wire is connected; changing pressures on the diaphragm cause it to deflect (6). This deflection is measured as a change in wire tension and a change in the natural vibration frequency of the wire element (6). Installed below the piezometric surface, height fluctuations of the unconfined phreatic zone cause changes in applied pressure, vibrating frequency, and subsequent output voltage readings allowing monitoring of pore pressure changes in engineering units. Drive point piezometers are installed by drilling to within approximately 5-ft of the desired sensor elevation, fitting the drill rod with an adaptor and attaching a special rod directly to the piezometer tip, and then pushing the sensor through soft material to the final depth. However, dense native gravels and sands which could potentially damage the tips were encountered during initial push-in installation. Therefore, the push-in installation method was discontinued and the borehole advanced to the intended depth of the sensors, then backfilled using specified methods.

Settlement Cells

Slope Indicator non-vented vibrating wire settlement cells were installed to measure vertical ground deformation beneath the MSE wall and embankment fill. The settlement cells were installed mounted on a 9-in by 9-in steel settlement plate. Sensors were placed within a 30-in deep minimum trench (Figure 5). The settlement cells were surrounded with a minimum of 6-in of sand above and below the instrument. Sensor cables connecting to the ADAS were protected by a 6-in corrugated conduit surrounded by 6-in of fine aggregate above and below. The settlement cell fluid-tube reservoirs were housed within the ADAS enclosure. Because non-vented settlement cells are sensitive to atmospheric pressure, barometric pressure measurements were required to correct settlement readings (7). A Vaisala PTB110 series barometer was used for atmospheric pressure readings and corrections were made by an algorithm within the datalogger program.

METHOD OF PERFORMANCE MONITORING

The performance monitoring program protocol involved three main parties: Project Engineer, contractor project managers, and the Instrumentation Supervisor. The Instrumentation

Supervisor was charged with providing a summary report that included data reduction, evaluation, and analyses. It was submitted to both project engineers and managers on a daily basis during fill placement or other grading activities. During construction periods, daily measurements for all instruments were collected by 5:00 PM local time and submitted within 24 hours of the most recent measurement. In addition, inclinometer data and fill data was provided daily. The Project Engineer evaluated the data daily and, if necessary, determined any action to be taken by the contractor or other team members. Alert thresholds for each sensor type were predetermined by project engineers and are discussed below.

Alert Thresholds

In the event that measurements exceeded a predetermined threshold level, the results were verified with additional readings and immediately reported to the Project Engineer to determine after further review if any action was required.

Inclinometers

Inclinometer installations had both a consecutive and cumulative alert threshold:

- lateral movement of 10% of the vertical movement under the embankment near that point, as determined by the corresponding settlement cell, in either axis between consecutive readings
- cumulative lateral movement of 1-in

Piezometers

The piezometer alert threshold was set at a measured pore pressure increase from initial baseline readings taken prior to construction in excess of 50% of the applied fill effective stress load. The threshold pressure was determined using the Approximate (2:1) Method (8) for stress distribution calculation for vertical pressure beneath embankment fills.

Settlement Cells

Settlement cells also had a consecutive and cumulative alert threshold:

- 1-in settlement or heave between consecutive readings
- total cumulative settlement exceeding 6-in

APPLICATION

To demonstrate the method and evaluate its application, monitoring data from an MSE wall is presented as a case study. The data is compared with soil foundation performance monitoring methods used during the I-15 highway reconstruction project (3)(4) and the results discussed.

Performance Monitoring Data

Performance monitoring data encompassing the duration of construction activities at the case study MSE wall is shown in Figure 6. It includes MSE wall and embankment fill height (H), vertical displacement (s), maximum lateral displacement (h_m), and pore pressure (u) data over time. Data in Figure 6 shows a strong relationship between MSE wall height, maximum lateral displacement, and settlement. Pore pressure readings did not appear to be affected by the placement of fill. Generally, the increased load would result in a relatively quick increase of pore pressure followed by a gradual return to measured pressure equal to or slightly elevated from before the fill placement. Most likely this was due to the relatively high permeability of subsurface fine-grained materials. During drilling operations it was observed that the fine-grained material was quite pervious and grout take in the boreholes was greater than expected.

Also shown in Figure 6 are the cumulative alert threshold levels for the inclinometers and settlement cells. Instruments approaching or exceeding cumulative alerts helped the engineers and project managers assess changing soil foundation conditions. Isolated consecutive reading inclinometer and settlement cell alerts occurred occasionally during fill placement. On review by the Project Engineer and Instrumentation Supervisor these were determined to be acceptable and not solely indicative of decreasing foundation stability. However, lateral and vertical displacement values between Days 47 and 58 following a construction schedule of ramp loading and a rapid fill placement resulted in an Alert. Work was stopped and two courses of fill were removed. Once the foundation material had stabilized a maximum fill placement rate of 2-ft per day (Figure 6) was instituted. The MSE wall design height was reached on Day 78 without failure or further incident.

Methodology Comparison

I-15 Reconstruction Project Performance Monitoring

The purpose of both the I-15 reconstruction project and the widening and realignment of the Case Study highway were the same: monitoring to control the rate of fill placement to prevent failures. Both localities were faced with the loading of soft soil foundations. When comparing the instrumentation design and monitoring programs, differences can be attributed to geography and time constraint between the two projects. The work at I-15 was done along a stretch of interstate within an urban environment. A greater volume and variety of instruments was included because one of the project goals was to determine the amount of settlement and avoid its occurrence near structures and subsurface utilities.

Time constraints of the I-15 project were due to a work schedule that required completion prior to the 2002 Winter Olympics. Sequencing of the I-15 project involved two major phases, each lasting approximately 2 years (4) to keep the route open to traffic. During the first phase all traffic was shifted to the existing lanes while initial construction of the new lanes began. After completing Phase One construction, traffic was shifted to the new lanes and Phase Two began on the remaining lanes open during Phase One. Lake Bonneville sediments made the work challenging because previous construction activities in the 1960s recorded as much as 3 to 6-ft of initial settlement over a period of 2 to 3 years (4). Engineers at I-15 were tasked with accelerating the rate of primary consolidation and completing construction in a time frame shorter than the soft sediments of Lake Bonneville might allow. In addition to requiring a greater number and type of instruments in the design, the monitoring program and alert threshold and action protocol developed at I-15 was tailored to address this challenge.

For the construction of individual MSE walls and embankments a two-stage construction schedule was developed. One of the techniques used to accelerate the rate of primary consolidation at I-15 was the use of surcharge, i.e. placing additional loads atop the fill to speed consolidation. Initial construction of MSE walls and embankment fill was halted and surcharge applied after an intermediate height was reached (approximately 26-ft) during Stage One. The temporarily halt allowed engineers to determine the percent completion of primary consolidation using the observational method discussed by Asaoka (9). When a satisfactory consolidation and stability was determined, surcharge was removed and Stage Two began to achieve design height (approximately 56-ft). When the fill height was within 6-ft of design height the frequency of instrument measurements was increased to one per day. After design height was reached daily readings continued for a week or until acceptable stability was achieved (3).

As described earlier, during each stage of construction engineers and instrumentation personnel at the I-15 highway reconstruction project primarily focused on two deformation indicators: the change in the maximum horizontal displacement over change in time (dh_m/dt) and the deformation ratio ($DR = dh_m/ds$), derived from changes in maximum lateral and vertical displacement (3)(4) (Saye & Ladd refer to the parameter as the deformation ratio and Bartlett et al. the displacement ratio; the Saye & Ladd usage has been selected for this paper). From these parameters the stability threshold levels were developed and response actions for the I-15 reconstruction project shown in Table 1. Figure 7 is from Barlett et al. (4) and plots cumulative horizontal displacement versus cumulative settlement to calculate the deformation ratio.

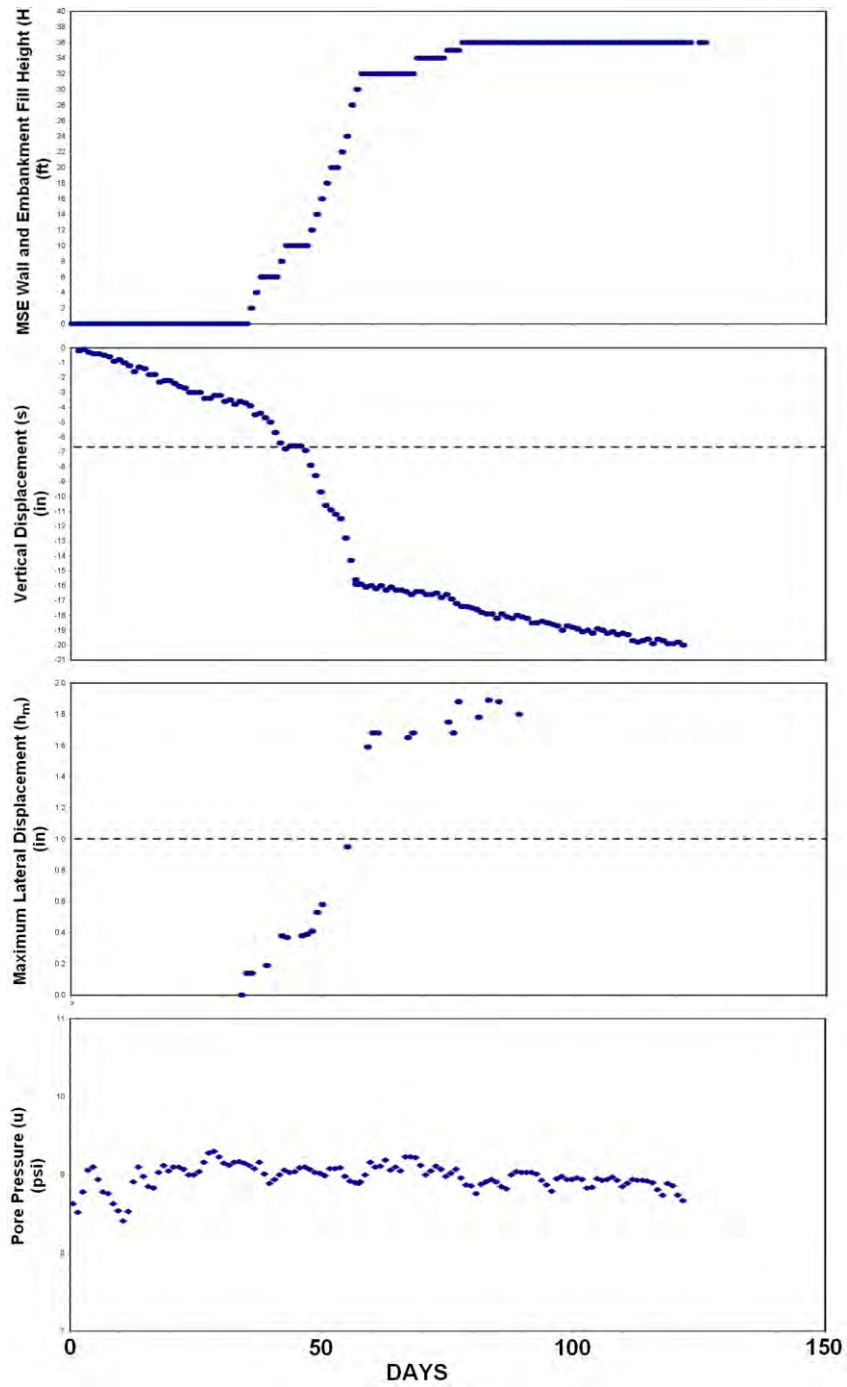


Figure 6 – Foundation Performance Monitoring Parameters: (H) MSE Wall and Embankment Fill Height; (s) Cumulative Settlement; (h_m) Maximum Lateral Displacement; (u) Soil Foundation Pore Pressure

Case Study Performance Monitoring

The highway at the case study was the primary man-made structure. Few surrounding buildings and subsurface utilities meant not having to have the volume or variety of instruments required in the I-15 monitoring program. Although the widening and realignment of the highway was not an infrastructure improvement necessary prior to a large international event like the Olympic Winter Games, soft compressible subsurface materials would present similar geotechnical challenges as the Lake Bonneville sediments did to the I-15 project. Although there are some differences in design between the two locations, the primary purpose of the monitoring programs developed at each site was the same; control the rate and placement of fill for MSE walls and embankment construction to prevent the occurrence of failures.

Alert Level	1	2	3
Horizontal Displacement Rate (in/day)	0.15	0.3	1.0
Displacement Ratio (DR)	0.1	0.2	0.3
Piezometric Head Increase	-----	>200% of Load Due to Fill Placement	Same as Threshold 2
Response Action	* Notify Field Construction Manager * Increase Monitoring Frequency	* Stop Fill Placement * Prepare Specific Action Plan * Implement Plan if Conditions Worsen	* Buttress Slope and Remove Fill * Notify Senior Project Management * Notify Utah DOT

Project sequencing of the case study was the same as that implemented at I-15 with two phases allowing the route to remain open to traffic. Instead of using staged construction, MSE walls and embankments constructed at the Case Study relied upon ramp loading. As described above, daily monitoring reports summarized data for interpretation by engineers. If thresholds were exceeded appropriate remedial action was determined and executed by project managers. The ADAS system made increasing frequent measurements time and cost efficient for the vibrating wire instruments. The time and cost of retrieving horizontal displacement values from the inclinometers still involved considerably greater time and cost because of the manual nature of such work.

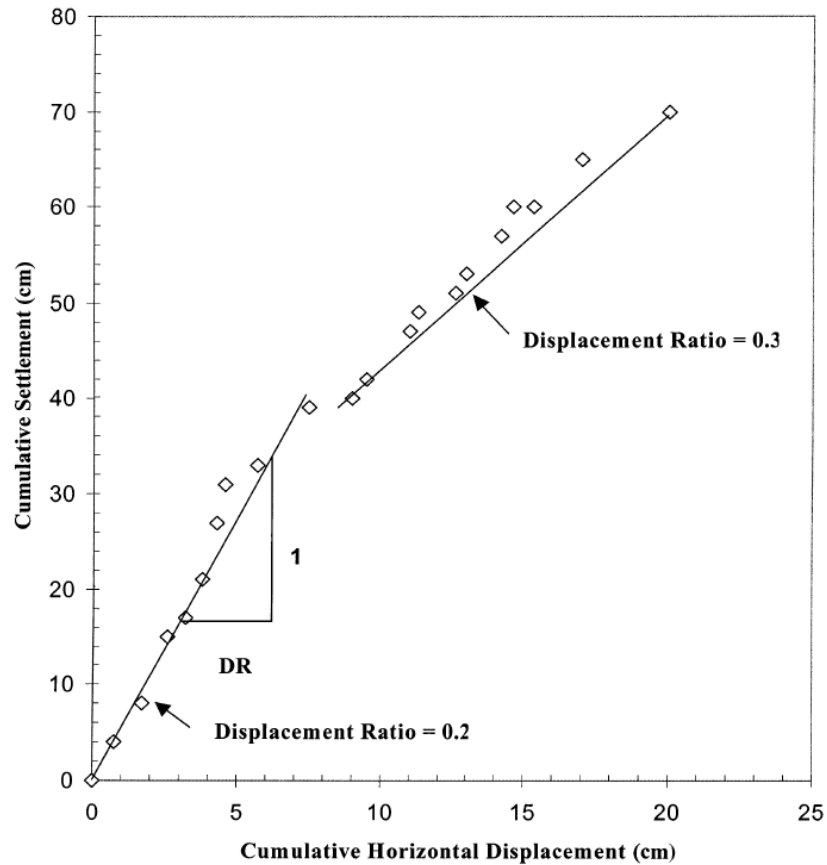


Figure 7 – Plot of Cumulative Horizontal Displacement Versus Cumulative Settlement to Calculate DR From Bartlett et al. (4).

Method Comparison

To evaluate the stability assessment methods and alert action levels derived from them, data from the Case Study will be used for comparison. Figure 8 depicts the maximum horizontal displacement over change in time (dh_m/dt) alert levels shown in Table 1 applied to the MSE wall and embankment fill Case Study data. Figure 9 shows the deformation ratio (DR). Using the dh_m/dt thresholds used at I-15, two Level 1 events and two Level 2 events would have occurred.

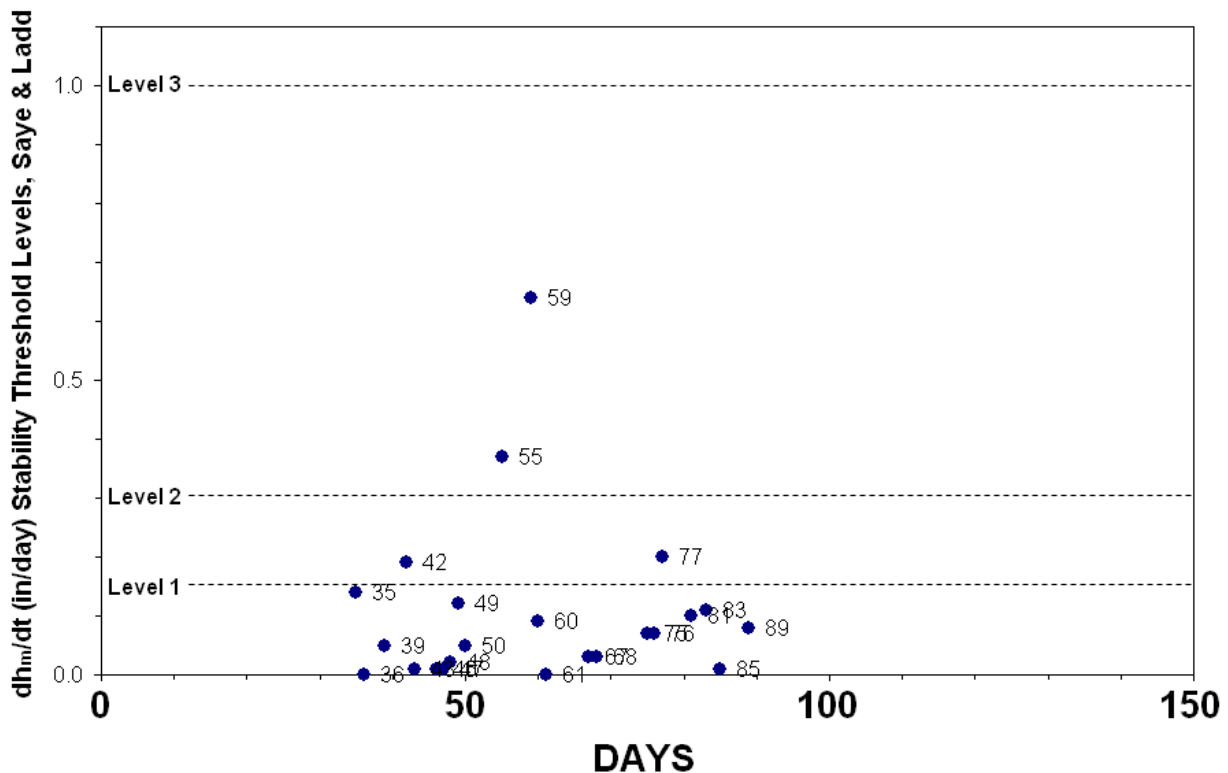


Figure 8 – Horizontal Deformation Rate (in/day) for the Case Study

Comparison of DR trends from Figure 7 of Bartlett (4) with that of the case study shows a similar change in the ratio. Bartlett et al. (4) describe how a significant change in the displacement ratio with time can indicate when the foundation behavior changes from a relatively stable condition associated with consolidation settlement to a state of excessive plastic deformation. The significant change in DR for the MSE wall case study data shown in Figure 9 occurred around Day 55 within the interval of rapid fill placement, Figure 5.

The DR values shown in Figure 9 and the time when the change occurs in correlation to the Case Study construction schedule fit the description for variations in the parameter discussed by Tavenas et al. (10). Tavenas et al. analyzed the development of lateral displacement under 21 embankments constructed on soft soil and clay foundations. They describe the variation as dependent on a change in foundation state from overconsolidated during the initial construction to a normally consolidated state during final stages of construction.

The analysis by Tavenas et al. produced embankment DR values during the initial construction phase varying between 0.06 and 0.36, with a mean of 0.18 and a standard deviation

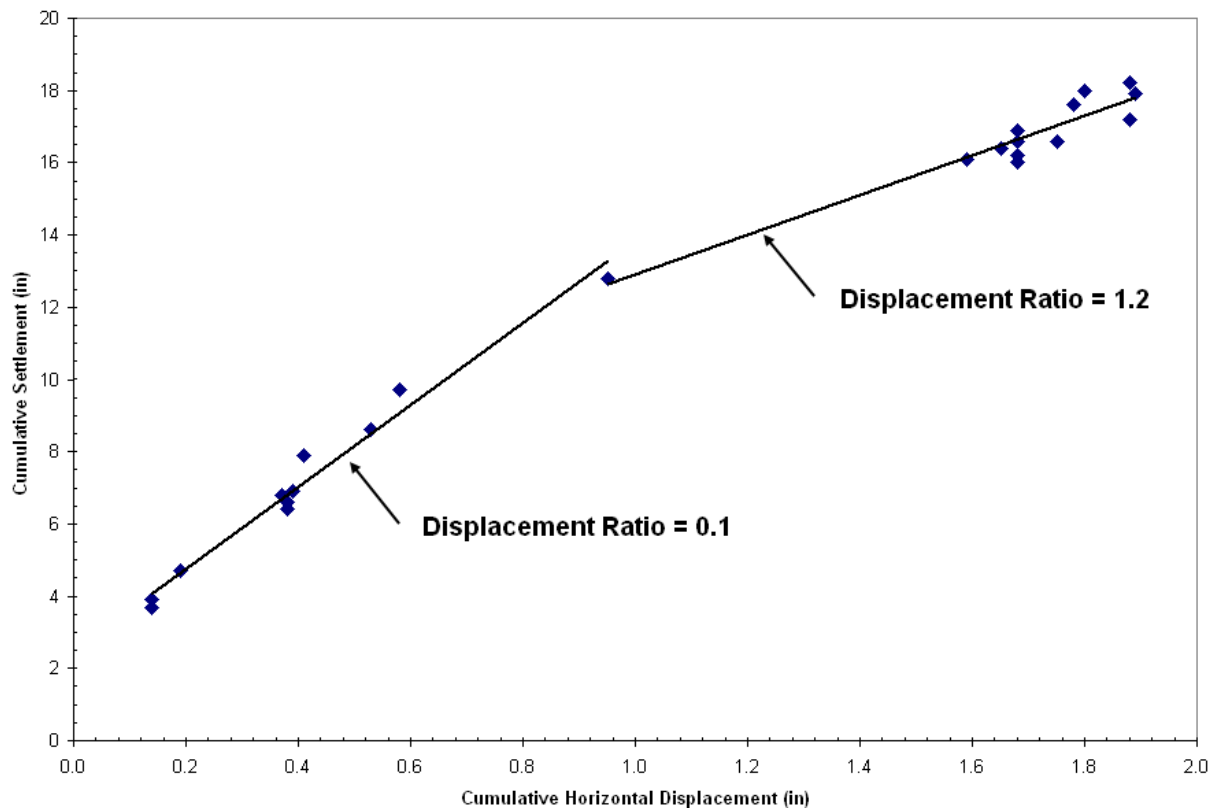


Figure 9 – DR for Case Study Data Showing a Significant Change in DR Trend Occuring Around Day 55.

of 0.09 (10). The DR value for the Case Study was 0.1 (Figure 9). During the final stages of construction, Tavenas et al. determined that the lateral displacement increments are significantly increased, becoming approximately equal to the settlement increments, which also increase (10). Mean DR values changed from 0.18 during initial construction to 1.0 when the foundation became normally consolidated. The time at which this occurs is dependent upon the geometry of the embankment, the applied load, preconsolidation differences, the rate of fill placement, and the rate of consolidation in the overconsolidated materials (10). For the Case Study, the variation occurred at a height of 28-ft with the DR value becoming 1.2 (Figure 9). The range for end of construction DR values presented by Tavenas et al. varied between 0.42 and 1.33, with a mean of 0.91 and a standard deviation of 0.2 (10).

Evaluation

The Case Study's foundation stability monitoring program was effective because it allowed project engineers and managers to evaluate the foundations soil displacement as construction progressed and MSE wall height increased. By being able to evaluate the changing

soil conditions beneath the MSE wall, the safest and most efficient construction schedule could be followed. This proved critical when measurements between Day 47 and 58 indicated the potential development of decreasing foundation stability. Fill placement was halted and after foundation stability was determined to be safe, staged construction continued with 2-ft maximum lift height increases.

The alert levels and thresholds set for the I-15 reconstruction project identified the greater magnitude of deformation measured after ramp loading when applied to data from the case study. However, the scale of each parameter's threshold levels appears out of proportion with the measured displacement. The dh_m/dt alert levels might have conveyed less urgency to project engineers because the Level 3 threshold was not exceeded, even after the ramp loading period. From comparisons between Figure 7 of Bartlett (4) and Figure 9 of the Case Study, the observation can be made that the distinct change in the DR parameter near Day 55 indicated a change in foundation behavior to a state of excessive plastic deformation. Although the materials at each locality can be similarly described as soft, compressible materials, their engineering properties differ enough so that the thresholds used at I-15 for the dh_m/dt and DR parameters could have been adjusted for use at the Case Study. In addition to considering the differing material properties, the fact that prefabricated vertical drains were not installed at the Case Study would also have to be considered in the adjustment of alert thresholds.

CONCLUSIONS

The project goals, geologic materials, and general inclinometer, settlement cell, and piezometer instrumentation arrays used had similar parallels between the I-15 highway widening project and the highway reconstruction project Case Study of this paper. As is common with monitoring of soft soil embankment foundations, both projects focused primarily on horizontal displacement as an indicator of changing stability. Although similar in design and concept, different monitoring protocols and alert thresholds were utilized at each locality to evaluate lateral and vertical displacement to control construction activities. The methodology used at the Case Study provided the design engineers with sufficient data to evaluate the developing adverse conditions. This was supported by the significant change in the displacement ratio, between Days 47 and 59 of the project during a period of rapid ramp loading. Because the contractor was directed to take remedial measures and remove fill, potential failure was avoided.

As projects employ new and advanced construction practices, the use of large-array, real-time instrumentation can provide important data that would otherwise be missed using conventional monitoring methods. The addition of in-place inclinometers (IPIs) and time domain reflectometry (TDR) sensors can further reduce manual labor and speed up data acquisition even further. Future highway projects will benefit from having automated geotechnical instrumentation installed and a soil foundation performance monitoring program in place to bolster project safety, time and economic efficiency, and better ensure project success.

REFERENCES:

1. Dunicliff, J., & Green, G. E. (1988). Geotechnical instrumentation for monitoring field performance. New York: Wiley.
2. Caltrans. (1998). *Method for Installation and Use of Embankment Settlement Devices*. California Department of Transportation, March 1998, 19 pg.
3. Saye, S. R., & Ladd, C. C. (2004). Analysis of Geotechnical Instrumentation to Assess Foundation Performance of I-15. *Geotechnical Special Publication*. 2 (126), 2103-2114.
4. Bartlett, S.B., Monley, G.C., Soderborg, A. and Palmer, A. (2001) "Instrumentation and construction performance monitoring for I-15 reconstruction in Salt Lake City, Utah." *Transportation Research Record 1772*, 40-47.
5. Orr, E. L., & Orr, W. N. (2000). Geology of Oregon. Dubuque, Iowa: Kendall/Hunt Pub.
6. Geokon (2009). *Instruction Manual Model 4500 series Vibrating Wire Piezometer*. 48 Spencer Street, Lebanon, NH, www.geokon.com.
7. Durham Geo Slope Indicator (2005). *VW Settlement Cells*. 12123 Harbour Reach Drive, Mukilteo, WA, USA, www.slopeindicator.com.
8. Liu, C., & Evett, J. B. (1987). *Soils and foundations*. Englewood Cliffs, N.J.: Prentice-Hall.
9. Asaoka, A. (1978) *Observational procedure of settlement prediction*. *Soils and Foundations*, 18(4), 87-100.
10. Tavenas, F., Mieussens, C. and Bourges, F. (1979). *Lateral displacements in clay foundations under embankments*. *Canadian Geotechnical Journal*, 16(3), 532-550.

Bridge over Snake River:
Geotechnical Engineering on Unstable Ground

Kirk Hood

Wyoming Department of Transportation
5300 Bishop Blvd.
Cheyenne, WY 82009
(307) 777-4418
Kirk.Hood@dot.state.wy.us

Jamie Martens

HNTB Corporation
715 Kirk Drive
Kansas City, MO 64105
(816) 527-2348
jamartens@hntb.com

Norman Norrish

Wyllie & Norrish Rock Engineers Inc.
17918 NE 27th St
Redmond, WA 98052
(425) 861-7327
nnorrish@msn.com

Prepared for the 61st Highway Geology Symposium, August, 2010

Disclaimer

Statements and views presented in this paper are strictly those of the author(s), and do not necessarily reflect positions held by their affiliations, the Highway Geology Symposium (HGS), or others acknowledged above. The mention of trade names for commercial products does not imply the approval or endorsement by HGS.

Copyright Notice

Copyright © 2010 Highway Geology Symposium (HGS)

All Rights Reserved. Printed in the United States of America. No part of this publication may be reproduced or copied in any form or by any means – graphic, electronic, or mechanical, including photocopying, taping, or information storage and retrieval systems – without prior written permission of the HGS. This excludes the original author(s).

ABSTRACT

The Wyoming Department of Transportation intends to improve US Highways 26/89 south of Jackson in Teton County, Wyoming beginning at milepost (MP) 140.69 and extending northerly through Hoback Junction terminating at MP 142.50. The route is located in mountainous terrain adjacent to the confluence of the Snake and Hoback Rivers and crosses Federal, State, County, and privately owned properties. The corridor is heavily traveled by commuters, commercial vehicles, and seasonal recreational traffic.

Landslides have significantly impacted the transportation infrastructure within the project limits. An active landslide is located near the west abutment of the existing bridge over the Snake River, and construction of the existing bridge in 1950 re-activated a portion of the slide mass. Since construction, the abutment has experienced periodic movement as evidenced by inclinometer readings and settlement of the abutment. Subsurface conditions consist of colluvium/landslide and alluvial terrace deposits overlying sandstone, siltstone, and shale of the Cretaceous-aged Aspen Formation.

As part of the corridor improvement, the existing bridge over the Snake River is to be replaced on an improved alignment. Key components of the project include installation of three rows of ground anchors in the vicinity of the west abutment for landslide mitigation, construction of a new, two-hinged arch span bridge over the Snake River, and construction of an approximately 1,000 linear foot long anchored soldier pile and lagging retaining wall to accommodate roadway realignment. Design challenges included definition of the “active slide”; development of stability models consistent with inferred stratigraphy, current topography and documented displacement history; and integration of reinforcement anchors with bridge foundation elements to avoid conflicts. Construction sequencing is vital to install and commission as many of the ground anchors as possible prior to the excavations required for the bridge foundation elements.

PROJECT DESCRIPTION

Project Overview

The Wyoming Department of Transportation (WYDOT) is improving US Highways 26/89/189/191 south of Jackson in Teton County, Wyoming (Figure 1). The routes are located in mountainous terrain adjacent to the Snake and Hoback Rivers and cross Federal, State, County, and privately owned properties. These corridors are heavily traveled by commuters to and from Jackson, commercial vehicles, and seasonal recreational traffic. The improvements have been divided into three separate sections. This project includes the Hoback Junction Section beginning at milepost (MP) 140.69 of US Highway 26/89 and extending northerly through Hoback Junction terminating at MP 142.50. Key components of the project include installation of ground anchors for landslide mitigation, construction of a new bridge over the Snake River (MP 141.30), and construction of an anchored soldier pile and lagging retaining wall to accommodate roadway realignment.

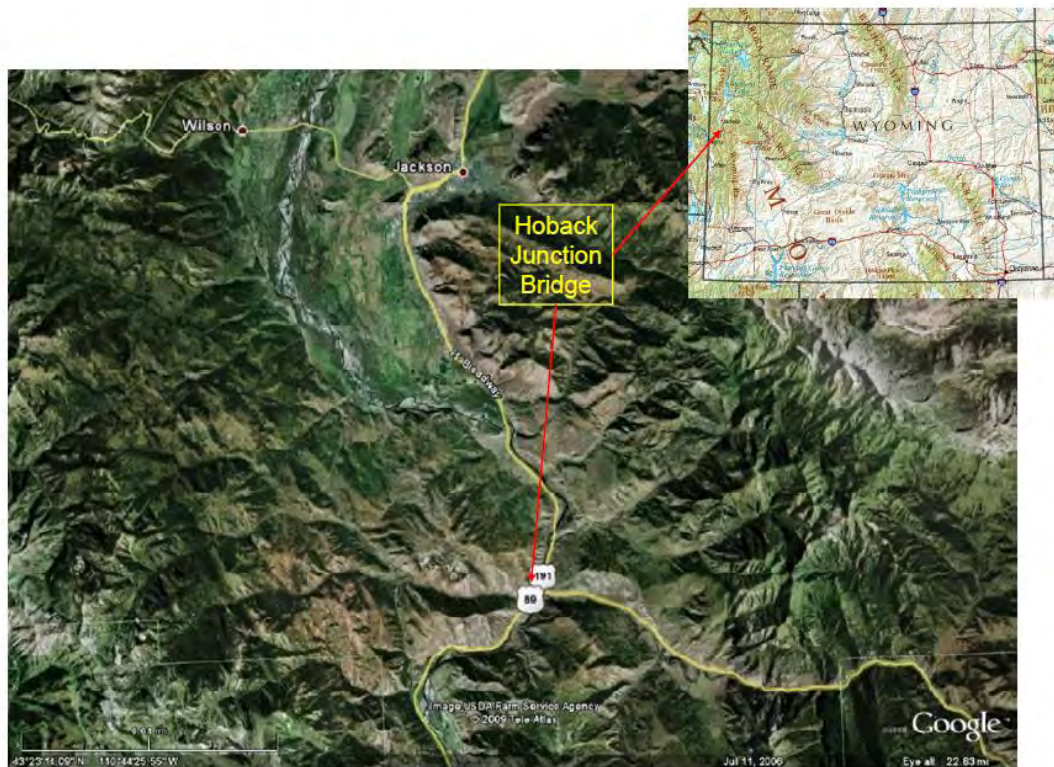


Figure 1 – Project Location Plan

Existing Structure Conditions

The existing roadway is over 30 years old and generally comprised of two, 12-foot wide lanes with various shoulder widths. The roadway has a reduced level of service, numerous substandard vertical and horizontal curves, and inadequate clear zones. Furthermore, landslide activity has adversely impacted the roadway quality and the condition of the existing bridge over the Snake River.

The existing bridge (Figure 2) was constructed circa 1950 and designed for H15 loading. Seismicity was not considered in the original structural design. The structure consists of a simple-span arch bridge founded on concrete pier walls. On the east side of the arch, three reinforced concrete t-girder approach spans are founded on reinforced concrete bents supported on spread footings. Four simple wide-flange girder approach spans founded on timber piling are present on the west side of the arch. Overall bridge length is approximately 579 feet with a bridge roadway width of 26 feet. The bridge deck over the arch is concrete. The concrete t-girder and the nail laminated floor planks on the approach spans are overlaid with asphalt. Numerous structural deficiencies were identified during a 2003 WYDOT inspection.



Figure 2 – Existing Bridge Looking North

Historical Instability

Landslides have significantly impacted the transportation infrastructure within the overall corridor and specifically within the project limits. An active landslide is located near the west abutment of the existing bridge. Construction of the existing bridge re-activated a portion of the slide mass resulting in the installation of the timber approach spans at the west abutment that traverse a portion of the suspected landslide. Since construction, the abutment has experienced periodic movement as evidenced by inclinometer readings and settlement of the abutment. In 1982 and 1983, WYDOT installed several inclinometers on both sides of the abutment. In the mid 1980's, the slope movement was relatively active after a series of unusually wet years, resulting in total movement in excess of four inches. Since the late 1980's, the movement has slowed, but slope inclinometers installed in 1999 indicate that the slide continues to move.

GENERAL GEOLOGIC SETTING

Hoback Junction is located within an overthrust belt from the Sevier Orogeny (Late Cretaceous) that resulted in significant folding and low angle thrust faulting creating elongate basins in which sedimentary and volcanic rocks were deposited during the Paleozoic and Mesozoic (*1*).

Key aspects of the geologic history of the project location include the following:

- Deposition of Cretaceous-Aged Aspen Formation – Thick shallow sea deposits of shale, sandstone and siltstone. The Aspen Formation is described as poorly consolidated shale, very unstable and subject to slumps and slides.
- Laramide Orogeny – Relatively recent mountain building episode forming the Tetons. Forces exerted from thrust faulting, normal faulting, and plutonic intrusions created folding of the rocks in the Hoback Junction area. The project area is located between parallel axes of the Willow Creek Anticline and the Willow Creek Syncline. The trough of the syncline is located near the southwest limit of the project. The strike of the sedimentary rocks is nearly normal to the bridge with a dip to the southwest at 25 degrees.
- Quaternary Alpine Glaciation – Glacial features, such as open parabolic (U-shaped) valleys, arêtes and cirques, are common in the area. A geologically younger Snake River, wider, higher in elevation, with more flow from glacial melt during the Pleistocene carried more and deposited larger sediment as terrace deposits. The terrace deposits formed a plain higher and wider than the present river. Eventually, lower flows, a small constant uplift of the region, and river downcutting, lowered the Snake River to its present state. Most likely during the Pleistocene, the river was undercutting the weak sediments of the Aspen, creating large slumps and landslides and forming the large areas of colluvial shale deposits overlying the terrace and alluvial sediments.
- Recent (within the last 10,000 years) river dynamics further undercut and cause lesser slumps and slides.

SITE AND SUBSURFACE INVESTIGATIONS

Previous Investigations

WYDOT completed numerous subsurface investigations of the subject area in 1982, 1984, 1985, 1999, 2005, and 2008 with a total of 31 exploratory borings drilled. Drilling advancement methods consisted primarily of hollow and solid stem augers, with soil samples obtained with driven split-barrel samplers in accordance with the Standard Penetration Test (SPT). Continuous samplers were also used in an attempt to define the slide plane. Limited rock core was obtained until the 2005 and 2008 investigations. Laboratory testing of soil and rock samples included classification, index properties, and strength (unconfined and direct shear) testing. As part of the previous drilling investigations, WYDOT installed casing for displacement monitoring in eight (8) boreholes using slope indicator equipment. However, instrumentation was not installed to monitor groundwater conditions. Finally, two (2) test shafts were installed in 1985 to evaluate potential construction methods.

Recent Investigation

Drilling and Testing Program

The objectives of the most recent 2009 drilling program for the bridge, retaining wall, and landslide investigation were to complete the following:

1. Investigate and characterize the engineering and geologic subsurface conditions;
2. Identify zones of soil and/or rock failure;
3. Install downhole instrumentation for long-term monitoring of groundwater conditions and slope stability; and
4. Characterize subsurface conditions at the foundation elements.

The rationale for the proposed location and depth of the boreholes, and the type of instrumentation was developed based on previous investigations, existing surface conditions, geologic mapping, and proximity to proposed bridge structures. The as-drilled boring locations for the previous and recent subsurface investigations including the location of instrumentation are shown on Figure 3.

The subsurface investigation was completed by WYDOT drilling forces in two phases of work between May and June, 2009. All borings were advanced through the overlying soils and into the weathered bedrock using hollow stem auger methods and SPT split barrel sampling at 5-foot (nominal) intervals followed by continuous NQ coring in the bedrock. Borehole logging was performed by both WYDOT and HNTB personnel.

Piezometers and slope inclinometer casing were installed in selected boreholes. The piezometers were screened with slotted 2-inch diameter PVC surrounded by filter pack sand. Clay cuttings and bentonite were used to fill the hole above and below the screened interval. Subsequent to installation, both standpipes were temporarily fitted with vibrating wire piezometers (VWPs) to measure changes in pore water pressure within the formation. VWP data was recorded for the two piezometers between June 2, 2009 and September 1, 2009. Slope indicator casing was installed in borehole H-1 to a depth of 67 feet. The baseline data was taken soon after installation. All instrumentation data collection was conducted by WYDOT personnel.

Rock and soil core samples were collected from the borings and preserved to prevent moisture loss by double enclosure within sealed plastic bags. The samples were labeled and submitted under chain-of-custody to the WYDOT Materials laboratory in Cheyenne for testing in accordance with State procedures. Laboratory testing was used for refinement of the field soil and rock classification, and to develop geomechanical properties for the key engineering units during design.

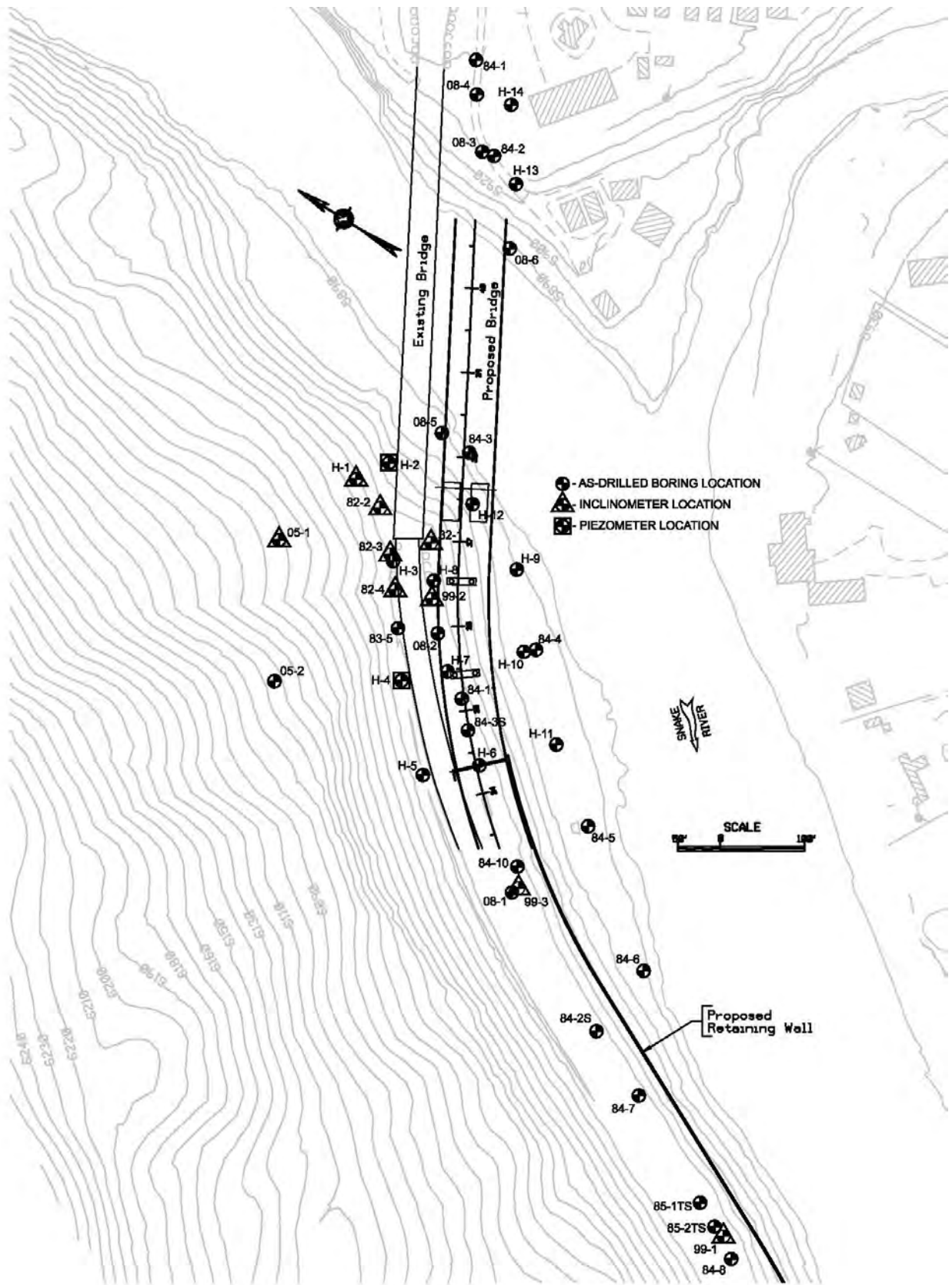


Figure 3 – Site and Boring Location Plan

Photogeologic Interpretation

In order to investigate the extent of the “active slide” area in the vicinity of the west abutment, high altitude aerial photographs from 1962, 1978, 1983 and low altitude photographs dated 2000 were analyzed using stereographic techniques. Many of the large (covering > 1/2 square mile) landslides in this area appear to be older features that were active immediately after deglaciation. With respect to the proposed bridge abutment relocation, the critical issue was whether the landslide upslope from the abutment is active or whether topographic/geologic conditions indicate the potential for reactivation. Additionally, because of the steep slopes and the nature of the landslide debris, it was important to determine if conditions exist that may lead to smaller slumps, debris flows, and other mass movement events that may potentially impact the abutment in the future.

Evidence was not observed on the aerial photographs for recent activity of the major slide mass above the proposed abutment. However, features are present within the slide mass that may lead to slide reactivation (Figure 4). An upslope bench appears to be a closed or at least partially closed depression and deposits above that bench appear to have an arcuate geometry. If the bench represents the top of a slide mass, loading with additional material from above combined with unfavorable groundwater conditions could lead to slide reactivation. Furthermore, any change in the resistance to sliding by toe removal could exacerbate the situation. Downslope from the bench, numerous features exist that indicate the potential for minor mass movement activity and older circular failures are present along with potential debris flow paths. Given the presence of landslide deposits in the subsurface and the steep slopes, additional small mass movement events were deemed highly probable in the project area.

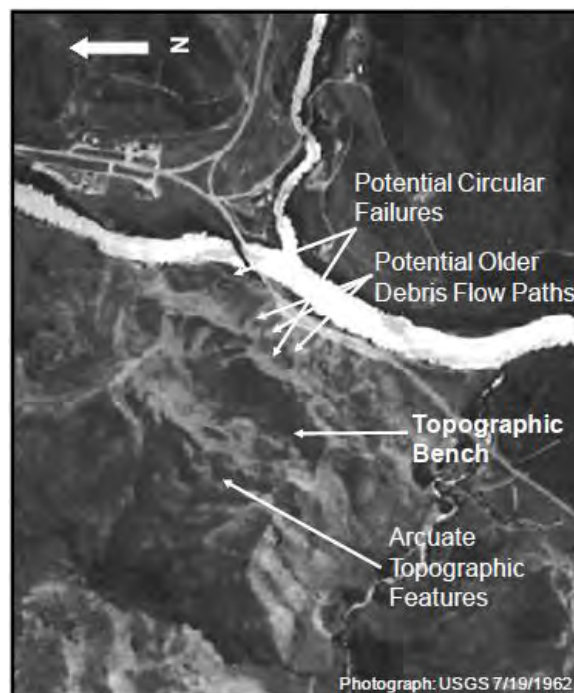


Figure 4 – Photogeologic Observations

Surface Mapping

A reconnaissance-level surface mapping effort was undertaken to field-identify the “active” slide proximal to the west abutment and to collect bedrock structural data. Observations of local topographic features led to the interpretation that a possible active slide is defined by an arcuate lateral scarp as shown in Figure 5. This interpretation was consistent with the anecdotal accounts of instability when excavations were made for the existing west approach spans in 1950. The timber bents evident at the west approach spans represent the design changes made during construction to accommodate the instability. The inferred active landslide was staked in the field and surveyed by WYDOT personnel.



Figure 5 – Inferred “Active” Landslide at West Abutment

Bedrock outcrops are limited in the vicinity of the bridge. The best exposures are along both banks of the Snake River with a few on ledge-forming slopes on the west abutment. Although the data set is limited, the most consistent discontinuity orientation is the bedding which exhibits an inclination of about 20 degrees to the west-southwest. This orientation is into the west valley wall and discounts bedding as a structural control for the historic landslides evident at this location.

SUBSURFACE CHARACTERIZATION

The 2009 drilling and testing program investigated both the landslide deposits and the subsurface conditions for the various foundation elements for the proposed bridge, retaining wall, and

landslide stabilization. Based on both surface exposure and subsurface sampling, the materials were categorized into the following units for engineering analysis:

Fill/Colluvium/Landslide Deposits: Material consists predominantly of moist to saturated sandy clay to clayey sand and gravel with occasional cobbles and boulders. Gravel, cobbles, and boulders generally consist of angular siltstone and sandstone fragments. The average measured SPT value is 20, indicating medium dense material. Moisture content test results range from 5 to 16 percent with an average of 11 percent. Typical total unit weight based on laboratory testing is 128 pcf. The measured percent passing the No. 200 sieve ranges from 10 to 57 percent with an average of 36 percent. The average measured liquid limit of the fine-grained material is 36 percent with an average measured plasticity index of 19 percent.

Alluvium/Terrace Deposits: Material consists primarily of clayey and silty sand and gravel with rounded cobbles. The average measured SPT value is greater than 50 indicating dense to very dense material. Difficult drilling conditions were encountered during the subsurface investigations including rough drilling, auger refusal on cobbles and boulders, and hole instability. The average moisture content test result is 7 percent with a total unit weight on the order of 136 pcf. The measured percent passing the No. 200 sieve ranges from 2 to 49 percent with an average of 17 percent. Plasticity testing on the fine-grained fraction indicates an average measured liquid limit of 28 percent and an average measured plasticity index of 11 percent.

Bedrock (Fractured and Unweathered) West Side of the Snake River: Bedrock consists of hard siltstone and fine sandstone (Figure 6) with interbedded seams (generally less than 3-ft thick) of softer claystone, clay, and bentonite. The upper 2 to 3 ft of the bedrock is typically weathered with the upper 15 to 20 feet described as fractured. The average measured unconfined compressive strength of the bedrock is 10,400 psi. For the softer claystone, clay, and bentonite seams, unconfined compressive strength testing indicates an average of 1,990 psi with an average measured rock quality designation (RQD) of 29 percent. The average measured unconfined compressive strength of the siltstone and fine-grained sandstone bedrock is 12,840 psi with an average measured RQD of 33 percent.



Figure 6 – Bedrock West Side of Snake River

Bedrock (Fractured and Unweathered) East Side of the Snake River: Bedrock consists of hard siltstone and sandstone with an average measured unconfined compressive strength of 10,100

psi. The average measured unconfined compressive strength of the siltstone is 8,070 psi with an average measured RQD of 38 percent. The sandstone generally consists of “salt and pepper” sandstone with laboratory test results indicating an average unconfined compressive strength of 10,580 psi. The average measured RQD is 60 percent.

ENGINEERING ANALYSIS AND DESIGN

Landslide

Probable Cause(s)

Landslides are typically the result of a combination of geologic conditions and external factors, often related to human activities. In the case of the west abutment landslide, some assertions concerning causation can be made with a high degree of certainty while others fall into the category of probable cause.

- The Cretaceous Aspen Formation is a well-documented “bad actor” in the region, and ash layers altered to bentonite provide the potential for low shear strength.
- Glacial meltwater was a probable major cause of valley wall over-steepening and instability.
- The site is located in a seismically active area and ground accelerations could have triggered historic slope instability.
- Excavation for west bridge abutment in 1950 triggered slide movement that represented the reactivation of a portion of a much larger landslide.
- More than 4 inches of movement of the west abutment during the 1980’s following several wet years was reported by WYDOT. No recent distress of pavement or the west abutment has been reported.
- Inclinerometers document creep type movement at depths at or above bedrock since 1999.
- The landslide is apparently not bedding-controlled.
- Anecdotal accounts of recent instability associate slope movement with high runoff years.

Based on the results of previous investigations, and the geologic and instrumentation analyses conducted for this project, accurate delineation of the “active” portion of the west abutment landslide complex is not possible. The agreed-upon course of action, therefore, was to apply engineering judgment and failure risk as guidance to stabilize a reasonably sized block of ground proximal to the west abutment structure. It was deemed not feasible to stabilize the entire upslope landslide mass.

Geotechnical Model

An assessment of the west abutment landslide was performed to evaluate the viability of landslide movement under measured or inferred engineering parameters for the site. These parameters, including the slide geometry, measured groundwater levels, and material properties, were integrated into a geotechnical model for analysis. Validation of the geotechnical model consisted of comparing the ratio of resisting forces (shear strength) to the driving forces (weight, groundwater pressure) expressed as a Factor of Safety (FS). A calculated FS less than unity (1.0) would be consistent with the observed landslide movement.

Based on surface mapping and borehole investigations, a geologic model was constructed that captured the inferred three-dimensional geometry of the engineering units. This geologic model was used to construct idealized two-dimensional cross sections along potential axes of movement for which stability analyses could be performed. The primary cross sections for analyses were through the west abutment and through the axis of the inferred “active” slide.

Back Analyses

Stability analyses for circular failure were performed using the software program, Slide Version 5.041 (2). For the initial two-dimensional analyses, the search algorithm determined the minimum FS for a circular failure surface. Search limits were set to preclude failures that extended upslope of the active slide identified by the field mapping. Three methods of analysis were performed: Spencer, Janbu Corrected and GLE/Morgenstern-Price. Groundwater and external forces were not included in the back analysis (conservative assumption) since the purpose of the back analysis was to confirm the shear strength assignments for use in forward design analyses.

The initial model consisted of a homogenous low shear strength for the colluvium/landslide debris material. For the primary cross sections, minimum FS values calculated were 1.11 (west abutment) and 1.52 (axis of the inferred slide). The interpretation of these results was that the shallow local topography through the slide was not compatible with the homogenous low shear strength model. This suggested the probability of a lower shear strength surface between the bedrock and the landslide debris along which previous movement(s) have occurred.

Coring in the 2009 boreholes was generally not initiated until the upper weathered rock had been penetrated using hollow stem auger methods. Thus, remnants of a suspected weak layer at the bedrock-overburden contact were probably not recovered. In some boreholes, plastic clay infillings were recovered from deeper in the bedrock section. Based on the site geology, it was reasonable to assume that such a weak, pre-sheared layer was present at or near the top of bedrock.

In order to assign shear strength parameters to the inferred paleo failure surface, a number of data sources were reviewed. Direct shear tests were performed on samples from lower depths with friction angle results ranging between 12 and 34 degrees. In addition, Atterburg Limit tests were performed on numerous samples. The measured Plasticity Index (PI) values were related to

residual friction angle using the approach published by Mesri and Shahien (3). Depending on stress level, the predicted residual friction angle was 22 to 23 degrees based on average PI values and 12 to 16 degrees based on the maximum PI value. The design shear strength parameters assigned to the pre sheared weak layer were friction angle of 20 degrees and cohesion of zero.

For the “weak layer” analyses, the analytical model could select circular arcs or a combination of circular arcs and straight line segments as the failure surface. In this case the minimum FS values for the two cross sections were 0.98 and 1.11, respectively. Figure 7 shows the results for the analyses through the axis of the inferred slide.

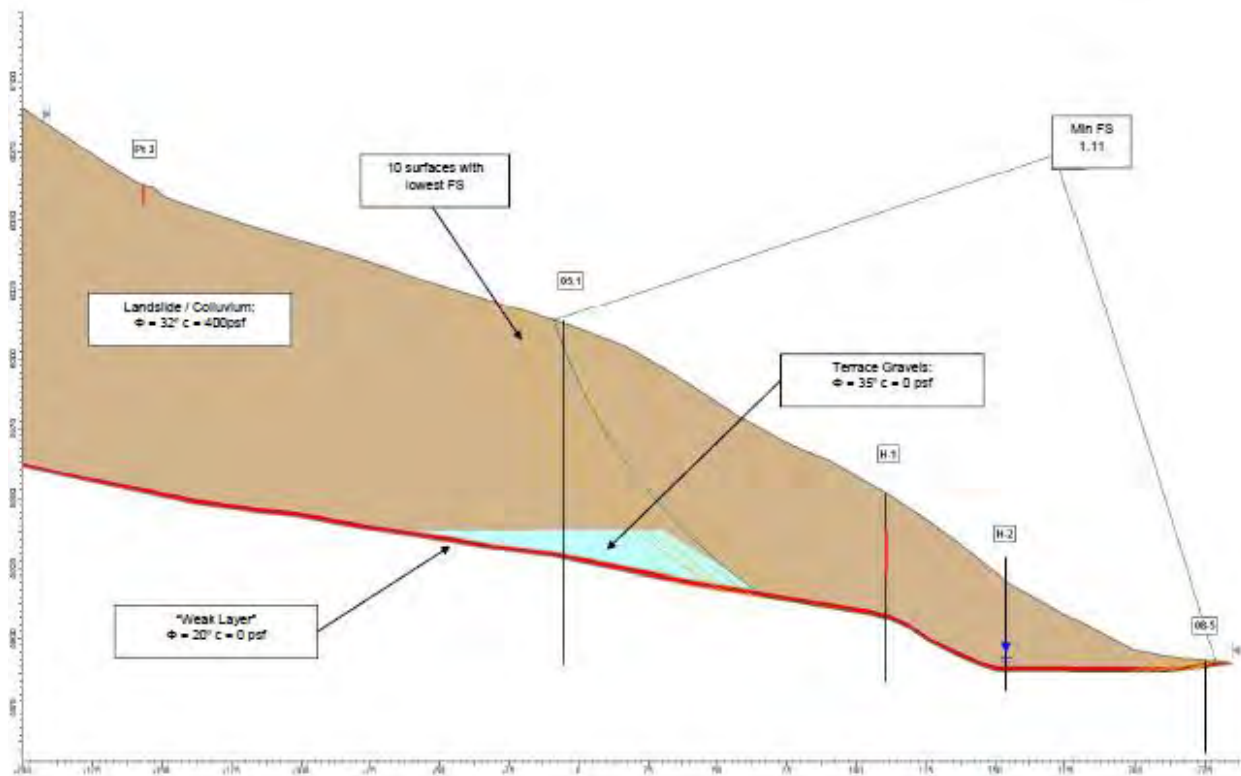


Figure 7 – Weak Layer Back Analyses: Slide Axis

These results were interpreted to be compatible with the existing slope geometries at both cross section locations and the weak layer model was therefore adopted for the forward analyses. The assumption that the current FS for the slopes is about unity (i.e. on the verge of failure) is the most conservative approach to the design. The remedial stabilization must increase the margin of stability from this low threshold to a value reasonable for the risk to the structure.

Stabilization Options

Various landslide stabilization techniques were evaluated for the project. Ground anchors were the selected option for the following reasons:

1. High strength per anchor;

2. Ability to specify required capacity per anchor;
3. Successful utilization by WYDOT for a nearby stabilization effort; and
4. Contractor familiarity with the required construction techniques.

Forward Analyses

The objective of the forward analyses was to determine the anchor force requirements necessary to achieve a FS for the reinforced slope consistent with the presence of the bridge structure. Based on discussions with WYDOT, the target FS value was established as 1.50 under static loading conditions. An anchor with a working load comparable to that used by WYDOT at a previously completed stabilization was assumed (528 kips). The analysis indicated three rows of anchors spaced on a 10-foot horizontal by 20-foot vertical pattern were required to achieve the target FS value.

Limited groundwater monitoring data was available for the project. To investigate transient groundwater conditions, a simple phreatic surface was modeled corresponding to a level slightly higher than the measured head in the lowermost piezometers. The corresponding FS value reduced to 1.38 for the cross section along the axis of the inferred slide. Furthermore, peak horizontal accelerations for the site were obtained from the USGS website. The FS for the 500-year event was approximately 1.2 and for the 2500-year event was approximately 0.9. These pseudo static analyses used seismic coefficients conservatively set at 50 percent of the peak accelerations in accordance with Pyke (4) and did not incorporate the transient groundwater condition. It was concluded that the proposed anchor stabilization was acceptable under static and transient loading, whether by groundwater or earthquake.

Design Criteria

Based on the stability analyses described above, the site topography and the geometric constraints associated with the proposed bridge structure, a conceptual anchor layout was developed. The design required two rows of anchors from the west abutment to the first interior bent (Bent 2), and three rows between Bent 2 extending to a location beyond the axis of the inferred slide. The following general design criteria were established:

1. Anchors to be located on uniform contour lines at nominal elevations 5950, 5930 and 5910.
2. Anchors spaced at 10 feet horizontal and extending from the west abutment to about 10 to 20 feet beyond the proposed bridge structure on the west side of the Snake River.
3. Two primary anchor azimuths (300 and 315 degrees) were specified with a transition area between. Within the transition area, final grading plan was taken into account. Due to curvature of existing ground surface, effective spacing was less than the target 10 feet and therefore some anchors were eliminated to avoid interference with the structure.

4. Target inclination was -20 degrees per optimization analysis. Inclination was varied from -15 deg to -25 deg to avoid interference.
5. If interference issues were not resolved with inclination variance, then anchor head elevation was varied by ± 10 feet.
6. Recommended design load was 528 kips. It was considered unlikely that solid bars would be selected by the contractor to achieve this load due to installation difficulties. Thus, 15-strand cable anchors were recommended.
7. Drain holes to be drilled in the lower slope to prevent buildup of groundwater pressure.

Final Design

The final design of the landslide stabilization required careful consideration of proposed bridge substructure elements, temporary construction excavation(s), construction sequencing, and final grading. In order to visualize potential interference issues, the above-mentioned design criteria were used to develop a 3D model incorporating the **existing** bridge, roadway, and subsurface conditions, and the **proposed** bridge elements, ground anchors, and final grading (Figure 8). Adjustments to the anchor inclination, azimuth, and head elevation were required to avoid potential conflicts with proposed bridge substructure elements. Furthermore, anchor installation had to be staged to maintain traffic and avoid undermining the existing bridge foundations.

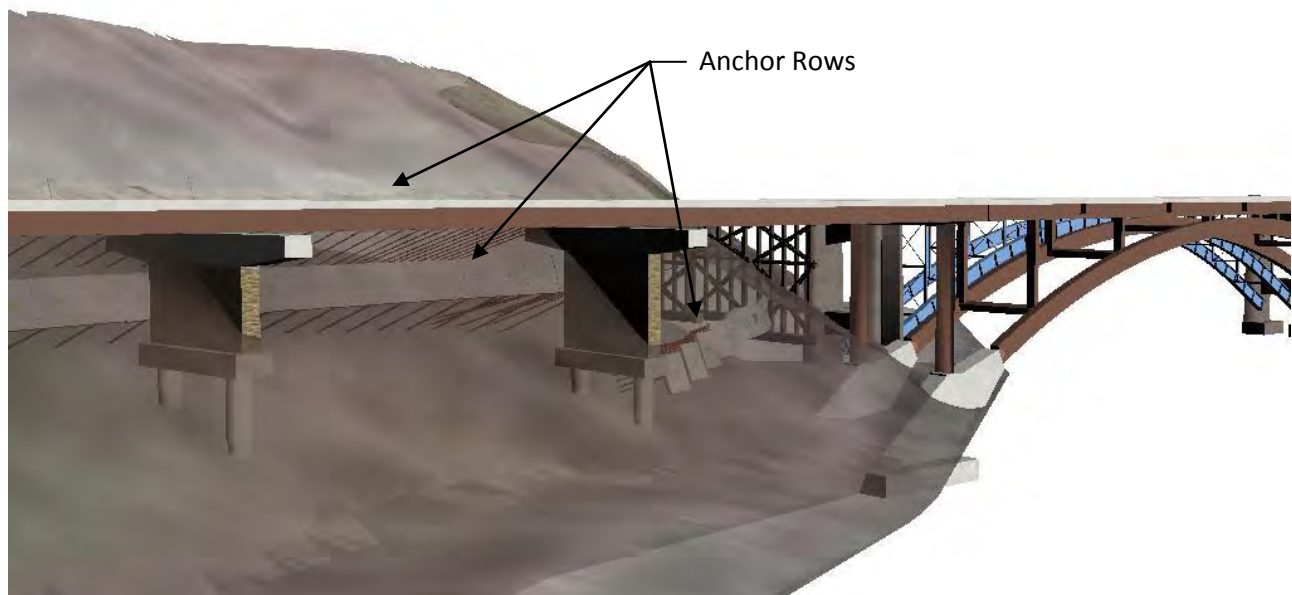


Figure 8 – Ground Anchor 3D Model

After refinement, the 3D model was uploaded to MicroStation V8i software, and queries were developed to obtain the horizontal and vertical position of the anchor head, azimuth of the bearing panel, and inclination of the ground anchor. This information was used to verify that the 3D model was in general agreement with the design criteria established. Furthermore, this data was used to evaluate potential adjacent anchor interference issues. Adjustments in the anchor inclination were required to maintain approximately 5 feet of clearance between the distal ends of the anchors. A partial plan view of the final ground anchor design is shown in Figure 9.

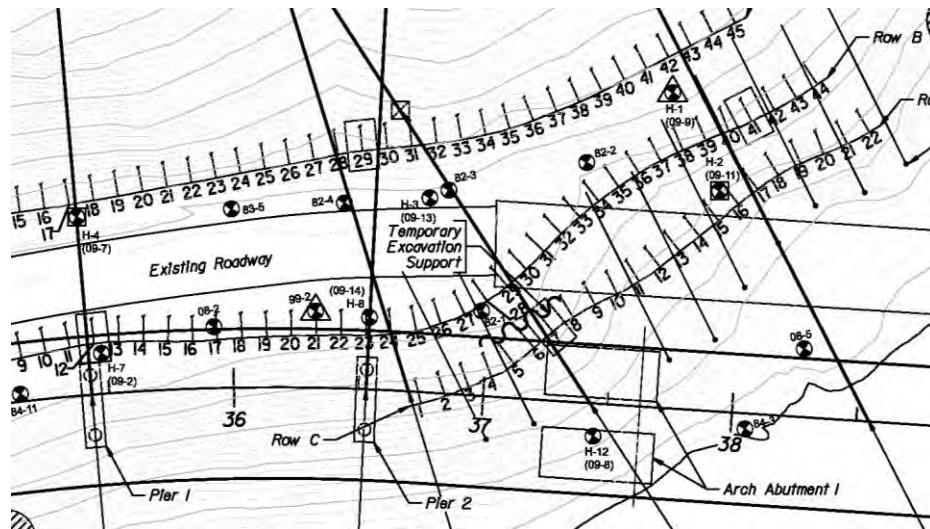


Figure 9 – Ground Anchor Plan View

Retaining Wall

Proposed Structure

As part of construction for the new bridge, an approximately 980 linear foot (LF) retaining wall was proposed between Sta. 24+50 and 34+31 (proposed west abutment). The current roadway is positioned on an approximately 40- to 70-foot wide sideslope bench with an existing roadway elevation between 5945 and 5950 feet. The proposed roadway alignment requires widening of the existing sideslope bench by 20 to 35 feet. Wall heights above the existing ground surface range between 5 feet and 30 feet with a typical height of 20 feet.

The original proposed retaining wall consisted of a post-tensioned system requiring extensive excavation to position the structural members and place the required select backfill. Initial slope stability analyses of the proposed system indicated less than desirable short- and long-term FS. Furthermore, temporary excavation support would be required for maintenance of traffic. Finally, the aggressive construction schedule and inability of the proposed system to adapt to the anticipated variable subsurface conditions necessitated a different wall system. After discussion with WYDOT, the selected wall system consisted of an anchored soldier pile and lagging wall in a fill condition.

Engineering Evaluation

Lateral earth pressure diagrams incorporating both static and dynamic loading were developed for structural analyses. Structural design of the wall identified various wall types based on the anticipated height. The tallest wall sections required three (3) rows of anchors with the shortest section requiring only a single row of anchors. The maximum tieback anchor load was approximately 195 kips. Longitudinal spacing of all steel elements (tieback anchors and soldier piles) was 8 feet.

Global stability analyses were conducted using Slope/W software at five (5) cross section locations. Anchors were included in the analysis at their design location and inclination. The design load at each anchor level was input into the slope stability model. Shear capacity of the anchors was not included in the model. However, shear resistance of the soldier pile was incorporated into the model for the double W14x68 section (Grade 50). Spencer's method was used to calculate the factor of safety for three different search routines: block, entry/exit, and grid. Based on the slope stability modeling, the minimum calculated factor of safety is on the order of 1.7 at the tallest wall section (Figure 10). The same stability models were also analyzed under seismic loading.

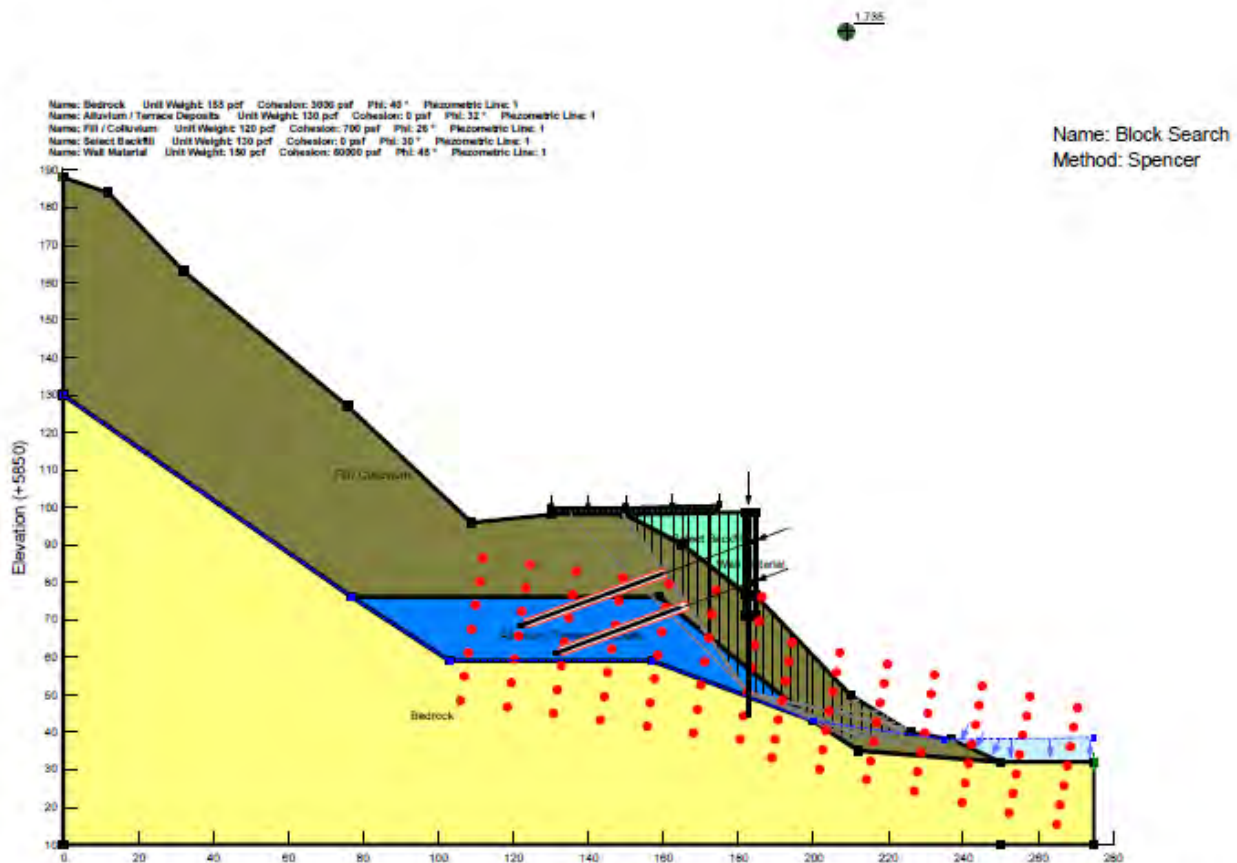


Figure 10 – Anchored Retaining Wall Long-Term Stability

Design Criteria

The following key design criteria were developed for the anchored retaining wall:

1. Construct the retaining wall in general accordance with the sequence identified in Paragraph 5.11.5 of FHWA's *Geotechnical Engineering Circular No. 4: Ground Anchors and Anchored Systems*.
2. Embed the soldier piles a minimum of 5 feet into the bedrock.
3. Employ an earth pressure coefficient between the at-rest and active earth pressure coefficient as wall movement will be controlled by anchor tensioning.
4. Include a uniform traffic surcharge of 250 psf.
5. Use multiple corrosion protection (Class I).
6. Require pre-production pull-out tests to verify the allowable bond stress.
7. Use free draining granular backfill requiring minimal compactive effort.

Bridge

Proposed Substructure Elements

The bridge abutments will be supported on end-bearing H-piles. Intermediate bents on the west side of the Snake River (Bents 1 and 2) will be supported on 4.5-foot diameter drilled shafts. Finally, the intermediate bents on either side of the Snake River will be supported on arch spread footings requiring the installation of temporary excavation support. Geotechnical design criteria for the substructure elements were developed in accordance with AASHTO LRFD Bridge Design Specifications, 4th Edition 2007 with 2009 Interim Revisions.

CONSTRUCTION ISSUES

Construction sequencing is considered critical to the success of the overall project. The construction sequence should strive to have all stabilization measures installed and functional prior to the commencement of excavations. However, this objective is not entirely feasible, particularly in the vicinity of the arch foundation on the west side. The compromise at this location was to leave out only those anchors necessary to provide space for the footing excavation and the associated temporary excavation support. As such, the contract documents included mandatory sequencing requirements for certain elements of the work, and a proposed construction sequence was provided to assist the contractor in developing his approach to the project.

Extensive monitoring was also required throughout the duration of the construction contract and also post-construction. A combination of load, displacement, and groundwater monitoring was

required to monitor the performance of the excavations and to enable timely remedial actions should the need arise. The monitoring takes advantage of existing instrumentation as well as the installation of new equipment.

CONSTRUCTION CONTRACT AWARD

The bid letting took place on April 22, 2010. A total of five bids were submitted ranging from \$25 million to \$31.3 million. The contractors submitting bids were Flatiron Construction Corp., WW Clyde, Ralph L. Wadsworth Construction Company, Wadsworth Brothers Construction, and Reiman Construction. As per WYDOT policy, the lowest bid was accepted from Wadsworth Brothers Construction for \$24,999,493.50. The Engineer's estimate was \$27,083,541.14. Work is anticipated to begin in June 2010 with final paving completed prior to October 15, 2011.

CONCLUSIONS

Key aspects of the Snake River Bridge replacement at Hoback Junction were the recent and historical evidence of slope instability, the requirement for extensive slope reinforcement for both slope stabilization and alignment structures, and the need to compress a large number of reinforcing elements into a very restricted working area. These challenges were overcome with a combination of detailed site characterization using high quality drilling and in situ testing techniques, assembly of geotechnical models that were consistent with existing and previous stability and therefore suitable for prediction of future stability, and incorporation of state-of-the-practice visualization software for final design and construction scheduling. All the foregoing supplemented with a liberal application of "dirty-boots" engineering.

REFERENCES

1. Mears, B. Jr.; Eckerle, W.P.; Gilmer, D.R.; Gubbels, T.L.; Huckleberry, G.A.; Marriott, H.J.; Schmidt, K.J.; and Yose, L.A. *A Geologic Tour of Wyoming from Laramie to Lander, Jackson and Rock Springs*. Public Information Circular No. 27, Geological Survey of Wyoming, 1986.
2. Rocscience. 2D Limit Equilibrium Slope Stability Analysis, Version 5.041. 2007.
3. Mesri, G., and Shahien, A. M. Residual Shear Strength Mobilized in First-Time Slope Failures. *Journal of Geotechnical and Geoenvironmental Engineering*, Vol. 129, No. 1, 2003, pp. 12-31.
4. Pyke, R. *Selection of Seismic Coefficients for Use in Pseudo-Static Slope Stability Analyses*. http://www.tagasoft.com/TAGAsoft/Discussion/article2_html. 2004.

Road and Housing Construction on Reclaimed Coal Mine Spoil Undergoes Settlement Damage in Southwest Indiana

Terry R. West and Nils I Johansen
Dept of Earth & Atmospheric Sciences, Purdue University, West Lafayette, IN
trwest@purdue.edu
and University of Southern Indiana, Evansville, IN, respectively

ABSTRACT

Coal mining in Pennsylvanian-aged rocks of southwestern Indiana has occurred for over 100 years. Seventeen counties from Terre Haute to Evansville have experienced both surface and underground coal mining. Since coal measures in Indiana dip southwest toward the Illinois Basin, geologic units show increased overburden thickness as they extend westward. Shallow strip mines prevailed in the early history of mining, but increased stripping capacity occurring in later years allowed for deeper extraction. Underground room and pillar mining was conducted on the deeper coal seams beyond the limits of strip mining at the time of extraction.

Early in mining history, reclamation of surface strip mines was virtually non-existent. Abandoned mine lands consisting of cast-over strip piles prevailed along the eastern boundary of the coal-bearing strata. In recent years, however, Federal mining laws have required that strip mines be properly reclaimed with the land surface restored to that which was present before mining. With this history in mind, we find that for recent strip mine areas, the overburden thickness is typically about 100 feet and the mined areas are carefully reclaimed to mimic their original contours. A primary consideration for reclamation is to allow the surface material to support vegetation, including row crops, pasture and forestation. Consequently, the surface material is left in a loose condition so as not to discourage plant growth.

Currently some reclaimed land is being sold by mining companies for development as housing tracts. Roads and house lots are then developed on the reclaimed land. In southern Warrick County, north of Evansville and near Interstate 164, problems have developed in a housing area on the reclaimed mine spoil. Foundation settlement leading to interior damage in homes has occurred. Streets have also undergone major settlement. In the paper these settlement problems are discussed and mitigation procedures are addressed.

Introduction

In southwest Indiana, within the sequence of Pennsylvanian-aged rock, coal mining operations have been conducted for over 100 years. Seventeen counties from Terre Haute south to Evansville have been sites for strip mining, underground mining or both during this period. Indiana has extensive areas of mined lands, 186,000 acres of underground mines, plus 284,000 acres at the surface. In southern Indiana,

rock units dip about 1° to the west toward the Illinois Basin. Shallow strip mines are located to the east with deeper mines to the west that developed with the passage of time as larger strip mining equipment became available. Thickness of the overburden removed above the coal which was typically less than 50 feet was extended to well over 100 feet as time progressed. Area strip mining, the procedure used at the study site, is illustrated in Figure 1.

In addition to surface mining, underground mining was also accomplished. In the early days, adit mine entrances from hillside locations prevailed, to be supplemented later by vertical shafts extended downward to the coal seams. Room and pillar mines were developed from these shaft entrance ways. Only more recently, a new underground mining technique has been added, longwall mining, but this procedure, which is outside of the scope of this presentation, is not considered here.

In some locations in the state, both surface mines in an upper coal unit and underground mines in a lower one, are encountered. An ongoing study by Fisher and West, 2009, is investigating the utilization of these sites for geothermal energy development. There are a number of sites, for example the Friar Tuck site near Dugger, IN, where major surface workings and coal processing plants overlie extensive underground mine workings (Kuo and West, 1990; West, et al., 1990; West and Lary, 1983; West, 2006). This was an early AML site (explained below) that has been extensively reclaimed.

Coal mine land reclamation for surface mines has improved significantly since the enactment of the Surface Mining Act (SMCRA) in 1977. Prior to that time, reclamation of cast over strip mine piles was not required which gave rise to long piles of cast over debris with an elongated lake occupying the final cut of the mining operation. Also a vertical wall was left intact as a hazard and vertical shafts to underground workings were sometimes left open. Such areas were designated as Abandoned Mine Land sites (AML) which are now being reclaimed through federal funds paid to states as a return on taxes on coal obtained from current surface mine projects. Requirements today call for separating top soil and subsoil materials, placement of the mined rock back into the strip mine excavation, and grading the surface to its original contours so that row crops, pasture and forest areas can be developed. The final cut must be filled in to reduce the steep slope of the highwall of rock which had remained at the end of the mining process.

In order to encourage growth of cultivated crops, care is taken not to compact the subsoil and top soil of the reclaimed surface area. It is an established fact that traffic over crop land densifies the soil which reduces crop productivity. Current farm practice attempts to minimize the traffic of heavy equipment onto the field. An example experienced by the first author (West, 1992, consulting report) pertains to this situation. It involved truck traffic across a farm field following an oil tank spill that ran across the neighboring field. This led to compensation for the land owner due to soil compaction from the truck traffic and anticipated loss of crop yield to follow. Because the anticipated use for reclaimed surface

mine land is for agricultural purposes, care is taken not to compact the upper layers of the reclaimed soil. This turns out to be counter-productive when the ultimate use of the land is to build residential sites and streets, and to promote business development. This concern is further addressed later on in this presentation.

Geologic Setting

The geology of Indiana is best considered by evaluating several maps of the state. These entail the physiographic regions map and the geologic or bedrock geology map of Indiana. The physiographic map is presented as Figure 2. There are two distinct areas involved, the northern glaciated portion and the southern area beyond the glacial boundary, where bedrock exposures prevail. There are two divisions of the glaciated area, the first formed by Wisconsin glaciations and the other where Illinoian drift prevails, which is located south of the Wisconsin glacial border. The extremely flat portion of Indiana consists of the Tipton Till Plain in central Indiana along with the Kankakee Outwash/Lacustrine Plain to the north. South of Terre Haute and Indianapolis, Illinoian drift prevails, which extends to the terminal glacial boundary to the south. Thickness of the glacial drift is less for the Illinoian glaciated area than it is for that of the Wisconsin. The Wabash Lowlands division is found on the southwestern part of Indiana, consisting of flat terrain developed on Pennsylvanian-aged rocks, composed mainly of shale, siltstone, sandstone and coal units. This comprises the area of interest for the current study.

The bedrock map of Indiana is presented as Figure 3. It shows the state with all surficial material removed, notably the glacial deposits of northern Indiana. The structure of the rock indicates a northwest trend, or strike, of the beds which dip gently to the west. For the southern part of the State this involves the exposed bedrock including a number of coal bearing units in the southwestern area. Ordovician aged rocks occur in the southeast corner of Indiana and from there the progression moves up the geologic column to Silurian, Devonian, Mississippian and finally Pennsylvanian rocks in western Indiana. Figure 4 shows the different bedrock units of the state along with their geologic age. Groups and formations of rocks are designated. The coal measures occur in the Pennsylvanian rocks as the coal members become younger toward the western boundary with Illinois. Figure 5 shows the different coal seams present in the Pennsylvanian rocks of Indiana.

Seven mineable units of coal are present in the Pennsylvanian. The Springfield Coal, also known as the Number 5 Coal, is a prominent seam that has been mined extensively, both in underground mines as well as being strip mined. It crops out in the eastern part of the Wabash Lowlands but as it dips westward, vertical shaft mines are required using the room and pillar mining procedure, prevalent in central Illinois.

Site Specific Details of the Housing Area

The site in question (near Chandler, IN) is located in a reclaimed strip mine spoil area. The land is part of the closed Ayrshire Mine that was a large strip mine operating up until about 20 years ago. Therefore, the spoil has been allowed to settle since that time and to compact under its own weight. The No.5 Springfield Coal was mined here, located at an average depth of 100 feet.

Streets were constructed throughout the site and housing lots were plotted and made available for sale. Two and one-half acre lots were the minimal size allowed, with water lines and utilities provided, but septic tanks were needed. The focus of this study is on a specific residence that has undergone major settlement causing distress both on the outside and inside of the structure. It is located on 3.25 acres and is adjacent to a remnant lake located immediately to the north.

The house is a two story frame structure built on a crawl space with strip footings below the outside walls and most interior walls as well. Brick veneer was not recommended for the site so vinyl siding was used instead. Construction of the house which began in 2005 was completed in 2006. Within six months of completion, cracks developed along the masonry blocks in the foundation walls and in the dry wall inside the home. Also the concrete floor of the garage moved away from the adjacent interior wall. Many door frames were affected so that a number of doors inside the home would not close properly. To investigate the nature of this problem a structural engineering firm was hired to evaluate the damage (Associated Engineers, Inc., 2008). It was concluded that cracking and settlement of the house persists but the house, of high quality construction, is not in danger of structural collapse.

With the knowledge that surface subsidence can be caused by the collapse of underground mines and that this problem is addressed in Indiana through the U.S. Office of Surface Mining (OSM), a second study was performed to determine if subsurface mine collapse was a possibility at the site (Quality Environmental Professionals, Inc., 2008). This report indicated that no underground mining had occurred below the site and therefore, OSM had no authority or responsibility to deal with the settlement problem. From this it is clear that the surface settlement is due to the continuing compaction of the mine spoil that was placed during the strip mining operation. Coal mine subsidence protection through OSM apparently is limited to the settlement from the collapse of underground coal mines but the densification of coal mine spoil from surface mining is not included in the law. This yields a major concern for the home owner in question as the house continues to settle, the walls crack and doors and windows do not open and close properly.

Site Visit

The problem at the housing site was brought to the attention of the second author of this paper and the first author was invited to join in the evaluation of the settlement problem. Dr. Terry West, who specializes in geology, geological engineering and civil engineering, joined Dr. Nils Johansen a professional engineer specializing in geological and geotechnical engineering. They both visited the site to obtain first hand information about the settlement problem.

The housing tract covers a large area of the reclaimed strip mine previously operated by AMAX Coal for their Ayrshire Mine. It is located in southwestern Warrick County about 14 miles northeast of Evansville and about a mile east of Interstate 164 in the small community of Chandler. The home in question is a two-story residence on Meadowlake Hills Road. In this area the access roads were built over mine spoil which has settled differentially yielding grade problems on the roads. Figures 6 and 7 are photographs showing some of the worst distress on the access roads in the area. The residential roads like Meadowlake Hills Road are raveling and contain pot holes. These secondary roads are predominantly chip and seal roads.

The two-story home, shown in Figure 8 is a frame structure with vinyl siding. The owner was instructed not to use brick veneer because of a concern for cracking in this more brittle material when settlement occurs. Vinyl siding being more flexible is more able to undergo settlement without developing exterior cracking.

The foundation plan for the home is shown as Figure 9. Strip footings below the perimeter walls and below some internal walls were constructed. These are 24 inches wide, 14 inches thick with 5/8" reinforcing steel placed in the footings. The "rebar" wraps around the corners to hold the footings together. Foundation construction was checked by a county building inspector after the trench was dug, when reinforcement bars were placed and after the concrete footings were poured.

Large volumes of water in the spoil were encountered during building construction. Perched water zones appear to be abundant in the spoil and large blocks of rock may be encountered as well. A cut-off wall was added later along the wall between the garage and the kitchen. This was added to stabilize the house which had settled differentially to cause interior cracking. This is a 4-inch slab of concrete over a series of piers that extend about 6 feet into the subsurface. A photo of this is shown as Figure 10.

Inspection of the house by the two authors verified that cracking had occurred in the exterior block wall foundation. Figure 11 shows this. In the garage the floor slab (a 4-inch thick concrete slab) has pulled away from the wall by more than an inch (Figure 12). Inside the home the walls are settling and have separated from the ceiling (Figure 13) and doors no longer close properly (Figure 14).

Following inspection of the Meadowlark Hills Road residence, a tour of the overall residential area was conducted. Only a few homes have been constructed in this sizeable building area which in total

is more than 10 square miles. A home on Fahd Avenue was examined (Figure 15). This house, built in 2002, began to settle immediately after construction. Rainfall accumulated against the foundation before it was backfilled, which aggravated the problem. Subsequently, 42 piers, 50 to 80 feet long were placed under the house involving steel tubes driven to refusal on resistant material. The insurance company for the home owner paid for this improved support of the residential home.

Another one story brick veneer home was observed on Fisherview Road (Figure 16). Brick construction was used despite the recommendation that vinyl siding should be used instead. This house supposedly has serious cracking problems in the interior, but does not show any obvious cracking on the exterior of the home. An inspection of the home's interior was not possible. On return to the home on Meadowlark Hills Road the general area of the large reclaimed mine tract was examined. Churches and graveyards were left intact during the mining process (Figures 17 and 18). However, the entire town of Millersburg was removed as mining proceeded over that location. As a final photo of the area, Figure 19 shows the lake north of the Meadowlark Hills Road residence with the home, featured here, on the left of the photograph.

Conclusions and Recommendations

On the basis of the information provided above, available literature and the site visit, several conclusions have been reached. It is apparent that the differential settlement and cracking of the residential areas is caused by post construction compaction of the mine spoil. It is unclear how much of the settlement is due to the weight of the house recently added to the site and how much settlement would have occurred without the added construction. It is a well-established fact that mine spoil in Indiana continues to settle after many years following mine reclamation (J. Nowacki, personal communication, 2010). Cast over mine spoil is extremely heterogeneous by nature of the mining and reclamation process, so that one building site could be considerably more susceptible to settlement than another.

The houses themselves, with strip footings only two feet wide should produce increased pressure only to depths of five or six feet below the footing, based on stress distribution analysis. It is clear, however, that the reclamation process which prescribes soil conditions for growing crops is specifically designed not to densify the soil which thereby enhances crop production capability. The two uses are therefore at cross purposes: 1) agricultural use versus residential construction. This needs to be recognized and dealt with prior to home and road construction.

Soils can be densified using compaction rollers pulled by dozers across the ground surface. However, the effects of such compaction only extends less than a foot below the ground surface. A possible solution would be to excavate the area of the imprint of the home, to a depth of six feet or so, and then replace the soil back in the excavation in 8 inch lifts, with compaction following each lift.

Another procedure with promise is dynamic compaction. This involves a crane and a heavy drop ball to compact the soil for some distance below the surface after the ball is dropped from a considerable height above the ground. This would be conducted in an area which covers the imprint of the building plus extending some additional dimension beyond it.

The assumption involved in these recommendations is that the compaction settlement is caused by near surface densification that occurs after home construction. If instead, settlement is caused by deep seated differential densification of the mine spoil, this densification of the near surface material will not entirely solve the problem. If deeper seated settlement prevails, another solution would be to drive support columns to refusal in the spoil cross section and place the strip footings over these pile supports. The effect of septic tank effluent is another concern. Several hundred gallons of liquid per day for a family household may induce some densification of the spoil.

The authors also learned that the developer is contemplating the construction of commercial buildings or even a mall facility to serve the growing community. Obviously the support procedures discussed above must be considered in the design of the foundations for such major structures.

Recommendations for future construction involve the densification of the housing site prior to construction. Densification of the upper six feet or so is likely to be sufficient for homes on strip footings and crawl space construction. There is another consideration for buildings in coal mine spoil areas. Mobil or manufactured homes will settle as a unit without significant cracking taking place. Such homes can be re-leveled on a regular basis to regain their original elevation after settlement occurs.

A recommendation for further study would be to examine the rate of natural compaction for mine spoil sites. Obviously a twenty year period of natural settlement is not sufficient to prevent the cracking of residential structures nor excess settlement of access roads. For road construction, removal of the spoil to a depth of six feet and recompaction of the soil in 8-inch lifts would also be in order.

References Cited

Associated Engineers, Inc., 2008, Structural Analysis of a Home Located in the Chandler, IN Area, consulting report, Madisonville, KY, July.

Fisher, R.A. and West, T.R., 2009, Engineering Opportunities Related to Underground and Surface Mines in Southwest Indiana. Indiana Society of Mining and Reclamation (ISMR) poster presentation, Jasper, IN, December.

Kuo, K.C. and West, T.R., 1990, "Reclamation of a Gob Pile in Southwest Indiana, An Innovative Approach", Proceedings, 1990 National Symposium on Mining, Knoxville, TN, p. 181-190.

Nowacki, J., May 2010, personal communication.

Quality Environmental Professionals, Inc., 2008, "Mine Subsidence Evaluation, Residence on Meadowlake Hills Road, Chandler, Indiana", consulting report, Indianapolis, IN, September.

Surface Mining Act of 1977 (SMCRA)

West, T.R., Kuo, K.C. and Petersen, W.K., 1990, "Site Investigation of a Coal Strip Mine Area, Southwest Indiana, USA, to Provide Geotechnical and Hydrologic Data for Reclamation Design", Proc., Sixth International Congress, International Association of Engineering Geology, pp. 1491-1500, Amsterdam, Netherlands.

West, T.R., 1992, "Compaction of Soil in Farm Field from Site Clean-up Equipment, Boone County, Indiana", consulting report.

West, T.R. and Lary, B.E., 1993, "Evaluating Erosion Rates of an Abandoned Coal Refuse Pile, Southwest Indiana Using Contrasting Techniques", Abstracts with programs, 36th Annual Meeting, Association of Engineering Geologists, San Antonio, TX.

West, T.R., 2006, Mass Wasting in a Disturbed Terrain, Abandoned Coal Mine Site Southwest, Indiana, Abstracts with Programs, 49th Annual Meeting, Association of Environmental and Engineering Geologists, Philadelphia, PA, November.

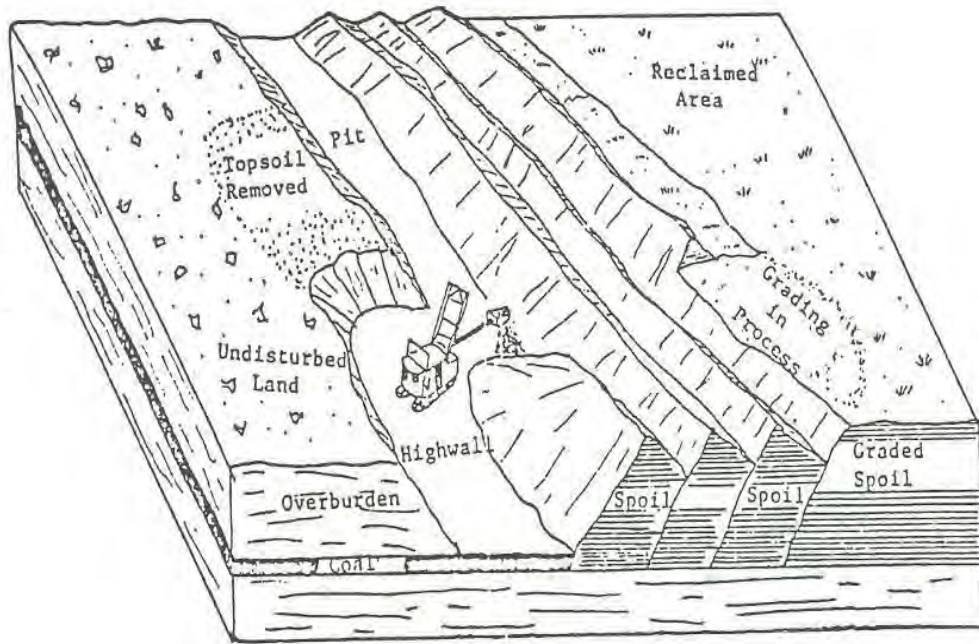


Figure 1. Coal strip mining including post mining reclamation.

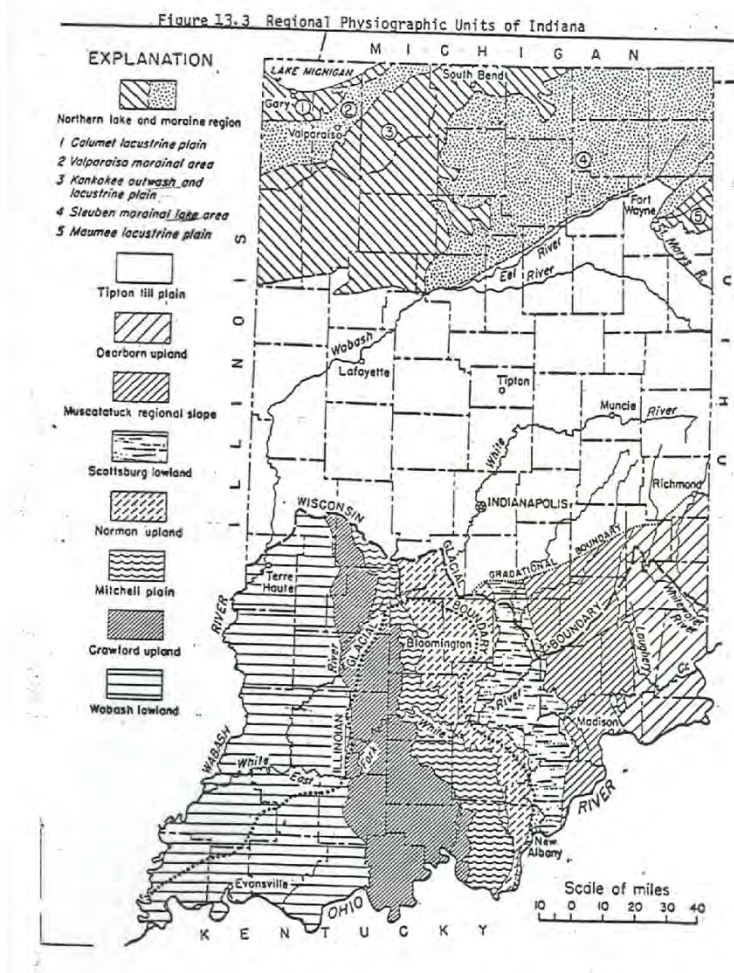


Figure 2. Physiographic Units of Indiana.

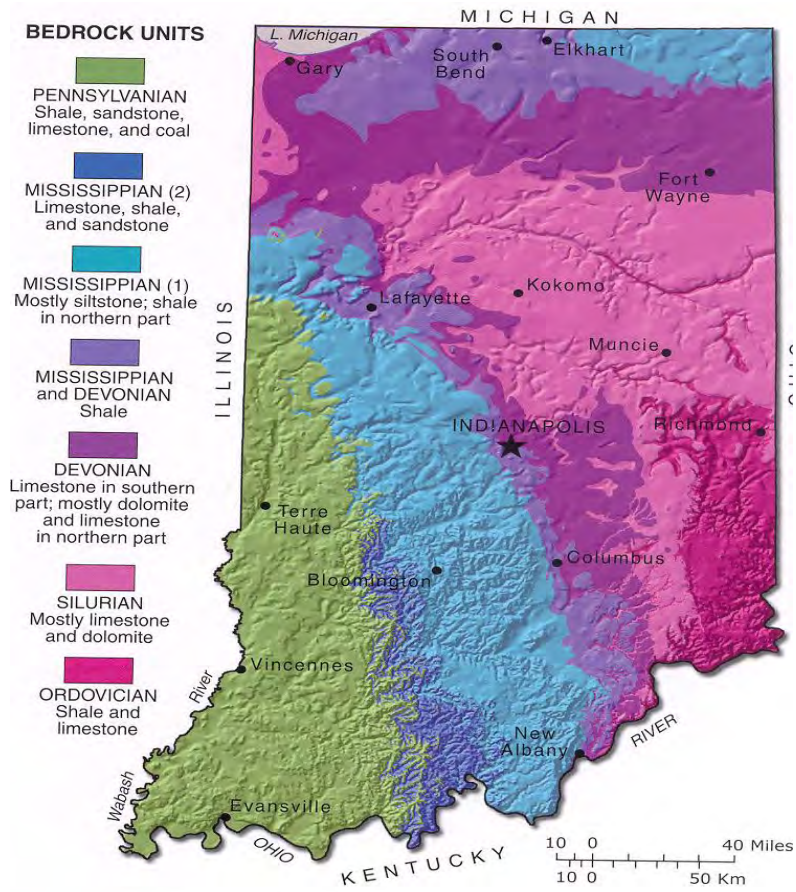


Figure 3.

Bedrock Geologic Map of Indiana

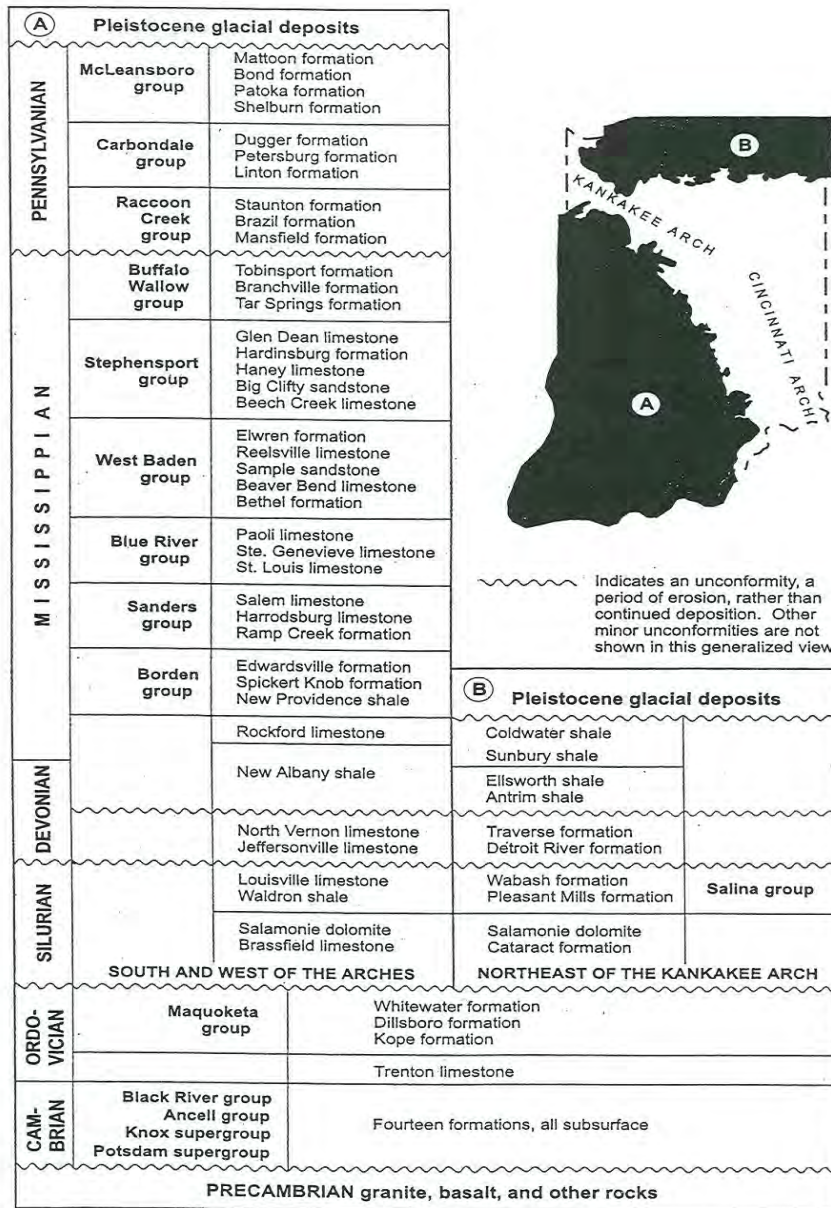


Figure 4. Bedrock Geology of Indiana.

TIME UNIT		THICKNESS (IN FEET)	LITHOLOGY	ROCK UNIT		
PERIOD	EPOCH			SELECTED MEMBERS AND BEDS	FORMATION	GROUP
PENNSYLVANIAN	ALLEGHENIAN	230 to 345		Danville Coal Mbr. (VII)	Dugger	Carbondale
				Hymera Coal Mbr.* (VI)		
				Coal Vb		
				Alum Cave Limestone Mbr.	Petersburg	
				Springfield Coal Mbr. (V)		
				Survant Coal Mbr.* (IV)		
	POTTSVILLIAN	145 to 450		Colchester Coal Mbr. (IIIa)	Linton	Raccoon Creek*
				Seelyville Coal Mbr. (III)	Staunton	
				Perth Limestone Mbr.	Brazil	
				Minshall and Buffaloville Coal Mbrs		
Upper Block Coal Mbr.	Mansfield					
Lower Block Coal Mbr.						
			Mariah Hill Coal Bed			
			St. Meinrad Coal Bed			

Figure 5. Geologic Units, Pennsylvanian Bedrock of Indiana.



Figure 6. Access road, Ayrshire Mine, Warrick County, Reclaimed Spoil Area.



Figure 7. Access road, Ayrshire Mine, Reclaimed Spoil Area.



Figure 10. 4-inch concrete slab over pile supports, Meadowlake Hills Road.



Figure 11. Exterior block wall with cracks in mortar joints, Meadowlake Hills Road residence.



Figure 12. Garage floor pulled away from wall, Meadowlake Hills Road residence.



Figure 13. Walls separated from the ceiling, Meadowlake Hills Road residence.



Figure 14. Doors unable to close, Meadowlake Hills Road residence.



Figure 15. Fahd Avenue residence, Chandler, Indiana.



Figure 16. Fisherview Road residence, Chandler, Indiana.



Figure 17. Church near previous town of Millersburg, IN, mining proceeded around the church.



Figure 18. Cemetery near Church, near previous town of Millersburg, mining proceeded around the cemetery.



Figure 19. View across pond in final cut toward Meadowlake Hills Road residence (on the left).

**Interstate 40 Emergency Rock Remediation,
Haywood County, North Carolina**

Daniel Journeaux, President

Janod Contractors Inc.
34 Beeman Way
Champlain, NY 12919
(518) 298-5226
daniel@janod.biz

Jody C. Kuhne, LG, PE

North Carolina DOT Geotechnical Engineering
Asheville Area Office
PO Box 3279
Asheville, NC 28802
(828) 298-3228
jkuhne@dot.state.nc.us

Noel Philippon

Janod Contractors Inc.
34 Beeman Way
Champlain, NY 12919
(518) 298-5226
daniel@janod.biz

Peter C. Ingraham, P.E.

Golder Associates Inc.
670 North Commercial St., Ste. 103
Manchester, NH, 03101
(603) 668-0880
pingraham@golder.com

Acknowledgements

The authors would like to recognize the contributions of their colleagues at NCDOT, Janod, Golder Associates and Phillips and Jordan. The field teams from these groups were extraordinary. Bon Chance!

Disclaimer

Statements and views presented in this paper are strictly those of the author(s), and do not necessarily reflect positions held by their affiliations, the Highway Geology Symposium (HGS), or others acknowledged above. The mention of trade names for commercial products does not imply the approval or endorsement by HGS.

Copyright Notice

Copyright © 2010 Highway Geology Symposium (HGS)

All Rights Reserved. Printed in the United States of America. No part of this publication may be reproduced or copied in any form or by any means – graphic, electronic, or mechanical, including photocopying, taping, or information storage and retrieval systems – without prior written permission of the HGS. This excludes the original author(s).

ABSTRACT

On Saturday morning, October 25, 2009 at 02:30 a massive rockslide occurred on Interstate 40 in North Carolina at Mile Marker 2.6 near the border with Tennessee. The volume of material that fell was roughly 80,000 cubic yards and some of the rock blocks were the size of city busses. Phillips and Jordan of Knoxville Tennessee were called under an emergency contract to remove slide material from the roadway and find a specialty subcontractor to address remediation of the remaining rock slope. Noel Philippon of Janod Contractors arrived on site Monday October 26th to assess the slope condition and develop a work plan with Phillips and Jordan, and Janod commenced initial scaling of the slide mass and scarp on October 28th. Initial scaling and material removal operations were closely monitored for movement as the slide was considered potentially still active.

Jody Khune, a geological engineer with North Carolina Department of Transportation (NCDOT), completed geologic mapping of the slide mass and scarp and concluded that the slope consisted of several potential wedge failures and further rockfalls could be expected from the failure plane. An initial plan was developed to remove the slide debris and the remaining wedge structure extending up to 900 feet above the roadway where the joint planes daylighted. When wedge removal proved to be too expensive, NCDOT short listed contractors to bid on installing 50,000 linear feet of post-tensioned rock anchors up to 130 feet long in 60 days to stabilize the wedge structure. The team of Phillips and Jordan and Janod were the successful bidders on the project and the contract work started on December 28, 2009. There were several challenges on the project that became exponentially more complicated due to the fact that the work was to be performed during the worst weather of the year for that area and in one of the most severe winters in the last 30 years. Due to the time restraints in designing such a complicated project there were several changes to the design that were proposed by Janod. We discuss in detail the design and construction challenges that were met and innovative construction methods used that exceeded expectations.

INTRODUCTION

In the early morning hours of October 24, 2009, a massive rockslide occurred at milepost 2.6 on Interstate 40 in Haywood County, North Carolina (Figure 1). The slide encompassed roughly 80,000 cubic yards of rock and debris, burying the westbound barrel with rock blocks the size of busses and covering the eastbound barrel car-sized rocks. Two vehicle strikes occurred: a westbound car that braked too late and struck the rock pile deploying the vehicle's airbag and an eastbound tractor trailer that pierced a saddle tank on a rock in the eastbound barrel. Luckily there were no serious injuries.

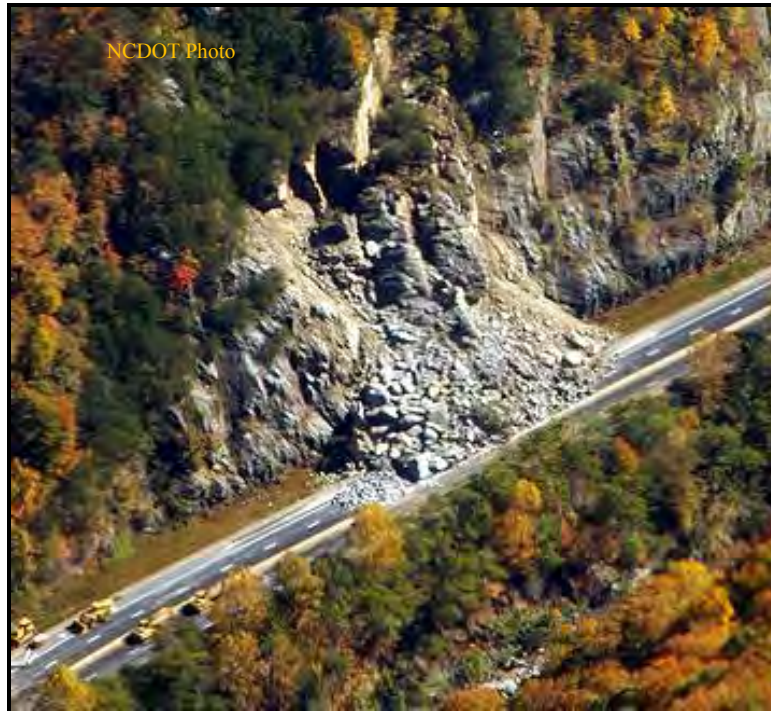


Figure 1 - Aerial View of I-40 Slide on October 26, 2009

The slopes had been cut in the 1960s as the Interstate was advanced through the Smoky Mountains. Several rock benches formed by the excavation are still visible, and suggest the rock cuts were made at a 4-on-1 slope commonly used in highway construction at the time (Figure 2). The strike and dip of geologic features were apparently not taken into consideration, and the Interstate has seen numerous rockfalls and slides since construction, including a major slide less than half a mile from the North Carolina- Tennessee border that closed I-40 for 10 weeks in 1997.



Figure 2 - Benched Rock Cut Adjacent to Slide

The slopes along the interstate were stabilized in the early 1990s using tensioned resin-anchored rock bolts. These bolts were supposedly tight grouted with cementitious grout to the collar, but observation of the bolts following the slide indicated that the holes were not tight grouted (Figure 3). Further, some of the bolts appear to have sheared off at the depth of the slide plane and “launched” out of the bolt holes as their tension was released (Figure 4). In 2009 the area received record rainfalls and NCDOT personnel noted more frequent rockfall activity and slides than normal. The I-40 slide happened after a long, rainy summer and autumn.



Figure 3 - Ungrouted Rockbolt



**Figure 4 - Popped Rockbolt
"Turkey Timer"**

Following the slide, NCDOT personnel, with assistance from Tennessee DOT, closed the Interstate and NCDOT geotechnical personnel commenced analyzing the slide. Terrestrial and aerial photographs were taken of the site, and the margins of the slide scarp and orientations of

the bedding and joint planes were mapped by the NCDOT Geological Engineer (Figure 5). Phillips and Jordan, under an existing emergency services contract with NCDOT, were called in to assess the slide and develop a plan for debris removal and roadway repair. Phillips and Jordan called in Janod Contractors, a specialty rock slope stabilization contractor, to address the metastable slide scarp and assist with the high angle work to complete the project. Janod's operations manager, who had worked on the 1997 slide as a foreman, arrived two days after the slide and began the safety and construction assessments needed to start removing the slide debris.



Figure 5 - NCDOT Geological Engineer Inspecting Slide Scarp

Similar to the 1997 slide, the fallen rock mass was described by joints forming a wedge feature with a line of intersection dipping at roughly 38 degrees out of the slope. The line of intersection daylighted near the toe of the slope and extended to nearly 900 feet above the roadway where it daylighted upslope. The initial concept for remediation was to remove the wedge entirely, as had been done in 1997 for the other wedge slide. However, as the slide debris was cleared and the lower scarp was trimmed, it became apparent that the remaining portion of the wedge was reasonably stable and could potentially be secured using tensioned ground anchors. NCDOT with support from Fisher and Strickler developed a design incorporating 506 post-tensioned anchors with lengths varying from 45 to 120 feet (Figure 6). Anchor lengths were established based on the depth to the planes forming the wedge, establishing a 10-foot bonded anchor zone starting at least 10 feet below the wedge planes. The design called for 1 3/8-inch diameter, Grade 150 bar anchors, tensioned to 140 kips, which yielded a calculated factor of safety of 1.3 derived from the anchor loads. The orientation (azimuth and plunge) of the anchors was critical, along with the aggregate anchor load anticipated. The design was assembled into a contract and bids were solicited for the work. The contract stipulated that the anchors would need to be installed in 60 days, which would be precedent-setting given the steep terrain, scale of

the project, and project start the week after Christmas. The Phillips and Jordan/Janod Team was selected to complete stabilization of the wedge feature.

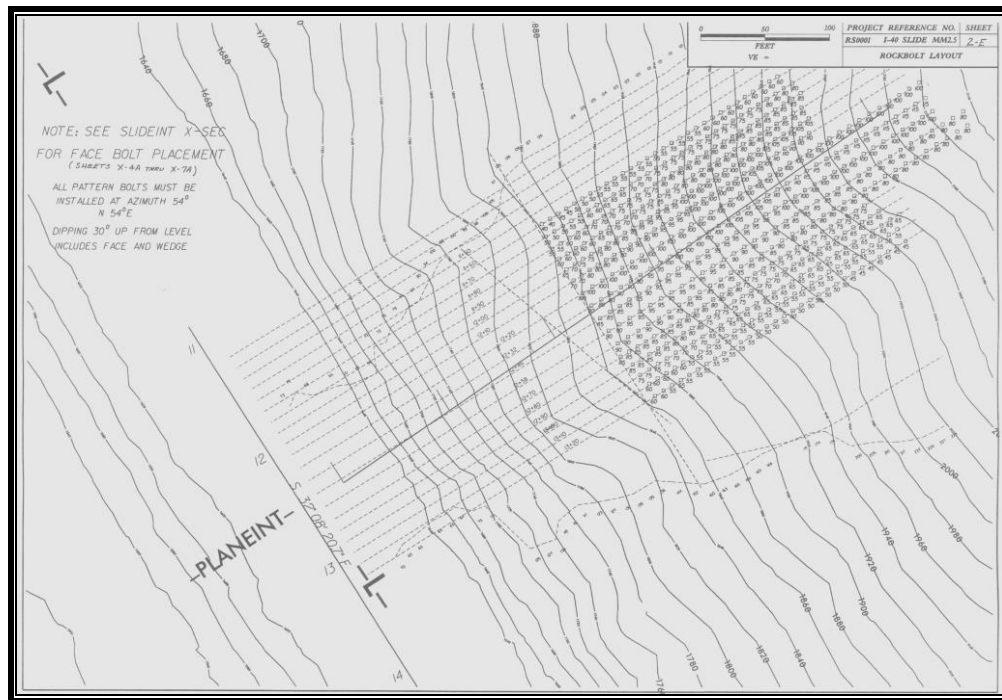


Figure 6 - Initial Anchor Layout

CONSTRUCTION

Following project award on December 18, 2009, the construction team began mobilizing materials, equipment and support personnel to the site. To accommodate the tight schedule, drilling would need to be done around the clock, equipment maintenance and repairs had to be completed on site, bar anchors had to be fabricated on site for on-time delivery to the anchor holes, and getting materials and equipment up the 900-foot slope would require innovative methods. Within a week, the site was receiving materials, maintenance supplies, compressors, and staff for a maintenance facility to keep 10 to 12 drills running 24/7 for two to three months straight (Figure 7). Additional staff from Golder Associates were added to Janod's crew to monitor submittal/approval processes, production, drill logs, drill hole acceptance, downhole video logging, anchor fabrications, installation, grouting, testing and acceptance. This allowed Janod to focus on production.

Critical to the schedule was acceptance of an alternative anchor design for anchors longer than 60 feet - the maximum length of continuous threadbars commercially available. Janod proposed using multistrand tendons comprising four Dywidag 7-wire strands to eliminate potential issues associated with having bar couplers in the unbonded length of the anchors. These would require several weeks lead time for fabrication and delivery, along with custom bearing plates for the anchor head assemblies. The change required increasing the anchor hole diameter to 4 ½ inches to accommodate the 4-strand anchors. It also increased the minimum

bond length requirement to 15 feet. NCDOT elected to increase all the bond lengths to 15 feet to address the uncertainty of ground conditions.



Figure 7 - On-Site Maintenance/Fabrication

As with all high angle projects, addressing site safety, access and mobility was the first priority. The construction team was familiar with the site, having been working on the demolition and removal of the slide mass from October to December. But with the design change to stabilization from blasting and removal, logistics issues for a greater number of staff, night operations, movement of materials, machines and plant upslope and proof testing of every anchor greatly increased the complexity of the project. Access was initially improved with a highline tramway installed to ferry supplies upslope (Figure 8). Removal of cleared trees was facilitated with a CH-53 helicopter, and proved so effective, the helicopter was used throughout the project to deliver light and grout plants, drill rigs and anchors to the working face (Figures 9). This practice proved so successful, that all of the ground anchors were installed using the helicopter.



Figure 8 - Highline System

The construction schedule started on December 28th. As the work began, the beginning of the worst winter locally in 30 years also started. Although in the south, the Smoky Mountains are known for producing snow and beautiful fall foliage. This winter would see record rainfalls in the south, additional rockslides on I-40 near the project in Tennessee and North Carolina, major road closures in Tennessee and a record flood in Nashville. Every storm it seemed, tracked through the I-40 corridor producing rain, sleet, high winds and snow. Site work was suspended for safety reasons on days when high angle access was hampered by weather.



Figure 9 - CH-53 Lifting Grout Plant

Design modifications were developed to address changing conditions as the slope was exposed or drilling revealed different ground conditions. Initial removal of the lower scarp by controlled blasting exposed a stable joint face that became the new terminus of the wedge feature rather than a planned presplit line. This extra face area provided space for additional anchors when they were needed later in the project. Deep soil conditions up to 18 feet deep were encountered on several of the anchor rows. Because of their location, scaling or grubbing of the soil was not practical. Deep soil conditions at the anchor heads had not been contemplated during the design and bidding process. Further, excavating below 4 or more feet in soil would trigger OSHA trench safety requirements. A two-stage grouted anchor design was developed where the bonded anchor length portion of the anchor would be grouted in place, the anchor tensioned using a temporary wood cribbing system on the ground surface, and a second filling of grout would lock in the tension with an upper bond zone. After the grout cured the cribbing would be removed and re-used. Two test anchors were installed and the first stage grouting was completed, but ultimately anchors in deep soil zones were relocated.



Figure 10 - Checking Anchor Hole Orientation

Due to the tight anchor spacing (roughly a 10 ft by 10 ft grid), it was very important to align the drilling equipment at the correct azimuth and inclination to prevent holes crossing at depth. In addition, because the wedge planes are not parallel to the ground surface, drilling a hole to the design depth at an incorrect azimuth or inclination could put the bond length within or above the failure plane rather than below it. NCDOT inspectors worked with Golder staff to measure all completed holes for azimuth and inclination and evaluated their acceptability on a hole-by-hole basis (Figure 10). Any holes drilled outside the prescribed tolerance were evaluated to see if they would still be beneficial to the design or needed additional length to satisfy the design. NCDOT added additional anchor locations at the bottom of the slope to make up for rejected holes.

Variable rock conditions were also encountered and forced field design changes in anchor length. Where drilling was terminating in softer rock, noted by faster drilling rates, anchor holes were extended deeper to terminate in at least 15 feet of harder rock. As drilling progressed, some holes were approaching 150 ft in length to reach competent rock. Although the multistrand cable anchors could accommodate this length, the elongation of the free stressing length in the strands during tensioning would exceed the maximum travel of the hydraulic test jacks. This required the use of larger jacks weighing over 300 lbs, which could not be safely moved under high angle conditions. Janod installed a Tyrolean hoist system across the upper portion of the slope (Figure 11) to safely move the heavy jacks between anchors.



Figure 11 - Tyrolean Hoist System, Inset - Moving a Jack

Variable rock zones similarly made development of flat bearing surfaces for the bearing plates problematic. Larger bearing plates were required in some instances because the intact rock strength after bearing pad preparation was not great enough to withstand proof test loads. Preparation of the bearing pads in harder rock at times took more than twice as long as it took to drill an individual anchor hole.

As the project progressed, there were continued difficulties installing multistrand tendons caused by bearing pad preparation, problems with the large jacks, and testing of strands with over 10 inches of elongation during stressing. Because the helicopter pilot was able to install full length bar anchors, Janod switched back to using 1-3/8" bar anchors for all anchors and developed a sleeved sheath for couplers in the free stressing length. Drilling continued with the 4 1/2 inch diameter downhole hammer drills. With the successful ability of Janod to drill the larger diameter holes straight and full depth, the ability of the helicopter to install full length anchors, and the slow nature of chipping out bearing surfaces, testing and locking off tensioned anchors, NCDOT proposed changing the design to use 1 3/4 inch Grade 150 continuous threadbar passive rock anchors. Each 1-3/4" passive anchor would provide the capacity of 2 tensioned anchors and would be easier to fabricate (no greased and sheathed section), they would not be limited to holes with less than 3 ft of soil, and would not require proof testing of each anchor (Figure 12). The use of passive anchors also eliminated the proposed two stage grouted anchors. NCDOT's design for the passive anchors required that 125 tensioned anchors be installed on the slope, which was roughly what had been installed and grouted at that time. Locations for the remaining anchors were identified based on soil depth and location in proximity to other tensioned anchors.



Figure 12 - Rock Bolt Fabrication and Staging

Anchors were generally grouted in blocks to keep the crews focused on the steps of drilling, fabrication, installation and grouting of the ground anchors. It also cut down on the effects of communication between anchor holes through the fractured rock mass forming the wedge. Due to the large number of fractures in the rock mass, grouting was difficult when working from the top down, as grout tended to migrate down into open holes that anchors had not yet been installed into. NCDOT allowed Janod to complete the drilling and insertion of all anchors in a work area prior to grouting them in order to minimize the loss of open holes to grout migration.

As the anchors were being completed, the major push was to reopen the Interstate. Final anchor locations were identified by NCDOT and the requirement for completing a TECCO stabilized soil slope prior to reopening the roadway was dropped so that NCDOT could redesign this area to accommodate the 29 foot depths of soil present. The Interstate re-opened on April 26, 2010. From the Contract Start Date of December 28th, 120 calendar days had elapsed, including 48 full days and 19 partial days the site was closed down by weather.

In the final tally, over 58,000 linear feet of drilling had been done, concurrent with scaling, bolt installation and testing. The mix of anchors included:

- 105 multistrand anchors (10,210 LF), tensioned to 140 kips
- 25 1 3/8 inch tensioned bar anchors (1,680 LF), tensioned to 140 kips
- 278 1 3/4 inch passive bar anchors (24,544 LF)
- 91 1 3/4 inch passive bar anchors (6,171 LF) on the vertical face
- 22 1 3/8 inch passive anchors (1,342 LF) completed after the highway reopened

- 35 holes (3,303 LF) drilled and not approved by NCDOT for azimuth and inclination
- 26 holes (2081 LF) drilled and approved by NCDOT but not used
- 29 holes drilled (911 LF) for the original TECCO design on the east side of the slope

CONSTRUCTION TECHNIQUES

Achieving the production in drilling and anchor construction noted above in rugged terrain and during winter could not have been done without considerable resources and experience in high angle work techniques. The number of drills, staff, anchors required, and the steep terrain (Figure 13) necessitated using specialized equipment, materials handling techniques, and modification of plant and power supplies to accommodate site conditions.



Figure 13 - Project Work Area (compressors at lower left for scale)

Air Supply

Running ten to twelve drill rigs simultaneously required significant planning. Janod mobilized six high capacity air compressors to the site and staged them all together. With the drills requiring both high and low pressure air, several large air tanks were placed on the mountain about halfway up. The individual air lines to the equipment were run off of these air tanks with dedicated high volume/high pressure airlines running to the compressors down below. The use of the air tanks reduced the loss in pressure of moving air for long distances through small air lines. As work progressed down and across the slope, additional air tanks were installed on the east side of the site and the compressors split between both sides of the site.

Moving Materials

With the top of the site more than 500 vertical feet off the highway below, moving material and supplies around the site was a major concern. Janod installed a highline hoist system (Figure 8) from the highway up to the air tanks on the west side, about half way up the slope. This system, typically equipped with a large basket, quickly and easily moved everything from drill bits and air tool oil to the lunches of the workers up the slope. By removing the basket, larger items such as coiled multistrand anchors could be moved up the slope.



Figure 14 - CH-53 Installing a Ground Anchor

During anchor testing, moving the hydraulic test jacks weighing up to 300 pounds each around the slope was facilitated using a Tyrolean cable hoist system developed in the Alps for work in high terrain. For this project, an upper highline supported by one intermediate tower and a lower highline supported by two intermediate towers was used. A third highline ran from the lower slope through a block on a trolley on the lower highline up through a second block on a trolley on the upper highline. Items were attached to a trolley on the third highline and could be moved anywhere on the upper slope by moving the third highline left or right.

The majority of the heavy lifting was accomplished with a twin turbine CH-53 helicopter flown by Construction Helicopters. In addition to being able to precisely locate and insert full length bar anchors weighing upwards of 1000 lbs (Figure 14), the helicopter was used to move grout plants to the top of the mountain above the site and stockpile all of the grout used. Other lifts by the helicopter included removing the trees cut from the slope at the start of the project, moving light plants around the slope, and also moving test jacks.

Drilling

Drilling production and installation of anchors in 3 ½ inch and 4 ½ inch holes using conventional bencher drilling equipment would have been impossible. For this project, the basic drill consisted a 3 ½ inch downhole hammer drill mounted to a custom-built air powered wagon drill (Figure 15). Special modifications to accommodate larger anchors for this job, included 4 ½ inch downhole hammers, and several drills were adapted to use hydraulic power for rotation and downfeed pressure. Hydraulic power was supplied by portable hydraulic power units mounted to carts that could be winched up and down the slope. During drilling on the vertical face, standard air-powered wagon drills were again used, this time running the 4 ½ inch downhole hammers. Janod also adapted two Ingersol Rand airtrack drills to operate on the slope and drill with the 4 ½ inch downhole hammers and hydraulic feed.



Figure 15 - Multiple Wagon Drills

Night Shifts

In an effort to complete the work by the original deadline, Janod elected to work two crews per day, eventually going with two 12-hr shifts. This required working under lights in the dead of winter. Dedicated generators were installed at the bottom of the slope and three phase power run up the slope to several temporary power panels complete with breakers. Power was then run to electric light towers (as well as any tools used by both the day and night shifts). To increase the amount of light, three diesel light plants were flown up the slope and installed at strategic locations (e.g., the grout plant) to supplement the existing lights.

CONCLUSIONS

Construction of large scale repairs to slopes requires capability and flexibility on the part of the project team. From the designer to the contractor and owner, expectations should include the need to adapt to changing conditions as they are identified. Greater success will be achieved by those who have more tools and flexibility to adapt and implement the necessary changes. This project was a good example of the teamwork needed to complete design and construction to

reopen a critical roadway following a rockslide. Through application of innovative construction techniques, adaptive design modifications and teamwork, this precedent-setting project was completed despite changing ground conditions and the worst winter weather in 30 years.

**Emergency Rock Slope Stabilization in the Ocoee Gorge
U.S. Route 64, Polk County, Tennessee**

Vanessa Bateman, P.E., P.G.

State of Tennessee, Department of Transportation
6601 Centennial Boulevard
Nashville, TN 37243
(615) 350-4133
Vanessa.Bateman@tn.gov

Jay R. Smerekanicz, P.G.

Golder Associates Inc.
670 North Commercial St., Ste. 103
Manchester, NH, 03101
(603) 668-0880
jay_smerekanicz@golder.com

Deana Sneyd, P.G.

Golder Associates Inc.
3730 Chamblee Tucker Road
Atlanta, GA 30341
(770) 496-1893
deana_sneyd@golder.com

Prepared for the 61st Highway Geology Symposium, August, 2010

Acknowledgements

The author(s) would like to thank the individuals/entities for their contributions in the work described:

John Kizer – Tennessee Department of Transportation
Peter C. Ingraham, P.E. – Golder Associates Inc.
Harry Moore, P.G. – Golder Associates Inc.
Dorothy R. Bourbeau – Golder Associates Inc.

Disclaimer

Statements and views presented in this paper are strictly those of the author(s), and do not necessarily reflect positions held by their affiliations, the Highway Geology Symposium (HGS), or others acknowledged above. The mention of trade names for commercial products does not imply the approval or endorsement by HGS.

Copyright Notice

Copyright © 2010 Highway Geology Symposium (HGS)

All Rights Reserved. Printed in the United States of America. No part of this publication may be reproduced or copied in any form or by any means – graphic, electronic, or mechanical, including photocopying, taping, or information storage and retrieval systems – without prior written permission of the HGS. This excludes the original author(s).

ABSTRACT

On November 10, 2009, a large rockslide struck U.S. Route 64 in the Ocoee Gorge in Polk County, Tennessee, following an intense rainfall event associated with tropical storm Ida. The slide obliterated the roadway and a sidewalk, blocked access to a boat ramp, and impacted area access as well as the local economy for five months. Approximately 15,000 cubic yards of rock, soil and forest vegetation buried the roadway to a height of nearly 25 feet. An adjacent historic concrete faced timber crib dam operated by the Tennessee Valley Authority (TVA) was not impacted by the slide. An initial smaller slide occurred early in the morning closing the roadway and mobilizing maintenance, repair and television crews to site. Observation of the slope during the initial cleanup indicated a larger slide mass was failing and provided sufficient warning to evacuate workers clearing the initial rock debris before the main slide fell, avoiding potential loss of life. Television news crews on site to cover the initial smaller slide obtained rare video footage of a major rockslide occurring.

Originally called the Copper Road because it was constructed to haul ore west along the Ocoee River valley to Cleveland, Tennessee, U.S. Route 64 is a vital east-west two-lane highway providing the only principal access between extreme southeast Tennessee and adjacent North Carolina. Detour routes around the area extended travel up to two extra hours. The roadway follows the winding Ocoee River, the site of the whitewater events of the 1996 Summer Olympic Games. The roadway is also the primary route for commuters from Polk County to jobs in neighboring Bradley and Hamilton Counties, a daily commute that ranged from one to two hours for citizens on the far side before the slide occurred. The river and roadway traverse the Cherokee National Forrest, providing access to outdoor enthusiasts. The roadway also serves as the primary route for emergency and commercial vehicles serving the towns, tourist camps and whitewater rafting outfits in the area, and is also the main east-west corridor for commercial trucking from Chattanooga and southeast Tennessee with North Carolina. The rock slope, like many within the Ocoee Gorge, has been monitored closely by the Tennessee Department of Transportation (TDOT) under their rockfall hazard program. Area TDOT maintenance workers, well aware of the issues posed by many of the rock slopes within the gorge, check the slopes and roadway for changes regularly during the winter freeze-thaw events and after significant rainfall.

The rocks in the Ocoee Gorge consist of late Precambrian, complexly folded, thin to medium bedded, low-grade metasediments, including slates, phyllites and metagraywackes. Differential weathering of thin beds of slate and phyllite bounded by more competent metagraywacke can lead to planar and wedge failure of steeply dipping beds, intersecting joints and cleavage planes. Exposure of these weak beds in the toe of the slope, in conjunction with over five inches of rain over a 24-hour period, led to planar sliding failure of a portion of the rock slope. Remediation included scaling of loose rock and soil; trim blasting of remaining beds on the slope to remove the potential for further rockfall; installation of pattern rock bolts throughout the slope; and installation of drains at the toe of the slope. Due to the proximity of the TVA dam, blasting vibrations had to be monitored. Limited access along the mountainous two-lane highway hampered rock slope mitigation construction.

INTRODUCTION

On November 10, 2009, at about 6:00 a.m., a small rock slide occurred on U.S. Route 64 in Polk County, southeast Tennessee, mile marker 17.6 in the Ocoee River Gorge (see Figure 1). The small slide partially blocked the highway, but occurred during light traffic with no reports of any accidents. The maintenance crew of Region 2 of the Tennessee Department of Transportation (TDOT) immediately closed the roadway and started to clear the road using a hydraulic breaker and other heavy equipment. The rockslide occurred following heavy rains from a tropical storm/nor'easter nicknamed "Nor-Ida". As heavy rains continued that morning, TDOT monitored the rock slope closely. At about 12:30 that afternoon, after hearing the slope continue to crack and groan, the TDOT geotechnical engineer ordered all maintenance crews, media and others to evacuate the rock slope. At about 1:00 p.m., a much larger rock slide occurred, comprised of about 15,000 cubic yards (cy) of rock, soil and forest debris that slid onto the roadway and into the Ocoee River. Two television crews captured the second slide on video, which made national news and many rounds amongst the engineering geology community. Review of the video indicates a possible key rock block slab about five feet (ft) long slid out from the toe of slope seconds before the main mass slid. The initial estimate of roadway closure was at least eight weeks.

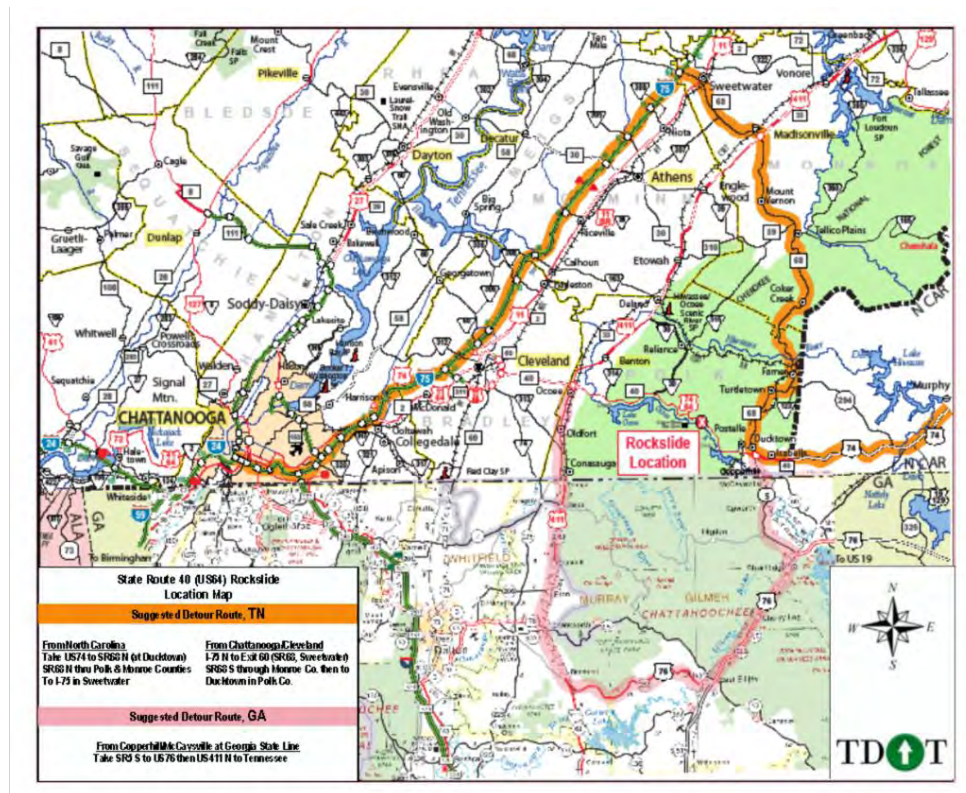


Figure 1 – Site Location Map Showing Detours Around Rock Slide Location (TDOT).

The second slide destroyed about 150 ft of two lane roadway, a sidewalk, and a put-in for white water rafting and other vessels on the Ocoee River (see Figure 2). The slide just missed a historic concrete-faced timber crib dam (Ocoee Dam No. 2) operated by the Tennessee Valley Authority (TVA), built in 1912. U.S. Route 64 is a vital east-west highway linking western

North Carolina with the Cleveland-Chattanooga area of southeastern Tennessee. It is the main east-west corridor for commercial trucking from Chattanooga and southeast Tennessee with North Carolina, and provides recreational access to the Cherokee National Forrest and Ocoee River. In 1996, whitewater events of the Summer Olympic Games were conducted at the site of the rock slide. Detours (Figure 1) around the slide area were extensive, up to two hours one-way, as roadways are spaced widely in the rugged mountainous region of the Southern Appalachians. The detours caused major socioeconomic impacts from late fall 2009 into spring 2010, adding significantly to commute times each way for citizens working in the neighboring counties of Bradley and Hamilton (the location of many of the area's jobs), and closing down the regionally critical tourism trade associated with outdoor activities and whitewater rafting on the Ocoee, delaying the start of rafting season by several weeks. Most significantly, the road closure adversely impacted emergency services to Eastern Polk County, cutting off Ducktown from a hospital with surgical capabilities necessitating a helicopter evacuation for any critical patients.

Improvements in the roadway, particularly those since the 1930's, have focused on adding some width, but in several places these improvements have removed the toe of planar beds steeply dipping toward the roadway. Some of the roadway, nearest to the Whitewater Center and before the entrance to the Gorge at Parksville Dam, have already been widened to a four lane route. However, this last section of roadway while extensively studied, has not been widened due to the area geology, unique cultural and environmental features, environmental opposition, potentially acid producing rocks, and the extreme potential expense of roadway construction in this mountainous terrain.



Figure 2 – Aerial Photograph of the Rockslide on November 15, 2009. Note TVA Dam and Partially Buried Whitewater Raft Put-In on Lower Right. View to the Northeast.

REGIONAL GEOLOGY

The project area is located within the Blue Ridge Physiographic Province of southeast Tennessee. U.S. Route 64 traverses mountainous terrain characterized by over steepened ridges locally associated with existing and historic landslides and narrow, steep-sided drainages and stream valleys containing little or no flood plain. These drainages and streams generally trend northeast-southwest and discharge into the Ocoee River. The corridor is predominantly underlain by rocks of the Great Smoky Mountain Group. These rocks generally consist of fine- to coarse-grained, interbedded metasedimentary rocks subjected to structural deformation that produced large-scale folds with local chaotic bedding. Low-grade metamorphism resulted in a pervasive slaty cleavage that generally overprints most of the bedding planes and is axial planar to large-scale folds.

The bedrock at the site consists of late Precambrian metaconglomerate, metasandstone, metagraywacke and locally graphitic and sulfidic slate, with thin discontinuous dark gray layers of “pseudodiorite”. Initial detailed field mapping correlated these rocks as equivalent to the late Precambrian Hothouse Formation of the Ocoee Series (Heron, 1968). Later mapping assigned these rocks as belonging to the Buck Bald Formation of the Ocoee Supergroup, consisting of quartz-feldspar pebble metaconglomerate, with interbeds of metagraywacke, slate and metasiltstone (Clark et al., 1993). More recent mapping indicates these rocks lie within the late Precambrian Dean Formation, within the Western Blue Ridge Greenbrier Thrust Sheet, consisting of metaconglomerate, metagraywacke, slate and metasiltstone (Thigpen and Hatcher, 2009) (see Figure 3).

The corridor occurs just west of the world-renowned Ducktown massive sulfide deposit. Sulfides, mainly in the form of the minerals pyrite and pyrrhotite, are reported to occur as disseminated crystals and in veins in the slate and to a lesser degree in the metamorphosed sandstone. These sulfides locally occur in much higher concentration in the troughs and crests of folds. The occurrence of sulfides has also been reported to increase with decreasing metamorphic grade; metamorphic grade generally decreases to the west within the corridor.

Road cuts within the corridor generally consist of interbedded metasandstone, metaconglomerate and variably phyllite and slate. Slope stability is largely controlled by joint sets and cleavage in the slate. Rock cuts are typically excavated at about ¼H:1V where the rock is massive and appears to be stable overall. Locally, the irregular appearance of the slopes, however, suggests rock falls have historically occurred. A fairly thin veneer (typically 0 to 20 ft) of residual soil mantles the bedrock on ridges within the corridor. The Ocoee River, along with associated drainages and tributaries, flows primarily on slightly weathered to fresh bedrock.

One key feature of the rock cuts through this section of the Ocoee River Gorge is the extensive weathering and some blast damage of the original rock cuts and bluffs. Most of the cuts that have been made in the area, with the exception of several areas improved during the winter of 2009 and over time, date back to the original construction of the road and many are still in their natural state. Very little presplit blasting was utilized during the construction of the rock cuts in the area, adding to the potential problems. Numerous rockslides and rockfalls have occurred in the area over the years ranging from small falls to larger road blocking events.

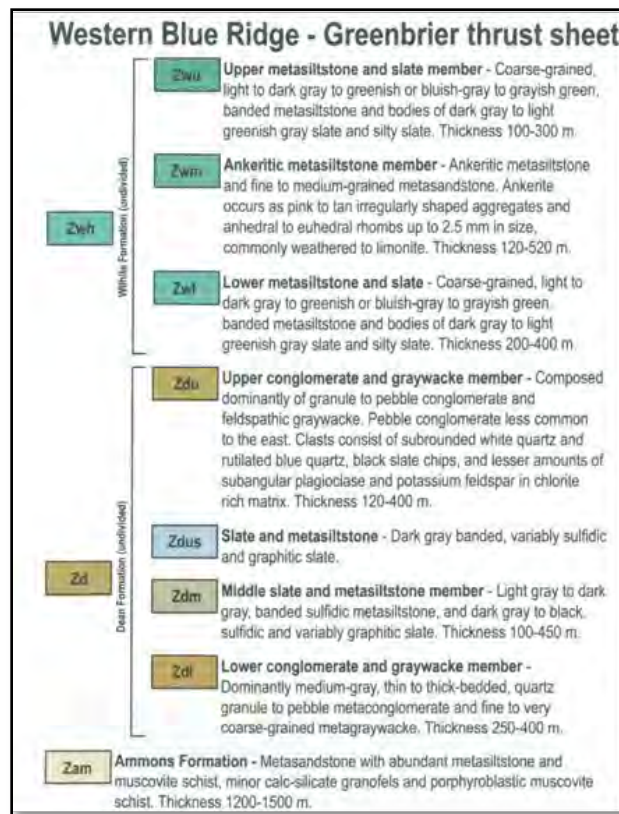
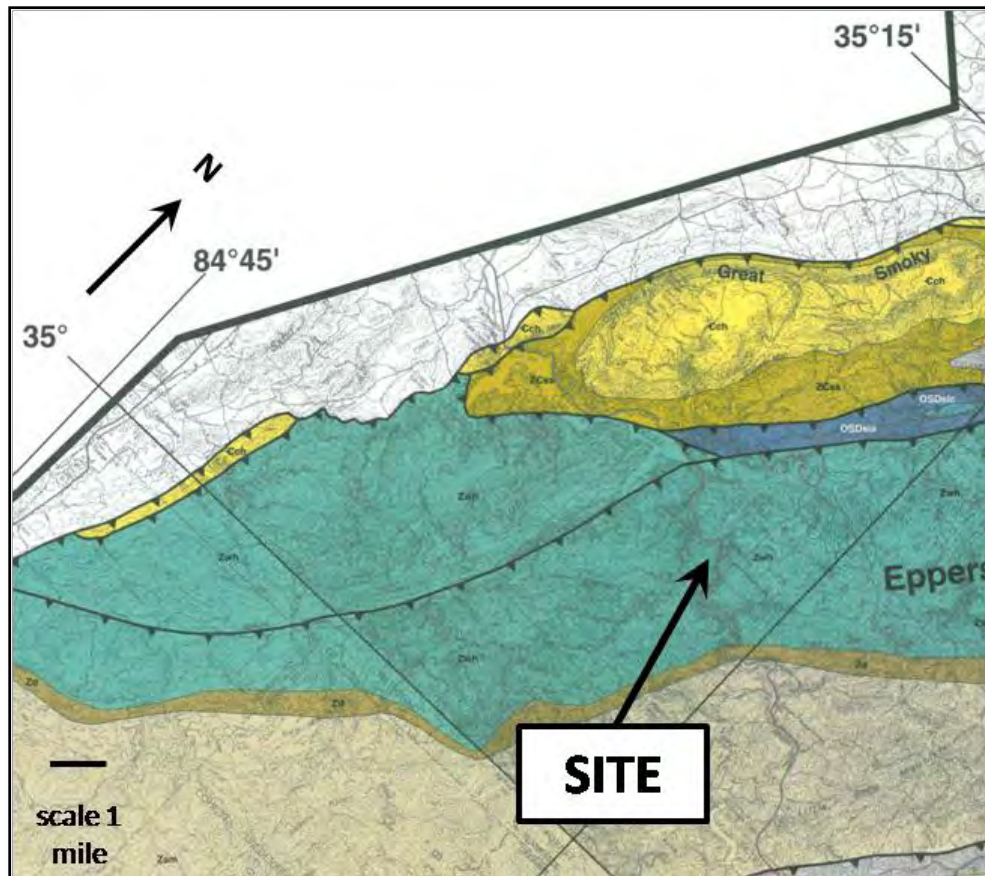


Figure 3 – Regional Geologic Map (Thigpen and Hatcher, 2009)

Bluffs, cliffs and slopes above the roadway show extensive loose rock and stacked rock. Hidden weak layers of rock/weathered rock/clay dipping toward the roadway and underneath the natural 1/2:1 to 1:1 slopes have also given way over time, as with the rockslide of 2005 that shut the roadway down for two months. Numerous natural slide scars can be seen along the roadway, many of which have no record at TDOT, and personnel who have been working in the area for the last 40 years report no knowledge of when these events occurred.

SITE GEOLOGY

The lithology of the site consists of metaconglomerate, metagraywacke and metasiltstone. The metaconglomerate consists of massive, thickly bedded (1 to 5 ft), medium to dark bluish gray (weathered), medium bluish gray (fresh), very hard (R6), coarse to very coarse grained (up to 0.75-inch dia.), weakly foliated metaconglomerate, with clasts consisting predominantly of quartz with some feldspar (probably potassium feldspar), with rare oxides. The metaconglomerate contains some iron hydroxide staining and replacement of calcite and oxides/sulfides. The metagraywacke is similar to the metaconglomerate, but consists of massive to medium bedded (0.5 to 3 ft), medium to dark gray (weathered), medium to light gray (fresh), rusty weathering, medium to coarse grained (up to 0.25 inch dia.), hard (R5-R6), weakly to moderately foliated greywacke. The metasiltstone consists of thinly bedded (less than 0.5 ft), medium to dark brownish and greenish gray (weathered), dark gray (fresh), very fine grained to aphanitic (where slaty), strongly foliated and cleaved (with at least three cleavages), weak (R1-R2) metasiltstone and slate. This unit occurs as pods, lenses and discontinuous beds, often containing rusty weathering and damp to wet seeps, and is susceptible to differential weathering. Both the metaconglomerate and metagraywacke contain dark gray, foliated pods and lenses of metasiltstone, interpreted to be rip-up mudclasts. Discontinuous quartz veins up to three inches wide commonly exist perpendicular to bedding, and less so concordant with bedding. Folding is minor at the rock slope site. Unlike many of the adjacent areas, the metaconglomerate and metagraywacke at this site are not a source significant potentially acid producing rock.

TDOT and Golder, Associates collected over 300 discontinuity measurements from adjacent rock outcrops in the Ocoee Gorge, as well as from the rockslide slope via rope rappel. From these data, four major discontinuity sets exist (see Figure 4). These are:

Set ID	Strike/Dip Right	Notes
1 m	038 / 56	Parallel to bedding, dip slope former
2 m	222 / 38	Perpendicular to bedding, quartz veins
3 m	171 / 50	Minor discontinuity set
4 m	314 / 84	“Evil Twin” release joint set

Of these, the 1 m set (above) contains the dip slope forming joint set, which is parallel to bedding and foliation (as contained within the metaconglomerate and metagraywacke). It is this set in which the rockslide originated.

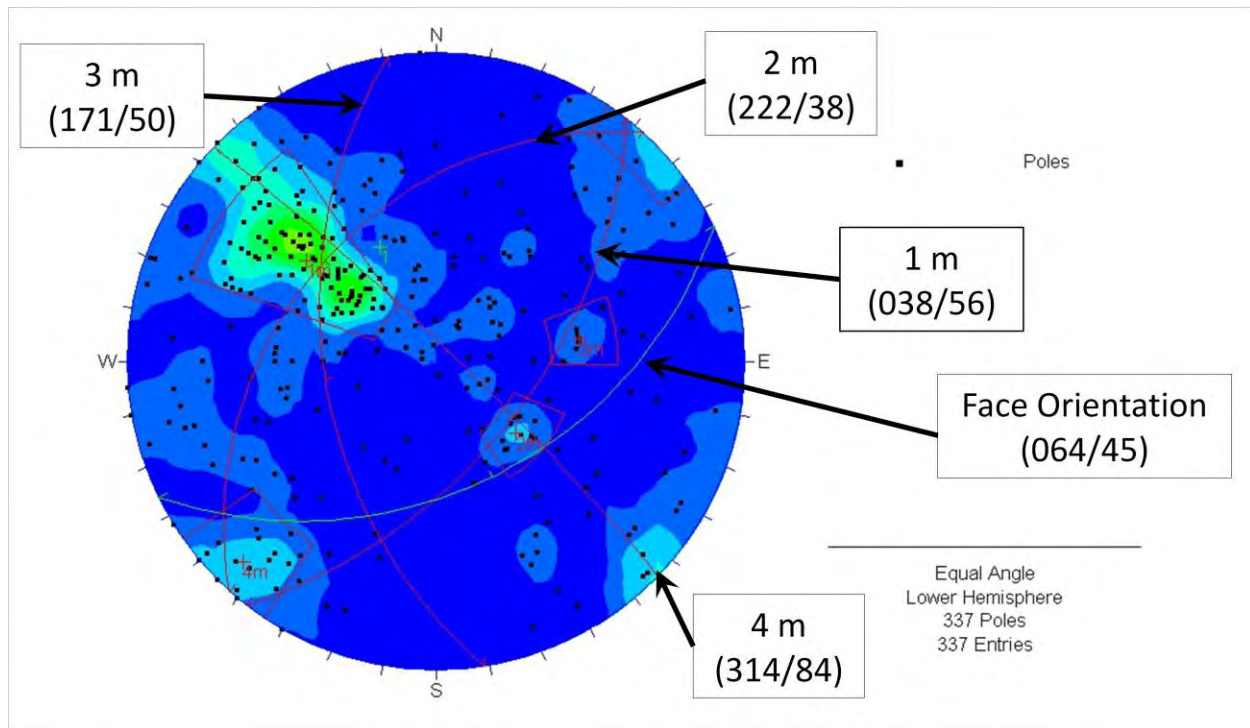


Figure 4 – Discontinuity Stereonet (Major Discontinuity Planes and Face Orientation in Strike/Dip Right Format).

The primary failure surface consists of a thin bed of highly to completely weathered metasiltstone between thickly bedded to massive metaconglomerate and metagraywacke of the 1 m discontinuity set. Following the failure, this material was found to have eroded to a completely weathered, saturated, light brown sticky silt and clay.

ROADWAY HISTORY

Adding to the geological challenges at the site is a roadway that has evolved over time, and was not designed for rockfall catchment or under current accepted standards. This section of roadway, while extensively studied for re-alignment over the past 40 years as part of TDOT's roadway program and with the encouragement of the Federal Appalachian Development Authority has not yet resulted in a re-alignment or significant upgrades to the roadway facility from a two lane road. Adjacent sections of this roadway from the east and west have all been, or are being constructed as a four lane divided highway. However, this particular section presents significant technical, cost and environmental challenges. Currently, a new alignment is being studied and is in the "environmental phase" of assessments.

Major improvements to the area, such as a major realignment or construction of a four lane road through this section of roadway, have not been performed due to the technical challenges, large cost and potential environmental and cultural impacts to the area. Much of the rock in the area, though not at this specific site, is highly susceptible to producing acid rock drainage and this area was damaged extensively by such drainage and acidic rain due to copper

and sulfate mining in the 19th and 20th centuries. Many of the old mines in and around Ducktown and Copper Hill still discharge significant acidic runoff. Pyrite cubes can be seen with the naked eye along many of the rock cuts and bluffs and net acid based accounting gives many of the tested samples in this area among the worst of the potentially acid producing rock of Tennessee. The topography also presents significant challenges: many of the potential new alignments, and even improvements of the existing road, lead to potential cross sections of numerous cuts at 200 to 300 ft in height in folded, faulted and otherwise structurally complex rock. Over the years tunnels, viaducts and other expensive structures have been proposed to reduce the height of these cuts and the significant fills (200 to 400 ft) that might be necessary depending on the alignment chosen.

The roadway through the Ocoee Gorge was initially constructed in the mid-1800's to haul copper from near Ducktown to a railhead in Cleveland, and was originally called the Old Copper Road. The Tennessee Department of Highways reconstructed the roadway in the 1930's and again in the mid-1960's, improving travel along the scenic Ocoee Gorge. Part of the improvement included shallow, vertical rock cuts at the toe of the rockslide area. The removal of the toe has caused successive failure of small rock blocks further up slope, as the weak metasilstone beds were exposed to weathering and water pressure build-up, causing TDOT maintenance crews to monitor the project area. Maintenance crews regularly inspect the roadway for changes and falls after freeze-thaw events in the winter and after any large rain events, and then notify the TDOT Geotechnical Division of changes and concerns. Numerous calls have been made to inspect sites over the years and spot improvements have been conducted as weathering and sliding changes impact the cuts.

Rockfall and rockslide repairs to the slope in this area have tended to be more reactive, partially because of plans to improve the entire corridor. Before the 2009 slide, this section of roadway contained 11 of the 36 worst rockfall sites statewide in Tennessee and had over 44 "Class A" (high potential for rockfall) sites within a 10 mile section. Numerous "Class B" Sites (medium potential for rockfall) are also contained within a 10 mile section. The need to improve so many sites in order to significantly reduce the risk to the public leads inevitably to the conclusion that in terms of rockfall and rockslide mitigation, the most effective method of repair is to mitigate (i.e., improve or realign) the section of roadway, rather than just concentrating on individual rock cuts and bluffs.

Unfortunately, with no good detour, a narrow two lane road with no shoulder and a significant ADT of more than 6,000 cars per day would require closing the road for any work along this section of roadway. Many areas cannot have more work performed other than some simple patchwork scaling due to the site constraints without closing the road for significant periods of time, an option that presents serious hardships to the people and economy of the area.

Due to the undercutting of the toe, and persistent minor rockfalls, the rockslide site was on the list of potential mitigation sites as part of TDOT's rockfall hazard rating system (Bateman, 2010); however, environmental, funding, permitting and community impacts precluded addressing the work sooner. TDOT's rockfall mitigation program started in 2008 and has, or is mitigating 18 sites statewide, not including the five emergency rockfall/rockslide projects from the winter of 2009/2010.

MITIGATION DESIGN

Due to the emergency nature of the roadway cleanup, the project contract was scoped in the field, and overall mitigation design elements were selected on site based on TDOT's experience in rock slope mitigation. The \$2.1M emergency contract was let to Blalock and Sons within days of the slide. The mitigation elements consisted of tree/vegetation removal, hand scaling, machine scaling, trim blasting, blast scaling, pattern rock dowel installation, and drain installation, as well as rockslide debris removal, put-in repair, and roadway reconstruction. Due to the predominant planar sliding mechanism, and relative uniformity of the bedding, TDOT chose pattern bolting to secure the rock face.

Due to the closure of the roadway at the rockslide site, and requirements for roadblocks to detour traffic several miles from the rockslide area, about 14 miles of US Route 64 were closed for several months. TDOT therefore used this time to perform additional rockfall mitigation and slope work on numerous sites on U.S. Route 64, including excavation of other problem rock slopes; remediation of a second smaller site which suffered a toppling rock fall January 18, 2010; and mitigation of the "15 mile per hour curve" which had a hanging wedge failure discovered during the investigation for improvements to this area. Interestingly, TVA's flume on the opposite side of the river experienced another wedge failure almost directly opposite from the 15 mph curve in late April 2010. This site was named for the posted speed limit required in order for two vehicles to safely pass one another in a very tight horizontal curve.

The contractor awarded the work, Blalock and Sons, chose to use large cranes for the majority of the high angle work. The full closure of the roadway allowed for the use of a 275-ton crane, assembled on site, as well as smaller 100-ton cranes. The sequence of work consisted of tree removal, hand scaling and trim blasting of boulders and soil left by the rockslide but potentially causing falling hazards to workers below. Work generally moved in a west to east and top-down fashion. High scalers worked from fall protection ropes anchored at the top, removing loose rocks and soil top-down. Following removal of the loose material, the contractor performed mechanical scaling using a crane-suspended pygmy excavator with a hoe-ram attachment (see Figure 5). The contractor also used a crane-suspended 20-ton crawler mounted drill rig for trim blasting and blast scaling, as well as a hand operated plugger drill. About 12,000 cy of rock were removed via hand scaling, machine scaling and trim blasting. Based on observed conditions (and sometimes while on rope rappel), TDOT inspectors determined the depth of rock removal for trim blasting to cease.

Blasting at the site had to be carefully monitored and the reaction of the rock face to the blasting studied due to the need to prevent potential damage to the dam, the need to stabilize the slope for pattern bolting, and the need to avoid further destabilizing large blocks or sections of the rock cut.



Figure 5 – Mechanical Scaling Using Pygmy Excavator with Hoe-Ram Suspended From 275-Ton Crane. View to East (Photograph Date January 19, 2010).

Blasting operations were scrutinized closely by the TVA, who was concerned about the stability of the dam at the toe of the slope. The contractor kept charge weights down to keep vibration levels within tolerable limits (generally less than 0.5 inches per second peak particle velocity). At the request of the TVA, the contractor erected a makeshift rockfall barrier comprised of blasting mats held vertically on a steel frame as a curtain to contain falling rock onto the roadway above the dam. No rockstrikes occurred on the dam during the rockfall mitigation work.

Adjustments were made to blast hole spacing, charge weights, amount of blasting area and delays as the project continued in order to remove rock, where possible, back to a smooth potential sliding plane, thus keeping the rock face as undamaged as possible. The lack of shoulder at the roadway, inability to re-align the roadway due to the site constraints and lack of catchment meant that the face needed to be as clean as possible to prevent future rockfall.

Of particular concern was a section of the original rock slope left hanging after the larger slide, affectionately called the “Evil Twin” (see Figures 6 and 7). This rock mass was bounded by a release surface on the west corresponding with discontinuity set 4 m, and the planar sliding discontinuities (set 1 m). TDOT placed crack gauges and took daily photographs of the loose rock blocks at the toe of the “Evil Twin” to track movement. By late November 2009, TDOT determined that the toe of the “Evil Twin” was indeed moving, and the rock mass would have to

be removed. This posed a special concern to the contractor, who was not allowed to stage equipment or personnel beneath this area until it was removed. Rope rappel inspection of the upper portions of the rock mass identified two joints of the same set (4 m) existed further to the east, which were used to limit rock excavation (see Figure 8).



Figure 6 – View of "Evil Twin" on Right (East) Side of Rockslide Scar Outlined in Red (Photograph Date November 10, 2009).



Figure 7 – View of "Evil Twin" on Right (East) Side of Rockslide Scar. Areas outlined in black are apparent older slide scars on rock face more than 40 years old. TVA dam in lower right, including placement of crack gauges (photograph date November 20, 2009).



Figure 8 – Evil Twin Area After Removal of Sliding Rock, But Before Scaling and Bolting. Note release surface formed by discontinuity set 4m dipping steeply to the east (right).

Figure 8 shows two photos of the removal of the Evil Twin. Note the original slide release surface was at a steeper angle than some of the joint sets on the new “walls” as the cut is transitioned back out into the hillside. Spray paint marks show potential bolting locations, and slope bolting operations can be seen on the left side of the photograph. The photo on the left shows a birds eye view from the 275-ton crane platform several days after right photo was taken and during clean-up of scaling operations in order to re-position the crane.

Following rock excavation, the sub-contractor, Hayward-Baker installed untensioned pattern rock bolts using an electric powered drill, also suspended by a crane. The bolts consisted of grade 150 #11 (1-3/8 inch) threadbar, installed to depths of 15 to 40 ft, depending on the bedding/slab thickness, and grouted with neat cement grout. The pattern was diamond shaped, with bolt spacings generally 10 ft. Bolt spacing to the east side of the “Evil Twin” area and above the east side old slide scar were placed on an 8 foot pattern due to the need to secure very large blocks. Bolts were finished with faceplates and nuts bearing on a mortar pad. About 11,200 ft of rock bolts were installed. Following completion of bolting, drains to reduce slope water pressures were drilled into the slope at the toe, and produced up to about 2 gallons per minute water flow. A few holes originally drilled for bolting were left open and replaced by adjacent holes due to the water flow. These were left open due to drilling of drain holes around the bolting holes that did not succeed in producing water. The holes left open are located on a section of vertical face on the eastern side of the slope in the area of the largest potential boulders.

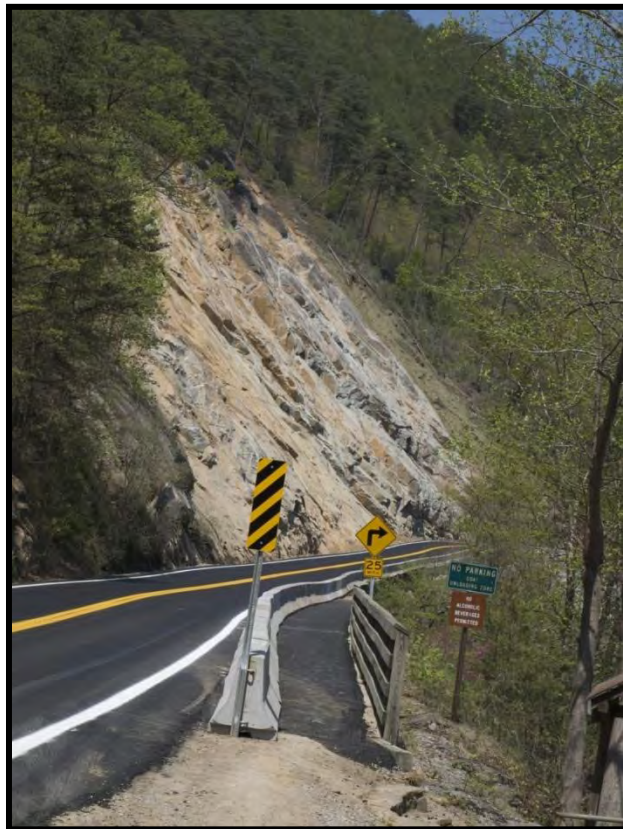
Spot bolting was used extensively around the edges of the rock cut to transition the cut back into the natural slope and to attempt to prevent excavation of rock from having to continue up to the top of the mountain. Boulders with a good footing, but with potential for movement, were particularly targeted with this spot bolting.



Figure 9 – View of Slope After Completion of all Operations and on the First Day the Road was Opened. Photo taken from behind the dam in parking area. Sidewalk to boat access ramp below the roadway.



Figure 10 – View from the Boat Ramp of Rock Bolts and “Guard Rock” Left as the Natural Transition Between the Slope and Pedestrian Walkway.



**Figure 11 –
View from west side of slope on day of roadway opening.**

Mitigation of the site, while following the original contract of scaling, trimming, blasting and bolting evolved over time as the project continued based on the results of the scaling, trimming, blasting and other removal work. Bolt pattern spacing and depths were designed, re-designed and adjusted based on how stable the area was after all the excavation was complete. All areas of the slope were inspected by TDOT geotechnical personnel after every blast and after every milestone of scaling and trimming. Work proceeded more quickly after the “Evil Twin” was successfully removed. One of the parallel potential sliding planes above the level of the plane that originally failed proved to be a good stopping place for part of the “Evil Twin” as all of the movement of the rock in this area was on this parallel plane which was up to 10 feet outward from the original sliding plane. The area was transitioned in a “stair-step” type pattern with the 4 m joint set often providing the wall for the next step up (see Figure 8). The main thrust of the bolting operations was in these transition areas. This allowed for some of the natural slope to be maintained at its original level closest to the dam and prevented impacting both the dam and the hanging bridge used to access the flume and the dam house on the south (far) side of the river.

Slope mitigation work lasted from November 17, 2009 to April 11, 2010, the day of the road opening (see Figures 9 through 11). This includes the roadway, sidewalk and put-in ramp repair. Due to the construction access method employed by the contractor, work had to occur in

a sequenced manner, as the large 275-ton crane blocked much of the access to work areas, and TDOT extended the estimated roadway reopening date from mid-January to mid April. To accelerate the schedule, the contractor employed a night shift from mid-February until early April (see Figure 12).



Figure 12 – Night Drilling Pattern Rock Bolts Using Electric Drill Suspended by 275-Ton Crane.

Due to the highly public nature of the rockslide repair, and the importance of the work to the local economy, TDOT installed a digital camera that obtained a site image every 12 minutes, and hooked the camera up to the TDOT website for the public to track progress. Every image could be viewed at anytime by using the camera/clock toggle on the website. The camera was mounted at a TVA blockhouse above a flume gate on the south (far) end of the dam. The camera, while seemingly intrusive at first to some, actually provided a useful tool for TDOT and its consultants, allowing discussions of observed conditions, review of rope rappelling inspection results, and tracking the contractor's activity. Numerous discussions and observations were compared by both on-site and off-site personnel immediately after blasting and scaling operations were completed. These on-site "real time" photographs allowed for faster identification and better analysis of problem areas where more work ended up being needed. Additionally, most of the blasts on-site were recorded and these movies were uploaded, often within minutes to hours of the blast. This assisted field personnel greatly as it was far easier to discuss structures and areas on the face with a real-time visual aid to the geologists and engineers not on site at the time. Also, it provided an excellent photographic documentation of the work as it proceeded along with changes to the site. The ability to analyze these photographs for patterns such as water flow, fall development and larger rock movement made the field work more effective and less dependent on verbal descriptions of potential problem areas. It was far easier to locate and discuss specific areas on site with a constantly updated photographic "map" of the face. Though originally dubious, several members of the team ended up relying extensively on

these web-cam photographs and opined that better resolution of the cellular camera would be been even more useful.

CONCLUSIONS

As with all rockfall mitigation projects, the mitigation design elements and approach must be flexible and adapt to the encountered conditions. The engineers and geologists on this project stayed one step ahead, working with the contractor in anticipating and addressing changing conditions. The innovative use of the webcam provided a new tool to evaluate and track project progress remotely, and allowed the public access to the site they otherwise wouldn't have had.

REFERENCES:

1. Hernon, R.M. *Geology of the Ducktown, Isabella, and Persimmon Creek Quadrangles, Tennessee and North Carolina*. Open-File Report 68-128. United States Geological Survey, 1968.
2. Clark, S.H.B., Spanski, G.T., Hadley, D.G. and Hofstra, A.H. *Geology and Mineral Resource Potential of the Chattanooga 1° × 2° Quadrangle, Tennessee and North Carolina – A Preliminary Assessment*. Bulletin 2005, United States Geological Survey, 1993, 35 p.
3. Thigpen, J.R. and Hatcher, R.D. Jr. *Geologic Map of the Western Blue Ridge and Portions of the Eastern Blue Ridge and Valley and Ridge Provinces in Southeast Tennessee, Southwest North Carolina, and Northern Georgia*. Map and Chart Series MCH097, Geological Society of America, 2009, scale 1:200,000.
4. Bateman, V.C. Developing and Implementing a Rockfall Management System and Mitigation Program for Tennessee. *Transportation and Research News* vol. 266, 2010, pp. 35-37.

GEOTECHNICAL ENGINEERING FOR A SUPER-LOAD DELIVERY OVER PENNSYLVANIA HIGHWAYS

Chris Ruppen

Michael Baker Jr., Inc.
4301 Dutch Ridge Road
Beaver, PA 15009
724-495-4079
cruppen@mbakercorp.com

Don Gaffney

Michael Baker Jr., Inc.
4301 Dutch Ridge Road
Beaver, PA 15009
724-495-4254
dgaffney@mbakercorp.com

Dave Saylor

Michael Baker Jr., Inc.
Airside Business Park
100 Airside Drive
Moon Township, PA 15108
412-269-4601
dsaylor@mbakercorp.com

Acknowledgements

The authors would like to thank the following companies for allowing presentation of this paper:

Michael Baker Jr., Inc
Airside Business Park
100 Airside Drive
Moon Township, PA 15108

AREVA NP INC.
3315 Old Forest Road
P.O. Box 10935
Lynchburg, VA 24506-0935

Disclaimer

Statements and views presented in this paper are strictly those of the authors, and do not necessarily reflect positions held by their affiliations, the Highway Geology Symposium (HGS), or others acknowledged above. The mention of trade names for commercial products does not imply the approval or endorsement by HGS.

Copyright

Copyright © 2010 Highway Geology Symposium (HGS)

All Rights Reserved. Printed in the United States of America. No part of this publication may be reproduced or copied in any form or by any means – graphic, electronic, or mechanical, including photocopying, taping, or information storage and retrieval systems – without prior written permission of the HGS. This excludes the original authors.

ABSTRACT

This fast track project required delivery of two new steam generators in September 2009 to support Three Mile Island's license renewal to continue operations through 2034. The delivery was managed by AREVA NP, Inc., with Baker providing route planning and engineering support. The route to TMI from their off-loading point in Maryland was characterized by its 75-mile length, hilly terrain, narrow rural roadways, and many water crossings. The steam generators on their transporter units; coming in at 825 tons, 153-feet long, 18-feet wide and 24-feet high each; were the largest loads ever transported on Pennsylvania and Maryland highways.

The geotechnical challenges included foundation support or temporary bypasses at several bridges, stability of sections of roadway, and consideration of pavement structure. One section of the route originated as an Indian hillside trail along a stream in the 1600's that hadn't progressed much past black-topping in the centuries since: it was in very poor shape with the entire roadway showing signs of creeping toward the adjacent river. Additional portions of the overall route required detailed pavement analyses, subgrade and settlement analyses, and design of temporary roadways to bypass bridges lacking the capacity to support the load. Temporary bypasses were designed with various gradations of aggregate with geotextile and geogrid reinforcement for additional aggregate stability.

Baker's geotechnical team uniquely combined existing techniques and theory to model the transporters. Embankments were analyzed for local and global stability, which found the existing roadways theoretically capable of satisfactorily supporting the transporters. Flexible pavement design methods are based on repetitive vehicle loads, but our model viewed each transporter as a temporary structural load and analyzed the structural response from a pavement-and-subgrade strength position. This required analysis of how the wheels of the transporter interacted with each other and how the stress from the combined wheels distributed through the pavement to the subgrade soils.

The true test came as the transporters passed. Any failure of the roads during the move would have been devastating to the project as it would have meant a complete stoppage in traffic while the road could be made safe to pass the transporters or the transporters could be rerouted. Success is measured in performance in line with analyses. Baker's geotechnical team's analyses permitted the transport of the generators without extraordinary and expensive stabilization construction or extended disruption of private land owners and traffic along the route.

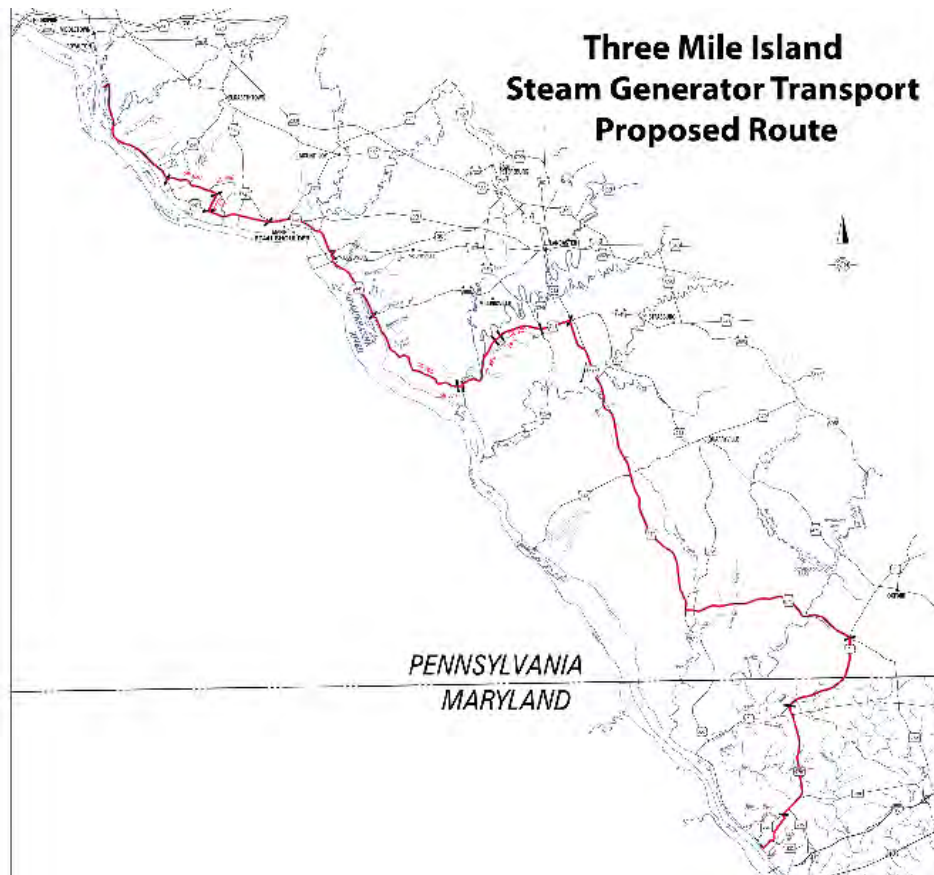
INTRODUCTION

The Route

Two Steam generators manufactured in France were transported for installation in the Three Mile Island nuclear power plant near Harrisburg, PA. They were shipped overseas to Port Deposit, MD, where they would start their final transportation leg.

An exhaustive investigation of alternative transportation modes and routes was performed prior to selection of the 11-day travel route from Port Deposit Maryland to Three Mile Island, both of which are on the Susquehanna River. Water transport was eliminated because of the shallow water and dams along the Susquehanna River. Rail transport was not feasible because of clearance issues with tunnels and low bridges. Overland transport was selected as the preferred mode.

Once the mode was determined, roadway alternatives were identified. State maintained roads were preferred for their standard minimum level of design, construction, and maintenance. The final route was nearly 75 miles long; traversing State maintained highways and a few local roads. Actual travel was accomplished over 14 days, with a maximum speed of 3 mile per hour.



The Load

Each generator was loaded onto a 153-foot-long by 18-foot-wide Self Propelled Modular Transporter (SPMT). Each SPMT was comprised of a pair of trucks that provided support for the generator in a specifically designed cradle that distributed its load uniformly and safely restrained it during transport. The aggregate weight of the SPMT and generator was approximately 825 tons. The SPMT was equipped with 52 four-wheeled axles for a total of 208 wheels. Maneuverability was maximized using mechanically independent axles and an electronically controlled hydraulic steering system. The transporter was powered and controlled by operators at both ends, using a computer interface to control axles.



The Challenge

The challenge was to pass the largest load ever to travel over Maryland and Pennsylvania highways minimizing disruption to the public and without damaging any infrastructure. Much of the infrastructure in this area of the country is historic and sensitive to disturbance. Many streams flow under roads via hand cut, stone arch bridges. Pavements, sensitive and restrictive structures, and underground utilities all required identification, investigation and analysis; with protective measures against potential damage or bypass alternatives designed.

PAVEMENT CHALLENGES

Pavements had to support the wheel loads of the transport and localized load concentrations of temporary structures. Rigorous pavement design calculations were not practical over the entire route and not possible without strength and stress/strain relationships for the existing pavement materials. The entire route was subjected to a field view, with stops at areas where specific improvements were contemplated or that appeared critical in any way. Test borings were taken in particularly sensitive areas and at bridge abutments to evaluate existing pavement conditions. Assumptions were made using typical modulus values and comparing stress profiles from SPMT wheel loads to those of legal highway wheel loads such as HS 20 loading. Various surfaces were investigated from standard concrete and bituminous pavements to aggregate driveways and brick lined medians.



Parking Areas

Eleven overnight and five contingency overnight parking sites were evaluated. Parking areas were provided by private and public parking lots, industrial sites, and highway shoulders. Parking area surface materials had to be evaluated for wheel loads and subgrade consolidation under the longer term load.

Settlement was a concern where the transporters were to be parked over night. Stresses from individual and combination wheel loads were calculated as point loads distributed through the pavement structure. Settlement was estimated to be comparable to conventional on-road vehicles.

Reconfiguration Areas

Reconfiguration of the SPMT wheel and axle alignment improved their adaptability. Two reconfiguration areas were required during the move. The SPMTs were initially placed under the generators as they were lifted off barges at the main harbor near Port Deposit, MD.

After the generators and SPMTs were driven off the barge at a marina in Port Deposit, they made a short 3-mile trip to the closed Bainbridge Naval Training Center where they were reconfigured and thoroughly checked for the highway trek ahead of them. The closed training facility provided the security and existing paved areas with enough open space to comfortably work on the transporters without interference.

The transporter as originally configured for the roadway was not wide enough to engage all of the bridge beams on the Conestoga River Bridge. Only if all the beams were engaged would the bridge have enough capacity to support the load. To widen the transporters, gantry cranes on both ends of the bridge had to be installed to lift the turbines off the transporters. Immediately before crossing the bridge, the SPMT wheelbase was widened. The process was reversed at the end of the bridge.

Foundation pads for the gantry crane were founded on micro piles extended into bedrock to reduce the risk of differential and total settlement. A transition of geologic units was encountered at one of the pads. On one end of the foundation pad area, test borings encountered bedrock at about 25 feet below the ground surface while the opposite end of the pad test borings extended to 80 feet without encountering competent bedrock. The shallow bedrock at 25 feet was limestone and the soft rock materials encountered at the deep boring was schist.



Crossover Areas

The transporters had to be directed around intersections on major highways U.S. Route 1 and S.R. 0030 because of their size. The transporter had to cross the median to access the opposite side of the highway in order to negotiate the ramps and exit the highway. Median areas were covered with steel plating to make them passable without disturbance. Traffic disruption was minimized by using this technique and staging the equipment movement.

Roadway Stability Area

One roadway segment was especially sensitive. Conestoga Boulevard originated in 1638 as an Indian trail that parallels Conestoga Creek. Over the years it has evolved into an asphalt-paved, state maintained road. The road is visibly creeping toward the stream. A roadway video-log of this section of roadway indicated over-stressed and locally failed pavement, with many

cracks paralleling the shoulder. By the time of actual field view, it had received a fresh bituminous overlay.



A subsurface investigation was performed with geotechnical laboratory testing to support slope stability analyses along this two-mile stretch of road. Baker looked at the load applied as a strip load much like a foundation load as well as individual and combination wheel loads for a shallow failure that could progress into a global failure. Baker found satisfactory factors of safety for all conditions investigated.

Other Pavement Areas

Underground utilities and railroad crossings were protected by 3-inch steel plating and plywood placed just ahead of the transporter. Prior to the move, utility companies raised power poles where they could raise them, and removed and replaced poles they could not raise. During the move many utilities had to be raised by hand, traffic signals were swung out of the way. All utilities were cleared from the path of the transporter prior to or during the move.



Other pavement areas of local concern were identified by various agencies. These areas were investigated, with pavement structure, history and condition considered. Typically it was concluded that the loads imposed by the SPMTs were not significantly greater than those historically seen by the pavement from other legal loads. If conditions warranted, steel plating and plywood was recommended.

Superload Permitting

The State of Pennsylvania, as part of its permit process, required automated pavement condition surveys of its State Routes immediately before and after each route was traversed by the SPMTs. This survey was LIDAR-based, and performed in accordance with PennDOT Publication 336. Technical specifications for this work were prepared for use in contracting these services.

BRIDGE AND CULVERT CHALLENGES

All bridges along the proposed route had to be evaluated for the anticipated load. Except for the single bridge where the SPMTs were reconfigured, bridges and culverts that were determined to be inadequate for the load were handled in one of three ways: specially designed temporary structures (overbridges) were placed and removed immediately ahead of and behind the SPMTs as they crossed the structure, the structure was braced to support the additional load without overstressing, a combination of these two techniques was used, or the structure was avoided entirely by a bypass using local roadways or a specially constructed temporary roadway.



Overbridges

Overbridges typically were the first choice and were used in multiple locations to span various size structures. Temporary bridges of 30', 50', and 80' were provided, based on a proprietary design. They were comprised of multiple steel I beams fabricated into sections that distributed the load to the ends. The ends were set on plywood pads on pavement and steel plates on aggregate. Specially designed haulers transported, placed and removed the overbridges. These haulers required their own special permits for oversized loads.

At one location micro piles and temporary bents were used to support an 80' overbridge while crossing a very poor condition stone arch and to permit improved turning radius in a difficult location. A subsurface investigation was performed at the structure for the micropile design.

Bracing

Various types of structural bracing were used. A three span P/S I beam bridge was braced using steel beams placed underneath the center three girders. The steel beams had greater stiffness than the P/S beams and accepted the load through bearing pads located every 9'. A box culvert situated longitudinally to the roadway carrying a stream underneath an old stone railway arch had three rows of posts supporting aluminum beams spaced at 5' for the entire 200' under the roadway. A 1926 closed spandrel arch had shoring towers under its entire 101' length.



In two locations old stone masonry walls were buttressed with fill to provide resistance to any outward loads. These included gabion walls to keep the fill out of adjacent streams

Determining the adequacy of the foundations for the bracing was another geotechnical responsibility addressed through field reconnaissance and subsurface investigations as warranted.

Bypasses

Two bridges over streams were not capable of supporting the weight of the transporters and were too long for the use of an overbridge. These structures had flat surrounding topography and relatively low grade difference between the roadway and stream. The alternative was to construct a temporary aggregate roadway adjacent to the bridge.

Large diameter concrete pipes were installed in the streambed to continue to pass the stream and an aggregate road was constructed over the pipes. A geotextile was placed on original ground to preserve the surface vegetation and potential historic artifacts. A geogrid was incorporated into the aggregate embankment and road at regular intervals to maximize the embankment slope and reduce the risk of rutting.

CONCLUSION

The real test was in the actual transport of the generators from Port Deposit to Three Mile Island. The move was concluded without significant damage to pavement, structures or other infrastructure. This success could not have been possible without the combined efforts of multiple disciplines from several companies working together.

In recognition of this effort, this project was selected for the American Council of Engineering Companies Diamond Honor award in Pennsylvania and National Grand Award for Engineering Excellence.

**Subsurface Stabilization of Problematic Soil Areas
President George Bush Turnpike - Dallas County, Texas**

Garry H. Gregory, Ph.D., P. E., D.GE
Gregory Geotechnical
2001 West 44th Avenue
Stillwater, Oklahoma 74074
(405)-747-8200
ggregory@gregeo.com
Adjunct Professor of Civil Engineering
Oklahoma State University
garry.gregory@okstate.edu

Prepared for the 61st Highway Geology Symposium, August, 2010

Acknowledgements

The author would like to thank the following entities for their contributions to the Project:

North Texas Tollway Authority – Owner
Carter-Burgess, Inc - Prime Civil Engineering Consultant – Segment IV – Section 24
Turner-Collie & Braden - Inc. Prime Civil Engineering Consultant – Segment IV – Section 25
Terra-Mar, Inc. - Prime Geotechnical Engineering Consultant

Disclaimer

Statements and views presented in this paper are strictly those of the author, and do not necessarily reflect positions held by their affiliations, the Highway Geology Symposium (HGS), or others acknowledged above. The mention of trade names for commercial products does not imply the approval or endorsement by HGS.

Copyright Notice

Copyright © 2010 Highway Geology Symposium (HGS)

All rights reserved. Printed in the United States of America. No part of this publication may be reproduced or copied in any form or by any means – graphic, electronic, or mechanical, including photocopying, taping, or information storage and retrieval systems – without prior written permission of the HGS. This excludes the original author.

ABSTRACT

When the North Texas Tollway Authority (NTTA) planned to construct Segment IV of the President George Bush Turnpike (PGBT) in Dallas, County, Texas, one of the challenging engineering aspects was subsurface stabilization of problematic soil areas along the proposed route. These problematic soil areas consisted of two closed landfills, a system of water treatment plant backwash lagoons, a deep rubble fill area, a steep slope area adjacent to an active landfill, and roadway embankments constructed of high plasticity clays. The PGBT design required a variety of improvements in the problematic soil areas including earthfill embankments to approximately 33 feet in height, MSE Walls to approximately 26 feet in height, and excavation cuts to approximately 23 feet deep in one of the closed landfill areas. These areas were stabilized with a variety of subsurface techniques including, dynamic compaction, lime-fly ash slurry injection, compaction grouting, deep soil mixing, vibro-concrete columns, geogrid reinforcement, and fiber-reinforced soil (FRS). Geotechnical instrumentation was installed to monitor vertical and lateral deformations in the stabilized areas to verify performance prior to construction of pavements. The geotechnical design was completed in late 2001 and construction was substantially completed in October 2005. To date the project has performed as expected in the stabilized areas.

INTRODUCTION

The President George Bush Turnpike (PGBT) consists of approximately 30 miles of six to eight lane toll road in north central Texas. The turnpike passes through portions of Dallas, Collin, and Denton counties, and through portions of the cities of Garland, Richardson, Plano, Carrollton, Farmers Branch, and Irving. The portion of the turnpike that is the subject of this paper is known as the “PGBT Superconnector” consisting of Segment IV, Sections 24 and 25, an approximate 6 mile north-south segment that connects I-35E to the I-635 airport extension. Segment VI was constructed at a cost of approximately \$339 million. This is the only segment in which the author was involved. The PGBT is owned and operated by the North Texas Tollway Authority (NTTA). Design of Segment IV was initiated in 2001, following route studies and acquisition in the previous few years. The final selected route of Segment IV was scheduled to pass over two closed landfills, a system of inactive water treatment plant backwash lagoons, a deep rubble fill area, and involved a steep slope area adjacent to municipal landfill. These areas are collectively referred to in the remainder of this paper as the “problematic soils areas.” Moreover, the proposed construction consisted of roadway embankments to be constructed of high-plasticity clay soils. The problematic soils areas are briefly described in the following sections.

Segment 25 - Farmers Branch Closed Landfill

A portion of Segment IV-Section 25 from station 1095+00 to station 1142+00 (approximately 0.9 miles) was scheduled to pass along the western edge of the Farmers Branch closed landfill. The landfill is a municipal solid waste facility which was closed in about 1983. The site consisted of approximately 20 acres in area with a maximum depth of waste of about 25 feet. While the main lanes were not designated to pass over the actual waste fill area, two ramps were required to achieve access from the main lanes on the west to Valley View Lane (a major arterial) on the east. The ramps were to be supported by drilled shafts outside the landfill area, but were required to be ground supported within the landfill footprint. The grades necessary for the ramps required approximately 10 feet of excavation into the existing solid waste, leaving approximately 15 feet of waste below the ramp elevations in the cut areas and the full 25 feet where the ramps extended to existing grade near the main lanes.

Segment 24 - DWU Sites and Carrollton Landfill

A portion of Segment IV-Section 24 from station 1216+00 to station 1345+73 (approximately 2.5 miles) was scheduled to pass over the Dallas Water Utilities (DWU) Backwash Lagoons and Solid Waste Area, and across a deep rubble fill area of the City of Carrollton Landfill.

DWU Lagoons

The lagoon areas consisted of inactive water treatment plant facilities and contained “sludge” consisting of fine grained soil solids and traces of flocculation chemicals such as alum

and lime which were by-products of back wash water from the adjacent water treatment plant filters. The material classifies as sandy and silty lean clay and fat clay (ASTM D 2487). This material is essentially inert and should not be confused with *wastewater* treatment plant sludge. The backwash sludge was approximately 12 feet thick in Lagoon Number 1, which is the largest lagoon area beneath the turnpike foot print. The sludge was soft to very soft and was highly compressible. The required roadway embankments in the lagoon area were about 22 feet in height and were predicted to cause up to 22 inches of primary settlement.

DWU Solid Waste Area

The DWU Solid Waste Area consisted of a closed construction debris landfill containing wood, paper, plastic, masonry and concrete debris, asphalt materials, and other miscellaneous construction debris. The thickness of the solid waste ranged from about 11 feet to 15 feet and contained a relatively high water table in a few areas. The solid waste was expected to experience a large magnitude of settlement under the proposed embankment heights of 15 to 25 feet.

Carrollton Landfill Rubble Fill Area

The turnpike was not anticipated to pass over the actual solid waste area of the Carrollton Landfill. However, a large closed portion of the landfill within the original permitted area consisted of rubble fill up to about 40 feet in depth. The rubble fill consisted predominantly of concrete, masonry, and asphalt rubble. However, the rubble fill was loosely placed and contained large voids. Several feet of earth fill had been placed over the rubble fill. The loose nature of the rubble with large voids was problematic since the overlying fill might later migrate into the void spaces and cause excessive settlement, and the rubble fill might shift into a more dense condition under the weight of the proposed embankments and also cause significant settlement.

Carrollton Landfill Municipal Solid Waste Area

As previously stated, the main lanes of the turnpike were not scheduled to pass over the portion of the landfill that actually contained municipal solid waste. However, the turnpike alignment would result in the side slope of the embankment fill protruding over the solid waste if the embankments were constructed with a slope ratio of 4 (4 horizontal to 1 vertical) as planned. This is the maximum slope ratio (maximum steepness) that is typically used for slopes in the general area which are constructed of fat clay soils. The protrusion of the side slope fill onto the solid waste area would have caused large settlement in the waste and would have required stabilization of the waste to support the embankment loads and reduce the settlement.

Contractual Relationships and General Time Frames

The author's firm was selected to provide specialized geotechnical engineering consulting and design services for stabilization of the problematic soils areas based upon the author's expertise and experience in subsurface stabilization. The author's firm was a subconsultant to the prime geotechnical engineering consultant. The author became involved in

the project in late 2000 and was involved through the design and construction phases of Segment IV, Sections 24 and 25. The author's firm also designed, installed, and monitored the geotechnical instrumentation during the construction phase of the project. The geotechnical design of subsurface stabilization in the problematic soils areas was completed in early 2002. Construction on Segment IV began in January 2003 and was substantially completed in October 2005.

GEOTECHNICAL DESIGN OF SUBSURFACE STABILIZATION

The geotechnical design of subsurface stabilization and related activities for each of the problematic soils areas is described in the following sections. The analysis and design of the subsurface stabilization methods were performed based upon FHWA recommendations (1) and upon the author's experience with similar projects and conditions. Settlement calculations and decomposition settlement rates in the solid waste areas were performed based upon methods recommended by Sowers (2) and later expanded by the author.

Farmers Branch Closed Landfill

Field Exploration

The Farmers Branch Closed Landfill was explored by 15 geotechnical borings performed by the prime geotechnical consultant. The author and/or the author's representative were present during drilling of the borings. The plan of borings and site layout are presented in Figure 1.

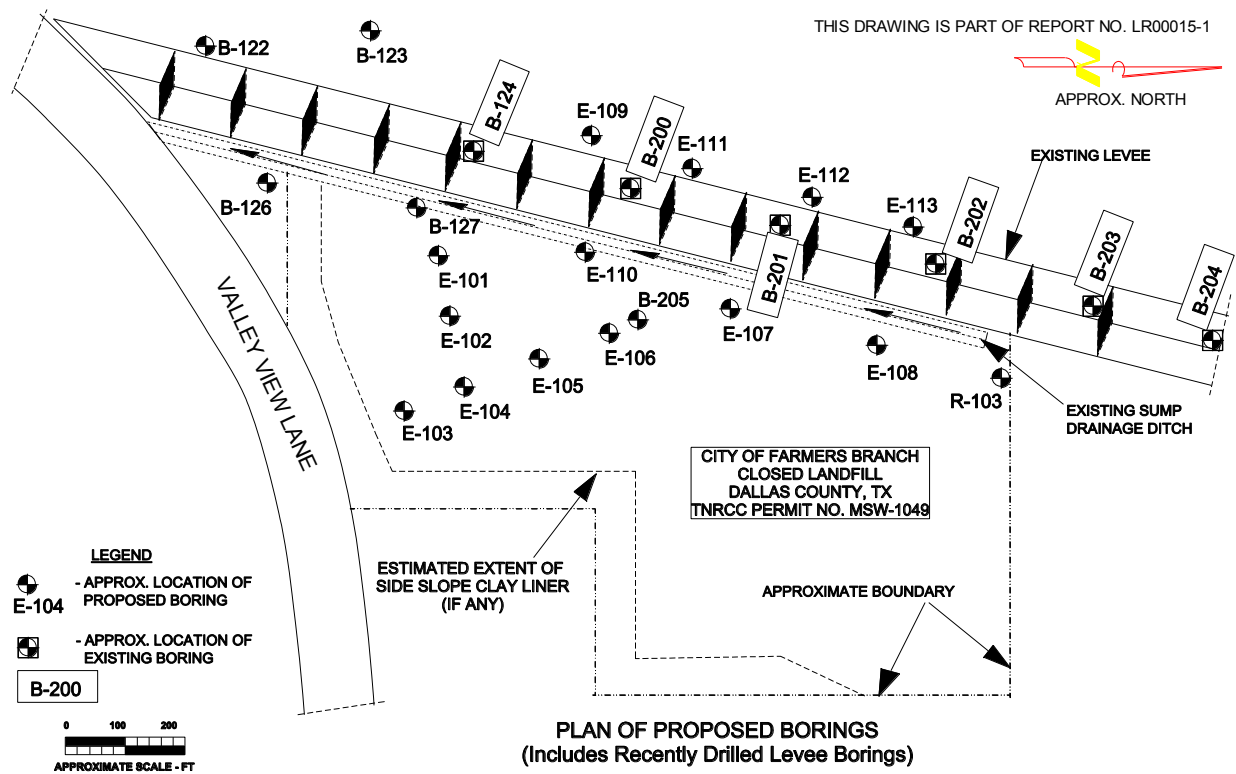


Figure 1 – Plan of Borings and General Layout

The municipal solid waste encountered in the borings consisted predominantly of highly decomposed waste with a large moisture content, similar to “sludge.” Photographs taken during the field exploration and of the typical materials encountered in the borings are presented in Figure 2.



Figure 2 – Field Exploration of Farmers Branch Closed Landfill

Stabilization Options Considered

Stabilization options considered included removal of the solid waste in the area of the proposed ramps (previously described) and replacement with select earth fill, dynamic deep compaction (DDC) followed by lime-fly ash injection, vibro stone columns (VSC), deep soil mixing (DSM), and vibro concrete columns (VCC). Consideration of DDC was eliminated due to the high water table and the thickness of the waste fill. VSC was eliminated due to concerns that the very low strength solid waste might not provide sufficient lateral support for the stone columns. Accordingly, the remove and replace, DSM, and VCC were evaluated and cost compared. The estimated cost of the remove and replace option was approximately \$6.7 million. This option would also produce the largest volume of excavated waste requiring disposal in a permitted and operating solid waste facility. The cost of the DSM option was estimated at approximately \$5.8 million. This method would produce more spoil for disposal, including intermixed solid waste, than the VCC option, but less than the remove and replace option. The cost of the VCC option was estimated at approximately \$2.8 million and would produce the least amount of solid waste to be disposed. Consequently, the VCC option was selected for the Farmers Branch Closed Landfill site.

VCC Option Details

The vibro concrete column method consists of constructing plain concrete columns in soft soil or solid waste with a vibrating probe that compacts the surrounding solid waste, and pumps concrete under pressure through the probe as it is withdrawn and re-penetrated to form a concrete column. The probe is re-penetrated into the lower end of the column and also into the upper end to form an upset section or “bulb” at the top and bottom of the column. The columns

are placed on a staggered (triangular) grid pattern and a geogrid-reinforced granular soil mat (often referred to as a Load Transfer Platform or LTP) is constructed over the tops of the columns to distribute the imposed loads. The VCC with the LTP can significantly reduce the long term settlement since the loads are essentially distributed to the VCC by the LTP, without relying on the interstitial solid waste for support. The VCC also provide stabilizing elements for the side slopes of the excavations through the solid waste to accommodate the ramps.

The required spacing of the VCC was evaluated with a 2-D finite element program assuming the grid pattern of columns represents a plane strain condition. The waste between columns was assumed to have very low strength to simulate settlement due to continued decomposition of the waste. The finite element method (FEM) solution mesh is presented in Figure 3.

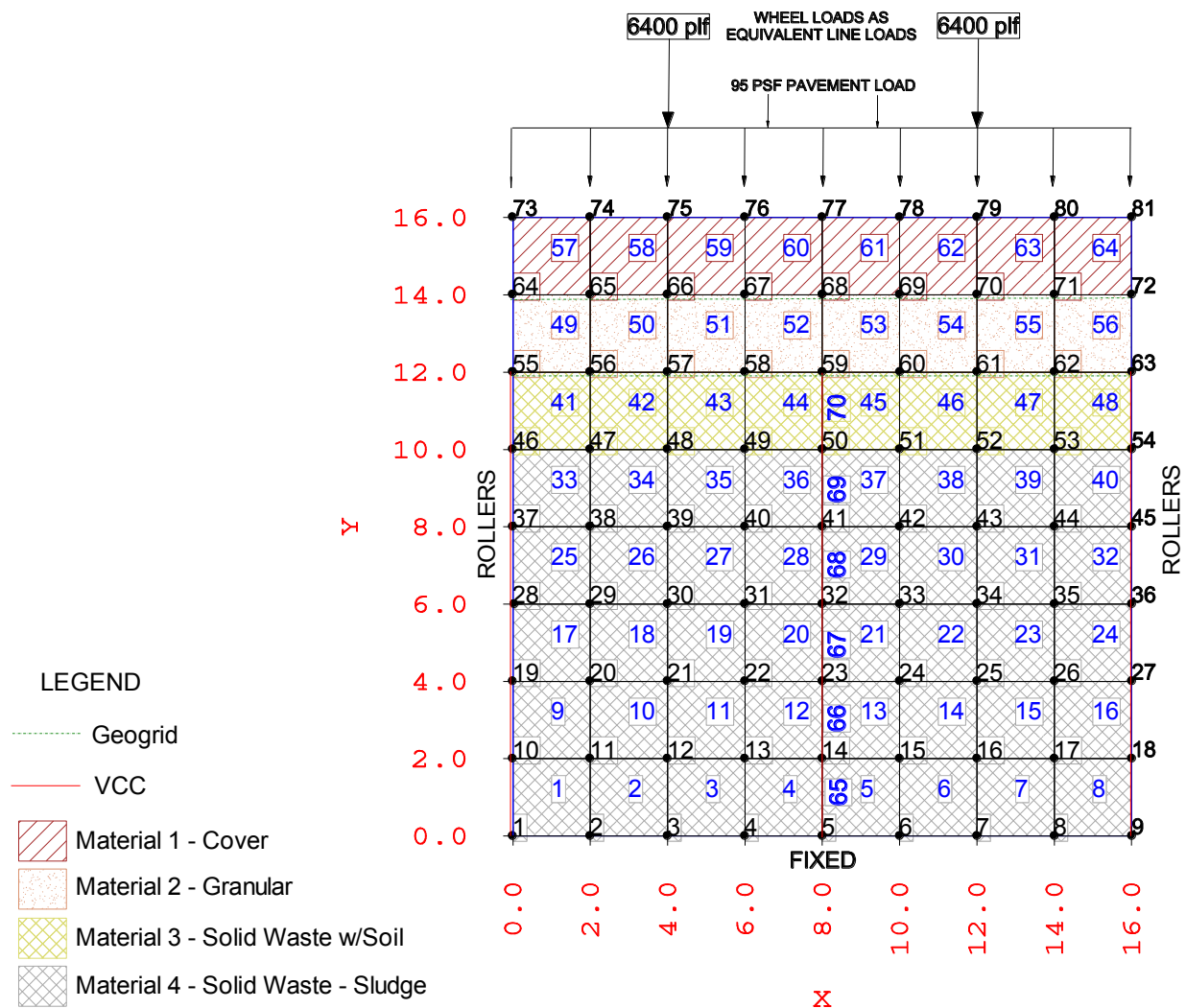


Figure 3 – FEM Solution Mesh for VCC

The FEM analysis indicated a maximum post construction settlement of about 3 inches with the vibro concrete columns on 8-foot centers. This settlement was determined to be within

an acceptable range for the ground supported pavements, with consideration that flexible pavement materials would be used for the pavement surfacing and that additional maintenance would be required compared to the remove and replace option. The VCC spacing was verified for slope stability purposes using the limit equilibrium method and considering the lateral support value of the VCC. These analyses produced a calculated factor of safety (FS) value greater than 1.7 for the long term condition. The general arrangement of the VCC is shown schematically in Figure 4.

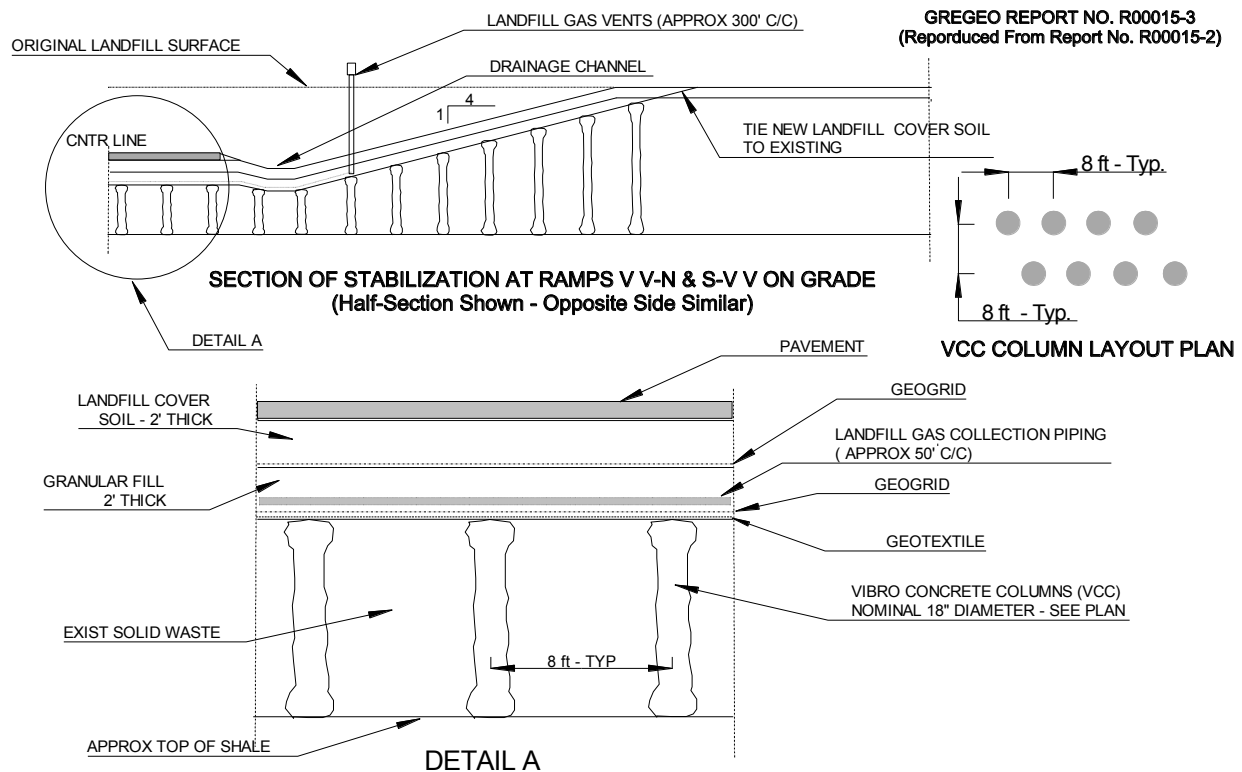


Figure 4 – VCC Details

The VCC were specified to extend to the underlying shale as shown in Figure 4. Since solid waste was to remain beneath the roadway, a landfill gas collection and venting system was specified.

DWU Sites and Carrollton Landfill

Field Exploration

The DWU Sites and Carrollton Landfill were explored by approximately 66 geotechnical borings drilled by the prime geotechnical consultant. The author and/or his representative were present during a majority of the drilling activities. Selected photographs of the area prior to stabilization, and of the field exploration activities in the DWU Solid Waste Area are presented in Figures 5 and 6.



Figure 5 – Typical Areas Prior to Stabilization



Figure 6 – Typical Field Exploration and Solid Waste Encountered

DWU Lagoon No. 1

A schematic plan view of the lagoon area is presented in Figure 7. The plan view shows the various options and applicable locations of the options considered for stabilization. The stabilization options are discussed in subsequent sections.

Sludge Description and Strength Parameters

The DWU Lagoon No. 1 contained about 12 feet of backwash sludge as previously discussed. Based upon field vane shear tests and unconsolidated undrained (UU) triaxial tests performed in the laboratory on recovered thin-walled tube samples, the sludge had an undrained shear strength ranging from about 200 pounds per square foot (psf) to about 800 psf, which is considered soft to very soft. The material also had high compressibility based upon CRS consolidation tests performed in the laboratory. Moisture content of the sludge averaged approximately 50 percent.

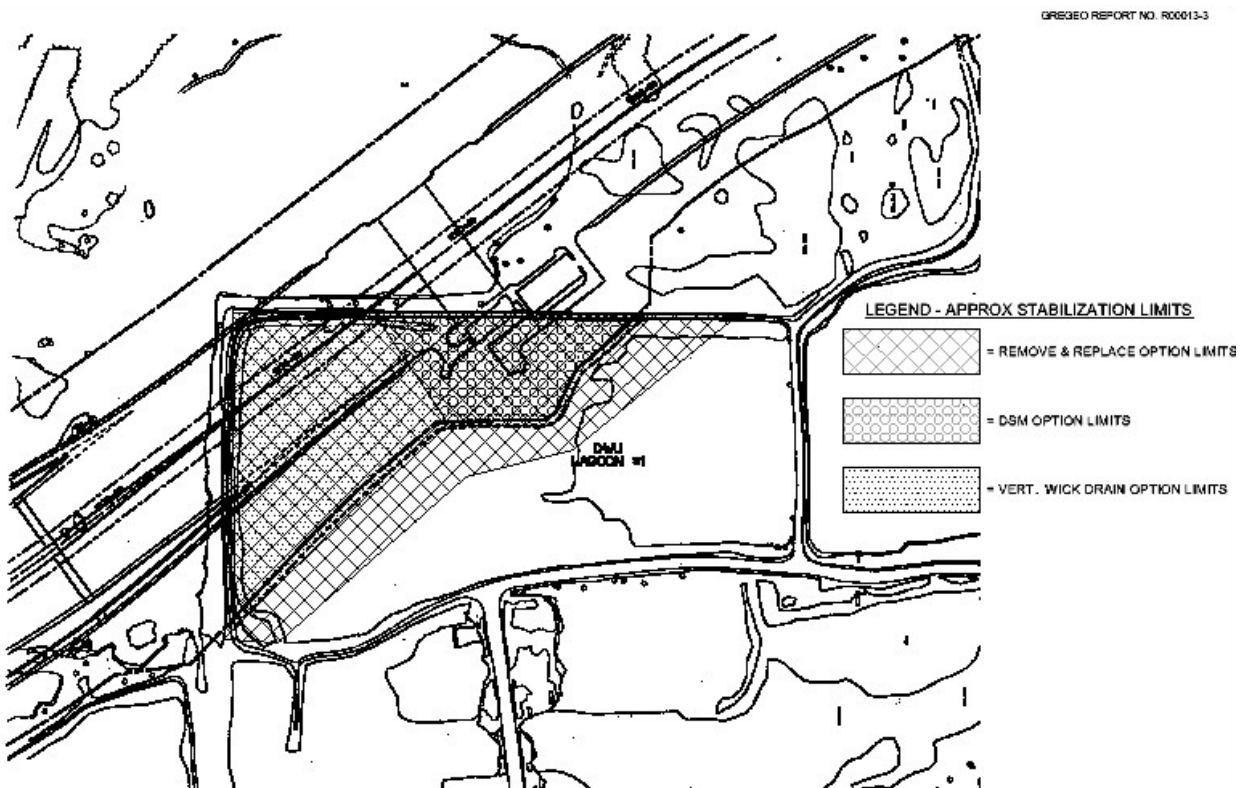


Figure 7 – DWU Lagoon –Stabilization Option Areas

Stabilization Options Considered

The options considered for stabilization of the lagoon area included remove and replace, vertical wick drains and staged embankment construction, and deep soil mixing (DSM). The remove and replace option would have resulted in approximately 200,000 cubic yards of sludge to be removed and disposed in a permitted landfill. Although the sludge is essentially inert, it was classified as a solid waste by the regulatory agencies and could only be disposed in a permitted solid waste landfill. The estimated cost of the remove and replace option was approximately \$6.1 million.

The most cost effective method of stabilization considered technically viable was the vertical wick drains and staged embankment construction. However, a significant portion of one of the main toll plazas was scheduled to be constructed in the lagoon area. The toll plaza was a time sensitive item that was on the critical path from a schedule standpoint. The estimated time to achieve the target settlement with the wick drain option was approximately 6 months. This time frame could not be accommodated for the toll plaza. However, the DSM option would allow construction to begin on the toll plaza approximately two to three weeks after completion of the DSM. Accordingly, the decision was made to stabilize the toll plaza area with DSM columns and the remainder of the lagoon area with vertical wick drains and staged embankment construction. The DSM and vertical wick drain areas are shown in Figure 7. The remove and

replace area that would have been necessary is also shown in Figure 7, but that option was not used.

DSM Column Option Details

The DSM column option consists of forming a series of columns in the soft soil (sludge) with a special pier drilling rig. The pier drilling rig is equipped with a large mixing auger with a hollow stem that will accommodate pumping cement slurry into the subsurface as the auger penetrates. The special auger mixes the unstable soil with cement slurry and forms in-situ soil cement columns. The columns are placed on a staggered (triangular) grid pattern and a geogrid is typically used to help distribute the embankment loads between columns. The DSM columns take on a larger percentage of the embankment load than the surrounding untreated soil due to the greater stiffness of the columns. The percentage of the load taken by the columns is related to the modulus ratio between columns and soil and the area replacement ratio. Maximum target settlement for the lagoon area was 2.5 inches following construction. The loads on the interstitial soil had to be reduced below 800 psf in order to not exceed this value. A practical modulus ratio value was determined to be 6:1 based upon laboratory pilot testing of untreated and cement stabilized sludge. This meant that the DSM columns would carry about 83 percent of the embankment load and the interstitial soil about 17 percent. This modulus value and a replacement ratio of slightly above 0.5 resulted in a calculated soil stress of about 782 psf. The schematic details of the DSM columns are presented in Figure 8.

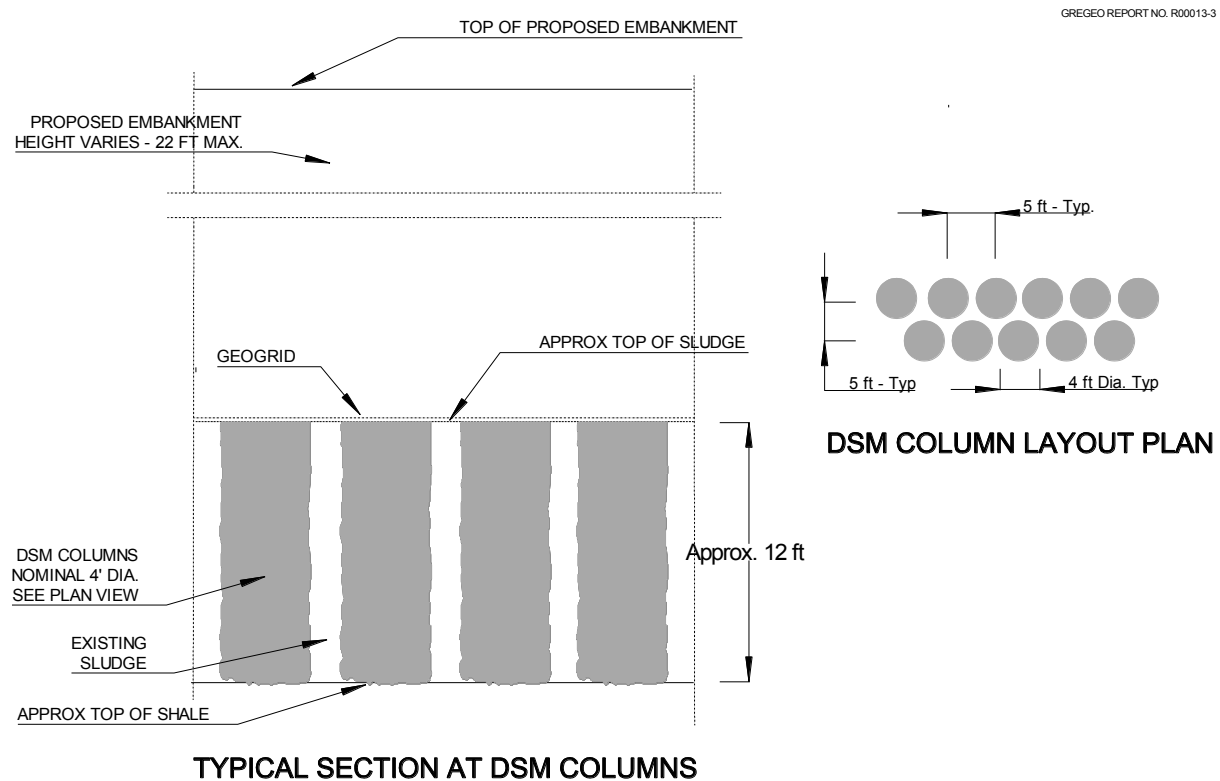


Figure 8 – DSM Column Details

The required column diameter and spacing were 4-feet and 5-feet, respectively. The estimated cost of the DSM columns in the toll plaza area was about \$1.7 million.

Vertical Wick Drain Option Details

Consolidation analyses in the wick drain area resulted in predicted settlements ranging from about 11 inches to 22 inches. The lower value of 11 inches was based upon using a preconsolidation pressure value of about 1.5 tsf indicated by the CRS consolidation tests. However, there had been no known preloading history for the sludge area. It was believed that the preconsolidation value may have been induced by slight cementing action due to the lime content of the sludge. Without considering the preconsolidation pressure, the predicted total settlement was 22 inches. This larger value was used in the analysis to determine the wick drain spacing required to reduce the remaining settlement to approximately 2.5 inches, the target value. The required wick drain spacing was determined using a radial drain analysis. The required spacing to reduce the remaining settlement to 2.5 inches within 6 months after embankment construction was determined to be four feet. The details of the vertical wick drain system are shown in Figure 9.

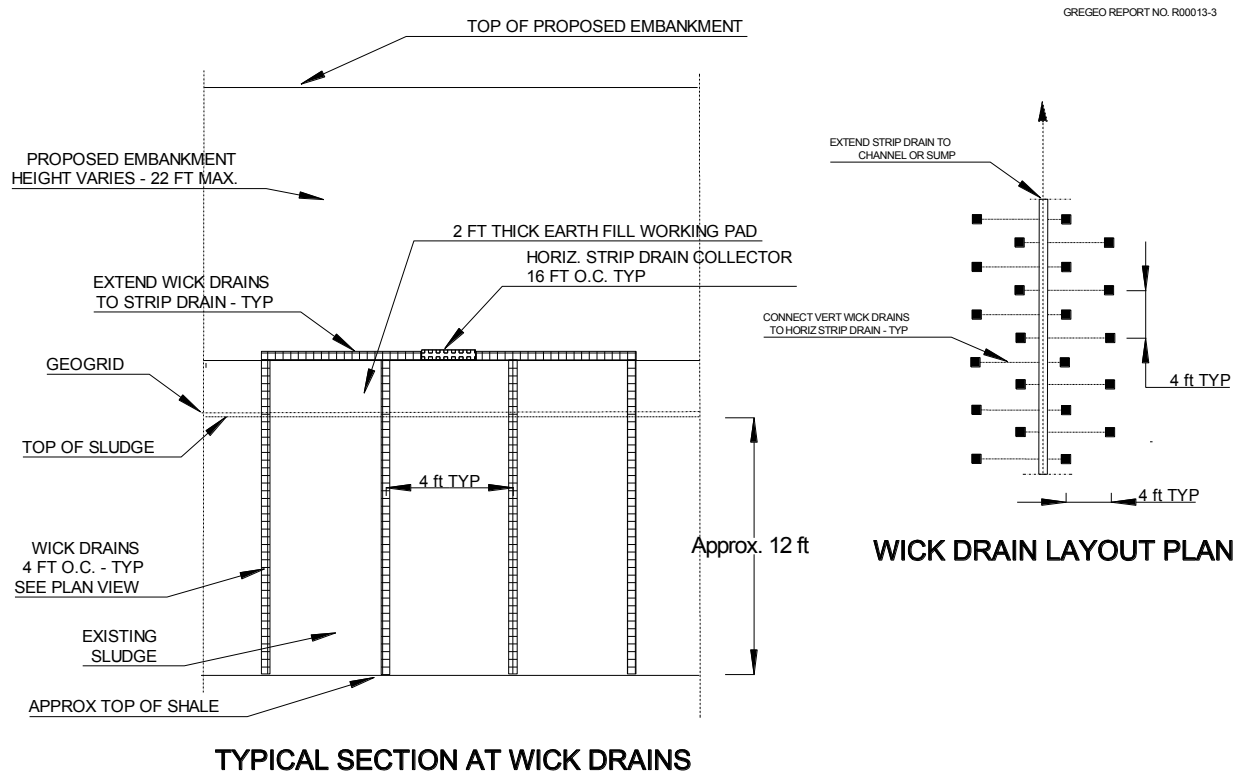


Figure 9 – Vertical Wick Drain Details

Due to the high cost of importing clean sand or aggregate for the horizontal drainage blanket, a system of strip drains was designed for the horizontal drainage system to collect and dispose of the water evacuated from the consolidating soil through the vertical wick drains. The horizontal strip drain system is also shown schematically in Figure 9.

Slope stability analyses were performed to evaluate whether the embankment could be constructed continuously over the wick drain area or if dormant periods would be required for dissipation of pore pressures within the sludge to prevent a slope failure involving the sludge during embankment construction. It was determined from the slope stability analyses that continuous embankment construction could be tolerated as long as the maximum rate of uniform fill placement was regulated to achieve the finished embankment height in no less than two months after beginning embankment fill.

The estimated cost of the vertical wick drain system in Lagoon No. 1 outside the toll plaza area was approximately \$893,000.

DWU Solid Waste Area

A schematic plan view of the DWU Solid Waste Area is presented in Figure 10. The plan view shows the approximate limits of the required stabilization area which consists of about 460,000 square feet. The stabilization options are discussed in subsequent sections.

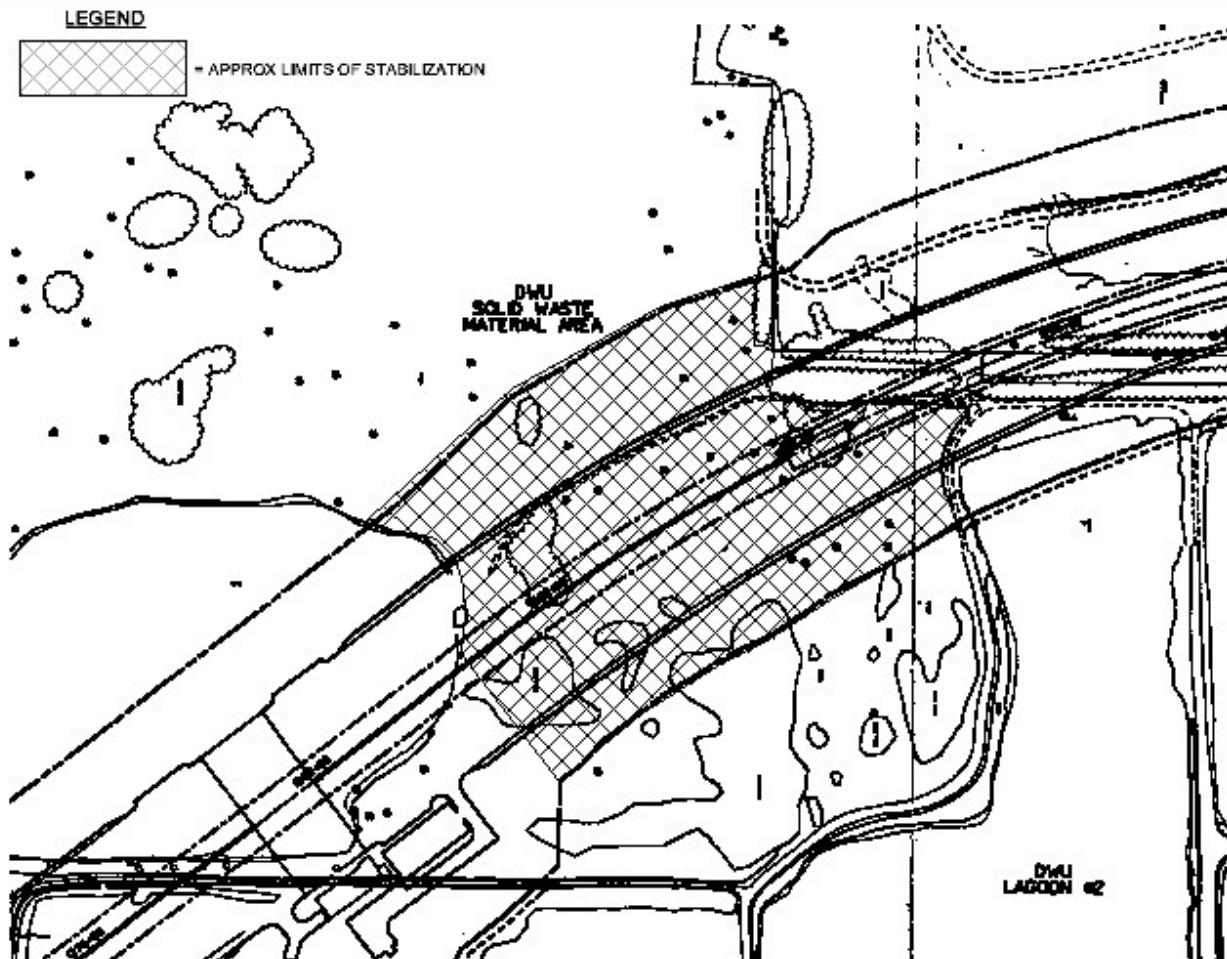


Figure 10 – DWU Solid Waste Area

Stabilization Options Considered

The DWU Solid Waste Area required consideration of two settlement mechanisms under the proposed embankment loading. Those settlement mechanisms are initial primary settlement during and for a relatively short time following construction, and decomposition settlement which would likely occur over many years as the solid waste continued to decompose. The options considered for stabilization of the DWU Solid Waste Area included the remove and replace option and deep dynamic compaction (DDC) followed by lime-fly ash injection. These options are discussed below.

Remove and Replace Option

The option to remove all the solid waste and replace with imported select fill would have resulted in the environmental impacts of removing over 200,000 cubic yards of solid waste and hauling it over public roadways to an acceptable disposal facility. Also, the cost of the remove and replace option was estimated to be approximately \$8.4 million.

DDC followed by Injection

DDC in solid waste areas is typically achieved by first constructing a crushed stone working pad, following by DDC with a large weight dropped on a grid pattern from a considerable height with a special crane. The drops are repeated until the desired optimum densification and pre-settlement are achieved. The dropping weight compacts the crushed stone working pad into the solid waste and improves stability. This is referred to as primary densification. Primary densification is typically followed by what is referred to as an “ironing” pass or passes. This consists of dropping a lighter weight, but with a larger footprint in an overlapping manner to flatten and smooth the rough surface left by the primary densification passes. Since some ground water was encountered in the DWU Solid Waste Area during site exploration, it would be necessary to install vertical “pressure relief wells” to help relieve pore water and pore air pressure during DDC to prevent high pore pressure build up from significantly reducing the beneficial effects of the DDC. This is accomplished by installing vertical stone columns which penetrate through the waste and tie into the crushed stone working pad. In DDC applications the stone column relief wells are typically constructed by repeatedly dropping a “pencil” weight to form the column hole, followed by backfilling the hole with crushed stone. The pencil weight is on the order of 10 to 12 feet in length and approximately the diameter of the proposed relief well. The relief well spacing was 50 feet on center on a triangular grid pattern. DDC typically reduces the primary settlement to a relatively small value by lowering (compacting) the solid waste surface by several feet.

As previously stated, the other settlement mechanism in solid waste is decomposition settlement. This can be significantly reduced by injecting the solid waste with lime-fly ash slurry following the DDC operation. The lime-fly ash slurry encapsulates the waste and raises the average pH, both of which significantly reduce decomposition. Also, the cementitious characteristic of the fly ash slurry tends to form a “skeleton” of stiffer material around the waste and provide additional support.

The estimated cost of the DDC and Lime-Fly Ash injection option was estimated to be approximately \$3.2 million. The much lower cost and less environmental impacts of this option compared to the remove and replace option resulted in the DDC and injection option being selected. Analysis of the combined DDC and injection option indicated that long term settlement in the DWU Solid Waste Area following embankment construction could be reduced to approximately 3 to 3.5 inches or less, which was determined to be acceptable by the design team.

Carrollton Landfill Rubble Fill Area

A schematic plan view of the Carrollton Landfill Rubble Fill Area is presented in Figure 11. The plan view shows the limits of the required stabilization area which was approximately 1,200,000 square feet. The stabilization options are discussed in subsequent sections.

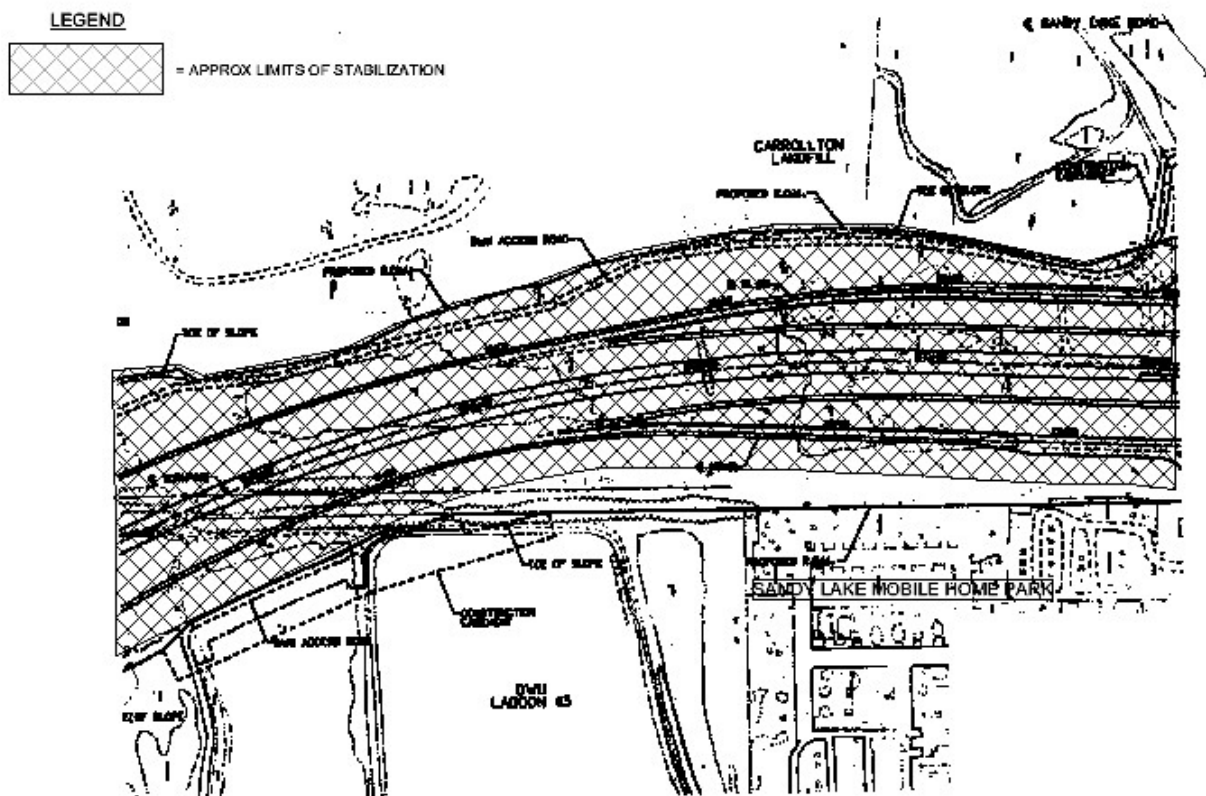


Figure 11 – Carrollton Landfill Rubble Fill Area

Stabilization Options Considered

The rubble fill area contained essentially inert materials such as concrete, masonry, and asphalt rubble as previously discussed. However, the primary concerns were that the overlying soil could migrate into the relatively large void areas in the rubble fill and/or the rubble fill could shift into a more dense condition due to the embankment fill loading, with resulting significant settlement following construction. The stabilization options considered for the rubble fill area included DDC, compaction grouting, double geogrid reinforcement, and combinations of these

methods. Due to the large depths of the rubble fill (up to 40 feet) the remove and replace option was not considered for this area.

DDC Stabilization Option

The DDC option was considered ideal for the rubble fill area because this technique had been used successfully numerous times under similar conditions. It was anticipated that the DDC would be effective in reducing the void ratio in the rubble and overlying soil to the point that tolerable settlements would result following construction. Since the rubble was essentially inert, injection with lime-fly ash would not be required, and a crushed stone working pad would also not be required. Post construction settlement in the rubble fill area was estimated to be in the range of 2 to 3 inches with the DDC option. This option also included one layer of geogrid placed on the subgrade prior to embankment construction to help reduce spot differential settlement.

Although the DDC option was a viable and attractive option, it was determined that DDC in the northern part of the area adjacent to the large existing mobile home park (see Figure 11) would cause a high level of disturbance to the residents. The DDC operation produces shock waves similar to a mild earthquake or blasting operations. Although no actual physical damage was anticipated, calculations for the area north of station 1303+00 indicated a scaled energy factor that classifies as “very disturbing” to humans within a distance equal to that of the mobile home park if DDC operations were conducted north of station 1303+00. Concerns with the potential for litigation from residents shutting down the project resulted in the decision not to use DDC in the northern area of the rubble fill.

The estimated cost of the DDC option south of station 1303+00, which is about 46 percent of the total rubble fill area, was approximately \$1 million. The southern area consisted of about 553,000 square feet. The DDC option was selected for the rubble fill area south of station 1303+00.

Double Geogrid and Localized Compaction Grouting Stabilization Option

The large remaining area of rubble fill north of station 1303+00 (about 648,000 square feet) could have been stabilized with compaction grouting which would have reduced the estimated post construction settlement to about 2 to 2.5 inches. However, the use of compaction grouting over the entire area would be very cost prohibitive, although less than the remove and replace option. An alternative option was to use two layers of geogrid over the northern area with one layer being placed on the subgrade and the other layer being placed about 3 feet above the subgrade in the embankment fill. The double geogrid layer would not significantly reduce the total settlement, but was expected to substantially reduce the spot differential settlement. The total settlement anticipated for the double geogrid area was approximately 3 to 5 inches, with perhaps more in spot areas. This was considered marginally acceptable for the roadway embankments by the design team. However, this magnitude of settlement was not acceptable for the MSE wall areas discussed in the next paragraph.

The ramp areas in the northern part of the site that were to exit to Sandy Lake Road required construction of MSE walls up to about 26 feet in height. Since the MSE walls could not tolerate the settlement predicted for the double geogrid option, compaction grouting in an 80-foot wide strip along the alignment of the MSE walls was selected for stabilization of the rubble fill areas at the wall locations. The predicted settlement of 2 to 2.5 inches with the compaction grouting option in the MSE wall areas was considered acceptable. The required area of the compaction grouting was approximately 201,000 square feet and the estimated cost was about \$1.4 million. The area of the double geogrid option was approximately 648,000 square feet, requiring about 144,000 square yards of biaxial geogrid. The estimated cost of the double geogrid option was approximately \$540,000. The double geogrid and localized compaction grouting option was selected for the rubble fill area north of station 1303+00.

Steep Embankment Slope Area Adjacent to Carrollton Landfill

As previously discussed in the introduction section, a portion of the roadway alignment was scheduled to pass close to the municipal solid waste area of the Carrollton Landfill. If the standard slope ratio of 4 (4H:1V) was used in this area, the side slope area would encroach onto the existing municipal solid waste resulting in large settlements unless extensive stabilization measures were taken. Consequently, a decision was made to construct the slope at a ratio of 2 with multi-layer uniaxial geogrid reinforcement to provide an adequate factor of safety against sliding failures of the slope. This area consisted of a length along the alignment of about 750 feet. Six or seven layers of geogrid were used to reinforce the embankment depending on the actual vertical height which varied over the 750-foot length. Fiber reinforced soil (FRS) was used as secondary reinforcement between the primary geogrid layers in the upper 6 feet of the embankment slopes. FRS consists of nominal 2 to 3-inch long polypropylene fibers that are mixed into the soil as the fill is placed and which significantly increase the shear strength of the soil (3, 4, and 5).

Shallow Slope Reinforcement for Embankment Slopes

The only available soil for constructing the general embankments was high plasticity clay classified as Fat Clay (CH) in accordance with ASTM D 2487. Extensive experience in the general geographic area of the project has shown that slopes constructed of these clay soils with vertical heights of about 15 feet or greater and side slope ratios of 4 or steeper will experience significant shallow slope failures over time. These slope failures are typically in the range of 4 to 6 feet in depth along the exposed slopes. Although the shallow failures generally do not initially impact the integrity of the roadway pavements and shoulders, if not repaired in a timely manner they will continue in a progressive failure mode and along with induced erosion will soon be causing damage to actual guardrails, shoulders, and pavements. The shallow slope failures are a nightmare from a maintenance and repair standpoint. Accordingly, a decision was made to reinforce a veneer area of 6 feet in thickness parallel to the slope faces on all embankment slopes of 15.5 feet or greater in vertical height.

GEOTECHNICAL INSTRUMENTATION

Due to the relatively large settlement magnitudes anticipated to take place as a result of embankment construction, a program of geotechnical instrumentation was designed and implemented to monitor settlement and lateral embankment movements during construction as a means to determine that target levels of remaining settlement had been reached prior to construction of actual pavements and similar facilities sensitive to movement. The geotechnical instrumentation was designed, installed, and monitored by the author's firm.

Description of Instrumentation

The instrumentation consisted of vibrating wire piezometers (VW Piezos), liquid filled vibrating wire settlement cells (S-Cells), and slope inclinometers totaling 146 instruments in all. The VW-Piezos were installed in subgrade areas beneath the proposed embankments to monitor increase and dissipation of pore pressure during and following embankment construction to help in estimating the percent of settlement that had taken place at any point in time. The S-Cells were installed beneath the embankments to monitor actual settlement with time. The inclinometers were installed in the side slopes of selected embankments to monitor lateral movements of the embankments due to settlement of the foundation soils.

Instrumentation Locations

The geotechnical instrumentation was installed in selected locations throughout the problematic soils areas previously described, except in the Farmers Branch Closed Landfill area. The Framers Branch Closed Landfill area involved a cut into the solid waste rather than fill and since vibro concrete columns were used to support the roadway, settlement monitoring was not required.

In addition to the problematic soils areas described previously, the instrumentation was also installed in an area of the project where a large depth (up to 50 feet) of soft clay soil was present beneath the proposed turnpike embankments in the area between stations 1162+80 and 1185+90. This area was designed by others and was not included in the description of problematic soil area stabilization design performed by the author's firm. This area however was included in the scope of geotechnical instrumentation performed by the author's firm and is included in this section on instrumentation. Selected photographs of the instrumentation installation and monitoring activities are provided in Figures 12 through 14. The geotechnical instrumentation monitoring showed vertical settlement magnitudes and rates, and lateral embankment movements all within the predicted limits during construction. The settlement magnitude in Lagoon No. 1 leveled off at approximately 11 inches. This indicated that the preconsolidation pressures indicated by the CRS consolidation tests were accurate, and were likely due to slight cementing action from the lime content of the sludge as previously discussed. Instruments in a small area within the DWU Solid Waste Area showed continued downward trends which if continued would have resulted in significantly larger settlement in that area than had been predicted. The downward curve was much steeper than in other areas. However, just prior to reaching the range of predicted settlement, the readings leveled off abruptly and the total settlement was within the predictions.



Figure 12 – Instrument Installation



Figure 13 – VW Piezos (left) and S-Cells (right) During Instrumentation Installation



Figure 14 – Instrument Terminal Station (left) and Monitoring of Instruments (right)

CONSTRUCTION ACTIVITIES

Construction Schedule and Photos

Construction of Segment IV began in January 2003 and was substantially completed in October 2005. Selected photographs of subsurface stabilization in the problematic soils areas during construction are included in Figures 15 through 21.



Figure 15 – Vibro Concrete Column Construction



Figure 16 – Vertical Wick Drain Construction



Figure 17 – Deep Soil Mixing – Soil Cement Columns



Figure 18 – Deep Dynamic Compaction (Ironing Pass on right)



Figure 19 – Lime-Fly Ash Injection (DDC in background on left)



Figure 20 – Compaction Grouting



Figure 21 – Biaxial Geogrid (left) and Fiber Reinforced Soil (right)

CONCLUSION

Innovative subsurface stabilization techniques in the problematic soils areas resulted in an economical stabilization program that had predicted settlements larger than the remove and replace option in most locations but that were within tolerable limits for roadway embankment construction and that saved many millions of dollars in construction cost and time. Geotechnical instrumentation installed and monitored during construction verified total settlement magnitudes and rates and indicated when target residual settlement levels had been reached so construction of movement sensitive items such as pavements could proceed in a timely manner. At the writing of this paper the project has been completed for approximately 5 years (with embankment construction completed for approximately 6 years). The project has performed as expected to date and settlement magnitudes have been within or less than predicted. No shallow slope failures or failures in the steep slope areas have been noted. Maintenance related to settlement has been less than anticipated.

REFERENCES

1. Elias, V., Lukas, R., Warren, J., and Welsh, J. *Ground Improvement Technical Summaries*, Publication No. FHWA-SA-98-086, Volumes I and II, FHWA, U.S. Department of Transportation, 1999.
2. Sowers, G. F., Settlement of Waste Disposal Fills. *Proc., 8th International Conference on Soil Mechanics and Foundation Engineering*, Moscow, USSR, 1973, pp. 207-210.
3. Gregory, G. H. and D. Chill. Stabilization of Earth Slopes with Fiber Reinforcement. *Proc., 6th International Conference on Geosynthetics*, Atlanta, Georgia, USA, March 1998.
4. Gregory, G. H. Theoretical Shear Strength Model of Fiber-Soil Composite. *Proc., ASCE Texas Section Spring Meeting*, Longview, Texas, USA, April 1999.
5. Gregory, G. H. Fiber-Reinforced Soil – A Key Role in Geosynthetics Applications for the 21st Century. *Proc., 13th GRI Conference on Geosynthetics*, Folsom, PA, USA, December 1999.

Safe and Sound – Design Build Program to Replace 554 Bridges in Missouri

John F. Szturo R.G.

Senior Geologist,
HNTB Corporation
715 Kirk Drive
Kansas City, MO 64105
Ph 816.527.2275
jszturo@hntb.com

Prepared for the 61st Highway Geology Symposium, August, 2010

Disclaimer

Statements and views presented in this paper are strictly those of the author(s), and do not necessarily reflect positions held by their affiliations, the Highway Geology Symposium (HGS), or others acknowledged above. The mention of trade names for commercial products does not imply the approval or endorsement by HGS.

Copyright Notice

Copyright © 2010 Highway Geology Symposium (HGS)

All Rights Reserved. Printed in the United States of America. No part of this publication may be reproduced or copied in any form or by any means – graphic, electronic, or mechanical, including photocopying, taping, or information storage and retrieval systems – without prior written permission of the HGS. This excludes the original author(s).

ABSTRACT

The Missouri Department of Transportation plans to replace 802 of Missouri's most worn out bridges in five years. The 802 bridges are divided into two groups. 248 have been identified for rehabilitation by multiple design bid build processes and 554 will be completely replaced by a single design build contract. The Missouri Highways and Transportation Commission selected KTU Constructors to replace 554 bridges in a single design-build contract.

Some key provisions of KTU's proposal: Quoted price of \$487 million. Committed to finish by Dec. 31, 2013 – 10 months earlier than required. Average bridge closure for 493 bridges will be 45 days – nearly half of what a normal MoDOT bridge project would take. MoDOT has the ability to move 120 bridges within KTU's proposed construction schedule to respond to local events and issues. Overall, the schedule will demand one bridge be turned over every two and a half days during the project duration.

The schedule will necessitate completing the subsurface investigations and foundation recommendations for all 554 bridges within the first 18 months of the project, or about two every three days.

Many creative ideas were used in the development of foundation types and costs for the winning proposal for all 554 bridges. Many more will have to be deployed to successfully deliver the project on time.

INTRODUCTION

Project background

In the spring of 2007, Missouri had 10,240 structures on state inventory, 1,613 were structurally deficient and 1,223 were functionally obsolete for a total of 2,836 deficient bridges (25 percent of bridges overall).

To reduce the inventory of deficient bridges to the point where the projected bridge construction funding levels could address the remaining deficient bridges and keep up with the number of newly deficient bridges, MoDOT initiated the Safe & Sound Bridge Improvement Program to replace or rehabilitate 802 of the worst bridges in the state.

The bridges were selected based upon the following criteria:

- No major river bridges (bridges on the Missouri or Mississippi River)
- No bridge greater than 1000' in length
- Bridges on minor routes with a National Bridge Inventory (NBI) rating of 3
- Bridges on major routes with a NBIS rating of 4 or less
- No bridges that required significant roadway work or additional right of way

In September 2008, MoDOT took 248 bridges grouped them by location, type of work, and schedule and let them in small packages using a normal bid processes. This project was called the Modified-Design-Bid-Build (MDBB) program. The design work would be completed with MoDOT in-house resources or by a consultant.

The remaining 554 bridges were grouped into one Design Build project. These bridges were all scoped as complete bridge replacements. The key components of the Design Build project are:

- No private financing or maintenance component
- Contractor will be paid for work as it is completed
- MoDOT does all construction inspection
- MoDOT coordinates utility relocations and ROW acquisition
- MoDOT coordinates traffic control for bridge closures
- MoDOT takes the lead for all Public Information

The goals for this project are:

- Deliver good bridges at a great value
- Minimize public inconvenience through increased construction speed and flexibility in schedule
- Complete construction no later than December 31, 2013

Quality design standards were maintained by requiring the contractor to use current MoDOT bridge design standards or submit Alternate Applicable Standards (AAS) for approval prior to bid submittal.

Two teams submitted responsive bids. In May of 2009, MoDOT awarded the Design Build contract to KTU Constructors. By late November, 2009, the first design build bridge was completed.

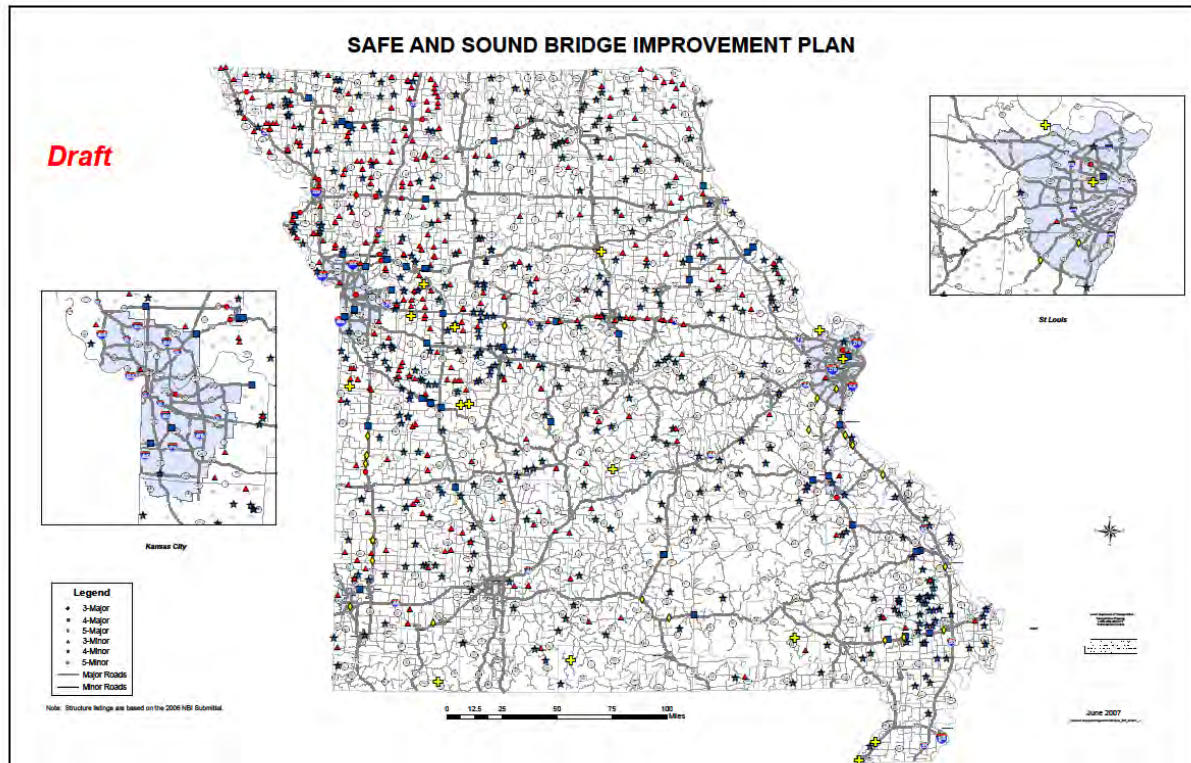


Figure 1 – Safe and Sound Bridge Locations

General

KTU Constructors (a joint venture of Kiewit, Traylor Brothers and United Constructors) (HNTB Corp and LPA Group providing design services) has been selected for the challenging task of replacing 554 primarily small, two-lane rural bridges within a short construction span of three years.

Design and construction of each bridge is a rather simple task, however the complexity results in the logistics of designing and constructing 554 scattered bridge sites in ten different MoDOT districts with distinct hydraulic, geotechnical and environmental characteristics. Logistics and standardization will become the backbone of the value of the project.

Nearly all bridges cross small to medium waterways with relatively few to be constructed over railroads or other road. An average of 45 days is allotted for constructing the bridges including demolition and disposal of existing bridge components. In order to achieve these aggressive targets, a well-conceived construction process is necessary. A strategic construction sequence was key to prioritizing bridges in such a way that otherwise deteriorated, load-posted bridges would not have been available for utilization during construction. With respect to the design approach, several superstructure and substructure scenarios are evaluated upfront based on

preliminary assumptions made during the procurement process. These scenarios are grouped in categories that dictate a number of design analyses to be performed. These “standardization” measures significantly reduce the design, fabrication and construction efforts.

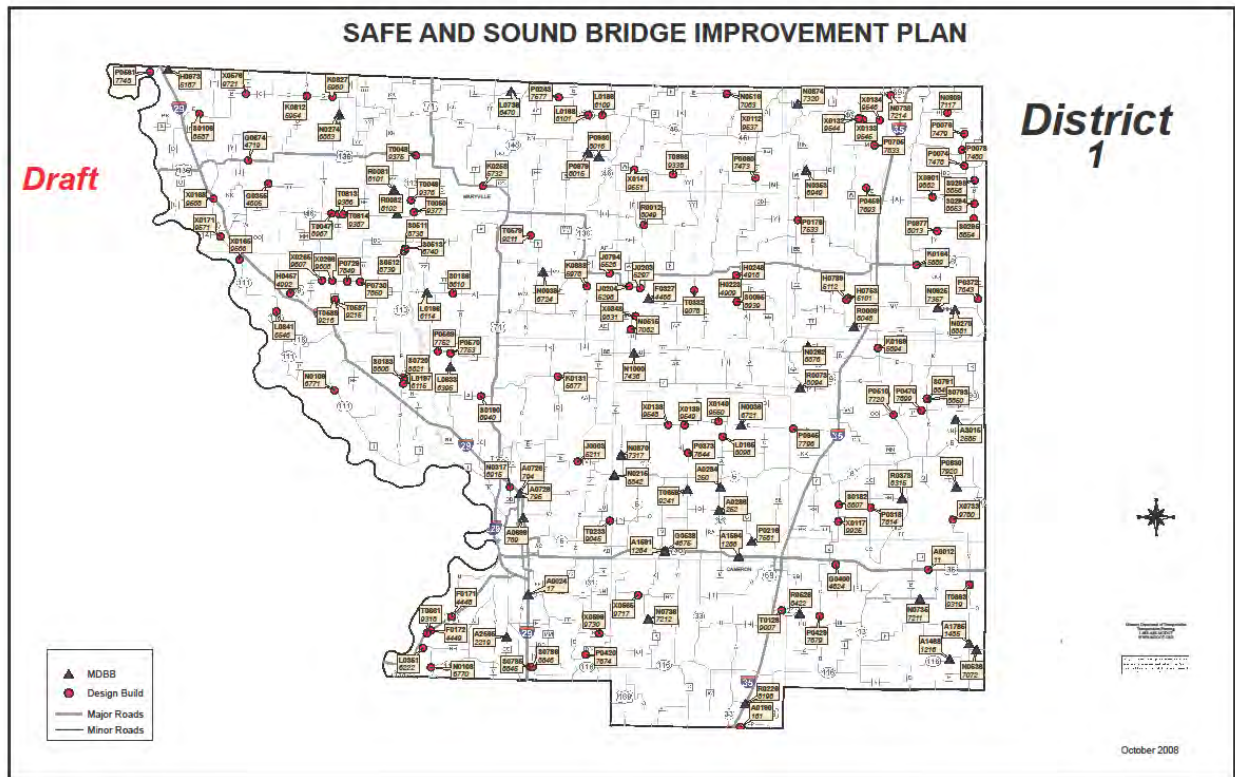


Figure 2 – Typical Bridge Locations by MoDOT District

This innovative, accelerated design and construction approach includes early evaluation of all 554 bridges and standardized spans, widths, and skews that help finalize the superstructure cross-sections. This process enabled the design team to minimize the number of superstructure and substructure design analyses through standardization process. The additional resources were evaluated by reaching out to other state DOT standards and their practices that help simplify and adopt details that accelerate design and construction process. The major focus was to deploy concrete pre-cast components for superstructure and pile bents for substructure design to minimize construction duration. To enhance the plan development process, standard plan sheets were created that are utilized for multiple bridges; these sheets are developed, QA/QC'ed once, then used multiple times.

Activities during pre-award Phase

During procurement, KTU sent inspection teams of construction and design personnel to all 554 sites to study field conditions, access for construction, bridge size, height above approach fill and the channel. The field data was stored in a database, along with MoDOT required bridge widths, ADT and other constraints.

During the engineering/design phase of procurement, four major disciplines of bridge, roadway, geotechnical and hydraulics performed pre-design activities to determine a best approach to constructing project bridges.

For bridges, the Geotechnical focus was to develop pile lengths with limited geotechnical data and work towards a matrix of foundation types by bridge arrangements.

For speed, ease of constructability, and risk management, driven pile was the foundation of choice. Spread footings and drilled shafts were deemed to pose undue risk and reduce the standardization factor. Each would have to be individually designed as to size and elevation. Reinforcing steel and concrete would also have to be ordered and designed for each column, further complicating logistics.

Nearly every one of the existing 554 bridges had some form of as built plans. Most of the bridges in the program were constructed during the period 1920 – 1940. Many utilized timber construction. Additionally, many of the bridges have been repaired and modified multiple times.

The existing bridges were founded on two primary foundation systems. Spread footings in areas where bedrock was shallow (less than 25') and timber piling. The timber piles were commonly short and of 10 to 20 tons capacity. Most of the plans had piling lengths and capacities but no boring or subsurface information. Top of bedrock elevation was unknown in most cases.

The geotechnical task force reviewed each bridge and plan set for existing foundations and boring information during the pre award phase. Since higher capacity steel H or Pipe piles were now desired, a method of back calculating new pile lengths from timber pile lengths and capacities was developed.

One of the approaches developed by the team was to use the information from existing timber piles, driving records, and back-compute a frictional component. This would be utilized to develop the pile lengths for the proposed steel piles, allowing the team to have more confidence in the pile lengths to be bid, thus reducing the risk within the bid.

In the end, pricing parameters for type and length of pile for each bridge was developed with little to no new subsurface information.

Taking the ideas/concepts from the disciplines along with the required site needs, the project team of designers and builders sat down and reviewed all 554 project bridges. During the review, a span arrangement, proposed foundations and potential road work was developed for all project bridge sites. This became the basis of the estimate phase. In addition to the project bridges, the preliminary maintenance of traffic (MOT) schemes were developed and used in the bid estimate.

Design

All design had to run in a sequence and schedule to maximize efficiency and meet project schedule. 554 Bridges were to be design in the span of 18 months, 390 working days, or about 7 bridges per week.

A complex work chart was developed between the disciplines of geotechnical, hydraulics, roadway, and bridge design. Each bridge demanded a strict order and time for each task. One missed task could put an entire bridge design off sequence and disrupt the schedule.

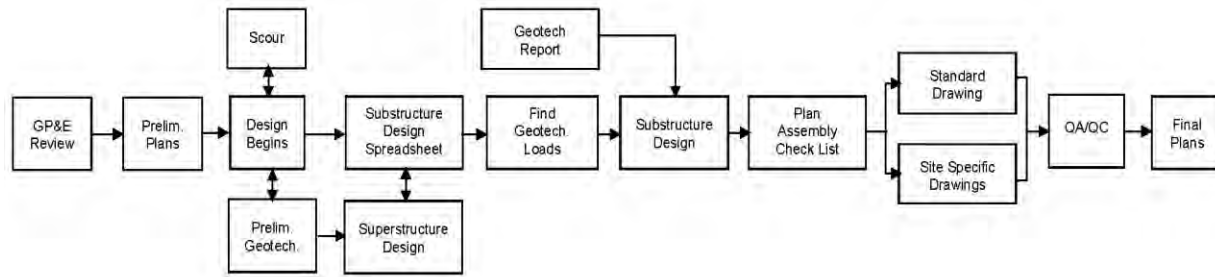


Figure 3 – Design Process

The Geotechnical Assembly Line

The key to success in meeting project schedule was standardization, strict schedule and up to the minute tracking. The initial period of the project was devoted to developing geotechnical engineering standards. The standards included

- Overall subsurface exploration approach and cost estimate
- Sequence, and protocol for data transfer and filing
- Proposed boring location plans
- Drilling, sampling, testing requests
- Boring log templates
- Laboratory data
- Grain size data for scour
- Rock core photographs
- Report templates
 - End bearing piles
 - Friction piles
 - Spread footings
 - Drilled shafts
- Plan production
 - Produce boring sheets for the plans
 - Interdisciplinary review of plans
- Quality control – quality assurance

The Assembly Line

1. **Screening** - At each bridge site, perform an initial geotechnical screening, organize and sort all existing data. Sort data from existing plans, as built data, rehabilitation plans, inspection reports, construction reports and available boring logs.

Screening Factors – Geology, type of crossing, seismic classification, expected foundation type, geologic hazards, and existing boring data

Result – Sort each bridge into groups by expected geologic condition, proposed foundation type and determine if existing information can be used to develop final design geotechnical recommendations. All bridges will utilize new foundations – no reuse or rehab of existing.

Individual teams were formed to work specific groups or types of expected bridge foundations. One group concentrated on end bearing piles, another on friction piles, another on special needs such as drilled shafts, spread footings or bridge and embankment slopes. Another group focused on performing checking, quality control and quality assurance. Nearly daily meetings were held to coordinate within the geotechnical team as well as between design disciplines.

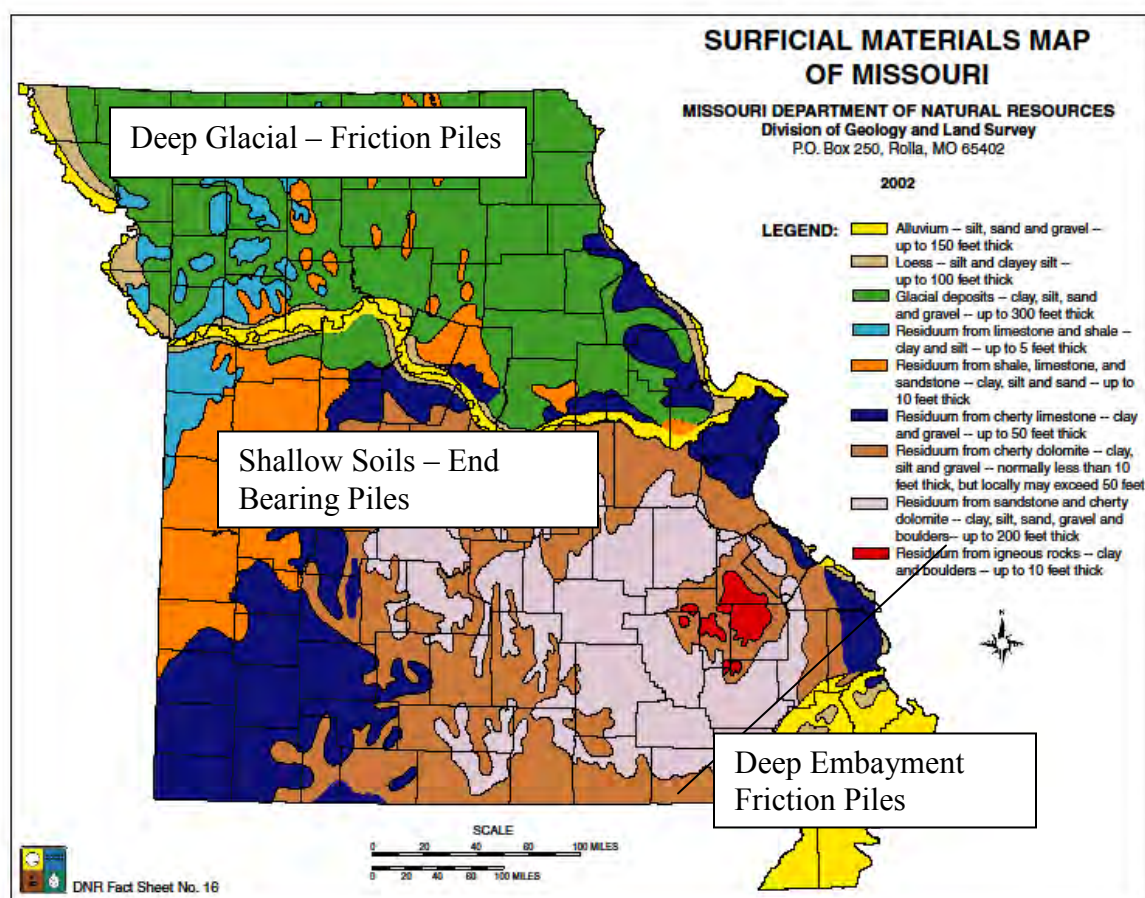


Figure 4 – General Foundation Types

2. **Develop bridge sounding request** - Use scoped bridge type, size, location and foundation type to develop sounding request. Assemble all pertinent documents into a pre design boring package (old bridge plans, maps, photographs). Prepare the boring location plan, sampling requirements, with instructions to drillers. Issue orders and track progress.

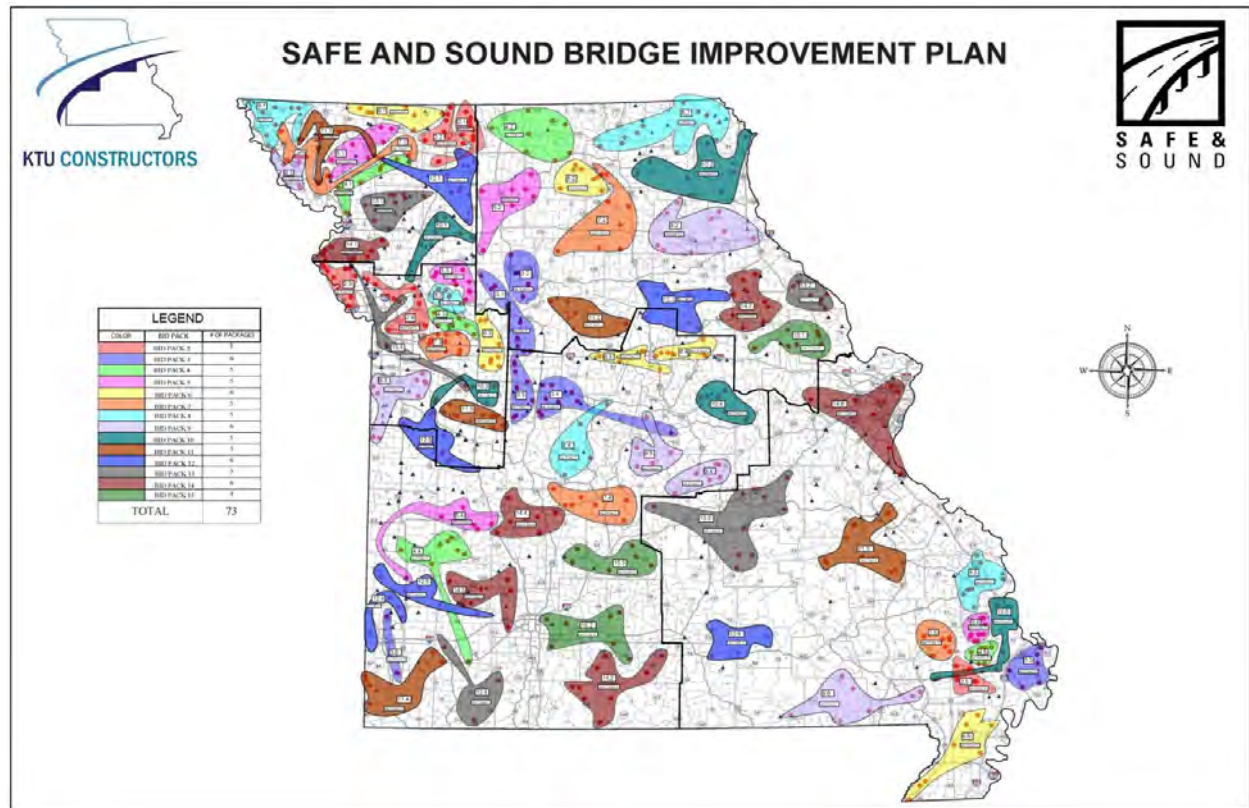
- General parameters - For locations where borings are needed, develop a boring program:
 - Assume 1 boring per bridge bent as per AASHTO
 - Number of borings, depths, types of sampling, and testing. Standardize by foundation type and other factors as much as possible.
 - Consider access to drill locations, traffic control, utility locations, year/sequence of construction, etc.
- 3. **Perform drilling, sampling, testing** - Managed by the builder. KTU contracted, purchased and managed the drilling, sampling and testing. Work was performed by subcontract drillers. Primarily two geotechnical firms used up to 6 rigs simultaneously and drilled out 484 locations in approximately 150 calendar days, or approximately 3 bridge sites per day.
- Field location of borings is performed by drillers
- Borings are logged by drilling subcontractor, to standards developed by the geotechnical team
- Schedule
 - Field boring logs to Geotech office the next day after completion of drilling,
 - Soil tests assigned by Geotech office and back to lab in one day
 - Final boring logs in electronic format to Geotech office within 2 days of drilling completion.
 - Soil test data (index/classification testing) to Geotech office within 2 days of test assignments.
 - Core photographs to Geotech office within 5 days of drilling completion
- 4. **Develop working profiles, assign laboratory testing** – It was very important that document control staff track and file the enormous amount of rapidly incoming boring and test data. CADD technicians then used the boring data to plot subsurface information for interpretation. Geotechnical engineers then viewed the boring data and subsurface plots to assign laboratory testing.
- 5. **Scour** – The geotechnical team furnished grain size data and soil classification to Hydraulics and Hydrology team for computation of scour. Scour depths were computed and returned to the geotechnical team for inclusion in the pile foundation design.
- 6. **Geotechnical Engineering Analysis and Foundation Recommendations** - Assume the preferred bridge to be some type of precast concrete beams supported by pile trestle type bents.
 - One span bridges will assumed to be supported by driven H piles at each abutment. Determine top of rock for end bearing pile. Receive pile loads from bridge designers and perform analysis to estimate friction pile length. Determine if friction piles are to be driven using Modified Gates formula or PDA.
 - Note individual geotechnical considerations during construction at each bridge site.
 - Multiple span bridges will assumed to be supported by driven H piles at each abutment with intermediate trestle bents consisting of H or Pipe piles. Drilled shafts and spread

footings will also be considered where applicable, mainly due to deep scour or long unsupported length of piles.

- Furnish Geotechnical Recommendation Memo to bridge designer – short, concise, one page memo to include items such as:
 - Pile type and length
 - Drilled shaft recommendations with tip elevation and allowable bearing
 - Spread footing elevation and allowable bearing
 - Settlement issues at embankments
 - Bridge end spill slopes and embankment slopes

CONSTRUCTION

The bridges were grouped together in “packages” of logical sequencing, in a local zone or circular pattern where a bridge crew could work efficiently rather than jumping around to different locations through the state.



CONCLUSIONS - The MoDOT Safe and Sound Design Build Bridge Replacement Project is a unique delivery system which enabled the replacement of hundreds of structurally deficient or obsolete bridges in a short amount time at a great value.

The systematic, standardization of design and construction was fundamental to the schedule and value. While each one of the 554 bridges was designed individually, the Geotechnical Engineering benefitted from the use of standardization, complex scheduling, and a systematic approach.

REFERENCES

Desai, B., Gutknecht, M., McMillan, S., 2010. Accelerated Bridge Improvement Program in Missouri: Safe and Sound BIP Replacement of 554 Bridges, 2010 FHWA Bridge Engineering Conference, Orlando, FL

**Using Light Weight Tire Derived Aggregate (TDA) as a Green Alternative for
Reconstruction of Landslide Road Failures**

William V. McCormick
Kleinfelder
2240 Northpoint Parkway
Santa Rosa, California 95407
(707)-571-1883
bmccormick@kleinfelder.com

Prepared for the 61st Highway Geology Symposium, August, 2010

Acknowledgements

Special thanks to the engineering staff at the Sonoma County Department of Transportation and Public Works for their enthusiasm for trying innovative solutions and their support of the geotechnical design team at Kleinfelder. Acknowledgements also go out to engineering support from the California Integrated Waste Management Board and Professor Dana Humphrey Ph.D. from the University of Maine for their technical review.

Disclaimer

Statements and views presented in this paper are strictly those of the author, and do not necessarily reflect positions held by their affiliations, the Highway Geology Symposium (HGS), or others acknowledged above. The mention of trade names for commercial products does not imply the approval or endorsement by HGS.

Copyright Notice

Copyright © 2010 Highway Geology Symposium (HGS)

All Rights Reserved. Printed in the United States of America. No part of this publication may be reproduced or copied in any form or by any means – graphic, electronic, or mechanical, including photocopying, taping, or information storage and retrieval systems – without prior written permission of the HGS. This excludes the original author.

ABSTRACT:

A 300-foot-long stretch of road in Northern California has been plagued with re-occurring landsliding for over 25 years. A driven-pile and lagging retaining wall constructed by road crews in the 1980's failed in response to heavy rains during the 2005-2006 rainy season, making the road unpassable. Available road reconstruction funds prevented a more robust retaining wall mitigation design and construction to stabilize and open the roadway.

Previous landslide failures and creek erosional transport at the base of the slope have resulted in significant volume loss of (clayey) earth materials that would be needed to reconstruct the slope, and stability analysis indicated that a stable slope could not be constructed with the weak native materials due to environmental setback restrictions. In addition, import of select earth materials was cost prohibitive.

An alternative design was developed using light weight (50 pcf) Tire Derived Aggregate (TDA, shredded waste tire fill) which was available free of charge in California as part of a tire recycling program from the California Integrated Waste Management Board. The light weight TDA significantly reduced the driving force for future sliding and supplied the needed volume of material needed to reconstruct the roadway fill prism within the road right-of-way and away from environmentally sensitive wetlands. The ultimate design consisted of removal of the landslide deposits and replacement into a geo-grid reinforced engineered soil buttress at the base of the slope and alternating layers of TDA and soil in the upper portion of the road prism. Over 330,000 tires were removed from landfills and utilized as permanent fill on this road.

INTRODUCTION

A 300-foot-long stretch of rural road in Santa Rosa, California, USA has been plagued with re-occurring landsliding for over 25 years that has displaced the entire width of roadway and has made it impassable for years at a time. The roadway sits on top of a 30-foot-high slope, which is an active landslide with wetlands and an eroding creek at the base. In addition, a perennial spring emanates mid-slope from one side of the landslide. The upslope side of the roadway is about 15 feet high, with a residence approximately 50 feet away from the head scarp of the active landslide. This predominantly translational type landslide is located within an area that has been interpreted by local geologists as being a large, ancient bedrock landslide. Materials within the active slide mass consisted mainly of highly plastic clays derived from soft bedrock consisting of interbedded soft claystone, siltstone and clayey sandstone underlying the active slip surface. The maximum depth of active landsliding is approximately 30 feet below existing grade.

The first landslide that displaced the roadway occurred in the early 1980's. In response county road crews constructed a 20-foot-high wall with metal lagging and steel H-piles on the order of 50+ feet deep. The retaining wall was constructed by driving piles to refusal and then tying them back with steel struts connected to shorter deadman piles on the uphill side of the road. The lagging was backfilled with granular import soils. In response to heavy and prolonged rainfall events in December 2005, the retaining wall and roadway prism were displaced by renewed landslide movement and the road was closed (Figure 1).



Figure 1 - Failed Tied-back H-beam Retaining Wall and Roadway Due to Landsliding.

Initial design efforts to mitigate the failed retaining wall and roadway concentrated on brute force type approaches such as new retaining structures consisting of deep piers and multiple rows of tieback reinforcement. This proved to be too costly for the local transportation department who had access to limited funds, so more cost-effective solutions were needed to be considered. One alternative was to reconstruct the slope and road prism with a standard earthen buttress. This alternative was determined to be unfeasible due to restrictions of the buttress footprint from encroaching into the wetlands and the costs associated with importing select fill materials to replace the clay-rich materials that had been eroded away by the creek at the base of the slope over time and the need to construct the slope steeper than would be considered adequately stable using plastic clay materials.

TIRE DERIVED AGGREGATE (TDA)

The use of Tire Derived Aggregate (TDA) has been documented for various engineering application since the early 1990's (Humphrey, 2003). TDA consists of waste tires that have been shredded into individual piece ranging in size from 2 to 12 inches in maximum dimension. One of the most popular uses of TDA is for general or light weight fill in road embankments and as a backfill for retaining walls. Some of the beneficial properties associated with TDA include 1) light weight, unity weight 40 to 60 pcf, 2) free draining, hydraulic conductivity 1 to 10 cm/s, 3) good thermal insulator, 4) durable, and 5) usually the cheapest solution.

It has been estimated that in the United States there are over 850 million scrap tires in open piles (Associated Press, 1996) and that one scrap tire is produced per person per year (an additional 300 million per year). According to Humphrey (2003), one cubic yard of compacted TDA fill contains approximately 75 shredded tires.

SONOMA MOUNTAIN ROAD LANDSLIDE

The Sonoma Mountain Road landslide project presented a unique combination of limiting factors when considering standard mitigation design and techniques. The local transportation department had limited funds and simply could not afford a tiedback retaining wall solution with an estimate cost of over \$2 million (US). Likewise, environmental jurisdiction regulations prevented encroachment into or disturbance of protected wetlands with an earthen buttress repair at the toe of the slope. As such, a mitigation scheme utilizing various engineering solutions in concert with each other was necessary to stabilize the roadway and to meet financial targets.

Due to the weak and plastic nature of the landslide slip surface and overlying clay-rich landslide deposits, it was paramount that removal of these materials within the prescribed limits of work be included in the design. In order to reduce costs associated with the slope repair, existing landslide deposits were to be re-used in slope reconstruction to reduce costs associated with importing vast quantities of select fill. Slope stability analyses using on-site native clay materials indicated that a wider earth buttress with a flatter slope would be required to reconstruct a stable road prism without other engineering alternatives. Once again, due to environmental space re-

restrictions, this option was deemed unfeasible. Stability analyses did indicate that an earth buttress constructed of native and imported fill within the prescribed work limits could be built that would have the required static Factor of Safety (F.O.S., 1.5), but it did not provide an adequate F.O.S under seismic loading (0.8) and the import of fill proved too costly for the transportation agency. Further stability analyses did show that a statically and pseudo-statically stable road prism could be reconstructed with a combination of existing native materials and light weight fill. Once again due to budgetary limitations, importing light weight aggregate such as volcanic rock was cost prohibitive to this project and another light weight source was needed.

The various limiting factors involved with this particular road failure project created the need to look beyond standard engineering applications and suppliers for the right solution. Fortunately in California, the California Integrated Waste Management Board (CIWMB) has a statewide recycling and reuse program that supplies TDA free of charge for civic projects. As part of the program, TDA is processed and delivered to individual project sites for use.

MITIGATION DESIGN AND CONSTRUCTION

The TDA import fill source from CIWMB enabled the project design and construction to move forward. Slope design utilizing TDA requires that the engineering and physical properties of the TDA be taken into account in conjunction with standard slope stability analysis. Humphrey (2003), in cooperation with the CIWMB, has developed a manual chronicling past uses and performance of TDA projects as well as design applications for using TDA. That manual includes guidelines on how reduce the potential for exothermic reactions (combustion/tire fires), calculation of overbuild for compression of the TDA, compaction and appropriate soil cover. Based on past performance of other TDA road embankment projects throughout the US, current uses of TDA should be limited to a maximum thickness of 15 vertical feet, with no more than a 10-foot thickness in any one layer (Humphrey, 2008, personal communication). Likewise, TDA layers should be separated and covered by a minimum of 3 feet of compacted soil for confinement and to sufficiently reduce the potential for exothermic reactions. In order to take advantage of the light weight properties of the TDA, a two-layer system with a total vertical thickness of 15 feet was utilized in the design and construction of this project.

In order to mitigate the active landslide, all of the landslide material within the project limits was removed to a minimum of 3 feet below the slip surface into more stable bedrock derived materials. The lower portion of the slope was reconstructed as a buttress with a toe keyway 30-feet-wide and 5 feet below the slip surface. The toe keyway was drained with a subdrain that drains into the wetlands area below the repair. Since this landslide was known to have significant subsurface groundwater and a spring, the lower 2/3 of the excavation was reconstructed with a continuous gravel blanket drain that was tied into the toe subdrain.

In order to meet the environmental restrictions and avoid disturbing the wetlands at the base of the slope, finished slope gradients would need to be 2H:1V (horizontal to vertical) or steeper to reach the restored road surface. Since the majority of the on-site fill material was highly plastic clay, slopes constructed at this gradient required additional reinforcement in order to maintain a stable configuration. As such the outer 15 feet (measured horizontally) of the slope was reinforced with alternating layers of uniaxial and biaxial geogrid layers. The uniaxial layers, spaced

every 3 vertical feet, were placed to increase the global stability of the slope face. The biaxial geogrid layers, spaced 1 foot apart in between the uniaxial layers, were placed to reduce the potential for surficial failures within the clayey slope face. Fill soils were compacted to a minimum of 90% relative compaction at moisture levels 2%-4% above optimum (ASTM D 1557).

As previously stated, the upper half of the slope reconstruction was designed as a two-layer TDA system. The lower layer was designed as a 10-foot-thick (maximum recommended compacted vertical height of any single layer) and the upper layer was designed as a 5-foot-thick layer. In order to maintain global stability and to aid in the placement of TDA, the outer portion of the slope must be designed as a soil “choker” to act as a lateral barrier for the TDA as it is being placed and compacted in 12-inch-thick lifts (Figure 2). The soil choker is raised prior to the placement of successive lifts of TDA. The compressibility of the TDA due to successive fill layers and loads must be taken into account in the overall design. This necessitates a calculation of the amount of overbuild for each individual TDA fill layer based on their individual overburden loads at finished grade, which varied across the road fill prism. For this project, the lower layer required a TDA overbuild of 1.0 to 1.8 feet and the upper layer required 0.7 to 1.3 feet.

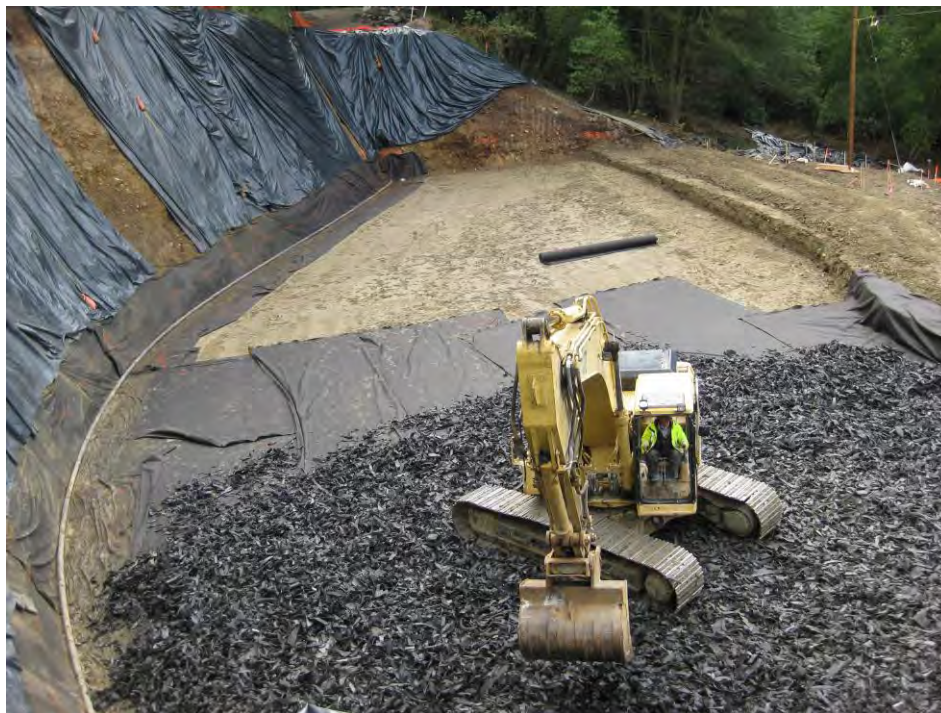


Figure 2 - Placement of Initial Lift of TDA Fill on Filter/Separation Fabric with Subdrain Pipe on Left and Soil “Choker” on the Right.

TDA requires the use of a filter/separation geotextile fabric for encapsulation purposes to prevent fines from overlying confining soil fill layers from infilling voids within the shredded tires and hence, created new voids and potential settlement issues within the compacted soils. One of the benefits of using TDA is its relative high permeability. TDA acts as its own “drain rock” for sub-

drain purpose, thereby eliminating the need for expensive granular import drain material. Construction with TDA initially begins by placing the filter fabric/geotextile across the surface to be filled, placement of the perforated subdrain pipe and then subsequent 12-inch maximum lifts of the TDA fill within the confines of the outer soil choker (Figure 2). The TDA is compacted, as in this case, with 6 to 8 passes of a smooth drum roller. Compaction testing is not required. In order to reduce the potential for exothermic reactions and to seal off the TDA from the surface, the TDA layers are covered by a minimum of 3 feet of compacted soil and ultimately by the reconstructed road section.

“GREEN” BENEFITS

Utilizing TDA as an engineered construction product has many benefits; financial as well as environmental. Typically, the cost of delivered TDA is about 50% less than other light weight import fill materials. In the case of this project and other civic projects in California, TDA was made available and delivered free of charge through a grant program from the CIWMB. Additional costs savings are also realized because it takes less time to place the TDA fill as compared to soil fill. Because of the time savings and reduced duration of heavy equipment use, this results in a lower carbon footprint for the project. Use of TDA resulted in an overall costs saving of 36% for the Sonoma Mountain Road project.

The greatest benefit of TDA, which reaches far beyond the limits of any one project and into the community at large, is the reuse of recycled waste tires. TDA production removes tires from the overall waste stream and reduces impacts on landfills. Since one cubic yard of compacted TDA is equivalent to approximately 75 waste tires, it is easy to see how even a small project utilizing TDA can make a difference in reducing the impacts of waste tires on the environment. For the Sonoma Mountain Road project, approximately 4,400 cubic yards or 330,300 waste tires were removed from the waste stream and utilized as permanent, environmentally friendly engineered fill (Figure 3).



Figure 3 - Road Signage for TDA use on Sonoma Mountain Road Project.

REFERENCES:

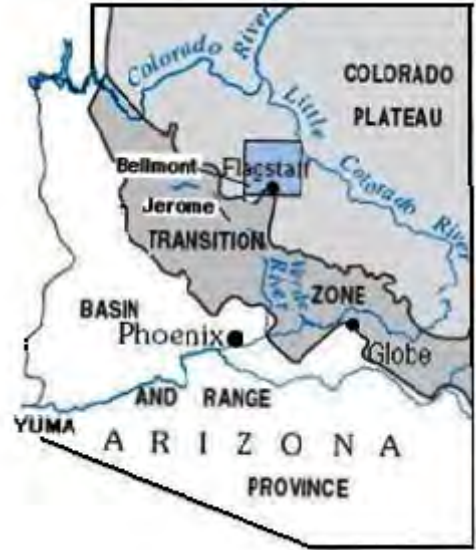
1. Associated Press, 1996, as printed in *USA Today*, September 30, 1996 p.23A.
2. Humphrey, D.N., 2003, Civil Engineering Applications Using Tire Derived Aggregate (TDA), pp 147.
3. Humphrey, D.N., 2008 (personal communication).

USING LIDAR LASER SCANNING FOR GEOTECHNICAL CHARACTERIZATION IN ROCK

*Nick M. Priznar, Engineering Geologist, ADOT,
Geotechnical Design Section*

*Virgil Coxon, Chief Surveyor, ADOT, Engineering
Survey Section*

*Dr. John Kemeny, University of Arizona, Dept. Mining
and Geological Engineering*



Abstract:

For several years two sections of ADOT have collaborated on the use of laser scanning for acquiring very accurate three dimensional data in previously inaccessible terrain for geotechnical assessments. The application LiDAR appears to hold promise to reduce field investigation costs, increase the amount of usable data collected, and greatly reduce the level of hazardous exposure to field personnel while performing rock mass characterization studies.

LiDAR was used to supplement and analyze rock mass discontinuity orientations on high cut slopes on I-8, MP 20, at Telegraph Pass, in Yuma County, Arizona, in 2007, and on I-40, MP 180.1, west of the Belmont Traffic Interchange, Coconino County, Arizona, in 2009. Additionally, LiDAR was used to estimate distress in a plastered rubble retaining wall on SR 89A within the Town of Jerome, Yavapai County, Arizona, in 2008.

Due to the limited and potentially hazardous access to the rock cut slopes, ADOT and its collaborators extracted orientation data from LiDAR point clouds that were originally generated to create digital terrain models for the highway corridors. Three dimensional data sets of discontinuity surfaces with similar orientation properties were grouped together and extrapolated from point cloud images. The average orientation of these groups was downloaded into commercially available slope stability programs and used to augment the analysis of the potentially unstable rock slopes.

LiDAR, as defined by Wikipedia, “is an optical sensing technology that measures properties of scattered light to find range and /or other information of a distant target. Monte (2002) describes the process of utilizing a portable LiDAR scanner device to create “optical pulses of light to remotely measure thousands of three-dimensional (3D) coordinate points for any object or surface. The collection of these coordinate points, (referred to as a **point cloud**), renders a 3D model of the scanned object.” Thus, when laser scanning is completed for a rock mass, a variety of discontinuity data can potentially be obtained from the point cloud data sets.

The advantages of Using LiDAR include the following enhancements to routine surface mapping techniques:

- Ability to characterize inaccessible or unsafe rock surfaces.
- Ability to collect a large amount of data in a relatively short period of time.
- Ability to extract extraneous information from the point cloud data set such as vegetation and traffic that interferes with analysis.
- Ability to quickly compare different segments of slopes and look for trends that may be contributing to kinematic instability.
- Potential to download large amounts of data into existing software.
- Ability to confirm existing observations and look for hidden relationships within a large statistical data set.
- Potential to routinely use LiDAR data to create products for other engineering disciplines required to develop a set of construction plans.



Characterizing slope conditions by rappelling down a cut face.

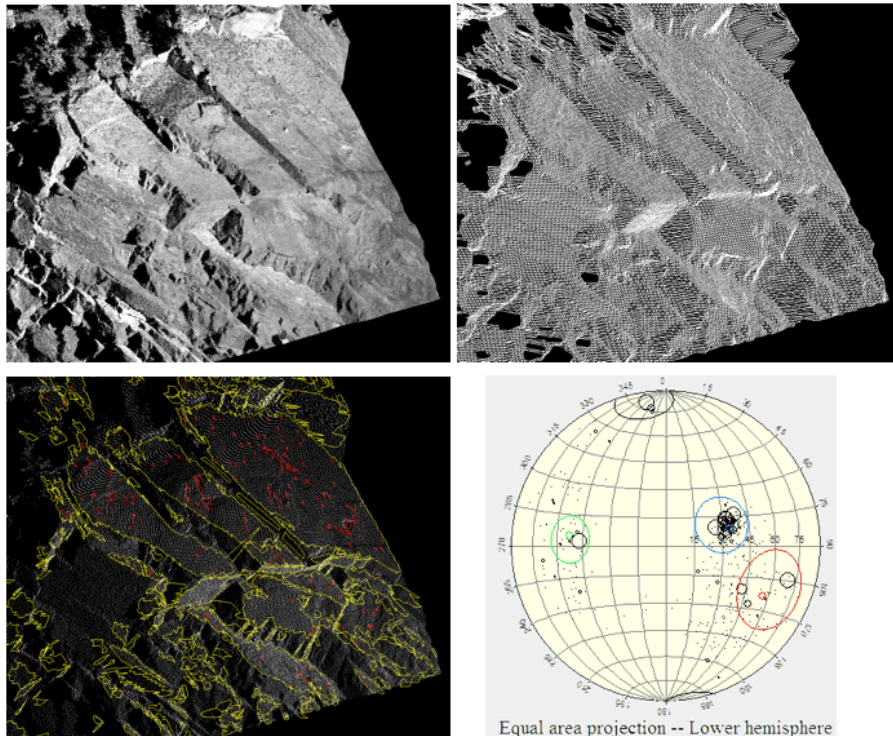


Image Courtesy of John Kemeny

Four images displaying the steps in processing LiDAR data from point cloud, to triangular net, to discontinuity identification, to stereo net analysis.

Using LiDAR to Estimate Rock Mass Discontinuity Orientations on High Cut Slopes: I-8, MP 20, Telegraph Pass, Yuma County, Arizona

The project area is located approximately 20 miles east of downtown Yuma, Arizona, in the Gila Mountains of southwestern Arizona. The area is dominantly composed of Precambrian through Mesozoic age, crystalline rocks that vary from granite, to granitic schist and gneiss. The typical outcrop exhibits persistent planar and angular discontinuity surfaces that are coincident and adverse



to slope orientations depending on the position of the highway alignment. Mafic dikes have intruded the crystalline rock materials, dilating intersecting shear zones exposed in the bedrock outcrops. Intermittently, weathered red, boulder laden sandstones, breccias, and fanglomerate are un-conformably deposited within topographic basins created in the older intrusive rocks. The alignment is bifurcated along a curvilinear grade separated alignment with a posted speed limit of 65 miles per hour. The existing $\frac{1}{4}$:1 slopes exposed along the alignment have a short sight distance and a very narrow shoulder, with chain link fence mounted on concrete half-barriers. Heights of the existing cuts range from 20 feet to over 100 feet.

To evaluate the kinematics of the site, an outcrop mapping technique was first employed by the geotechnical investigation team. Only a limited number of orientations were available above the top of the cuts and the rock outcrops accessible at the toe of the cuts were providing a biased data set. The existing steel rock fall fence was also interfering with measurement of the orientations of the kinematics data. Working behind the fence exposed the investigators to an increased risk of rock fall. Suspected changes in discontinuity orientations higher up in the cuts were excluded from the data set.

To overcome the difficult topography ADOT's Survey and Mapping Section were utilizing LiDAR Scanning to create a digital terrain model of the site. After evaluating the options a decision was made to attempt using the point cloud data from the geometrics survey to abstract kinematic information to supplement the exiting discontinuity data sets. With this larger data file the project team would have a greatly improved basis for slope modeling decisions.

After receiving the data and processing the point cloud it, was possible to delineate a triangular mesh that models a close approximation of the slope geometry and features. This model was used to identify the dominant joint and fracture sets on the slopes and obtain a close approximation of the discontinuities orientations that could be utilized for kinematic analysis.

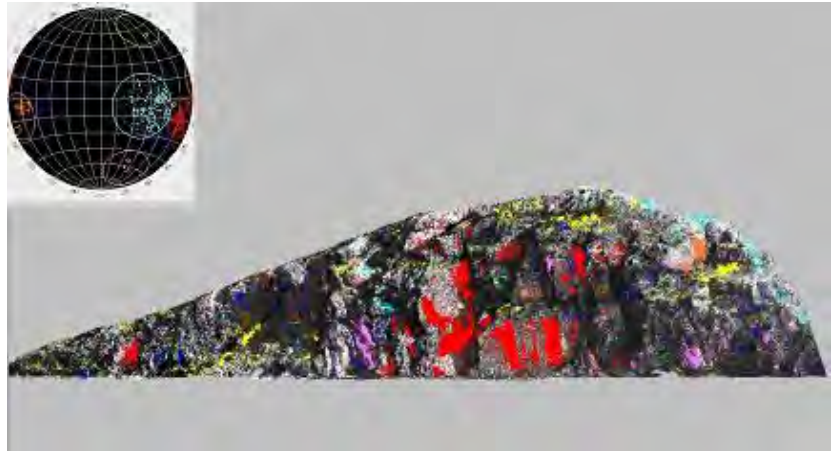
Using the technique outlined by (Handy et al. 2004) and (Monte, 2004); "a grid perpendicular to the scanner's line of sight is imposed onto the point cloud. Within the grid, groups of individual coordinate points ranging

from 5 to 10 per cell were selected. The cell centers were then calculated from the points within the cell boundaries. The edges and faces of the triangular mesh were generated from the cell centers”.

As described in FHWA-CFL/TD-08-006, “The most important processing step is the delineation of fracture “patches” from the triangulated surface mesh. The term “patch” is used rather than fracture, because a single large fracture maybe delineated into several smaller patches, depending on the flatness and roughness of the fracture. Fractures are detected by using the basic assumption that they are flat. Flat surfaces are automatically found in the triangulated mesh by first calculating the normal to each triangle, and then finding groups of adjacent triangles that satisfy a flatness criterion.”

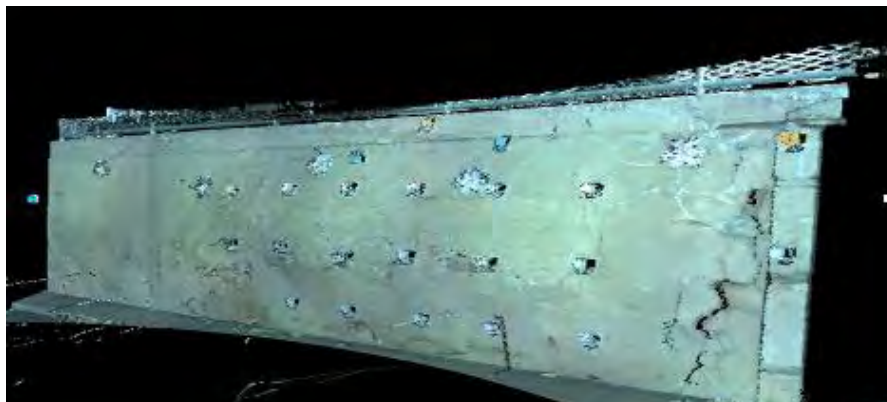
In this project, the fracture surfaces (patches) were identified by calculating the normal to each triangle created by three points from the triangulated surface mesh. Groups of adjacent triangles that met the flatness criteria and had similar orientation properties were grouped together. After the groups were identified, their average orientations were plotted on equal area stereo net. Relatively large contiguous groups of separated patches that have a relatively common orientation are indicators of the LiDAR based estimate of the dominant fracture and joint surface orientations on the slope.

The LiDAR scans resulted in a very large data set that was free of field bias and greatly reduced the risk to the field personnel from rock fall while collecting orientation data. The method also recovered very useful geologic data from previously inaccessible areas of the slopes, enhancing both the data set that was recovered and the field work safety.



There were areas of the slope that were not well covered by the digital terrain modeling survey and gaps in the continuity of the data obtained were observed. These areas appeared as shadows on the images and supplemental field observations were required to insure that important discontinuity surfaces were not omitted.

Using LiDAR to Measure Changes in the Positions and Distress of Rock Mass in a Rubble Retaining Wall

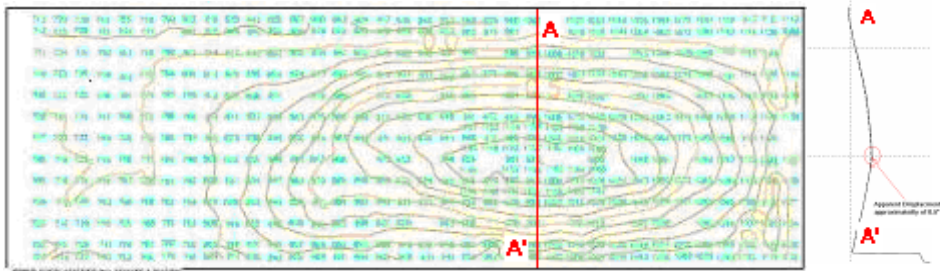


Scanned image of deteriorated rubble retaining wall in Jerome, Arizona

LiDAR was successfully utilized to monitor a failing rubble retaining wall on SR 89A, at MP 344, in the Town Of Jerome in Yavapai County. The existing highway alignment was constructed in 1919 and dominantly consists of a 20 feet wide roadway with 6% to 10% grades and poor sight distance. There are no known “As-Built” drawings or permit records for this wall and it was assumed that its construction was part of the residential development of the town and not part of a highway construction project. The face of the wall had been exhibiting deterioration for over 20 years. The bulging and lateral deviation of the wall face appeared to be accelerating and a determination was made to survey the site, on a regular periodic basis.

Several attempts to apply traditional surveying techniques (by consultants) to monitor the wall did not achieve discernible results. The combined level of instrument and human errors were well within the limits of apparent measured wall movement. Precision LiDAR rescanning of the wall surface was employed from established benchmarks over a 14 month period utilizing state plane coordinates for the point cloud data sets. Using Leica's Cyclone 5.X post-processing software the point clouds were edited and converted into CADD file formats. This allowed the data to be directly imported into a Micro Station Inroads data file and the offset distance from selected points on the structure could be measured from a convenient reference line.

Two types of images were generated from the LiDAR scanning: a vertical digital terrain model (VDTM) of the wall surface, and cross sections. The VDTM could be compared from each survey to determine if the area of distress was changing. The cross sections from each survey could be stacked in multiple views and an estimate could be made to determine if there were any observable lateral displacements of the wall surface. If there were lateral displacements; a comparison of previous measurements were made to determine if the rate of wall movement was accelerating.



Additionally, displacement between pre-selected reference points was calculated by aligning two point clouds visually as accurately as possible. At that point, one coordinate value from the earlier survey was picked as an origin. All of the coordinate values from the later survey within a circle of one degree of angular horizontal deviation were examined. The coordinate value (from the later survey) that represented the minimum horizontal distance between each survey was selected. The corresponding horizontal distance was conservatively used to represent the apparent lateral deviation of that wall position, within the selected survey time period.

The data suggested that the estimated total lateral deformation of the wall face was approximately 0.9 feet. The estimated average total displacement for over the past 20 year's period was 0.045 feet per year. The observed maximum displacement over a 14 month period was 0.042 feet per year. The data also indicates that at the time of the last scan, lateral displacement was not accelerating, but may have been occurring at a roughly uniform annual rate. However, it may have been occurring over an increasing larger surface area, as the wall deformation continued.

Another LiDAR scanning method presently under development is the ability to utilize the data scans to detect changes in rock fabric directly from the point cloud data files. This method has been outlined by Dr. John Kemeny and cited in FHWA-CFL/TD-08-006. This methodology is directly applicable to monitoring rock fall and changes in rock fabric on highway cuts.

In this method “periodic scans are processed to evaluate rockfall using “change algorithms”. Change algorithms can be found in a number of the point cloud processing software. The change algorithms subtract two point clouds (data sets) and produce a “difference cloud”, which is point cloud providing information on the relative difference between the two scans at points throughout the area that was scanned. From the change, the movement of a rock block can be tracked, or the size of a block that has moved can be monitored. The total accumulated rockfall rate can also be calculated. Before the change algorithm can be applied, the two point clouds must be aligned as accurately as possible. In general, Iterative Closest Point (ICP) algorithms (Besl, 1992) are used to align the scans with the highest accuracy (higher than can be achieved by surveying alone).”

This method appears to be attractive due to the lesser amount of data manipulation that is required before a change in rock position is detected. It appears to be more versatile over a convoluted or irregular surface and does not need to be tied into an existing coordinate grid system. However the former technique lends itself more readily to the development of plans and specifications and the development of earthwork quantities. It would appear that some integration of both of these techniques would present the most optimal use of LiDAR for highway projects.

ARIZONA DOT LiDAR TEST STUDY SITE

As part of a pooled study project, ADOT is testing the effectiveness of LiDAR on a rockfall mitigation site in north central Arizona. ADOT will rely on terrestrial based LiDAR to supplement rock slope stability and rock fall analysis. The intent is to use LiDAR to identify the structural geologic discontinuities that control rock fall and also identify the structural trends that will augment redesign of the existing cut.



A change detection analysis in both the rock fabric (relaxation of blocks) and rock fall (movement of blocks) of the existing slopes will be attempted. Two scans of the site were

conducted before and after the winter season. After processing the point cloud data, a site correlation will attempt, to verify identified changes in the point clouds within areas of observed rock fall. A digital terrain model and cross sections will also be created in sufficient detail so that plan sheets, cross sections and volume estimates may be accurately calculated to design any corrective measures.

The project area is located west of the Belmont traffic interchange, in Coconino County; on West Bound I-40 @ MP 180.1. This site is located approximately 11 miles west of Flagstaff, Arizona within the Kaibab National Forest and adjacent to the Navajo Army Depot.

In this area, I-40 is classified as a divided rural interstate which runs east-west and consists of 2-12 feet lanes, with 4 foot inside shoulders and 10 foot outside shoulders in both directions. The alignment in this area is along a curve with a 75 mph speed limit. The existing rock slopes were excavated approximately (3/4: 1) to (1/2:1) and range 80 feet or more in height. The entire cut is approximately 1200 feet long. The natural landform ranges to 100 feet above the exiting roadway. The terrain is analogous to moderately rolling hills to mountainous. Approximately 8,500 vehicles pass this cut every day. The sight distance is approximately 800 feet under good conditions. The normal annual precipitation in the area is approximately 25 inches per year. The average elevation is approximately 7,200 feet above sea level.

As-Built Roadway Conditions

The existing high roadway cut slopes were constructed in extrusive basalt flows and breccias to accommodate the interstate highway alignment. The as-built plans indicate the cut was originally excavated with controlled blasting techniques. However, the slope may have also been damaged by blasting during this process. The existing cut produces a significant volume of rock fall and requires maintenance activities to clear out the cut ditch several times a year. The adverse orientation of some of the joint planes tends to form wedges and planes that become unstable in times of increased precipitation and ice development. A significant rock fall event took place in February 2005 over a period of time when a number of heavy rainfall and snow events occurred. Water appears to infiltrate in rock discontinuities and may be accelerating deterioration of the slope. Large boulders up to 6 feet in diameter have fallen on to travel lanes despite the existing catchment ditch. The major focus of rock fall is near the east end of the cut section, coincident with a highly fractured zone in the slope face.

Regional Geologic Site Conditions:

The geology of the region has been mapped by the USGS, (1984), as a group of extrusive and pyroclastic lithologies associated with the San Francisco Volcanic Field, ranging in age from Holocene to Pliocene. (0.1 to 5.3 MYA). Generally they are composed of basalts, andesite, dacite, rhyodacite, and rhyolite flows and domes. Regionally present are a series of moderately eroded cinder cones and associated pyroclastic deposits. Underlying these deposits is an erosional unconformity on top of the Permian Kaibab Formation (286 MYA). This contact is recognized as a former topographic surface which consisted of low hills and low gradient streams and pediments which were formed on the Kaibab Formation and are now concealed by volcanic deposits.

In the project vicinity, moderately high roadway cuts (60 to 80 feet in height) in basalt flows have been constructed to accommodate the highway alignment. Numerous

curvilinear and undulating to near vertical cooling joints in the cut face form wedges, and boulders. In places, multiple flow pulses and basalt breccias are chaotically intercalated in a highly fractured rock mass.

Some of the joint planes dip adversely into the roadway and are potentially hazardous to the traveling public. The rock cut can be divided into two distinct sections, a western and eastern side. The western side of the cut is composed of massive basalt with discontinuous and random joints. The lower two-thirds of the cut is massive, while the top portion appeared to be more fractured. It is separated from the east cut by a drainage area. The east side of the cut is described below:

According to a recent report from (Ninyo & Moore, 2005) “The major focus of rockfall is near the east end of the cut section, coincident with a highly fractured zone in the cut face. The intensity of the fractures in the basalt in this area is significantly different from the rest of the cut section, in that rock particles are laminar in shape. And the joint patterns are distorted. This pattern is typical of the margins of basalt flows (that occur) along steep topographic relief.”



The figure to the right illustrates the laminar shaped rock fall material that forms in the distorted joint patterns at the test site.

Preliminary Results of LiDAR Investigation (as of June 2010)

LiDAR scanning was conducted of a highway slope along Interstate 40 westbound at milepost 180. The rock slope is approximately 1200 feet long and ranges in height from 40 to 120 feet. Scanning was conducted in November 2009 by ADOT personnel using a, Leica HDS 3000, LiDAR scanner. A registered color point cloud of the entire slope was produced by ADOT personnel, and this point cloud was then broken up into 5 sections for analysis with the Split FX point cloud processing software. Section 1 is the most eastern part of the slope and Section 5 is the most western part of the slope. There are several reasons for breaking the slope into 5 sections. First of all, since the point cloud of the entire slope contains over 15 million points, this allows for manageable subsets of point cloud data. Secondly, the geologic structure varies along the length of the slope, and this allows geotechnical analysis of subsections of the slope. The analysis below is for Section 2, and the boundaries for Section 2 are roughly shown in Figure 1 below.



Figure 1. Approximate location of the Section 2 point cloud (between red lines).

The point cloud from Section 2 is shown in Figure 2 and contains about 4 million points. The length of this point cloud is about 230 feet and the height ranges from 60 to over 100 feet. The average dip of the rock slope in Section 2 is 65.5 degrees and the average dip direction is 208 degrees.



Figure 2. Point cloud of Section 2

Geologic Structure of Section 2

The geologic structure in Section 2 is complex and contains several sets of sub-vertical cooling joints as well as one set of sub-horizontal discontinuities. Pre-split blasting was used to excavate the slope with a minimum of blast damage, but the presence of blasting-induced fractures is still possible. There are randomly oriented discontinuities in the rock mass, and fracturing associated with the pre-split blasting may include separation along these pre-existing discontinuities.

The geologic structure in the Section 2 point cloud was analyzed using the following steps in the Split FX program:

- 1. A triangulated surface was created from the point cloud.**
- 2. Fracture “patches” were automatically found by finding collections of triangles that conform to a flatness criterion.**
- 3. Fractures that appear as traces and not surfaces on the rock slope were extracted by manually delineating the fracture traces on the point cloud.**
- 4. The orientation of the fracture patches and traces were plotted on a stereo net, and joint sets are determined.**
- 5. Measurements of average joint spacing for each joint set were determined using manual measurement tools in the program.**

The results of the structural analysis of Section 2 are shown below. Figure 3 presents the stereo net of fracture patch and trace orientations. The fracture patches are small circles on the stereo net and the size of the circle correlates with the size of the patch. The fracture traces are shown as triangles on the stereo net. Figure 4 shows the location of the fracture patches and traces along the rock face (trace fractures are shown as circular disks).

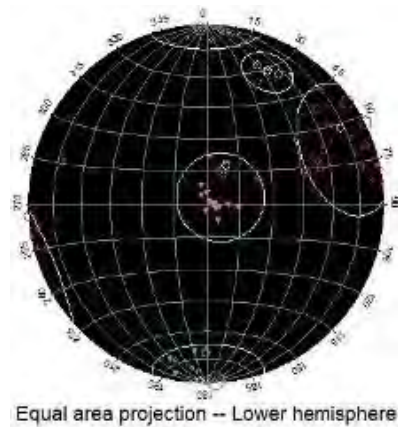


Figure 3. Stereo net showing fractures in Section 2. fracture patches and trace

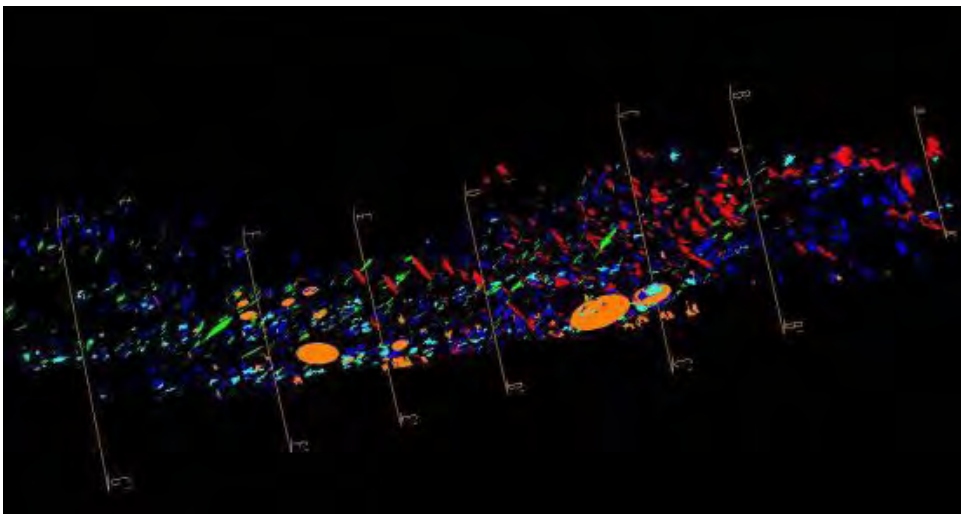


Figure 4. Location of fractures along Section 2. The trace fractures are shown as circular patches.

As shown in Figure 3, four primary fracture sets were detected. Two of the sets are associated with sub-vertical cooling joints, one set is sub-horizontal, and the fourth set is parallel to the rock face. The average dip and dip direction and the Fisher constant for each set are shown in Table 1 below. The set that is parallel to the rock face may partially consist of blasting fractures between the pre-split holes, but at least some of these fractures appear to be natural as shown in Figure 5 below. It should be noted that the Fisher constants for the two cooling joint sets are, low indicating significant scatter in joint orientation for these sets.

Table 1. Orientation and joint spacing information for the four fracture sets shown in Figure 3.

Set	Average Dip	Ave. Dip Direction	Fisher constant	Ave. joint spacing
1	74.8	240.7	25	8.1 ft
2	88.6	2.2	51	3.3 ft
3	19.4	206.1	144	3.5 ft
4	70.5	204.4	142	Not determined



Figure 5. Picture of the part of the Section 2 rock slope showing pre-split half-casts and some natural fractures sub-parallel to the slope.

Slope Stability of Section 2

Using the structural data presented in Table 2, a slope stability analysis was conducted using the Rocscience Swedge program. The Swedge software program takes the mean dip angle, the corresponding dip direction and Fisher constant for each set and performs a probabilistic slope stability analysis. In particular, to determine the probability of failure for potential wedges between any two discontinuity sets and the rock face, it randomly picks a fracture from each set and determines the factor of safety. It does this 10,000 times for each pair of discontinuity sets. If the result of the two picks and the rock face does not result in a removable wedge, it labels the pick as an invalid wedge. The probability of failure is the percentage of trials that results in a failed wedge. There are four discontinuity sets in Section 2, but since one set is parallel to the face, slope stability calculations were conducted between the other three sets and the average rock face orientation (dip 65.5 and dip direction 208.1). Friction angles of 35 degrees, zero

cohesion and zero pore pressure were assumed for each joint set. The results are shown in Table 2 below.

The results indicate that unstable wedges are primarily associated with the two sub-vertical cooling joints (labeled sets 1 and 2 in Table 2), and some wedge failure is expected to occur along these even though the probability of failure is low (around 3%). More specifically, for 10,000 trials between sets 1 and 2, 313 were valid wedges and 294 of those resulted in failure. Thus for valid wedges, the probability of failure is about 94%. However, since invalid wedges will also occur in the field, the field probability of failure should be 294 failed wedges out of 10000 trials, or about 3%. Based on the average joint spacing listed in Table 1, the average block volume associated with these wedge failures is expected to be about 36 cubic feet.

Table 2. Slope stability results for Section 2.

Wedge	Cases	Valid wedges	Failed wedges	Stable wedges	Prob. of Failure
Sets 1 and 2	10000	313	294	19	2.94%
Sets 1 and 3	10000	8297	8	8289	0.08%
Sets 2 and 3	10000	7108	3	7105	0.03%

References:

Bellian J., Jennette D., Kerans C., Gibeaut J., Andrews J., Ysseldyk B. and Larue D., 2002. 3-Dimensional Digital Outcrop Data Collection and Analysis Using Eye-safe Laser (LiDAR) Technology. AAPG Meeting. Houston, Texas. March 10-13.

Chamunda T. L., Kay G. B., 2005, Rockfall Assessment SR 89A (Oak Creek Canyon Switchbacks) and Westbound I-40 at Mile Post 180.1 Coconino County, Arizona, Task Order No. 14, Prepared for the Arizona Department of Transportation, : Nino & Moore, Geotechnical and Environmental Sciences Consultants, Phoenix, Arizona (unpublished)

Haire S. A., Kay G.B., 2008, Geotechnical Evaluation Report, I-8 Telegraph Pass, Yuma County, Arizona. Traccs No. 008 Yu 017 H5453 01D, Contract No. 03-25, Task Order No.09. Prepared for the Arizona Department of Transportation: Nino & Moore, Geotechnical and Environmental Sciences Consultants, Phoenix, Arizona

Kemeny J. M., Turner K, 2000, Ground-Based LiDAR Rock Slope Mapping and Assessment, FHWA-CFL/TD-08-006

Monte J. M., 2004, Rock Mass Characterization Using Laser Scanning and Digital Imaging Data Collection Techniques, MS Thesis, University Of Arizona, Dept of Mining and Geological Engineering

Olmstead F.H., Loeltz O.J., Irelan B., 1973, Geohydrology of the Yuma Area, Arizona and California, Geological Survey Professional Paper 486-H, USGS, Water Resources of Lower Colorado River-Salton Sea Area

Ulrich G. E., Billingsley G.H., Hereford E.W., Nealey L.D., & Sutton R.L., 1984, Map Showing Geology Structure, and Uranium Deposits of the Flagstaff 1° X 2° Quadrangle, Arizona, Department of the Interior, United states Geological Survey, Prepared in Cooperation with the United States Department of Energy, Miscellaneous Investigation Series, Map I-1446

Software:

Cyclone and Cloud Worx, Point Cloud Processing Software, products of Leica, HDS Division, San Ramon, California

Micro Station, CAD Software for 2-and 3-Dimensional Design and Drafting, a product of Bentley Systems.

Split FX, 2010, Point Cloud Processing Software for Geotechnical Analyses, a product of Split Engineering LLC, www.spliteng.com.

Swedge, 2010, 3D Surface Wedge Analysis Program for Slopes, a product of Rocscience Inc., Toronto/Ontario, Canada, www.rocscience.com.

Assessment of the Garvin Landslides

Christopher R. Clarke, P.E.

Geotechnical Lab Supervisor

Oklahoma Department of Transportation, Materials Division

200 N.E. 21st Street, Oklahoma City, OK 73105-3204

(405) 522-4994

cclarke@odot.org

James B. Nevels, Jr., P.E., Ph.D

Geotechnical Consultant

605 Mimosa Dr., Norman, OK 73019

(405) 818-2897

jnevels1@cox.net

Prepared for the 61st Highway Geology Symposium, August, 2010

Acknowledgements

The authors would like to thank the employees of the ODOT Geotechnical Branch for their work in performing the site investigation, Division 2 Construction and Maintenance employees for their valuable information in the history of the project, and the faculty and students of the University of Oklahoma School of Civil Engineering and Environmental Science for performing borehole shear testing (BST).

Disclaimer

Statements and views presented in this paper are strictly those of author(s), and do not necessarily reflect positions held by their affiliations, the Highway Geology Symposium (HGS), or others acknowledged above. The mention of trade names for commercial products does not imply the approval or endorsement by HGS.

Copyright Notice

Copyright © 2010 Highway Geology Symposium (HGS)

All Rights Reserved. Printed in the United States of America. No part of this publication may be reproduced or copied in any form or by any means – graphic, electronic, or mechanical, including photocopying, taping, or information storage and retrieval systems – without the prior written permission of the HGS. This excludes the original author(s)

ABSTRACT

A shallow landslide in a highway cut-section slope occurred on January 13, 2005 in high plasticity residual clay soils creating a costly maintenance problem. The site location was approximately 3.1 miles east of Garvin in McCurtain County, Oklahoma along the westbound lanes of US-70. The north facing cut-section slope failure, designated as slide A, was investigated in 2005, and repairs were recommended and completed in the summer of 2006. The repair solution applied was a counterfort trench drain system. Two additional slides occurred in February 2010 and March 2010, designated as slide B and slide C, respectively. These two new landslides are relatively the same size as slide A, and are spoon-shaped. The standard Oklahoma Department of Transportation (ODOT) Roadway Design slope design of 3:1 was applied to the north facing cut-section slope in the original construction.

This paper continues with the refinement of the mechanisms of stability degradation discovered with slide A, addresses in more detail the site investigation and geologic description, and further assesses the back-calculated shear strength. Upon further review the mobilized shear strength at the time of these recent slides, as well as the original slope failure, was more likely the fully-softened shear strength rather than the assumed residual shear strength.



Figure 1 - Garvin Landslide (Slide A) in 2005

FIGURE 1 Garvin landslide.

section excavation in this highway widening project began on May 31, 2001 and was completed on October 15, 2001, see Figure 1. Slide A was reported to have occurred on January 13, 2005, which is a period of 42 months and 16 days from the completion of the cut section excavation. Preceding and during this period the climate at this site was dryer than normal, based on data from the Idabel Mesonet Weather Station.; however, numerous rainfall events did occur. Research into causes of landslides historically implicates rainfall as one of the key triggering mechanisms (1, 2, 3). At this site, the Thornthwaite Moisture Index (TMI) was utilized to indicate the changes in the water balance over the time frame in question. TMI analysis over this time period reveals that during the cut section excavation the TMI is near the historical average, and then following the end of the excavation construction (October 15, 2001) the TMI takes a dramatic and steady drop until December 2003, indicating a dry period. Then the TMI increases with time, indicating a wetting period, until the landslide occurs on January 13, 2005. A back-calculated slope stability analysis based on the center cross-section of slide A reveals that the operating shear strength is nearly at the stiff clay's fully softened shear strength ($c' = 0$, $\phi' = 14.5^\circ$). Recent research (4, 5) into shallow slide failures in high plasticity embankment slopes also shows that the failure mechanisms involved in these slopes are related to moisture infiltration into the slope surface and diffusion of moisture from cracks into the clay matrix that leads to decreases in soil suction and shear strength. In this case, the stiff clay is known to be structured, having slickensides that form parallelepipeds and cracks that open up various times of

the year. Research into fully softened shear strength generally supports its development as a long-term process (6, 7). This paper looks into the effect that soil suction plays in reducing the mobilized shear strength and the degradation of the friction angle to a fully-softened shear strength, through a case history.

Since the repair of slide A, two additional landslides have occurred being referred to as slides B and C in March and April 2010, respectively, while slide A has suffered no further distress. The question comes down to what actually is the safe cut section slope ratio with regard to first time landslide development.

SITE CHARACTERIZATION

The location of the landslide site is west of Idabel, Oklahoma in a reconstruction project of the westbound lanes of US-70 in McCurtain County by the Oklahoma Department of Transportation (ODOT). The cut section is located in a Hollywood soil series map unit (HoB) according to the National Resources Conservation Service (NRCS) of the U.S. Department of Agriculture McCurtain County Soil Survey (8). A check with the USDA Natural Resources Conservation Service (NRCS) Web Soil Survey 2.2 program indicates that the soil series at the site location has been re-correlated to the Cadeville soil series (CaC). The Cadeville soil series can physically be described as a residual soil formed in clayey marine or stream sediments over limestone. This residual soil can be further characterized as having a shallow depth, a high plasticity, a medium subangular blocky structure, predominantly moist state, medium to stiff consistency, mottled color, and having a high shrink-swell potential. The Cadeville soil series soil taxonomy classification is a fine, mixed, active, thermic Albaquic, Hapludalfs (9). The soil taxonomy implies the following two facts that are of significance in the engineering analysis of the landslide: 1) The soil series has an aquic soil moisture regime meaning that one or more subhorizons are saturated in normal years and 2) an abrupt textural change occurs between the between the A and E horizons (an ochric epipedon).

The Cadeville soil is overconsolidated due to desiccation. A complete Cadeville soil profile is presented in Figure 2, and as can be seen this soil series develops with discontinuous and fragmented limestone float underlain by shaly clays. The site geology is the Washita geologic unit (Kw), and consists dominantly of shaly clays with minor amounts of limestone (10). Based on the borings in the slide cross-sections and exposures of the limestone in the roadway cut, the limestone in the Washita unit is believed to form lenses separated by shaly clays. Further based on these cross-section borings, the slide mass has developed in the shaly clays.

The slide mass was symmetrically divided by three cross-sections, surveyed, and tied to the construction plan stations. Predominately all investigative work was concentrated on the center cross-section (cross-section B). Hand auger borings were made in the outer two cross-sections to confirm the center cross-section findings. A noticeable observation during site investigation was visibility of surface cracks within and outside the slide mass on all site visit occasions.

A total of 108 rainfall events occurred during the 42 month and 16 day period (1281 days) from the end of the cut section excavation to the date the landslide occurred. Typical

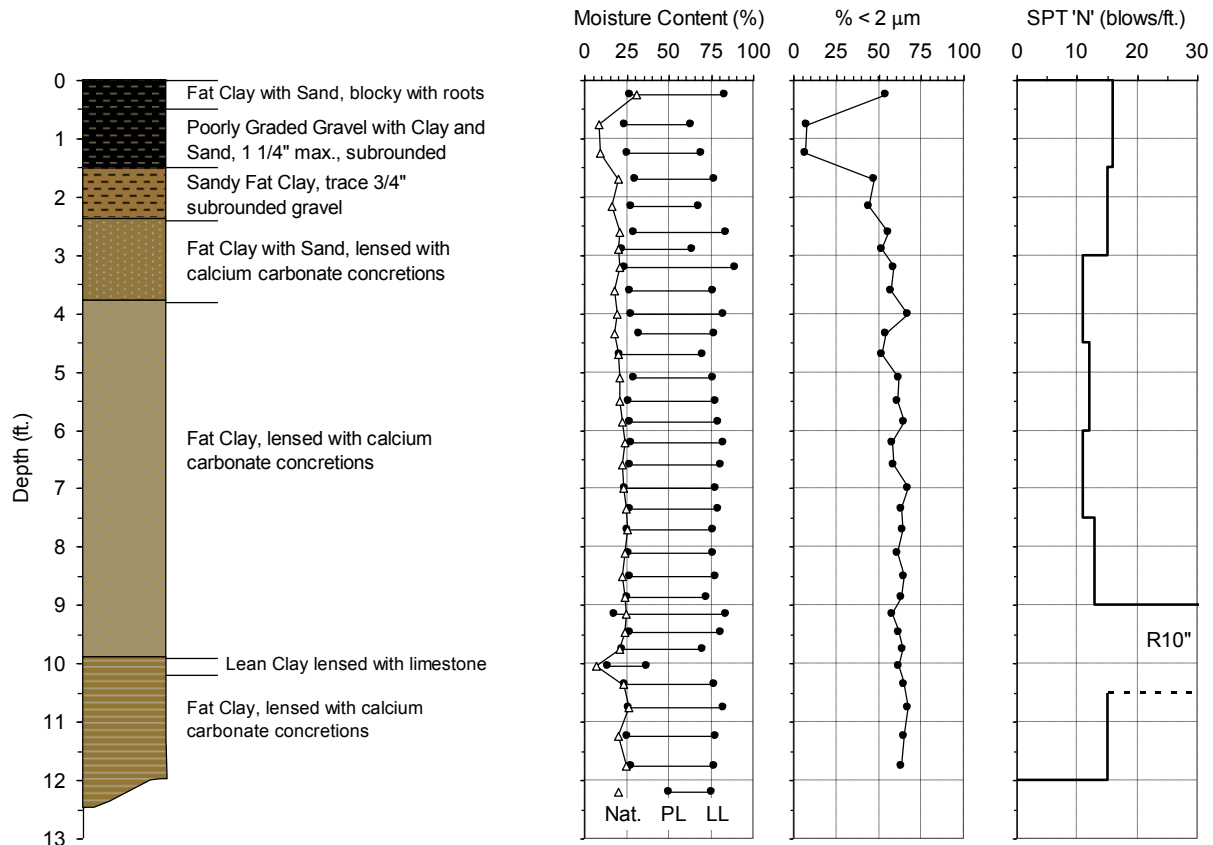


Figure 2 - Cadeville Soil Series Profile

yearly rainfall events are shown for 2003 in Figure 3, and Figure 3 is meant to show the sporadic nature of the rainfall events (highs and lows). Table 1 presents the sporadic rainfall events leading up to the slope failure. The TMI for weather data at the Idabel Mesonet Site is calculated for the time period from the start of the cut section excavation to the date the landslide occurred, see Figure 4.

GEOTECHNICAL INVESTIGATION

The geotechnical investigation consisted of two phases: an in-situ study of the center cross-section with some supplemental hand auger borings in the two outer cross-sections and a laboratory testing program. The in-situ study of the center cross-section consisted of three continuously-sampled Standard Penetration Test (SPT) borings, three CPT soundings, four continuously-sampled hand auger borings, and two continuously-sampled thin-walled tube borings. Samples from SPT and hand auger borings were taken at 0.4-ft. (0.12-m) intervals. The most recent and appropriate ASTM standards employed respectively are ASTM D 1586, D 5778, D 1452, and D 1587 for the above in situ sampling and testing. The laboratory

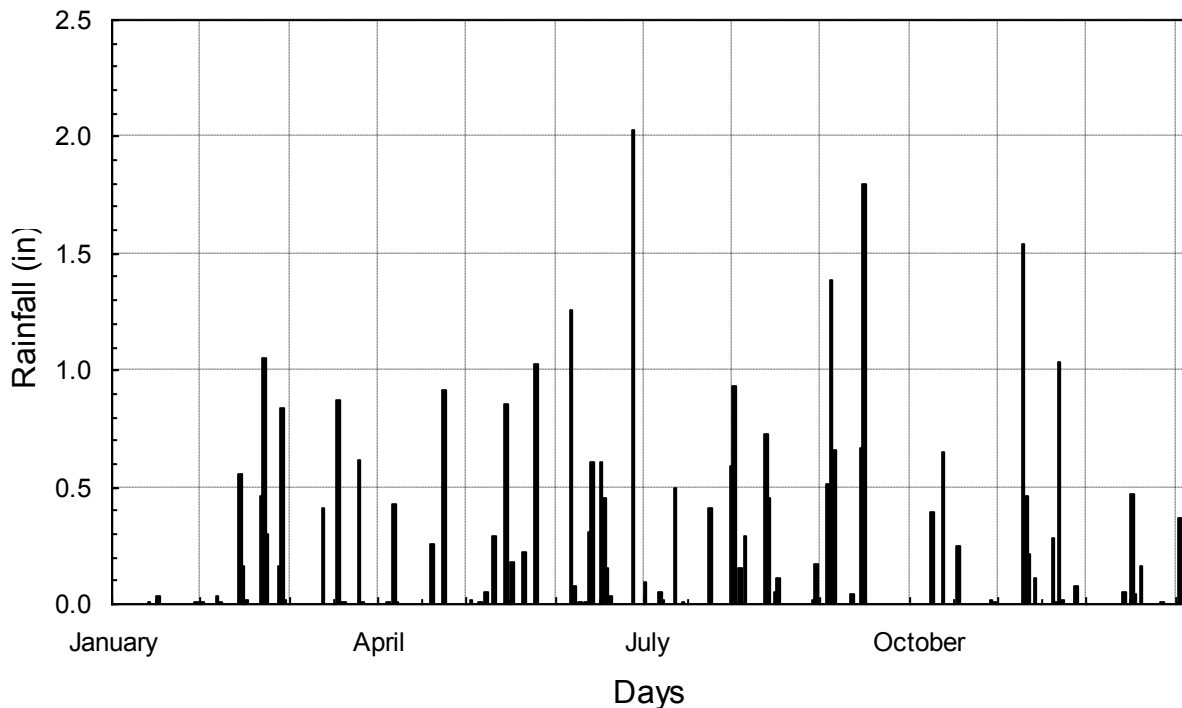


Figure 3 - 2003 rainfall

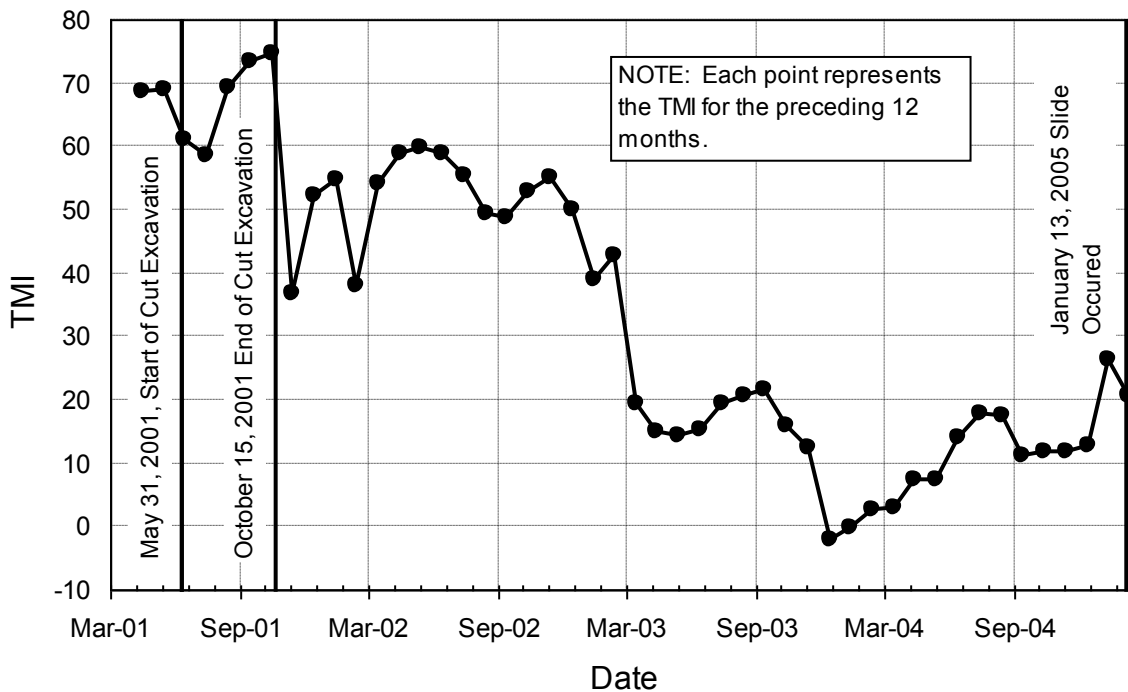


Figure 4 - Thornthwaite moisture index (TMI) at Idabel Mesonet site

Table 1 - Rainfall events preceding the slope failure

Date	Rain (in.)	Date	Rain (in.)	Date	Rain (in.)
November	1 0.54		26		21
	2		27		22 0.37
	3		28		23
	4		29 0.41		24
	5		30		25
	6	December	1		26
	7		2		27
	8		3		28
	9		4		29
	10		5 0.35		30
	11		6 0.44		31
	12		7	January	1
	13		8		2 1.43
	14		9		3 1.97
	15		10		4
	16		11		5
	17 0.45		12		6
	18		13		7 0.59
	19		14		8
	20		15		9
	21		16		10
	22 0.44		17		11
	23 1.22		18		12 1.07
	24		19		13 Slope failure
	25		20		

testing program consisted of moisture content, classification and index properties, and total wet density tests. The most recent and appropriate ASTM standards (11) applied, respectively ASTM D 2216, D 421, D 422 (including hydrometer tests), D 4318, D 2487 and AASHTO T 233.

SLOPE STABILITY ANALYSIS

The GSTABL7 with STEDwin Version 2.0 computer program was used to back-calculate the mobilized shear strength at failure. The slip surface used in this back-calculation was estimated from the landslide surface feature survey (scarp, surface geometry, and toe) and from the peak moisture depth from the moisture content versus depth profiles. The estimated slip surface is presented in Figure 5. Several slope stability techniques (modified Bishop, Janbu, random, and trial wedges) were tried and they arrived at essentially the same mobilized drained shear strength at failure ($c' = 0$, $\phi' = 14.5^\circ$). The trial wedge was selected as the most representative failure pattern for this landslide, see Figure 6. The classification of this landslide

is that of a translational slide because of the $D_r / L_r = 0.12$ and the presence of preexisting shear planes (slickensides) (7).

ANALYSIS AND DISCUSSION

Based on the climatic conditions over the past five years prior to the landslide, the climate at the site was dryer than normal. In Figure 3, the randomness of rainfall at this location is depicted and is typical over the 42 month and 16 day period prior to the landslide. Significant facts about the rainfall is that a total of 108 rainfall events occurred over the 42 month and 16 day time period leading to the landslide and the spacing of the rainfall was very similar to that shown in Figure 3 and Table 1. The TMI shown in Figure 4 shows the effect of the water balance from the start of the cut section construction until the landslide occurrence. During the cut excavation, the TMI average is slightly higher than the historical TMI average of 50, which means the climate was near normal rainfall. From the end of the cut excavation on October 15, 2001 until approximately the middle of November 2002, the TMI fluctuates yet the mean TMI in this time frame is close to the historical average TMI of 50 indicating normal rainfall. There appears to be a dramatic drop in the TMI from approximately December 2002 to the middle of December 2003, which implies a further drying condition, and corresponding increase in soil suction. Then the TMI from mid December 2003 increases, flattens out briefly, decreases briefly, and then increases until the point of failure January 13, 2005. This second period reflects a wetting up period and a decrease in soil suction.

The key points in the site characterization that contribute to this investigation are the facts that the in situ soil is highly structured (having slickensides and parallelepipeds), and the soil profile consists of high plasticity index soils, see Figure 2. Also shown in Figure 2 is the significant amount of clay content in these samples with depth. The R10 was a thin 0.4-ft (0.12-m) lens of limestone underlain by shaly clay. Looking at the back-calculated shear strength parameters from Figure 6 from the GSTABL7 program it appears that these shear strength parameters are well below the peak drained shear strength.

Aubeny and Lytton (4, 5) have recently reported on the mechanisms of stability degradation that lead to shallow slide failures in embankment slopes constructed of high plasticity clays. The failure mechanism involves moisture infiltration into the slope surface through cracks in high plasticity clays that leads to decreases in soil suction and soil shear strength. The soil shear resistance within a slide mass can be considered to be a function of the net mechanical stress and matric suction (4, 5). Such shear resistance can be characterized by a generalized Mohr-Coulomb relationship for an unsaturated soil (4, 12, 14). The difference between this recent research (4, 5) and this case study is the fact that the shallow seated landslides reported herein occurs in highly structured (slickensides and the like), naturally occurring stiff, overconsolidated clays instead of compacted high plasticity clay slopes. The torsional ring shear test was ran to establish a lower limit of shear strength resulting in a $c'_r = 0$ and a $\phi'_r = 5.3^\circ$, which is significantly lower then the back-calculated trial wedge shear strength ($c' = 0$, $\phi' = 14.5^\circ$).

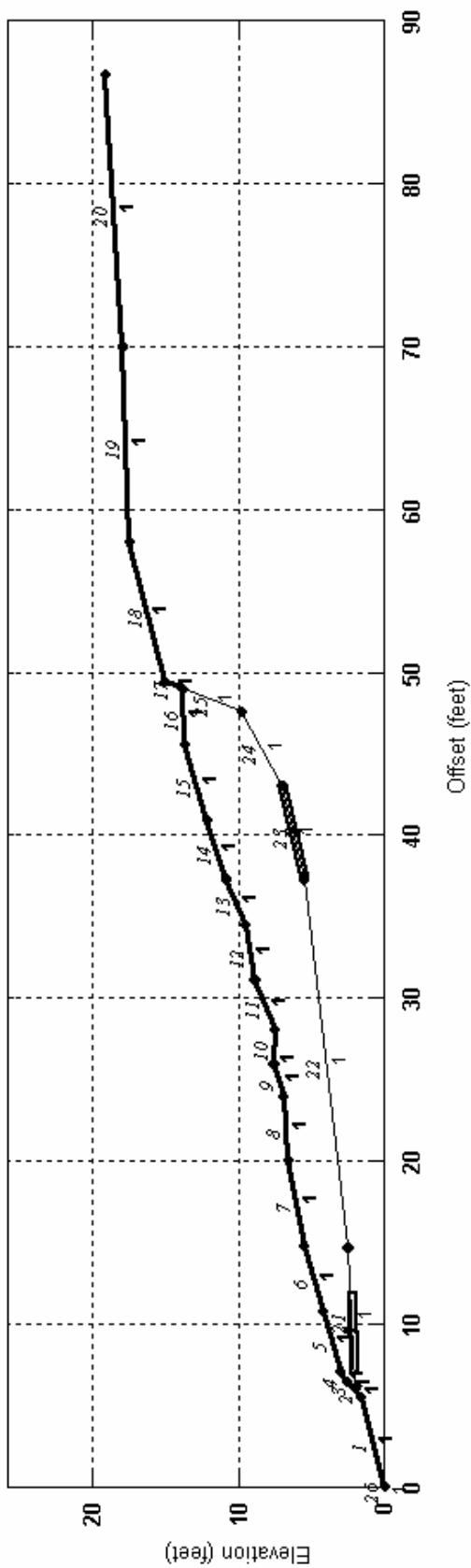


Figure 5 - Estimated slip surface for center cross-section

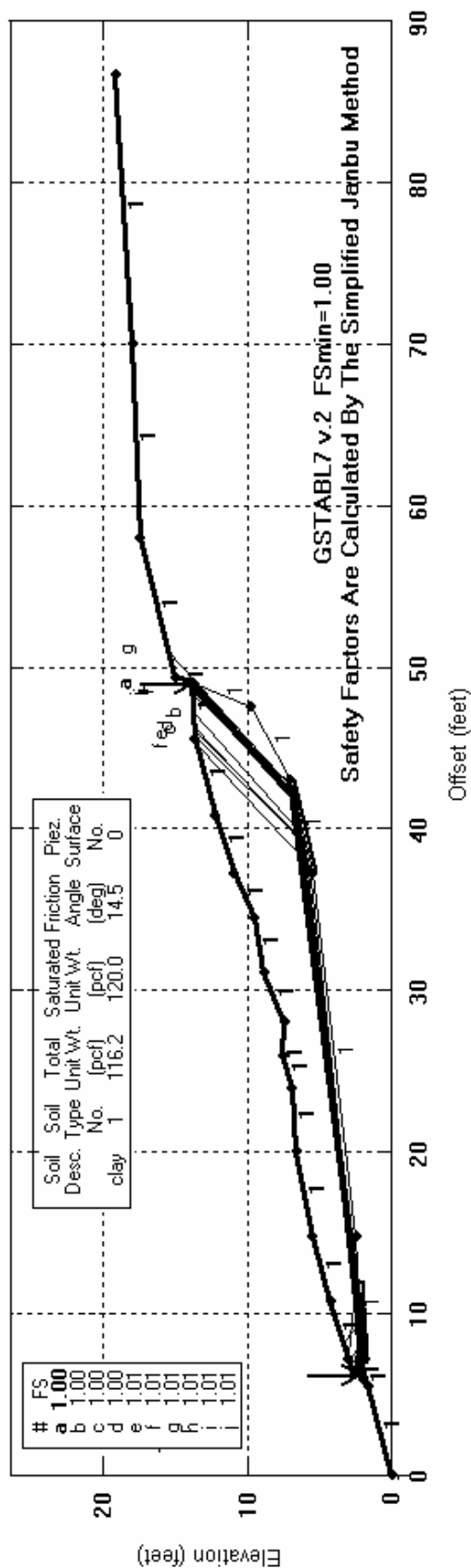


Figure 6 - Trial wedge at failure ($c' = 0, \phi' = 14.5^\circ$)

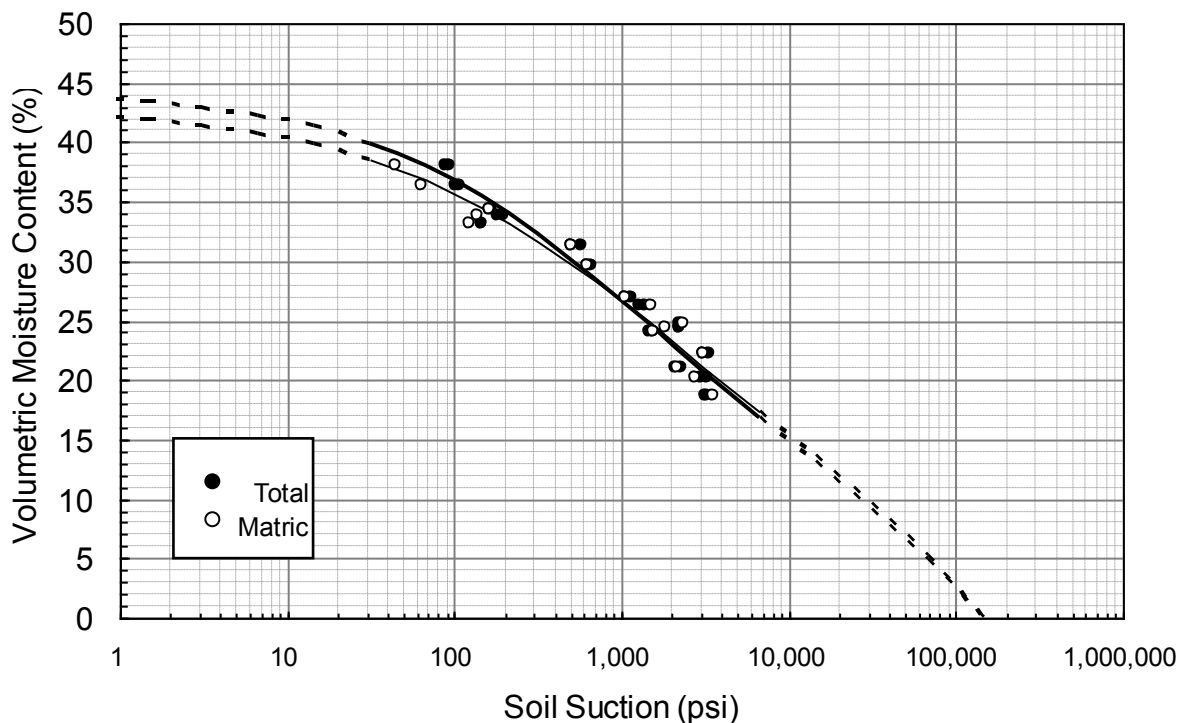


Figure 7 - Soil-Water Characteristic Curve

From the SWCC shown in Figure 7, the matric suction developed for volumetric moisture contents reported in Table 2 appears to develop in the range up to 3600 psi (25,000 kPa) in this soil slope and slide mass. It has been reported by Lu and Likos (12) that at high soil suctions, the total soil suction is dominated by and nearly equal to the matric soil suction. Recalling from Figure 4 there is a dramatic drop in TMI indicating an increase in soil suction from mid December 2002 to mid December 2003 and then there gradual increase in TMI, a flattening off, a sudden drop, a gradual increase, and finally a sharp increase from mid December 2004 to the time of failure on January 13, 2005. From mid December 2004 to January 13, 2005 based on the TMI there is a sharp decrease in soil suction. A decrease in soil suction further means a reduction in shear strength. There is a relatively well-used correlation between total soil suction and TMI by Russam and Coleman (15). A revised correlation between the TMI and total soil suction (D. R. Snethen, personal communication) was used to estimate total suction. Using this revised correlation, total suction was estimated from mid-October 2002 to the time of failure, see Figure 8 and Table 3. As can be seen, the total suction steadily increases until December 2003, and then decreases until December 2004. Slide A occurs after a dramatic drop in total suction.

Table 2 - Saturation and Volumetric Moisture Content from Thin-Walled Tube Samples

Sample	Depth (feet)	Gravimetric Moisture Content (%)	Dry Unit Weight (pcf)	Moist Unit Weight (pcf)	Degree of Saturation (%)	Volumetric Moisture Content (%)
4F1	2.3 - 2.6	39.4	72.4	101.0	79.8	45.8
4F2	2.6 - 3.1	27.6	91.1	116.2	86.8	40.2
4F3	3.1 - 3.4	16.8	105.6	123.3	75.1	28.4
	3.4 - 4.0	-	-	-	-	-
4G1	4.0 - 4.4	21.9	93.2	113.6	72.4	32.7
4G2	4.4 - 4.9	22.7	95.8	117.5	79.8	34.8
4G3	4.9 - 5.3	20.5	93.3	112.4	67.9	30.6
4G4	5.3 - 5.8	21.1	99.7	120.8	81.6	33.7
4G5	5.8 - 5.9	20.9	96.3	116.4	74.4	32.2
	5.9 - 6.0	-	-	-	-	-
4H1	6.0 - 6.5	22.1	99.1	121.0	84.2	35.0
4H2	6.5 - 7.0	23.0	99.1	121.9	87.8	36.5
4H3	7.0 - 7.3	23.2	80.6	99.3	57.0	30.0
5G1	4.0 - 4.4	(14.0)	(99.4)	113.3	(53.8)	(22.3)
5G2	4.4 - 4.8	(20.7)	(94.1)	113.5	(69.9)	(31.2)
5G3	4.8 - 5.3	(13.9)	(103.6)	118.0	(59.1)	(23.1)
5G4	5.3 - 5.6	(12.8)	(106.1)	119.7	(58.1)	(21.8)
5G5	5.6 - 6.0	(20.0)	(101.7)	122.0	(81.2)	(32.6)
5H1	6.0 - 6.6	23.4	98.8	121.9	88.5	37.0
5H2	6.6 - 7.2	24.9	95.8	119.7	87.6	38.2
5H3	7.2 - 7.5	(21.3)	(87.7)	106.4	(61.9)	(29.9)
				Range:	53.8 - 88.5	21.8 - 45.8

Values in parentheses are estimated from adjacent borings

Dashes (-) indicate missing data

Lytton (4, 5) has found the practical limit of wetting to be near a matric suction of 1.5 psi (10 kPa). If this value is assumed to exist on the previously identified slip surface, the modified shear strength can be determined by:

$$\tau_f = (\sigma_n - u_a) \tan \phi + (u_a - u_w) f \tan \delta$$

where

- τ_f = shear strength at failure, psi
- σ_n = total normal stress on slip surface, psi
- $(u_a - u_w)$ = matric suction on slip surface, psi
- u_a = pore air pressure, assumed negligible, psi
- u_w = pore water pressure, psi

- f = coefficient which is a function of degree of saturation (4)
 θ = volumetric moisture content (as decimal)
 ϕ' = angle of internal friction for saturated, drained conditions, degrees

For matric suction near 1.5 psi, the product $f\theta$ approaches unity. When the shear strength term due to suction is taken into account, the back-calculated angle of internal friction drops to 6.3° for a F.S. =1.0.

In summary, it can be concluded that the site was in an unsaturated soil state prior to the occurrence of slide A. The cyclic infusion of moisture into a highly structured and cracked natural clay slope affects the net mechanical stress and matric suction (total) components of the shear resistance in the slide mass. With regard to the matric soil and total suction in this case history Figure 8 clearly shows variation in total suction leading to a dramatic drop just prior to the landslide occurring.

However, the mobilized shear strength for this landslide appears to be close to the fully-softened shear strength for a first time landslide and not the estimated shear strength related to the unsaturated soil condition. In Figure 9, a summary of the shear strength for the cut section estimated for the design 3:1 slope. Since the occurrence of slides B and C, the question is what actually is the safe cut section slope ratio with regard to first time landslide development. Using the back-calculated assumed fully softened shear parameters in Figure 6 ($c' = 0$ and $\phi' = 14.5^\circ$) in Figure 7 a FS = 1.68 was found by flattening the existing slope to a 4:1 slope ratio.

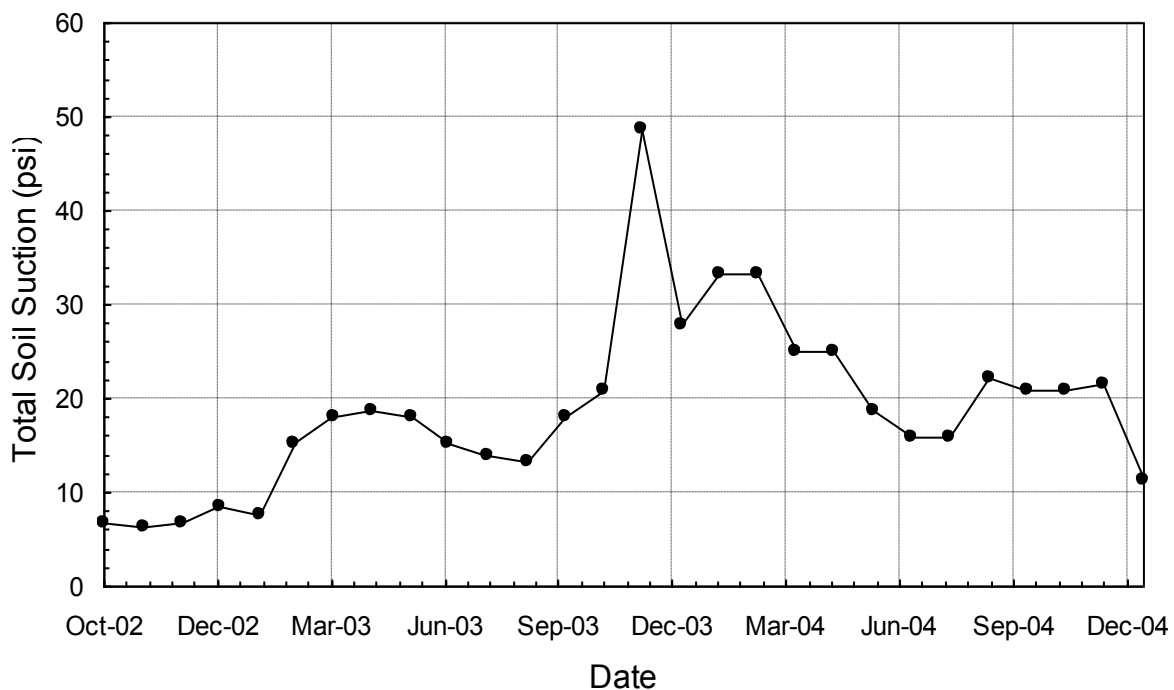


Figure 8 – Time versus Estimated Total Soil Suction

Table 3 - Time versus Estimate Total Soil Suction

Date	TMI	Total Soil Suction (psi)	Climatic Category
October-02	52.9	6.67	Humid
November-02	55.0	6.39	Humid
December-02	50.0	6.81	Humid
January-03	38.9	8.47	Humid
February-03	42.6	7.64	Humid
March-03	19.3	15.3	Moist Subhumid
April-03	15.0	18.1	Moist Subhumid
May-03	14.4	18.8	Moist Subhumid
June-03	15.2	18.1	Moist Subhumid
July-03	19.4	15.3	Moist Subhumid
August-03	20.7	13.9	Moist Subhumid
September-03	21.6	13.2	Moist Subhumid
October-03	15.8	18.1	Moist Subhumid
November-03	12.4	20.8	Moist Subhumid
December-03	-2.0	48.6	Humid
January-04	-0.3	27.8	Humid
February-04	2.7	33.3	Moist Subhumid
March-04	2.8	33.3	Moist Subhumid
April-04	7.3	25.0	Dry Subhumid
May-04	7.3	25.0	Dry Subhumid
June-04	13.9	18.8	Moist Subhumid
July-04	17.7	16.0	Moist Subhumid
August-04	17.5	16.0	Moist Subhumid
September-04	11.0	22.2	Moist Subhumid
October-04	11.8	20.8	Moist Subhumid
November-04	11.9	20.8	Moist Subhumid
December-04	12.9	21.5	Moist Subhumid
January-05	26.3	11.4	Humid

CONCLUSION

In summary, we conclude from this case history the following points:

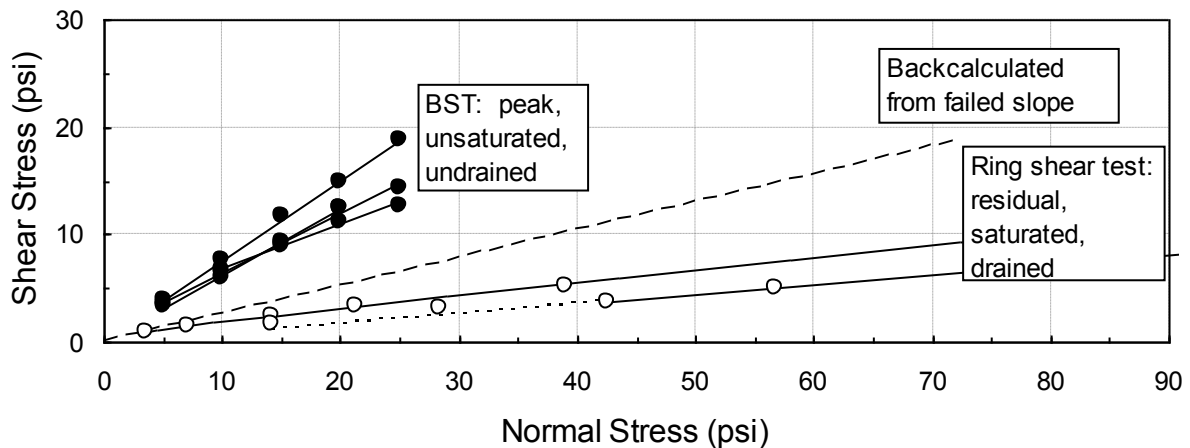


Figure 9 - Range of Shear Strengths

1. This case study concerns a problem in unsaturated soil mechanics. The site characterization describes an essentially dry soil condition developing following the cut section construction. Qualitative evidence based on the TMI suggests that soil suction varies considerably at this landslide site.
2. Matric suction and total soil suction play key roles in the triggering mechanism equation. The application of shear strength based on unsaturated soil mechanics (employing matric suction) has great potential. However, utilization of the approach stems on a practical coupling of the matric suction in shear strength measurement.
3. This case history appears to lend credence to the degradation of the internal angle of friction of the soil towards a fully-softened value. The cyclic effect of water infiltration into a cracked soil structure was evidently enough for the development of the large cumulative shear strains needed for the development of the full-softened shear strength condition.
4. From Figure 9 the logical conclusion is that the assumed fully softened shear parameters ($c' = 0$ and $\phi' = 14.5^\circ$) is the most likely mobilized shear strength at the time of failure.

REFERENCES

1. Bromhead, E. N. *The Stability of Slopes*. 2nd Edition. Blackie Academic & Professional, London, 1992.
2. Abramson, L. W., T. S. Lee, S. Sharma, and G. M. Boyce. *Slope Stability and Stabilization Methods*. John Wiley & Sons, Inc., New York, 1996.
3. Cornforth, D.H. *Landslides in Practice: Investigation, Analysis, and Remedial/Preventative Options in Soils*. John Wiley & Sons, Inc., New Jersey, 2005.
4. Aubeny, C. P. and R. L. Lytton. *Long-Term Strength of Compacted High-PI Clays*. Report No. FHWA/TX-03/2100-1, Texas Transportation Institute, College Station, Texas, 2003.
5. Aubeny, C. P. and R. L. Lytton. Shallow Slides in Compacted High Plasticity Clay Slopes. *ASCE Journal of Geotechnical and Geoenvironmental Engineering*, Vol. 130, No. 7, 2004, pp. 187-197.
6. Duncan, J. M. and S. G. Wright. *Soil Strength and Slope Stability*. John Wiley & Sons, Inc., New Jersey, 2005.
7. Turner, K.A., and R. L. Schuster. *Landslides: Investigation and Mitigation*. Special Report No. 247, TRB, National Research Council, Washington, D.C., 1996.
8. *Soil Survey for McCurtain County, Oklahoma*. United States Department of Agriculture, Soil Conservation Service, Washington, D.C., 1974.
9. Buol, S. W., F. D. Hole, R. J. Southard, R. C. Graham, and P. A. McDaniel. *Soil Genesis and Classification*. 5th Edition. Iowa State Press, Ames, Iowa, 2003.
10. Hartronft, B. C., C. J. Hayes, and W. McCasland. *Engineering Classification of Geologic Materials, Division Two*. Oklahoma Department of Highways, Research and Development Division, Oklahoma City, Oklahoma 1966.
11. American Society for Testing and Materials (ASTM) 2005 Section 4, Volume 04.08 Soil and Rock (I), West Conshohocken, Pa.
12. Lu, N., and W. J. Likos. *Unsaturated Soil Mechanics*. John Wiley & Sons, Inc., New Jersey, 2004.
13. Fredlund, D.G., and H. Rahardjo. *Soil Mechanics for Unsaturated Soils*. John Wiley & Sons, Inc., New York, 1993.
14. Russam, K., and J. D. Coleman. The Effect of Climate Factors on Subgrade Moisture Conditions. *Geotechnique*, Vol. 11, 1961, pp. 22-28.

Rockfall Mitigation Field Techniques and Design

Dane A. Wagner
KANE GeoTech Inc.
7400 Shoreline Drive, Suite 6
Stockton, CA 95219
(209) 472-1822
dane.wagner@kanegeotech.com

William F. Kane
KANE GeoTech Inc.
7400 Shoreline Drive, Suite 6
Stockton, CA 95219
(209) 472-1822
william.kane@kanegeotech.com

Prepared for the 61st Highway Geology Symposium, August 2010

Disclaimer

Statements and views presented in this paper are strictly those of the authors, and do not necessarily reflect positions held by their affiliations, the Highway Geology Symposium (HGS), or others acknowledged above. The mention of trade names for commercial products does not imply the approval or endorsement by HGS.

Copyright Notice

Copyright © 2010 Highway Geology Symposium (HGS)

All Rights Reserved. Printed in the United States of America. No part of this publication may be reproduced or copied in any form or by any means – graphic, electronic, or mechanical, including photocopying, taping, or information storage and retrieval systems – without prior written permission of the HGS. This excludes the original author(s).

ABSTRACT

Rockfall is a geologic hazard that results in the catastrophic loss of life and substantial property damage to roadways, railways, and infrastructure. Over the past fifty years, rockfall mitigation practice has seen rapid advancement, with the greatest technological strides occurring in the last ten years. During this time, the design methodology has also matured from empirical field methods to a system of quantitative analysis producing design loads and forces. The design of mitigation systems must take into account a variety of factors and physical characteristics to properly provide safety. Current design practices today focus on both the safety and economic costs of mitigating hazardous slopes by involving a qualified geotechnical investigation and analysis with a consideration on practicality. Analysis methods such as the Rockfall Hazard Rating System (RHRS) and the Colorado Rockfall Simulation Program (CRSP) have allowed for the determination of site specific mitigation options. Choosing the proper mitigation approach must incorporate analyses with crucial information from the field and may involve active, passive, or a combination of mitigation solutions. After the proper mitigation system has been selected for the specific site, system design incorporates the quantitative data from the analyses to engineer for the variety of loads subjected upon the system; including those on the system, the foundation, and the anchors and/or bolts. This paper reviews the state of current rockfall mitigation practice and provides a comprehensive approach to analysis and design for use by geologists and engineers.

INTRODUCTION

In this paper “rockfall” is defined as “the movement of rock of any size from a slope that is so steep that the rock continues down slope. Movement may be by free-falling, bouncing, rolling, or sliding”. The fall may involve more than one rock but does not include large volumes of rock, rock avalanches, or landslides including rock (1).

Rockfall is a naturally occurring geologic condition that creates a hazard to transportation routes, structures, and human life. The failure to recognize this hazard can be catastrophic. As human activity increases in and around steep, rocky slopes, ethical considerations and increased liability requires an emphasis on rockfall hazard mitigation. Rockfall exists as the result of natural and human activities that create slopes in which rocks move down slope under the force of gravity. This natural hazard results in millions of dollars spent in mitigation or maintenance of hazardous slopes.

The first comprehensive attempt to review rockfall mitigation methodology was made by Brawner (2). This guide explains the causes of rockfall, rock slope failure modes, investigation, analysis, mitigation, and provides specifications and construction guides. Since its publication, the procedures for evaluating rockfall hazard and the technology have evolved. The purpose of this paper is to provide an introduction to rockfall mitigation and provide a guideline to:

1. Approach potential rockfall hazards in the field
2. Site analysis
3. The design of practical and economical solutions

Due to the numerous factors that contribute to rockfall and the hazards associated with it this paper is not intended to be a comprehensive treatment of the subject. Readers should refer to the reference list for more detailed discussions of the various aspects of rockfall mitigation.

PREVIOUS WORK

Ritchie (3) provided one of the earliest guides to rockfall mitigation. He produced a practical guideline on the identification and mitigation of rockfall hazards based on field experience rather than on the theory of rock mechanics. The result of his investigation was the development of a table showing recommended mitigation methods for differing slope heights and angles. The measures consisted of the installation of barriers and catchment ditches, Figure 1. Ritchie (3) showed only the locations of barriers and did not specify barrier heights or energy capacities.

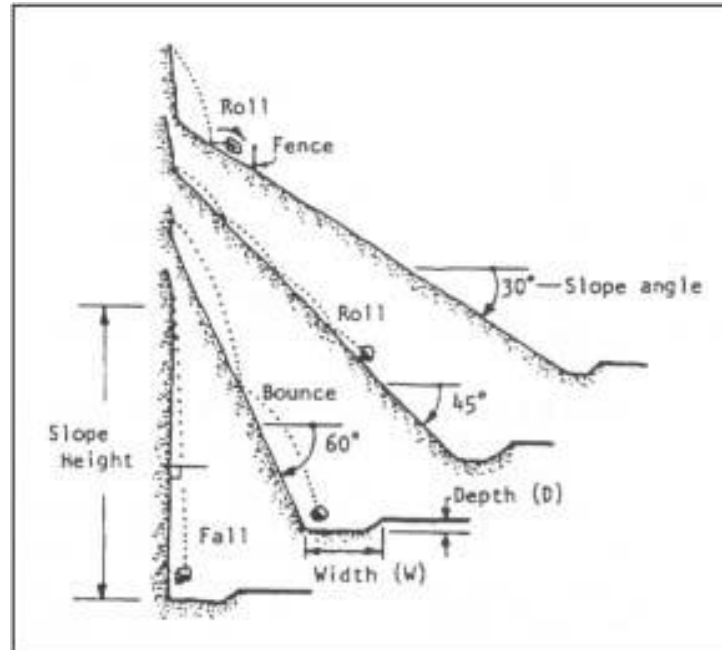


Figure 1 - Rockfall Travel Modes (3)

The development of rockfall barriers that can be built to specifications regarding height and energy absorbance led to the simultaneous development of computer simulation programs. These programs simulate rockfall events for a particular location and provide a consistent prediction of rockfall bounce heights and energies. Foremost among these was the Colorado Rockfall Simulation Program (CRSP) developed by Jones and Higgins (4). Correlated with field data, CRSP provides an alternative to actually test-rolling rocks at site, which in most cases is time consuming and impractical.

At the same time, some method of assessing the risk of rockfall was necessary. The Rockfall Hazard Rating System (RHRS) (5) was created for highway departments as a way to quantify the relative hazard rate by providing a numerical value for each slope and therefore prioritize mitigation and optimize the allocation of resources. This, in turn, had the effect of reducing liability by treating the most hazardous slopes first. The original RHRS was produced by the Oregon Department of Transportation; since then many states have adopted the RHRS and made modifications to suit their needs.

ROCKFALL HAZARD IDENTIFICATION

The first step to identifying potential rockfall hazards is the determination of the cause(s) of the rockfall. In many situations more than one factor can contribute to the hazard. The two major causes of rockfall are the structural features of the rock unit and the lithology of the rock unit or units. Other factors, in combination with unfavorable geology that can also influence rockfall are groundwater, animals, and vegetation.

The important geologic structural discontinuities include the bedding, jointing, and faulting of the rock mass. Bedding is the plane of contact between the layers of

differing textures of rock. Jointing is a defined crack in the rock where no movement has occurred. Joint sets are relatively regular-spaced, parallel or sub-parallel joints that can divide the rock into blocks. A fault is a fracture along which movement has occurred.

Groundwater can cause high pore water pressure within joints, reducing effective stress along the joint, and causing movement. Expansion of ice can force blocks to move out and fall. Alternatively, thawing of soft material beneath boulders can reduce support and lead to movement. Burrowing animals can also undermine and reduce rock support. Also, root wedging into joints and fractures can be responsible for many rockfall events.

ROCKFALL HAZARD INVESTIGATION PRACTICE

Preliminary Work

The first step in rockfall hazard mitigation usually is field work to collect data for analysis and to determine the relative risk involved. The Rockfall Hazard Rating System (RHRS) is used to compare and determine the greater hazard between locations. Required field data includes information on the rock slope structure: beds, faults, and joint dips and dip direction are recorded as these are considered the greatest factors in the development of rockfall (5). However, in some situations the materials are unconsolidated talus slopes or boulders weathered out of a fine grained matrix such as glacial till.

The slope profile for each rockfall analysis will be different and vary in slope height, slope angle, rock type, slope surface, soil cover, and vegetative cover. The slope profile cross-section should include the rockfall source area, contour changes along the slope, the slope base, and the run-out distance for the rockfall. The slope height is significant because the rockfall source area will contribute to the energy of falling rock, the higher the source area the more potential energy. The slope angle may be the greatest factor affecting the velocity and mode of a falling rock (3). Therefore, it is important to have an accurate slope angle for analysis. The slope angle can be determined from a topographic map or in the field. If the slope is determined in the field the slope profile should reflect changes in the slope angle.

The slope surface greatly affects the trajectory of rock moving down slope. The regularity or irregularity of the slope is a major factor in determining if the rock rolls, bounces, or slides; rock shape is the other major factor. An irregular slope will provide locations for rocks to bounce or launch away from the slope. The common rock shapes are spherical, cylindrical, and discoidal. The hardness of the slope will also affect how the rock behaves and how energy is transferred, harder slopes will not absorb energy but a softer soil slope will transfer energy to the slope as the rock impacts the surface. Soil thickness and type should be recorded as a thick layer of loose soil would reduce rockfall energy impact. Vegetation cover can also have an affect by reducing the velocity and bounce heights (2).

The accuracy at which topographic maps are available for sites is variable at best. Some topographic maps may only be available at a 1:24,000 scale, commonly lacking the detail needed for accurate slope data. The accuracy of the slope profile will affect the analysis, thus it is important to obtain the most accurate topographic maps possible. While the use of LIDAR or similar mapping provides an extremely accurate model of topography, in many cases it is not yet cost effective. When an accurate topographic map is not available to create a cross-section of the rock face then a cross-section will need to be created with special consideration taken for the roughness of the slope as it greatly affects rockfall trajectories.

Run-out distance and or ditches are vital during analysis and design because they affect the mitigation options. Run-out distance can lower energy of a falling rock and reduce barrier size. Ditches can also reduce rockfall energy or contain rockfall.

ANALYSES

Rockpack III (Stereographs)

Modeling rock slopes for stability involves two phases: kinematic analyses and limiting equilibrium analyses. A kinematic analysis is performed initially using field data and estimated joint strength parameters. It serves as a “first cut” to identify rock masses that require further analysis and could theoretically fail based largely on geometry. The second phase, limiting equilibrium, involves examining those slopes which may be close to failure.

Kinematic analysis is conducted to eliminate locations that are of low concern with regard to instability. Analyses involve plotting stereonet with an estimated friction angle and determining which discontinuities daylight in the cut face and are steeper than the friction angle.

Stereographic projection is a graphical method of representing three-dimensional geologic features (such as joints, faults, etc.) in two dimensions. On stereographic projection, a plane is represented as a curved line called a great circle. Linear features (dip vectors or the intersection of planes such as a wedge) are represented as points.

Kinematic analysis involves plotting stereonet for the various discontinuities using dip vectors to represent the orientation of the joints and a great circle to represent the slope face. The estimated internal angle of friction for the discontinuities is drawn as an inner circle offset from the hemispherical circle by a distance measured in degrees of friction angle.

Dip vectors of discontinuities plotting within the friction angle circle, that is, dipping steeper than the coefficient of friction for the discontinuity, and less than the dip of the bench or slope face, that is, “day lighting” in the slope, have the potential for failure. Experience has shown that the dip vector must also trend within $\pm 20^\circ$ of the bench/slope dip vector trend (6).

Wedge failures, formed by the intersection of two discontinuities, can be assessed in a similar manner. Joint intersections plotting within the friction circle, and less than the bench or slope face dip, have failure potential.

Once the slopes most susceptible to sliding have been identified, limiting equilibrium analysis is used to estimate a factor of safety against sliding. Limiting equilibrium is based on a comparison of the sum total of forces resisting sliding to the sum total of forces tending to cause the rock mass to move down-slope, the “safety factor.” Resisting forces are functions of the strength of the joint and the normal component of weight across the discontinuity. Driving forces consist of the component of weight acting parallel to the discontinuity. Water can increase the driving forces and decrease the resisting forces.

In general, a safety factor of 1.5 for static conditions and 1.1 for seismic conditions is considered satisfactory for potential planar features. Although for temporary slopes, such as temporary cuts and some mine slopes, safety factors as low as 1.05 may be acceptable.

Rockfall Hazard Rating System

The Rockfall Hazard Rating System (RHRS) is used to rate a rock slope for potential instability due to rockfalls (5). It is primarily used by various state departments of transportation in the United States to rate and list highway rock cut sections that may need stabilization. However, it can also be applied to other situations where rock slopes exist such as mining and quarry operations. RHRS involves two phases of inspection: an initial assessment phase and the detailed rating phase.

The initial assessment phase categorizes slopes as either A, B, or C based on overall hazard. A-rated slopes indicate high hazard probability. C-rated slopes indicate low hazard probability. Slopes receiving an A-rating are investigated further and are given priority while B-rated slopes, because of their low to moderate hazard, are investigated as thoroughly as temporal limitations allow. C-rated slopes are not investigated beyond the preliminary rating phase because of their low level of hazard (5). Slopes categorized by an A-rating are codified using the detailed rating phase. The system of rating slopes as A, B, or C requires skilled and experienced personnel in the area of rockfall mitigation.

The detailed rating phase and score calculation is derived from twelve categories influencing the overall rock stability of a slope and its associated risk, Figure 2. The scoring scale ranges from 1 to 100 and is determined with an exponential function. A higher score indicates a higher hazard level. Thus, addressing the higher hazard areas with priority reduces liabilities as the most hazardous and rotationally dangerous slopes are mitigated first.

CATEGORY		RATING CRITERIA AND SCORE				
		POINTS 3	POINTS 9	POINTS 27	POINTS 81	
SLOPE HEIGHT		25 FT	50 FT	75 FT	100 FT	
DITCH EFFECTIVENESS		Good catchment	Moderate catchment	Limited catchment	No catchment	
AVERAGE VEHICLE RISK		25% of the time	50% of the time	75% of the time	100% of the time	
PERCENT OF DECISION SIGHT DISTANCE		Adequate site distance, 100% of low design value	Moderate sight distance, 80% of low design value	Limited site distance, 60% of low design value	Very limited sight distance, 40% of low design value	
ROADWAY WIDTH INCLUDING PAVED SHOULDERS		44 feet	36 feet	28 feet	20 feet	
GEOLOGIC CHARACTER	CASE 1	STRUCTURAL CONDITION	Discontinuous joints, favorable orientation	Discontinuous joints, random orientation	Discontinuous joints, adverse orientation	Continuous joints, adverse orientation
		ROCK FRICTION	Rough, irregular	Undulating	Planar	Clay infilling or slickensided
	CASE 2	STRUCTURAL CONDITION	Few differential erosion features	Occasional erosion features	Many erosion features	Major erosion features
		DIFFERENCE IN EROSION RATES	Small difference	Moderate difference	Large difference	Extreme difference
BLOCK SIZE		1 FT	2 FT	3 FT	4 FT	
QUANTITY OF ROCKFALL/EVENT		3 cubic yards	6 cubic yards	9 cubic yards	12 cubic yards	
CLIMATE AND PRESENCE OF WATER ON SLOPE		Low to moderate precipitation, no freezing periods, no water on slope	Moderate precipitation or short freezing periods or intermittent water on slope	High precipitation or long freezing periods or continual water on slope	High precipitation and long freezing periods or continual water on slope and long freezing periods	
ROCKFALL HISTORY		Few falls	Occasional falls	Many falls	Constant falls	

Figure 2 - Rockfall Hazard Rating System Chart (5)

Colorado Rockfall Simulation Program

It is possible to estimate how far a rock will travel along a slope by conducting actual rock rolling tests. While these tests may be useful in verifying criteria, they can be expensive and are limited by the small number of rocks that can be rolled. In contrast, literally thousands of simulated rolls can be made using the Colorado Rockfall Simulation Program (CRSP). CRSP uses a computer algorithm based on actual rockfall tests to predict the distance a rock will stop from the toe of a slope, the velocity of the rock, how high the rock is likely to bounce, and the kinetic energy of the rock at any

point. The program requires a slope profile and an estimate of parameters such as rock unit weight and size, slope roughness, and normal and tangential coefficients of restitution along the slope. CRSP can then compute the dynamic parameters of rockfall events, that is, the velocity, kinetic energy, and bounce height.

By modeling a slope using CRSP, it is possible to make some reasoned judgments on the need for rockfall mitigation such as a fence or barrier, wire mesh drapery, a berm, or rock bolting. If mitigation is indicated, it provides data to aid in the selection and design of a rockfall mitigation system. The CRSP algorithm has been validated by field data. It is routinely used as a design tool by many state highway transportation departments.

When using CRSP as a resource for a given site the investigation should include representative profiles derived from the field investigation and topographic map, necessary information for determination of surface conditions, information on boulder sizes, shapes, and properties. The representative path of a given rock or boulder will vary on the slope conditions unique to the site. In this respect it is important to model the path of the moving rock. The representative path may be directly down slope or be redirected into a chute or channel. An up-to-date and properly scaled topographic map is a critical tool in the investigation and will provide the proper input data. The slope surface conditions will affect the manner in which the rock will travel down-slope. Rocks traveling on a smooth slope will more likely roll on the slope in comparison with an uneven slope which can cause the rock to bounce and launch into the air. The difference in the hardness of the slope also plays a major role in the energy of the traveling rock; a hard bedrock slope will absorb and dissipate less energy than an unconsolidated soil slope. The boulder size and shape affects the trajectory and velocities of the rockfall. The dimensions of the boulder and the unit weight will provide a mass, which in combination with the velocity will provide the energy of the traveling boulder. The shape of the boulder greatly affects the trajectory as differing geometries will cause rolling, sliding, flipping, and bouncing.

Analyses Points (AP) represent locations on the slope profile in which data of the traveling rock for the individual location can be obtained. The output data that can be obtained at the AP include energies and bounce heights. Analyses Points should be placed at significant locations to characterize the rockfall behavior and to evaluate the necessary rockfall mitigation and impact energies at those locations. Velocity, bounce heights, and kinetic energies can be determined at these locations. Figure 3 shows a typical CRSP output profile with analysis points.

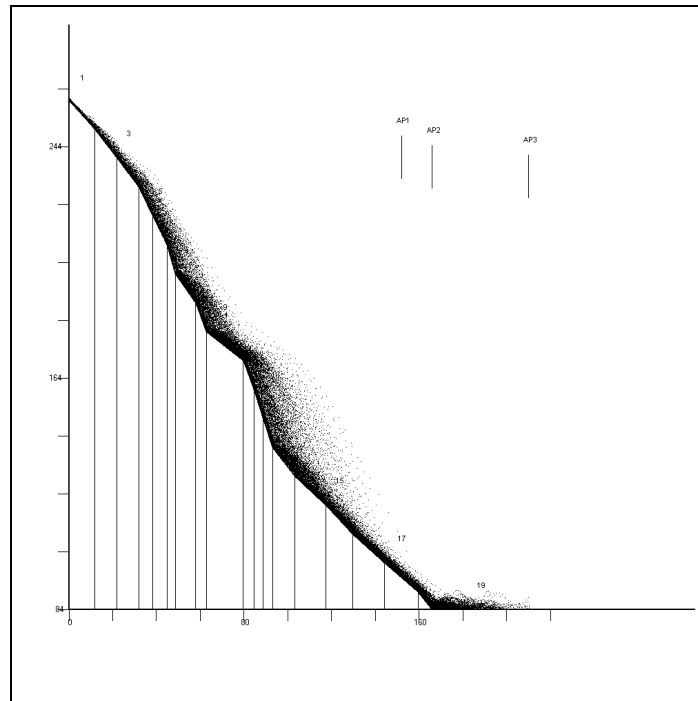


Figure 3 - Typical CRSP Profile Showing Analysis Points (AP#)

MITIGATION METHODS

After analyses are performed and an understanding of the potential hazard is determined, a mitigation option that best fits the site can be chosen. It must be emphasized that each site has individual characteristics which may include property boundaries, access, constructability, maintenance, design life, and cost. All factors should be considered as each factor can and does influence the others.

The mitigation methods for the prevention of rockfall and rockfall hazards can be separated into three areas: stabilization, protection, and warning (1) (2).

Stabilization / Protection / Warning

Stabilization is the reduction of driving forces and/or the increase of resisting forces associated with the failure, thus preventing movement of hazards down-slope. The stabilization of rockfall on slopes can be accomplished by: excavation, scaling the slope or reducing slope angle, reduction of pore water pressure, or installation of a support system (1). Combinations of all these approaches are often used as well.

Protection allows failure to occur in the form of rockfall, but prevents the hazard from reaching the protected facility. Protection is accomplished by structures that stop or store rockfall, re-direct rockfall, or avoid the hazard (2).

Warning and instrumentation can provide data and information on occurring movement or an immediate warning that a failure has occurred. Warning systems are valuable tools and can prevent major disasters from occurring. Warnings can be provided by as little as a posted sign or include a comprehensive instrumentation program with remote access and alerts for road or rail closures.

Active Systems

Active systems are characterized by a force that is applied to the slope to prevent the down-slope movement of rock. This can come in the form of a pressure applied to a rock by tensioned rock bolts or a tensioned anchored mesh. It can also take the form of an addition to the resisting forces that can prevent movement such as dowels or buttresses.

Anchored Mesh

Anchored mesh systems actively apply pressure to the rock face to prevent movement of the rocks on the slope. Anchors are drilled and installed, mesh is placed, and the anchors tensioned. The load is applied to the anchors and is transferred to the mesh which is actively putting a force on the slope. It is important that a high strength mesh be used because the load of the tensioned anchors is transferred to the slope by the mesh. Wire mesh, such as standard chain link and double twisted wire mesh are not suitable in an active anchored system. This is because the material is of low strength leading to plastic deformation and failure under the loading conditions. High strength materials are made from high tensile strength steel with roughly four times the tensile strength. However, high strength steel will not deform plastically and will rupture abruptly when the failure limit is reached.

Pinned cable nets can be an affordable alternative, albeit with certain limitations. Wire rope strengths and cable connections need to meet loading requirements. When cable nets are used in anchored systems it is important to use cable nets without clips at the intersections. The clips can pop off under tensioning or loading, leaving loose wire ropes. Wire rope cable nets also expose more surface area corrosion; this should be considered in the life of the system.

Bolting

A rock bolt is a tensioned bar that actively applies a force. It is installed by drilling a hole in the rock and inserting a threaded or deformed bar in the middle of the hole and then grouting a determined length at the base of the hole. A load is then applied to the bar and a steel plate and nut is usually locked off at that load. The load is then removed and the remainder of the hole is grouted.

Bolting can be done in a pattern or used in individual spots. Bolting patterns should be based on the results of the kinematic analysis which defines the type of failure

being mitigated. Bolting can also be done as “spot bolting” where bolting is performed on an as-needed basis and individual rock or outcrops are addressed.

Shotcrete

Shotcrete, or gunite, has been used as a rockfall mitigation tool mainly for the prevention of weathering and spalling of rock slopes. Shotcrete application is the spraying of concrete, portland cement, aggregate and water, by a pneumatic pressurized gun or nozzle. The shotcrete is reinforced with welded wire mesh or steel fibers and applied to a thickness of three to six inches. The use of shotcrete as a rockfall mitigation tool is expensive and can be replaced in most cases with a tensioned anchored mesh system.

The benefits to using an anchored mesh system is that it is relatively inexpensive, free-draining, and aesthetically pleasing as vegetation can grow through the mesh. The anchored mesh acts to retain loose and spalling rock. Shotcrete still has advantages in preventing weathering, especially in situations where differential weathering creates overhanging hazards.

Concrete Buttress

Concrete buttresses are formed concrete that are used to support large overhanging rocks. In most cases the form is built up from the toe of the slope to the base of the overhang it is supporting. These structures can be large and expensive. The concrete buttress must be anchored into the rock face to support the overhanging rock. The cost of the concrete forming can be very expensive as the size and height of the buttress increases.

Retaining Walls

Retaining walls are not often an economical solution for exposed rock slopes. There are instances where they may be the best solution. Retaining walls are most commonly used for soil cuts in roads and railways when global slope stabilization is necessary. In rockfall mitigation retaining walls become viable when global slope stability is a concern and the retaining or tie-back wall is required to stabilize the slope and can be modified to protect from rockfall as well.

Passive Systems

Passive systems, in contrast to active systems, allow rock movement to occur but focus on preventing rockfall from reaching roads, railways, and other protected areas. Protection is done by retaining, controlling, and catching the rockfall. Passive systems are often the most cost-effective solution as some rockfall source areas are not accessible, or the construction of an active system would be too expensive.

Ditches and Berms

Ditches and berms are widely used and are one of the best and most effective rockfall protective measures. Numerous studies have been dedicated to ditches and catchments areas providing a large database for improving the effectiveness of protection. In some instances right-of-way or limited access considerations make ditches and berms an uneconomical choice.

Drapery Systems

Drapery systems applied to slopes allow rockfall to occur but in a controlled fashion. The drapery is applied to the slope and rockfall is controlled by preventing freefall and bouncing of the rocks, thereby preventing rockfall into the protected area. Draperies allow rockfall to travel down-slope and accumulate at the base for removal. The drapery system selected to provide mitigation will vary depending on site conditions and rock types. Rock size, shape, and hardness are very important factors when selecting a drapery system. As the rock size and hardness increase so does the necessity for a more robust system.

The use of drapery systems are an important tool in rockfall mitigation, and our opinion of these systems are as follows. Double twisted wire mesh is a suitable solution for most drapery situations. The material prevents unraveling with the double twist in the wire mesh. Double twist wire mesh limitations are the size, shape, and hardness of the rock. Double twisted wire mesh is suitable for rockfall with a maximum size of 1-ft x 1-ft and hard, sharp rocks have been known to tear mesh. The system will still perform with small tears in the mesh but care should be taken in the investigation stage to prevent under-design of a system.

Double twisted wire mesh with wire rope included in the manufacturing process is a product where the extra strength of the wire rope increases the ruggedness of the material. As a rule of thumb, this increases the size of the rock that can be contained with the product to 2-ft x 2-ft. The same limitations of the double twisted wire mesh are still present with sections between the wire rope.

Very high strength steel (approximately 260-ksi) chain link wire mesh used as a drapery system is a higher strength material and can withstand impacts of hard, sharp rocks with a maximum rockfall size of 3-ft x 3-ft. Chain link only has a single twist and some engineers and geologists believe that this can cause unraveling if the product is torn. However, this is unlikely with the high strength steel used.

High strength twisted steel wire and wire rope nets with wrapped junctions have proven a suitable drapery for rockfall up to approximately 6-ft x 6-ft. Because of the larger opening size of about one foot, these systems may also need an underlayment of chain link mesh to protect against smaller rockfall.

Ring net drapery should be used as drapery when block sizes are 6-ft x 6-ft. Ring nets are extremely durable, thus allowing use with large rockfall and jagged rocks. Chain link mesh may also be needed to prevent smaller rocks from passing through the ring net.

Rigid Barriers

Rigid barriers include jersey barriers, gabion baskets, reinforced concrete block walls, concrete retaining walls, and steel and timber lagging walls. These types of walls are capable of retaining and withstanding low energy rockfall impacts but can become severely damaged with high energy impact. Repair and possible replacement is often necessary, driving maintenance costs higher in comparison to the installation of proper rockfall mitigation. In many cases these structures under high impact load of rockfall will fail and allow rockfall to enter the traveled way. Overall these structures are not cost effective for rockfall protection in comparison with other rockfall mitigation available.

Flexible Barriers

Flexible barriers on the market today have improved considerably since their introduction and use rockfall mitigation. The first barriers were designed with wire mesh and posts suitable only for low energy rockfall. Subsequently, cable nets and stronger rigid posts were used. Brake rings were introduced to absorb additional energy from rock impacts in the netting.

Flexible barriers have undergone extensive testing and design changes, and new innovations have been introduced. Ring nets are frequently used for the netting of the barriers, flexible (battered) posts support the nets, and brake rings and support ropes now significantly reduce energy from rockfall impacts. Barriers have been designed that are capable of absorbing rock impacts of more than 1,800 foot-tons (5,000 kilojoules). When planning such barriers, it is important to allow for the deformation of the barrier during impact and provide an adequate distance for the net to expand.

Barriers can be installed both at the base or toe of the slope and along the slope wherever placement may most effectively reduce the energy of the rockfall. Tools such as CRSP can predict the energy for a specific rockfall event.

Tunnels and Sheds

When rockfall cannot be mitigated with other means, tunnels and sheds may be options. These structures allow rockfall to pass over roads and railways. Rockfall tunnels and sheds are expensive and only used when all other types of rockfall mitigation are ruled out. This generally occurs with high steep slopes that produce large amounts of energy. One important design criterion is to design the roof large enough to capture and contain the rockfall; the use of a soft material like sand can help dissipate energy of the rockfall (2).

Table 1 shows a summary of rockfall mitigation approaches based on empirical and quantitative analyses.

Table 1 – Rockfall Mitigation Summary		
System	Type	Energies
Anchored Mesh	Active	--
Bolting	Active	--
Shotcrete	Active	--
Retaining Walls	Active	--
Drapery	Passive	--
Rigid Barrier	Passive	< 30 ft-tons
Flexible Barrier	Passive	5 to 1,500 ft-tons
Ditch & Berm	Passive	> 1,500 ft-tons

DESIGN

Several approaches can be used when designing and specifying rockfall mitigation measures. In the case of barriers, one of three requirements must usually be met. These are:

- Provide calculations demonstrating system can resist potential rockfall impact loads.
- Provide analyses showing system behavior under potential rockfall impact loads such as finite element method (FEM) analysis.
- Provide certified test results that system can withstand potential rockfall impact loads.

Structural calculations for each member of a barrier during dynamic impact are virtually impossible. Few, if any, agencies attempt to require this information. Advanced analytical methods such as FEM for dynamic impact of rock on barriers is available. One such program is FARO (7) (8). Such programs require numerical, constitutive models for the components and are usually cost prohibitive. However, in some specialized instances they may be the best approach.

Certified test results are the best and most reliable means of ascertaining that a barrier can meet energy requirements. These tests are performed and certified under the auspices of such entities as the European Union (ETAG) or the Swiss WSL. As yet, there is no American agency charged with certifying barriers for use in the United States. Most American owners will accept the European certifications.

Post Foundation Design for Rockfall Barriers

The purpose of the supporting posts in a rockfall barrier system is to maintain the height of the catchment net. As such, foundation performance is not critical to the operation of the system as, for example, anchor embedment is. However, post

foundations are subject to loading during an impact and must be designed accordingly to ensure limited maintenance after impact.

Foundation loads during impact can be obtained from barrier manufacturers. These loads may have been determined by direct measurement during testing or by extrapolation from measured impact and anchor loads. The post foundations are loaded by an overturning moment applied to the post. Post anchor bolts can be loaded in shear, tension, compression or a combination of loads. Foundation design must consider loads on both the anchor bolts and the foundation as a whole in the surrounding geologic material.

Anchor bolts specified by the manufacturer are adequate. Anchors are generally threaded bars ranging from A36 to high strength steel, with or without corrosion protection.

Actual measurement data of loads on foundations are rare but directly govern design. Turner et al. (9) published data from Diotallevi, et al. (10) derived from an actual instrumented foundation. The loads were 7.55-kips in shear and 12.88-kips in compression. They then proceeded to design a post foundation based on these published loads.

Depending on the geomaterial present, the foundation type will vary. When installed on hard, competent bedrock, anchor bolts are grouted directly into drilled holes. Generally, only the tension anchor must be checked for capacity. This can be done using the Post Tensioning Institute (11) bond strengths for anchors.

Foundations in colluvial materials or soils can be either shallow pier-type foundations or drilled shafts. Turner et al. (9) used Broms' (12) approach and the loads described above to design a foundation in soil for a 350 ft-ton (1000-KJ) barrier. The foundation size was a cubical 2.5-ft x 2.5-ft x 2.5-ft. Repeating this exercise for a drilled shaft using the L-PILE (13) program yields a shaft 5-ft deep x 2-ft in diameter with the same volume of concrete, approximately 15.7-ft³. Therefore, the required amount of steel reinforcement will be the same.

Turner, et al. (9) did not publish an estimated horizontal displacement after impact. The estimated horizontal displacement under dynamic load for the drilled shaft was 1.3-in (no damage to the foundation). It would be expected that the cubical foundation displacement would be much greater as it was only one half as deep.

Thus at low barrier energies the foundation type depends more on constructability and preference. The advantage of the shaft is that, because it is deeper, less rotation will occur on impact. At higher energies the size of a pier-type foundation becomes extremely wide in order to accommodate the high dynamic passive pressure placed on the subgrade. In these cases, a drilled shaft will most likely be more constructible.

Anchor Design

Anchor design for both rockfall barriers and draperies is a matter of determining the load the anchor must support. This can be estimated for draperies and, as described earlier, is obtained from the manufacturers for rockfall barriers. Estimated anchor depths can then be determined by using tables (14) or calculated from the shear strength properties of the soil or rock.

Specifications and Plans

Specifications for rockfall barriers fall into two categories: result specifications and method specifications. Result specifications are based on the results of the engineering geologist's field work and rockfall analyses. Essentially design-bid, these specifications call for a particular layout, design height and energy with the winning contractor responsible to supply an engineered system that meets these requirements. Result specifications may also include desired attributes such as stainless steel fittings, ring nets, or high strength steel mesh. Contractors who are awarded the project then must produce an engineered system to meet the requirements.

Method, or final product, specifications are much more detailed and constitute the design for the actual mitigation measure. They will include anchor depths, locations, post foundation design, barrier type (usually describing a particular manufacturer's barrier or equal) and details on the various connections and members; they must be stamped by an engineer and are used by the contractor to construct the mitigation measure.

Problems arise when Specifications and Plans are put out to bid that are either partially or wholly methods specifications, stamped by an engineer with the requirement that the contractor or engineer provide additional stamped plans for a construction design. Engineering statutes in all states require that engineers either perform the work that they are stamping or have responsible charge of that work. For example, the Hawai'i Engineering Code states:

“Misconduct in the practice. Misconduct in the practice of the profession of engineering, architecture, land surveying, or landscape architecture means without limitation the following:

“ . . . "Plan stamping"; i.e. sealing, stamping, or certifying any document which was not prepared by or supervised by the licensee; . . . ”

It is illegal and subject for disciplinary action for engineers to stamp the work of another engineer for which they had no control, also known as “plan stamping.” Once a contractor or manufacturer has tasked an engineer with a design for rockfall mitigation per specifications that engineer has full charge, responsibility, and legal liability for the design. Conflicts often occur when the engineer that produced the bid documents insists that his or her design be followed exactly without providing the necessary calculations or analyses to the design engineer for verification. Once the bid document engineering work has been turned over to the actual design engineer, the Specification engineer

cannot force changes per his or her personnel preference but only review the design engineer's work to determine whether it is sound and meets the overall design criteria. An example of this might be where the Specification engineer has specified that a post foundation only need to be 2-ft deep where the design engineer calculates the foundation to be 4-ft deep. The Specification engineer has no legal right to require that the design engineer change his foundation depth to 2-ft. To attempt to do so may constitute an ethical violation. Often engineers are asked to stamp the shop drawings of a manufacturer for submittal by the manufacturer or contractor. This is also a violation.

CONCLUSIONS

Rockfall mitigation has developed from an empirical approach to a quantitative methodology using the most modern technology. However, the general process remains the same. Site characterization by aerial image, literature review, and field mapping is still essential. Numerical modeling using sophisticated software such as CRSP, FARO and L-PILE allow for the specification of particular mitigation methods and products and their design. Standardized testing and certification provides assurance that products meet the demands of the application. The work toward an American standard will continue the trend to higher quality and better design.

Some legacies of the past remain. Plan stamping still appears to be relatively common in rockfall mitigation construction. Besides being illegal, it transfers liability from the *de facto* design engineer who produced the stamped bid documents to another engineer who is willing to take an illegal risk by stamping the work of others. Plan stamping should be discouraged by all members of the rockfall mitigation community and those engineers who participate in the activity should be reported to their respective boards for disciplinary action. To do otherwise endangers the public in a field which has made tremendous advances in protecting people and property in the last two decades and puts the contractor and manufacturer at liability risk.

REFERENCES:

1. Caltrans (1985) *Rockfall Mitigation*, Report No. FHWA/CA/TL-85/12, California Department of Transportation, Sacramento, California. 147 p.
2. Brawner, C. (1994). *Rockfall Hazard Mitigation Methods, Participants Workbook*. Federal Highway Administration, Washington, DC, 1994.
3. Ritchie, A. M. (1963), *The Evaluation Of Rockfall and Its Control*, Highway Research Board, highway Research Record No. 17, Washington, DC, 1963.
4. Jones, C. L., Higgins, J. D., Andrew, R. D. (2000). "Colorado Rockfall Simulation Program Version 4.0." Colorado Department of Transportation, Denver, CO, 127 p.

5. Pierson, L. A., Davis, S.A., Van Vickle, R. (1990). *Rockfall Hazard Rating System Implementation Manual*, Federal Highway Administration, Washington, DC, 1990.
6. Hoek, E., and Bray, J. (1974), *Rock Slope Engineering*, Institution of Mining and Metallurgy, London, 358 p.
7. Volkwein, A. (2005). "Numerical Simulation of Flexible Rockfall Protection Systems." *Proceedings, Computing in Civil Engineering*, ASCE, Cancun, Mexico.
8. Wendeler, C., Mc Ardell, B. W., Rickenmann, D., Volkwein, A., Roth, A., and Denk, M. (2006). "Field Testing and Numerical Modeling of Flexible Debris Flow Barriers." *Proceedings, Physical Modeling in Geotechnics, 6th ICPMG '06*, pp. 1573- 1578.
9. Turner, R., Duffy, J. D., Turner, J. P. (2009). "Post Foundations for Flexible Rockfall Fences." *Proceedings, Highway Geology Symposium*, pp. 125 - 139.
10. Diotallevi, P., P., Gottardi, G., Govoni, L. (2007). "High Resistance (Maccaferri) Rockfall Barrier, (500kJoule)." CTR/05/07/B, Full Scale Impact Test Certification, University Of Bologna, DISTART Department (Faculty of Engineering) and Consorzio Triveneto Rocciatori s.r.l of Fonzaso, July 25, 2007.
11. Post-Tensioning Institute, (2004). "Recommendations for Prestressed Rock and Soil Anchors." Post-Tensioning Institute. Phoenix, Arizona. 2004. 98 p.
12. Broms, B.B., 1964. "Lateral Resistance of Piles in Cohesionless Soils." *Journal of the Soil Mechanics and Foundations Division*, ASCE Vol. 90, No. SM3, pp. 123 - 156.
13. L-Pile Plus 5.0, (2004) "Computer Program L-Pile Plus Version 5.0 Technical Manual, A Program for the Analysis of Piles and Drilled Shafts Under Lateral Loads." Ensoft, Inc. Austin Texas, 2004.
14. Hunt, H. E. (1984). *Geotechnical Engineering Investigation Manual*, McGraw Hill, New York. 983 p.

FLEXIBLE FACING ANALYSIS FOR SOIL NAILING

Ghislain Brunet

Maccaferri, Inc
10303 Governor Lane Blvd.,
Williamsport, MD 21795-3116
Ph: 301-223-6910
gbrunet@maccaferri-usa.com

Paola Bertolo

OFFICINE MACCAFERRI S.p.A.
Via Kennedy 10
40069 Zola Predosa, Bologna, Italy
Paola.Bertolo@maccaferri.com

Giorgio Giacchetti

External Consultant - OFFICINE MACCAFERRI S.p.A.
Via Kennedy 10
40069 Zola Predosa, Bologna Italy
giorgio.giacchetti@maccaferri.com

Prepared for the 61th Highway Geology Symposium, August 2010

Disclaimer

Statements and views presented in this paper are strictly those of the author(s), and do not necessarily reflect positions held by their affiliations, the Highway Geology Symposium (HGS), or others acknowledged above. The mention of trade names for commercial products does not imply the approval or endorsement by HGS.

Copyright Notice

Copyright © 2010 Highway Geology Symposium (HGS)

All Rights Reserved. Printed in the United States of America. No part of this publication may be reproduced or copied in any form or by any means – graphic, electronic, or mechanical, including photocopying, taping, or information storage and retrieval systems – without prior written permission of the HGS. This excludes the original author(s).

ABSTRACT

Soil nailing is a technique in which soil slopes, excavations or retaining walls are reinforced by the insertion of relatively slender elements - normally steel reinforcing bars. The bars are usually installed into a pre-drilled hole and then grouted into place or drilled and grouted simultaneously. A rigid or flexible facing system is used to stabilize the soil between the anchors.

Flexible facing systems have been used for many years to maintain and improve stability between the anchor systems. Despite this long use, the design methods usually take into account only the anchor design to reach the expected safety factor. No calculation method exists to help the designer choose the correct facing type and evaluate the facing behavior against the load of the unstable material layer. The geotechnical properties and the load can change with time (e.g.: by softening and weathering phenomena).

To solve this lack of knowledge Maccaferri has developed the BIOS System (Best Improvement of Slopes). With this new approach it is easy for the designer to verify the effectiveness of the selected facing system, checking the work both for Ultimate and Serviceability Limit State.

The Ultimate limit state check is necessary to avoid total collapse of the entire system. The serviceability limit state check is necessary to avoid having the system be under designed with respect to the potential deformation of the mesh. This check takes into account the long term behavior of the slope material. Large debris displacement over time can produce unacceptable deformation of the system between the nails. This can lead to interference with the protected structure or deeper stability problems in the slope.

INTRODUCTION

The use of steel mesh for soil nailing facing has been increasingly frequent over recent years. The system, known in the technical literature as Flexible Facing (CIRIA, 2005), has, without doubt, advantages of an aesthetic nature and it may be used to successfully consolidate slopes generally with vegetation. However, the state of the art is still not mature as is often shown by the lack of design approaches or the sometimes improper use of the meshes. This paper analyses the general behavior of the flexible facing and proposes the new BIOS (Best Improvement of Slopes) design approach which has been widely used by Maccaferri for the design of excavation slopes and the consolidation of natural slopes.

THE CONCEPT OF SOIL NAILING

The aim of soil nailing is to improve the soil stability when there are unfavorable stability conditions. The stability is achieved by inserting reinforcement bars in the soil, which are then grouted and fixed soundly to the ground for their entire length (nailing). The nailing mobilizes friction forces along the entire length and contributes to the improvement of the stability conditions when there are displacements in the soil (Schlosser F. et al., 2002; Soulas R., 1991; BS 8006; Byrne, R.J et al., 1998). The stabilizing friction forces are generated passively with the start of the soil failure. The frequency and the length of the nails must be calculated in accordance with EN 1997 1 or FHWA.

The protection of the exposed surface of the soil reinforced by the nails is obtained with the facing, the aim of which is to hold the soil between the nails, prevent erosion phenomena and assume an aesthetic function. The facing may obviously only collaborate with the passive action of the nails.

APPLICATION OF THE FLEXIBLE FACING

On sub-vertical excavation faces the facing is usually made from a rigid structure (Hard Facing – shotcrete or precast elements), which is able to control in an optimum manner all the displacements induced by the variation of the stresses.

On slopes of up to approximately 60° the facing may also be made with flexible structures (Flexible Facing – wire mesh or wire mesh geocomposites); the preferential field of application of the flexible facing is the natural slope or the relatively small excavation face, where significant variations to the stresses are not expected.

Geosynthetics are used for the facing of moderately steep slopes where only a simple short-term protection is sufficient, which favors the growth of vegetation. They are sometimes reinforced by lightweight wire meshes (soft facing).

Experience shows that, except in the case of perfectly flat and smooth surfaces, it is not possible to place the mesh in continuous contact with the soil (Ferraiolo and Giacchetti, 2004). If it were technically possible to pre-tension the mesh, forces would be developed tangential to the plane of the mesh; these could generate pressures against the soil only at the points of contact with protuberances or cavities (See Figure1); in all the other positions the pressure against the soil would be zero. It may be said that, in a certain sense, the mesh enables the surface of the anchor plate to be expanded (Besseghini et. al., 2009), but this increase is absolutely negligible due to the intrinsic deformability of the net itself.

It is worth to note that the deformability of the net is mainly related with the weaving of the mesh, and the contribution of the material strength (e.g. different steel grade) is absolutely negligible.



Figure 1. Unlevel slope facing with soil nailing

It should be noted that in the soil nailing system defined above, the pre-tensioning of the mesh by means of the nail plates does not offer any advantage. Simple numerical models show that pre-loading the nail plate (Figure 2 - A) slightly disturbs the stresses in the soil below the plate itself (Figure 2- B), but it does not generate active stabilizing forces; furthermore the nails do not have the free section (which is present in the ties) that enables the forces to be transferred from the surface (the plate) to a far away point (the foundation).

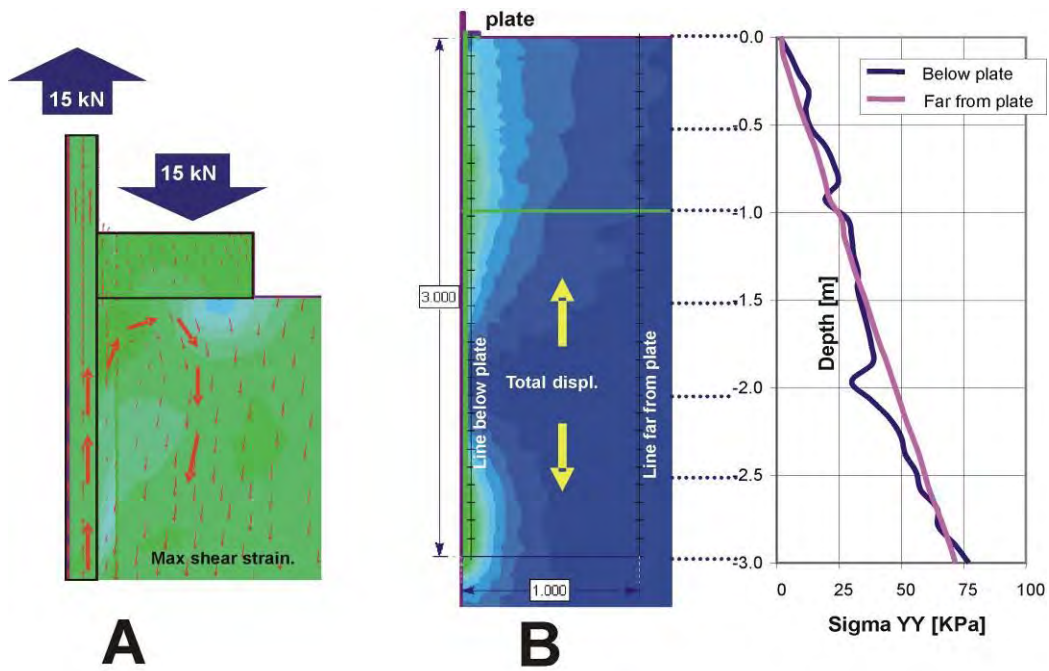


Figure 2: Results of the axial-symmetric FEM model of the anchor: (A) Maximum force fields and direction of the displacements below the plate; (B) Total displacement fields and trend of the vertical pressures YY below the plate (blue line) and far from the plate (purple line)

Existing projects have demonstrated that the mesh between the anchors doesn't provide continuous pressure on the soil. Figure 3 shows a displacement between two soil nails using high efficiency single-twist mesh for flexible facing stabilization system. By applying a small pull out pressure by hand only, the mesh was displaced by more than 355 mm (14 inches). On the same project in California, with nails spaced at only 2.1 m (7 ft) of distance (see figure 4 and 5), the displacement from a small pull out pressure (small means the pressure related to a human action, without using mechanic equipments, as shown in Figure 3) was of 152 mm (6 inches).



Figure 3. Photos of flexible mesh facing high performance single-twist mesh.



Figure 4. Distance of 2.1 m (7 ft) between anchors



Figure 5. Non-uniform pressure between two short distances nails using high performance single-twist mesh.

BEHAVIOUR OF THE FLEXIBLE FACING

Various studies and laboratory tests have been carried out with regard to the behavior of the meshes (Ruegger R., & Flumm D., 2000; Bonati & Galimberti 2004; Torres et al., 2000; Muhunthan B. et al., 2005) using various sized samples fastened to test frames with a range of constraint conditions. The results of the research highlight that the movement of the meshes subject to puncturing, at the point of application of the load, ranges from several decimetres to several meters, with a non-linear development of the response, the trend of which depends mainly on the combination of the mesh weaving, the size of the test sample and the type of constraint with which the sample is fixed. There are large displacements during the initial phase of application of the load in all the tests. Only subsequently does the mesh start to appreciably oppose the load. The mesh may not therefore be modelled with a pressure uniformly distributed on a surface through the action of the nails and, for this reason too, it is to be considered as a passive element.

Large displacements of the meshes are found in the case of tests carried out with 3 x 3 m (10 ft x 10 ft) frames (Bonati and Galimberti, 2004): for example, with the same constraint conditions (fastened on all sides), the double-twist mesh reinforced with steel cables -

RockMesh - is very deformable compared with the HEA cable panel, but much more rigid than the single-twist meshes with high-strength wire. With a load of 1,500 daN (1.5 tons, i.e. slightly less than a cubic metre of soil) (3300 lb) the HEA panel deforms by 15 cm, the RockMesh by 38 cm (15 inches) and the single-twist mesh by 55 cm (22 inches). Full scale puncturing tests have been carried out more recently at Pont Boset, Aosta (Italy), reproducing a constraint system frequently used for the consolidation of rock faces and soil slopes, and simulating the load on the mesh by means of a jack placed at 45° to the plane of the mesh (Figure 6) (Bertolo et. al. 2007; Bertolo et. al., 2009).



Figure 6 - Pont Boset (Aosta Valley, Italy) test site developed by Turin Polytechnic in collaboration with Officine Maccaferri (Bertolo et al. 2009)

The test is particularly interesting as it summarizes in a realistic manner the different types of puncturing that is sometimes carried out on the meshes (puncturing with pressure at the center of the sample and puncturing with the anchor plate). On the one hand the results confirm the non-linear behavior of the meshes and on the other hand they highlight that in reality the displacements are much greater than those envisaged on the basis of tests carried out on samples at a reduced scale or fastened in a perfect manner (Figure 7).

DESIGN MODELS

Taking into consideration the results of the in-situ tests, simplified numerical design models have been implemented which enable the effectiveness of the flexible facing formed with different types of meshes to be assessed. For example, a natural slope has been considered with regular morphology, an angle of inclination of 54° and a height of 14.0 m

(46 ft), consisting of highly weathered rock with a weight of 24.0 kN/m^3 (150 lb/ft^3), a cohesion of 20 kPa (417 lb/ft^2), a shear resistance angle of 20° and a Young's modulus of 800 kPa ($16,700 \text{ lb/ft}^2$). The calculation has been carried out with the non-associated flow rule obtaining a global safety factor of 1.05 (Phase 2 7.0, 2009). By inserting solely the $3 \times 3 \text{ m}$ ($10\text{ft} \times 10 \text{ft}$) anchors, but not the flexible facing, the global safety factor for the slope increases to 1.30. The instability of the soil between the nails only manifests itself in the long term, as a reaction to the softening processes. Only after this new instability condition has been established does the flexible facing enter into play and collaborate with the anchors.

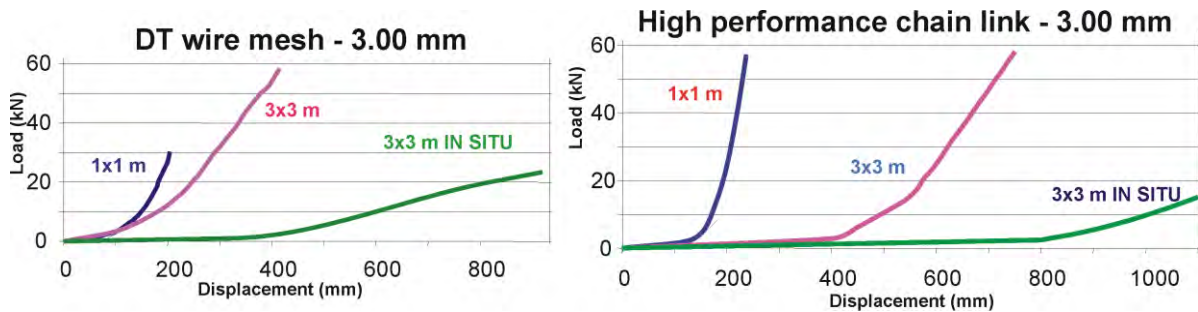


Figure 7: Graphs of the puncturing tests on $1 \times 1 \text{ m}$ ($3 \text{ ft} \times 3 \text{ ft}$) samples in the laboratory (blue line), $3 \times 3 \text{ m}$ samples in the laboratory (purple line) and $3 \times 3 \text{ m}$ ($10\text{ft} \times 10 \text{ft}$) samples in situ (green line), in the case of double-twist mesh (on the left) and single-twist high performance mesh. The displacement law depends on the size of the sample and the constraints. The dramatic displacement of the in-situ single-twist mesh may be seen.

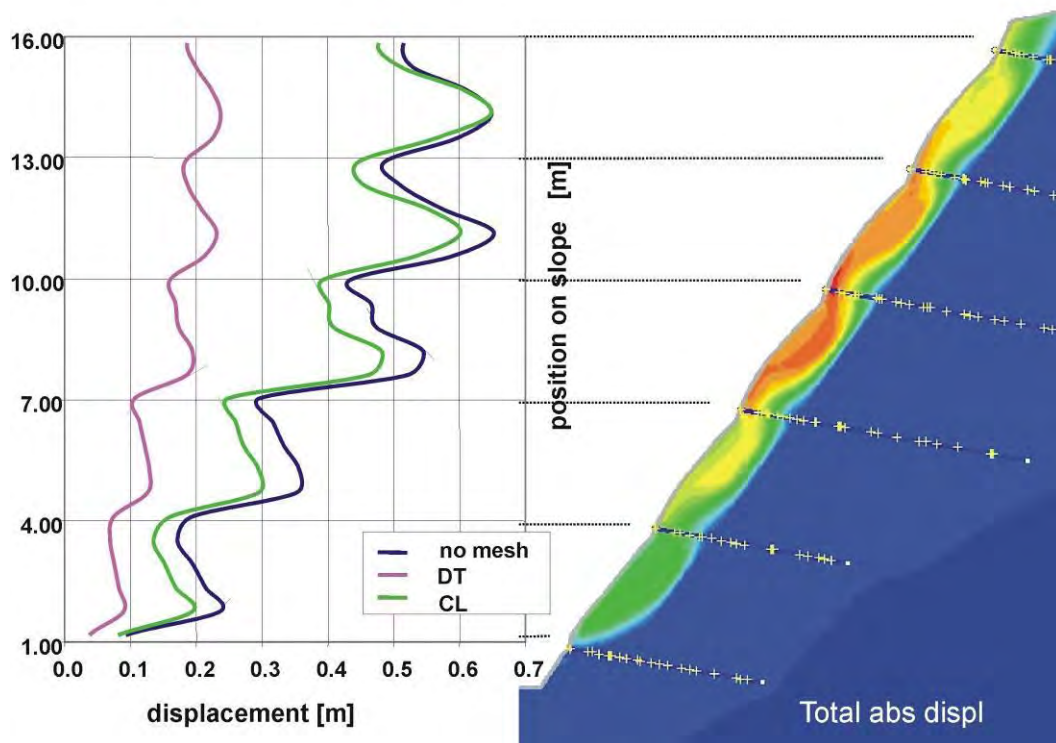


Figure 8: Total displacements on the slope and the relative total displacement graphs recorded with double-twist mesh (purple line), high-performance single-twist mesh (green line) and without the flexible facing (blue line). While the double-twist mesh is effective thanks to its membrane stiffness, the single-twist mesh has practically no effect.

The short-term stability of the material between the nails is a necessary condition for the purpose of installation of the flexible facing.

In the simplified numerical models, the flexible facing may be represented as a membrane with a known strength and displacement modulus, connected by means of an interface with zero tensile strength (the displacement modulus of the meshes have been determined in the Pont Boset tests). If the numerical model is run with the soil in softening conditions and with a flexible facing, it may be seen that (a) the tensile strength of the flexible facing has no influence on the geotechnical system and (b) the membrane displacement of the flexible facing plays an important role in the stability of the softened soil. In the example shown in Figure the displacements of the slope have been calculated without a facing (blue line), with a flexible facing consisting of a high-performance single-twist mesh (green line) and with a flexible facing consisting of a double-twist mesh (purple line). The displacements obtained show that the single-twist mesh, even though it has a high tensile strength, does not oppose the soil displacements, while the double-twist mesh actually collaborates with the anchors in opposing the total displacements of the slope thanks to its high membrane stiffness; in addition, the flexible facing which is not very deformable minimizes the stripping processes which affect the nails. The final result is that the double-

twist mesh keeps the global safety factor of the slope approximately 10% higher than that for the single-twist mesh.

SIMPLIFIED APPROACH: BIOS

The use of sophisticated numerical models requires efforts and processing times which may not be considered reasonable in normal design practice; the preferred approach is therefore the limit equilibrium method where the design models used are necessarily very simplified. The conceptual approach commonly used assumes that the system of mesh and anchors in some way plays an active role in the consolidation (Cravero et al., 2004; Saderis A., 2004; Flumm D. & Ruegger, 2001; Castro, 2008); however, this approach is not in line with either the concept of soil nailing or with the passive behaviour of the meshes.

Models have been proposed more recently which also consider the displacement of the mesh in the consolidation of rock faces (Bertolo & Giacchetti, 2008, Valfrè, 2007). In the Maccaferri BIOS approach, the loads transmitted from the soil to the flexible facing have been calculated with the “two wedges method”, with the assumption that the forces act directly on the steel mesh as a distributed load and that the two wedges are contained in the space existing between the two adjacent rows of nails; the angle of inclination of the two wedges is varied in the calculations to maximize the acting force. The total force will be (Majoral et al., 2008):

$$T_{tot} = T_1 + T_2 \quad (1)$$

with:

$$T_1 = \frac{(W_1 + Q_1) (\tan \theta_1 - \tan \varphi'_1) + U_1 \cdot \tan \varphi'_1 - K_1}{\tan \theta_1 \cdot \tan \varphi'_1} \cos \theta_1 \quad (2)$$

$$T_2 = \frac{(W_2 + Q_2) (\tan \theta_2 - \lambda_s \cdot \tan \varphi'_2) + \lambda_s \cdot U_2 \cdot \tan \varphi'_2 - K_2}{\lambda_s \cdot \tan \theta_2 \cdot \tan \varphi'_2} \cos \theta_2 \quad (3)$$

where:

- 1 (kN) (Weight of wedge 1;
- 1 (kN) (Weight of wedge 2;

2	kN)	(Overload acting on wedge 1;
1	kN)	(Overload acting on wedge 2;
2	kN)	(Angle at the base of wedge 1;
1	°)	(Angle at the base of wedge 2;
2	°)	(Resultant of the pressure of the water acting at the base of
1	kN)	wedge 1;	Resultant of the pressure of the water acting at the base of
2	kN)	wedge 2;	Cohesion force acting at the base of wedge 1;
1	kN)	(Cohesion force acting at the base of wedge 2;
2	kN)	(Slip factor at the base.

s

and the safety factor is calculated with

$$FS = \frac{K_1 + K_2 + W_1 \cdot \cos \alpha_1 - U_1 \cdot \tan \varphi'_1 + W_2 \cdot \cos \alpha_2 - U_2 \cdot \tan \varphi'_2}{W_1 \cdot \sin \theta_1 + W_2 \cdot \sin \theta_2}$$

The analysis of the facing is carried out in 4 phases:

1.1 Phase 1 – Short-term solution

The short-term behaviour of the slope is analysed firstly, to check that the safety factor of the slope between two nails is greater than 1.0 ($F_s > 1.0$). This procedure checks the correctness of the geotechnical input assumptions.

1.2 Phase 2 – Long-term check

The softening of the soil which occurs in the long term is simulated assuming the progressive loss of the strength parameters c' and φ' until the acting and resisting forces are equal ($FS=1$). The procedure enables the volume of unstable soil which may move between the nails to be evaluated.

1.3 Phase 3 – Ultimate limit state check

This phase evaluates whether the steel mesh between two adjacent nails may fail. The problem may not be resolved with the limit equilibrium procedure, so a comparison is made between the unstable volume of soil in the long-term situation and the maximum volume of soil which the mesh may support.



Figure 9. Debris accumulation contained by the soil nailing system with the steel cables inserted with RockMesh is transferring efficiently the load from the rocks to the anchors. .

The maximum volume of soil may not be easily calculated since the mesh takes up the characteristic configuration of a sack lying down to a greater or lesser degree towards the end of the slope, the shape of which depends on the ground slope and the deformability of the mesh. It is therefore necessary to introduce approximations of a geometrical nature on the deformed shape of the mesh and set up the system with the conditions based on the initial assumptions, with the limits of deformability and strength of the structure known from the tests.

The following initial assumptions apply (Figure 10 – left):

- The deformed shape is divided into 3 sections: the first limb, rectilinear, with length X inclined with an angle α with respect to the slope, the angle of which is indicated by β ; the second limb, curved, with length $(\pi+\alpha) r$ that characterizes the sack shape of the soil; the third limb, rectilinear, lies on the slope, with the same inclination and a length $X-L$;
- The second stretched limb is tangential to both the first and third limbs of the mesh;

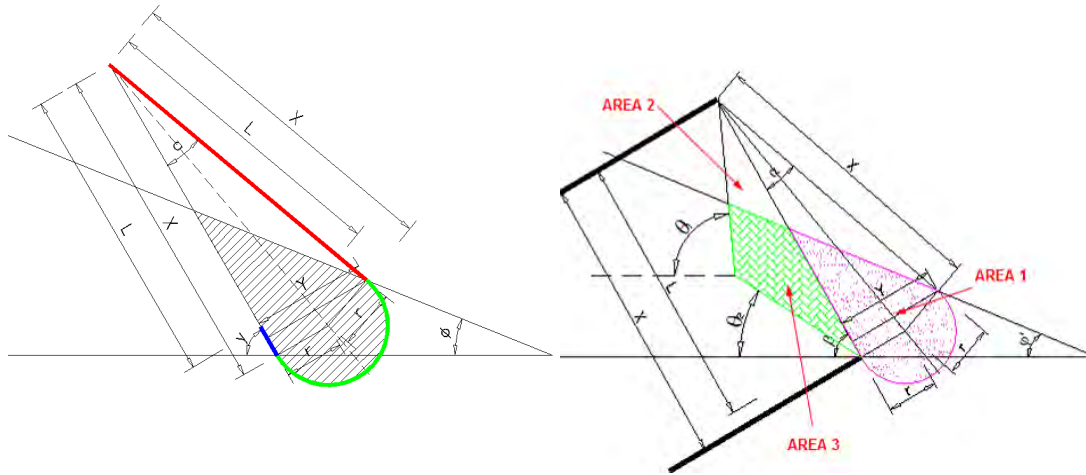


Figure 10: left: division of the mesh into segments – right: deformation model of the mesh

- The mesh, completely stretched, deforms and reaches a maximum length at the failure limit of not more than:

$$L_{tot} = L + \varepsilon \cdot L \quad (4)$$

where

ε percentage deformation under failure conditions obtained from large scale puncturing tests and tension;

L distance of the mesh between two nails in a direction parallel to the slope.

- The area of the section corresponding to the sack is equal to that of the circular sector with an angle at the center equal to $(\pi+\alpha)$ and radius r ;

Area 1 and Area 2 can be obtained with geometric calculation, while Area 3 is the difference between the volume of long-term unstable soil and area 2. The total volume thereby obtained must be compared with the unstable volume under the long-term conditions; if the unstable volume is greater than that necessary for failure of the mesh, the flexible facing will be put at risk.

1.4 Phase 4 – Design limit state check

The designer must check whether the deformations of the flexible facing induced by the expected long-term load are acceptable. Since it is a load-deformation problem, the limit equilibrium method does not provide direct solutions. Consequently, the load-deformation curves obtained from the puncturing tests are used to obtain the volume of soil which determines the maximum permissible deformation. If the volume determined in this way is greater than that expected in the long term, the flexible facing satisfies the design requirements. The maximum permissible deformation is decided upon by the designer on the basis of one or more criteria of a geotechnical nature (effects of the deformation of the mesh on the stripping of the anchors, triggering of erosion processes, effect of settlement induced at the boundary of the soil nailing) and a functional nature (maximum size permitted for the sacks of debris), and in consideration of the appearance.



Figure 11. Excessive debris accumulation

CONCLUSIONS

This paper proposes the BIOS system developed by Maccaferri for the construction of flexible facing using steel meshes. The system highlights that the fundamental property for this type of application is the membrane stiffness of the flexible facing, while its tensile strength has limited influence, as the forces in play are generally very low. With the BIOS system it is possible to reduce both the time for design of the facing and the cost of the works. However, it is absolutely essential that the designer verifies the context in which the facing is to be applied, analyzing the stress conditions, ground stratigraphy, permissible deformations, water in the soil, and erosion phenomena.

BIBLIOGRAPHY

- Bertolo P., Ferraiolo F., Giacchetti G., Oggeri C., Peila D., e Rossi B., 2007: Metodologia per prove in vera grandezza su sistemi di protezione corticale dei versanti – GEAM Geingegneria Ambientale e mineraria, Anno XLIV, N. 2, Maggio-Agosto 2007.
- Bertolo P., Oggeri C., Peila D., 2009 – Full scale testing of draped nets for rock fall protection - Canadian Geotechnical Journal, No. 46 pp. 306-317.
- Bertolo P. , Giacchetti G., 2008 - An approach to the design of nets and nails for surficial rock slope revetment – in Interdisciplinary Workshop on Rockfall Protection, June 23-25 2008, Morshach, Switzerland.
- Besseghini F., Deana M., Di Prisco C., Guasti G., 2008 – Modellazione meccanica di un sistema corticale attivo per il consolidamento di versanti di terreno, Rivista GEAM Geingegneria ambientale e Mineraria, Anno XLV, N. III dicembre 2008 (125) pp. 25-30 (in Italian)
- Bonati A., e Galimberti V., 2004: Valutazione sperimentale di sistemi di difesa attiva dalla caduta massi – in atti “Bonifica dei versanti rocciosi per la difesa del territorio” - Trento 2004, Peila D. Editor.
- BS 8006, 1995 - Code of practice for Strengthened/reinforced soils and other fills.
- Byrne R.J, Cotton D., Porterfield J., Wolshlag C., e Ueblacker G., 1998: Manual for design & construction monitoring of soil nail walls - U.S. Department of transportation – Federal Highway Administration. FHWA A-SA-96-06R – Washington D.C
- Castro D., 2008 – Proyetos de investigaciòn en la Universidad de Cantabria - II Curso sobre protecciòn contra caida de rocas – Madrid, 26 – 27 de Febrero. Organiza STMR Servicios técnicos de mecànica de rocas.
- Cravero M., Iabichino G., Oreste P.P., e Teodori S.P. 2004: Metodi di analisi e dimensionamento di sostegni e rinforzi per pendii naturali o di scavo in roccia – in atti “Bonifica dei versanti rocciosi per la difesa del territorio” – Trento 2004, Peila D. Editor.
- EN 1997 1, 2005 - Eurocode 7: Geotechnical design - Part 1: General rules
- Ferraiolo F., e Giacchetti G., (2004): Rivestimenti corticali: alcune considerazioni sull'applicazione delle reti di protezione in parete rocciosa – in atti “Bonifica dei versanti rocciosi per la difesa del territorio” – Trento 2004, Peila D. Editor.
- Flumm D., Ruegger R. (2001): Slope stabilization with high performance steel wire meshes with nails and anchors – International Symposium Earth reinforcement, Fukuoka, Japan.

- LCPC, 2001: Parades contre les instabilités rocheuses - Guide technique - Paris.
- Majoral R., Giacchetti G., Bertolo P., 2008 – Las mallas en la estabilización de taludes – II Curso sobre protección contra caída de rocas – Madrid, 26 – 27 de Febrero. Organiza STMR Servicios técnicos de mecánica de rocas.
- Muhunthan B., Shu S., Sasiharan N., Hattamleh O.A., Badger T.C., Lowell S.M., Duffy J.D., 2005: Analysis and design of wire mesh/cable net slope protection - Final Research Report WA-RD 612.1 - Washington State Transportation Commission Department of Transportation/U.S. Department of Transportation Federal Highway Administration.
- Phear A., Dew C., Ozsoy B., Wharmby N.J., Judge J., e Barley A.D., 2005: Soil nailing – Best practice guidance - CIRIA C637, London, 2005.
- Ruegger R., e Flumm D., 2000: High performance steel wire mesh for surface protection in combination with nails and anchors – Contribution to the 2nd colloquium “Construction in soil and rock” – Academy of Esslingen (Germany).
- Saderis A., (2004): Reti in aderenza su versanti rocciosi per il controllo della caduta massi: aspetti tecnologici e progettuali – Tesi di Laurea in Ingegneria per l’Ambiente e il Territorio, non pubblicata, Politecnico di Torino.
- Schlosser F., (Chairman), 2002: Additif 2002 aux recommandations clouterre 1991 pour la conception, le calcul, l’exécution et le controle des soustènements realises par cluage des soil – Presses Ponts et chaussées.
- Phase 7.0, 2009: Software manual - Rocscience Inc - Toronto.
- Soulas R., (Chairman), 1991 : Recommandations clouterre 1991 pour la conception, le calcul, l’exécution et le controle des soustènements realises par cluage des soil – Presses Ponts et chaussées.
- Torres Vila J.A., Torres Vila M.A., e Castro Fresno D., 2000: Validation de los modelos fisicos de analisis y diseno para el empleo de membranas flexible Tecco G-65 como elemento de soporte superficial en la estabilizacion de taludes.
- Valfrè A., 2007: Dimensionamento di reti metalliche in aderenza per scarpate rocciose mediante modellazioni numeriche – GEAM Georingegneria Ambientale e mineraria,

Use of Dimensional Modeling for Sizing Flexible Barriers Installations That Mitigate Debris Flow and Shallow Landslide Natural Hazards

Corinna Wendeler¹, Louis Bugnion², and Frank Amend³

¹Geobruigg AG, Hofstrasse 55, Romanshorn, Switzerland, CH-8590, (T) +41-71-466-8178, (F) +41-71-466-8150, corona.wendeler@geobruigg.com

²Swiss Federal Institute for Forest, Snow and Landscape Research (WSL), Birmensdorf, Switzerland, (T) +41 81 4170 268, (F) +41 81 4170 110, louis.bugnion@wsl.ch

³Geobruigg North America, PO Box 7453, Rocky Mount, NC 27804-0453, (T) +1-252-937-2552, (F) 252-451-1254, frank.amend@geobruigg.com

ABSTRACT

The previous large-scale fires in California and the resultant mudflow disasters that were produced have demonstrated that some kind of properly designed flexible barrier could be useful in handling the complex forces present in a fluid/slurry torrent and could be a tool to effectively stop debris flows, shallow landslides, and/or mitigating such hazards. Intensive research has been conducted which identified flow volumes, velocity, and density resulting in pressure as the primary design parameters and have acknowledged specific engineering criteria necessary for use in these types of applications. Such research has included 1:1 laboratory testing with small-scale, artificially generated debris flows, real-scale 1:1 field-testing as well as computer simulations modeling the behavior of barriers during such events.

A design model for debris flow (based on a finite element software program, but not included in the paper) has been calibrated and verified by real-scale field-testing and is the only known valid model for tested barrier type ((GB) ring-net barriers) in debris flow applications. During the model's development, it became clear that each application site where a debris flow barrier would be considered requires specific dimensioning to be completed for each barrier as no "one-size-fits-all" criteria exists for a properly designed solution. Furthermore, the loading associated with debris flows vastly differs from that of rockfall, thereby necessitating different barrier design criteria.

A much more complex phenomenon is shallow landslides and attempts to construct viable models for dimensioning barriers to mitigate them is an on-going process. Initial progress for developing the methodology will be presented in this paper along with resultant testing attempting to prove the models' comprehensiveness.

INTRODUCTION

Debris Flow:

Debris flow mitigation requires the estimation of the expected volumes of debris and velocities from debris flow events as well as the characterization of the expected debris flow compositions, measurement of channel geometry, and determination of expected barrier orientations. From this information, engineers can dimension barriers appropriate for these conditions. Dimensioning of the barriers is accomplished using a general design concept developed from that learned in various field testing efforts, from back-calculating forces exerted on barriers from observations of performance of barriers that had been impacted to date in actual debris flow events in the field, and from verification of the concept using a unique computer simulation program that predicts barrier response and performance. Each site requires a unique barrier design with differing barrier heights, capacities and support infrastructure.

Shallow Landslide:

Landslides are gravity driven flows including rock fall, debris-flow, deep-seated landslides and shallow landslides. Shallow landslide refers to slope failure with a depth of the sliding surface up to 6.5 feet [1]. They can mobilize up to 7,100 ft³ of water saturated soil material and debris. Most of the time they take place during heavy rainfall thus their initiation is very much influenced by the structure and composition of the soil layers. Typically the presence of low permeability bedrock close to the ground surface enhances the risk of failure. The vegetation type and distribution within the soil layer will also play an important role in the stability of the slope [2].

In contrary to deep-seated landslides that are principally slow and creeping mass movements, shallow landslides release and come to a rest within tens of seconds. They are quite unpredictable and no measures can be taken during their occurrence. In spite of their limited volume compared to other phenomenon like debris-flows they can be very destructive due to their high bulk density of and to large front velocities. Habitations, roads and railway lines in the vicinity of steep terrain are primarily concerned with the shallow landslide hazard.

Debris flow and shallow landslide mitigation requires the estimation of the expected volumes of debris and velocities from debris flow events as well as the characterization of the expected debris flow compositions, measurement of channel geometry, and determination of expected barrier orientations. From this information, engineers can dimension barriers appropriate for these conditions. Dimensioning of the barriers is accomplished using a general design concept developed from that learned in various field testing efforts, from back-calculating forces exerted on barriers from observations of performance of barriers that had been impacted to date in actual debris flow events in the field, and from verification of the concept using a unique computer simulation program that predicts barrier response and performance. That way a designer can produce a unique barrier solution for site with differing barrier heights, capacities and support infrastructure.

Up to now research was done on the shallow landslide phenomena addressing various aspects of the initiation and flowing processes. The presence of pore water in the ground was studied regarding soil permeability, soil porosity and flow rates. Concepts like pore water pressure, soil suction and effective normal stress were introduced to assess the stability of slopes [3], [4], [5].

As many efforts were made understanding the rheology of landslide material and process that conditions the ability of the material to flow. The complexity of material made of particles from μm sizes like clays up to cm sizes like gravel passing over silt and sand made the task very difficult. Laboratory works including tri-axial compression tests, rotating drum and small-scale chute experiments [6] were carried out in order to define viscosities and yield stresses values. However the application of results obtained in laboratory for the modeling of full-scale flows was difficult at best.

TESTING

Debris Flow:

The first 1:1 field test to have been conducted on flexible barriers to determine performance under debris flow loading was completed in 1996 at the USGS Debris flow flume in Blue River, Oregon. During 6 tests conducted at this site, instrumentation was used to record flow velocities, forces on various barrier elements, and debris flow character and barrier response in a general way. The most important finding from these tests from a design standpoint was the fact that despite the relatively large openings of ring nets, they can be very effective for purposes of retaining even fine-grained mudflows. Additionally, the tests demonstrated that ring nets perform better than woven wire rope nets due to the higher flexibility, higher energy absorption, better load distribution to the support infrastructure, less need for repair, and better adaptability to the irregular terrain that can be expected in debris flow channels.



Figure 1 & 2. Debris in Ring Nets during Test Simulation in Oregon.

Another series of 1:1 field tests took place between 2005 and 2008 at Illgraben, Canton Valais, which is one of the most active debris flows channels in Switzerland. The Swiss Federal Institute for Forest, Snow and Landscape Research (WSL) has been running a debris flow observation station in the Illgraben since the year 2000. The observation station is equipped with the following instrumentation: rain gauges measuring rainfall intensity, geophones along the channel to determine the front velocity, laser and radar devices to measure the flow height, a force plate for density measurement and finally a shear wall with pressure and geophone measurement devices over the flow height to get an approximation of the velocity and pressure profile over the flow height. At the end of this channel next to the river Rhone a test barrier was installed with cable force measurement devices in each support rope. Three different test barrier setups were successfully tested by several debris flows and also overtopped by several thousand cubic meters of material. Data from these tests has been invaluable in determining the response of barriers to such loading, and thus has contributed to creation of the barrier dimensioning concept.



Figure 3. Illgraben Debris Flow Test Site

Shallow Landslide:

The most comprehensive testing to-date was conducted at a disused quarry located in the Veltheim community in the canton Aargau (Switzerland). The test slope is a 26 feet wide by 135 feet long channel with an average inclination of 30°. The sides of the channel are about 3.2 feet high and the bed surface is made of bedrock covered by sediments. At the top of the slope a release apparatus was built. It consists of a 6 feet high wall whose 2.6 foot lower section is a trap door that can be opened per distance. The lateral sides as well as the bottom surface above the wall are reinforced and made impermeable. The release apparatus has a capacity up to 1,766 ft³ material.



Figure 4 & 5. Filled release apparatus and trap door

The landslide material was prepared by a digger out of earth material and gravel. The largest cobbles have a size up to 8 inches. Water is added until saturation and the whole is stirred up into a homogenous mixture. The material is then transported per truck and poured into the reservoir. The duration between material mixture and release lasts between 2 to 3 hours preventing material sedimentation in the release apparatus.

The flexible barrier is installed at the end of the 131 foot long channel. It consists of three fields between the posts with a maximum span width of 16.5 ft. The 11.5 foot high posts are hold upslope with retaining cables. From post to post support ropes at the top and bottom hold the SPIDER wire mesh. This wire mesh consists of high tensile wire with mesh sizes of 5.1 inches that holds back most of the largest particles. Additionally a second layer of a chain-link mesh with smaller meshes prevents large draining of finer material. All support ropes are equipped with brake elements which get elongated under increasing load level.



Figures 6, 7, & 8. Impact pressure sensor, force plate and force cell

Shallow Landslide Measurement Devices: The main goals of the instrumentation and data acquisition at the Veltheim test site were to quantify the full-scale shallow landslide tests in terms of velocities, flow heights, impact pressure and basal forces, and to measure the loading and deformation of the flexible barrier under impact. Several measurement devices were installed along the channel or built in the flexible barrier as follows:

- Laser distance sensors were located downward from the release apparatus. At one location, 2 distance sensors were placed next to each other in order to obtain 2 similar signals slightly shifted in time.
- A square-shaped force plate with was mounted in the channel bed surface downward from the release apparatus. It measured shear and normal basal forces at the flow bottom. The force plate was enclosed in a concrete foundation built flush to the channel bed surface.
- Impact pressures were measured downward from the release apparatus by two obstacles with measuring surfaces installed in the middle of the channel.
- A total of 4 force cells were built in the barrier upper and lower support ropes as well as in two retaining cables. They could measure forces up to 200 Kn. After the release the filled barrier was measured using a tachometer. Single mesh nodes, shackles and posts are recorded with 3D coordinates.

All the data from the measurement devices were recorded with quick acquisition rate and the results were smoothed with a moving average method over 0.1 s time intervals.

Shallow Landslide Results: The results from six experiments conducted between September 2008 and October 2009 are presented with release of 1,766 ft³ material. Not all devices were installed or worked properly at the time of the experiments so that the data available varies from one experiment to another.

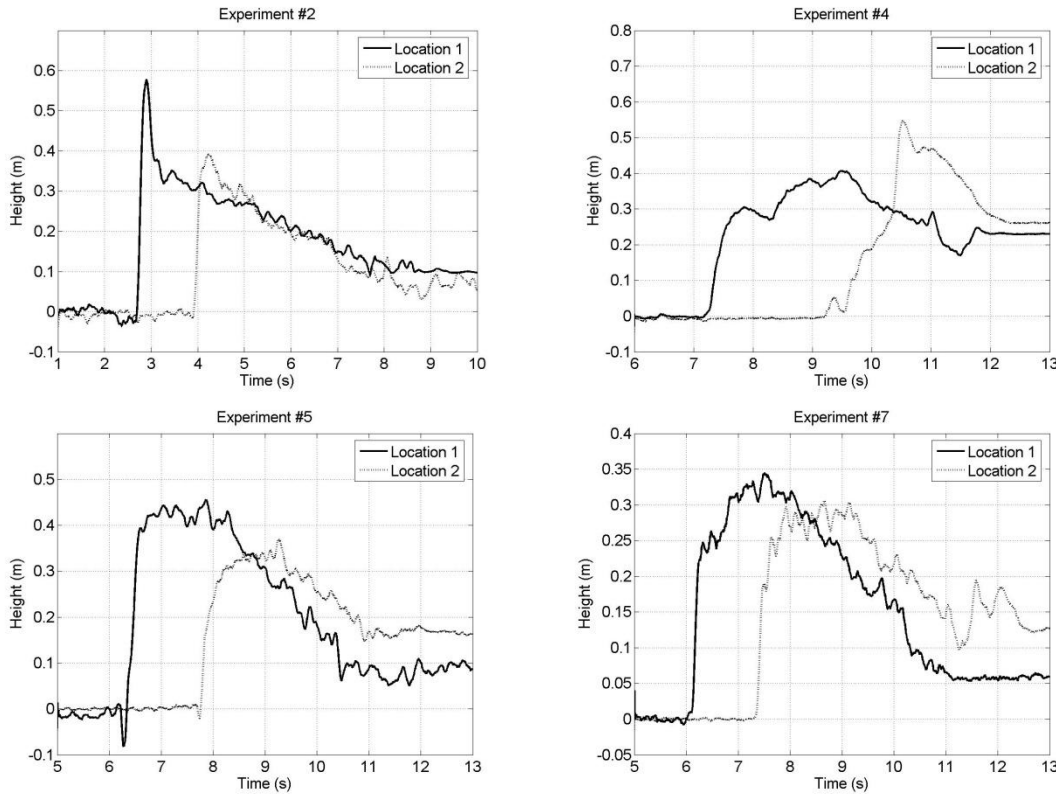
Experiment	Mean velocity (front velocity at location 1/2) (m/s)	Maximum flow height at location 2 (m)	Density (kg/m ³)	Water content (% of mass)	Main component
#2	9.5 (9/11)	0.4	1900	14	Gravel
#4	6.9 (8.6/6.1)	0.5	1850	22	Sand + fines
#5	8.7 (8.9/9.1)	0.35	1920	21	Gravel + sand
#7	9.8 (9.1/11.1)	0.3	1760	17	Gravel +Sand
#77	9.5 (10/11.1)	0.3	1760	17	Gravel +Sand
#8	7.9 (8.3/8.3)	0.35	1840	25	Sand + fines

Table 1: Summary of the experiments #2 to #8

The mean velocity and the amount of deposited material were not only dependant on the material composition but also on the channel bed surface. If the channel was dry and covered with sediments like in experiment #4 the flow was slower and large amount of material deposited. If the bed surface was wet or covered with little sediment the flow was faster and little material deposited.

Flow heights:

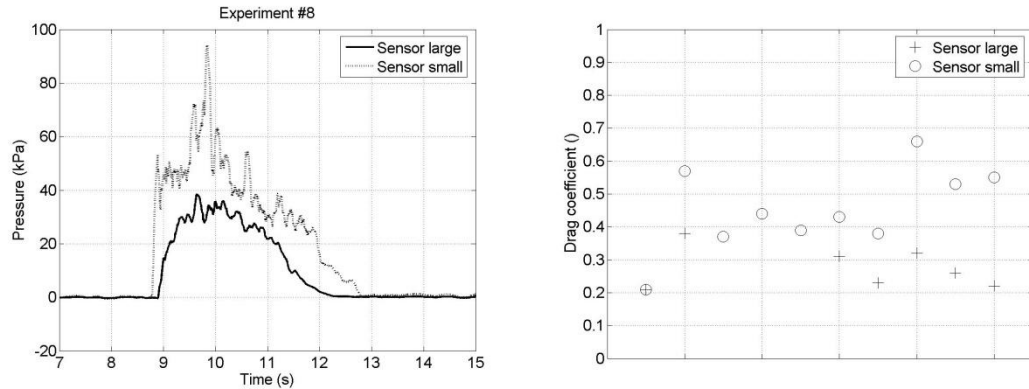
The flow heights at location 1 and 2 are plotted in Figures 9, 10, 11, & 12. Maximum flow heights are larger for slower flow with same starting volume. The maximum flow heights decrease between location 1 and 2 when the flow front is accelerating (experiments #2, #5 and #7) and increase when the flow front decelerates (experiment #4). It shows that the flow is either spreading (maximum acceleration at the front) or compacting (minimum acceleration at the front). This interpretation of the flow height changes is consistent with the flow surface velocities and friction coefficients discussed in section 3.2 and 3.3.



Figures 9, 10, 11, 12. Flow heights versus time at location 1 and 2 for experiments #2, #4, #5 and #7

Impact pressure:

Impact pressures were measured 13 feet downward from the force plate. An ideal dynamic pressure measurement is not supposed to disturb the flow. In the present case the obstacle size has the same order of magnitude as the flow height. The flow was therefore deviated over and on the sides of the obstacle.



Figures 13 & 14. Impact pressures for experiment #8 and drag coefficients for experiments #4 to #8

The smaller cell measures because of size effects due to particle sizes higher impact pressures leading to higher drag coefficients (see Table 2).

Experiment	c_w small cell () first/second shot	c_w big cell () first/second shot
#4	0.21	0.21
#5	0.57	0.38
#6	0.37	-
#7/#77	0.44/0.39	-/-
#8/#88	0.43/0.38	0.31/0.23

Table 2: Drag coefficients for experiments #4 to #8

2.3 Interaction shallow landslide impact – flexible ring net barrier

A particular ground adaptation is necessary for the flexible shallow landslide barriers in comparison to the flexible debris flow barriers which have a special basal opening (see Figure 16, [7]). Fixing the mesh to the ground helps keep the lower support rope near the ground during the impact [8]. An additional benefit is that flows with small flow heights can be completely stopped with only liquid streams passing through the barrier.



Figures 15 & 16. Particular ground adaptation with a fixed mesh for shallow landslide barriers (left) and extra projected basal openings for debris flow barriers (right)

After eight tests with varied mixtures, some with several releases, the results applicable for barrier design were obtained and are illustrated in Table 3. First calculations of barrier design are given in [8]. Most important parameters for barrier design are the dynamic impact of the surge and the static load case for the expected filling height.

With the measured drag coefficient for each test the intensity of the flow hitting the barrier can be estimated. For an engineering approach we assume the flow acts equally over the channel width to the bottom support rope (see Figure 17, [7]).

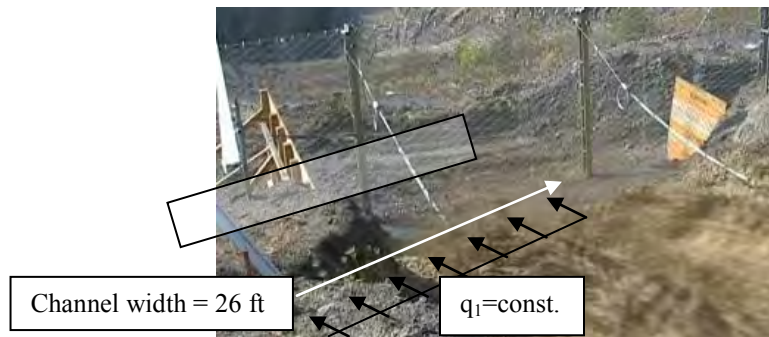


Figure 17. Impacted area on flexible barrier and assumed constant pressure distribution in the middle field

Assuming constant pressure acting to the middle field and to one third of each border field (see Figure 24), a load distribution to lower support rope calculation can be performed. These calculations can then be compared to actual test results with the comparison data contained in Table 3 below.

Experiment	Impact to middle field (kN/m)	Calculated equation (kN)	Measured Test Results (kN)	Deviation (%)
#4	1.8	11	12	-8.0
#5	16.6	76	79	-3.7
#6	36.5	116	98	+18.0
#7	17.0	83	85	-2.3
#8	10.6	53	55	-3.6

Table 3. Comparison of the calculated rope equation with measured rope force from testing

CONCLUSIONS

Debris Flow:

Field observations have proven that flexible barriers can be used to stop debris flows with debris volumes of up to several thousand cubic feet. Due to the flexible nature of these barriers, they are ideal for mitigating such dynamic impacts in a cost effective, quick and relatively nonintrusive manner. A basic barrier dimensioning model based on back-calculations of prior impacts to barriers, 1:1 field testing and a novel computer calculation program called DEBFLOW has been created to help provide some objective basis for dimensioning such barriers. Even these barriers that were originally dimensioned based on Rickenmann approach can also be classified by the new developed multi-level pressure surge model.

The application of these barriers can be considered a complete success, performing exactly as intended. Some minor modifications to the barriers will be undertaken to prevent subsequent damage and to better facilitate maintenance.

Shallow Landslide:

The results of full-scale shallow landslide experiments are presented from a test setup of 1,766 ft³ of landslide were released on a 26 feet wide by 135 feet long channel with an average inclination of 30°. The material was made of gravel, sand and clay saturated with water. Flow heights, basal stresses, front velocities and surface velocities were measured. At the end of the test slope a flexible barrier with high tensile steel net installed. Forces in the support ropes and retaining cables were recorded during impact.

A method was developed to estimate the maximum dynamic load in the barrier during impact of the flow. By assuming constant drag coefficient over the channel width the forces in the lower support rope were calculated and compared with the measured forces solving the rope equation. The results could then be utilized to size the appropriate barrier.

References

- [1] Kantonale Gebäudeversicherungen (2005), Objektschutz Rutschungen.
- [2] Schwarz M. (2008), Characterization of the vegetation cover at the test site of Rüdlingen, *Internal CCES-TRAMM report*.
- [3] Terzaghi K. (1925), *Erdbaumechanik*, Franz Deutike, Vienna.
- [4] Iverson R.M. (1997), The physics of debris-flows, *Reviews of Geophysics*, 35, 245-296.
- [5] Springman S. et al. (2009), Landslide triggering experiment in a steep forested slope in Switzerland, *Proceedings of the 17th International Conference on Soil Mechanics and Geotechnical Engineering*, doi:10.3233/978-1-60750-031-5-1698.
- [6] Iverson R. M. et al. (2009), The Perfect Debris Flow? Aggregated Results from 28 Large-scale Experiments, submitted.
- [7] Wendeler C. et al. (2010), Structural design of flexible steel barriers for torrent debris flow mitigation, in preparation.
- [8] Bugnion L. et al. (2008), Shallow Landslide Full-Scale Experiments In Combination With Testing Of Flexible Barrier

The Latest in Testing Procedures and Technological & Installation Developments in Rockfall Protection Barriers

John Kalejta Jr. & Frank Amend
Geobruigg North America, LLC
Geobruigg Protection Systems
551 Cordova Rd., PMB 730
Santa Fe, NM 87505
Tel: 505-220-1404

E-mail: john.kalejta@geobruigg.com; frank.amend@geobruigg.com
www.geobruigg.com

Abstract:

The latest rockfall protection barriers are tested under the most rigorous vertical drop conditions according to the Swiss Federal Institute for Forest, Snow and Landscape Research (WSL). More recently, rockfall barriers have been tested and certified under the ETAG 27 guideline of the European Organization of Technical Approvals (EOTA). The EOTA test certification is comprised of two so-called Service Energy Level (SEL) tests: the barriers are loaded with two hits of 33% of the nominal energy without intermediary maintenance. The Maximum Energy Level (MEL) test is then performed with 100% of the nominal energy.

Geobruigg's newest rockfall barriers, the GBE series, have verified a residual useful height corresponding to the highest category, A, of the ETAG 27. In other words, after the MEL test, a residual height of at least 50% of the nominal barrier height was attained in the impact field. The latest in technologically advanced rockfall barriers, the GBE series, with full European Technical Approval certificates and CE marking, protect against impact energies up to 2,000 kJ with over 50% residual height in the impact field, require no secondary mesh (500 & 1,000 kJ) and have simple anchorages due to lower

force transmission. Higher energy versions of the GBE barrier, up to 5,000 kJ, are under development.

The time spent installing rockfall protection barriers is a large factor in project cost calculations. These new technological breakthroughs were developed to facilitate rapid installation by contractors through modular design, the use of lightweight components and partial factory pre-assembly. Recent installation cases in New Mexico, Tennessee & Arizona will be presented. The ultimate goal of any rockfall project is the most economical solution to the rockfall and safety problems without compromise of the technical solution.

Design Parameters For Choosing A Rockfall Barrier:

To establish the optimum rockfall barrier for a project requires a determination if the eventual event will likely be a single rockfall or several rocks (rockslide) and if the rockfall event will occur during a single time interval or over an extended period of time. In the case of repeated events with high energy levels and distinct time domain, the barrier(s) should be designed with reference to the Maximum Energy Level (MEL) while applying a suitable safety factor.

The Service Energy Level (SEL) verifies the effectiveness of the rockfall barrier system to minor events, which might occur on a more infrequent basis. In this case it is not necessary to proceed with repair or maintenance after each event. The determination of the appropriate rockfall barrier must take into account:

- the energy that can be dissipated by the rockfall barrier(s) is greater than or equal to the design energy of the application.
- the barrier height is greater than the design bounce height.

- the maximum barrier deformation, when subjected to a MEL impact, should be smaller than the design distance between the area that must be protected and the rockfall barriers. (For DOT applications, other factors must be considered, i.e. placement of concrete jersey barrier in front of the rockfall barrier, etc.).

Product Characterization:

The materials used to fabricate a marketed rockfall barrier should be identical to that of the certification test barrier design. In addition, the corrosion protection for the ropes, nets, posts, hardware, etc. should be evaluated. These checks verify that the tested barrier is the same one as described in the design documents and that which will be installed on a project.

Cost Savings For Installations Of New Rockfall Barriers:

In recent years, technologically outdated rockfall barriers have typically been costly and very difficult to construct. Installation costs can vary between 100-200% of the material costs based on such factors as: time of year of installation, crew size, site access, traffic control, energy & height of the rockfall barrier, site ground conditions, large steel posts, large diameter support ropes, heavy ring nets or woven cable nets, etc. New technological advancements with regards to lightweight components have contributed greatly to reducing the cost of installations. Mutually adapted barrier components can be installed by hand, with a crane, by boom truck or on difficult access sites, by helicopter. (See Fig. 1).

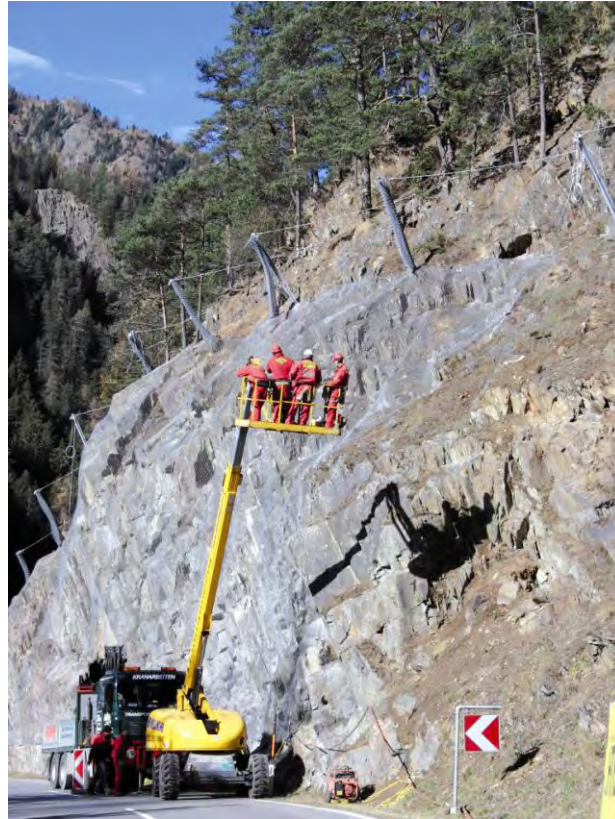


Figure 1: Difficult Installation Site

These new lightweight barrier components would include the following:

- A single anchor suffices for mounting the rockfall barrier ground plate. To prevent twisting, an additional short anchor is drilled, with the ground plate serving as a template.
- The HEA post profiles are light and therefore easy to handle.
- The braking elements are mounted only at the ends of the barrier (and intermediately only every 200 ft.) and close to the ground.
- The TECCO[®] G80/4mm high-tensile steel wire mesh panels are pre-mounted to the posts during production and erected together onsite with the upslope anchor ropes. (See Fig. 2).



Figure 2: X-Sectional View of Construction - GBE Rockfall Barrier

- The top and bottom support ropes are simply pulled through the pulleys on the post and mesh and then tensioned.
- The TECCO[®] mesh can then be easily pulled over the support ropes like a curtain.
- The mesh sections are quickly connected with shackles.
- Unlike older ring net and woven net rockfall barriers, no secondary mesh is required. (See Fig. 3).



Figure 3: Installed GBE Rockfall Barrier

Case Studies:

USACE Jemez Dam Rockfall Project:

Project parameters: GBE-1000A rockfall barrier – Jemez Dam, NM

400 Lft. x 10 ft. high. Post spacing = 40 ft.

Owner: U.S. Army Corps of Engineers – Albuquerque District

Contractor: Groundhog Excavating, Inc.

Note: Construction of barrier completed in 8 working days. (See Figs. 4 & 5).



Figure 4: Installed GBE Rockfall Barrier, Jemez Dam, NM



Figure 5: Installed GBE Rockfall Barrier, Jemez Dam, NM

TNDOT Rockfall Project:

Project parameters: GBE-1000A rockfall barrier – US 64, Ocoee, TN

500 Lft. x 12 ft. high. Post spacing = 36 ft.

Owner: Tennessee DOT

Contractor: Ameritech Slope Constructors

Note: Construction of barrier completed in 12 working days. (See Fig. 6).



Figure 6: Ongoing Installation of GBE Rockfall Barrier, Ocoee, TN



Figure 7: Installed GBE Rockfall Barrier, Ocoee, TN

ADOT Rockfall Project:

Project parameters: GBE-500A rockfall barrier – I-8 Telegraph Pass

360 Lft. x 8 ft. high. Post spacing = 30 ft.

592 Lft. x 10 ft. high. Post spacing = 31 ft. – 2 in.

GBE-1000A rockfall barrier

600 Lft. x 10 ft. high. Post spacing = 30 ft.

Owner: Arizona DOT

Contractor: Fencecorp

Note: Construction of barrier completed in ___working days.

(See Fig. 8 & 9).

Conclusions:

The current rockfall barrier market is evolving and changing rapidly. Many governmental agencies and state highway departments are now requiring installation of tested and certified rockfall barriers that are covered under the ETAG 27 guideline. The GBE series of rockfall barriers fulfills this requirement. The other major advantage of these new technologically advanced rockfall barriers is their relative ease of installation.

A skilled construction crew of 4 men can install 100 linear feet of a GBE barrier in less than an hour once the post foundations and anchors have been prepared. It can be noted that an average rate of production for the GBE series of rockfall barriers is 80 linear feet per day versus 30-40 linear feet per day for older ring net or woven net rockfall barriers. This translates in a huge savings in construction labor and is very beneficial in the railway industry or highway construction where work is often time limited.

**North Slope Landslide A Investigation, US 62
Chickasha, Oklahoma**

By

James B. Nevels, Jr., Ph.D., P.E., LLC
Geotechnical Engineering Consultant, 605
Mimosa Dr., Norman, OK 73069-8622,
Cell No. (405) 818-2897,
e-mail: jnevels1@cox.net .

Introduction. Shallow landslide failures in highway embankments constructed in medium to high plasticity create costly maintenance problems. The site location of the embankment landslides recently and currently under investigation are in Grady County, Oklahoma within the Chickasha city limits along the west approach embankment over the old St. Louis & San Francisco Railroad line on US 62 highway. The south slope embankment slope failures (consisting of three separate slides) were investigated in 2005 and concluded with a detailed report and repair recommendations in 2006. They were relatively deep seated slides rotational landslides and were repaired at a contract cost of \$490,000 plus in 2008.

The north embankment slopes are now under study consist of two landslides, but they are noticeably shallow seated landslides. This paper investigates the mechanisms of stability degradation that leads to the shallow slope failures north embankment slope. The landslides were given the name **North Slope Landslides A and B**. A large contributing factor in these slope failures was the right of way restrictions that required the side slopes to be constructed steeper than the standard Oklahoma Department of Transportation (ODOT) side slopes set at 3:1 in order to accommodate the four lane highway widening. Unique to this investigation is the application of moisture diffusion and matric suction associated with the mechanisms of stability degradation. Further in the investigation a detailed back analysis is made to estimate the slip surface, and in doing so the use of dynamic cone soundings (DCP) supplemented with borings and closely spaced moisture content sampling are made. Critical to the study is the evaluation of the fully softened shear strength reasoned to be the operating shear strength of this first time slide. The GSTABL7 computer programs are utilized in the slope stability analysis. This paper concentrates on the larger landslide - **Landslide A**. The scope of this paper is to estimate the mobilized shear strength at the time of failure so that this shear strength can be utilized in the repair solution for **Landslides A and B**. New approaches in the use unsaturated soil mechanics have been advanced in recent years by Fredlund, D. G. and Rahardjo, H (1) and Lu, N. and Likos, W. J. (2).

The field investigation and laboratory processing and testing for the embankment investigation are in accordance with the current Oklahoma Department of Transportation (ODOT) geotechnical specifications for roadway design (October 31, 2005). These specifications stipulate embankment design requirements from a geotechnical

engineering perspective. The field work for this investigation was initiated on December 05, 2009 and nearly complete as of May 01, 2010.

Site Description. The site location is in the west side of Chickasha in Grady County, Oklahoma at the juncture of the west approach embankment over the old St. Louis & San Francisco Railroad line along US 62 highway. The site of the referenced project is located on US 62 0.93 miles southeast from the junction of US 62 and US 81 northbound. The North Slope Landslide location is circled in the northeast quarter of the Grady County Soil Survey sheet number 39, see Figure 1. As noted in Figure 1 the embankment is located on an alluvial deposit of Line Creek. A photograph of the **North Slope Landslide(s) A and B** from just outside of the New Holland Farm Implement Company property is given respectively in Figures 2 and 3. A view of the site from google map is shown in Figure 4. The approach embankment was constructed in a somewhat restricted right of way resulting in embankment slopes approximate slope ratio of 2.75:1. Construction of the embankment took place in the summer and fall of 1970.

The **North Slope Landslide(s)** were reported to have occurred in April 2005. They consist of one large and one small slide. The landslides appear to be very shallow seated as seen in Figures 2 and 3. The landslides were contained within the embankment slope as seen also in the above photographs in Figures 2 and 3.

The borrow source location for the embankment material was identified from the remaining construction records was recorded to have come from a pit approximately four miles west of the west embankment site on the south side of US 62 in a McInain silty clay loam,

Site Soils and Geology. The surface soils at site are mapped as the Port silt loam (40), 0 to 1 percent slopes according to the Grady County Soil Survey (August 1978)(2). A check with the USDA Natural Resources Conservation Service (NRCS) Web Soil Survey 2.2 program (4) indicates that the soil series at the site location has been re-correlated to the Yahola fine sandy loam 0 to 1 percent slopes, occasionally flooded. The extended soil information in the Web Soil Survey 2.2 is presented in Appendix A (to be included in the final detailed report).

The Grady County Soil Survey (August 1978) provides no geological information other than generalized geologic descriptions associated with the in-place soil series. According to the Oklahoma Department of Transportation (ODOT) Engineering Classification of Geologic Materials, Division Seven, 1969 (Red Book) (5), the underlying geology for this project alignment is the Dog Creek-Blaine subunits unit (Pdb) undifferentiated. This unit consists of dark red shales interbedded with minor amounts of fine-grained gypsiferous sandstones that locally grade into pure gypsum. Mudstone conglomerates a few feet in thickness occur sparingly within the strata. The total thickness of the unit varies from 130 to 230 feet. The unit forms broad flat to gently rolling prairie topography. According to the Oklahoma Geological Survey Hydrological Atlas 4 by Roy H. Bingham and Robert L. Moore 1975 (6), the geology is recorded as the Oil Creek and Joins formation. This formation consists of mostly red-brown silty shale and some fine-grained sandstone. The formation contains one or two layers of thin dolomite (or gypsum) in the lower part. Thicknesses of the unit averages about 200 feet

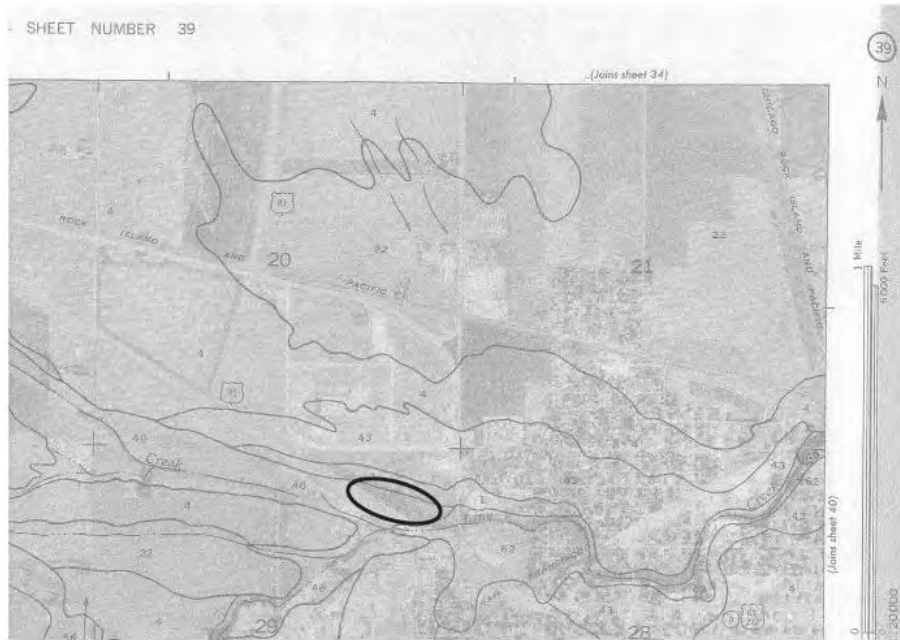


Figure 1. North slope landslide location Grady County Soil Survey sheet no. 39.



Figure 2. Landslide A.



Figure 3. Landslide B.



Figure 4. Google map of Landslide A and B location.

near Minco and about 130 feet near Chickasha. The Oklahoma Geological Survey does provide a definitive geologic publication, Geology of Grady County in Bulletin No. 73 by Carl C. Branson, 1954 (6) that identifies the site geology as Dog Creek Shale and Blaine Formation of Permian geologic age as described above.

Field Investigation. The survey plan for this landslide investigation consisted of five cross-sections in the large landslide **A** and one cross-section between the landslide **A** and the smaller landslide **B** to verify the original embankment design slope. Initially three cross-sections labeled A, B, and C were planned but were later supplemented with cross-sections 2 and 3 for **Landslide A**, see plan view of **Landslide A** in Figure 5. The five cross-sections were planned to be roughly centered around the center cross-section B, see plan view presented in Figure 5. The exterior extent of the **Landslide A** was measured from the center cross-section B in the upper extent of the landslide and from flag number 20 in center cross-section B for the lower extent. The five cross-sections in **Landslide A** were relatively equally spaced and were surveyed from a known benchmark on the northwest wing wall of the westbound railroad bridge.

One of the principal tasks of the field investigation was gauge the consistency of the embankment material with depth as well as to predict the slip surface(s) of the slide mass. A total of 36 dynamic cone penetration (DCP) soundings were made in the five cross-sections in this effort according to the ASTM D 6951-03 (7) standard. Summary plots of the five dynamic cone soundings versus depth per cross section, and the individual cross-section slopes for **Landslide A** are presented in Appendix B. A total of three hand auger borings were also made to further confirm the consistency of the embankment material according to ASTM D 1492-80(2000) standard. The boring logs are presented in a tabular and a gINT log format, see Appendix C (to be included in the final detailed report). A auger boring at the base of the embankment on cross section B five feet from the right of

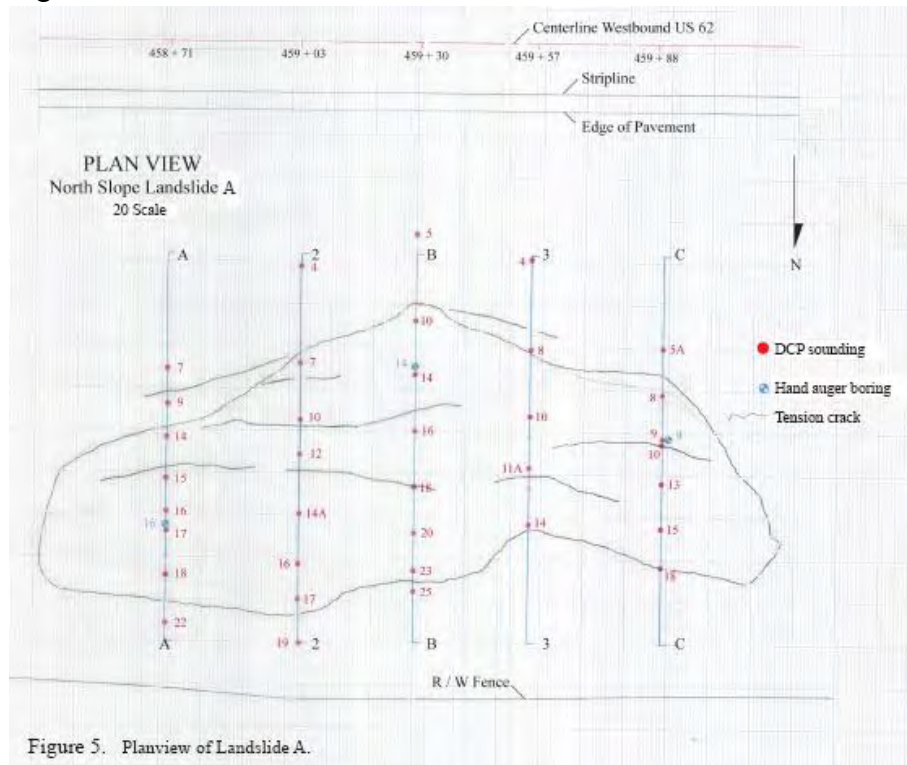


Figure 5. Planview of Landslide A.

way fence fixes the water table at a elevation of 1087 feet or approximately 9.0 feet beneath the embankment.

A large representative sample of the embankment material was taken from a test pit near the toe of cross-section 2. The borings from the larger south slope landslide reported in 2006 are presented in Appendix D (to be included in the final detailed report). All three borings indicate consistent medium to high plasticity, moist, red clay with shale fragments with depth.

Laboratory Testing. The laboratory tests performed on the soil samples taken in this investigation were in agreement with the most current and applicable AASHTO test procedures (8), since the embankment was constructed under AASHTO quality control standards. The laboratory testing schedule included the determination of the natural moisture content (AASHTO T265), Atterburg limits (AASHTO T89 and T90), grain size distribution (AASHTO T88), laboratory moisture-density relations of soils (AASHTO T99A). The determination of a unconsolidated undrained triaxial compression and an consolidated undrained triaxial compression tests were determined according to AASHTO T-296 and T-297 respectively. The test results are presented in Appendix E in a tabular and graphical format (to be included in the final detailed report).

The moist unit samples of the embankment material were taken from selected chunk specimens that were sampled from the three auger borings with depth for measuring the in-place wet unit weight, see corrected wet unit weights (converted to dry density) plotted on the moisture versus dry density. Experience has shown that hand augering in stiff clay soils that the augering process does produce relatively intact and undisturbed chunk specimens sufficient for in-place wet unit weight determination. The test data from the representative sample of the embankment material taken from a test pit near the toe of cross-section 2 is presented in Appendix E.

Analysis. According to ODOT Division 7 records since construction, the present **North Slope Landslides A and B** occurred at the same time frame as the south slope embankment slope failures (consisting of three separate slides) that were investigated in 2005 landslides as first time landslides. The operating shear strength at the slope failure is assumed to be a drained shear strength for all cases and further a fully softened drained shear strength. The effort here was to perform a back-calculation to predict the developed shear strength parameters (c'_d and Φ'_d) based on reasonable estimates of the slip surface and measured average soil properties of the embankment material for each of the five cross-sections. Cross section B was used for this purpose.

The estimate of the slip surface was set by the lowest dynamic penetration index (DPI) versus depth in tenths of a foot. A study of the DCP soundings in the five cross sections shown in Appendix B point out the following important conclusions: a) within 3 to 5 feet of the ground slope surface the degree of compaction and moisture content are in highly variable as measured by the DPI, b) below this depth the 3 to 5 foot depth the DPI becomes very stiff, and c) the estimated slip surface was variable. In cross sections A, B, and 2, the variability of the slip surface suggests that the development of the landslide mass in **Landslide A** is a result of progressive slope failure(s). In Figure 3 **Landslide B**

is reasoned to the start of another series slope movements advancing up slope and eventually joining up with **Landslide A**.

A trial and error approach for the global slope stability was analyzed by the GSTABL7 with STEDwin version 2.005 slope stability software by Garry H. Gregory, September 2006 to determine the fully softened shear strength parameters (c' and Φ') for a assumed factor of safety (FS) equal to one at the time of failure. This software uses an iterative approach where the soil property data, slope geometry, water table, and analysis technique is inputted into the GSTABL7 program. Because of the shallow depth of the slip surface indicated in the in the five cross sections shown in Appendix B, the Block2 analysis option in the GSTABL7 program was selected to model the landslide in the back calculation which approximates a shallow wedge failure pattern. After many trial runs with variation in the soil properties, an estimate of the fully softened shear strength parameters (c' and Φ') was found to be 30 psf (0.21psi) and 16° respectively, see Figure 6.

Details of the soil analysis from the test pit indicate an important point in the analysis in that there is considerable variation in the dry densities as seen dry density versus moisture plot, see Figure 7. The fully softened shear strength was estimated from a unconsolidated undrained (UU) triaxial test that corrected using the Gregory reduction factor (RF_M) = $I_s^{(\log CI)}$ where CI is the cohesion index. As can be seen in Figure 8, the shear strength parameters (c' and Φ') do not agree. This is partly due to the fact that a UU triaxial shear test was used instead of a consolidated undrained test with pore pressure (CU). However, the question might be what actual shear strength are we really dealing with here, refer to Figure 7.

Based on the test data shown in Appendix E, the embankment soil with depth is probably still unsaturated. To confirm this contention refer to Table 1 where the degree of saturation of soil samples are calculated from moisture content and wet unit weight test data. As can be seen from Table 1 from the three auger borings within the estimated depth of the not all of the soil samples are saturated. The question is can saturated soil mechanics principles be applied in an unsaturated soil problem. The back calculated analysis shear strength parameters (c'_d and Φ'_d), 30 psf (0.21psi) and 16° respectively nearly match the generalized Mohr-Coulomb shear strength equation by Aubeny and Lytton (9)

$$\tau_f = (\sigma_n - u_a) \tan\Phi' + f\theta (u_a - u_w) \tan\Phi' \quad (1a)$$

where the shear strength is controlled the mechanical stress ($(\sigma_n - u_a) \tan\Phi'$) and the matric suction ($u_a - u_w$) and the cohesion intercept (c') is assumed to equal 0. The f in the equation is a factor ranging from $1/\theta$ to 1 depending on the degree of saturation (θ). At full saturation equation (2a) reduces to

$$\tau_f = (\sigma_n - u_w) \tan\Phi' \quad (1b)$$

The apparent matric suction has an approximate equivalent effect to the cohesion intercept in the saturated soil mechanics equation

$$\tau_f = c' + \sigma_n \tan\Phi' \quad (1c)$$

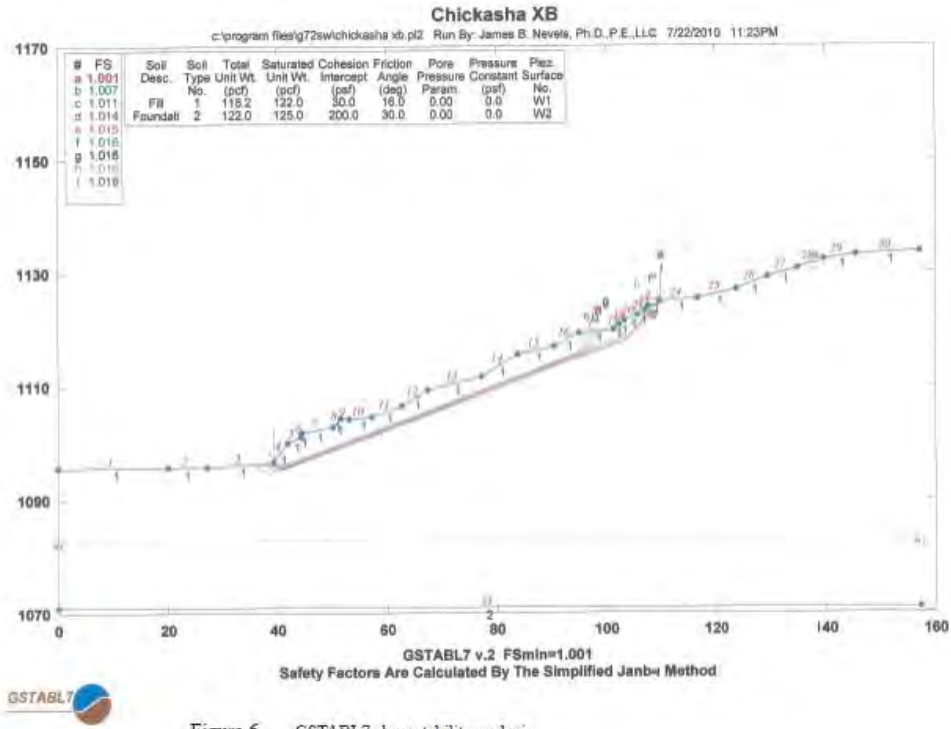


Figure 6. GSTABL7 slope stability analysis.

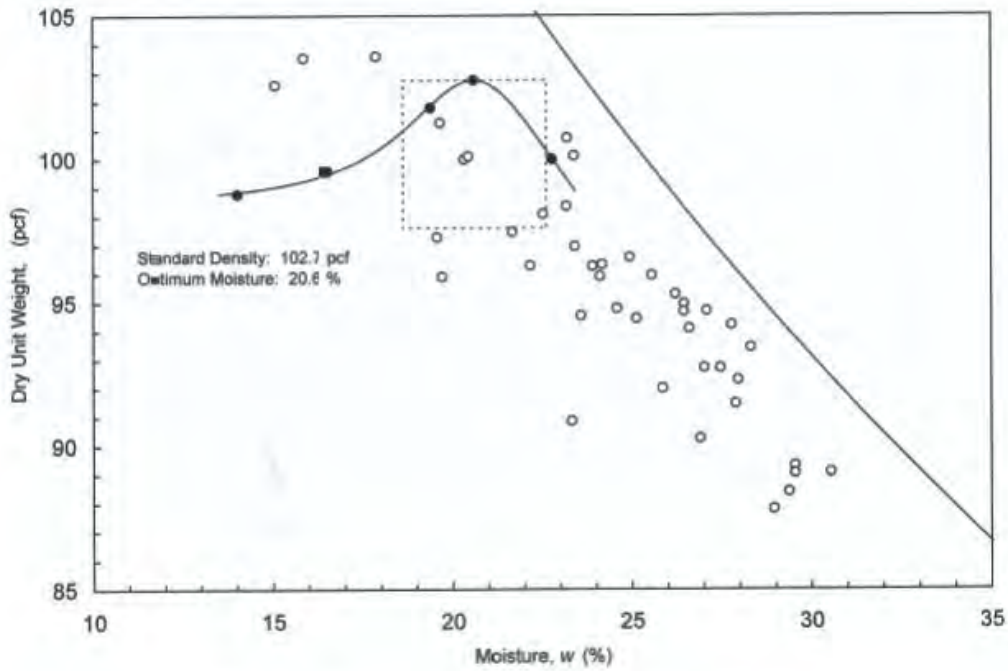


Figure 7. Moisture - density relationship with estimated in-place densities.

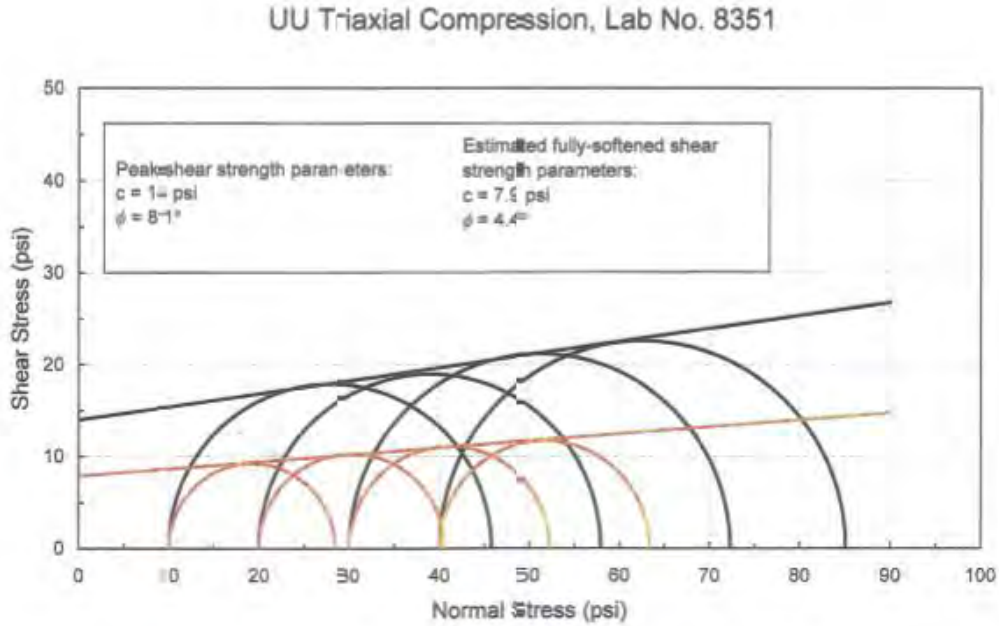


Figure 8. Estimated fully softened shear strength with the Gregory RfM.

Table 1. Degree of Saturation.

Cross Section	Boring No.	Moisture Class ¹	Moisture Content, %	Degree of Saturation
A	16	A	21.09	0.89
		B	19.71	0.83
		C	21.09	0.89
		D	22.53	0.95
3	7	A	24.98	1.06
		B	18.36	0.76
		C	22.49	0.95
		D	26.90	1.14
C	9	A	25.82	1.09
		B	22.17	0.94
		C	27.98	1.18
		D	30.67	1.30

1. Moisture Class : A- average MC in the boring, B- driest MC in 3 to 5 foot depth, C- wettest MC in 3 to 5 foot depth, D- average MC in 3 to 5 foot depth.

Conclusion. In compacted clay embankment slopes the moisture infiltration into the slope can lead to a condition of near full soil saturation. But this should not be construed

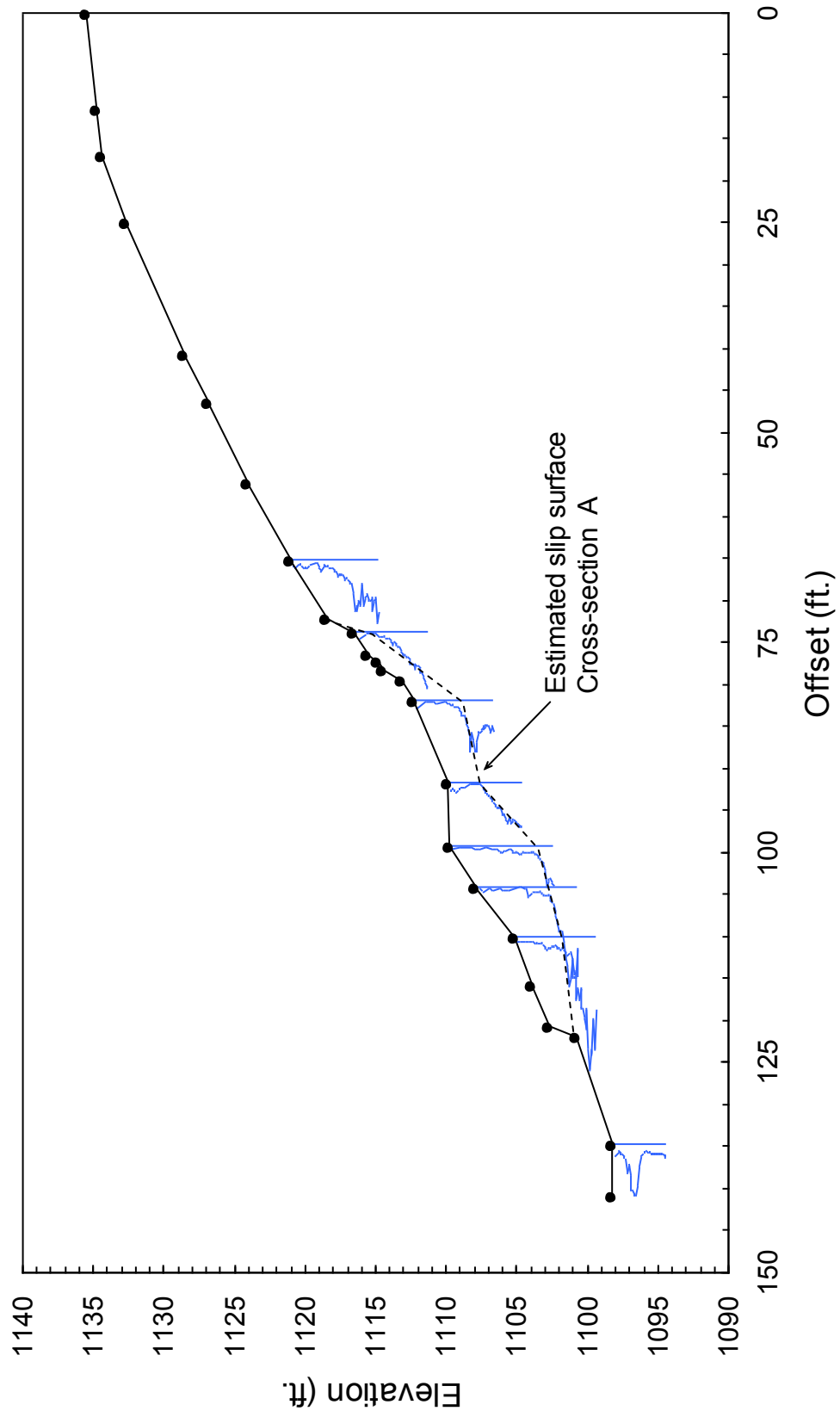
as a regional water table as it is associated only with the localized wetting of the surface of the slope. The pore water pressures in these shallow landslides will in general be negative in embankment material above a water table. Unsaturated soil mechanics principles are better suited in rationally explaining the mechanisms in shallow landslides in embankment clay soils.

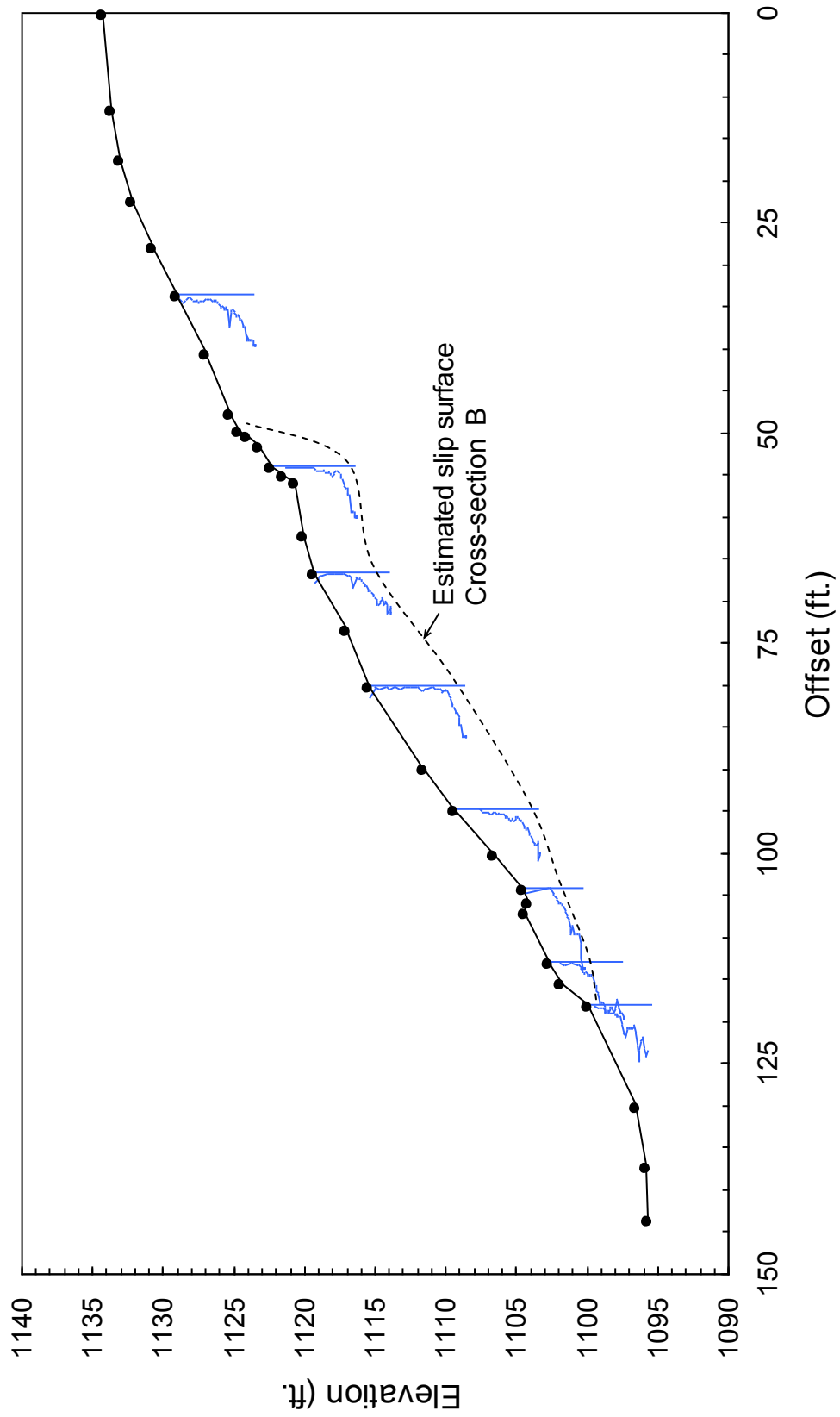
References.

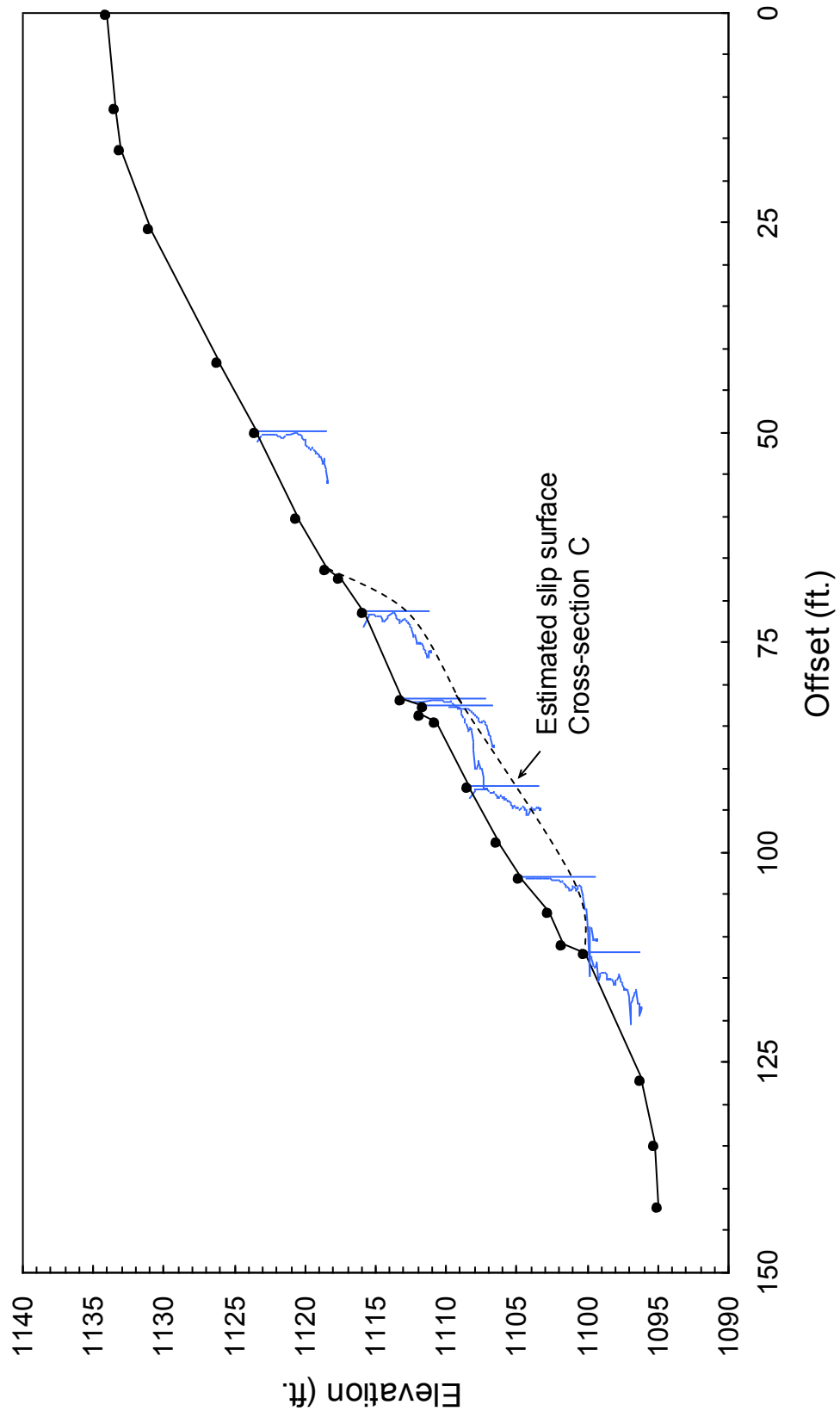
1. Fredlund, D. G. and Rahardjo, H., *Soil Mechanics for Unsaturated Soils* , John Wiley & Sons, Inc., New York, 517pp.
2. Lu, N. and Likos, W.J., *Unsaturated Soils Soil Mechanics*, John Wiley & Sons., Inc., New York, 556pp.
3. Soil Survey of Grady County (1978), USDA, Soil Conservation Service.
4. Engineering Classification of Geologic Materials, Division 7, Oklahoma Highway Department, Research and Development Division, 1969.
5. Oklahoma Geological Survey Hydrological Atlas 4 by Roy H. Bingham and Robert L. Moore, 1975.
6. Geology of Grady County in Bulletin No. 73 by Carl C. Branson, 1954.
7. AASHTO, Twenty Fifth Edition, 2005.
8. ASTM, 2009, Volume 04.03
9. Aubeny, C.P., and Lytton, R. L., *Shallow Slides in Compacted High Plasticity Clay Slopes*, Journal of the Geotechnical and Geoenvironmental Engineering, ASCE, July 2007.

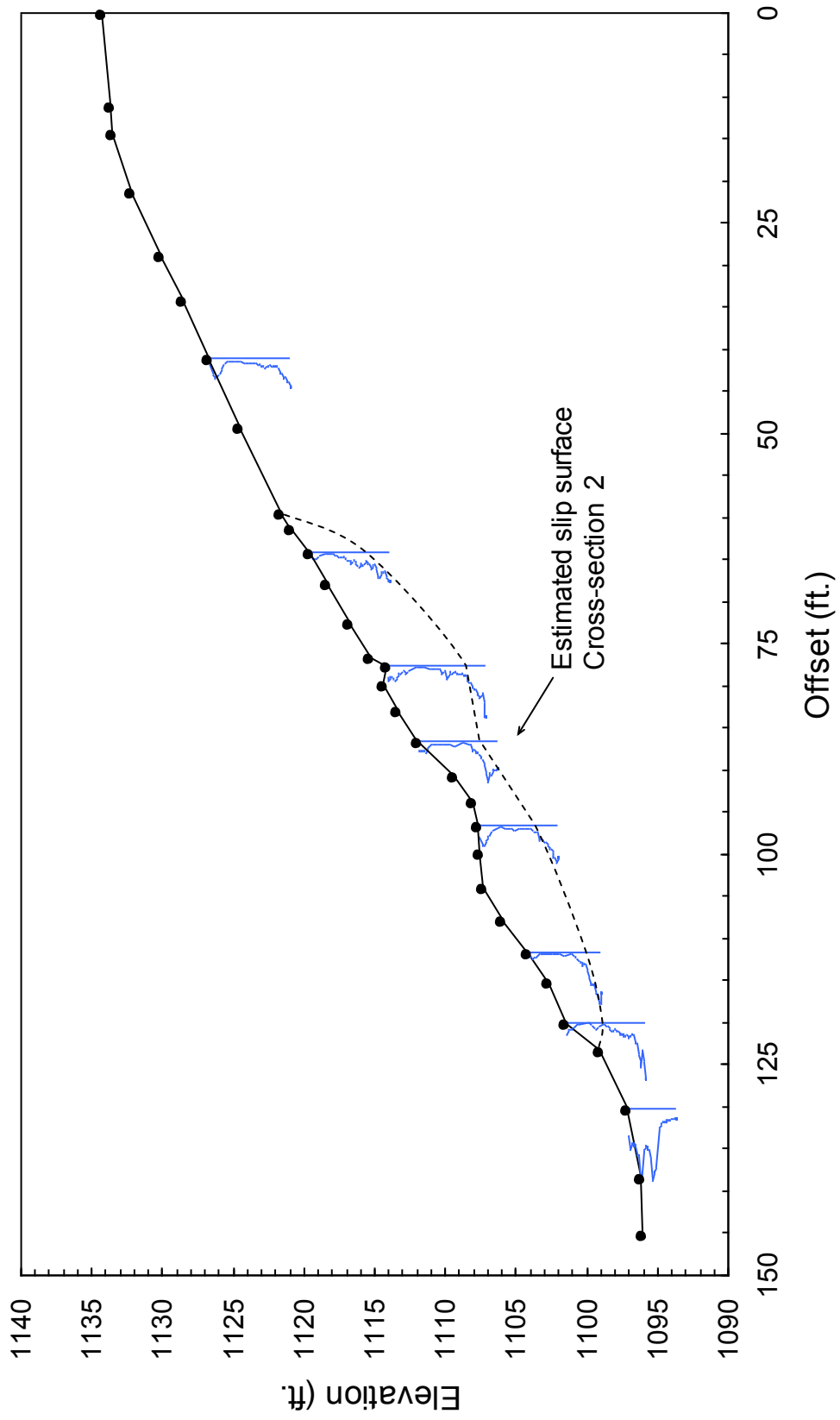
APPENDIX B

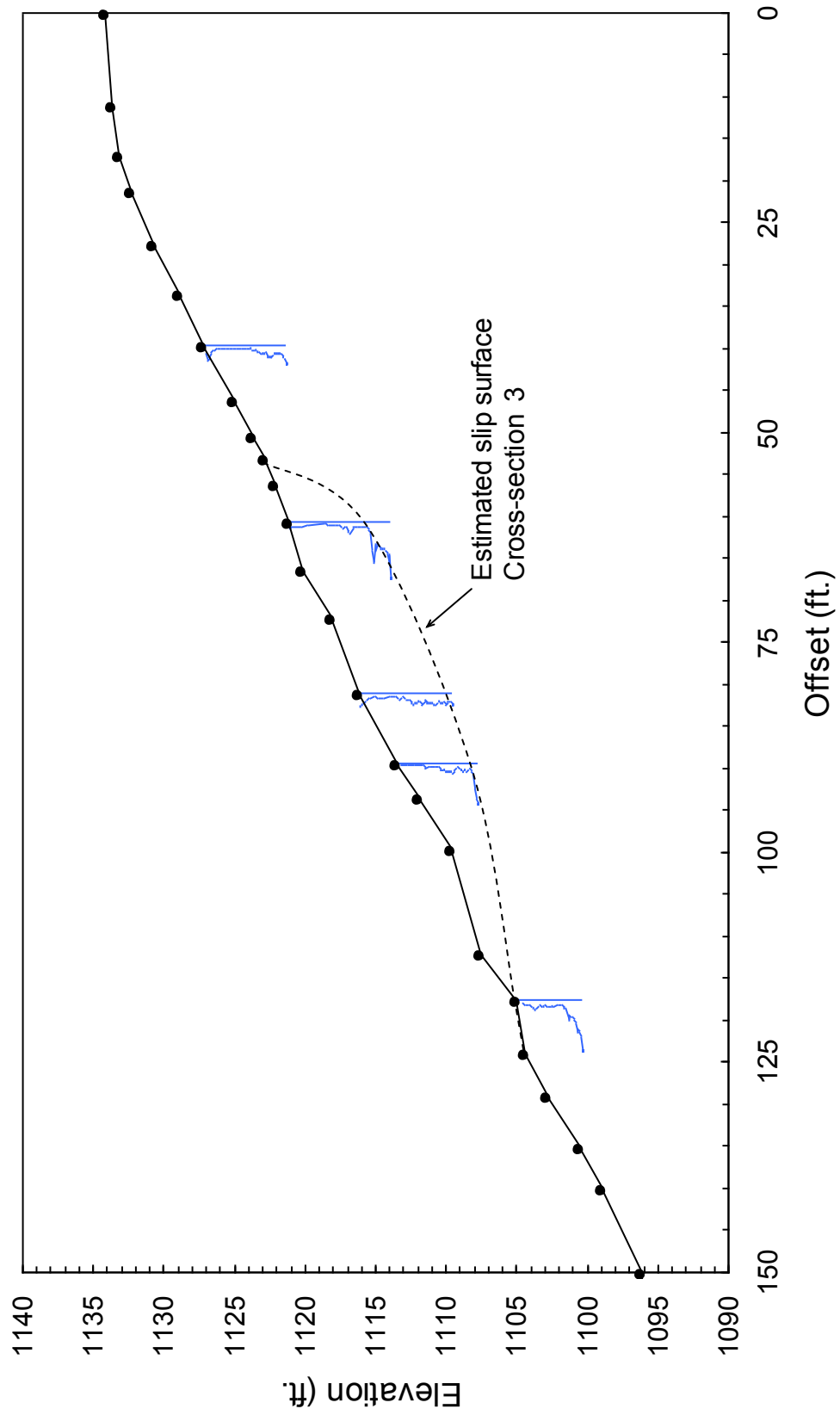
Summary of DCP Soundings











Influence of Various Cementitious Additives on the Durability of Stabilized Subgrades

Pranshoo Solanki

Research Associate, School of Civil Engineering and Environmental Science, University of Oklahoma
202 West Boyd Street, Room 334
Norman, OK, 73019-1024;
(405) 325-4236
pranshoo@ou.edu

Musharraf M. Zaman

David Ross Boyd Professor and Aaron Alexander Professor, Associate Dean for Research and Graduate Education, College of Engineering, University of Oklahoma
202 West Boyd Street, Room 107
Norman, OK, 73019
(405) 325-2626
zaman@ou.edu

Jeff Dean

Pavement Design Engineer, Oklahoma Department of Transportation
200 N. E. 21st Street, Room 2C2
Oklahoma City, OK, 73105
(405) 522-0988
jdean@odot.org

Prepared for the 61st Highway Geology Symposium, August, 2010

Acknowledgements

The author(s) would like to thank the individuals/entities for their contributions in the work described:

Vincent Reidenbach – Geotechnical Engineer, Oklahoma Department of Transportation
Christopher Clark – Geotechnical Lab Supervisor, Oklahoma Department of Transportation
Financial support for this study was provided by the Oklahoma Department of Transportation.

Disclaimer

Statements and views presented in this paper are strictly those of the author(s), and do not necessarily reflect positions held by their affiliations, the Highway Geology Symposium (HGS), or others acknowledged above. The mention of trade names for commercial products does not imply the approval or endorsement by HGS.

Copyright Notice

Copyright © 2010 Highway Geology Symposium (HGS)

All Rights Reserved. Printed in the United States of America. No part of this publication may be reproduced or copied in any form or by any means – graphic, electronic, or mechanical, including photocopying, taping, or information storage and retrieval systems – without prior written permission of the HGS. This excludes the original author(s).

ABSTRACT

A comparative laboratory study was conducted to evaluate the durability of three different subgrade soils stabilized with hydrated lime, class C fly ash (CFA), and cement kiln dust (CKD). Cylindrical specimens were compacted and cured for 7 days in a moist room having a constant temperature and controlled humidity. After curing, the specimens were tested for freeze-thaw (F-T) cycling, vacuum saturation and tube suction. The residual unconfined compressive strength (UCS) value after F-T cycling and vacuum saturation was compared with those of the raw soil specimens to determine the influence of cementitious stabilization on durability. The residual UCS values revealed that the addition of cementitious additive substantially increased the durability of stabilized specimens. The extent of improvement in durability, however, was dependent on the characteristics of both soil and additive. Also, durability evaluated using vacuum saturation test produced good correlations with residual strength of specimens subjected to F-T and W-D cycles indicating that vacuum saturation could be used as a time-efficient and inexpensive method for evaluating durability of stabilized soils. It was also found that the final dielectric constant values (DV) measured by conducting tube suction tests are influenced by the method of specimen preparation. However, the final DV is not affected by the specimen size.

INTRODUCTION

Durability (or long-term performance) of pavement materials induced by changes in climatic conditions namely, freeze-thaw (F-T) and wet-dry (W-D), have been recognized by pavement engineers as a major factor in poor pavement performance. In cold regions, F-T action is considered to be one of the most destructive actions that can induce significant damage to a pavement structure. The freezing of the moisture present in the pore spaces of soil structure results in the formation of ice lenses. During times of temperate weather, the ice lenses thaw, and the structural capacity of the roadway may be dramatically reduced (1). The repeated action of F-T deteriorates the integrity of the pavement structure indicating possible changes in the engineering properties of pavement material such as resilient modulus and unconfined compressive strength. The importance of considering durability in mixture design has been highlighted by AASHTO (2), Transportation Research Circular E-C086: Evaluation of Chemical Stabilizers (3), and a recent NCHRP Web-Only Document: Recommended Practice for Stabilization of Subgrade Soils and Base Materials (4).

Consequently, this study was undertaken with the objective of exploring the influence of different cementitious additives on the durability of stabilized subgrades commonly encountered in Oklahoma. Three different cementitious additives namely hydrated lime, class C fly ash (CFA), and cement kiln dust (CKD) were used. The durability of 7-day cured stabilized samples was evaluated by conducting F-T cycling, vacuum saturation, and tube suction tests.

OVERVIEW OF PREVIOUS STUDIES

A review of previous studies reveals no widely accepted laboratory procedure to evaluate the durability of cementitiously stabilized subgrade soils. Hence, a summary of different experimental procedures available in literature for evaluating durability of stabilized soil specimens is provided in this section.

Freeze-Thaw and Wet-Dry Cycling

Soil specimens subjected to freeze-thaw (F-T) or wet-dry (W-D) cycles provide an indication of how those specimens will maintain engineering parameters in the field under diverse environmental conditions. Among “conventional” laboratory procedures, the ASTM D 559 and ASTM D 560 test methods are the only existing standardized procedures for evaluating effect of W-D and F-T cycles on cement-stabilized soil specimens, respectively. These methods consist of mixing soil and additives at optimum moisture content and compacting with standard effort in a 4 in (100 mm) diameter Proctor mold. After compaction, specimens are cured for 7 days in a humidity room and then subjected to a series of F-T or W-D cycles. After completion of each cycle, the specimens are brushed on all sides with a wire brush and the effect of F-T or W-D cycles is measured in terms of percent weight loss. As a result of the variability associated with the brushing process, many agencies and researchers omit the brushing portion of the test and replace it with unconfined compressive strength (UCS) testing after completion of all 12 cycles (5).

In a combined laboratory and field study from Oklahoma, Miller and Zaman (6) investigated the durability of CKD-stabilized soil by performing UCS on samples subjected to F-

T and W-D cycles separately. Tests were conducted on three 7-day cured combinations of soil and additives, namely CKD with sand, CKD with shale, and quicklime with shale. One W-D cycle consisted of immersing samples in water for 5 hours, followed by oven drying for 24 hours at 160°F (71°C). Samples that survived were subjected to UCS after 0, 1, 3, 7, and 12 W-D cycles. The UCS tests were conducted after the drying cycle so that moisture conditions would be uniform for each sample tested. The same procedure was used to prepare and cure samples during F-T testing. One F-T cycle consisted of placing samples in a freezer at -9°F (-23°C) for 24 hours and then placing the samples in a moisture chamber under controlled humidity of 95% and temperature of about 73°F (23°C). UCS tests were conducted after 0, 1, 3, 7, and 12 cycles. Specimens were tested at the end of the thawing period. CKD-stabilized shale specimens showed an increase in UCS values for the first three W-D cycles, beyond which samples did not survive immersion in water. On the other hand, specimens stabilized with quicklime survived only one W-D cycle. Sand specimens stabilized with CKD showed an increase in UCS values over the full 12 W-D cycles. Contrary to W-D cycles, all the specimens survived the full 12 F-T cycles.

Arora and Aydilek (7) conducted F-T tests on silty sand (SM) stabilized with 40% class F fly ash in combination with cement or lime. It was found that the strength of specimens stabilized with class F fly ash and cement increased with increasing number of F-T cycles. The increase in strength was more enhanced for mixtures that contained 7% cement than for mixtures with 4% and 5% cement. Also, lime-stabilized specimens survived during F-T cycles, but their strengths decreased with increasing number of F-T cycles.

Vacuum Saturation

The vacuum saturation method was proposed by Dempsey and Thompson (8) as a rapid and economical method for predicting the durability of stabilized materials. Currently, vacuum saturation test is outlined in ASTM C 593 as a durability test for Class C fly ash, lime-fly ash, and lime-stabilized soils. This method consists of mixing soil and additives at optimum moisture content and compacting with standard effort in a 4 in (100 mm) diameter Proctor mold. After compaction, specimens are cured for 7 days and placed in a vacuum chamber that is subsequently evacuated to a pressure of 24 in Hg. (610 mm Hg., 11.8 psi). After 30 minutes, the chamber is flooded with de-ionized water, and the vacuum is removed. The specimens are allowed to soak for 1 hour and are then tested for UCS. Only a few studies (e.g., 9, 10, 11) are available in the literature on this topic.

In a recent study, Parker (11) conducted vacuum saturation tests on silty sand and lean clay stabilized with different types of additives, namely class C fly ash, lime-fly ash, lime or Type I/II Portland cement. It was found that the silty sand specimens stabilized with lime-fly ash had significantly higher UCS after vacuum saturation than specimens stabilized with CFA, lime, or cement. Also, clay specimens stabilized with CFA or lime-fly ash had significantly higher UCS values than specimens stabilized with cement or lime. This study also proposed strong correlations between residual UCS values after F-T cycling and vacuum saturation.

Tube Suction Test

The Tube Suction Test (TST) was developed by the Finnish National Road Administration and the Texas Transportation Institute to evaluate the moisture susceptibility or

the amount of “free” water present within a soil system (12, 13). The TST involves measurement of surface dielectric values (DV) of the test specimens. During the test, the increase of moisture in the specimen is monitored with a dielectric probe, which measures the dielectric properties at the surface of the specimen. The DV is a measure of the unbound or “free” moisture within the specimen. High surface dielectric readings indicate suction of water by capillary forces and can be an indicator of a non-durable material that will not perform well under saturated or freeze-thaw cycling conditions (14). Guthrie and Scullion (15) suggested that aggregate base specimens having final dielectric readings less than 10 be characterized as satisfactory with respect to moisture and/or frost susceptibility, while specimens with final readings above 16 be considered unsatisfactory. Aggregate base specimens with final dielectric values between 10 and 16 are expected to exhibit marginal long-term durability. To the author’s knowledge, there are no recommended lower and upper DV values for stabilized soil specimens. Hence, in the present study, DV values will be used to evaluate comparative moisture susceptibility of stabilized soil specimens.

In recent years, TST results have been correlated with bearing capacity, frost heave, and several other parameters (14, 15, 16, 17, 18, 19, 20, 21). Little (17) evaluated moisture susceptibility of low, moderate, and high plasticity soils using TST. Moisture susceptibility was determined indirectly by measuring the DV of stabilized specimens using a PercometerTM. Tests were performed on three versions of each soil: untreated, lime-treated with unsealed curing, and lime-treated with controlled curing (seal-cured). It was found that for low-plasticity soils, lime acted as a fine filler and increased the water content after capillary soaking. No significant difference was seen on the DV over that of the untreated soil. For moderate plasticity and high plasticity soils, lime treatment, with seal-curing, resulted in slightly lower moisture contents and substantial and statistically significant reductions in DVs.

In a recent study, Zhang and Tao (21) conducted TST for evaluating durability of cement-stabilized low plasticity soils. A series of specimens were molded at six different cement contents (2.5, 4.5, 6.5, 8.5, 10.5 and 12.5%) and four different molding moisture contents (15.4, 18.5, 21.5, and 24.5%). It was found that the final stable DV values of stabilized specimens were all above the value of 30. The maximum DVs generally decreased with an increase in cement content. With an increase in the molding moisture content, it was less effective for cement to reduce the maximum DV. Also, it was reported that at a low cement dosage, specimens molded on the dry side of compaction curve can suck in free water faster than those compacted on the wet side until enough amount of cement is used. Furthermore, the test results indicated that the water-cement ratio of cement-stabilized soil had the dominant influence on the maximum DV.

MATERIALS

In this study, three soils namely Port series soil (P-soil), Kingfisher series soil (K-soil), and Carnasaw series soil (C-soil) were used to evaluate the durability. A summary of the soil properties determined in the laboratory and the corresponding standard testing identification are presented in Table 1. According to the USCS, P-soil is classified as CL-ML (silty clay with sand) with a liquid limit of approximately 27 and a plasticity index (PI) of approximately 5. K-soil is classified as CL (lean clay), according to the UCSS with an average liquid limit of approximately 39% and a PI of approximately 21. As per the USCS, C-soil is classified as fat clay (CH) according to USCS with a PI value of 29.

Table 1 – Testing Designation and Soil Properties

Method	Parameter/Units	P-soil	K-soil	C-soil
ASTM D 2487	USCS Symbol	CL-ML	CL	CH
AASHTO M 145	AASHTO Designation	A-4	A-6	A-7-6
ASTM D 2487	USCS Name	Silty clay with sand	Lean clay	Fat clay
ASTM D 2487	% finer than 0.075 mm	83	97	94
ASTM C 430	% finer than 0.045 mm	54	89	87
ASTM D 422	% finer than 0.002 mm (clay content)	11	45	48
ASTM D 4318	Liquid limit	27	39	58
ASTM D 4318	Plastic limit	21	18	29
ASTM D 4318	Plasticity index	5	21	29
...	Activity	0.24	0.47	0.69
ASTM D 854	Specific gravity	2.65	2.68	2.64
ASTM D 698	Optimum moisture content (%)	13.1	16.5	20.3
ASTM D 698	Max. dry unit weight (kN/m ³)	17.8	17.4	16.3

USCS: Unified Soil Classification System

Table 2 – Chemical and Physical Properties of Stabilizers used in this Study

Chemical compound/Property	Percentage by weight, (%)		
	Lime	CFA	CKD
Silica (SiO ₂) ^a	0.6	37.7	14.1
Alumina (Al ₂ O ₃) ^a	0.4	17.3	3.1
Ferric oxide (Fe ₂ O ₃) ^a	0.3	5.8	1.4
Silica/Sesquioxide ratio (SSR)	1.9	3.0	6.0
SiO ₂ /(Al ₂ O ₃ +Fe ₂ O ₃)	68.6	24.4	47
Calcium oxide (CaO) ^a	95.9 ^{**}
Calcium hydroxide (Ca(OH) ₂) ^a	0.7	5.1	1.7
Magnesium oxide (MgO) ^a	0.1	1.2	4.4
Sulfur trioxide (SO ₃) ^a	0.1	2.2	1.7
Alkali content (Na ₂ O + K ₂ O) ^a	31.8 [*]	1.2	27
Loss on ignition ^b	46.1	0.2	6.7
Free lime ^b	98.4	85.8	94.2
Percentage passing No. 325 ^c	12.58	11.83	12.55
pH (pure material) ^d	17.0	6.0	12.0
Specific surface area (m ² /gm) ^e	...	708	17
28-day UCS (kPa)	...	708	17

^aX-ray Fluorescence analysis; ^bASTM C 114; ^cASTM C 430; ^dASTM D 6276; ^eEthylene glycol monoethyl ether method (Cerato and Lutenegeger 2001); UCS: Unconfined compressive strength; *Ca(OH)₂ decomposes at 512°C; **Before ignition

As noted earlier, three different cementitious additives, namely hydrated lime, class C fly ash (CFA), and cement kiln dust (CKD), were used. Hydrated lime was supplied by the Texas Lime Company in Cleburne, Texas. It is a dry powder manufactured by treating quicklime (calcium oxide) with sufficient water to satisfy its chemical affinity with water, thereby converting the oxides to hydroxides. CFA from Lafarge North America (Tulsa, Oklahoma) was brought in well-sealed plastic buckets; it was produced in a coal-fired electric utility plant. CKD used was provided by Lafarge North America located in Tulsa, Oklahoma. It is an industrial

waste collected during the production of Portland cement. The physical and chemical properties of the stabilizing agents are presented in Table 2.

LABORATORY PROCEDURE

Conventional Freeze-Thaw Test

Table 3 – A Summary of OMC-MDD of Soil-Additive Mixtures

Type of Soil	Type of additive	Percentage of additive	OMC (%)	Maximum dry density	
				kN/m ³	pcf
P-soil	None	0	13.1	17.8	113.4
K-soil		0	16.5	17.4	110.6
C-soil		0	20.3	16.3	103.7
P-soil	Lime	6	15.9	16.9	107.2
K-soil		6	16.5	16.8	106.6
C-soil		6	22.7	15.6	99.0
P-soil	CFA	10	12.8	18.1	114.9
K-soil		10	15.3	17.4	111.0
C-soil		10	18.6	16.6	105.3
P-soil	CKD	10	15.2	17.2	109.3
K-soil		10	17.3	17.1	108.6
C-soil		10	21.7	16.0	101.8

1 pcf = 0.1572 kN/m³; OMC: optimum moisture content; MDD: maximum dry density; CFA: class C fly ash; CKD: cement kiln dust

The freeze-thaw (F-T) test was performed in accordance with the procedure outlined in ASTM D 560. Specimens were prepared by mixing raw soil with a specific amount of additive. The amount of additive (6% for lime and 10% for CFA and CKD) was added based on the dry weight of the soil. The specimens were molded with a Harvard Miniature device (diameter = 1.3 in i.e., 33 mm and height = 2.8 in i.e., 71 mm). The Harvard Miniature procedure was calibrated in accordance with the ASTM D 4609 test method using each soil and additive mixture so that at the standard Proctor optimum moisture content (OMC) and the Harvard Miniature procedure produced a specimen having the standard Proctor maximum dry density (MDD). All specimens were compacted at the OMC and MDD of the soil-additive mixture, as presented in Table 3. After compaction, the specimens were cured for 7 days at a temperature of 73.4 ± 3.1°F (23.0 ± 1.7°C) and a relative humidity of approximately 96%, as recommended by the ASTM D 1632 test method. A total of two replicates were prepared for each combination and then subjected to 0, 1, 4, 8 and 12 F-T cycles after 7 days of curing. Each F-T cycle consists of freezing for 24 hours at a temperature not warmer than -10°F (-23.3°C) and thawing for 23 hours at 70°F (21.1°C) and 100% relative humidity. Free potable water was made available to the porous plates under the specimens to permit the specimens to absorb water by capillary action during the thawing period. After the completion of appropriate F-T cycle, unconfined compressive strength (UCS) tests were conducted by loading specimens in a displacement control mode at a strain rate of 1% per min.

Vacuum Saturation Test

The vacuum saturation test was performed in accordance with the ASTM C 593 test method with slight modifications. This method consisted of mixing soil and additives, namely 6% lime, 10% CFA, or 10% CKD, and compacting with standard effort in a Proctor mold (diameter = 4 in i.e., 100 mm and height = 4.5 in i.e., 115 mm). After compaction, the specimens were cured in a humidity room at $73.4 \pm 3.1^\circ\text{F}$ ($23.0 \pm 1.7^\circ\text{C}$) rather than at 100°F (37.8°C), as specified in the ASTM procedure. Following curing, the specimens were placed in a vacuum chamber that was subjected to a vacuum pressure of 11.8 psi (81.3 kPa; 24 in Hg). After 30 minutes, the vacuum was removed and the chamber flooded with water and the specimens were allowed to soak for 1 hour. After the saturation period, the water was drained and the specimens were immediately tested for UCS by loading the specimens in a displacement control mode at a strain rate of 1% per min. A comparison of the differences in UCS values between specimens subjected to this procedure (UCS after vacuum saturation) and those not subjected to this procedure (UCS before vacuum saturation) provided a relative measure of durability of the stabilized specimens. The vacuum chamber consists of a 1 in (25 mm) thick Plexiglas lid. The specimens were placed in an upright position on a perforated steel plate so that water could enter the soil from all surfaces.

Tube Suction Test

Since there is no standard protocol for conducting tube suction tests, the durability of specimens was evaluated by preparing specimens by using the following three different methods:

1. *Method-1*

Compaction: Standard Proctor compaction (five layers/lifts) at the OMC and a target dry density of 95-100% of MDD

Cylindrical specimen size: diameter = 4 in (101.6 mm), height = 8 in (203.2 mm)

2. *Method-2*

Compaction: Superpave gyratory compactor (single layer/lift) at the OMC and a target dry density of 95-100% of MDD

Cylindrical specimen size: diameter = 4 in (101.6 mm), height = 4 in (203.2 mm)

3. *Method-3*

Compaction: Superpave gyratory compactor (single layer/lift) at the OMC and a target dry density of 95-100% of MDD

Cylindrical specimen size: diameter = 6 in (152.4 mm), height = 6 in (152.4 mm)

After compaction, the specimens were cured for 7 days in a controlled environment with a temperature of $73.4 \pm 3.1^\circ\text{F}$ ($23.0 \pm 1.7^\circ\text{C}$) and a relative humidity of approximately 96%. Then, the specimens were dried in an oven at $104 \pm 9^\circ\text{F}$ ($40 \pm 5^\circ\text{C}$) for two days. After oven drying, the specimens were allowed to cool down at room temperature for 30 minutes, and then applied with a thin layer of grease around the lateral surface and placed on a porous stone in an open dish containing approximately 0.4 in (10 mm) of de-ionized (DI) water. Since the quality of the porous stones has significant influence on the final DV (22), clean porous stones were used. Furthermore, the top surfaces of the specimens were covered with a plastic sheet and plate to avoid loss of moisture due to evaporation. During wetting of the specimens in DI water, the increase in dielectric value (DV) with time due to capillary rise of water was measured. Four

measurements were taken along the circumference of the specimen in separate quadrants and the fifth reading was taken at the center of specimen and an average of all five readings was calculated. Measurements were taken daily for 10 days using a dielectric probe (or Percometer™) and the final 10th day reading was reported. A photographic view of the TST setup is shown in Figure 1. To ensure adequate contact of the probe on the top of surface of the specimen, a surcharge of 4.86 lb (2.2 kg) was applied (Figure 1). After 10 days of TST, specimens prepared by using Method-1 and Method-2 were cut into five and three equal layers, respectively, and oven dried for moisture content.

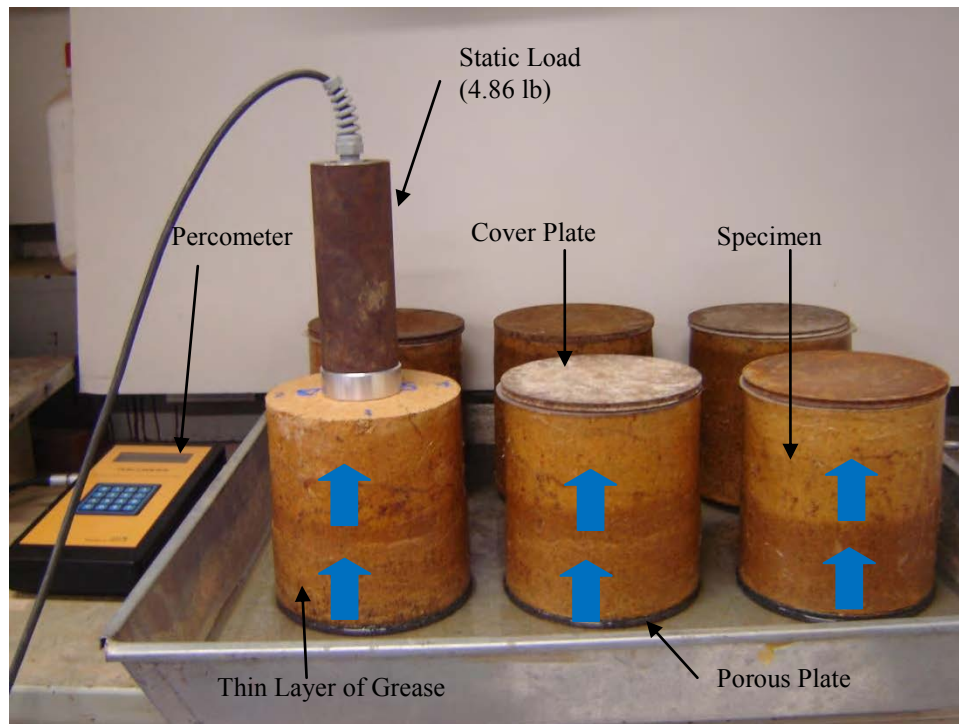


Figure 1 – Setup for Tube Suction Test

PRESENTATION AND DISCUSSION OF RESULTS

Effect of Freeze-Thaw Cycles

The individual results of the UCS tests after 0, 1, 4, 8 and 12 F-T cycles are graphically illustrated in Figures 2 (a), (b) and (c) for P-, K-, and C-soil, respectively. All the specimens tested in this study, in general, showed reduced UCS values with an increase in the number of F-T cycles. For example, the UCS value of raw, 6% lime-, 10% CFA-, and 10% CKD-stabilized K-soil specimen after 12 F-T cycle is approximately 97%, 89%, 93%, and 90% lower than a comparable specimen with a zero F-T cycle.

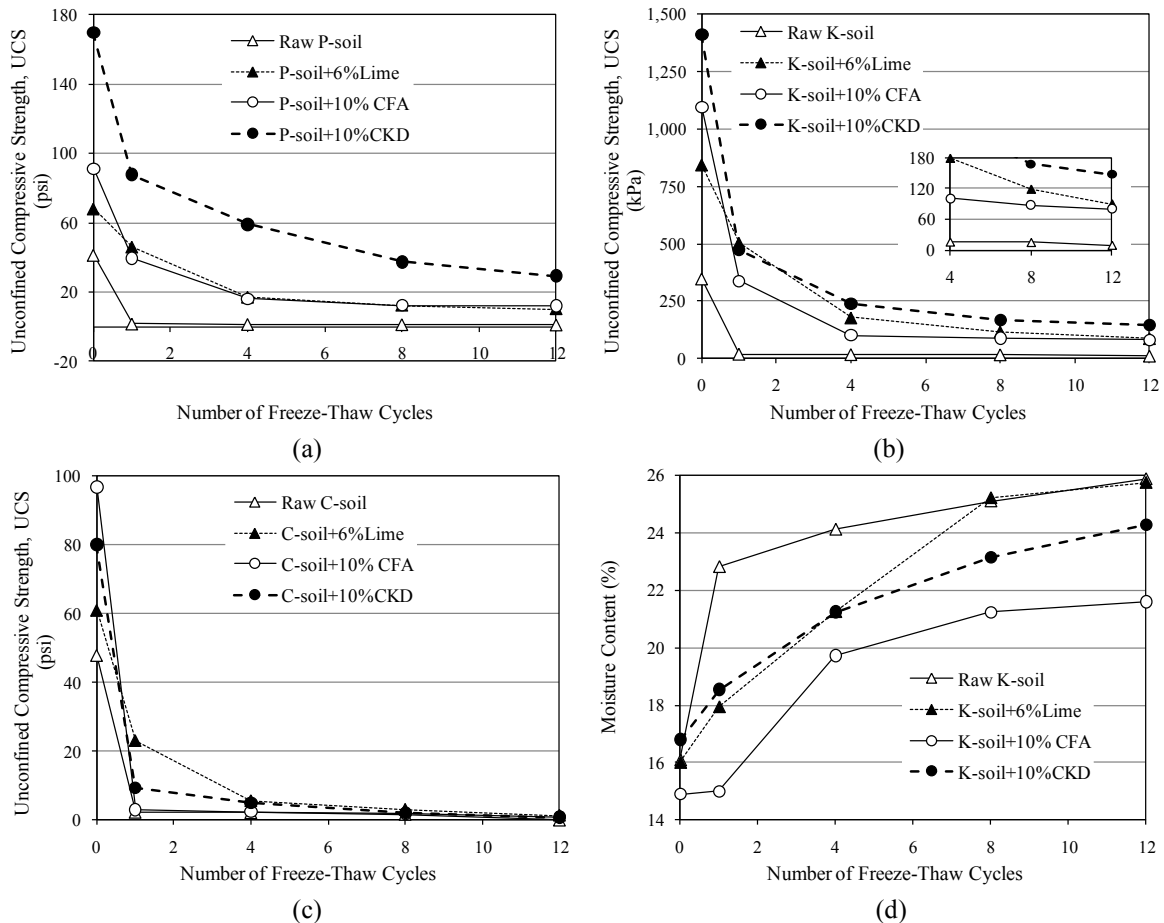


Figure 2 – UCS of Raw and Stabilized (a) P-Soil, (b) K-soil, (c) C-soil specimens at the End of 0, 1, 4, 8 and 12 Freeze-Thaw Cycles; (d) Moisture Content of Raw and Stabilized K-Soil Specimens at the End of 0, 1, 4, 8 and 12 Freeze-Thaw Cycles

A similar qualitative trend was observed for the P- and C-soil specimens, where the UCS values exhibited a decrease as the number of F-T cycles increased up to 12. The decrease in UCS values can be explained by a combined effect of pore structure and the increase of moisture content (Figure 2d for K-soil specimens) during the thawing portion of the cycle. Increase in moisture content during the thawing phase results in ice lenses within the void space of the specimens in the freezing phase; formation of ice lenses distorts the structure of raw and stabilized specimens. On the other hand, higher density of stabilized soil specimen indicates fine pore structure. The capillary force exerted on a pore wall depends on the pore size- the smaller the pore, the higher the suction force. As water enters and exits the pores, it can generate considerable pressure and degrade the surrounding material (23). Although lime-stabilized specimens had higher moisture content than corresponding CFA-stabilized specimens (Figure 2d), they also had lower density indicating open pore structure which reduces the damage induced by F-T cycles (106.6 pcf for K-soil-lime versus 111.0 pcf for K-soil-CFA mixtures). It is also clear from Figures 2 (a) through (c) that the reduction in UCS values from F-T cycle 0 to 1 is higher than the reduction in UCS between other F-T cycles. For example, the UCS values of 6% lime-stabilized K-soil specimens decreased by approximately 40% between F-T cycles 0 – 1

and 34% between F-T cycles 1 – 4, respectively. It is speculated that freezing and thawing opened up the pores, reducing the damaging effects of later F-T cycles.

The effect of F-T action on UCS values varies from one soil-additive mixture to another, as shown in Figures 2 (a) through (c). Table 4 shows the average percentage decrease in UCS values of raw and stabilized P-, K-, and C-soil specimens due to F-T action. It is evident that for P-soil specimens, a silty clay with sand, the percentage reduction in UCS values of 10% CKD-stabilized specimens is lower than the corresponding 6% lime-stabilized specimens, followed by 10% CFA-stabilized specimens. For example, the average UCS value of CKD-stabilized specimens subjected to 4 F-T cycles is approximately 65% lower than the corresponding average UCS values of stabilized specimens with no such cycles. The corresponding percentage decrease is 75% and 82% for lime- and CFA-stabilized specimens, respectively. Although the percentage reduction in UCS values for lime-stabilized specimens subjected to 1 F-T cycle is higher than the corresponding CKD-stabilized specimens, the UCS values for CKD-stabilized specimens were higher than the corresponding UCS values of the lime-stabilized specimens. Specifically, the UCS values of CKD-stabilized specimens is 87.8 psi (605 kPa), which is approximately 91% higher than the corresponding UCS values of lime-stabilized specimens after 1 F-T cycle (Figure 2a). Consequently, CKD-stabilization provided better resistance than lime- and CFA-stabilization towards F-T durability of P-soil specimens.

Table 4 – Percentage Decrease in UCS Values of Raw and Stabilized P-, K- and C-soil Specimens Due to F-T Cycles

Additive Type	Number of F-T Cycles			
	1	4	8	12
<i>P-soil</i>				
None	96	96	97	97
6% Lime	33	75	82	85
10% CFA	57	82	87	87
10% CKD	48	65	78	83
<i>K-soil</i>				
None	95	95	96	97
6% Lime	40	79	86	89
10% CFA	69	91	92	93
10% CKD	66	83	88	90
<i>C-soil</i>				
None	95	95	96	100
6% Lime	62	91	95	98
10% CFA	97	98	98	99
10% CKD	88	94	98	99

Contrary to the behavior of stabilized P-soil specimens, F-T tests on both K-soil (lean clay) and C-soil (fat clay) stabilized specimens projected 6% lime-stabilized specimens showing the highest UCS values followed by 10% CKD and 10% CFA. For example, the average UCS value of 6% lime-stabilized C-soil specimens subjected to 1 F-T cycles is 23 psi (159 kPa), as compared to 9 psi (65 kPa), and 3 psi (21 kPa) for 10% CKD- and 10% CFA-stabilized specimens, respectively. Furthermore, the percentage reduction in UCS values from Table 4 supports the fact that 6% lime stabilized specimens are more durable against F-T cycles as

compared to specimens stabilized with 10% CKD and 10% CFA. It is believed that the highest calcium content in lime, among all additives used in this study (Table 2), will produce higher amount of cementitious products (e.g., calcium silicate hydrate, calcium aluminate hydrate) after combining with pozzolana (silicious and aluminacious material). Since K- and C-soil have very high clay contents, indicating higher amount of pozzolana as compared to P-soil (Table 1), more cementitious compounds are expected in K- and C-soil. Thus, one can conclude that the durability of C- and K-soil specimens against F-T cycles is higher with lime as compared to CFA and CKD.

Vacuum Saturation Test

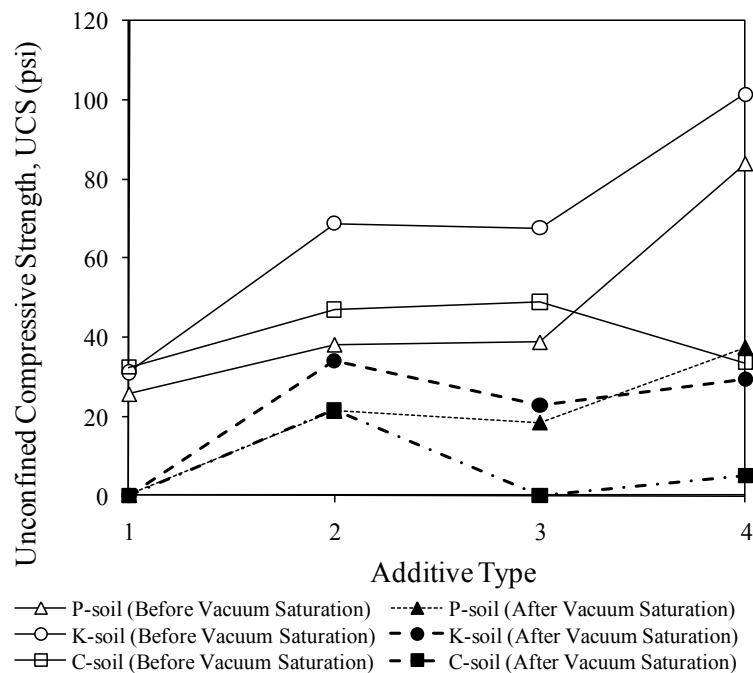


Figure 3 – UCS of Raw and Stabilized Soil Specimens Before and After Vacuum Saturation Test

A summary of the UCS results conducted on P-, K-, and C-soil specimens subjected to vacuum saturation procedure (UCS after vacuum saturation) and those not subjected to vacuum saturation procedure (UCS before vacuum saturation) is presented in Figure 3. The raw soil specimens deteriorated during the soaking stage and could not be tested for UCS. All of the stabilized specimens lost strength compared to the control specimens tested after 7 days. During vacuum saturation testing, the UCS of the P-soil specimens stabilized with lime, CFA and CKD decreased by an average of 44%, 53%, and 55%, respectively. Although lime-stabilized specimens showed the lowest percentage decrease, the average UCS value of CKD-stabilized specimen was the highest (37 psi, i.e., 258 kPa) after vacuum saturation test, among all the additives used in this study. Similar to the trends of UCS values after F-T cycles, 6% lime-stabilized specimens of K- and C-soil specimens showed the lowest percentage decrease in UCS values after vacuum saturation. For example, K-soil specimens stabilized with 6% lime, 10% CFA, and 10% CKD showed a percentage decrease in UCS values of approximately 51%, 66%, and 71%, respectively. Also, it is evident from Figure 3.11 that for K- and C-soil specimens, the

UCS values after vacuum saturation of 6% lime-stabilized specimens is higher than the corresponding 10% CKD-stabilized specimens, followed by the 10% CFA-stabilized specimens. Since the UCS values of stabilized P-, K-, and C-soil specimens after vacuum saturation showed similar trends to the UCS values after F-T cycling, similar reasons, as mentioned in the preceding section, can be used to justify the observed trends.

Tube Suction Test

A summary of the final 10th day dielectric constant values (DVs) for the raw and stabilized P-, K-, and C-soil specimens is summarized in Figures 4, 5, and 6, respectively.

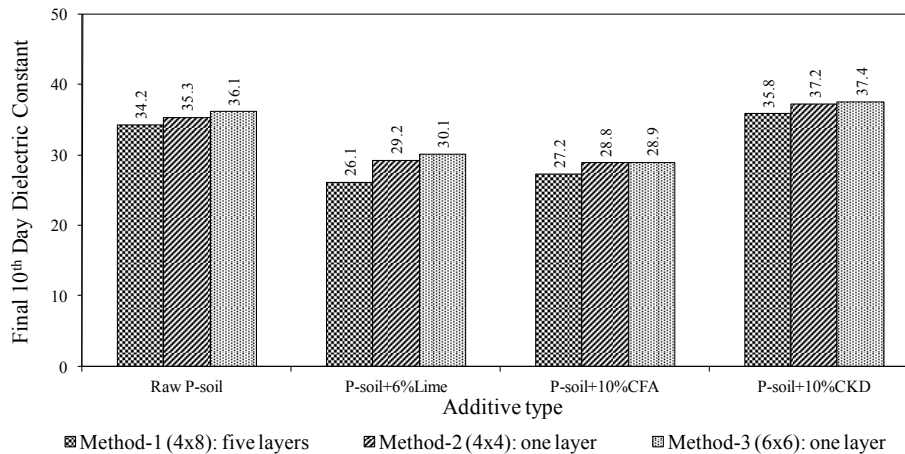


Figure 4 – Final 10th Day Dielectric Values of Raw and Stabilized P-Soil Specimens

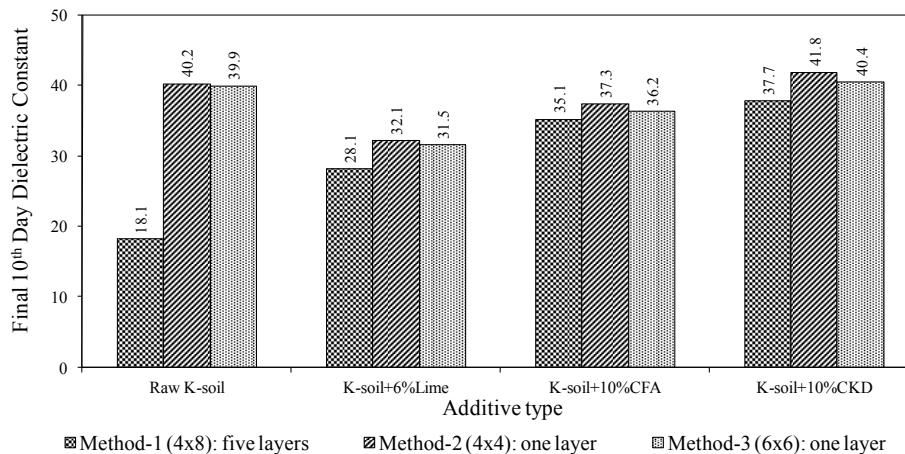


Figure 5 – Final 10th Day Dielectric Values of Raw and Stabilized K-Soil Specimens

Effect of Method of Specimen Preparation

It is clear from Figures 4 through 6 that the specimens prepared by using Method-1 showed a lower DV as compared to corresponding specimens prepared by using Method-2 and Method-3, which provided similar DVs. For example, raw K-soil specimens provided a DV of 18.1, 40.2, and 39.9 when specimens were prepared in accordance with Method-1, Method-2, and Method-3, respectively. This difference in DV between specimens prepared by using Method-1, Method-2, or Method-3 could be attributed to the variation of the moisture content values along the height of the specimens, as shown in Figures 7 (a), (b), and (c), respectively, for

P-, K-, and C-soil specimens. Specimens prepared by using Method-1 showed that the moisture content of the bottom layer is very high as compared to the moisture content of the top layer. This difference in moisture content between the bottom and top layer varies between 1.3 – 3.9%, 1.3 – 6.9%, and 1.0 – 6.7% for P-, K-, and C-soil specimens, respectively. On the other hand, all the P-, K-, and C-soil specimens prepared by using Method-2 showed a difference in moisture content of less than 0.5% between the bottom and top layer. Since the measured signal using Percometer™ depends only on the dielectric properties of top 0.8 – 1.2 in (20 – 30 mm) of material (24, 25), it is expected that the specimen having uniform moisture content will provide the representative behavior. Also, it is important to note that the specimens compacted in a single layer (Method-2 and Method-3) are more representative of the field conditions, where stabilized subgrade layer is compacted in one lift.

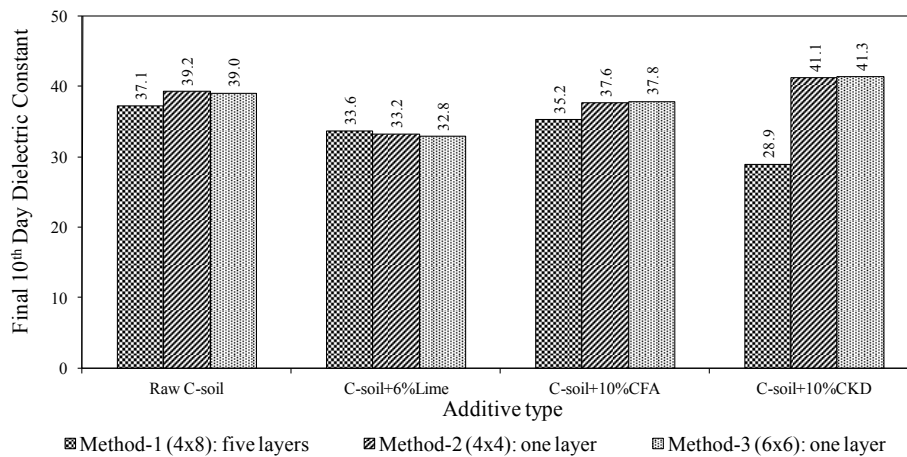


Figure 6 – Final 10th Day Dielectric Values of Raw and Stabilized C-Soil Specimens

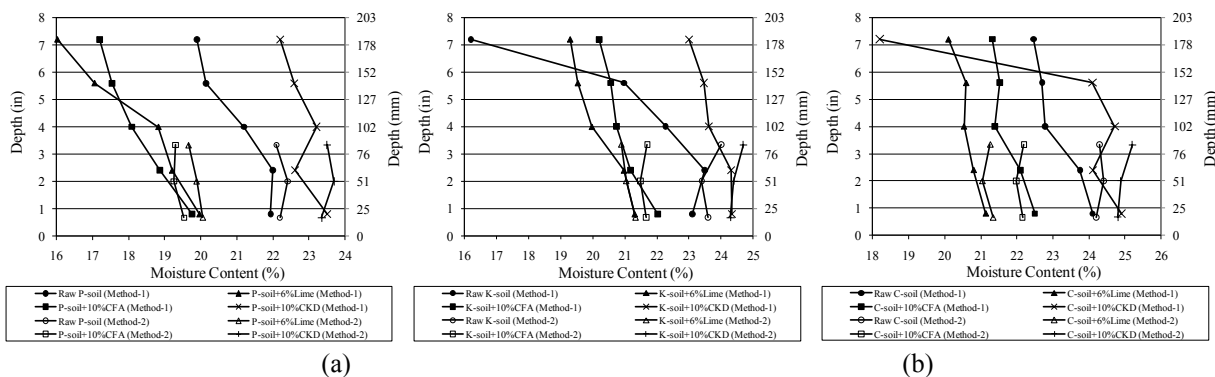


Figure 7 – Variation of Moisture Content Along the Height of Stabilized (a) P-soil, (b) K-soil and (c) C-soil Specimens

Effect of Additive and Soil Type

Since Method-2 and Method-3 provided similar and representative DVs of stabilized soil specimens, DVs obtained by using Method-2 were used for further evaluation on the effect of additives and soil type on durability. The raw P-, K-, and C-soil specimens showed an average DV of approximately 35.3, 40.2, and 39.2, respectively (Figures 4 – 6). Stabilization with 10% CFA is more effective in reducing the DV of P-soil specimens followed by 6% lime. For

example, DV values reduced by 18% and 17% by treating P-soil with 10% CFA and 6% lime, respectively. Similar to the qualitative trend noticed in preceding sections, K- and C-soil specimens showed more effectiveness with 6% lime by decreasing the DVs of corresponding raw soil specimens by 20% and 15%, respectively. These results are consistent with the observations made by Little (17), and Barbu and McManis (20). The percentage decrease in DV due to 10% CFA was found to be approximately 7% and 4% for K- and C-soil specimens, respectively, which is consistent with the observations reported by Guthrie et al. (10) and Parker (11). It is an indication that lime and CFA stabilization has more or less the same degree of effectiveness in reducing the DV for K- and C-soils.

On the other hand, the DVs of 10% CKD-stabilized P-, K-, and C-soil specimens exhibited an increase, an opposite trend as compared to lime- and CFA-stabilized specimens. For example, P-, K-, and C-soil specimens prepared with 10% CKD showed an average increase of approximately 5%, 4%, and 5% as compared to raw specimens. Hence, CKD was found to exhibit no significant improvement in DVs for the P-, K-, and C-series. Similar behavior of an increase in DV with addition of 2% CKD in limestone base material was reported by Si and Herrera (26). This behavior of an increase in DV of CKD-stabilized specimens may be attributed to the presence of extra CKD in the specimen, which is not reacting with the host material; hence it absorbs water, increasing the moisture content (Figures 7a – c) and dielectric constant.

DISCUSSION

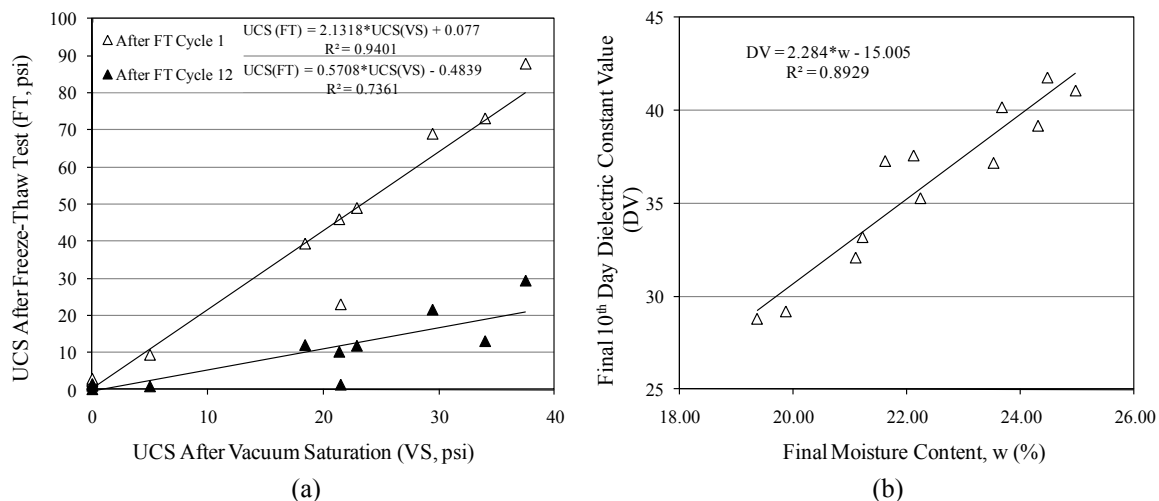


Figure 8 – Correlation between (a) UCS After the Freeze-Thaw (FT) Test and UCS After the Vacuum Saturation (VS) Test (b) Final Dielectric Constant Value and Moisture Content (Method-2)

Based on aforementioned UCS results, P-soil specimens, a silty clay with sand, showed better performance with 10% CKD against F-T cycles. On the other hand, K- (lean clay) and C-soil (fat clay) specimens showed a higher degree of improvement against F-T cycles with 6% lime. Similar qualitative trend of P-, K-, and C-soil specimens were observed for the retained UCS values after vacuum saturation tests. It is also important to note that C-soil specimens stabilized with lime, CFA, and CKD showed lowest retained UCS values as compared to corresponding specimens of P- and K-soil. This can be attributed to the acidic nature of C-soil

(pH = 4.17), which will decrease the rate of cementitious reactions. Furthermore, analyses of the test results indicated that the UCS values after 12 F-T cycle were lower than the corresponding values associated with the UCS values retained after vacuum saturation. This observation suggests that the 12 F-T cycles are more severe than the vacuum saturation test for these particular fine-grained soils. Figure 8 (a) shows a plot of UCS after F-T cycles (1 and 12) versus UCS after vacuum saturation. The R^2 value associated with this correlation is comparatively high at 0.9401 and 0.7361 after F-T cycle 1 and 12, respectively. Thus, a strong correlation exists between UCS values retained after vacuum saturation and F-T cycles.

The final DVs of all the raw and stabilized specimens were above the value of 16. Referring to the maximum DV criterion proposed by Guthrie and Scullion (15), which was mainly for coarse soils or aggregates, the soil tested in this study were moisture susceptible with its maximum DV above 16. However, based on increase of 7-day UCS by 345 kPa (50 psi) over raw specimens criterion, recommended by several highway agencies (Table 3.2) for the selection of additive content, 10% CKD-stabilized P-soil and all stabilized K-soil specimens should be durable. Thus, the maximum DV criterion seems more conservative since no specimen satisfied the maximum DV criterion, consistent with the observations reported by Zhang and Tao (21). Also, no correlation was observed between the final DV after TST and durability evaluated by using retained UCS values after F-T or vacuum saturation test. For example, P-soil specimens stabilized with 10% CKD showed best performance against F-T cycles among all the additives used in this study. On the other hand, TST projected 10% CKD-stabilized specimens showing the worst performance with a very high DV of approximately 37.2. Figure 8 (b) shows that the final DV is affected by the moisture content of specimens. However, it is worth noting that the final DV is dependent on material type and is influenced by properties such as clay content, saturation history, degree of bonding of water molecules around soil particle, optimum moisture content, and plastic limit (25).

CONCLUSIONS

The following conclusions can be drawn from the aforementioned results of this study:

1. All the specimens tested in this study showed decreases in the UCS values with increases in the number of F-T cycles. Such decreases could be explained by the increases in moisture absorbed by specimen during the thawing portion of the cycle and pore structure of the stabilized specimen.
2. For the percentages of additives used in this study, results showed that lime provides higher resistance against F-T cycles for lean clay (K-soil) and fat clay (C-soil). On the other hand, CKD-stabilization is more effective with silty clay (P-soil) against damage caused by F-T cycles. A similar qualitative trend of behavior was observed for retained UCS after vacuum saturation test.
3. The test results indicated that the 12 F-T cycles are more severe than the vacuum saturation test for the particular soils used in this study. Also, a strong correlation exists between UCS values retained after vacuum saturation and F-T cycles.
4. The final dielectric constant values measured by conducting tube suction tests are influenced by the method of specimen preparation. However, final DV is not affected by the specimen size, as evident from similar results obtained by using Method-2 and -3.

5. Stabilization with 10% CFA is more effective in reducing the DV of silty clay specimens, followed by 6% lime. However, 6% lime proved more effective in reducing DV of lean clay and fat clay specimens. On the contrary, 10% CKD was found to show no significant improvement in DVs for the soils used in this study. Also, a strong correlation was found between the final DV and moisture content of specimens suggesting that DV is affected by the amount of moisture present in the specimens.
6. The maximum DV criterion for selecting durable aggregate base material seems more conservative for raw and stabilized soil specimens.
7. No correlation was observed between the final DV after TST and the durability evaluated by using retained UCS values after F-T or vacuum saturation tests.
8. For all the soils used in this study, raw and stabilized C-soil (fat clay) specimens showed worst performance in F-T UCS and vacuum saturation tests. This can be attributed to the acidic nature of C-soil (pH = 4.17) which will decrease the rate of cementitious reactions.

REFERENCES:

1. Guthrie, W. S. and A. Hermansson. Frost Heave of Variably Saturated Aggregate Base Materials. *Transportation Research Record: Journal of the Transportation Research Board*, vol. 1821, 2003, pp. 13 – 19.
2. AASHTO. *Guide for Mechanistic-Empirical Design of New and Rehabilitated Pavement Structures*. Final Report prepared for National Cooperative Highway Research Program (NCHRP) 1-37A, Transportation Research Board, National Research Council, Washington D.C., 2004.
3. Petry, T. M. and K. Sobhan. *Evaluation of Chemical Stabilizers*. Transportation Research Circular E- C086, Transportation Research Board, National Research Council, Washington, D.C., 2005.
4. Little, D. N. and S. Nair. *Recommended Practice for Stabilization of Subgrade Soils and Base Materials*. NCHRP Web-Only Document 144, Contractor's Final Task Report for NCHRP Project 20-07, Transportation Research Board, National Research Council, Washington, D.C., 2009.
5. Shihata, S. A. and Z. A. Baghdadi. Simplified Method to Assess Freeze-Thaw Durability of Soil Cement. *ASCE Journal of Materials in Civil Engineering*, vol. 13 (4), 2001, pp. 243 – 247.
6. Miller, G. A. and M. Zaman. Field and Laboratory Evaluation of Cement Kiln Dust as a Soil Stabilizer. *Transportation Research Record: Journal of the Transportation Research Board*, vol. 1714, pp. 25 – 32, 2000.
7. Arora, S. and A. H. Aydilek. Class F Fly-Ash-Amended Soils as Highway Base Materials. *ASCE Journal of Materials in Civil Engineering*, vol. 17 (6), 2005, pp. 640 – 649.
8. Dempsey, B. J., and M. R. Thompson. Vacuum Saturation Method for Predicting Freeze-Thaw Durability of Stabilized Materials. *Highway Research Record*, Vol. 442, Highway Research Board, Washington, D.C., 1973.

9. McManis, K. L. and A. Arman. Class C Fly Ash as a Full or Partial Replacement for Portland Cement or Lime. *Transportation Research Record: Journal of the Transportation Research Board*, vol. 1219, pp. 68 – 61, 1989.
10. Guthrie, W. S., M. B. Roper and D. L. Eggett. Evaluation of Laboratory Durability Tests for Stabilized Aggregate Base Materials. *Transportation Research Board 87th Annual Meeting*, CD-ROM Publication, Transportation Research Board, National Research Council, Washington, D.C., 2008.
11. Parker, J. W. *Evaluation of Laboratory Durability Tests for Stabilized Subgrade Soils*. MS Thesis, Brigham Young University, Provo, U.T., 2008.
12. Syed, I., T. Scullion and J. P. Harris. Durability of Recycled and Stabilized Pavement Materials. *Geotechnical Special Publication*, vol. 89, 1999, pp. 25 – 36.
13. Guthrie, W. S., P. M. Ellis and T. Scullion. Repeatability and Reliability of the Tube Suction Test. *Transportation Research Record: Journal of the Transportation Research Board*, vol. 1772, 2001, pp. 151 – 157.
14. Scullion, T. and T. Saarenketo. Using Suction and Dielectric Measurements as Performance Indicators for Aggregate Base Materials. *Transportation Research Record: Journal of the Transportation Research Board*, vol. 1577, pp. 37 – 44, 1997.
15. Guthrie, W. S. and T. Scullion. *Interlaboratory Study of the Tube Suction Test*. Research Report 0-4114-2, Texas Transportation Institute, College Station, TX, 2003.
16. Saarenketo, T. and T. Scullion. *Using Electrical Properties to Classify the Strength Properties of Base Course Aggregates*. Research Report 1341-2. Texas Transportation Institute, Texas A&M University System, College Station, T.X., 1996.
17. Little, D. N. Evaluation of Structural Properties of Lime Stabilized Soils and Aggregates. *Mixture Design and Testing Protocol for Lime Stabilized Soils*, Vol. 3, National Lime Association report, 2000.
18. Syed, I., T. Scullion and R. B. Randolph. Tube Suction Test for Evaluating Aggregate Base Materials in Frost- and Moisture – Susceptible Environments. *Transportation Research Record: Journal of the Transportation Research Board*, vol. 1709, 2000, pp. 78 – 90.
19. Saarenketo, T., P. Kolisoja, N. Vuorimies, and S. Ylitapio. *Suction and Deformation Properties of Base Course Aggregates*. Final Report 10/2001, Finnish National Road Administration, Helsinki, Finland, 2001.
20. Barbu, B. and K. McManis. Study of Problematic Silts Stabilization. *Transportation Research Board 84th Annual Meeting*, CD-ROM Publication, Transportation Research Board, Washington, D.C., 2005.
21. Zhang, Z. and M. Tao. Durability of Cement Stabilized Low Plasticity Soils. *ASCE Journal of Geotechnical and Geoenvironmental Engineering*, vol. 134 (2), 2008, pp. 203 – 213.
22. Barbu, B. G. and T. Scullion. *Repeatability and Reproducibility Study for Tube Suction Test*, Report 5-4114-01, Final report submitted to Texas Transportation Institute, College Station, T.X., 2005.

23. Prusinski, J. R., and S. Bhattacharja. Effectiveness of Portland Cement and Lime in Stabilizing Clay Soils. *Transportation Research Record: Journal of the Transportation Research Board*, vol. 1632, 1999, pp. 215 – 227.
24. Adek. *Operating Instructions and Technical Data*. Percometer v.7, Estonia, 2007.
25. Saarenketo, T. *Electrical Properties of Road Materials and Subgrade Soils and the Use of Ground Penetrating Radar in Traffic Infrastructure Surveys*. PhD Thesis, University of Ulu, Finland, 2006.
26. Si, Z. and C. H. Herrera. Laboratory and Field Evaluation of Base Stabilization using Cement Kiln Dust. *Transportation Research Record: Journal of the Transportation Research Board*, vol. 1989, 2007, pp. 42 – 49.

UNDERSTANDING THE BEHAVIOR OF INTEGRAL ABUTMENT BRIDGES THROUGH FIELD INSTRUMENTATION

**Bryce Hanlon¹, Karrthik Kirupakaran², Gerald A. Miller³,
and K. K. "Muralee" Muraleetharan⁴**

¹EST, Inc., 3201 South Berry Road, Norman, OK 73072, Phone: 405-307-8378,
Email: bryce.hanlon@estinc.net

²School of Civil Engineering and Environmental Science, The University of Oklahoma, 202 W.
Boyd, Room 334, Norman, OK 73019, Phone: 405-365-6566, Email: karrthik@ou.edu

³School of Civil Engineering and Environmental Science, The University of Oklahoma, 202 W.
Boyd, Room 334, Norman, OK 73019, Phone: 405-325-4253, Email: gamiller@ou.edu

⁴School of Civil Engineering and Environmental Science, The University of Oklahoma, 202 W.
Boyd, Room 334, Norman, OK 73019, Phone: 405-325-4247, Email: muralee@ou.edu

ABSTRACT:

Integral Abutment Bridges (IAB) or jointless bridges are bridges without any joints within the bridge deck or between the superstructure (decks and girders) and the abutments. An IAB provides many advantages during construction and maintenance of a bridge. The behavior of abutments in an IAB is, however, poorly understood. Soil-structure interactions occurring during heating and cooling of the bridge at the abutments are complex, especially in skewed and long span IABs. This paper describes a field instrumentation effort to understand these soil-structure interactions.

The North bound I-44 Bridge over the Medicine Bluff Creek in Comanche County near Lawton, Oklahoma was instrumented for this project. This is a 210 feet long, three span IAB with a 10⁰ skew. Three abutment piles were instrumented with strain gages, earth pressure cells and tilt meters were placed on abutment walls, crack meters were placed between the bridge deck and the pavement, and thermistors were placed on the bridge deck and the girders. The data

collection began in June 2009. Some results from these instruments during heating and cooling of the bridge are discussed to gain insight into the soil-structure interactions between the bridge, abutments, piles supporting the abutments, and the surrounding soil.

INTRODUCTION

Integral Abutment Bridges (IAB) or jointless bridges are bridges without any joints within the bridge deck or between the superstructure (decks and girders) and the abutments. The use of integral abutment bridges has been increasing during recent years. An IAB provides many advantages during construction and maintenance of a bridge (Mistry 2000). The main advantage of an IAB is the elimination of the expansion joints in the structure. Roadway runoff through open or leaking joints in a conventional bridge leads to deterioration of girders and bearings. Bearings are also difficult to maintain and costly to replace. Water within deck joints can also freeze during cold weather and not be able to properly accommodate thermal contraction and expansion of the bridge. Therefore expansion joints in a conventional bridge lead to higher maintenance costs. Thermal contraction and expansion in an IAB is accommodated by the movement of the abutments. Abutments are commonly supported on steel piles that are oriented with their weak axis parallel to the longitudinal axis of the bridge to allow for easy movement of the abutments. Simpler joints between approach slabs and pavements accommodate the relative movements between the bridge and the pavement. Monolithic IABs also provide superior performance during extreme loading events such as earthquakes and blast loading.

Soil-structure interactions at the abutments occurring during thermal loading of a bridge are complex, especially in skewed and long span IABs. Because of the uncertainties in

understanding these interactions, many Departments of Transportations (DOTs) have been reluctant to build longer and skewed IABs. These uncertainties also affect the ability of the agencies to properly predict the long term behavior of these bridges. This paper describes a field instrumentation effort to understand these soil-structure interactions.

BRIDGE DESCRIPTION

The IAB mentioned in this study is the North bound I-44 Bridge over the Medicine Bluff Creek in Comanche County near Lawton, Oklahoma. The location of the bridge is shown in Figure 1. This is a 210 feet long, three span IAB with a 10^0 skew (Figure 2). The exterior spans are 60 feet long, and the interior span is 90 feet long. The structure was designed for two lanes of traffic with a roadway of 24 feet. A 13 feet shoulder is provided along the east side of the bridge deck and a 4 feet sidewalk along the west side of the deck. The structure includes a concrete deck supported on four girders. Each abutment wall is supported on 7 HP 10x42 steel piles and the central piers are supported on two 60-inch diameter drilled shafts per pier. The abutment piles are embedded 2 feet into the bottom of the abutment wall. The abutment piles are oriented with their weak axis parallel to the longitudinal bridge axis to offer the least resistance to bending during thermal movements of the bridge.

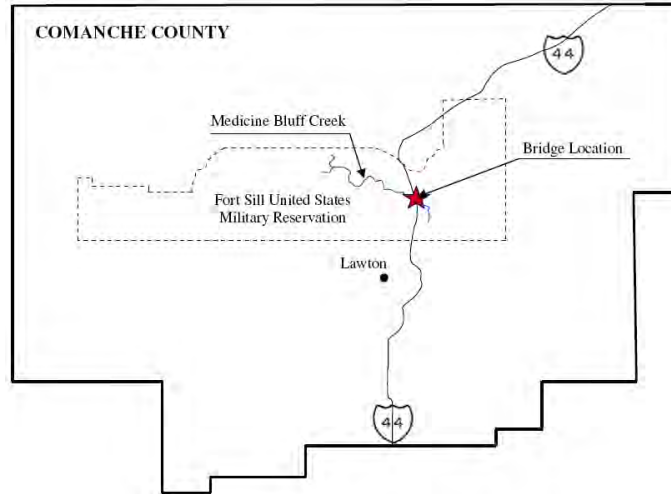


Figure 1. Location of the Instrumented Bridge on North Bound I-44

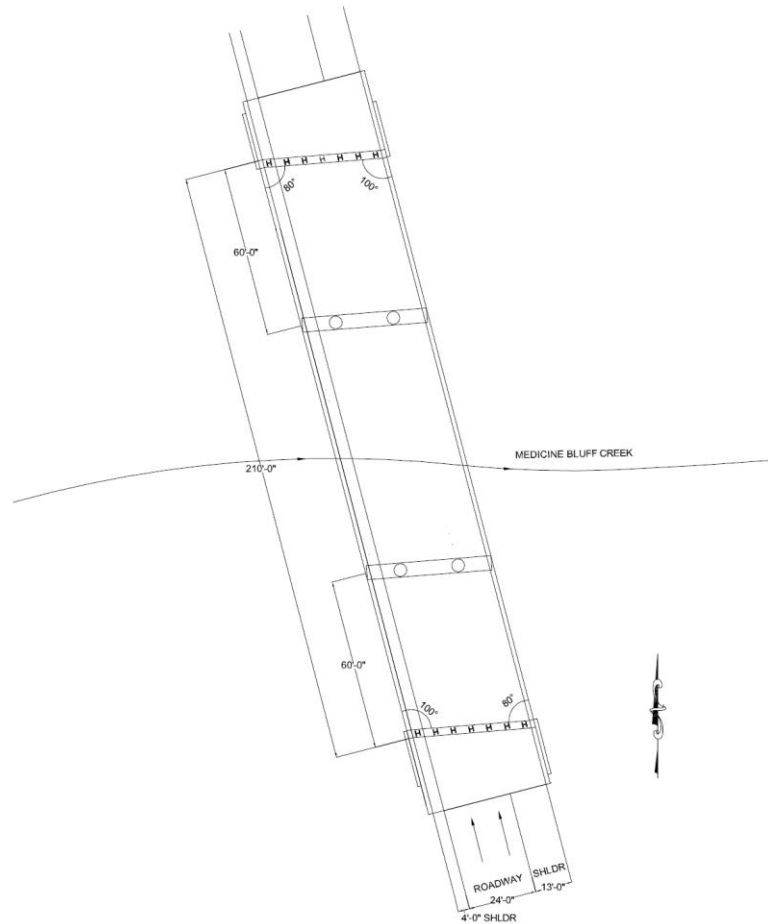


Figure 2. Details of the Instrumented Bridge

BRIDGE INSTRUMENTATION AND DATA COLLECTION

The bridge was instrumented with 46 separate instruments to capture the behavior during thermal loading. Five different types of instruments (pile strain gages, earth pressure cells, crack meters, tilt meters, and thermistors) were used. Abutment piles instrumented with vibrating wire strain gages (SG) are shown in Figure 3. The NE and SE piles were instrumented at three depths while the SW pile was instrumented at two depths. At each depth, two strain gages were placed on the web on the opposite sides (north and south sides) so that the bending strains can be separated from the axial strains. Therefore a total of 16 strain gages were attached to the piles. The locations of strain gages are shown in Figure 4.

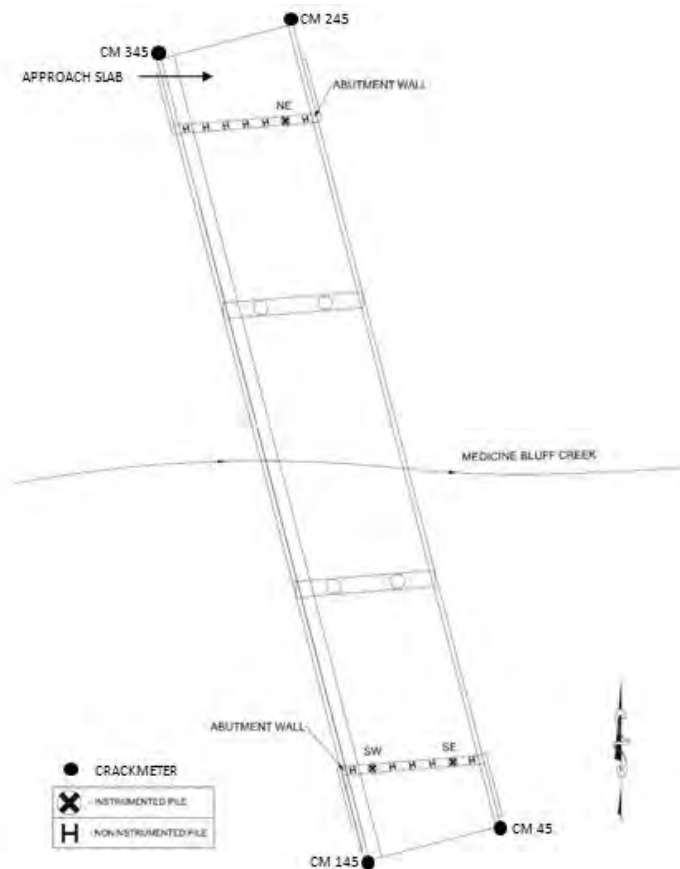


Figure 3. Locations of Crackmeters and Instrumented Piles

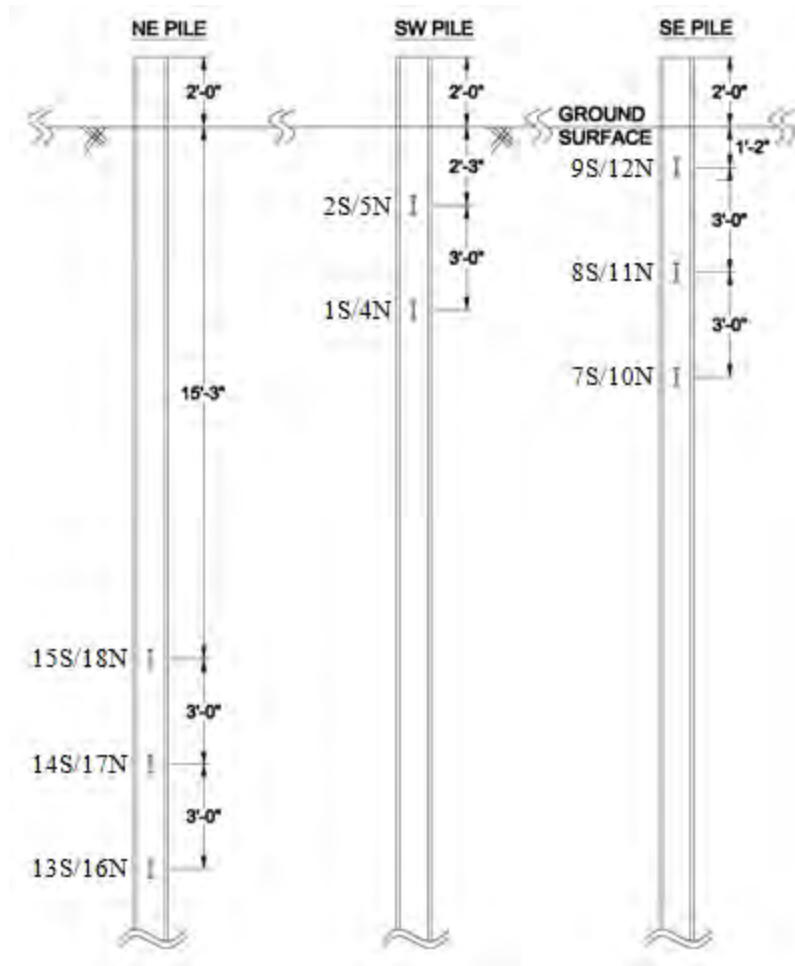


Figure 4. Locations of Strain Gages on Abutment Piles

Earth pressure cells (EPC) are located behind the abutment walls at different heights to measure the distribution of stresses behind the abutment walls. Six earth pressure cells, 4 on the north abutment and 2 on the south abutment, were installed to measure the earth pressures changes during heating and cooling of the bridge. The locations of earth pressure cells on the bridge are shown in Figure 5. The locations of the earth pressure cells were chosen to determine the variation of earth pressure on the abutment walls. On both the north and the south abutment walls, cells were positioned equidistant from each other at the same height on the wall to

measure the variation in pressure along the length of the wall. On the north wall, a cell was placed directly below the middle cell to see if there is a variance with respect to depth along the abutment wall. The locations of earth pressure cells on north abutment wall are shown in Figure 6.

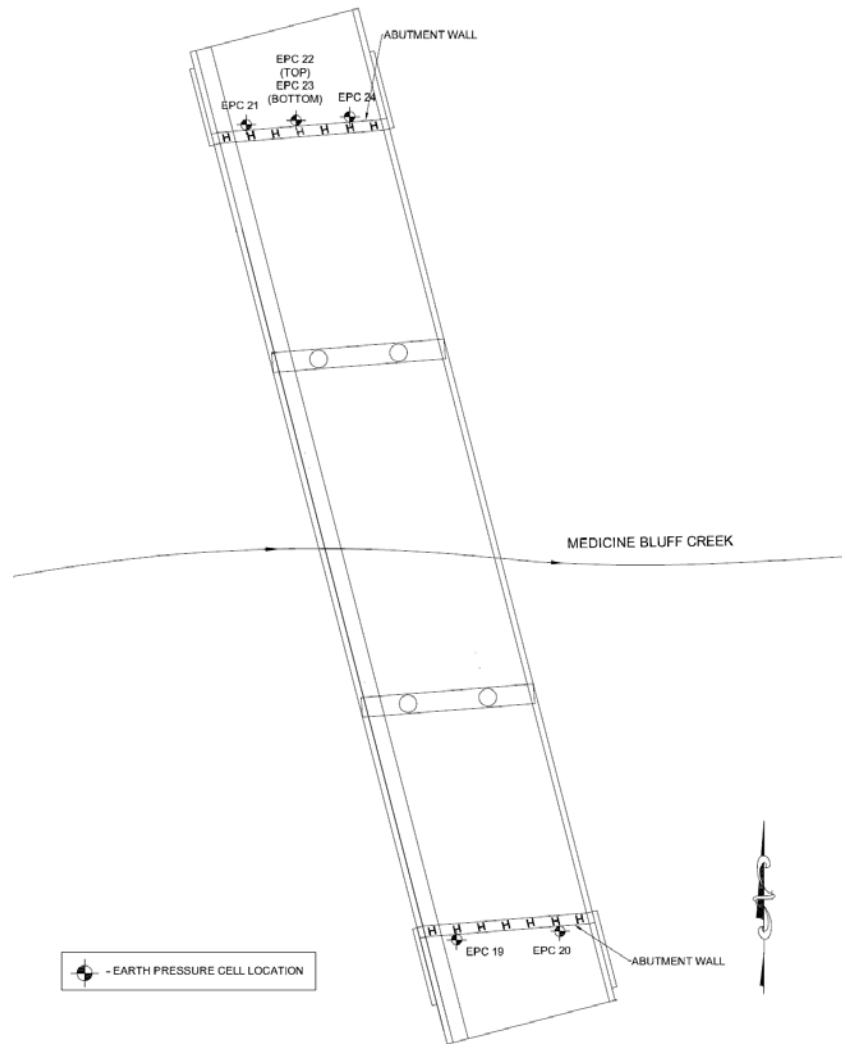


Figure 5. Locations of Earth Pressure Cells

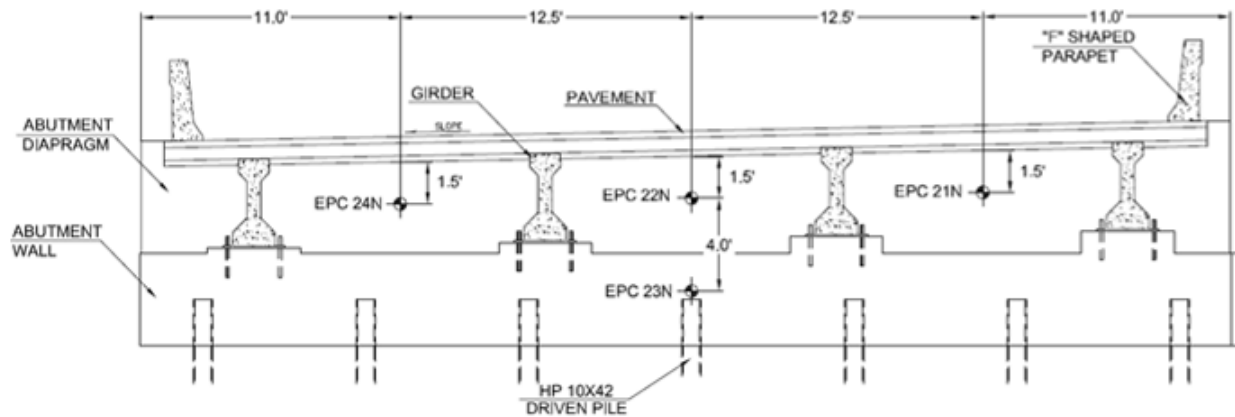


Figure 6. Locations of Earth Pressure Cells on North Abutment Wall

At the each abutment, two vibrating wire tiltmeters were attached to measure the rotation of the abutments about a horizontal axis. Tiltmeters were installed directly below the bridge deck. A total of 4 crackmeters (CM) were attached between the pavement and the approach slab to measure the translation of the bridge during heating and cooling. The locations of crackmeters are shown in Figure 3. Crackmeters were exposed to the direct sun light and to avoid damage to the instruments due to overheating, the crackmeters were covered by 2 inch diameter foam tubing. The foam was designed to protect the gage from direct sunlight, rain, and other outside elements. Finally, 16 thermistors were attached to the girders and the deck to measure the temperature changes. Thirteen thermistors were installed on the north side of the bridge, while only three were installed on the south side. The north side locations nearly cover the entire profile of the bridge, so the south locations will be mainly used for comparison. To make sure the temperatures of the bridge were being measured at the thermistor locations and not the ambient temperatures, the thermistors were covered in 0.5 inch thick foam.

All instruments were connected to a Geokon Micro-1000 data-logging unit through the use of 16-channel multiplexer cards. The system is programmed to acquire and store data from all the instruments every hour. The stored data are downloaded every month and processed on a personal computer using a spreadsheet. Data collection from the instruments started in June 2009 and is currently ongoing.

RESULTS AND DISCUSSION

Typical data collected from the instruments over a 5-day period (August 17 to August 21, 2009) are presented and discussed here.

Crack Meter Data

Longitudinal movement of the abutments for a five day period of field monitoring is presented in Figure 7. Based on the results, it appears that the readings for the crackmeters are consistent from day to day and show a distinct pattern that follows the shape of the change in temperature versus time. The crackmeter reading goes down as the temperature goes up, which means the gap in the expansion joint is closing as the bridge is expanding due to thermal loading. It shows bridge is expanding when heated and thus pushing out on the top of the abutment walls and the approach slab causing the expansion joint to close.

Crackmeters
North and South Abutments
8/17/2009 12:00 am - 8/21/2009 11:00 pm

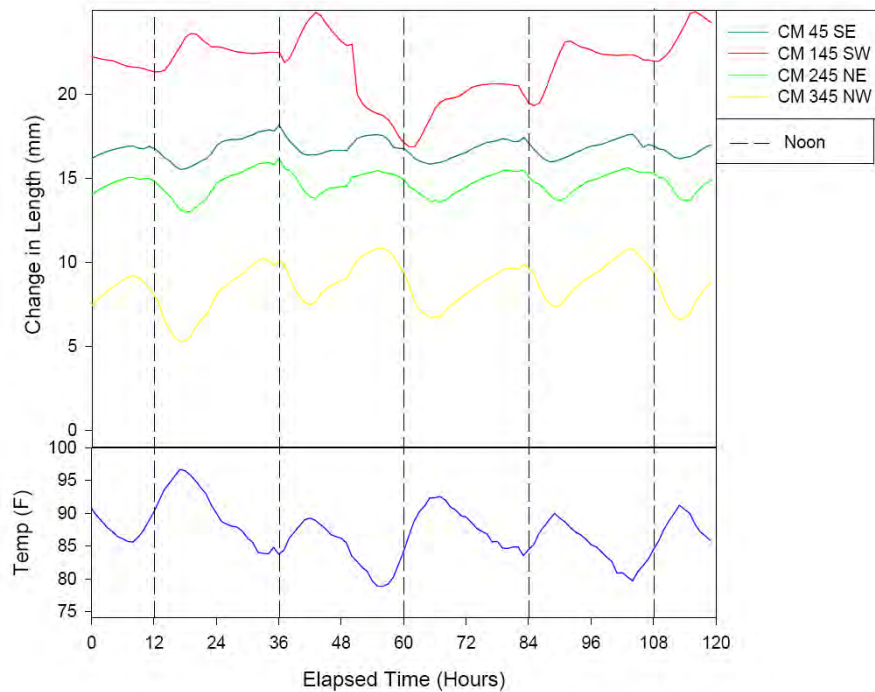


Figure 7. Measured Crackmeter Displacements

Earth Pressure Data

The variations in earth pressures are shown in Figure 8. When the temperature increases, the earth pressure also increases. As the bridge expands due to heating, the abutment walls tend to push on the soil backfill, thus increasing the earth pressure on the wall. The pressures measured in the obtuse corner of the north abutment (EPC 24N) were more than three times as high as any of the other pressures measured on the north wall. The changes in earth pressures for the two south abutment cells were identical. Both corners on the south side had far less pressure than was observed at the obtuse corner of the north abutment wall. The earth pressure cells on

the north abutment indicate that the skew of the bridge affects the earth pressures across the wall. Krier (2009) used a finite element computer program to investigate soil-structure interactions in IABs and concluded corner forces will be larger at the obtuse corners of a skewed IAB. The primary reason for this difference is that the length connecting the obtuse corners is smaller than that of the acute corners and hence the obtuse corners will carry larger loads for a given displacement of the abutments. The reason why the obtuse corner of the south abutment doesn't show a higher pressure is not known at this time.

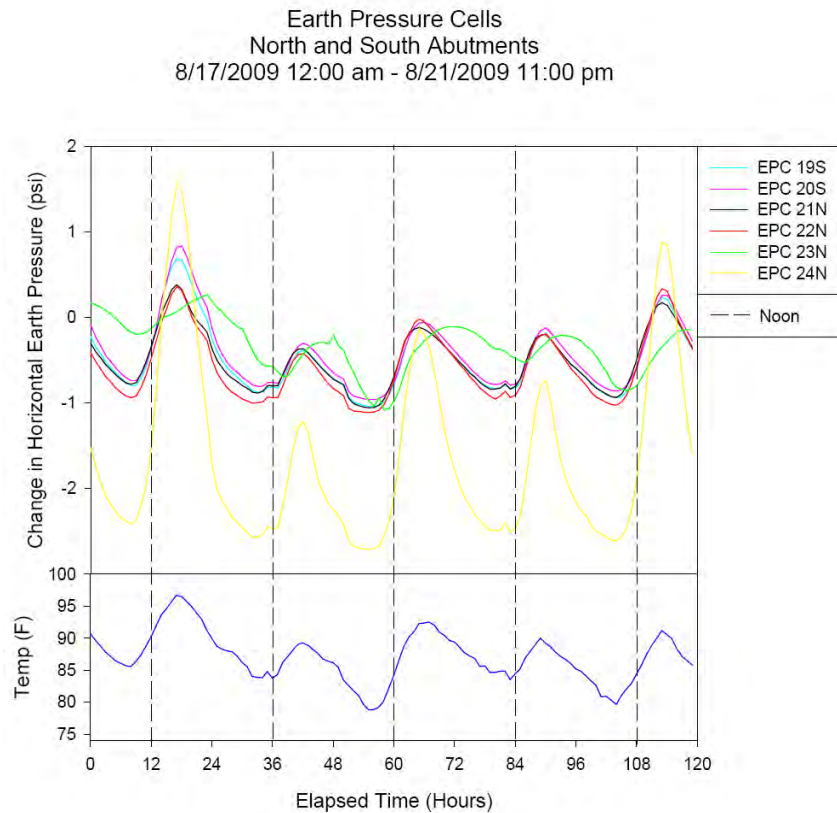


Figure 8. Measured Earth Pressures on Abutment Walls

File Strain Data

The variations in axial loads experienced by the piles inferred from strain gages are shown in Figure 9.

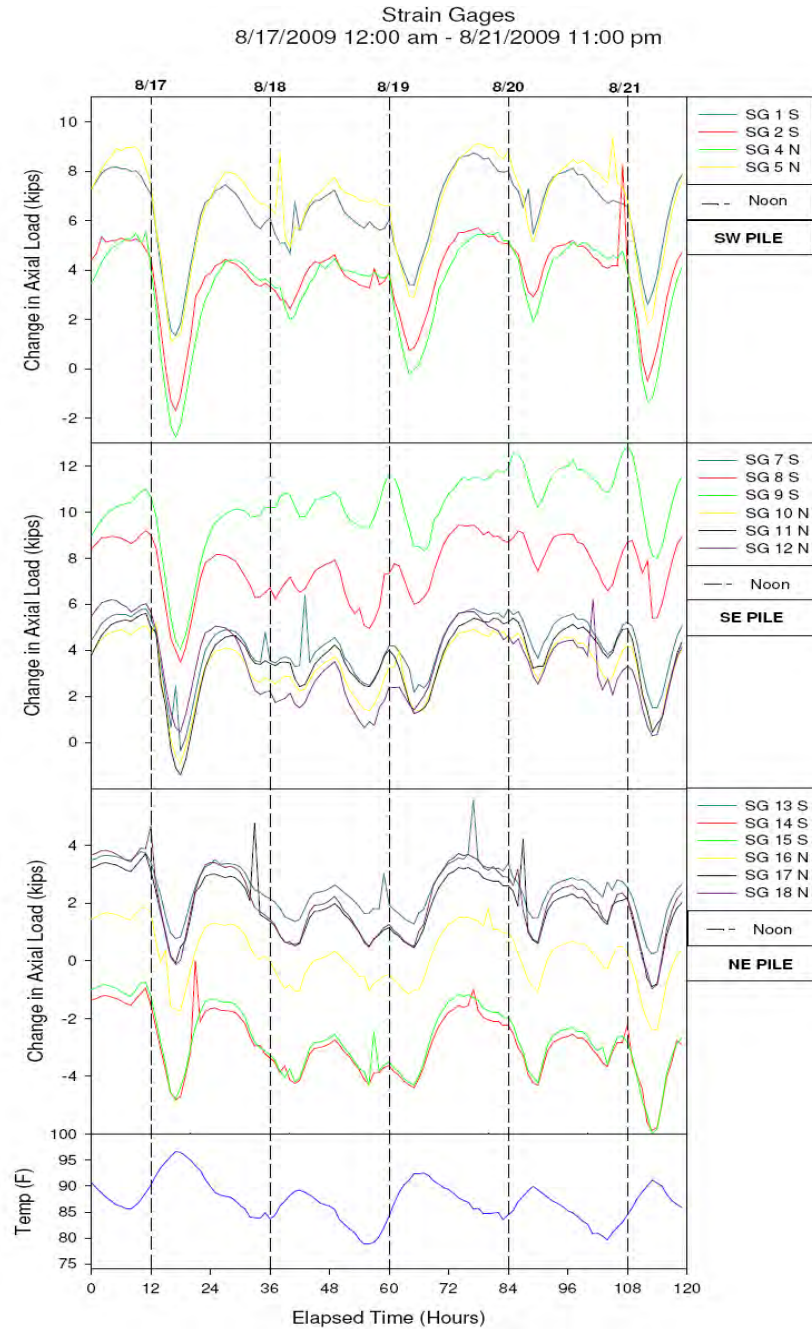


Figure 9. Axial Loads on Abutment Piles

The data shows as the temperature of the bridge increases, the axial loads on the piles also increase (tending toward negative values or compression). As the bridge is heated up by the increase in temperature, the bridge deck expands and increases the downward and lateral forces on the piles. The changes in axial loads were found to be higher on the shallower depth strain gages (south abutment piles) when compared to deeper strain gages (the northeast pile).

CONCLUSIONS

This study presents field monitoring of a skewed IAB in Oklahoma. From the interpretation of the field data, the following conclusions can be drawn on the performance of this bridge

- Contraction and expansion of the bridge as measured from crackmeter data correlate well with decreases and increases in ambient temperature.
- North abutment wall is experiencing higher changes in earth pressures on obtuse corner of the wall.
- Piles are experiencing higher daily variance in axial loading closer to the surface.

ACKNOWLEDGEMENTS

This research was supported by the Oklahoma Transportation Center (OTC Project No. OTCREOS7-1-37) and this support is acknowledged.

REFERENCES

Krier, D. (2009). "Modeling of integral abutment bridge considering soil-structure interaction effects." *Ph.D. dissertation*, School of Civil Engineering and Environmental Science, University of Oklahoma, Norman, Oklahoma.

Mistry, V.C. (2000). "Integral abutment and jointless bridges." *Conference on High Performance Steel Bridges*, Baltimore, Maryland, November (<http://www.nabro.unl.edu/articles>).

Soil Suction for Pavement Foundations

Rifat Bulut, Oklahoma State University, School of Civil and Environmental Engineering, 207 Engineering South, Stillwater, Oklahoma 74078, Phone: 405-744-7436, Fax: 405-744-7554, E-mail: rifat.bulut@okstate.edu

Abstract

Pavements are typically constructed on compacted soils that are usually unsaturated (i.e., soil pores are occupied with both water and air). In unsaturated soils, pore-water pressure is negative as compared to positive pore-water pressures in saturated soils. As water content of an unsaturated soil changes negative stress (or suction) in pore-water also changes. Suction plays a very significant role in the behavior of unsaturated pavement foundations. Soil suction variations have significant effects on the shear strength, volume change, and moisture flow in unsaturated subgrade materials. This paper reports on several soil suction measurement methods, and use of soil suction in pavement foundations. These techniques have been widely used in engineering practice and in research laboratories. Each of these techniques has its own limitations and capabilities, and active research into improving these techniques and their use in engineering practice is ongoing in universities, research laboratories, and private sector. This paper outlines working principles, calibration, measurement, and application areas of the tensiometer, thermal conductivity sensor, thermocouple psychrometer, transistor psychrometer, chilled-mirror psychrometer, and filter paper method.

Introduction

Significant advancements have been made particularly during the last two decades with respect to the development of the theoretical frameworks, experimental methods and numerical techniques related to unsaturated soil mechanics applications in geotechnical engineering practice. Several disciplines such as soil science, hydrogeology, petroleum, agricultural, geotechnical and geo-environmental engineering have contributed towards our current understanding of the mechanics of unsaturated soils. It has been proved that there are two stress state variables in unsaturated soils as compared to a single state variable in saturated soils (Fredlund and Rahardjo 1993). The main stress state variable in saturated soils is the effective stress principle. However, the net mean total stress and suction are the two stress variables responsible for the behavior of unsaturated soils. Therefore, the measurement or knowledge of the suction stress in pavement foundations is very important for understanding the behavior of those foundation materials, their analysis and design under traffic and environmental moisture effects.

Pavements are typically constructed using compacted soils that are in a state of unsaturated condition (with degrees of saturation between about 80% and 90%). Several design and maintenance measures are usually undertaken to maintain unsaturated conditions of the

pavement to achieve favorable engineering properties of soil (i.e., high shear strength). The conventional procedures for pavement design are often an over-simplification of in-situ conditions and are based on empirical procedures that do not take into consideration of the principles of unsaturated soil mechanics. However, in recent years, interest in determining the soil suction of unsaturated subgrade soils beneath a pavement has increased markedly. It is important to establish realistic estimates of expected subgrade moisture contents (suctions) to account for the effects of this variable on predicted pavement performance.

There is more than ever a greater need for reliable soil suction measurement techniques as soil suction becomes an integral part of engineering practice in many situations involving unsaturated soils. Soil suction is a result of capillary action, surface energy properties of soil particles, and ionic concentration of the pore water. In engineering practice, soil suction is composed of two components: matric suction and osmotic suction. The sum of matric and osmotic suction is total suction. Matric suction results when only capillary action and surface energy properties are active in the soil. Osmotic suction comes from the dissolved salts contained in the soil water. Significant contributions have been made by soil and geo-engineers in the measurement of soil suction. However, there is still need for research into the measurement of both matric and total suction in the field and laboratory. Almost all suction measurement methods have shortcomings including such aspects as the range of application, cost, reliability, and practicality.

This paper reports on several commonly used direct and indirect soil suction measurement methods. Direct methods measure the negative stress in the pore water directly, while indirect suction measurement techniques measure the moisture equilibrium condition of the soil instead of suction. A tensiometer measures the negative stress (matric suction) in the pore water directly. Indirect methods (i.e., thermocouple psychrometer, transistor psychrometer, chilled-mirror psychrometer, filter paper method, and thermal conductivity sensor) determine the moisture equilibrium condition of the soil by different means as partial vapor pressure (i.e., relative humidity), a specific porous medium (i.e., paper), and other physical properties (i.e., thermal) of a porous medium (i.e., ceramic). These techniques have been widely used in engineering practice and in research laboratories.

Tensiometers – Matric Suction

The commonly used device for direct measurement of matric suction in soils is a tensiometer. The tensiometer makes use of high air entry discs (cups) as an interface between the matric suction in the soil and the measuring system. Tensiometers can be used in the laboratory and in the field. A basic tensiometer consists of a high air entry disk connected to a pressure measuring system through a small plastic tube. For suction measurements, the tube is filled with deaired water and the ceramic porous disk is fully saturated. The ceramic tip is inserted into the soil. It is important that the ceramic disk is in good contact with the soil. Once equilibrium is achieved between the soil and the tensiometer, the matric suction can directly be read from the measuring system.

The matric suction that can be measured in a simple tensiometer is usually less than 100 kPa. The response time of tensiometers is very quick (i.e., seconds to minutes), and strongly depends on the degree of contact between the porous cup and the soil. Recently, a high-capacity, small

tensiometer has been developed (Ridley 1993) for suction measurements up to 1500 kPa. However, the application of this new tensiometer for field suction measurements is still under investigation due to its detailed and labor-intensive measuring system. This paper describes the very basic tensiometer where suctions less than one atmospheric pressure can be measured.

There are several types of tensiometers available from Soilmoisture Equipment Corporation (www.soilmoisture.com). The conventional Bourdon-vacuum gauge tensiometer has a diameter of approximately 2 cm and various lengths up to 1.5 m. The tensiometer can be installed in the field to depths of up to 1.5 m for suction monitoring of near ground surface with time. The jet fill type tensiometer is an improved version of the regular Bourdon tensiometer. A water reservoir is provided at the top of the tensiometer for the purpose of removing the air bubbles that diffuse into the measuring system. Another type of tensiometer available through Soilmoisture Equipment Corporation is a small tip tensiometer as shown in Figure 1. The tensiometer is prepared for suction measurements using a similar procedure to that described for the regular tensiometer. The small tip tensiometer is well-suited for both laboratory and as well as field suction measurements and monitoring. The smaller tip air entry ceramic disk with the flexible plastic tubing allows the installation of the tensiometer into a relatively small soil specimen during laboratory experiments.

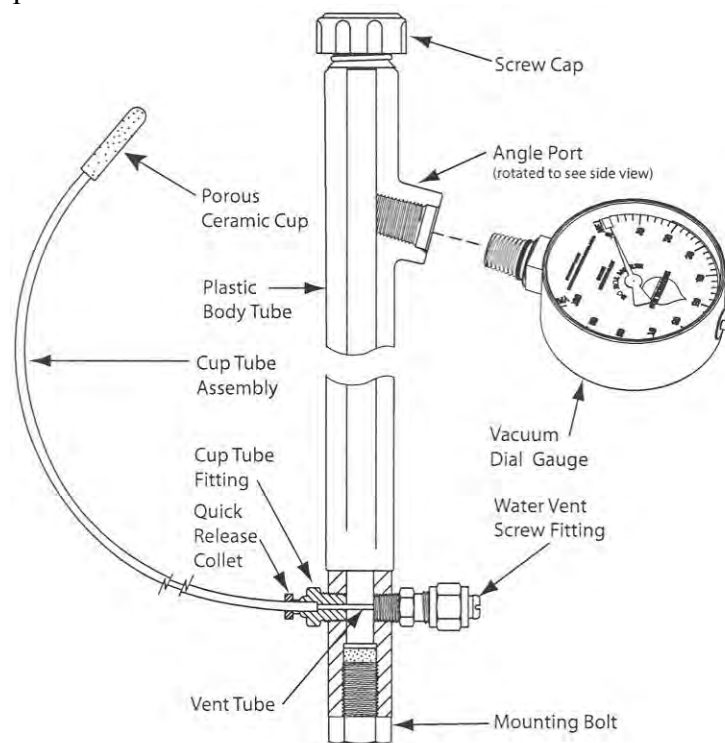


Figure 1. A small tip tensiometer (Soilmoisture Equipment Corporation).

A proper servicing of the tensiometers prior to installation and during measurement is very important for reliable and continuous monitoring of matric suctions with time, and at equilibrium. Details on the preparation, installation, and usage of the tensiometers can be found in Fredlund and Rahardjo (1993). After installation of the tensiometer, air bubbles may develop within the tensiometer due to several possible reasons. Dissolved air may come out of the

solution as the water pressure decreases to a negative value. Air in the soil may diffuse through the water in the ceramic disk (cup) and come out of the solution inside the measuring system. Air bubbles must be removed from the tensiometer periodically using a vacuum pump.

Tensiometers have been used to measure matric suctions in soils for number of different geotechnical applications. For instance, Sweeney (1982) installed tensiometers along a cut slope for monitoring changes in matric suction throughout the depth of the profile with time. The hydraulic head plots obtained from suction measurements and depth indicated the direction of moisture flow in the unsaturated zone. In another study conducted by Tadepli (1990) a small tip tensiometer has been installed in a consolidation specimen to measure changes in matric suction during the collapse of a compacted silt. Figure 2 shows a comparison of matric suction measurements between tensiometer and thermal conductivity sensor on some laboratory compacted soil specimens (Dawson 2007). The thermal conductivity sensor is described below.

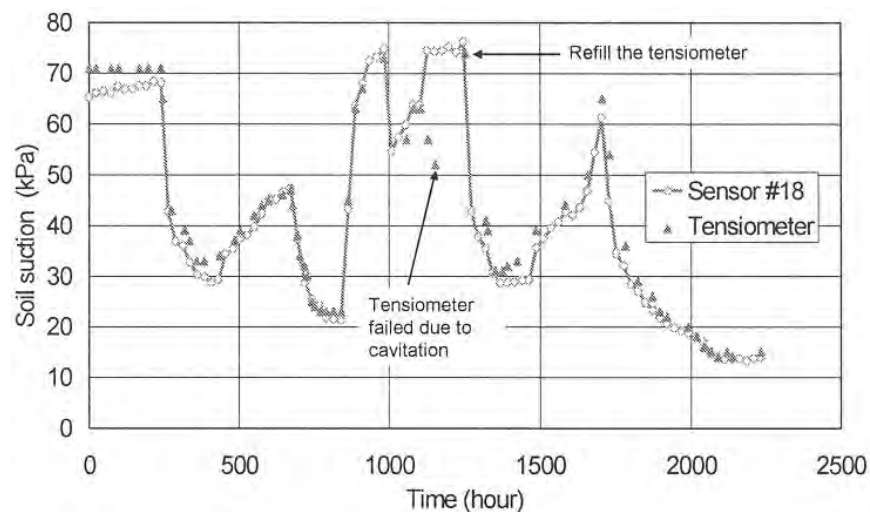


Figure 2. Tensiometer matric suction measurements with time, and their comparisons with thermal conductivity sensor measurements (Dawson 2007).

Thermal Conductivity Sensors – Matric Suction

A thermal conductivity sensor employs a porous block, typically ceramic, as a medium to measure matric suction indirectly. If a matric suction gradient exists between the soil and porous block, water flux will occur until their suctions are equal. The thermal conductivity of the block consists of the thermal conductivity of the solid and the fluid (air or/and water) that fills the voids in the porous block. The thermal conductivity of water is about 25 times that of air. Therefore, as the moisture content of the porous block increases, the thermal conductivity of the block increases. The moisture content of the block is measured by heating the porous block with a heater embedded in the centre of the porous block and measuring the temperature rise during heating. The temperature rise is related to the thermal conductivity of the porous medium and the moisture content. The temperature rise can then be used as an index of matric suction in the soil. The time to equilibrate depends on the temperature gradient and the hydraulic conductivity of the

porous medium and surrounding soil. The basic design of thermal conductivity sensor essentially follows the design of Phene et al. (1971) as shown in Figure 3. Over the years, the performance of the thermal conductivity sensor has been improved. Thermal conductivity sensors have been used in the laboratory as well as in the field (Fredlund and Wong, 1989; Oloo and Fredlund, 1992; O'Kane et al., 1998; Marjerison et al., 2001; Zhang et al., 2001; Nichol et al., 2003). Currently, thermal conductivity sensors are available commercially (e.g. Campbell Scientific, Inc. and GCTS). The Campbell Scientific thermal conductivity sensor CSI 229 has a matric suction measurement range from 10 to 1500 kPa whilst the GCTS thermal conductivity sensor FTC-100 has a matric suction measurement range from 1 to 1500 kPa. For the CSI 229, a 50 mA current is used with a 20-30s heating time. Typically the ambient temperature and the temperature after the heating period is recorded from which the matric suction is inferred from the calibration curve. For the FTC-100, a 200 mA current is used with a 60s heating period. The heating curve is recorded for three minutes during a measuring cycle. The diameter and length of the CSI 229 thermal conductivity sensor porous block are 15 mm and 25 mm, respectively, whilst those of the FTC-100 thermal conductivity sensor are 28 mm and 38 mm, respectively. The CSI 229 is more sensitive at matric suctions less than 300 kPa (He, 1999). The resolutions of the FTC-100 suction measurements in the ranges of 1-10, 10-100, 100-1000 kPa are 0.1, 1, and 5-10 kPa, respectively (UST, 2004).

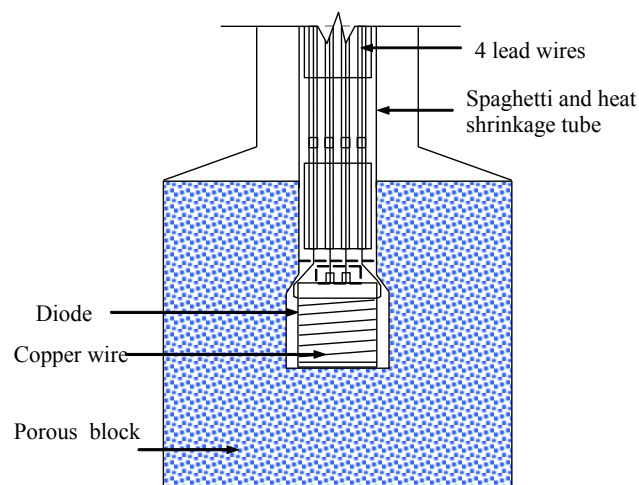


Figure 3. Cross-section of a thermal conductivity sensor (from Phene et al., 1971).

The main problem with the thermal conductivity sensor is the variable uniformity of the porous block from sensor to sensor. This means that a separate calibration curve is required for each thermal conductivity sensor. In addition, the thermal conductivity sensor shows hysteretic behavior on drying and wetting. Reece (1996) suggested that the thermal conductivity of the CSI 299 be normalized with the thermal conductivity measured after oven drying the sensor. With the normalization, Reece (1996) obtained a linear calibration curve between the inverse of the normalized thermal conductivity and the natural logarithm of matric suction up to 1200 kPa. Above a matric suction of 1200 kPa, a non-linear calibration curve is obtained. The hysteretic effect was not considered in the interpretation of matric suction measurement. Zhang et al.

(2001) evaluated thirty CSI 229 sensors and showed that the effect of hysteresis in the CSI 229 thermal conductivity sensor should be taken into consideration when measuring matric suction.

The equilibration time of the thermal conductivity sensor is dependent on the contact condition between the central element (heater and temperature sensor) and the porous block. Even the contact condition between the sensor and the soil affects the response of the CSI 229 (Zhang et al., 2001). Zhang et al. (2001) found that equilibration time of the CSI 229 thermal conductivity sensor can vary from several hours to several tens of hours irrespective of the suction level due to contact condition between the sensor and the soil. Nichol et al. (2003) installed eighteen FTC-100 type of thermal conductivity sensors in the field at depths of 0.2m and 4.5m. They found long-term drift of the thermal conductivity sensors. However O'Kane et al. (1998) and Marjerison et al. (2001) did not experience such problems in their long term monitoring of matric suction with thermal conductivity sensors.

In a recent study conducted by Nguyen (2006), thermal conductivity sensors were installed beneath the pavement, shoulder and slide slope to monitor matric suction and temperature changes with time. The installation layout of the sensors in the highway cross-section is shown in Figure 4. The long-term matric suction measurements between the years 2000 and 2005 at location 3-10 (as shown in Figure 4) beneath the pavement are depicted in Figure 5. The matric suction measurements in the field showed a direct relationship to rainfall and regional evaporation at the monitoring site (Nguyen 2006).

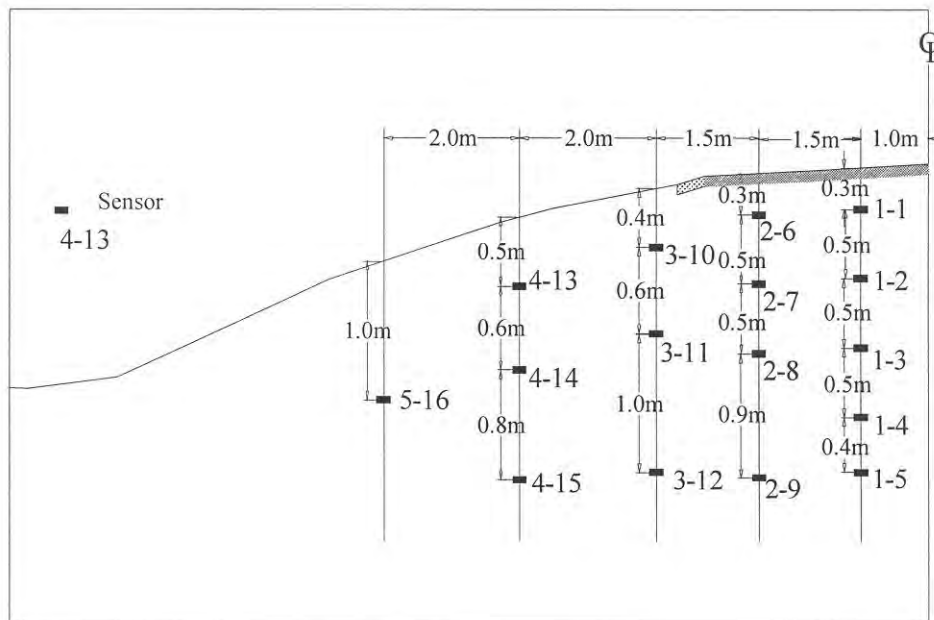


Figure 4. Layout of thermal conductivity sensors in a pavement cross-section (Nguyen 2006).

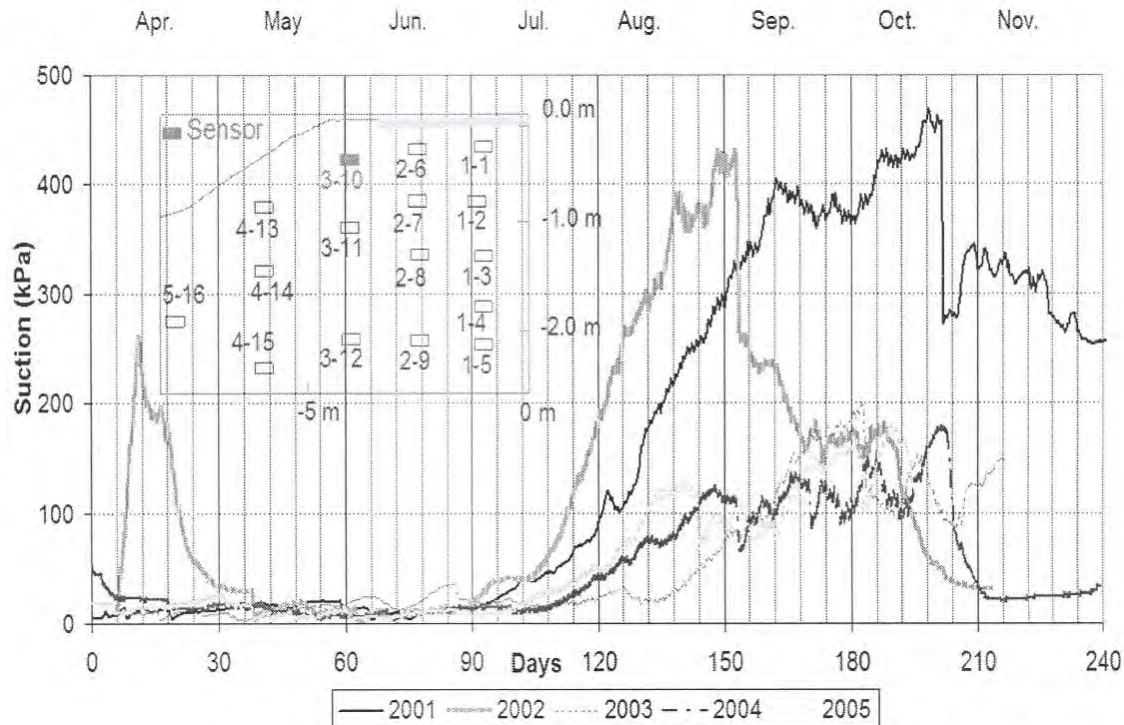


Figure 5. Long term matric suction monitoring beneath the pavement at location 3-10 as shown on the figure (Nguyen 2006).

Thermocouple Psychrometers – Total Suction

There are two types of thermocouple psychrometers for determining total suction measurements in soils: the wet-loop type sensor described by Richards and Ogata (1958) and the Peltier type sensor described by Spanner (1951). The wet-loop sensor is only used with the psychrometric measurement technique, whereas the Peltier sensor can be used with both the psychrometric and hygrometric measurement methods. The primary difference between these two sensors is the manner by which water is applied to the sensing junction. The wet-loop sensor is wetted by manually placing a drop of water on a small ring that is at the sensing junction. The wet-loop type sensor technique has been improved in a new psychrometric device which is called transistor psychrometer and it is discussed in the next section.

Thermocouple psychrometers that are commercially available from Wescor, Inc. are the PST-55 stainless steel and PCT-55 ceramic cup. The PST-55 sensor has a non-removable stainless steel shield, which has a larger pore size. A schematic drawing of a PST-55 sensor is given in Figure 6. The PCT-55 sensor has a removable ceramic shield. The Wescor HR-33T is a single-channel datalogger and can be used to determine the total suction of a sample using either dew point (hygrometric) or wet bulb (psychrometric) methods. The Wescor/Campbell CR7 datalogger and the new Wescor datalogger PSYPRO use only the psychrometric method. The PSYPRO data logger has 8 channels. The CR7 series data logger has several channel configurations (14, 28, 40, 70 and 140 channels). Using either method with any of the instruments, a cooling current is used to cool the thermocouple junction below the dew point of the air surrounding the sample causing

water to condense on the junction (Figure 6). Water evaporation and condensation is equilibrated and a voltage is created. This voltage is converted to total suction using standard salt solutions in the case for calibration. A range of sodium chloride (NaCl) and potassium chloride (KCl) solutions of known osmotic suctions is typically used to establish the relationship between total suction and microvolt output. Calibration solutions are chosen to cover the anticipated range of total suction to be measured. Correct calibration of thermocouple psychrometers is extremely important because the accuracy of all subsequent measurements and interpretations will be based on these data.

For routine measurements across the entire range, a minimum of four calibration solutions are typically selected to characterize each psychrometer's response to changes in total suction at a given temperature. Thermocouple psychrometers are typically calibrated by direct immersion into a small container of calibration solution or by suspension of the sensor over the solution in the container. The immersion method has often been selected because this configuration helps to control the temperature fluctuations better. The pore size of typical screen-cage and ceramic-cup housing is sufficiently small to prevent liquid from entering the air-filled sensor cavity (Pinnock 2005) at low pressures. A water bath is usually employed to maintain temperature stability. The microvolt output from a thermocouple psychrometer is very sensitive to ambient temperature fluctuations. Under isothermal conditions, the equilibration between thermocouple psychrometer sensor and vapor pressure from the salt solution is usually established within an hour.

Careful cleaning and thorough drying of the psychrometers before and after calibration and measurements are essential to reliable instrument performance. Contaminants, such as salts, can affect cooling, evaporation, and microvolt output. The pore size of the protective housing on the thermocouple psychrometer prevents most of contaminants, such as soil particles, from entering the sensor cavity. The most serious contamination occurs if dissolved contaminants migrate through or accumulate on the protective housing. Psychrometers can be cleaned with distilled or deionized water. The practical range over which total suction measurements can be made with thermocouple psychrometers is between about 300 kPa and 7000 kPa. Total suction values between about 300 kPa and 500 kPa should be evaluated very carefully since this is the range most affected by temperature fluctuation. Suction values below 300 kPa should be carefully evaluated for validity. Application of thermocouple psychrometers to infer total suction of unsaturated soils in geotechnical engineering research and practice has greatly broadened in the recent years. In one recent application, Mibirizi and Bulut (2010) monitored the total suction change of cylindrical Shelby tube soil samples over time with thermocouple psychrometers to determine unsaturated soil moisture diffusion coefficients following drying and wetting cycles (Figure 7). In another application, Blatz and Graham (2003) embedded Wescor PST55 in triaxial specimens to measure suction during isotropic loading and shearing.

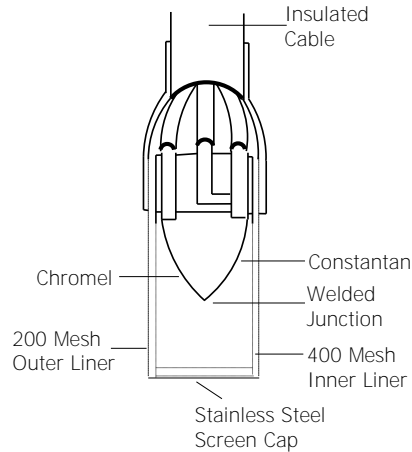


Figure 6. Schematic drawing of a thermocouple psychrometer.

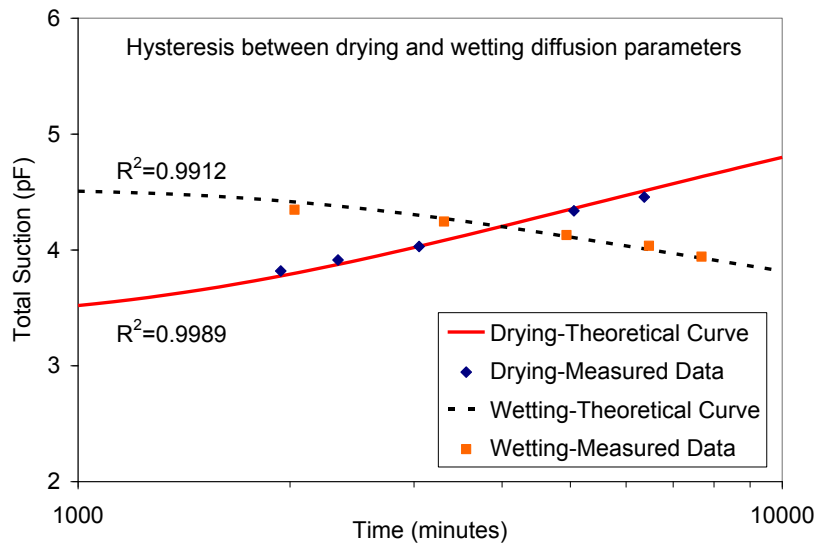


Figure 7. Wetting and drying diffusion coefficient measurements using thermocouple psychrometers (Mabirizi and Bulut 2010).

Transistor Psychrometer – Total Suction

Transistor psychrometer consists of a thermally insulated container that holds the psychrometer probes and a datalogger for measurement and recording of output. The instrument is very similar in operation to the thermistor psychrometer (Woodburn et al., 1993). The transistor psychrometer is an electronic wet and dry bulb thermometer in which a wet and dry transistor probe is used instead of wet and dry thermometer bulbs as in thermistor psychrometers. The sensor is used for inferring the relative humidity of the air space in equilibrium with a soil sample. The temperature depression of the wet transistor, which holds a standard-size water drop, is measured with the

sensors in the probe (Figure 8). The wet and dry transistors are employed as heat sensors and the voltage output from the probe is used to infer total suction.

Improvements in performance have been made that allow the device to measure a much wider range of total suction, from about 100 kPa to about 10000 kPa. Much of the improvement is due to calibration procedure and advances in micro-chip technology (Woodburn et al., 1993). The range and accuracy in measurements are also attributed to sensitivity of the transistors to changes in temperature. Soil Mechanics Instrumentation (Woodburn et al., 1993) produces two types of thermally insulated containers for the transistor probes: 12-probe unit and 8-probe unit. The 8-probe psychrometer is equipped with an insulated lid for better temperature control. Each probe can measure total suction in about one hour. Twelve and eight soil total suction measurements can be made within an hour with the 12- and 8-probe units, respectively.

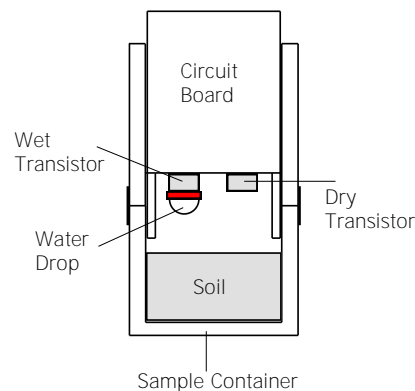


Figure 8. Schematic drawing of a transistor psychrometer probe.

The calibration of the psychrometer probes, determined from the relationship between millivolt output from the transistor and a known osmotic suction value of a salt solution, should be carried out carefully. The calibration curve can be affected by several factors: temperature fluctuations, hysteresis, and water drop size. The transistor probes are first equilibrated for at least 4 hours at zero total suction over distilled water and the output is adjusted to the initial zero reading before any calibration process or soil suction measurements. Afterwards, the different voltage outputs are recorded from the datalogger following one hour equilibration period for each suction level. The relationship between relative humidity and total suction (e.g., Kelvin equation) is used to determine the soil total suction. The thermally insulated container provided for the probes maintains a fairly constant temperature during the period of the test. Greater accuracy and reproducibility of results is obtained in a room where temperature is controlled to about $\pm 0.5^\circ\text{C}$ (Woodburn et al., 1993). Transistor psychrometer can only do point measurements (e.g., applicable for small soil specimens of 15 mm in diameter and 13 mm in height). The limitation of soil specimen size when using the transistor psychrometer is also widely recognized.

Transistor psychrometers have been used around the world. In Australia and New Zealand this instrument has been used for unsaturated expansive soils applications (Woodburn, 2005). It has

practically replaced thermocouple psychrometers in many laboratory soil suction measurements. Recent studies by Bulut et al. (2000, 2002) showed that transistor psychrometer has a better capability of measuring total suction at lower levels when compared with other psychrometric methods.

Chilled-Mirror Psychrometer – Total Suction

A chilled-mirror psychrometer uses the chilled mirror dew point technique to infer total suction under isothermal conditions in a sealed container (Figure 9). The chilled-mirror psychrometer discussed in this paper is a product of Decagon Devices, Inc. and is known as a WP4 Dew Point Potentiometer (www.decagon.com). Measurement of total suction with the WP4 is based on equilibrating the liquid phase of the water in a soil sample with the vapor phase of the water in the air space above the sample in a sealed chamber. A Peltier cooling device is used to cool the mirror until dew forms and then to heat the mirror to eliminate the dew. Temperature of the sample is measured with an infrared thermometer. An optical sensor is also employed to detect the dew formed on the mirror. A thermocouple attached to the chilled mirror measures the dew point temperature. A small fan is also employed to circulate the air in the sensing chamber and speed up vapor equilibrium. Both the dew point and soil sample temperature are then used to determine the relative humidity above the soil sample within the closed chamber.

The chilled mirror technique offers a fundamental characterization of humidity in terms of the temperature at which vapor condenses. Therefore, the calibration of the instrument with different concentrations of salt solutions is not necessary. However, the performance of the instrument should be checked prior to total suction measurement by measuring the total suction of a salt solution with a known osmotic potential (WP4 User Manual). When the temperature readings have stabilized, the instrument will determine the relative humidity of the enclosed space above the soil sample and will display the total suction of the sample. Temperature control is very important. The measured difference between dew point and sample temperatures must be kept small. The WP4 chilled-mirror psychrometer is a very robust instrument that is suitable for rapid total suction measurements, usually less than 10 minutes. It is important to avoid contamination of the instrument. The sample cup should be filled to less than full capacity to minimize the potential of contaminating the chamber. If necessary, the mirror and fan can be cleaned according to procedures outlined in the user's manual.

Bulut et al. (2002) performed a complete evaluation of the WP4 instrument using the relationship between osmotic suction and salt solution concentration. Bulut et al. (2002) compared the accuracy of the chilled-mirror psychrometer with the filter paper method for total suction measurements of undisturbed soil samples from the Dallas-Fort Worth area. Bulut et al. (2002) found that the degree of error associated with the WP4 psychrometer is higher than with the filter paper method at low suction levels, but very good correlation between the two methods at high total suction levels.

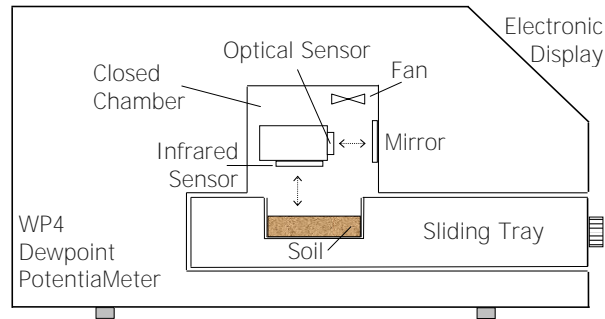


Figure 9. Schematic drawing of the WP4 chilled-mirror psychrometer.

Leong et al. (2003) evaluated the accuracy of a chilled mirror dew point device using compacted soil samples. A thorough calibration of the instrument using several standard salt solutions was performed. The equilibration time during calibration and total suction measurement was short, less than 15 minutes. The total suction measurements on the compacted samples were compared to the sum of matric and osmotic suctions of the same soils that were measured independently. The matric suction of the soils was measured with the null-type axis-translation apparatus and the osmotic suction of the samples was estimated from electrical conductivity measurements of the soil water solution obtained from a pore fluid squeezer device. The test results showed that total suctions obtained using the chilled mirror dew point device were always greater than the sum of the matric and osmotic suctions measured independently. In ASTM D6836-02, the chilled-mirror hygrometer is used in Method D for determining the desorption soil water characteristic curve for suction range above 1000 kPa as the limitation of the chilled-mirror hygrometer for low suction levels is widely recognized.

Filter Paper Method – Total and Matric Suctions

The filter paper technique is the only method from which both total and matric suction can be inferred. Using the filter paper method, the soil specimen and filter paper are brought to moisture equilibrium either in contact (matric suction) or not in direct contact (total suction) in a constant temperature environment (Figure 10). Direct contact between the filter paper and the soil allows water in the liquid phase and solutes to exchange freely, whereas separation between the filter paper and the soil by a vapor barrier limits water exchange to the vapor phase only and prevents solute movement. Matric suction measurements using the filter paper method are similar to the total suction measurements except that intimate contact must be provided between the filter paper and the soil (Figure 10). After equilibrium is established between the filter paper and soil, the water content of the filter paper is measured. Then, by using the appropriate filter paper calibration curve, the suction of the soil is estimated. The calibration curves are usually obtained from the processes of wetting and drying the filter papers through vapor transfer (salt solutions) and drying and wetting the filter papers through fluid transfer (porous plates). The filter paper method is a simple technique and can be reliable if the basic principles of the method are understood and a strictly practiced laboratory protocol is carefully followed.

As accuracy of the filter paper technique is dependent on the accuracy of the filter paper water content versus suction calibration curve, the calibration technique of the filter paper method has been investigated by numerous researchers (e.g. Houston et al. 1994, Bulut et al. 2001, Leong et al. 2002). Calibration equations should be developed specifically for the specific filter paper being used. The most commonly used filter papers are Whatman No. 42 and Schleicher & Schuell No. 589-WH.

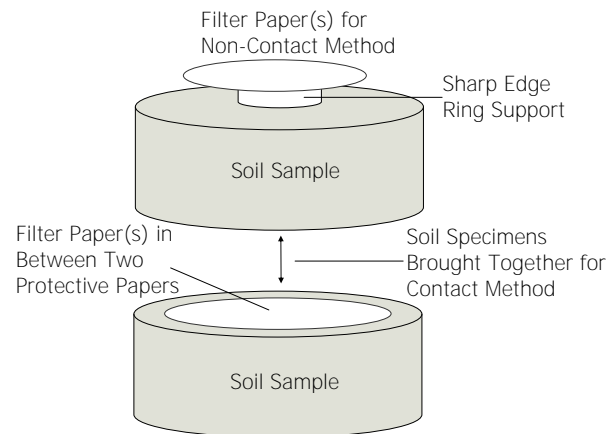


Figure 10. Schematic drawing of soil total and matric suction measurements.

Until Houston et al. (1994) all suction measurements were based on a single calibration curve. Houston et al. (1994) developed two calibration curves for Fisher quantitative coarse (9.54 A) filter paper: one for total suction and one for matric suction and reported that the curves were different. Bulut et al. (2001) developed two calibration curves for Schleicher & Schuell No. 589-WH filter papers: one by the process of wetting from initially dry filter papers through vapor flow using NaCl solutions and one by the process of drying from initially saturated filter papers through fluid flow using pressure plates and membranes. Leong et al. (2002) developed different calibration curves for total and matric suctions for Whatman No. 42 and Schleicher & Schuell No. 589-WH filter papers from initially dry filter papers using NaCl solutions and pressure plate. For instance, the calibration curves constructed by Leong et al. (2002) are given in Figure 11. In a more recent study, Bulut and Wray (2005) re-evaluated the filter paper method based on a new calibration curve and the most recent published literature.

The differences in the filter paper calibration curves in the literature are attributed to several factors such as the suction source for the calibration, thermodynamic definitions of suction components, and equilibration time (Fredlund and Rahardjo, 1993; Houston et al., 1994; Bulut et al., 2001; Leong et al., 2002; Bulut and Wray, 2005; Walker et al., 2005). Walker et al. (2005) evaluated total suction measurements of a soil sample using transistor psychrometer and filter paper method. Walker et al. (2005) adopted the filter paper calibration curve in Hamblin (1981) and found that total suction measurements from the filter papers were significantly smaller than the total suction measurements from the transistor psychrometer. Walker et al. (2005) suggested that the total suction calibration curves represent a transient condition during the calibration

period and that a unique, single calibration curve should be used for both total and matric suction measurements. In other words, Walker et al. (2005) suggested that if sufficient time is allowed for equilibration, the total suction calibration curve will tend towards the matric suction calibration curve. Bulut et al. (2001) and Bulut and Wray (2005) stated that a single calibration curve based on water vapor measurements is adequate for both total and matric suction measurements. Leong et al. (2002) attributed the differences between the calibration curves to the initial condition of the filter paper whether it is from the dry or wet condition. Leong et al. (2002) stated that if the calibration curves are from the initially wet filter paper condition, then it may be possible that both calibration curves are similar. However, two different calibration curves are obtained when the initially dry filter papers are adopted. Leong et al. (2002) and Bulut and Wray (2005) discussed in detail the different calibration curves of filter papers and the time required for equilibration. The filter paper method has been extensively used all around the world for both laboratory and field studies. For instance, in a recent study, Chao et al. (2008) used the filter paper method in obtaining the soil water characteristic curves for remolded expansive clay soils in Colorado.

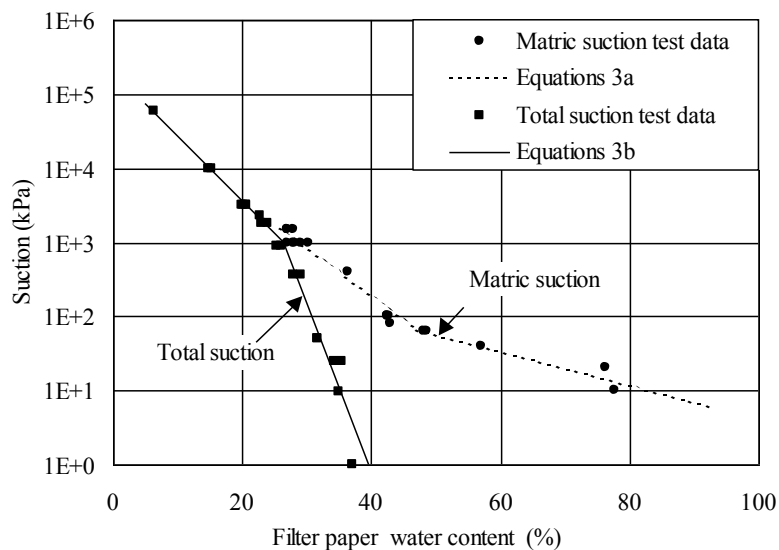


Figure 11. Total and matric suction calibration curves for Whatman No. 42 (Leong et al., 2002).

It is extremely important to minimize temperature gradients during the calibration with salt solutions as well as during total suction measurement. During calibration, it is suggested that temperature fluctuations should be maintained within an accuracy of $\pm 0.1^\circ\text{C}$ or better. It would be ideal to maintain a similar accuracy during total suction measurements, but it may be difficult to obtain such accuracy in a geotechnical engineering laboratory. Therefore, this accuracy may be relaxed to some degree. Temperature fluctuations are extremely critical at high relative humidity levels. Bulut and Wray (2005) described the sensitivity of suction at high relative humidity levels and illustrated that minor changes in relative humidity result in very large changes in suction. Filter papers should also be allowed to equilibrate for a sufficient time. Recent literature suggested that an upper limit of equilibration time of 14 days is sufficient for

filter paper calibration over salt solutions and distilled water, and one week of equilibration period is usually considered satisfactory for most soil suction measurements.

Discussions

The understanding and wide acceptance of unsaturated soil mechanics principles has produced a gradual change in geotechnical engineering practice. Soil suction variations in subgrade materials have significant effects on the shear strength, volume change, and moisture flow in unsaturated geo-materials. The performance of pavements could largely be controlled by strength of the subgrade soil which in turn is a function of the soil suction. For instance, with the recent popularity of mechanistic pavement design procedure (MEPDG), direct or indirect measurements of the shear strength (or modulus) of compacted soil layers have become popular. Due to unsaturated nature of these subgrades, soil suction is an important factor in determining the shear strength (or modulus) of those materials. Much work has been performed in regard to modulus-based quality control of compacted subgrade soils, and a number of in-situ test devices have been extensively studied to determine the pavement layer moduli. Although the new MEPDG procedures have taken the right path by shifting from density to modulus for quality acceptance, the dependence of modulus on moisture content (or suction) variations with climatic and environmental effects still need to be investigated in detail in terms of the principles of unsaturated soil mechanics. Thus, in order to apply the unsaturated soil mechanics principles to pavement materials successfully, the measurement and/or prediction of soil suction is essential.

This paper has summarized basic working principles, calibration, measurement, and application of several soil suction measurement methods based on the most recent literature. Table 1 summarizes key characteristics of suction measurement methods. The source/manufacturer mentioned in the paper is meant for reference and does not represent product endorsement by the author. The list is also not meant to be exhaustive. Accurate total suction measurement is still difficult with current technology, especially for total suction levels below about 100 kPa. Difficulties with the primary methods measurement techniques basically arise from two main sources. The first stems from the fact that relative humidity in the soil air phase changes only a small amount within the typical range of suction interest. Most measurements of interest to studies of unsaturated soils lie in the narrow relative humidity range from about 0.94 and 1.00. The second main source of difficulty arises from the fact that minor temperature fluctuations may lead to large errors in determination of total suction. Unless a strictly practiced laboratory protocol is followed, the filter paper method may give questionable results. However the filter paper method is simple and is the most affordable indirect suction measurement method. The thermal conductivity sensor measures the properties of the porous medium associated with its moisture condition from which matric suction is inferred. The thermal conductivity sensors have proven to be a promising means of measuring long-term field suctions.

Table 1. Summary of soil suction measurement methods.

Method	Suction	Suction Range (kPa)	Equilibrium Time	Source/ Manufacturer
Tensiometer	Matric	0-80	Seconds to minutes	Soil Moisture Equipment: www.soilmoisture.com
Thermocouple Psychrometer	Total	300-7000	1 hour	Wescor: www.wescor.com Campbell Scientific: www.campbellsci.com
Transistor Psychrometer	Total	100-10000	1 hour	Soil Mechanics Instrumentation: Australia
Chilled-Mirror Psychrometer	Total	500-30000 (or higher)	10 minutes	Decagon Devices: www.decagon.com
Filter Paper Method	Total/ Matric	50-30000 (or higher)	5 to 14 days	Whatman: www.whatman.com Schleicher & Schuell: www.schleicher-schuell.com
Thermal Conductivity Sensor	Matric	1-1500	Hours to days	Campbell Scientific: www.campbellsci.com GCTS: www.gcts.com

References

- Aitchison, G.D. and Richards, B.G. 1965. A broad-scale study of moisture conditions in pavement subgrades throughout Australia, *Moisture in Soils Beneath Covered Areas*, Butterworths, Australia, 198-204.
- Albrecht, B.A., Benson, C.H., and Beuermann, S. 2003. Polymer capacitance sensors for measuring soil gas humidity in drier soils, *Geotechnical Testing Journal*, 26(1): 1-9.
- ASTM D5298-94. 1994. Standard test method for measurement of soil potential (suction) using filter paper, 1994 Annual Book of ASTM Standards, ASTM, Philadelphia, PA.
- ASTM D6836-02. 2003. Standard test methods for determination of the soil water characteristic curve for desorption using a hanging column, pressure extractor, chilled mirror hygrometer, and/or centrifuge, 2003 Annual Book of ASTM Standards, ASTM, Philadelphia, PA.
- Blatz, J.A. and Graham, J. 2003. Elastic-plastic modelling of unsaturated soil using results from a new triaxial test with controlled suction, *Geotechnique*, 53(1): 113-122.
- Bulut, R. and Leong, E.C. 2008. Indirect measurement of suction. *Journal of Geotechnical and Geological Engineering*, Vol 26, pp. 633-644.
- Bulut, R. and Wray, W.K. 2005. Free energy of water – suction – in filter papers, *Geotechnical Testing Journal*, 28(4): 355-364.
- Bulut, R., Aubeny, C.P., and Lytton, R.L. 2005. Unsaturated soil diffusivity measurements, *International Symposium on Advanced Experimental Unsaturated Soil Mechanics*, Trento, Italy, June 27-29.
- Bulut, R., Lytton, R. L., and Wray, W. K. 2001. Soil Suction Measurements by Filter Paper, *Expansive Clay Soils and Vegetative Influence on Shallow Foundations*, ASCE Geotechnical Special Publication No. 115 (eds. C. Vipulanandan, M. B. Addison, & M. Hasen), Houston, Texas, 243-261.

- Bulut, R., Hineidi, S. M., and Bailey, B. 2002. Suction Measurements – Filter Paper and Chilled Mirror Psychrometer, Proceedings of the Texas Section American Society of Civil Engineers, Fall Meeting, Waco, Texas, October 2-5.
- Bulut, R., Park, S.-W., and Lytton, R.L. 2000. Comparison of total suction values from psychrometer and filter paper methods, Unsaturated Soils for Asia, Proceedings of the Asian Conference on Unsaturated Soils, UNSAT-ASIA 2000, Singapore, 18-19 May, 269-273.
- Bouyoucos G. J. and Mick A. H. 1940. Comparison of absorbent materials employed in the electrical resistance method of making a continuous measurement of soil moisture under field conditions, Proc. Soil Science Society of America, 5: 77-79.
- Chao, K.C., Nelson, J.D., Overton, D.D., and Cumbers, J.M. 2008. Soil water retention curves for remolded expansive soils. Unsaturated Soils: Advances in Geo-Engineering, pp. 243-248.
- Dawson, A. 2007. Water movement in road pavements and embankments. Summary Final Report. www.watmove.com.
- Feng, M. and Fredlund, D.G. 2003. Calibration of thermal conductivity sensors with consideration of hysteresis, Canadian Geotechnical Journal, 40(5): 1048-1055.
- Fredlund, D. G. and Rahardjo, H. 1993. Soil Mechanics for Unsaturated Soils, New York: John Wiley & Sons, Inc.
- Fredlund, D.G. and Wong, D.K.H. 1989. Calibration of thermal conductivity sensors for measuring soil suction, Geotechnical Testing Journal, 12(3): 188-194.
- Hamblin, A.P. 1981. Filter paper method for routine measurement of field water potential, Journal of Hydrology, 53: 355-360.
- He, L-C. 1999. Evaluation of instruments for measurement of suction in unsaturated soils, MEng Thesis, School of Civil & Structural Engineering, Nanyang Technological University, Singapore.
- Houston, S.L., Houston, W.R. and Wagner, A.M. 1994. Laboratory filter paper measurements, Geotechnical Testing Journal, 17(2): 185-194.
- Leong, E.-C., He, L., and Rahardjo, H. 2002. Factors affecting the filter paper method for total and matric suction measurements, Geotechnical Testing Journal, 25(3): 322-333.
- Leong, E.-C., Tripathy, S., and Rahardjo, H. 2003. Total suction measurement of unsaturated soils with a device using the chilled-mirror dew-point technique, Geotechnique, 53(2): 173-182.
- Mabirizi, D. and Bulut, R. 2010. A unified testing method for measuring unsaturated soil drying and wetting diffusion coefficients in laboratory. Transportation Research Record: Journal of Transportation Research Board. (in pres).
- Marjerison, B., Richardson, N., Widger, A., Fredlund, D.G., and Berthelot, C. 2001. Installation of sensors and measurement of soil suction below thin membrane of surface pavements in Saskatchewan, Proc. 54th Canadian Geotechnical Conference, Calgary, Alta, 16-19 September, 1328-1334.
- Ng, C.W.W., Springman, S.M., and Alonso, E.E. 2009. Monitoring the performance of unsaturated soil slopes. In Laboratory and Field Testing of Unsaturated Soils, Springer.
- Nguyen, Q. 2006. Long-term matric suction measurements in highway subgrades. MS Thesis. University of Saskatchewan, Saskatoon, Canada.
- Nichol, C., Smith, L. and Beckie, R. 2003. Long term measurement of matric suction using thermal conductivity sensors, Canadian Geotechnical Journal, 40(3): 587-597.

- O'Kane, M., Wilson, G.W., and Barbour, S.L. 1998. Instrumentation and monitoring of an engineered soil cover system for mine waste rock, *Canadian Geotechnical Journal*, 35: 828-846.
- Oloo, S.Y. and Fredlund, D.G. 1995. Matric suction measuring in an expansive soil subgrade in Kenya, *Unsaturated Soils: Proc. 1st International Conference On Unsaturated Soils*, Paris, France.
- Phene, C.J., Hoffman, G.J. and Rawlins, S.L. 1971. Measuring soil matric potential in-situ by sensing heat dissipation within a porous body: I. Theory and sensor construction, *Proc. Soil Science Society of America*, 35: 27-33.
- Pinnock, D. 2005. Personal Communication, Wescor, Inc., Utah, USA.
- Reece, C. F. 1996. Evaluation of a line heat dissipation sensor for measuring soil matric potential, *Soil Science Society of America Journal*, 60(4): 1022-1028.
- Reeves, B. 2003 Personal Communication, QA/QC Manager, Schleicher & Schuell, Florida, USA.
- Richards, L.A. and Ogata, G. 1958. A thermocouple for vapor pressure measurement in biological and soil systems at high humidity, *Science*, 128: 1089-1090.
- Ridley, A.M. 1993. The measurement of soil matric suction, PhD thesis, Imperial College of Science, Technology and Medicine, University of London.
- Siemens, G.A. and Blatz, J.A. 2005. Soil suction measurement using the Xeritron Sensor in two different types of infiltration tests on a swelling soil, *International Symposium on Advanced Experimental Unsaturated Soil Mechanics*, Trento, Italy, June 27-29.
- Skinner, A., Hignett, C., and Dearden, J. 1997. Resurrecting the gypsum block for soil moisture measurement, *Australian Viticulture*, October/November 1997.
- Spanner, D.C. 1951. The Peltier effect and its use in the measurement of suction pressure, *Journal of Exp. Bot.*, 2: 145-168.
- Sweeney, D.J. (1982). Some insitu soil suction measurements in Hong Kong's residual soil slopes. *Proceedings of the 7th Southeast Asia Geotechnical Conference*, Hong Kong, Vol. 1, pp. 91-106.
- Tadepalli, R. (1990). Study of collapse behaviour during inundation. MSc Thesis, University of Saskatchewan, Canada.
- UST 2004. <http://www.soilvision.com/subdomains/unsaturatedsoil.com/sensor.shtml>.
- Walker, S.C., Gallipoli, D., and Toll, D.G. 2005. The effect of structure on the water retention of soil tested using different methods of suction measurement, *International Symposium on Advanced Experimental Unsaturated Soil Mechanics*, Trento, Italy, June 27-29.
- Woodburn, J.A. 2005. Personal Communication, Soil Mechanics Instrumentation, Australia.
- Woodburn, J. A., Holden, J. C., and Peter, P. 1993. The Transistor Psychrometer: A New Instrument for Measuring Soil Suction, *Unsaturated Soils*, ASCE Geotechnical Special Publication No. 39 (eds. S. L. Houston and W. K. Wray), Dallas, Texas, 91-102.
- Zhang X., Leong, E.C., Rahardjo, H. 2001. Evaluation of a thermal conductivity sensor for measurement of matric suction in residual soil slopes, *Proc. 14th Southeast Asian Geotechnical Conference*, Hong Kong, 611 – 616.

Influence of Moisture Content on the Pullout Capacity of Geotextile Reinforcement in Marginal Soils

Kianoosh Hatami

School of Civil Engineering and Environmental Science (CEES), University of Oklahoma,
Norman, OK, USA 73019
(405)-325-3674
kianoosh@ou.edu

Lina M. Garcia

School of Civil Engineering and Environmental Science (CEES), University of Oklahoma,
Norman, OK, USA 73019
(405)-325-3674
linagarcia@ou.edu

Gerald A. Miller

School of Civil Engineering and Environmental Science (CEES), University of Oklahoma,
Norman, OK, USA 73019
(405)-325-4253
gamiller@ou.edu

Prepared for the 61st Highway Geology Symposium, August, 2010

Acknowledgements

The funding for this study was provided through ODOT Award No. SPR 2214 and the Oklahoma Transportation Center Award No. OTCREOS7.1-19. The authors are grateful for their useful discussions with ODOT engineers Mr. Jeff Dean, Drs. Butch Reidenbach and Jim Nevels, and Mr. Chris Clarke over the course of this study. The geotextile was donated by TenCate Geosynthetics. Undergraduate research assistants, Lee Blackburn, Matt Long, Derek Reid, Kyle Olson, Max Newton and Jeremy Christiansen helped with the setup and execution of the tests.

Disclaimer

Statements and views presented in this paper are strictly those of the author(s), and do not necessarily reflect positions held by their affiliations, the Highway Geology Symposium (HGS), or others acknowledged above. The mention of trade names for commercial products does not imply the approval or endorsement by HGS.

Copyright Notice

Copyright © 2010 Highway Geology Symposium (HGS)

All Rights Reserved. Printed in the United States of America. No part of this publication may be reproduced or copied in any form or by any means – graphic, electronic, or mechanical, including photocopying, taping, or information storage and retrieval systems – without prior written permission of the HGS. This excludes the original author(s).

ABSTRACT

As part of an on-going research program at the University of Oklahoma, pullout tests were carried out to determine the influence of moisture content on the soil-geotextile interface strength in reinforced soil structures constructed with marginal soils. The tests were carried out on an Oklahoma marginal soil at moisture content values on the dry and wet sides of its optimum moisture content. The test setup and procedure, and some preliminary test results are described in this paper.

The measured data indicate that the pullout capacity of geotextile reinforcement in marginal soils can be measurably reduced as a result of increase in the soil moisture content. Consequently, it is suggested that the influence of soil moisture content should be included in the future revisions of design guidelines for reinforced soil slopes and embankments that could contain significant amounts of fines.

INTRODUCTION

Over many years there have been problems with slope failures and landslides along the highways in Oklahoma. Many of these failures occur in eastern Oklahoma due to steeper topography, poor soil types or a combination of both. A recent example of these failures is the massive slope failure on Highway 82 in Latimer County in southeastern Oklahoma (**Figure 1**). Repairs and maintenance work associated with these failures cost transportation agencies millions of dollars annually.

A desirable solution for the construction or repair of slopes and embankments is to use geosynthetics and large quantities of coarse-grained, free-draining soils to stabilize these structures. However, such coarse-grained soils are not readily available in Oklahoma and many other parts of the U.S. Consequently, the production and transportation costs for these materials can be prohibitive amounting to millions of dollars. A possible solution to this problem would be to use locally available soils that are of marginal quality (e.g. soils with more than 15% fines content) but are significantly less expensive. Soils with up to 50% low-plasticity fines are currently considered for reinforced soil slopes (e.g. Elias et al. 2001, Berg et al. 2009).



Figure 1 – A massive highway slope failure in Latimer County, Oklahoma

However, marginal soils with greater fines contents and higher plasticity have also been considered as possible construction materials for reinforced soil structures provided that adequate drainage, construction control and performance monitoring are provided in their design and construction (e.g. Farrag and Morvant 2004, Berg et al. 2009). One main concern in internal stability of reinforced soil slopes constructed with marginal soils is the pullout capacity of reinforcement when the soil moisture content increases significantly. Current design guidelines and test protocols for reinforced soil slopes in North America (e.g. Elias et al. 2001, AASHTO 2002) do not include specific procedures to account for the reduction in interface strength due to increased moisture content.

In this study, a series of pullout tests were carried out to examine the influence of moisture content on the soil-geotextile reinforcement interface strength using an Oklahoma marginal soil. The tests were carried out at moisture content values on the dry and wet sides of the soil optimum moisture content (OMC). In the following sections, the test setup and procedure are described and the test results are discussed.

TESTING PROGRAM

Pullout Tests and Material Properties

Pullout tests were carried out in a fine-grained soil called Minco silt. The soil was found in west central Oklahoma about 20 miles west of El Reno (south of Geary) inside the Canadian County. The soil properties from laboratory tests are given in **Table 1**. Minco silt is classified as a CL-ML soil according to the Unified Soil Classification System (USCS) and was chosen as a possible candidate for a locally available and inexpensive soil for the construction of reinforced soil slopes due to its low plasticity. Its optimum moisture content and maximum dry unit weight from standard Proctor tests were determined to be OMC = 12.7% and $\gamma_{dmax} = 17.2 \text{ kN/m}^3$ (109.5 pcf), respectively (**Figure 2**).

The pullout tests were carried out at three different moisture content values OMC-2%, OMC and OMC+2%. The tests for each moisture content value were carried out at three different overburden pressures 10 kPa (209 psf), 20 kPa (418 psf) and 50 kPa (1044 psf). A woven polypropylene (PP) geotextile (**Figure 3**) with material properties given in **Table 2** was used as the reinforcement. Tensile response of the geotextile was determined as per the ASTM D4595 test protocol (ASTM 2009) and was compared with the manufacturer's data (**Figure 4**).

Table 1- Minco silt properties	
Minco silt (CL-ML) property	Value
Liquid Limit, %	23
Plastic Limit, %	19
Plasticity Index, %	4
Specific Gravity	2.6
Gravel, %	0
Sand, %	29.7
Fines, %	70.3
Maximum Dry Unit Weight, kN/m^3 (pcf)	17.2 (109.5)
Optimum Moisture Content, %	12.7

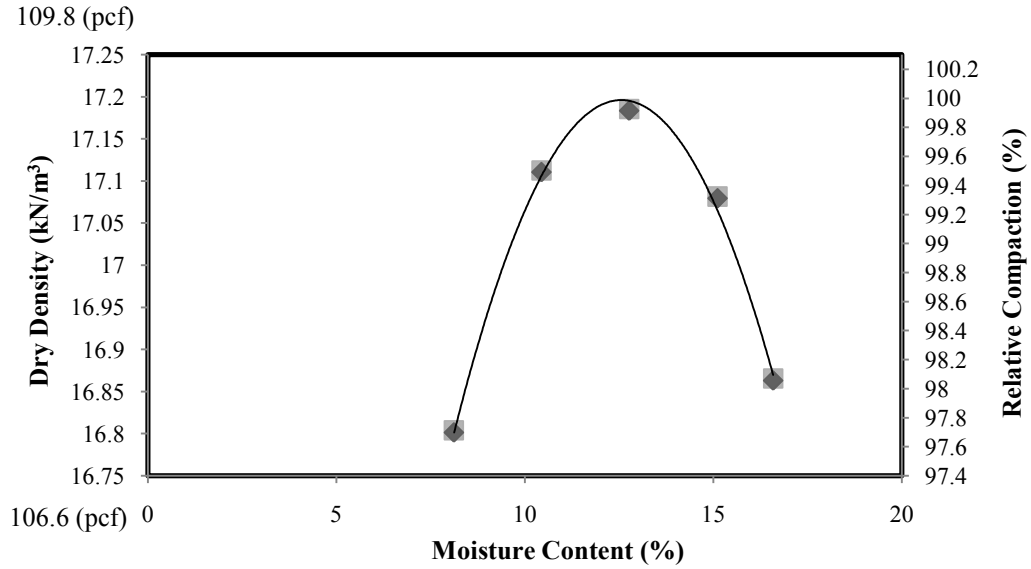


Figure 2 – Standard Proctor test results on Minco silt

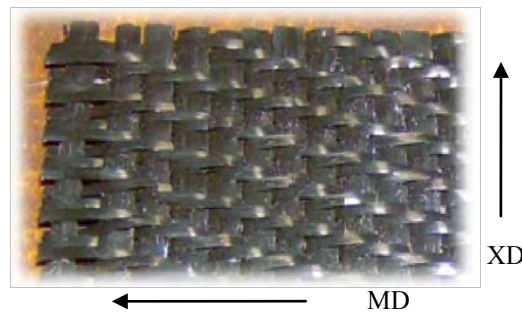


Figure 3 – Woven geotextile reinforcement used in the study. MD and XD refer to machine direction and cross-machine direction, respectively.

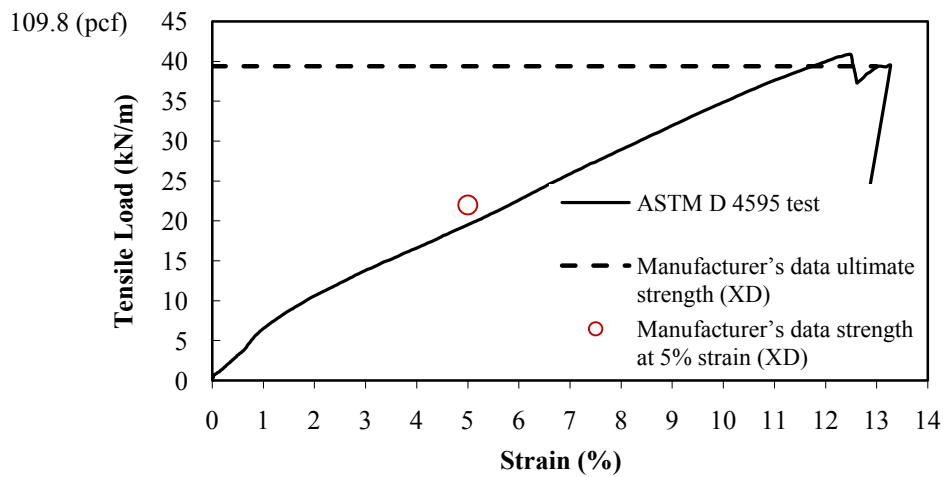


Figure 4 – Mechanical response of geotextile reinforcement as per ASTM D4595 test protocol and as compared with the manufacturer's data.

Property	Test Protocol	Value/description
Polymer type	-	Polypropylene
Fabric	-	Slit-film, Woven
Mass per unit area (g/m ²)	ASTM D5261	
Percent open area (%)	CWO-22125	
O ₉₅ (mm), Apparent opening size (U.S. Sieve)	ASTM D4751	0.600 (30)
Permittivity (s ⁻¹)	ASTM D4491	0.52
Puncture resistance kN (lb)	ASTM D4833	0.8 (179.8)
Trapezoidal tearing strength kN (lb)	ASTM D4533	0.76 (170.8) MD, 0.49 (110.2) XD
Grab tensile strength kN (lb)	ASTM D4632	1.78 (400.1) MD, 1.10 (247.28) XD
Elongation (%)	ASTM D4632	15 (MD), 6 (XD)
Survivability class	AASHTO M288	2,3
Applications	AASHTO M288	Separation, Stabilization, Reinforcement
Wide-width ultimate tensile strength kN/m (lb/ft)	ASTM D4595	47.3 (3241.0) MD, 39.4 (2699.7) XD

Note: MD and XD refer to machine direction and cross-machine direction, respectively.

Test Equipment

Nominal dimensions of the large-scale pullout test box (**Figure 5**) are 1800 mm/6 ft (L) × 900 mm/3 ft (W) × 750 mm/2.5 ft (H). The size of the box and its basic components, including metal sleeves at its front end exceed the requirements of the ASTM D6706 test protocol (ASTM 2009). Boundary effects were further minimized by lining the walls of the test box with plastic sheets. The test box has an 18 mm (¾ inch)-thick transparent panel wall on one side to allow for visual observation of the soil deformation during the testing period. A surcharge assembly including an airbag and reaction beams on the top of the soil surface was used to apply overburden pressures up to 50 kPa (1044 psf) on the soil-geotextile interface. The pullout load on the reinforcement specimen was applied using a 100 mm (4-inch) bore and 457 mm (18-inch) stroke, 90 kN (20 kip) servo-controlled hydraulic actuator. In the tests carried out in this study, only one half of the box length (i.e. 900 mm/3 ft) was utilized.



Figure 5 – Pullout test box at the end of sample preparation.

Two rows of tensiometer probes were placed above and below the geotextile to measure the matric suction in the vicinity of the soil-reinforcement interface (**Figures 6 and 7**).

Tensiometers were suitable to measure suction values up to about 100 kPa (14.5 psi). Reinforcement displacements were measured using four wire-line extensometers attached to different locations along the geotextile length (**Figure 6a**). An earth pressure cell (EPC) was placed on the top of the soil underneath the airbag to verify the magnitude of the overburden pressure applied on the soil and the soil-geotextile interface.



Figure 6 - (a) Wireline extensometers attached to the geotextile and tensiometer probes near the soil-geotextile interface, (b) tensiometer readout dials

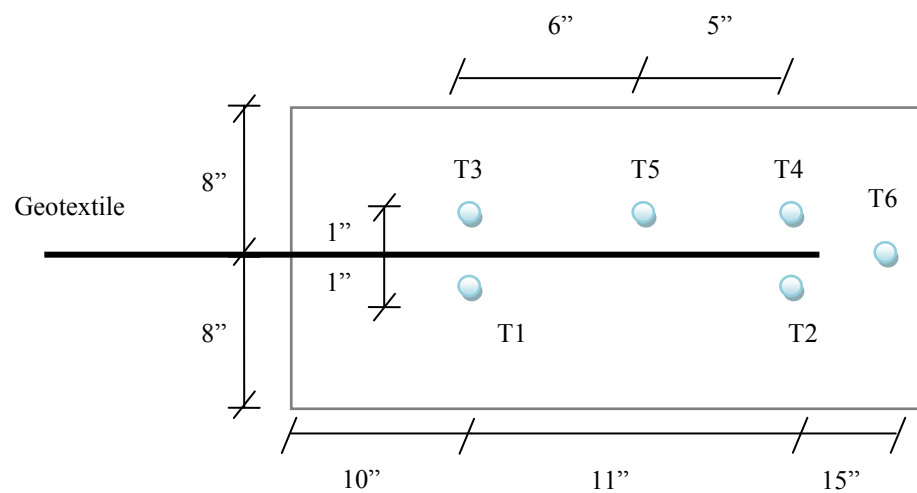


Figure 7 - Schematic diagram indicating the locations of tensiometers in the pullout test box (elevation cross-section view)

Test Procedure

After the soil was transported from the borrow site to the laboratory, the soil was dried to a natural moisture content of 0.4%, and then it was passed through the #4 sieve. The coarser particles and chunks were crushed and sieved again through the #4 sieve. Then the soil was mixed with water to reach the desired moisture content for each test. The wet soil was stored in thirty three 25 kg (55 lb) buckets and sealed for more than 24 hours to promote moisture equilibrium. The soil moisture content in each bucket was measured using the oven drying method.

The pullout box was lined with plastic sheets to preserve the soil moisture content and to minimize the friction between the soil and the sidewalls during testing. Next, the soil was placed and compacted in the test box in eight 50 mm (2 inch) lifts. Compacting Minco silt in the box to 95% of its maximum dry unit weight was found to be challenging for the case of OMC+2%. Therefore, in order to maintain a consistent compaction level in all test cases, the soil in all cases was compacted to 86% of its maximum dry unit weight (i.e. $\gamma_d = 14.81 \text{ kN/m}^3 = 94.3 \text{ pcf}$) which was achievable for the soil at OMC+2%. The corresponding bulk unit weight of the soil was $\gamma = 16.40 \text{ kN/m}^3$ (104.4 pcf). The soil target unit weight in the test box was reached using volumetric compaction control. The instrumented geotextile and the tensiometers were placed at the mid-height of the box (Figure 6a). The length and width of the geotextile specimen were 0.61 m (2 ft) and 0.30 (1 ft), respectively. The pullout box filled with compacted Minco silt at its target moisture content was sealed with plastic sheets on the top. The soil was monitored for 4 to 5 days until all tensiometers showed constant readings.

The pullout tests were carried out at a nominal rate of 1 mm/min as per the ASTM D6706 test protocol. The pullout phase of the test usually took between 40 minutes and 1½ hours depending on the overburden pressure. After the test was completed and the reinforcement underwent pullout failure, the test assembly was carefully dismantled. First, the surcharge assembly was removed from the top of the box. The exposed soil was examined for any signs of cracking or deformation, followed by careful excavation. It usually took about 5 to 7 hours to carefully dig the entire soil out of the test box. All together, a complete test required approximately 24 hours of hands-on preparation, 5 to 6 days of observation and monitoring, and 0.65 to 1.5 hours to run the pullout test. The soil was excavated from the test box in eight 50 mm (2 inch) layers. Soil samples were taken from each layer before and after each pullout test to determine their moisture content.

RESULTS

Measured results of pullout force vs. clamp displacement for Minco silt at nominal moisture content values OMC-2% (10.7%), OMC (12.7%) and OMC+2% (14.7%) are shown in **Figure 8**. These results show that the reinforcement pullout resistance is greater when subjected to greater overburden pressure (or normal stress, σ_n) magnitudes. They also show that reinforcement displacement at peak pullout load is greater at greater overburden pressures. This means that the extensible geotextile reinforcement when subjected to greater overburden pressures needs to be stretched to larger extents before it can be pulled out of the soil. Results in **Figure 8** show consistently higher maximum reinforcement pullout resistances at OMC-2%

compared to the values in the OMC and OMC+2% cases for all overburden pressure magnitudes examined. As expected, increasing suction led to higher maximum reinforcement pullout resistance in otherwise identical test specimens.

Results shown in **Figure 8d** indicate that the failure envelopes (showing average normal and shear stresses on the geotextile considering both top and bottom geotextile surfaces) of the Minco silt-geotextile interface can be considered as linear for all moisture content values tested. These results also show that the adhesion intercept of the soil-geotextile interface slightly (but consistently) decreased with increasing soil moisture content. Hatami et al. (2008) and Khoury et al. (2010) have reported similar observations from suction-controlled interface direct shear tests using a woven geotextile and an artificial fine-grained soil. Results in **Figure 8d** also show that the interface friction angle decreased by about 16% as a result of increasing the soil moisture content from OMC-2% to OMC+2%.

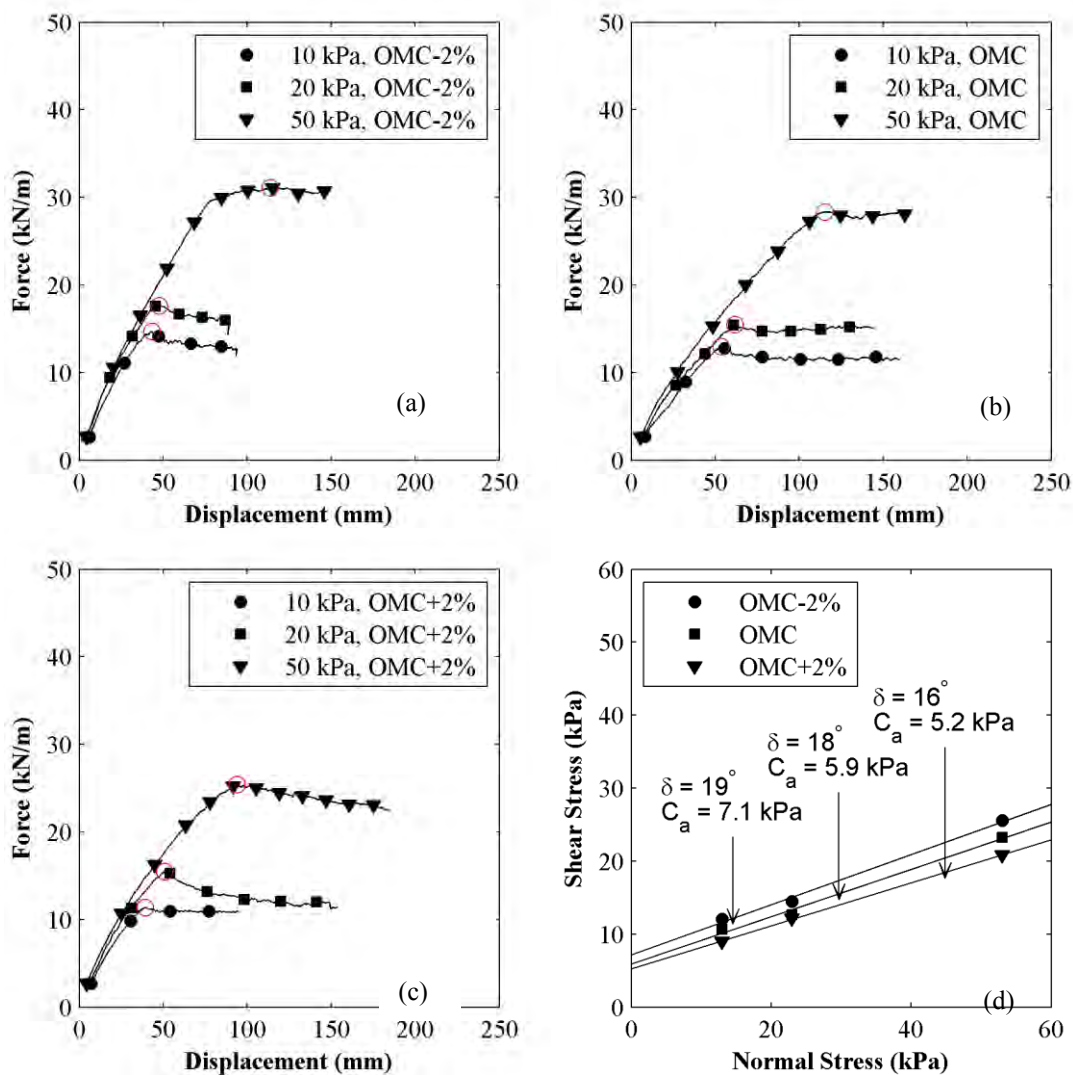


Figure 8 - (a)-(c) Pullout test data in Minco silt at different moisture content values, (d) comparison of failure envelopes for soil-geotextile interface from the test data shown in (a)-(c). C_a and δ refer to the interface friction angle and adhesion intercept, respectively.

A stronger pullout reinforcement performance in fine-grained soils on the dry side of optimum has also been reported in limited previous studies (e.g. Bergado 1991, Farrag 1995). These observations are consistent with increasing shear strength resulting from increasing matric suction as soil moisture content is reduced.

CONCLUSIONS

A series of large-scale pullout tests were carried out on a selected marginal soil (Minco silt) and a geotextile reinforcement fabric. These tests were carried out at three different moisture content values (OMC-2%, OMC and OMC+2%). The objective of this study was to quantify the influence of increasing the soil moisture content on the soil-reinforcement interface strength. The soil moisture content in different pullout test cases included values representing typical construction on dry side of optimum (i.e. OMC-2%) and conceivably greater values that could occur during the service life of reinforced soil slopes and embankments constructed with marginal soils. Based on the results of pullout tests, the following conclusions and observations are made:

Consistently greater maximum reinforcement pullout resistances were obtained at OMC-2% than for OMC and OMC+2% for overburden pressure magnitudes of 10 kPa (209 psf), 20 kPa (418 psf) and 50 kPa (1044 psf). These pressure magnitudes represent overburden pressures acting on higher level reinforcement layers in field structures where reinforcement pullout (as opposed to reinforcement rupture) is typically the dominating failure mechanism.

The soil-reinforcement interface tested at greater moisture content (and hence lower suction) values exhibited reduced shear strength due to both lower adhesion and friction angle values. The reduction in the interface adhesion intercept from OMC-2% to OMC+2% was found to be approximately 25%. Due to the overall low magnitudes of interface adhesion, this difference is believed to be of little practical significance. However, in more cohesive plastic soils it is expected that this difference will be significant. The interface friction angle was found to decrease by about 16% for the same amount of increase in the soil moisture content.

It should be noted that the marginal soil used in this study (Minco silt) was systematically prepared and placed in the pullout test box at different (i.e. molding) moisture content values. Therefore, the clay portion of the soil is expected to be more flocculated on the dry side of the optimum and more dispersed on the wet side of the optimum with inherently different mechanical properties. Consequently, the tests carried out in this study do not precisely simulate wetting of a fine-grained soil compacted and placed on the dry side of the optimum. Nevertheless, these preliminary results indicate that the influence of soil moisture content on the pullout capacity of reinforcement in reinforced soil structures constructed with marginal soils could be significant and requires further investigation. In an on-going study by the writers, a moisture reduction factor is being developed for the internal stability analysis of reinforced soil structures constructed with marginal soils.

REFERENCES:

1. AASHTO (2002). "Standard specifications for highway bridges." 17th ed. *American Association of State Highway and Transportation Officials*, Washington, DC.
2. Abu-Farsakh, M. Y., Almohd, I., and Farrag, K. (2006). "Comparison of field and laboratory tests on geosynthetics in marginal soils." *Transportation research record*. TRR No. 1975: 124-136.
3. ASTM (2009). "Book of Standards." Volume 4.13: Construction: Geosynthetics, American Society for Testing and Materials, ASTM International.
4. Berg, R.R., Christopher, B.R., and Samtani, N.C. (2009). "Design and Construction of Mechanically Stabilized Earth Walls and Reinforced Soil Slopes." Volume II, NHI Courses No. 132042 and 132043, Publication No. FHWA-NHI-10-025, FHWA GEC 011 – Volume II, November 2009.
5. Berg, R.R., and Swan, R.H. (1990). "Investigation into geogrid pullout mechanisms. Performance of reinforced soil structures." *British Geotechnical Society*.
6. Bergado D.T., Cisneros C.B., Sampaco C.L., Alfaro M.C., and Shivashankar R. (1990). "Effect of compaction moisture contents on pullout of steel geogrids with weathered clay backfill." *Geotextiles, Geomembranes and related products*, Den Hoedt (ed.), Balkema, Rotterdam: 803.
7. Chua, K. M., Aspar, W., and De La Rocha, A. (1993). "Simulating failures of geosynthetics-reinforced earth structures under saturated conditions." *Geosynthetics '93* – Vancouver, BC, Canada: 417-430.
8. Farrag, K., 1995. "Evaluation of the effect of moisture content on the interface properties of geosynthetics." *Geosynthetics '95*: 1031-1041.
9. Farrag, K., and Morvant, M. (2004a). "Evaluation of interaction properties of geosynthetics in cohesive soils: LTRC Reinforced Soil Test Wall." *Technical Summary Report 379*, LTRC, July.
10. Farrag, K., and Morvant, M. (2004b). "Evaluation of interaction properties of geosynthetics in cohesive soils: Lab and field pullout tests." *Technical Summary Report 380*, LTRC, July.
11. Hatami, K., Khoury, C.N., and Miller, G.A. (2008). "Suction-Controlled Testing of Soil-Geotextile Interfaces." *GeoAmericas 2008, The First Pan American Geosynthetics Conference & Exhibition*, Cancun, Mexico: 262-271.
12. IFAI (2009). "Geosynthetics Specifier's Guide." Industrial Fabrics Association International.
13. Khoury, C.N., Miller, G.A., and Hatami K., (2010). "Unsaturated Soil-Geotextile Interface Behavior." *Geotextiles and Geomembranes* (in press).

Effect of Sample Preparation Method on Aggregate Shape Characteristics

Dharamveer Singh

Doctoral Candidate,

School of Civil Engineering and Environmental Science, University of Oklahoma
202 West Boyd Street, Room 211, Norman, OK, 73019

Phone: (405) 325-9453, Fax: (405) 325-7508, E-mail: dvsingh@ou.edu

Musharraf Zaman

David Ross Boyd Professor and Aaron Alexander Professor,
Associate Dean for Research, College of Engineering, University of Oklahoma
202 West Boyd Street, Room 107, Norman, OK, 73019

Phone: (405) 325-2626, Fax: (405) 325-7508, E-mail: zaman@ou.edu

Sesh Commuri

Associate Professor,

School of Electrical and Computer Engineering, University of Oklahoma
101 David L. Boren Blvd, Room 1050, Norman, OK, 73019

Phone: (405) 325-4302, Fax: (405) 325-3442, E-mail: scommuri@ou.edu

Disclaimer

Statements and views presented in this paper are strictly those of the author(s), and do not necessarily reflect positions held by their affiliations, the Highway Geology Symposium (HGS), or others acknowledged above. The mention of trade names for commercial products does not imply the approval or endorsement by HGS.

Copyright Notice

Copyright © 2010 Highway Geology Symposium (HGS)

All Rights Reserved. Printed in the United States of America. No part of this publication may be reproduced or copied in any form or by any means – graphic, electronic, or mechanical, including photocopying, taping, or information storage and retrieval systems – without prior written permission of the HGS. This excludes the original author(s)

ABSTRACT

Hot Mix Asphalt (HMA) is a mixture of aggregates and asphalt binder, aggregates contributing to approximately 96 % of the total weight of the HMA mixture. The performance of HMA greatly depends upon the aggregate shape characteristics such as angularity, 2D form, texture and sphericity. These aggregate shape parameters may change while they go through different process of HMA production and sample preparation. Hence, it is important to study these aggregate parameters and quantify their effect on the performance of HMA mixes.

A laboratory study was undertaken to evaluate the effect of sample preparation methods on the aggregate shape characteristics. The loose HMA mix was collected from the Haskell Lemon plant in Norman. A Superpave Gyratory Compactor (SGC) was used to prepare samples of 6 inches diameter and 6.7 inches height at four different target air voids (6 %, 8%, 10%, and 12%). These samples were then cut and cored to get final samples of size 4 inches diameter and 6 inches height as specified in the American Association of State Highway and Transportation Officials (AASHTO) for conducting the performance testing (dynamic modulus, flow number, and flow time) of the HMA mix. Aggregates were retrieved from these samples after burning in the National Center for Asphalt Technology (NCAT) oven. In addition, original aggregate and loose HMA mix aggregate samples were used to compare them with other aggregates retrieved from SGC compacted samples. A total of six different types of aggregate were used in this study: original aggregates, plant mix aggregate, 6% air voids aggregates (AV), 8% AV, 10% AV, and 12% AV. Each aggregate type was divided in two sizes of coarse aggregates: passing a 3/4" sieve-retained a 1/2" sieve (+1/2"), and passing a 3/8" sieve-retained a #4 sieve (+#4). A total of 24 aggregate samples were used to measure aggregate shape characteristics using an Aggregate Imaging System (AIMS).

A statistical method, called Analysis of Variance (ANOVA), was used to compare six types of aggregate shape parameters. It was found both size of coarse aggregates exhibit more sensitivity to changing their shape parameters. The texture and 2D form of coarse aggregate particles changes while they undergo different process of sample preparation and HMA production. No significant change was observed in angularity and sphericity for all types of aggregates. These results are expected to develop the better understanding of HMA mixture behavior in light of aggregate properties pertaining to aggregate shape.

INTRODUCTION

Aggregate degradation can cause particles to lose their shape and texture (1). Degradation of aggregates may occur at plant site as the aggregates are exposed to impact and/or abrasive forces during the production of hot mix asphalt (HMA). Degradation can also occur during the compaction of HMA. Changes in aggregate gradation, aggregate shape characteristics (angularity, shape and texture) during the production and compaction of HMA can lead to differences between mixes used in the field and laboratory compacted specimens (2, 3). Pintner et al. (4) reported that sources of aggregates that have been found to be suitable based on standard mechanical degradation tests (e.g. Los Angeles Abrasion, Washington Degradation, etc.), may produce substantial fines during crushing, handling, and placement. They compared the fines produced in the laboratory and in the field due to handling and placement. It was reported that laboratory tests produced more fines, in general, compared to field.

Lynn et al. (5) evaluated 22 different mixtures during production and construction. It was reported that aggregate degradation result from plant mixing and field compaction activities. The increase in fine content relative to the baseline gradation varied from 0.1 % to 3.5 % for truck sampled material. It was mentioned that volumetric properties were affected by aggregate degradation. In a similar study, Page et al. (6) determined the amount of degradation to a typical north Florida limestone material and the subsequent effects degradation have on air voids. It was found that north Florida limestone aggregates used in their study degrade significantly as they were processed through the HMA plant from stockpile. However, these studies were limited to measurement of fines. The change in aggregate shape characteristics due to degradation was not evaluated in these studies. On the other hand, aggregate degradation can also occur during gyratory compaction of samples which may change the original gradation and shape of aggregates (7). Peterson et al. (8) mentioned that the current gyratory protocol produces specimens with significantly different mechanical properties than those of field cores produced with the same material and compacted to the same level of air voids. Hence, it becomes important to compare aggregate shape characteristics of samples compacted by a gyratory compactor.

The change in aggregate shape characteristics due to degradation during plant and laboratory can influence the performance of a HMA mix. For example, a higher amount of rounded, natural sands and more rounded aggregates will generally result in a lower VMA (9). Rough-textured surfaces, such as those of crushed rocks, result in stronger mixes by providing more friction between aggregate faces. The asphalt binder is thought to create stronger mechanical bonds with rough-textured aggregates than with smooth aggregates (10, 11). Performance of asphalt pavements greatly depend upon the aggregate shape characteristics, namely, angularity, 2D form, texture and sphericity (12-14). Several researchers have conducted laboratory tests to investigate the effect of aggregate shape parameters on the performance of HMA mixes. More angular aggregates, with rough surface texture increase rutting resistances (15-18). Johnson et al. (19) conducted performance testing (dynamic modulus, rut resistance) of HMA on four different asphalt mixes by varying the quantity of fine aggregate angularity (FAA). It was found that dynamic modulus and rut resistance are strongly related to FAA. In a similar study done by Pan et al. (20) reported that surface texture of coarse aggregate particles show the best correlation with the permanent deformation of HMA.

Hence, it is important to evaluate the change in aggregate shape characteristics due to HMA production process and laboratory preparation of sample. An Aggregate Imaging System (AIMS) was used in this study to determine the various shape characteristics, namely, aggregate angularity, texture, 2D Form and sphericity. The present study is expected to develop a better understanding of HMA mixture behavior in light of aggregate shape characteristics.

OBJECTIVES

The main objective of this study was to evaluate the change in aggregate shape characteristics (angularity, shape, texture) of coarse aggregates due to HMA production process and sample preparation in laboratory.

AGGREGATE IMAGING SYSTEM (AIMS)

The AIMS is an automated system that captures images of aggregates at different resolution, field of view, using different lighting schemes. It can be used for the analysis and classification of the shape characteristics of both fine and coarse aggregates in an accurate manner. The classification methodology can be used to evaluate the effects of different processes, such as crushing techniques and blending, on the aggregate shape distribution. It also lends itself to the development of aggregate specifications on the basis of the distribution of shape characteristics (21). Gatchalian et al. (22) used AIMS to measure changes in aggregate characteristics caused by abrasion forces in a micro-Deval apparatus. The AIMS gives detailed information on shape properties of aggregates in a short time (23). Masad et al. (24) indicated that particle geometry of an aggregate can be fully expressed in terms of three independent properties which influence the performance of HMA: shape (form), angularity, and texture (see Figure 1). The definition of different shape characteristics can be found elsewhere (25).

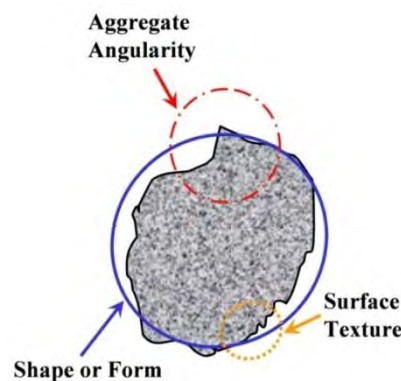


Figure 1 Components of an Aggregate Shape: Shape, Angularity, and Texture (Masad et al. (24))

COLLECTION OF MATERIAL AND SAMPLE PREPARATION

The loose HMA mix, of type S3 64-22, was collected from the production plant in Norman, Oklahoma. The nominal maximum size of aggregate was 19 mm. The aggregates in the collected HMA mix included 1" rock (20%), manufactured sand (44%), asphalt sand (11%) and

recycled asphalt pavement (RAP) (25%). A majority of coarse aggregates was limestone. The original aggregate of each type was also collected from the stockpiles at the plant. The total aggregate was divided into six different groups. The original aggregate containing all types of aggregates was named as “original aggregates (O).” The loose HMA was divided into five different groups. One group was left uncompacted and is called “plant mix” (PM), while the other four groups were used to compact samples at different target air voids: 6 %, 8 %, 10 % and 12 % air voids. These groups are named AV6, AV8, AV10 and AV12, respectively. Furthermore, all six aggregates were divided into two different sizes: one passing a 3/4” sieve and retained on a 1/2” sieve (called +1/2”) and the other passing a 3/8” sieve and retained on a #4 sieve (called +#4). Table 1 a summary of the test matrix.

Table 1 AIMS Test Matrix

Type of Aggregate	Aggregate Sizes	
	Coarse Aggregates	
	+ (1/2")	+ (#4)
O	X	X
PM	X	X
AV6	X	X
AV8	X	X
AV10	X	X
AV12	X	X

Different levels of target air voids were selected to simulate the degradation of aggregates in the field. It was reported by Lynn et al. (5) that degradation in the SGC correlated well with degradation associated with the compaction of the HMA mixture in the field. Based on this assumption samples were compacted at different air voids (6 %, 8 %, 10%, and 12 %) to simulate the field conditions. The weight of the loose HMA sample to be compacted in the SGC mold depends upon the target air voids levels. For compacting a given dimension of a sample, the weight of the loose mix increases as target air voids decreases. The gyratory compactor actuators exert forces on the specimen during compaction in order to apply vertical pressure and angle of gyration. Particles are pushed more when weight is increased. It is believed that such method may change the aggregate shape characteristics. Three samples were compacted for each target air voids levels. A total of 12 samples were compacted. Initially 6” diameter x 6.7” height samples were compacted using SGC. These samples were cut and cored to get final samples of size 4” diameter and 6” height. The sample size 4” diameter x 6” height is recommended by the American Association of State Highway and Transportation Officials (AASHTO) for conducting the performance testing (dynamic modulus, flow number, and flow time) of the HMA mix.

AIMS TESTING ON AGGREGATES

Aggregates were processed before conducting the AIMS testing. The compacted samples at all different air voids, and the plant mix loose HMA were burnt in the NCAT oven to retrieve the aggregates. All aggregates (O, PM, AV6, AV8, AV10, and AV12) were washed and allowed to dry for 24 hours at 110°C temperature. After drying, each aggregate type was separated into two different sizes of coarse aggregates particles: +1/2” and +#4. Each coarse aggregate type

was separated into two random samples of 56 aggregates. Pine's AIMS was used to evaluate the shape, texture, angularity, and sphericity of coarse aggregates. A total of 24 samples were tested in the AIMS. The AIMS was set up and operated, as per the specifications provided by Masad et al. (24). The 0.25x objective lens was installed and the camera was set to coarse position. Fifty six particles were then placed on the AIMS testing grid. The AIMS completes testing on coarse aggregates in two phases. The first phase uses only back light, and it measures the 2D form and angularity. The second phase uses the top light to obtain the measurements for sphericity and texture. After both of these phases are completed for a sample, the AIMS's software analyzes the images.

The mean, median, and standard deviation for all shape characteristics (gradient angularity, radius angularity, 2D form, texture, and sphericity) for all types of coarse aggregates are shown in Table 2. The classification of each type of aggregates was done based on cluster analysis developed by Masad et al. (25), shown in Table 3. The texture classifies aggregates in five different groups: polished, smooth, low roughness, medium roughness, and high roughness. These categories are based upon the texture index of each aggregate as shown in Table 3. Likewise, all other shape characteristics were divided into different groups.

Table 2 Descriptive Statistics of Shape Parameters for Coarse Aggregates

Type	Gradient Angularity Index						Radius Angularity Index					
	+1/2"			#4C			+1/2"			#4C		
	Mean	Stdev	Median	Mean	Stdev	Median	Mean	Stdev	Median	Mean	Stdev	Median
O	3319	1234	2941	2883	705	2812	11.11	3.69	11.11	11.41	3.33	11.00
PM	2703	670	2677	2892	1331	2693	10.24	3.34	9.91	10.13	3.03	9.57
AV6	3156	1269	2884	3300	1485	2944	10.86	3.36	10.79	10.95	3.75	10.48
AV8	2984	1367	2756	3341	1643	2856	10.53	3.70	10.13	10.74	3.36	10.68
AV10	2770	928	2657	3351	1601	2927	10.52	3.58	10.08	11.13	3.71	10.70
AV12	2852	1004	2663	3355	1557	2898	10.43	3.53	9.58	11.19	3.58	10.55

Type	2D Form						Texture					
	+1/2"			#4C			+1/2"			#4C		
	Mean	Stdev	Median	Mean	Stdev	Median	Mean	Stdev	Median	Mean	Stdev	Median
O	7.72	2.31	7.53	7.97	1.81	7.71	159	67	148	103	46	94
PM	7.03	1.56	6.60	6.97	1.48	6.68	149	49	148	89	45	88
AV6	7.52	2.10	7.18	7.84	2.37	7.50	178	67	180	124	57	124
AV8	7.44	2.09	7.08	8.09	2.19	7.84	199	74	193	126	65	122
AV10	7.39	2.25	7.25	8.06	2.20	7.70	191	61	189	132	70	122
AV12	7.38	1.88	7.16	8.23	2.62	7.54	184	71	185	123	59	115

Type	Sphericity					
	+1/2"			#4C		
	Mean	Stdev	Median	Mean	Stdev	Median
O	0.72	0.11	0.71	0.66	0.09	0.65
PM	0.72	0.08	0.74	0.68	0.11	0.69
AV6	0.72	0.11	0.72	0.68	0.11	0.69
AV8	0.71	0.09	0.71	0.68	0.11	0.69
AV10	0.73	0.10	0.74	0.66	0.13	0.66
AV12	0.71	0.10	0.72	0.68	0.11	0.68

Table 3 Classification of Aggregates Shapes

Aggregate Physical Property	Range and Description				
	High Roughness	Moderate Roughness	Low Roughness	Smooth	Polished
Texture	>460	350-460	275-350	165-275	<165
Angularity- Gradient Method	Angular >5400	Sub-Angular 4000-5400	Sub-Rounded 2100-4000	Rounded <2100	
Angularity-Radius Method	High Angularity >16	Angular 10-16	Sub- Angular 7-10	Sub-Rounded 5-7	Rounded 0-5
Sphericity	High Sphericity >0.8	Moderate Sphericity 0.7-0.8	Low Sphericity 0.6-0.7	Flat/Elongated <0.6	
2D Form	Elongated >10.5	Semi-Elongated 8-10.5	Semi-Circular 6.5-8	Circular <6.5	

RESULTS AND DISCUSSION

A statistical method, called ANOVA, was conducted using SPSS Base 9.0 statistical software. The null hypothesis for this analysis was that the difference in the mean of aggregate shape parameters for all aggregate types was equal to zero ($H_0 = \mu_O = \mu_{PM} = \mu_{AV5} = \mu_{AV7} = \mu_{AV9} = \mu_{AV12}$). The p-value of <0.000 indicates that the null hypothesis was rejected and the means of the data sets are not statistically equal. Table 4 shows the results of ANOVA.

Table 4 ANOVA Test Results

Type	Coarse Aggregates					
	+1/2"			+#4		
	F-Value	p value	Significant	F-Value	p value	Significant
Gradient Angularity	1.217	0.300	No	1.300	0.262	No
Radius Angularity	0.819	0.536	No	1.826	0.106	No
Sphericity	1.674	0.139	No	1.305	0.260	No
Texture	8.312	<0.000	Yes	12.464	<0.000	Yes
2D Form	3.092	0.009	Yes	7.423	<0.000	Yes

Effect on Angularity of Coarse Aggregates

The p-value for gradient, and radius angularity for +1/2" and + #4 sizes of coarse aggregates was observed >0.05. This indicates no statistically significant difference in angularity for different types of aggregates, thus sample preparation method does not influence the angularity significantly. The mean of gradient angularity and radius angularity for all types of aggregates ranged between 2100-4000, and 10-16, respectively, which indicates that all materials are in angular range. Graphs were plotted between percentage of particles and types of aggregates. Figure 2 and Figure 3 show plots for gradient angularity for +1/2" and + #4 sizes of coarse aggregates, respectively. It can be seen from Figure 2 and Figure 3 that percentage of

rounded particles are higher in all types of aggregates (PM, AV6, AV8, AV10, and AV12) compared to original aggregates (O). This shows that plant production process and laboratory sample preparation method increase rounded particles; however, the increase in rounded particles does not change angularity significantly because of the larger range of angularity (Table 3).

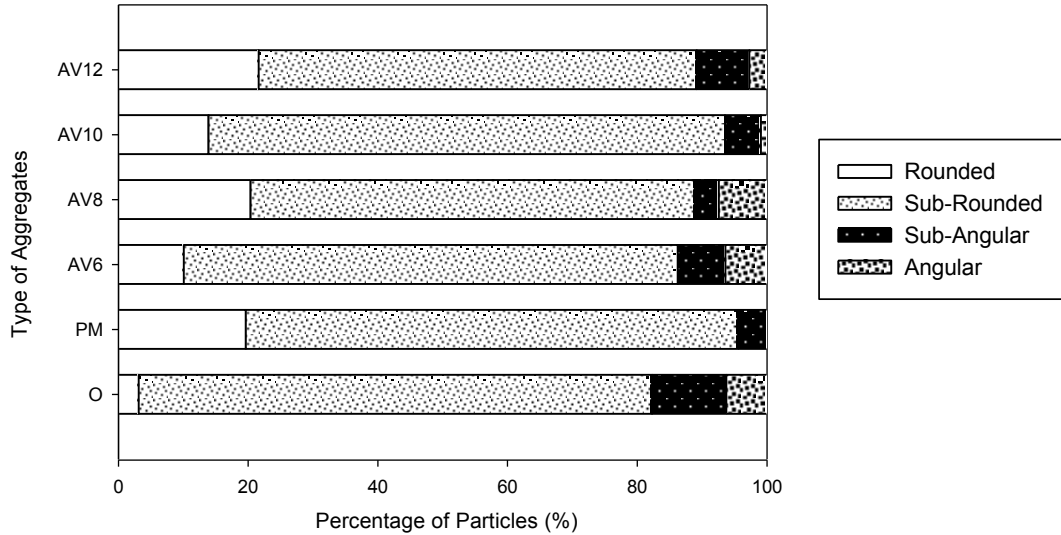


Figure 2 Percentage of Particles for Gradient Angularity for +1/2” Coarse Aggregates

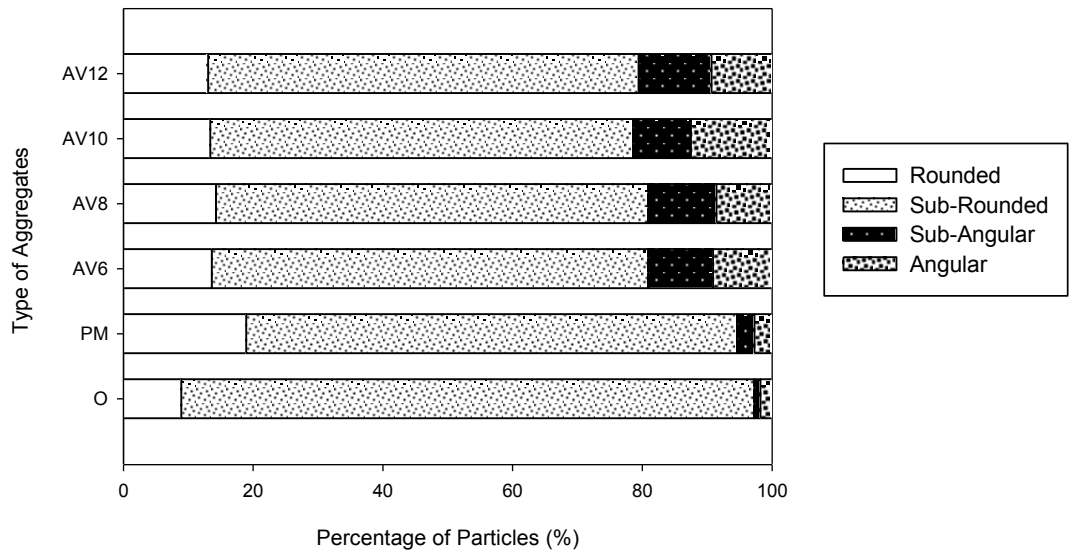


Figure 3 Percentage of Particles for Gradient Angularity for + #4 Coarse Aggregates

Effect on Texture of Coarse Aggregates

Texture showed a significant difference for both sizes of coarse aggregates (+1/2” and + #4), with p-value <0.000 (Table 4). It indicates that texture is different for all types of

aggregates. To further evaluate the difference in texture among aggregates types, a multi-comparison test was conducted using the Games Howell Method. The multi-comparison test is useful in identifying groups of aggregates where difference in shape parameters is significant.

A statistically significant difference was observed in texture between O aggregates and AV6, AV8, AV10, and AV12 aggregates, a similar trend was observed for PM aggregates. The O and PM aggregates did not show any significant difference. It was observed that laboratory preparation method increases the texture of coarse aggregates particles. For both sizes of coarse aggregates particles (+1/2" and +#4), the mean of texture increased from 159 to 200, and 103 to 132, respectively, as samples undergo different preparation method.

To further understand the reason for increase in texture for laboratory processed aggregates, graphs were plotted between percentage of particles and all types of aggregates for +1/2" and +#4 sizes of coarse aggregates as shown in Figure 4 and Figure 5. Figure 4 shows the graph for +1/2" size of coarse aggregates, while Figure 5 is for +#4 size of coarse aggregates. It can be seen from Figure 4 and Figure 5, that distribution of particles is almost the same for O and PM aggregates. The percentage of polished particles decreases during laboratory process. All other aggregates compacted at 6 %, 8 %, 10 %, and 12 % target air voids levels were observed to have less percentage of polished particles compared to O and PM aggregates. Due to smaller number of polished particles and an increased number of rough particles the texture of coarse aggregates particles increased. With the increased texture the performance of laboratory compacted samples can be significantly different from field compacted hot mix asphalt. It is recommended that proper care should be taken while comparing the laboratory and field sample performance.

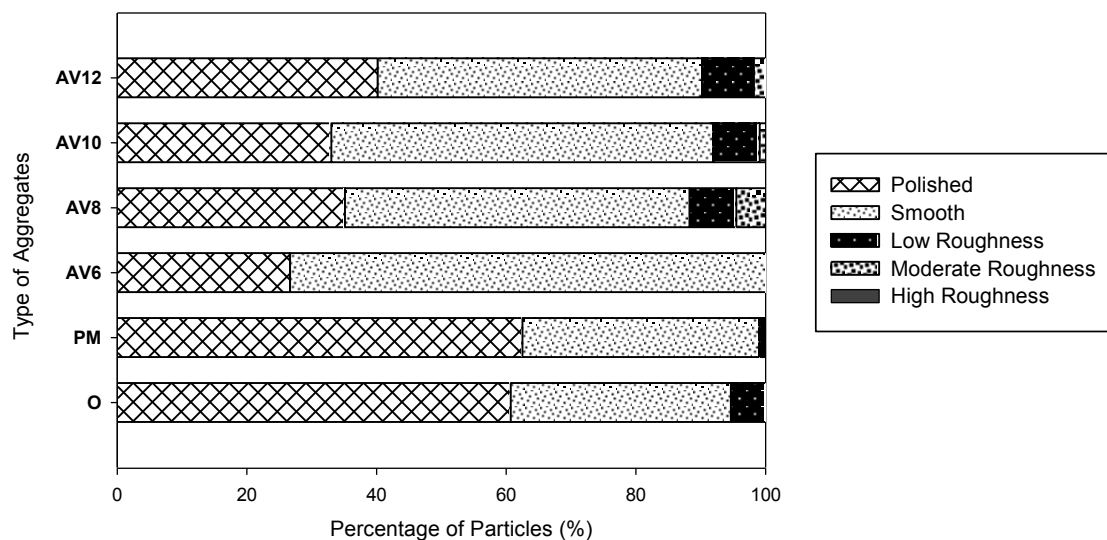


Figure 4 Percentage of Particles for Texture for +1/2" Coarse Aggregates

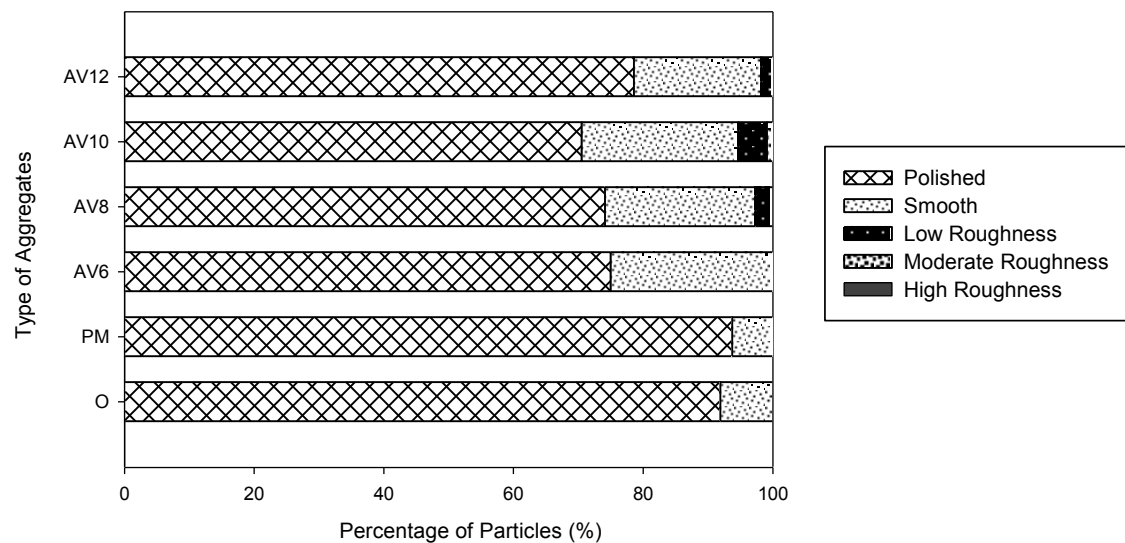


Figure 5 Percentage of Particles for Texture for + #4 Coarse Aggregates

Effect on 2D Form of Coarse Aggregates

For both sizes of coarse aggregates (+1/2" and + #4), the 2D form showed a significant difference with p-value <0.000 (Table 4). It indicates that the 2D form is different for all types of aggregates. To further evaluate the difference in 2D form among aggregates types, a multi-comparison test was conducted using the Games Howell Method.

A statistically significant difference was observed between O and PM aggregates. The median value of the 2D form for original aggregates was noticed 7.53; it decreased to 6.60 for plant mix aggregates. It indicates that original aggregates were more elongated compared to plant mix aggregates that might lose their form during the production process. No statistical significant difference was observed among different types of aggregates compacted at different air voids levels (AV6, AV8, AV10, and AV12).

In order to understand the change in the 2D form for PM coarse aggregates particles, graphs were plotted between percentage of particles and types of aggregates for both sizes of coarse aggregate as shown in Figure 6 and Figure 7. Figure 6 shows the graph for +1/2" size of coarse aggregates, while Figure 7 depicts distribution for + #4 size of coarse aggregates. It can be seen from Figure 6 and Figure 7 that distribution of particles is almost the same for O and different target air voids particles (AV6, AV8, AV10, and AV12). However, the particles distribution is different for O and PM aggregates. The percentage of circular particles increased in PM aggregates, that demonstrates that particles go under rolling, and degradation while production at plant site. However, the percentage of circular particles reduced when samples are prepared in the laboratory. Because of the higher number of circular particles and the lower number of semi elongated and elongated particles the 2D form of coarse aggregates particles decreases for PM aggregates. Round particles have the potential to fit very densely together because the smoothness of the surface and the lack of angular edges, which together reduce the

internal friction. The decrease in internal friction and the ability of uncrushed aggregates to compact more easily into a dense arrangement reduces void space, which ultimately leads to a reduction in VMA.

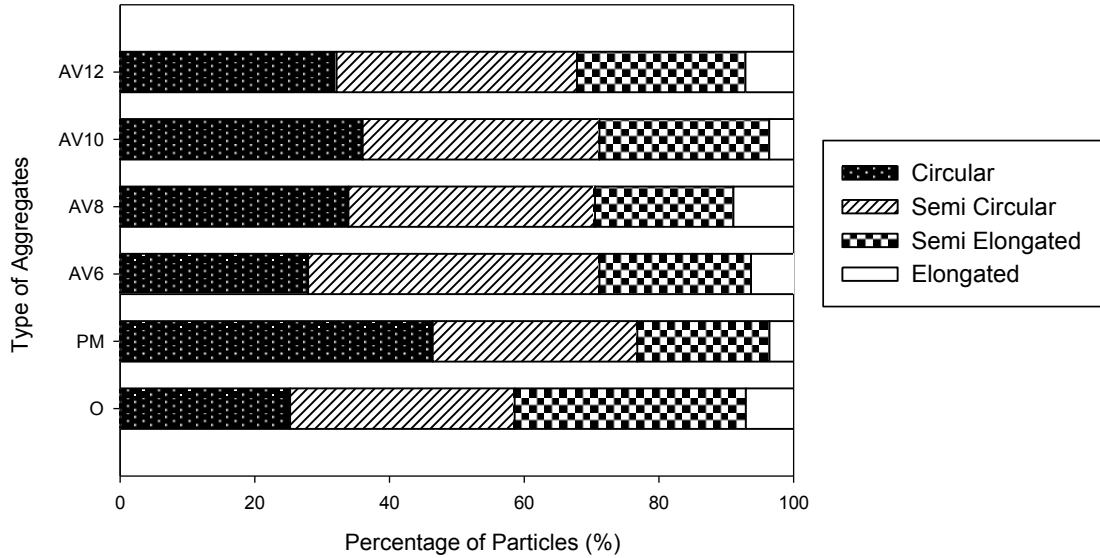


Figure 6 Percentage of Particles for 2D Form for 1/2" Coarse Aggregates

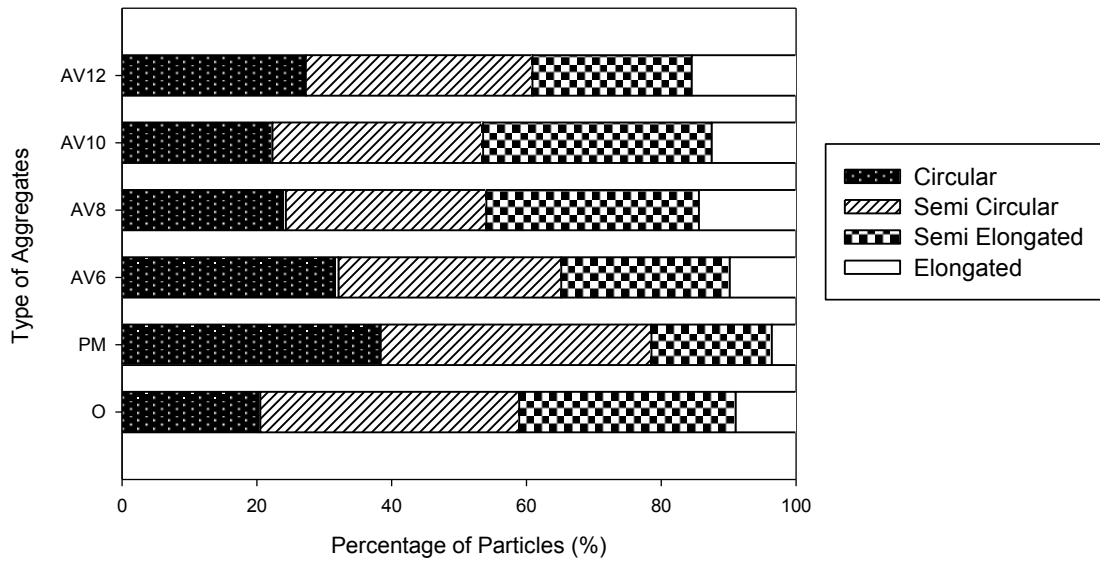


Figure 7 Percentage of Particles for 2D Form for #4 Coarse Aggregates

Effect on Sphericity of Coarse Aggregates

The sphericity value gives a good indication of the proportions of a particle's dimensions. The chart shown in Figure 8 and Figure 9 were plotted to distinguish among flat, elongated, and flat and elongated particles. Superimposed on this chart are the 3:1 and 5:1 limits for the ratio of longest dimension to the shortest dimension. The plots were generated for all types of aggregates for +1/2" and +#4 sizes. All aggregates pass the 5:1 Superpave requirement (both had less than 10% of particles with a dimensional ratio less than 5:1), but they had different distributions in terms of flat and elongated particles as shown in Figure 8 and Figure 9. This type of analysis in Figure 8 and Figure 9 reveal valuable information about the distribution that would not have been obtained if the aggregates was classified based on the 5:1 ratio only. Such details on the distribution are needed to understand the influence of shape characteristics on asphalt mix performance.

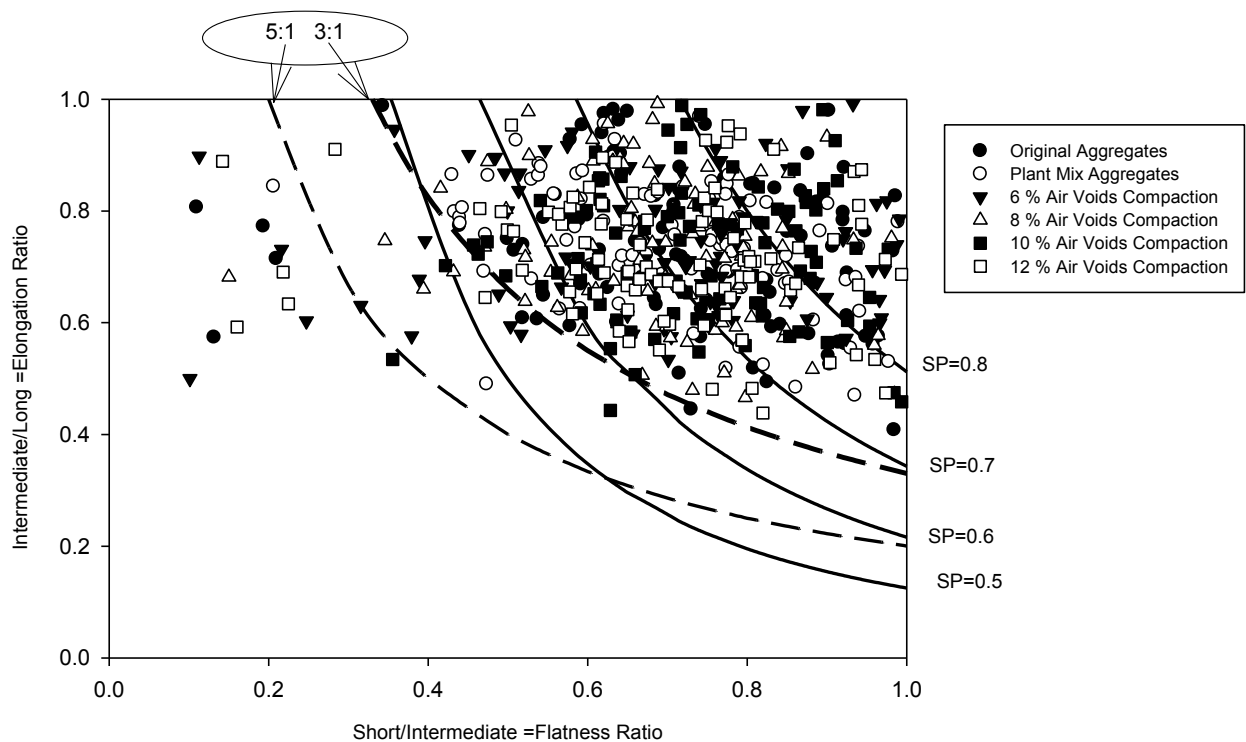


Figure 8 Sphericity Graph for +1/2" Coarse Aggregates

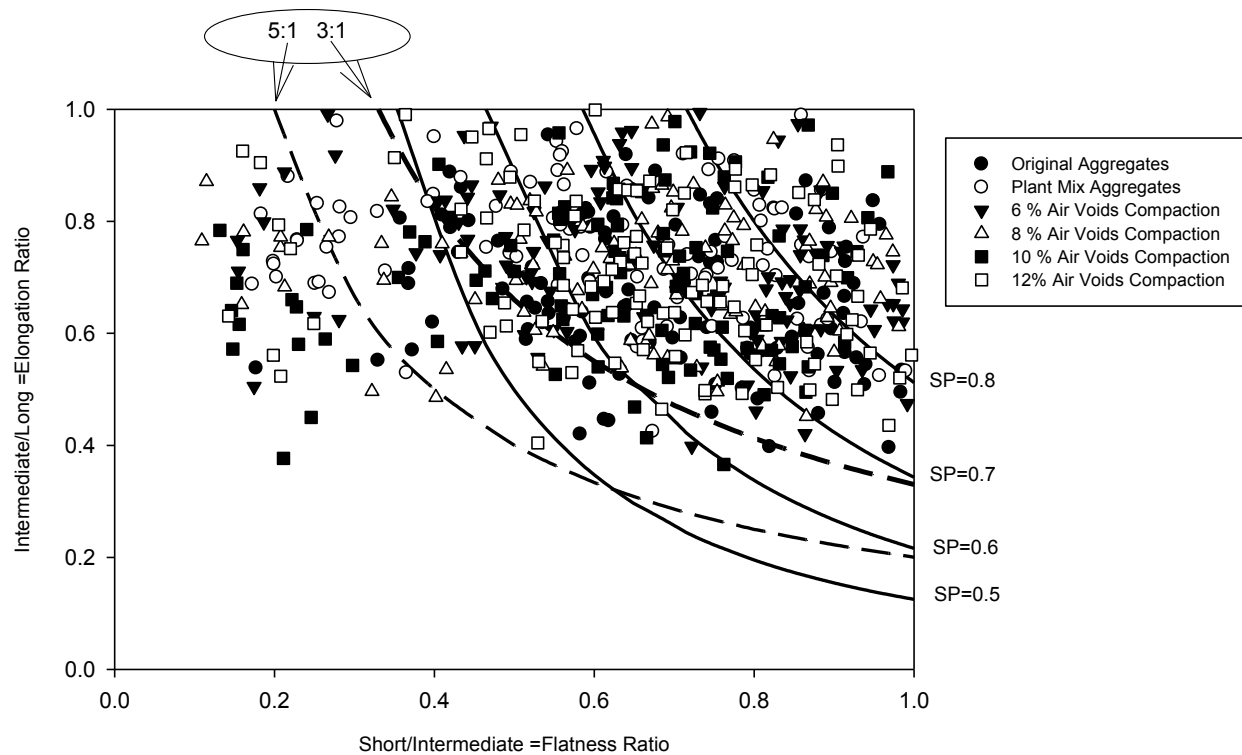


Figure 9 Sphericity Graph for + #4 Coarse Aggregates

CONCLUSIONS

A laboratory study was undertaken to evaluate the effects of sample preparation method on the aggregate shape characteristics. A total of six different types of aggregate were used in this study: original aggregates, plant mix aggregate, 6% air voids aggregates (AV), 8% AV, 10% AV, and 12% AV. The SGC was used to prepare samples at four different target air voids. Aggregates were retrieved from these samples after burning in a NCAT oven. The coarse aggregates were categorized in two groups; one passing a 3/4" sieve – retained a 1/2" sieve (+1/2") and another passing a 3/8" sieve – retained a #4 sieve (#4). A total of 24 aggregate samples were used to measure aggregate shape characteristics using the AIMS. A statistical method, called ANOVA, was used to compare six types of aggregate shape parameters. It was observed that laboratory preparation method increases the texture of coarse aggregates particles, when they undergo different compaction and preparation method. Furthermore, original aggregates were more elongated compared to plant mix aggregates; because plant mix aggregates might lose their form during the production process. No significant change was observed in angularity and sphericity for all types of aggregates. All aggregates pass the 5:1 Superpave requirement (both had less than 10% of particles with a dimensional ratio less than 5:1), but they had different distributions in terms of flat and elongated particles.

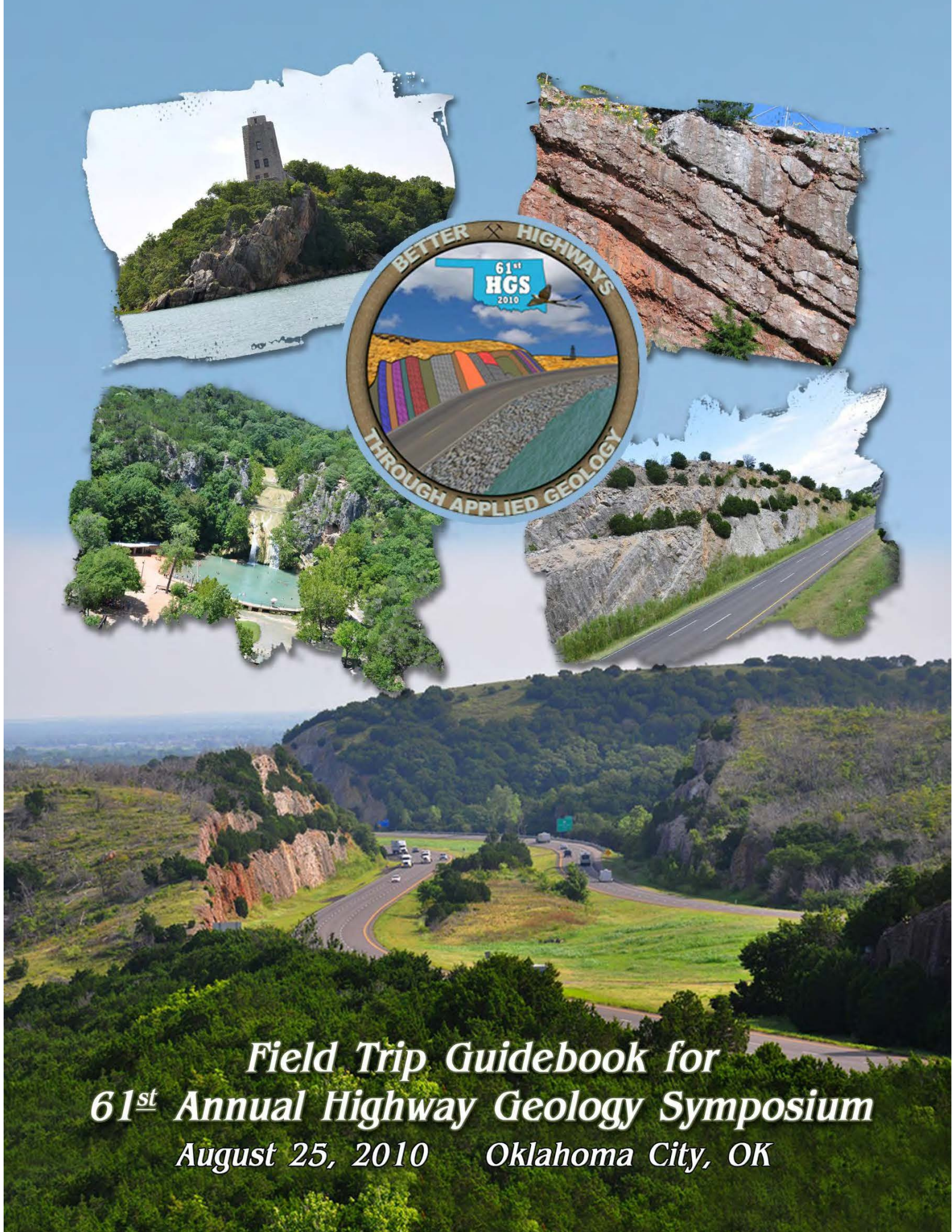
ACKNOWLEDGMENTS

The authors wish to express their sincere gratitude to Haskell Lemon Construction Company, Oklahoma City, Oklahoma for their assistance during every phase of this project. The financial support of Volvo Construction Equipment Company, Shippensburg, PA and the Oklahoma Transportation Center, Oklahoma City, OK are also greatly appreciated.

REFERENCES

1. Chadbourn, B. A., E. L. Skok, Jr., D. E. Newcomb, B. L. Crow, and S. Spindler. Effect of Voids in Mineral Aggregate on Hot-Mix Asphalt Pavements. Report MN/RC-2000-13. Minnesota Department of Transportation, St. Paul, 1999.
2. Mahmoud, E., and E. Masad. Experimental Methods for the Evaluation of Aggregate Resistance to Polishing, Abrasion, and Breakage. *ASCE Journal of Materials in Civil Engineering*, vol. 19, No. 11, 2007, pp.977-985.
3. Wu, Y., Parker, F., and P. Kandhal. Aggregate toughness/ abrasion resistance and durability/soundness tests related to asphalt concrete performance in pavements. *Transportation Research Record*, No. 1638, Washington, D.C., 1998, pp. 85–93.
4. Pintner, R. M., Vinson, T.S., and E.G. Johnson. Nature of fines produced In aggregate processing. *ASCE Journal of Cold Regions Engineering*, vol. 1, No. 1, 1987, pp. 10-21
5. Lynn, T., James, R.S., Wu, P.Y., and D.M. Jared. Effect of Aggregate Degradation on Volumetric Properties of Georgia’s Hot-Mix Asphalt. *Transportation Research Record*, No. 1998, Washington, D.C., 2007, pp. 123-131.
6. Page, G. C., J. A. Musselman, and D. C. Romano. Effects of Aggregate Degradation on Air Voids of Structural Asphalt Mixture in Florida. *Transportation Research Record*, No. 1583, Washington, D.C., 1997, pp. 19–27.
7. Collins, R., Watson, D., Johnson, A., and Y.P. Wu. Effect of Aggregate Degradation on Specimens Compacted by Superpave Gyrotory Compactor. *Transportation Research Record*, No. 1590, Washington, D.C., 1997, pp. 1-9.
8. Peterson, R.L, Mahboub, K.C., Anderson, R.M., Masad, E., and L. Tashman. Superpave® Laboratory Compaction Versus Field Compaction. *Transportation Research Record*, No. 1832, Washington, D.C., 2003, pp.201-208.
9. Aschenbrener, T. and C. MacKean. Factors that Affect the Voids in the Mineral Aggregate of Hot-Mix Asphalt. *Transportation Research Record*, No. 1469, Washington, DC, 1994, pp. 1-8.
10. Ahlrich, R.C. Influence of Aggregate Properties on Performance of Heavy-Duty Hot-Mix Asphalt Pavements. *Transportation Research Record*, No. 1547, 1996, pp. 7-14.
11. Roberts, F.L., Kandhal, P.S., Brown, E.R., Lee, D., and T.W. Kennedy. Hot Mix Asphalt Materials, Mixture Design and Construction, 2nd Edition. NAPA Education Foundation, Lanham, Maryland, 1996.
12. Wang, L., D. Stephen Lane, Yang Lu, and C. Druta. Portable Image Analysis System for Characterizing Aggregate Morphology. Report No. FHWA/VTRC 08-CR11, Virginia Transportation Research Council, 2008.
13. Atkins, N. H. Highway Materials, Soils, and Concretes. Prentice Hall, Upper Saddle River, NJ, 2003, pp. 121-142.

14. Fletcher, T., C. Chandan, E. Masad, and K. Sivakumar. Measurement of Aggregate Texture and its Influence on Hot Mix Asphalt Permanent Deformation. *ASTM Journal of Testing and Evaluation*, Vol. 30, No. 6, 2002, pp. 1-8.
15. Kandhal, P.S., and R.R.B. Mallick. Effect of Mix Gradation on Rutting Potential of Dense-Graded Asphalt Mixtures. *Transportation Research Record*, No. 1767, Washington, D.C., 2001, pp. 146-151.
16. Sousa J.B., Craus J., and C.L. Monismith. Summary Report on Permanent Deformation in Asphalt Concrete. Strategic Highways Research Program IR-91-104, 1991.
17. Brown, R.R., and C.E. Bassett. Effects of Maximum Aggregate Size on Rutting Potential and Other Properties of Asphalt –Aggregate Mixtures. *Transportation Research Record*, No. 1259, Washington, D.C., 1990, pp. 107-119.
18. Button, J.W., Perdomo, D., and R.L. Lytton. Influence of Aggregate on Rutting in Asphalt Concrete Pavements. *Transportation Research Record*, No. 1259, Washington, D.C., 1990, pp.141-152.
19. Johnson, E., Li, X., Zofka, A., and Marasteanu, M.O., and T.R. Clyne. Investigation of Superpave Fine Aggregate Angularity Criterion for Asphalt Concrete. *Transportation Research Record*, No. 1998, Washington, D.C., 2007, pp.75-81.
20. Pan, T., Tutumluer, E., and S.H. Carpenter. Effect of Coarse Aggregate Morphology on Permanent Deformation Behavior of Hot Mix Asphalt. *ASCE Journal of Transportation Engineering*, Vol. 132, No. 7, 2006, pp. 580-589.
21. Al-Rousan, T., Masad, E., Myers, L., and C. Speigelman. New Methodology for Shape Classification of Aggregates. *Transportation Research Record*, No. 1913, Washington, D.C., 2005, pp.11-23.
22. Gatchalian, D., Masad, E., Chowdhury, A., and D. Little. Characterization of Aggregate Resistance to Degradation in Stone Matrix Asphalt Mixtures. *Transportation Research Record*, No. 1962, Washington, D.C., 2006, pp. 55-63.
23. Flecher, T., Chandan, C., Masad, E., and K. Sivakumar. Aggregate Imaging System for Characterizing the Shape of Fine and Coarse Aggregates. *Transportation Research Record*, No. 1832, Washington, D.C., 2003, pp. 67-77.
24. Masad, E., D. N. Little, L. Tashman, S. Saadeh, T. Al-Rousan, and R. Sukhwani. Evaluation of Aggregate Characteristics Affecting HMA Concrete Performance. Research Report ICAR 203-1, The Aggregate Foundation of Technology, Research, and Education, Arlington, VA, 2003.
25. Masad, E.A. Aggregate Imaging System (AIMS) Basics and Applications. Report No.FHWA/TX-05/5-1707-01-1. Texas Transportation Institute, The Texas A&M University System College Station, Texas, 2005.
26. Masad, E., Olcott, D., White, T., and L. Tashman. Correlation of Fine Aggregate Imaging Shape Indices with Asphalt Mixture Performance,” *Transportation Research Record*, No. 1757, Washington, D.C., 2001, pp. 148–156.



*Field Trip Guidebook for
61st Annual Highway Geology Symposium
August 25, 2010 Oklahoma City, OK*



State Crystal - Hourglass Selenite
(Source: Wikipedia)



State Rock – Barite Rose
(Source: Wikipedia)

Field Trip Guidebook for the 61ST Annual Highway Geology Symposium

August 25, 2010
Oklahoma City, Oklahoma

Field Trip Organizing Committee:

Kenneth Luza, Ph.D., Oklahoma Geological Survey
Stanley T. Krukowski, Ph.D., Oklahoma Geological Survey
Jim Nevels, P.E., Ph.D., Geotechnical Consultant
Scott Cosby, Oklahoma Department of Transportation
Vincent Reidenbach, P.E., Ph.D., Oklahoma Department of Transportation
Jeff Dean, P.E., Oklahoma Department of Transportation

Field Trip Speakers:

Kenneth Luza, Ph.D., Oklahoma Geological Survey
Stanley T. Krukowski, Ph.D., Oklahoma Geological Survey
Jim Nevels, P.E., Ph.D., Geotechnical Consultant
Kenneth S. Johnson, Ph.D., Oklahoma Geological Survey
Jeff Dean, P.E., Oklahoma Department of Transportation

Special Thanks to Bob Rose, ODOT Division Seven Engineer and his crew for their assistance provided for the Symposium Field Trip.

Cover Photos:

Clockwise from Top Left; Tucker Tower at Lake Murray;
Collings Ranch Conglomerate exposed along I-35 off-ramp to scenic overlook;
I-35 Cut looking to the north; Turner Falls.
Bottom Photo: I-35 through the Arbuckles,

Inside Back Cover:

Oklahoma Geological Provinces and Trip Map

Back Cover:

Phillips 66 oil well on south side of State Capitol

Guidebook Layout and Design:

Oklahoma Geological Survey
Mallory Malwick
Jeff Dean, P.E., Oklahoma Department of Transportation
Scott Cosby, Oklahoma Department of Transportation

Symposium Hosts

Oklahoma Department of Transportation



Oklahoma Geological Survey



Field trip Sponsors



Box Breakfast



Lunch



Beverages

Table of Contents

Field Trip Objectives	1
Oklahoma Geology Introduction	3
Oklahoma Geological Survey	
Road Log	15
Oklahoma Geological Survey / Oklahoma Department of Transportation	
Arbuckle Mountains Geology	26
Oklahoma Geological Survey	
I-35 Construction through the Major Arbuckle Mountain Cut	34
Oklahoma Department of Transportation	
I-35 Construction through the Ardmore Basin	37
Oklahoma Department of Transportation	
Lake Murray State Park and Regional Geology	54
Oklahoma Geological Survey	
Tucker Tower and Local Geology	59
Oklahoma Geological Survey	
Bridge Construction in Karst Terrain	63
Oklahoma Geological Survey / Oklahoma Department of Transportation	
Turner Falls Overlook	68
Oklahoma Geological Survey	

Field Trip Objectives

Welcome to Oklahoma; “Native America”, for the 61st Annual Highway Geology Symposium (HGS) being held at the Skirvin Hilton in Oklahoma City. Oklahoma City is an important livestock market center, and home to several prominent energy companies. Founded during the Land Run of 1889, the population of Oklahoma City swelled to more than 10,000 overnight. While here we hope you soak in the culture of Oklahoma’s capital, and especially the **Bricktown** area of Oklahoma City with its many amenities.

The full day field trip will visit several stops within the Arbuckles region of south central Oklahoma. The stops will highlight the complex geology of the Arbuckle Mountains which include steeply dipping and vertical layers of limestone, dolomite and shale. Highway geology will focus on the engineering challenges faced during the design and construction of a 150 ft cut through the Arbuckles as part of the I-35 alignment through this section of the state. These challenges include pre-splitting tilted carbonate rocks, conglomerates, sinkholes, faults and joint systems as well as highly plastic clay shales. Additional locations will include Lunch at Lake Murray, and a mid afternoon geology tour of the Turner Falls area.

We hope you have a relaxed and informative day in the spectacular geological diversity of south central Oklahoma.

OKLAHOMA GEOLOGY INTRODUCTION

Kenneth V. Luza, Stanley T. Krukowski, and Kenneth S. Johnson
Oklahoma Geological Survey

REGIONAL GEOLOGY

The soils, topography, and vegetation of Oklahoma depend on its local geology and climate. The highest elevation (4,973 ft) in Oklahoma is on Black Mesa in the northwest corner of the Panhandle; the lowest elevation (287 ft) is in the southeast corner of the State. Mean annual precipitation varies from less than 20 in. in the Panhandle to over 55 in. in the Ouachita Mountains. The distribution of vegetation in Oklahoma is very diverse: piñon pine–juniper is found in the northwest; central Oklahoma is a mosaic of forest, woodland, and grassland vegetation; and cypress bottoms occur in sloughs and back swamps in southeast Oklahoma.

Oklahoma is a region of complex geology where several major sedimentary basins occur near mountain ranges and uplifts (Fig. 1). About 99% of all outcrops are sedimentary. Remaining outcrops are (1) igneous rocks, mainly in the Wichita and Arbuckle Mountains; (2) metamorphic rocks in the eastern Arbuckles; and (3) mildly metamorphosed rocks in the core of the Ouachita Mountains. Rocks formed during every geologic period occur in Oklahoma. About 46% of Oklahoma has Permian rocks exposed at the surface. Other extensive outcrops are Pennsylvanian (about 25%), Tertiary (11%), Cretaceous (7%), Mississippian (6%), Ordovician (1%), and Cambrian (1%); Precambrian, Silurian, Devonian, Triassic, and Jurassic rocks each are exposed in less than 1% of Oklahoma (Fig. 2).

Upper Cambrian through Mississippian rocks in Oklahoma are represented by marine sediments deposited in broad epicontinental seas. This basin, which extended across almost all parts of the southern Midcontinent, was a shelf-like area that received thick and extensive sediments of marine carbonates interbedded with thinner marine shales and sandstones. The sedimentary units thicken into protobasins such as the Anadarko, Ardmore, Arkoma, and other basins. Sediments were deposited later upon and across the present-day major uplifts. Strata subsequently were stripped away during Pennsylvanian uplift and erosion.

Orogenic activity during the Pennsylvanian Period sharply uplifted crustal blocks, subdividing the broad and shallow-marine protobasins into a series of well-defined basins. Orogenic activity was limited to folding, faulting, and uplift. Pennsylvanian orogenic pulses caused, or contributed to, (1) folding and thrusting of the Ouachita fold belt; (2) raising of the Wichita, Criner, Arbuckle, and Nemaha Uplifts; and (3) pronounced down-warping of the Anadarko, Ardmore, Arkoma, and Marietta Basins (Fig. 1).

Pennsylvanian strata in Oklahoma consist of sequences of marine and non-marine shale, sandstone, conglomerate, and limestone that thicken markedly into rapidly subsiding basins. Thick wedges of terrigenous clastic sediments were derived from nearby uplifts, and thinner carbonate sequences were deposited on shallow-water shelf areas distal to the uplifts. Successively younger Pennsylvanian units commonly overlap older units at the margins of the

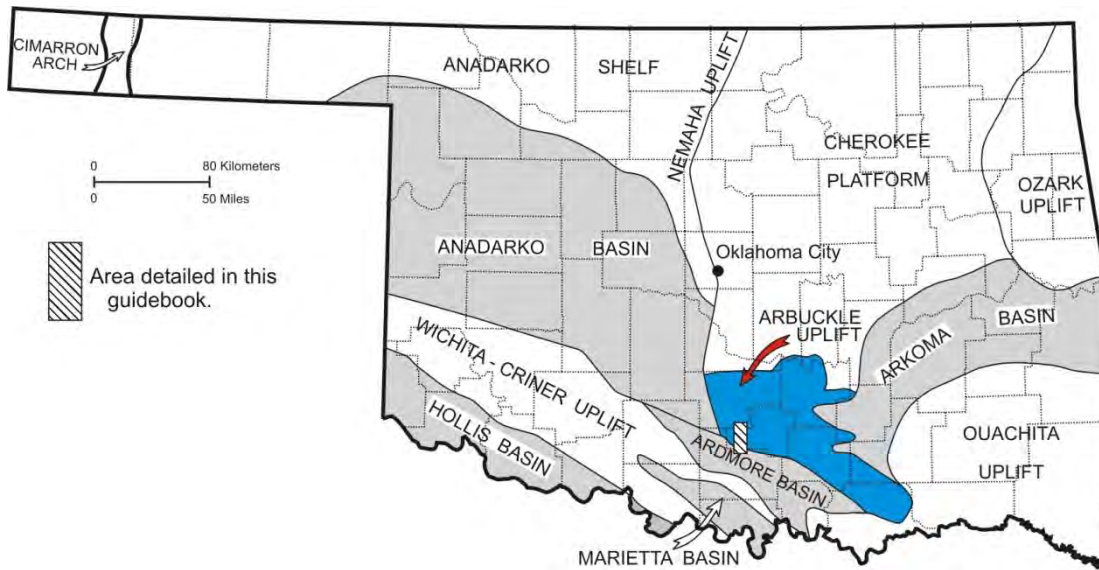


Fig. 1. Major geologic provinces in Oklahoma.

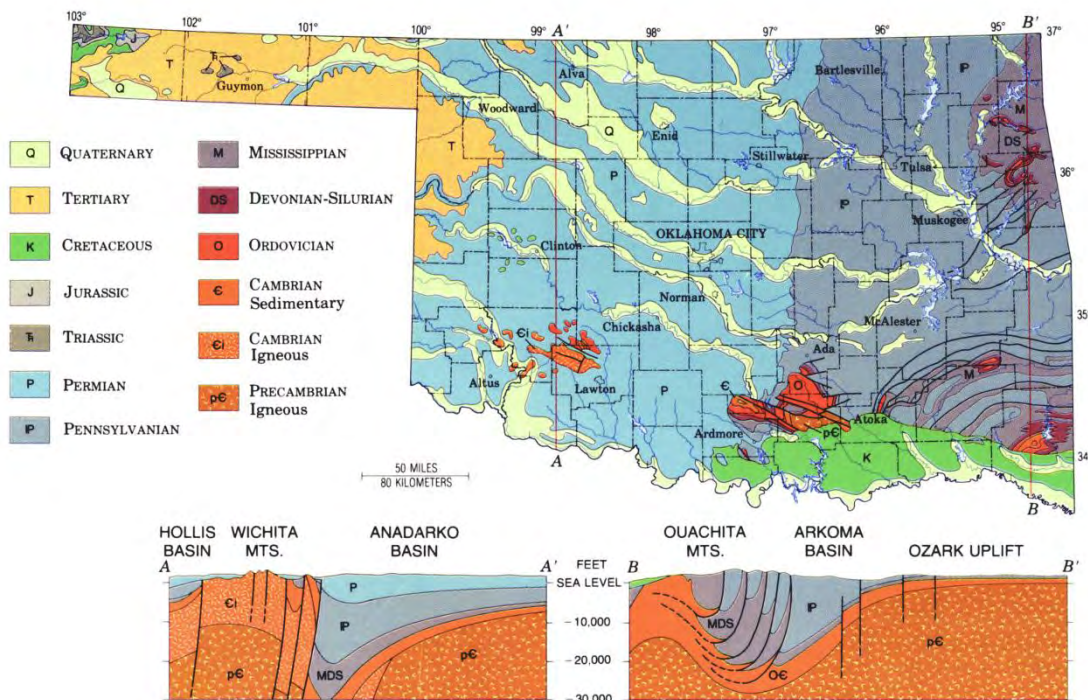


Fig. 2. Generalized geologic map and cross sections that show the subsurface configuration of rock units in Oklahoma.

basins and across some uplifts. Thin coal beds are abundant in Desmoinesian strata, mainly in the Arkoma Basin and the Cherokee platform. Total thicknesses of Pennsylvanian strata in various basins are 10,000–15,000 ft in the Anadarko, Ardmore, Arkoma, and Marietta Basins, and about 4,000 ft in the Hollis Basin. In most shelf or platform areas, Pennsylvanian strata typically are 1,500–4,000 ft thick.

Permian strata are limited to the western half of Oklahoma. Clastics were eroded from the Ouachitas in the east, the ancestral Rocky Mountains to the west, and the Wichita Mountains in southwest Oklahoma. Sediments accumulated mainly in the Anadarko Basin, Hollis Basin, and the Panhandle. Early Permian carbonate and shale, both gray and redbeds, are overlain by a major evaporite and redbed sequence in Middle and Late Permian. Evaporites (salt and gypsum/anhydrite) thickened in basins that continued to subside faster than adjacent uplifts and arches. Permian strata are as much as 7,000 ft thick in the Anadarko Basin, 4,000 ft thick in the Hollis Basin, and 1,000–3,000 ft thick in nearby shelf or platform areas.

The major outcrops of Mesozoic rocks are in the Gulf Coastal Plain of southeast Oklahoma. Cretaceous strata occur in an east-west belt about 175 mi long and as much as 40 mi wide. Beds mostly consist of non-marine sandstone and clay units at the base. The sequence passes upward into marine limestone and shale beds and terminates with non-marine sandstone beds. A second area of Mesozoic rocks, Triassic and Jurassic, is in the northwest corner of the Oklahoma Panhandle. Especially prominent is the Morrison Formation, a non-marine deposit known for its uranium occurrences in the western United States.

Tertiary sediments are confined to the High Plains of western Oklahoma and the Panhandle. The principal unit, the Ogallala Formation, consists of Pliocene sand and clay deposited by streams that originated in the Rocky Mountains; caliche units are also a conspicuous constituent. Some volcanic ash and lacustrine deposits also occur.

Three major mountain regions, Ouachita, Arbuckle, and Wichita Mountains, occur in southern Oklahoma (Figs. 1 and 2). The Ouachita Mountains in southeast Oklahoma form an arcuate fold belt that consists mostly of Mississippian and Early Pennsylvanian sandstone and shale units (Stanley, Jackfork, Johns Valley, and Atoka formations). Locally, sediments about 30,000 ft-thick were deposited in a great trough through Morrowan and Atokan time. The depocenter shifted northward in Atokan time to the southern part of the Arkoma Basin. The trough was destroyed during the Ouachita orogeny (Desmoinesian), with northward thrusting and complex folding of Ouachita-facies rocks to form the present-day Ouachitas. Resistant units of steeply dipping sandstone form long, sinuous mountain ridges and hogbacks that tower 1,000–1,500 ft above intervening shale valleys.

The Arbuckle Mountains in south-central Oklahoma make up an area of low to moderate hills containing 15,000 ft of folded and faulted sediments ranging in age from Cambrian to Pennsylvanian (Ham, 1969). About 89% of these sedimentary rocks are limestone and dolomite units; the remainder is shale and sandstone units. Rocks in this part of southern Oklahoma were thrust upward and folded and faulted during several mountain-building episodes in the Pennsylvanian. The sedimentary cover was eroded from the underlying Precambrian granites in

a 150-square-mile area in the southeast part of the Arbuckle Mountains, making this the largest exposure of Precambrian rocks in the State.

In the Wichita Mountains of southwest Oklahoma, granite, rhyolite, and gabbro are the dominant rocks. These are Middle and possibly Early Cambrian in age, and are flanked by scattered outcrops of Cambrian and Ordovician limestone and dolomite units similar to those of the Arbuckles. The Wichita fault blocks were thrust upward and slightly northward during several Pennsylvanian uplifts, at which time the cover of pre-Pennsylvanian sediments were eroded. The igneous rocks form mountains that rise 500–1,000 ft above the surrounding plain of Permian red beds.

A portion of the Ozark Uplift occurs in northeast Oklahoma. This deeply dissected plateau formed in gently dipping Mississippian limestone and chert beds. Caves, solution cavities, and other karst features are more prevalent here than in any other part of Oklahoma.

Much of the geologic discussion above was taken from Johnson and Mankin (1971), Johnson and McCasland (1971), Johnson and others (2001), and Johnson (2008a-c). General discussions of Oklahoma geology are presented by Ham and Wilson (1967), Ham (1969), and Johnson and others (1988).

GEOLOGY OF FIELD–TRIP REGIONS

The focal point of the field trip is the Arbuckle Mountains, but stops also will be made in the Ardmore area to the south (Fig. 3). The field trip traverses nearly the same path shown on cross section A-A' (Fig. 4a and 4b), commencing on the Permian "redbeds" and thence to the Arbuckle Mountains and the Ardmore Basin. The three regions are described separately in the order in which they will be traversed.

Central Redbed Plains—The Central Redbed Plains consist of red Permian shale and sandstone beds that form gently rolling hills and broad, flat plains. Strata dip gently westward 10 to 50 ft per mile toward the Anadarko Basin, and are exposed in long, parallel north-south belts with east-facing escarpments capped by more resistant sandstone beds.

Our drive to the Arbuckles parallels the strike of these beds, and so only 500–1,000 ft of Permian rocks in the Wellington Formation, Garber Sandstone, and Hennessey Shale (ascending order) are traversed during our 60-mile-long trip across the red beds. The Wellington and Hennessey are chiefly red-brown shale. They contain several red-brown and brown sandstone beds 5–30 ft thick. The Garber is mainly red-brown sandstone with some interbedded red-brown shale.

Early Permian sediments of the Central Redbed Plains were derived from eastern Oklahoma. These sediments are interbedded alluvial, deltaic, and shallow-marine deposits. They were laid down near the shore of the large inland sea that covered western Oklahoma and extended northward from west Texas to Nebraska and the Dakotas. The red color results from staining by red iron oxides (chiefly hematite) deposited along with the sand and mud.



Fig. 3. Road map and stops along field-trip route. Stops 3 and 4 are shown on map in Stop 3.

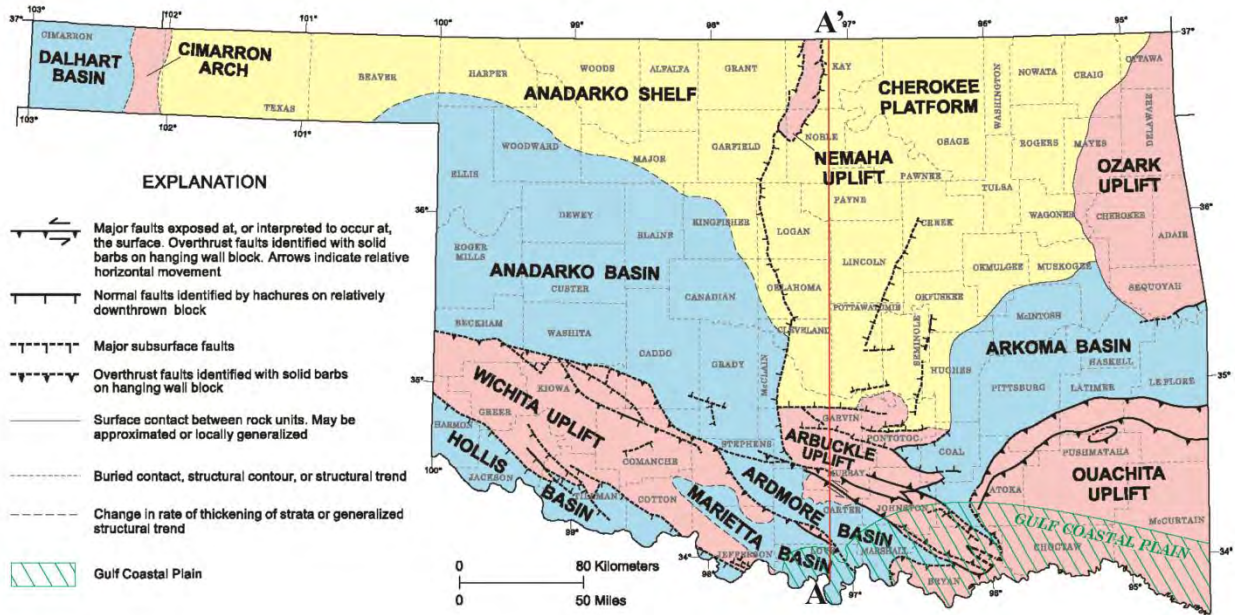


Fig. 4a. Major geologic provinces of Oklahoma and geologic cross section (modified from Northcut and Campbell, 1995).

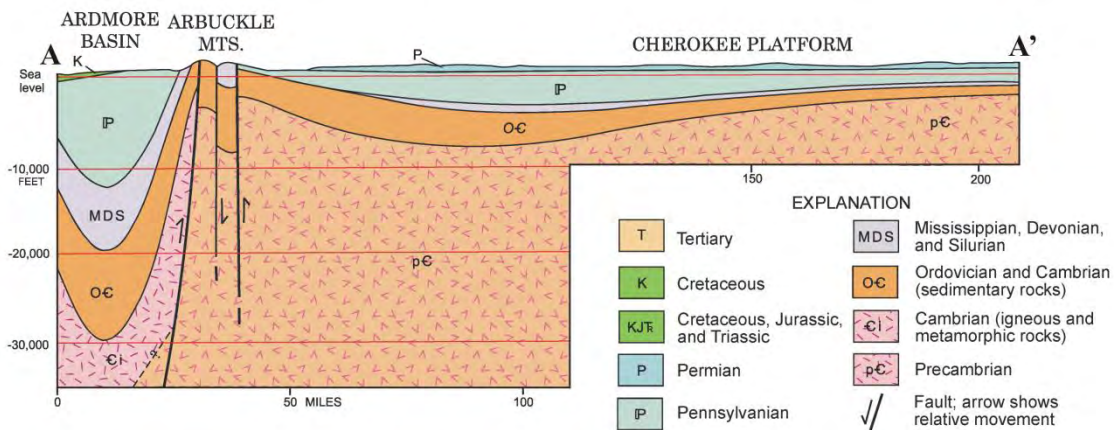


Fig. 4b. Geologic cross section near field trip route; vertical exaggeration 10x.

Oklahoma averages 50 earthquakes per year. Earthquake magnitudes range from 1.8 to 2.5, with shallow focal depths (less than 3 miles). Over half the annual earthquakes are concentrated in a 25- by 37-mile area along a deep, subsurface fault zone in west McClain and Garvin counties and southeast Grady County (Fig. 5). I-35 nearly parallels this fault zone between the cities of Norman and Pauls Valley. Another principal area of seismic activity is in Love, Carter, and Jefferson counties, near field trip stops 2, 3, and 4.

Arbuckle Mountains—The geological province known as the Arbuckle Mountains consists of a huge inlier of folded and faulted Paleozoic and Precambrian rocks. It is covered on the east, north, and west by gently westward-dipping Pennsylvanian and Permian strata and on the south by gently southward-dipping Cretaceous sediments of the Gulf Coastal Plain (Fig. 6).

The inlier is a roughly triangular area of 1,000 sq mi in south central Oklahoma. The geology is characterized by outcrops of mostly carbonate rocks. Immediately to the east begins the 200-mile-long exposure of the Ouachita Mountains, principally a sandstone-shale sequence that is quite unlike the Arbuckles in stratigraphic and structural development. At 100 mi to the west are the Wichita Mountains. They are characterized chiefly by extensive outcrops of Cambrian igneous rocks. Thus the three uplifted segments of southern Oklahoma actually share little in common, despite their similar age and geographic proximity, and each has a profoundly different geologic nature.

Referring to the Arbuckle outcrops as the “Arbuckle Mountains” is somewhat misleading because about 80 % of the area consists of gently rolling low hills and plains. Only in the western area—that of the Arbuckle anticline—is topographic relief sufficient to evoke comment from a newcomer. The greatest relief is along highways U.S. 77 and I-35. In this area, the Washita River flows at an elevation of 770 ft. Three miles away is the top of the east Timbered Hills—the crest of the Arbuckle anticline—at an altitude of 1,377 ft, nearly the highest point in the Arbuckles. The total relief of 607 ft is impressive only because it is more than 6 times greater than any other topographic feature between Oklahoma City and Dallas. Whether considered plains or hill country, the Arbuckles is a region of irresistible interest to geologists. Its 11,000 ft of fossiliferous Late Cambrian through Devonian strata constitute the best outcrops and greatest area of exposure of this sequence in the entire Midcontinent. Stratigraphic names taken from the Arbuckles, such as Arbuckle, Simpson, Viola, Sylvan, Hunton, and Woodford, have been widely applied in the subsurface as far away as West Texas, Illinois, and Nebraska. The 150-square-mile exposure of Precambrian granites in the eastern Arbuckles is the largest and best exposed outcrop of such rocks in the central United States between the Llano area of Texas and the Black Hills of South Dakota. Over 20,000 ft of Mississippian and Pennsylvanian clastics are present in the region, partly in synclinal grabens of the Arbuckles and to a much greater extent in the adjoining Ardmore Basin. Fusulinids from thin Pennsylvanian limestones in the sequence are widely used for standards of reference.

The process of strong uplift and deep erosion that produced the Arbuckles of today also exposed to the surface rocks that normally are buried. Many of the rocks are commercially

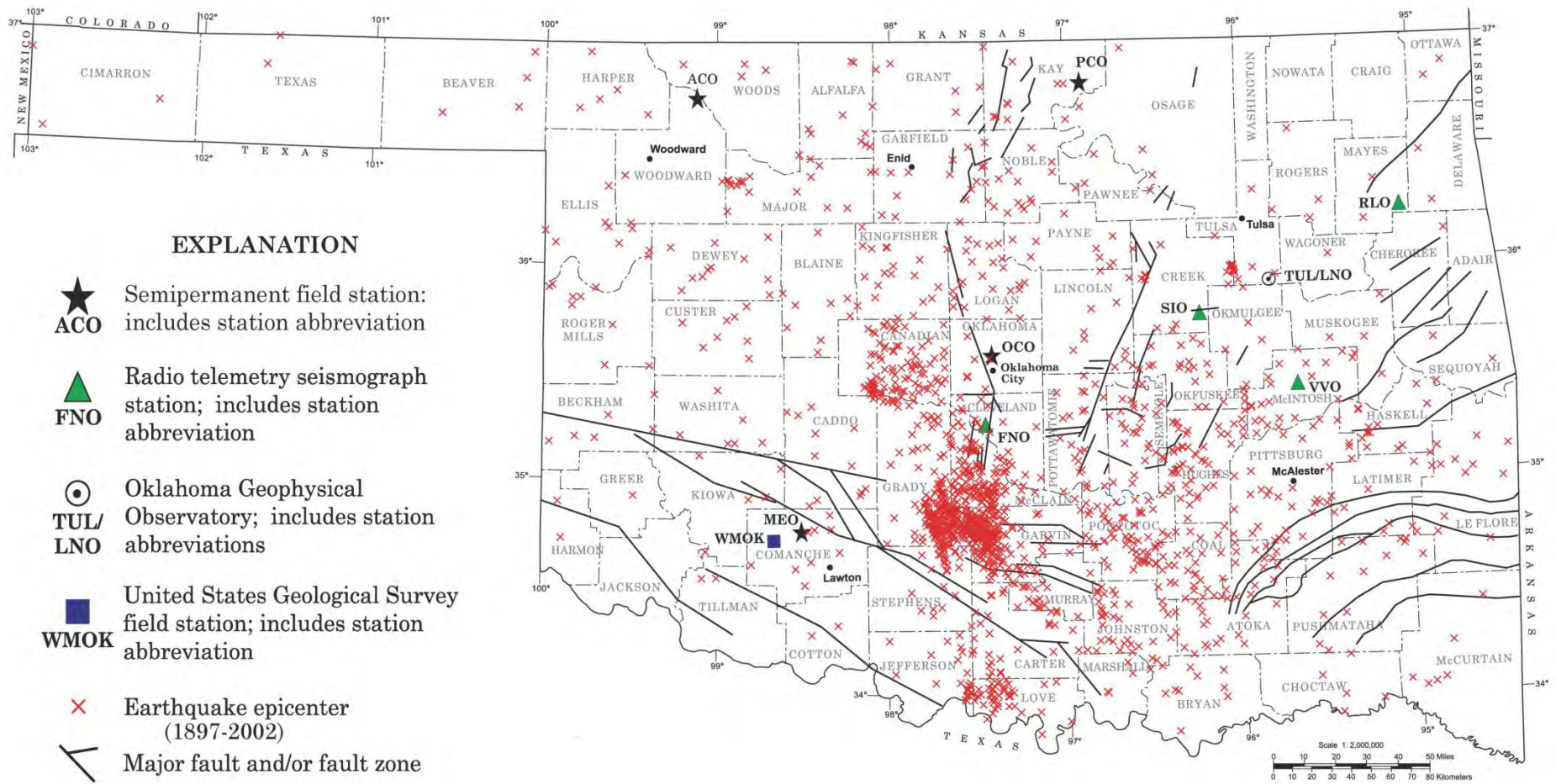


Fig. 5. Earthquake map of Oklahoma.

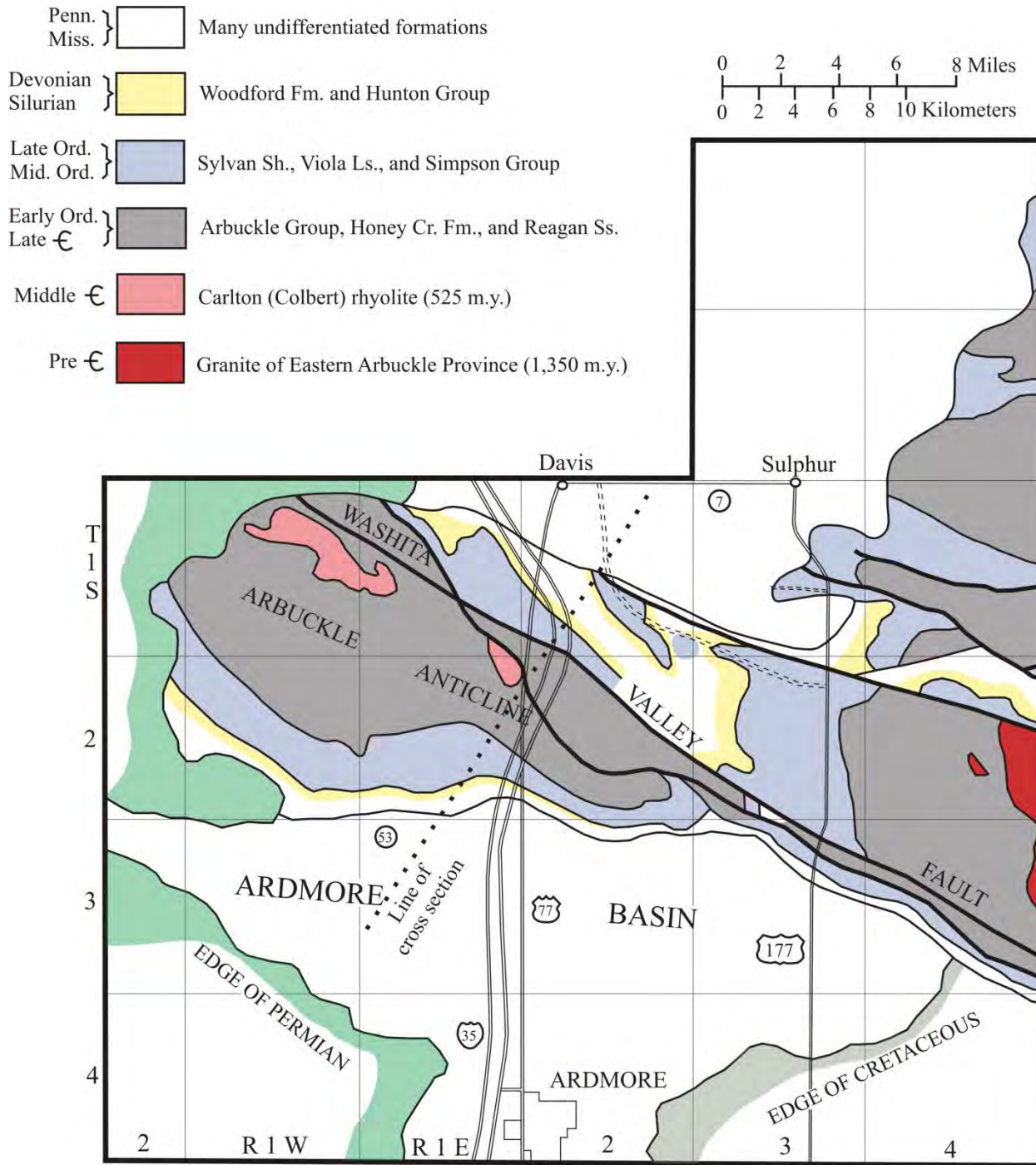


Fig. 6. Generalized geologic map of Arbuckle Mountains (Ham, 1969; Chaplin and Gomez, 2006); cross section in **Stop 1A**.

valuable. For example, limestone from thick and widely distributed outcrops of the Arbuckle and Viola Formations are quarried extensively for crushed stone. High-purity silica sand from the Simpson Group is used for glassmaking, proppant sand, and other industrial applications. Cement-making raw materials come from the Viola Limestone and Sylvan Shale. High-purity dolomite is mined from the Arbuckle Group for various uses including animal feed supplements. Precambrian granite provides dimension stone for buildings and monuments.

Ardmore Basin—The Ardmore Basin, located just south of the Arbuckle Mountains, is a downwarped remnant of the Southern Oklahoma Aulacogen that contains about 35,000 ft of Late Cambrian through Late Pennsylvanian (Missourian) sediments. It has a northwest trend averaging 15 mi wide and about 50 mi long. The general structure is that of a syncline, but several large anticlines are present within the basin. Dips are steep, particularly along the basin margins of the basin, commonly with 45° to 90° angles.

Pre-Mississippian strata, present only in the subsurface, are similar to those in the Arbuckle region. The Ardmore Basin continued to subside during the Mississippian and Pennsylvanian, receiving over 20,000 ft of thick shale interbedded with thin sandstone, limestone, and conglomerate units. These rocks were then tightly folded during Pennsylvanian orogenies that culminated in the uplifting of the Arbuckle Mountains (Fig. 7).

Shale outcrops are typically dark gray, gray, and brown in the Ardmore Basin, and range in thickness from 100 ft to several thousand. The interbedded sandstone, limestone, and conglomerate beds are typically 10–50 ft thick, and because they are more resistant than the shale beds, they form conspicuous sub-parallel ridges standing as high as 10 ft above adjacent lowlands.

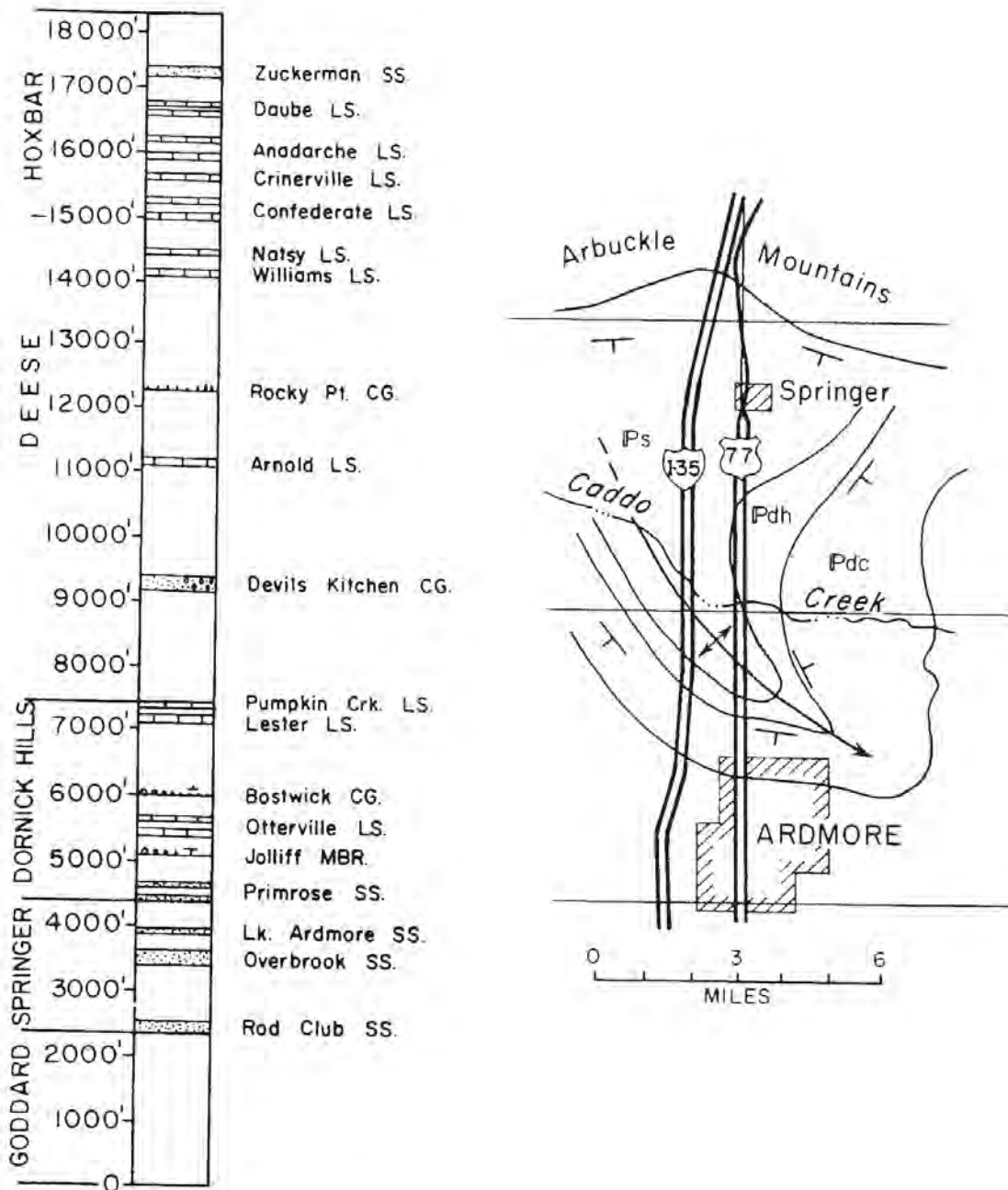


Fig. 7. Stratigraphic section of outcropping beds in the Ardmore Basin and generalized geologic map showing northwest-trending Caddo Anticline (*s Springer; *dh Dornick Hills; and *dc Deese Groups).

References

- Chaplin, J.R.; and Gomez, L.D., 2006, Field guide to some selected geological features in the western Arbuckle Mountains, southern Oklahoma: Oklahoma Geological Survey, Unpublished Open-File Report, 137 p.
- Ham, W. E., 1969, Regional geology of the Arbuckle Mountains, Oklahoma: Oklahoma Geological Survey Guidebook 17, 52 p.
- Ham, W. E.; and Wilson, J. L., 1967, Paleozoic epirogeny and orogeny in the central United States: *American Journal of Science*, v. 265, p. 332–407.
- Johnson, K. S., 2008a, Geologic history of Oklahoma, *in* Johnson, K. S. and Luza, K. V. (eds.), Earth Sciences and mineral resources of Oklahoma: Oklahoma Geological Survey Education Publication 9, p. 3–5.
- Johnson, K. S., 2008b, Geologic map of Oklahoma, *in* Johnson, K. S. and Luza, K. V. (eds.), Earth Sciences and mineral resources of Oklahoma: Oklahoma Geological Survey Education Publication 9, p. 6.
- Johnson, K. S., 2008c, Geologic cross sections of Oklahoma, *in* Johnson, K. S. and Luza, K. V. (eds.), Earth Sciences and mineral resources of Oklahoma: Oklahoma Geological Survey Education Publication 9, p. 7.
- Johnson, K. S.; Amsden, T. W.; Dennison, R. E.; Dutton, S. P.; Goldstein, A. G.; Rascoe, B., Jr.; Sutherland, P. K.; and Thompson, C. M., 1988, Southern Midcontinent region, *in* Sloss, L. L. (ed.), Sedimentary cover—North American craton, U.S. Geological Society of America, The Geology of North America, v. D-2, p. 307–359.
- Johnson, K. S.; and Mankin, C. J., 1971, Geology of Oklahoma—a summary, *in* Proceedings of the 22nd annual highway geology symposium, p. 1–7.
- Johnson, K. S.; and McCasland, Willard, 1971, Highway geology in the Arbuckle Mountains and Ardmore area, southern Oklahoma: 22nd Annual Highway Geology Symposium, Norman Oklahoma, 31 p.
- Johnson, K. S.; Northcutt, R. A.; Hinshaw, G. C.; and Hines, K. E., 2001, Geology and petroleum reservoirs in Pennsylvanian and Permian rocks of Oklahoma, *in* Johnson, K. S. (ed.), Pennsylvanian and Permian geology and petroleum in the southern midcontinent, 1998 symposium: Oklahoma Geological Survey Circular 104, p. 1–19.
- Northcutt, R. A.; and Campbell, J. A., 1995, Geologic provinces of Oklahoma: Oklahoma Geologic Survey Open File Report 5-95, 1 sheet, scale 1:750,000, 6-page explanation and bibliography.

ROAD LOG

Oklahoma City is and largest city and the capital of Oklahoma. It is the 31st most populace city in the nation with an estimated 551,789 residents in 2008; its metropolitan area has an estimated population of 1,206,142. The city limits extend into Canadian, Cleveland, and Pottawatomie counties; however, large areas are rural or suburban. Area-wise the city ranks 8th largest in the U. S.



Oklahoma City and Bricktown in foreground (photograph by David K. Luza)

Oklahoma City is an important livestock market, and home to several prominent energy companies. The city, situated in the middle of an oil field, boasts about the oil derricks on the grounds of the state capitol. Various heavy and light industries, Tinker Air Force Base, and the federal government are also vital sources of employment. Founded during the Land Run of 1889, the population of Oklahoma City swelled to more than 10,000 overnight. The worst terror attack in U.S. history prior to September 11, 2001 occurred here on April 19, 1995.



Phillips 66 oil well on south side of Oklahoma's State Capitol

Metropolitan Area Projects (MAPS) began in December 1993 when voters approved the MAPS sales tax, and ended in August 2004. The project is Oklahoma City's capital improvement program that upgraded sports, recreation, entertainment, cultural, and convention facilities. Nine elements of MAPS include the new AT&T Bricktown Ballpark; renovation of the Myriad (now Cox Business Services Convention Center); improvements at the state fairgrounds; the Bricktown Canal; a new Library/Learning Center; new trolleys; a near-rebuilding of the Civic Center Music Hall; improvements to the North Canadian River; and construction of the Ford Center. Most of these are within walking distance of the downtown area, and Highway Symposium participants are encouraged to visit the various elements of MAPS.

A mayor-appointed 21-member oversight board reviews project components and makes recommendations to the City Council. Every-day operations are the responsibility of the MAPS office composed of Oklahoma City employees.



Bricktown just east of the Santa Fe Railroad tracks (Photograph by David K. Luza)

<i>Cumulative mileage</i>	<i>Interval</i>	
0.0	0.0	Start field trip from the Skirvin Hotel lobby, Broadway and Park, in Oklahoma City.
0.1	0.1	Proceed west on Park to Robinson, TURN LEFT (south) on Robinson.
0.3	0.2	Myriad Gardens (right) and Cox Convention Center (left).



Myriad Gardens in the spring (photograph by David K. Luza)

The Myriad Botanical Gardens has 17 acres of breathtaking outdoor gardens that surround the Crystal Bridge Tropical Conservatory. The conservatory is a 224-foot long living plant museum with palm trees, tropical plants and flowers, waterfalls, and exotic animals. You will have to return for a tour next year, because the gardens are undergoing a yearlong renovation that began in April 2010.

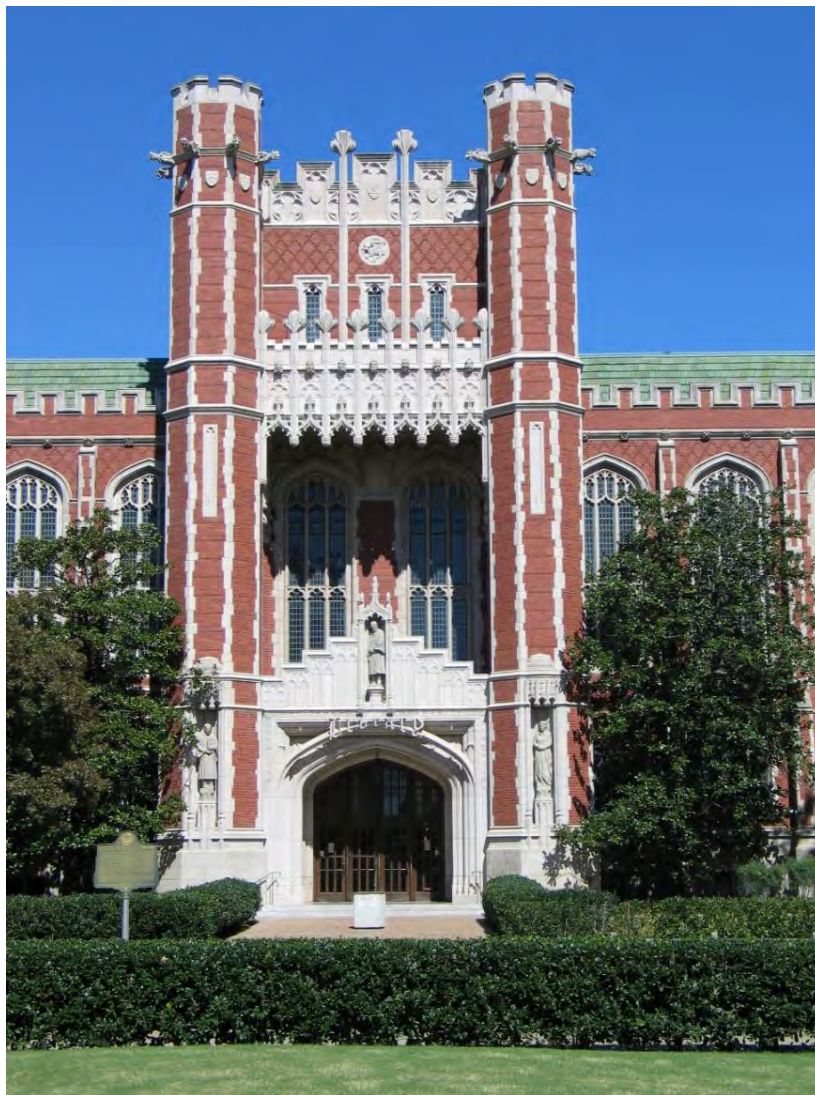
The Cox Convention Center boasts a 15,000-seat arena, 100,000 sq ft of exhibit space, a 25,000-sq ft ballroom, 27,000 sq ft of meeting rooms, and more. Designed for major national and international events, the Center can accommodate its clients with a staff that provides professional guest services that rival any in the country.

0.4	0.1	Ford Convention Center (left).
0.6	0.2	Third and Robinson, TURN LEFT.
0.7	0.1	TURN RIGHT, follow the on ramp to I-40 eastbound.
0.8	0.1	TURN RIGHT, EXIT 151B to I-35 southbound.
2.3	1.5	North Canadian River bridge.

Oklahoma River: Seven miles of the North Canadian River was converted into a series of “river lakes” with landscaped banks and trails and recreational facilities. Now known as “The Oklahoma River,” the various segments of the river are separated by a series of locks that control the water flow and level. Joggers, walkers, skaters, and bikers use the trails extensively. Fishing along the river is another popular pastime; a city fishing permit and state fishing license are required. Noodling is prohibited in the Oklahoma River; however, for the more adventuresome, it is allowed from the NW 10 Bridge downstream to the MacArthur Bridge.

Oklahoma City Oil Field began producing oil on December 4, 1928, when the Oklahoma City Number One was completed south of the city at a depth of 6,355 ft. It produced about 6,000 BPD. It was the first time that oil was produced inside an urban area. A 1930 city ordinance limited drilling to one well per city block. The ordinance also restricted activity to specific sections within the city. On April 10, 1933, the State Legislature passed House Bill Number 481, which brought oil production under control of the state. Legal challenges and potential violence required the Governor to establish martial law on several occasions during the Field's early history. Today the Field's legacy remains with several producing wells throughout the city. The State boasts the only oil well ever having been drilled and producing oil on the grounds of the State Capitol.

7.2	4.9	I-35/I-240 interchange.
18.7	11.5	I-35/Robinson Street bridge in Norman.
19.7	1.0	I-35/Main Street bridge in Norman.



Main library at The University of Oklahoma

Norman is county seat of Cleveland County and third largest city in Oklahoma. The population was 95,694 at the 2000 census. The city is named after Abner E. Norman, a surveyor who worked for the U.S Land Office. Norman was founded after the Land Run of April 22, 1889. The post office was established on May 27, 1889. Norman's largest employer is the University of Oklahoma, established in December, 1890; the first students enrolled in the fall, 1892. The Norman campus enrollment is about 20,000 students. The Oklahoma Geological Survey, which was authorized by Oklahoma's State constitution in 1907, is located on campus.

The National Severe Storms Laboratory and Mid Continent Severe Storms forecast center are located in a research park south of the main campus. Norman is home to many weather-related private businesses such as Weathernews Americas, Inc., Vieux and Associates, Inc., Weather Decision Technologies, WeatherBank, Inc., and Computational Geosciences, Inc. Other major employers include SouthWest Nano Technologies, a producer of single-walled carbon nanotubes; Bergey Windpower, a producer of small wind turbines; Johnson Controls, Hitachi; Astellas Pharma; Albon Engineering; Xyant Technology; Office Max's National Sales Center; Sitel; U.S Postal Service National Center for Employee Development; and Sysco Foods.

0.0	0.0	RESET ODOMETER TO ZERO AT MAIN STREET BRIDGE.
1.8	1.8	Canadian River Bridge; entering McClain County.

The **Canadian River**, a major tributary of the Arkansas River, has its source in Colorado and runs through New Mexico, the Texas Panhandle, and Oklahoma along its 900-mile length. Many Oklahomans refer to the Canadian as the South Canadian River to differentiate it from the North Canadian River. The river was the south boundary between Oklahoma and Indian Territory in 1889.

There are two probable explanations for its name. Because the river runs through steep canyons in New Mexico and Texas, Spanish explorers may have used the Spanish word *cañada* (meaning "canyon") to refer to the river. More likely, French voyageurs or traders gave the river its name after they observed other French-Canadian traders camping along its bank. The river was used by prehistoric natives for transportation; as a trade route; as a source for water; and as sites for settlement. Anglo-Americans explorers, surveyors, traders, and emigrants proceeded along the south bank of the Canadian on their way to Santa Fe and California.

Much of the Canadian's flow is managed by flood-control measures along its tributaries, so that today, the river moves slowly along its course. The banks and flood plain, as well as the streambed, are typically associated with mud flats, sand bars, and quicksand. The Canadian River Commission has jurisdiction over all major activities that utilize the water resources of the Canadian River including recreation, industry, mining, municipal utilities, etc. Passing over the I-35 Canadian River Bridge, one can observe on either side a mining operation producing construction sand from the stream channel.

5.0	3.2	Goldsby, Exit 104.
-----	-----	--------------------

Goldsby, located in northern McClain County, had a population of 1,204 at the 2000 census. It was named after Frank W. Goldsby, a prominent and early-day resident. One of the largest casinos in Oklahoma, Riverwind Casino, is located west of I-35 on State Highway 9. The casino is owned by the Chickasaw Nation.

14.7 9.7 Purcell, Exit 95.

Purcell is the county seat of McClain County. The population was 5,571 at the 2000 census. It is located on a bluff that overlooks the Canadian River valley. The official motto and registered trademark of Purcell is “Heart of Oklahoma.” Founded as a railroad town in 1887, the town was named in honor of the Atchison, Topeka, and Santa Fe railroad director, Edward Benton Purcell, of Manhattan, Kansas. Numerous quarter-horse farms are located in the vicinity of Purcell.

22.7 8.0 Communication’s tower.
24.3 1.6 Wayne/Payne, Exit 86.

Wayne is a town in southern McClain County. The population was 519 at the 2000 census. Pennsylvania railroaders in the 19th Century named towns after places from which they came and famous Pennsylvanians. Wayne was named after “Mad” Anthony Wayne, a U.S. Army general in the American Revolutionary War. **Payne** is a small unincorporated town west of Wayne, named after its first postmaster, Jeff D. Payne. The post office was established on December 15, 1904; and closed October 31, 1922.

Mid-America Technology Center is located west of I-35. It is one of 49 technology centers located throughout Oklahoma. The center provides vocational training in subjects such as equine production, horticulture, graphic communications, pre-nursing, welding, and automotive repair. Local and county taxes are the primary sources of funds for the technology centers.

31.1 6.8 Paoli, Exit 79.

Paoli, located in northern Garvin County, had a population of 649 at the 2000 census. It was named after Paoli, Pennsylvania, near Philadelphia, by railroad workers from there. The post office was established on June 27, 1888.

Copper and native silver were mined east of Paoli in the early 1900s. In 1971, Teton Exploration Drilling Company Incorporated acquired a Paoli prospect with Wolf Ridge Minerals Company. Teton utilized standard uranium exploration techniques to demonstrate that the Paoli copper-silver deposits occurred in solution fronts. Host rocks for copper-silver solution fronts at Paoli are sandstone paleochannels in the Permian Wellington Formation. The sandstone typically is greenish-gray, friable, well-sorted, fine- to medium grained, sub-rounded, quartzose, and without visible carbon. The unoxidized ore consists of chalcocite, digenite, chalcopyrite, covellite, and pyrite; and oxidized ores are characterized by covellite, bornite, malachite, hematite, and goethite.



Copper mineralization (mostly malachite) in the Wellington Formation

34.9 3.8 Washita River; Bureau of Land Management Mustang Relocation Program, South of the river.

The Wild Horse Annie Act of 1959 and the Wild Free-Roaming Horses and Burros Act of 1971 gave wild horses and burros the right to live on the public lands free from harassment. The U.S. Bureau of Land Management's (BLM) responsibility is to preserve and protect healthy herds as components of the public lands. The BLM has conducted the Adopt-A-Horse or Burro Program since 1973.

The Pauls Valley facility is a resting point for horses and burros that arrive from public lands in New Mexico, before they are shipped to adoption locations in the central and eastern United States. There are 12 pastures totaling 400 acres that provide the animals with a natural, safe environment prior to placing them in new homes. The facility can hold 600 animals. A drive-up interpretation center near the pastures allows visitors to view the animals roaming and grazing there.



BLM's Mustang Ranch

37.9 3.0 Pauls Valley, Exit 72.

Pauls Valley is the county seat of Garvin County. The population was 6,256 at the 2000 census. In 1847, Smith Paul and his family settled on land which became known to locals as "Smith Paul's Valley". The post office was established on August 21, 1871. The first newspaper was published in 1887. The Pauls Valley townsite was laid out in 1892. Today, Pauls Valley claims to have more brick streets than any other town in the U.S.

44.8 6.9 Wynnewood, Exit 66.

Railroad workers from Pennsylvania named **Wynnewood**, Oklahoma, after a town in their home state. Wynnewood was known as Walner prior to the railroad coming through. The original location was a rocky ford on the Washita River known as Cherokee Crossing. Wynnewood experienced a small population explosion after the Civil War when many veterans of the Confederacy settled there. About 2,300 people live in Wynnewood.

The largest industry is the Wynnewood Refining Company owned by the Gary-Williams Energy Corporation. The refinery processes 70,000 BPD of crude oil to produce gasoline, diesel, JP-8 and JP-5 jet fuel, asphalt, liquid petroleum gas (LPG), and solvents. Purchased from Kerr-McGee Corporation in 1995, the refinery employs 185 people.

Famous people born in Wynnewood include R&B singer, musician, and bandleader Roy Milton; General Tommy Franks, Commander of U.S. Army invasion forces during Operation Enduring Freedom in Afghanistan and Operation Iraqi Freedom in Iraq; and Donna Shirley, former manager of the Mars Pathfinder project at NASA's Jet Propulsion Laboratory (JPL).

46.9	2.1	Wynnewood, Exit 64 to state highway 17A.
52.5	5.6	Rest area, Exit 59.
55.4	2.9	Exit 55 to State Highway 7; east to Davis and Chickasaw National Recreation Area in Sulphur.

Sulphur, Oklahoma, situated in the center of the Chickasaw Nation, is home to the Oklahoma School of the Deaf and the Oklahoma Veterans Center. The town is the gateway to the Chickasaw National Recreation Area, famous for therapeutic mineral waters and mud that originate from springs charged with sulphur and bromine along Rock Creek.

Prehistoric natives discovered the natural springs thousands of years ago. White European settlers discovered the area in the late 19th Century. The city of Sulphur Springs grew around the springs and became an attraction especially for the waters' therapeutic qualities. Testimonials about miraculous cures from those "taking the waters" spread throughout the United States and resulted in trainloads of tourists seeking cures. The chiefs of the Chickasaw and Choctaw tribes, fearing that the springs would be contaminated by increased use, decided to transfer the land to the U.S. government in 1902 for its protection. In 1904, the Department of Interior officially opened Sulphur Springs Reservation to the public. Congress changed the name to Platt National Park, in honor of Senator Orville Platt of Connecticut, in 1906. Lake of the Arbuckles and Platt National Park were combined to form Chickasaw National Recreation Area in 1976.

A member of the Oklahoma Main Street project, historic downtown Sulphur remains a tourist attraction. Many hopeful visitors still take to the therapeutic waters, but most tourists browse the gift and antique shops; they may camp overnight at the CNRA. Both residents and visitors collect the mineral waters for its medicinal value. Drinking fountains and spigots are situated near the springs and wells for the convenience of visitors.

60.2	4.8	Exit 51 to U.S. highway 77 and Turner Falls.
60.7	0.5	Honey Creek Bridge; .
62.7	2.0	TURN RIGHT to scenic overlook
63.0	0.3	Park bus in northwest corner of parking lot— STOPS 1A and 1B.

The Honey Creek Bridges carry I-35 over Honey Creek and US-77 (fig 1). Foundation soundings showed that a medium-hard shale bed, the Mississippian Delaware Shale (overturned and dipping 70° to the southwest), is the bedrock beneath 12 to 24 feet of alluvial cover deposited by Honey Creek and the Washita River. The cut section on the south end of the bridge exposes the Sycamore Limestone, which conformably underlies the Delaware Creek and indicates the steepness of the dips in the area.

Initially, it was determined that it would be most economical to drive point-bearing piles under both abutments and piers 1 and 4, and that spread footings should be used under piers 2 and 3 close to the stream bed. When the contractor drove piling and began excavation, the depth to shale at pier 3 beneath the north bound lanes was found to be erratic and greater than anticipated (fig 1). A change in plans was required at pier 3 of the north bound lanes and piling was added due to the additional depth to shale.

The bridges consist of spans of 50 - 75 - 90 - 75 - 50 foot concrete T-girder rigid frames. The arch effect attained is both functional and aesthetically pleasing, and it serves to blend the northern entrance into the natural beauty of the Arbuckle Mountains.

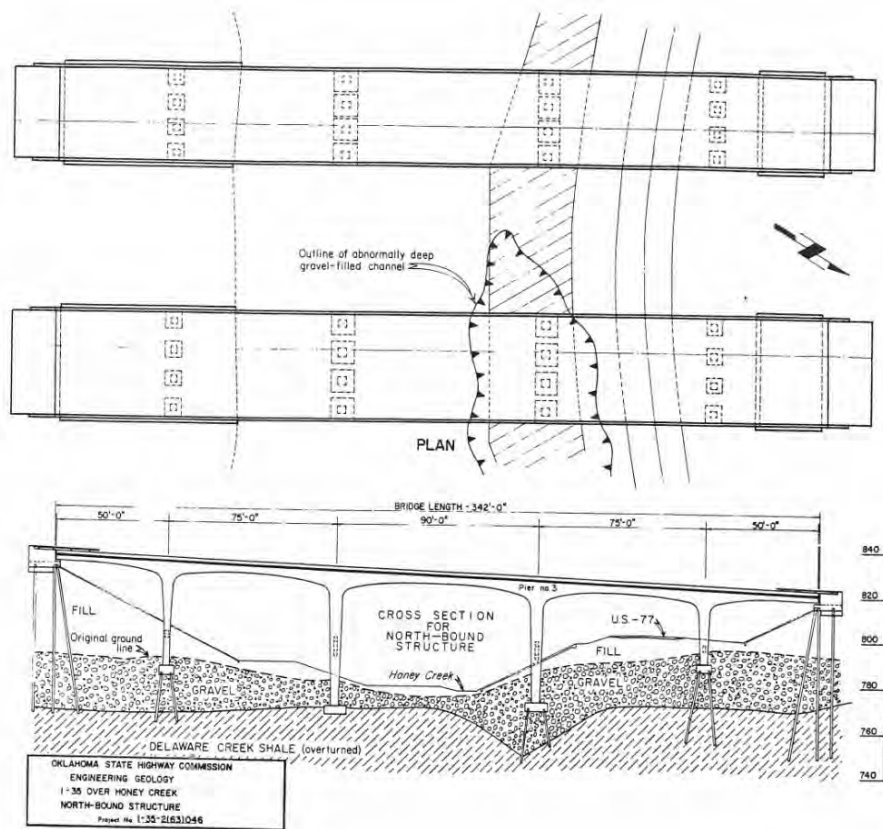


Figure 1. Plan view and cross section of I-35 Honey Creek bridges on north side of Arbuckle Mountains.



Vendome artesian well drilled in 1922 by Townsley and Lewis, Sulphur, Oklahoma



Men waiting to fill water bottles at Bromide Springs, Platt National Park (*Oklahoma Geological Survey Collection, Western History Collections, University of Oklahoma*)

STOP 1A. ARBUCKLE MOUNTAINS GEOLOGY

Leaders: Kenneth V. Luza and Stanley T. Krukowski, Oklahoma Geological Survey

Introduction

By early Paleozoic time, Oklahoma had three major tectonic/depositional provinces: the Oklahoma Basin, the Southern Oklahoma Aulacogen, and the Ouachita trough (Fig. 1). The Oklahoma Basin was a broad, shelf-like area that received a sequence of remarkably thick and extensive, shallow-marine carbonates interbedded with thinner marine shale and sandstone beds. The Southern Oklahoma Aulacogen was the depocenter for the Oklahoma Basin. It was a west-northwest-trending trough where sediments are generally similar to those elsewhere in the basin, but they are two to three times as thick. The aulacogen embraced the Anadarko, Ardmore, and Marietta protobasins, along with the Arbuckle Anticline, Criner Uplift, and Wichita Mountain Uplift. The Ouachita trough was the site of deepwater sedimentation along a rift at the southern margin of the North American craton. These sediments were thrust some 50 mi northward to their present position in the Ouachita Mountain Uplift.

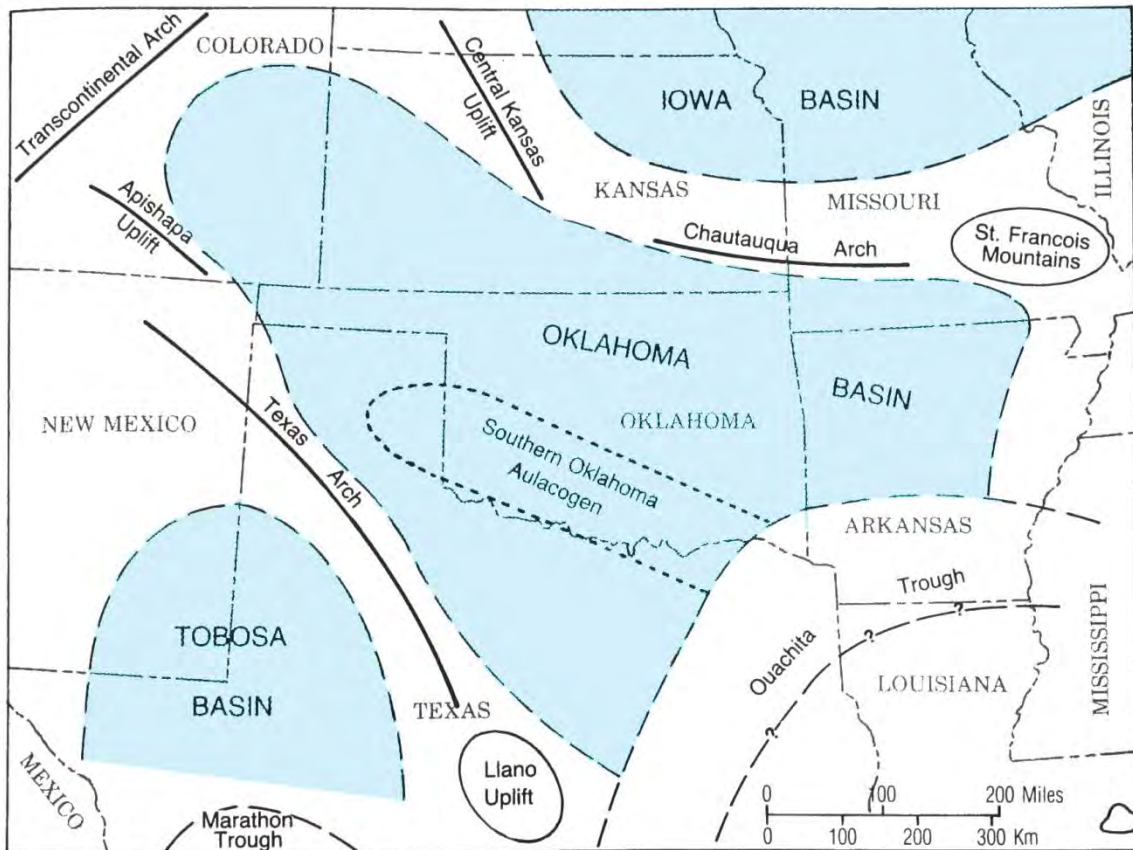


Fig. 1. Map of southwestern United States showing approximate boundary of the Oklahoma Basin and other major features in early and middle Paleozoic time (after Johnson and Cardott, 1992).

These three provinces persisted through the middle Paleozoic until Pennsylvanian time, when the Oklahoma Basin and the aulacogen were divided into a series of well-defined marine

basins by sharply uplifted crustal blocks. The Ouachita Trough was destroyed by uplift and northward thrusting during the Pennsylvanian. Orogenic activity throughout the State was limited to folding, faulting, and uplift, and was not accompanied by igneous activity. Early and Middle Paleozoic sediments tend to be quite persistent laterally, and so the same formations are recognized in most geologic provinces outside the Ouachita Mountains. In contrast, Late Paleozoic (mainly Pennsylvanian) strata are markedly different from basin to basin, and even within the same basin. Post Paleozoic strata are laterally persistent, but thickness and distribution are generally limited.

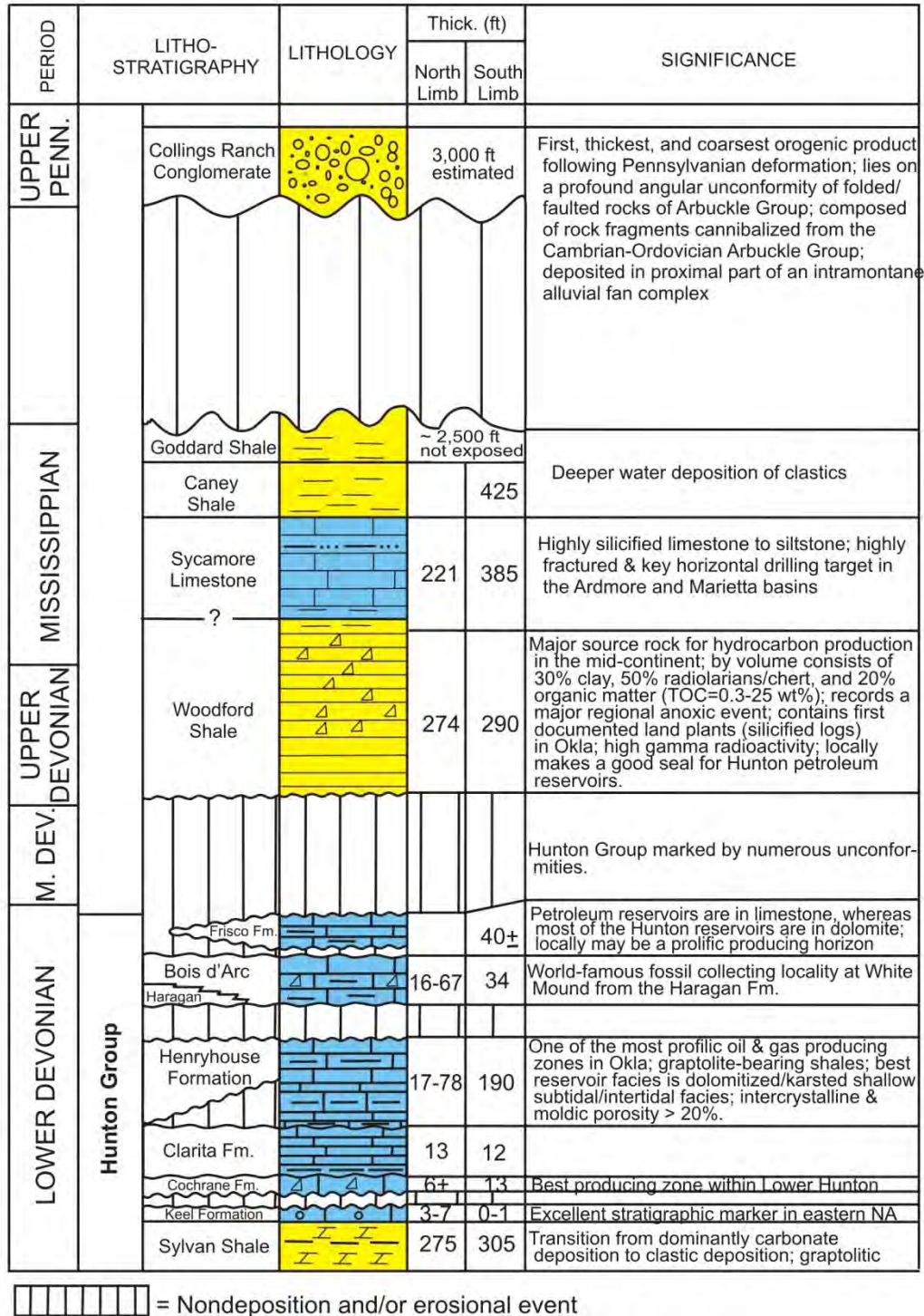
Throughout most geologic time, the region encompassed by the Arbuckle Mountains Province existed within an aulacogen along a passive continental margin. During the Precambrian through Early Cambrian, the Southern Oklahoma Aulacogen experienced considerable rifting that resulted in the emplacement of both intrusive and extrusive igneous rocks, not only in the Arbuckle Mountains region but also in the Wichita Mountains area to the west. In the Arbuckle Mountains region along I-35, these crystalline rocks are represented by the Colbert Rhyolite (dated at 500–550 mya), which makes up the core of the Arbuckle Anticline.

By Late Cambrian, rifting of the Southern Oklahoma Aulacogen ceased, and the area underwent an extensive period of slow subsidence and marine deposition that lasted until the Early Devonian (Fig. 2). Rock units formed during that time were chiefly marine carbonates deposited under supratidal, and intratidal to very shallow subtidal conditions (i.e., the Lower Ordovician Arbuckle Group: nearshore and shallow subtidal terrigenous clastics and carbonates (i.e., the Middle Ordovician Simpson Group), and deeper water shelf carbonates and clastics (i.e., the Upper Ordovician through Lower Devonian Viola Group, Sylvan Shale, and Hunton Group). By the Late Devonian and Early Mississippian, subsidence of the Southern Oklahoma Aulacogen increased, and a greater differentiation between shelf and deep-basin deposition occurred. Units reflecting deeper water sedimentation include the Woodford Shale, Sycamore Limestone, the Caney Shale (also known as the Delaware Creek Shale), and the Goddard Shale.

Deformation and uplift of the Arbuckle Mountains occurred as a series of orogenic events that most likely started in the Late Mississippian. Evidence for this interpretation is suggested by the occurrence of conglomerate facies within Chesterian formations of the Ardmore Basin (Caney and Goddard Shales), indicating initial emergence and shedding of sediments off the Arbuckle highlands. The main orogenic event, however, started in the Atochen, and is marked by strong folding and uplift along the Amarillo-Wichita-Criner trend. This orogenic event, termed the Wichita Orogeny, exposed Early Cambrian igneous rocks in the Wichita Mountains and in the northwest Arbuckle Mountains, and lifted the Criner Hills (located just to the south of the Arbuckle Anticline) and Tishomingo-Hunton areas (located to the east of the Anticline) some 15,000 feet above the Ardmore Basin.

The main Arbuckle Orogeny most likely began in the Early Virgilian. At that time the Arbuckle Anticline formed (Fig. 3), and the Wichita fold systems, which included the Criner Hills and Tishomingo-Hunton highlands, were rejuvenated. Sediments shed from the emergent landmass during the Arbuckle Orogeny included the Collings Ranch Conglomerate (still preserved on the north side of the Arbuckle Anticline). The Collings Ranch subsequently was folded and faulted in early Late Virgilian time, and represents the last stages of the Arbuckle Orogeny. This is suggested by the lack of deformation in latest Virgilian units of the Vanoss Conglomerate, which is relatively flat-lying in areas immediately north of the Arbuckle highlands.

Fig. 2. General lithostratigraphic framework near I-35 in the Arbuckle Mountains (adapted from Chaplin and Gomez, 2006). Lower Paleozoic section on next page. Predominantly carbonate lithology shown in blue; and predominantly clastic lithology shown in yellow.



PERIOD	LITHO-STRATIGRAPHY	LITHOLOGY	Thck. (ft)		SIGNIFICANCE
			North Limb	South Limb	
UPPER ORDOVICIAN	Viola Group	Welling Ls.			Hydrocarbon source rock; graptolite-bearing rocks; asphalt-bearing (active oil seeps); fracture porosity; quarried and crushed for road material and aggregate for cement work; forms steep resistant ridges; deepest cuts in the mountains; contains earliest record of vertebrate life in Oklahoma (fish scales & plates)
		Viola Springs Fm.	710	684	
MIDDLE ORDOVICIAN	Simpson Group	Poolville Member			Bromide sands are prolific reservoirs in southern Okla.; Capable of producing in excess of 600,000 barrels of oil per well w/recovery factors as high as 400 barrels of oil per acre/feet at depths less than 6,000 ft; contains probably the largest and most diverse echinoderm fossils ever collected from a single formation anywhere in the world; large trilobites
		Corbin Ranch Submbr			
		Bromide Fm.	80	120	
		Mtn. Lake Member	266	300	
		Tulip Creek Fm.	297	395	
		McLish Fm.	450	475	
		Oil Creek Formation		747	
LOWER ORDOVICIAN	Arbuckle Group	Joins Fm.		294	Asphalt-bearing sands; exhumed reservoir; high purity silica sands; capable of producing in excess of 1 million barrels of oil per well w/recovery factors as high as 800 barrels of oil per acre/feet, at depths less than 7,000 ft
		West Spring Creek Fm.		1,528	
		Kindblade Formation		1,440	
		Cool Creek Formation		1,300	
		McKenzie Hill Formation		900	
		Butterly Dolomite		297	
		Signal Mountain Limestone		415	
		Royer Dolomite		717	
		Fort Sill Limestone		155	
		UPPER CAMBRIAN	Timbered Hills Group	Honey Creek Limestone	
Reagan Sandstone				240	
Colbert Rhyolite				4,500 ft drilled, 7,500 ft estimated; core of Arbuckle anticline; 525 mya; emplacement of both extrusive/shallow intrusive rocks	

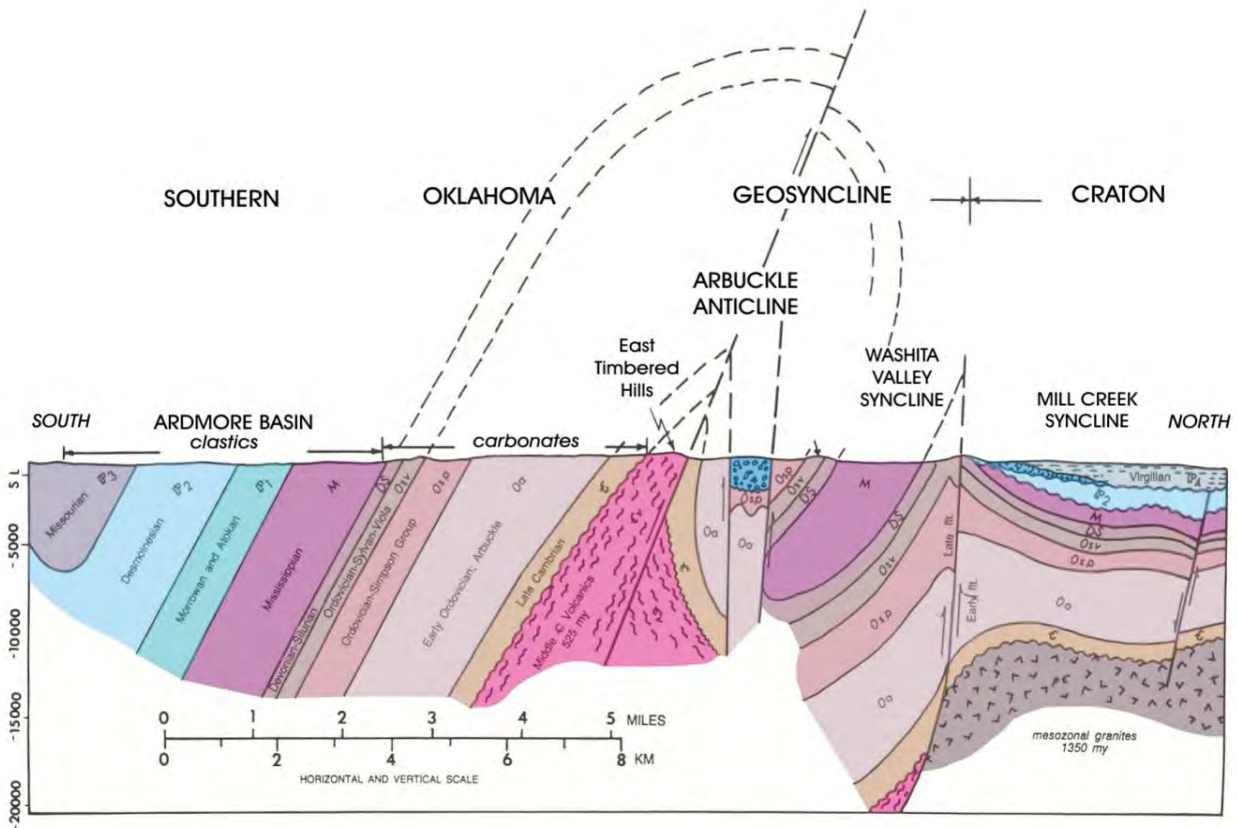


Fig. 3. Structural cross section of the Arbuckle Mountains just west of I-35. The line of the cross section shown on Fig. 6 is in the introductory section (modified from Ham, 1969).

Stop 1A

At this Stop the Washita Valley Fault trace runs slightly north of west, just south of the Geologic Cross Section sign, and separates the Washita Valley Syncline in the north from the Arbuckle Anticline in the south (Fig. 4). Throughout most geologic history, the fault trace



Fig. 4. Trace of Washita Valley Fault (bold line) exposed on ridge west of geologic sign. The fault separates Ordovician Kindblade Formation from Collings Ranch Conglomerate.

separated the rapidly subsiding Oklahoma Aulacogen to the south from the shelf to the north; however, this separation between depositional regimes probably was not accentuated until the Late Devonian.

Classifications of the fault zone have varied. At times the Washita Valley Fault was called a gravity fault, a wrench fault, or an overthrust by different researchers. Problems in its classification probably stem from the fault being reactivated at several different times in the geologic past; movement along the fault would change depending on the tectonic framework at each time. Initially, the Washita Valley Fault probably started as a rift-forming normal fault in the Late Precambrian through Early Cambrian. Evidence comes from the fact that 4,500 ft of Cambrian rhyolite flows are truncated along the south side of the fault zone, but are absent on the north side of the fault. These rhyolites presently crop out near the radio towers on the hill to the west, forming the core of the Arbuckle Anticline. During the Wichita and Arbuckle Orogenies in Late Pennsylvanian, uplift and compression occurred, reactivating the fault, and subsequently produced more of a late stage overthrust-style fault system with left-oblique movement during the formation of the Arbuckle Anticline.

At this site the Washita Valley Fault zone forms the contact between the Kindblade and West Spring Creek Formations of the Early Ordovician Arbuckle Group to the south, and the Late Pennsylvanian Collings Ranch Conglomerate to the north (Figs. 5 and 6). The latest interpretation is that the Collings Ranch formed as an alluvial fan complex within a pull-apart intramontane basin, representing one of the final synorogenic conglomerates deposited during the Arbuckle Orogeny. Uplift and compression continued throughout the time of Collings Ranch deposition, and so, much of the conglomerate was eroded prior to the final tectonic activity. Continued deformation after deposition of the conglomerate is seen on the east side of I-35 in outcrops that exhibit broad synclinal folding with some faulting (Fig. 6).

Texturally, the conglomerate is unsorted, clast-supported, and locally contains graded, and rare, inverse graded bedding. Clasts vary from pebble to boulder size, predominantly made of rock fragments derived from Arbuckle Group carbonates. The unit is moderately cemented by calcite. Sediments that constitute the Collings Ranch were most likely deposited in the proximal part of an alluvial fan complex as channelized flows, spread out laterally as sheet deposits, and/or as lobate-shaped debris flows. Bedded intervals tend to grade from boulder debris flows at their base, up into mud-dominated debris flows. The mud-dominated, debris-flow deposits tend to be weakly cemented, and so, during weathering, the outcrops form distinct recessive bands (Fig. 5). Each interval, boulder-debris to mud-debris, most likely represents an individual tectonic pulse that occurred during the Arbuckle Orogeny. Overall, the conglomerate coarsens upward, suggesting that the alluvial fan complex was prograding basinward to the north.

The monument (Fig. 7), north of the cross section, recognizes Karcher, Haseman, Ohern, and Perrine of the University of Oklahoma, for completing the first seismic reflection survey in August 1921. Their survey was conducted along Vines Branch a few miles north of Dougherty, a town near here. The reflection technique became the major method of petroleum exploration throughout the world.



Fig. 5. Collings Ranch Conglomerate exposed along off-ramp to scenic overlook. Beds within conglomerate probably represent different debris flows in the alluvial fan complex.



Fig. 6. Broad synclinal fold within the Collings Ranch Conglomerate, exposed in the median on both sides of I-35 near scenic overlook turn-off. Structural deformation continued throughout deposition of the conglomerate into Late Virgilian.

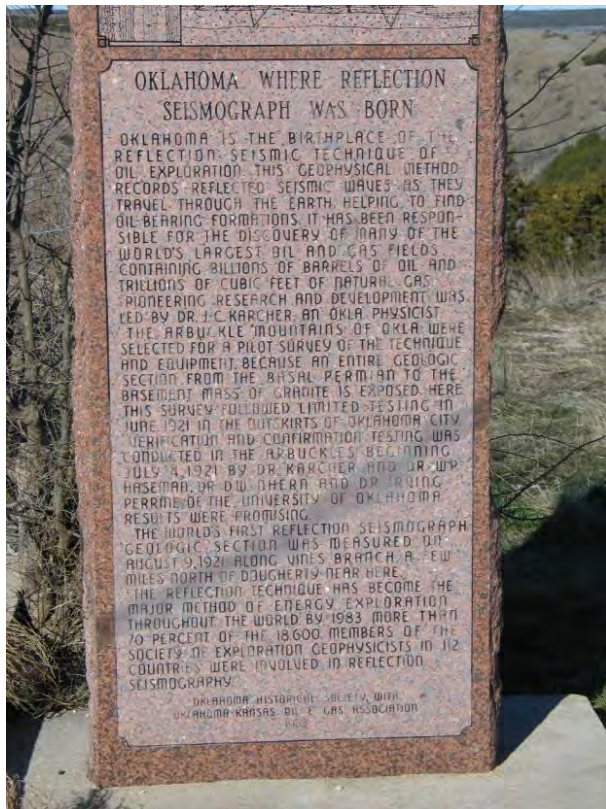


Fig. 7. The Oklahoma Historical Society and the Oklahoma-Kansas Gas Association erected this monument in 1983 to recognize the first seismic reflection survey that was conducted near here.

References

- Chaplin, J.R.; and Gomez, L.D., 2006, Field guide to some selected geological features in the western Arbuckle Mountains, southern Oklahoma: Oklahoma Geological Survey, Unpublished Open-File Report, 137 p.
- Ham, W. E., 1969, Regional geology of the Arbuckle Mountains, Oklahoma: Oklahoma Geological Survey Guidebook 17, 52 p.
- Johnson, K. S.; Amsden, T. W.; Dennison, R. E.; Dutton, S. P.; Goldstein, A. G.; Rascoe, B., Jr.; Sutherland, P. K.; and Thompson, C. M., 1988, Southern Midcontinent region, *in* Sloss, L. L. (ed.), Sedimentary cover—North American craton, U.S. Geological Society of America, The Geology of North America, v. D-2, p. 307–359.
- Johnson, K. S.; and Cardott, B. J., 1992, Geologic framework and hydrocarbon source rocks of Oklahoma, *in* Johnson, K. S. and Cardott, B. J. (eds.), Source rocks in the southern midcontinent, 1990 symposium: Oklahoma Geological Survey Circular 93, p. 21–37.
- Johnson, K. S.; and McCasland, Willard, 1971, Highway geology in the Arbuckle Mountains and Ardmore area, southern Oklahoma: 22nd Annual Highway Geology Symposium, Norman Oklahoma, 31 p.
- Stanley, T. M.; Miller, G. W.; Cardott, B. J.; and Krukowski, S. T., 2006, The Arbuckle Mountains field trip for Devon's 2nd annual geology and geophysics conference, Oklahoma City, unpublished report, 28 p.

STOP 1B. I-35 CONSTRUCTION THROUGH THE MAJOR ARBUCKLE MOUNTAIN CUTS

Leader: Jim Nevels

The site geology of the three major cuts that you will see in the stop were intensely explored in 1968-69 by the geologic staff of Research and Development Division which was adjoined with the Materials Division at that particular time in the Department's history. The basic corridor of study for these cuts was the existing US 77 alignment with numerous exposures of cut-sections. The old US 77 roadway was excavated by blasting where necessary in very winding alignment following the terrain breaks. This construction used prison labor was built in the 1920's.

The cut-sections were not drilled out in depth at all because at this time the Department did not operate adequately equipped drill equipment for this rock exploration. Teams of geologists along with geological support from the Oklahoma Geological Survey in Norman scouted out the final alignment assessing the strike and dip of the different formations with a Brunton compass. The steeply dipping, faulted jointed, and weathered limestones and dolomites (as well as the reddish-brown limestone conglomerates) of the Arbuckle Mountains do not pre-split in the same manner as flat-lying and less fractured rock. However, considering the alternative of conventional rock blasting and some of the negative that it might have such as a high volume of overbreakage, pre-splitting excavation was selected even though the higher cost of the pre-splitting offsets the anticipated cost of handling the overbreakage due to conventional rock blasting.

Presplit hole spacing using 4-foot centers were attempted, but it was soon discovered that 2-foot spacings worked best. Column-type charges were used. A solid $\frac{1}{2}$ to $\frac{3}{4}$ inch column charge was placed to within 5 feet of the top of the drill hole. Here it can be noted that the more massive Collings Ranch Conglomerate pre-splits much better than the steeply dipping layered limestones. Note that in the larger cuts there are three rock benches planned at 12 foot widths. The widths were selected at the time based on standard practice.

My personnel experience during this period of the rock cut excavation was working on the survey crew that laid out the eight aerial targets to be used for the final rock cut pay quantity flight estimate for the contractor. When blasting occurred the survey crew was required to simply leave the site until further notified by construction radio.

Leave STOP 1. Return to I-35 southbound.

63.3	0.3	I-35 Entrance to southbound traffic.
64.0	0.7	Exit 47 to State Highway 77.
65.5	1.5	Scenic overlook.
65.9	0.4	Exit 46
67.9	2.0	Woodford outcrop.
69.0	1.1	Exit 42 to State Highway 53.

Expansive soils and shales at the I-35 and State Highway 53 bridge caused the footing of the pier of the southbound bridge of I-35 to move 2.25 in. southward. At this location, the Springer Formation is composed of alternating layers of soft plastic clay-rich shale beds, and more competent sandstone beds. The clayey shale tends to swell and flow laterally.

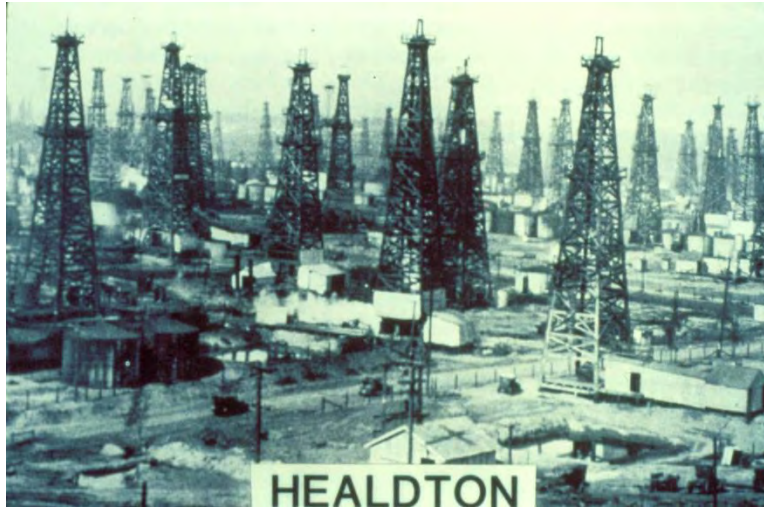


Seasonal wetting and drying caused the north footing of the west bridge to move 2.25 in. southward

69.3	0.3	Bridge.
71.2	1.9	Springer, Exit 40.
78.5	7.3	Ardmore, Exit 33.

Ardmore is a business, cultural, and tourism city as well as the county seat of Carter County. The population was 23,711 at the 2000 census. The town is named after Ardmore, Pennsylvania, a town along the Main Line of the Pennsylvania Railroad. In the early 1900s, the Ardmore area became well known for growing cotton. It became known as the world's largest inland cotton port. When cotton farmers quickly depleted the fertile soil, the cotton industry almost disappeared. In 1913, the Healdton oil field was discovered west of Ardmore. The field became one of the largest in the state. This discovery and many others created an energy-based economy for Ardmore.

Today, Ardmore is the principal center of trade for a ten-county region in south central Oklahoma. Ardmore's major employers are Michelin North America Inc. and Mercy Memorial Health Center. Several hundred employees work for regional distribution centers such as Best Buy, Dollar Tree, Inc. (Marietta), Dollar General Corporation, and others. Velero Energy Corporation has an 85,000 BPD oil refinery in northeast Ardmore. The Samuel Roberts Noble Foundation is located in Ardmore, one of the nation's 50 largest private foundations. The foundation primarily supports agricultural bioresearch activities.



Healdton oil field discovered in 1913 west of Ardmore

79.4	0.9	Ardmore, Exit 32.
80.5	1.1	Ardmore, Exit 31.
83.4	2.9	Highway construction site near Exit 29, STOP 2.

STOP 2. I-35 CONSTRUCTION THROUGH THE ARDMORE BASIN

Leader: Jeff Dean, Oklahoma Department of Transportation

Introduction

This section of Oklahoma Interstate 35 in southern Carter County, was originally constructed in 1968. It begins at the Carter-Love County line and extends north 7.1 miles to the US-70 West interchange. (Figure 1) The original pavement section consisted of 9 inches of plain jointed P.C. concrete on a base of 4 inches of fine aggregate bituminous base, F.A.B.B. The subgrade was treated with hydrated lime to a depth of 6 inches.

The project lies within the Ardmore Basin which extends from a mile south of the Carter-Love county line through Ardmore to the south edge of the Arbuckle Mountains. Geologically, this area is just as distorted and disturbed as the Arbuckle Mountains, but due to the predominance of shale in the basin as opposed to limestone in the Arbuckles, the area is covered with abnormally thick clay soils. The rock units in this area are tilted (dip) at angles approaching vertical, with dip angles of 70 to 80 degrees being common. (Figure 2) The Springer and Goddard shale formations present here are thousands of feet thick and due to

their tilted nature, have weathered much more deeply than the more typical flat-lying rock formations present in most of Oklahoma. These shales produce soil-like conditions to depths of 15 to 18 feet thick instead of the more typical 6 to 8 feet. This situation has produced the highly weathered, swelling soils that dominate this portion of the I-35 alignment. (Reference 1)



Figure 1 – Project Location

The Devils Kitchen (DK) sandstone and conglomerate is present beginning at the south end of the northbound ramps at the US-70 east junction, milepost 29.0, and extends to the US-70 west junction, milepost 31.5. The Devils Kitchen is mostly soft, interbedded sandstone which contains some angular, fine gravel-sized, weather chert conglomerate. The sandstone is present in thicknesses of approximately 500 feet plus. The strike is approximately 330 degrees (N 30 W) and dip is about 80 degrees to the northeast. It consists of two sandstones separated by about 10 or so feet of shale and forms part of the natural dam at Lake Murray. (Reference 3)

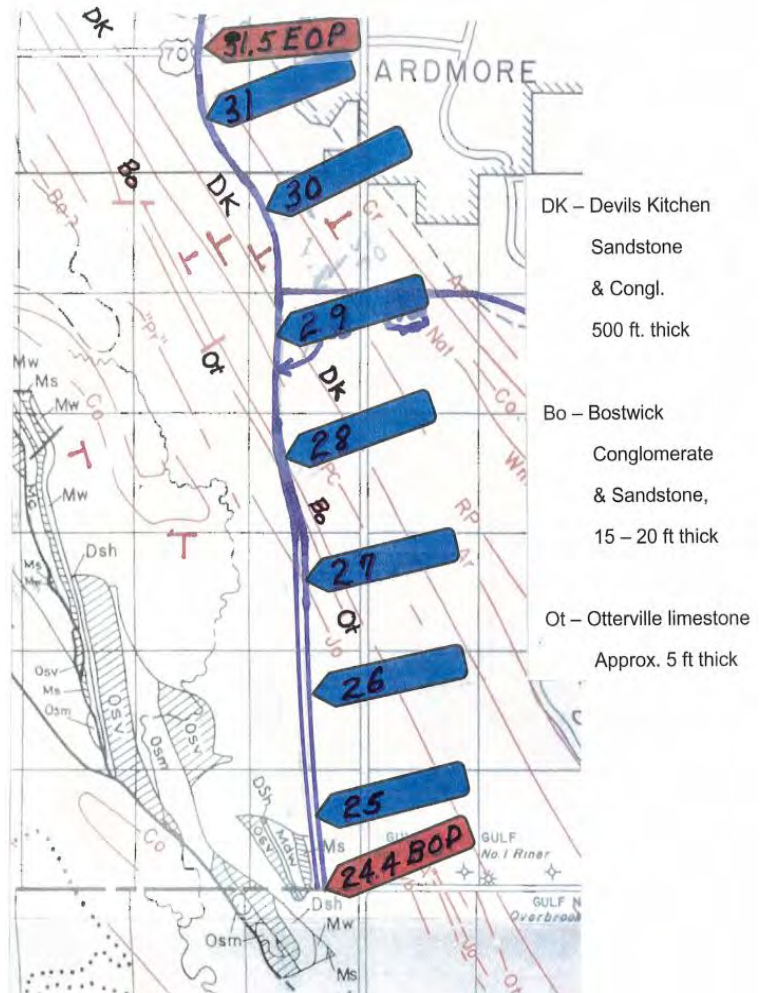


Figure 3 - Geology of I-35 Project (Reference 1)

Soils

Sixty two percent of the 7.1 mile extent consists of clay soils. Of these, 57 percent are high shrink-swell (Vertic) soils. These clays are several feet thicker than normal. This excessive thickness is due to the steep dip of the shale beds. This situation allows surface water to travel through the soil by way of the bedding planes and produce extraordinarily deep soils. They retain these soil-like properties and shrink-swell activity to a depth of 15 feet or more. The predominant soils as mapped by the NRCS consist of the Nomangee, Wilson, and Durant soil series. They are all very deep, very slowly permeable, swelling (Vertic) clays having a dominant smectite mineralogy. These soils make up approximately 45 percent of the clay soils along the 7.1 mile alignment. Four other highly plastic clay soils make up the remainder of the remainder to total 62 percent. They are the Bergstrom, Clarita, Heiden, and Steedman soil series (NRCS).

Project History

Soon after the 1968 completion of this section of Interstate 35, the wetting and drying activity of the heavy clay soils began to cause undulations in the pavement. As these undulations progressed, cracks began to develop in some of the pavement panels and the ride quality began to deteriorate. Pavement panels were repaired or replaced and asphalt overlays were placed in an attempt to restore the ride in the pavement. Through the following years, additional asphalt overlays were placed in order to maintain an acceptable ride quality for the pavement. By 2002, the total thickness of the asphalt overlays had reached up to 14 inches in places. By 2002, despite numerous panel repairs and overlays, the pavement continued to suffer the effects of the heaving clay soils and the costs of maintaining this section of the interstate continued to increase. Given these mounting costs, the decision was made to reconstruct the pavement. Recognizing the severity of the problem soils within the project extents and their effects on the pavement, an extensive soils and geologic investigation was undertaken in order to design a new pavement section that would withstand the detrimental effects of these heavy clays. The soils investigation included numerous test borings, significant soil sampling and testing, a seepage investigation, and a detailed review of the local geology.

New Project Development

The results of the soils investigation found extensive deposits of heavy clays and numerous locations of shallow groundwater seepage throughout the length of the project. The soils tests revealed, as expected, deep deposits of highly plastic clays having plasticity indices ranging from the 20's to the mid 50's. Further analysis of the data indicated an active zone of up to 18 feet in depth. The active zone refers to the upper stratum of the soil profile which exhibits the majority of the shrinking and swelling. This zone undergoes frequent fluctuations in moisture content as affected by climatic cycles. Given these soil characteristics and the depth of this active zone, it became apparent that more extensive measures than the typical 8 to 12 inches of lime stabilization would be needed to find a solution to this problem.

Several options were evaluated as potential solutions to stabilizing these swelling clays. One option evaluated included removing the top 6 feet of the subgrade and reconstructing it with controlled 8 inch lifts of soil compacted at 90 to 95% of standard density and at a moisture content of optimum to 2% wet of optimum. Further evaluation of this option raised concerns about the ability of the contractor to maintain such strict control of the earthwork operations. Failure to adhere to these requirements would lead to the same conditions which caused the early deterioration of the original pavement. This option was rejected. Another option recommended removing the top 6 feet of the subgrade and replacing it with quarry stone. A cost analysis estimated that up to an additional \$5,000,000 would be needed if this option was to be used and it was also rejected.

Another option considered replacing the top 6 feet of the subgrade with a more select soil, with plasticity indices less than 20, which would not be prone to the high shrink swell activity as the soils currently in place. This option was ruled out due to the predominance of heavy clay soils within close proximity to the project. Any soil that might meet the select requirements would require a considerable hauling distance which would add a significant cost to the project.

Further research and literature reviews led to the option of using a moisture barrier to control the swelling clays. The theory behind using a moisture barrier was that if one could control moisture content within the active zone of the soil profile, there would be minimal expansion or contraction within that zone regardless of the extremes in the climatic cycles. Further reviews of the use moisture barriers to control heavy clays lead to several questions which needed to be addressed. These questions involved material selection and placement within proximity of the pavement. There have been several case histories detailing the use of geomembranes or heavy plastic sheeting placed in vertical trenches along the pavement shoulder that have achieved good success for the most part. **(Reference 5)** The concept of the vertical moisture barrier was to encapsulate the upper portion of the soil profile such that fluctuation in moisture content would be kept to a minimum. Vertical moisture barriers had a much higher rate of success provided they were placed to a depth deep enough to maintain this constant, uniform moisture content within the active zone. There have been past projects, incorporating vertical moisture barriers, which did not achieve the anticipated success. The previous undulations and cracks in the pavement returned within a short time after completion of the restoration project. Field investigations attributed this to not placing the barrier deep enough into the active zone of the soil profile. Theoretically this depth needs to be at least 2/3 to 3/4 the depth of the active zone of the soil profile for the barrier to be effective.

Given this design criteria and the 18 feet active zone depth of the soils, within the project extents, the use of a vertical moisture barrier would require trenching and placement of the barrier to a depth of about 14 feet. While this depth might be considered prohibitive, equipment was located which could perform the job at a reasonable production rate. The deciding factors which eliminated this as an option were the numerous utilities such as fiber optic lines and high pressure gas lines as well as several shallow drainage structures which made placement of a continuous, vertical, moisture barrier difficult.

Upon elimination of the vertical moisture barrier option, attention was given to using a horizontal moisture barrier placed on top of the subgrade across the grading section of the new roadway. The issue of concern with this option involved finding an impermeable membrane material that would have the durability to withstand the effects of construction loads and future traffic loads.

The new pavement design called for a base course of 8 inches of crushed aggregate with a 4 inch layer of open graded Portland cement concrete base on top of it. The new pavement would be 12 inches of continuously reinforce concrete, CRCP. The horizontal moisture barrier would have to not only have a high tear resistance but also have the necessary puncture resistance to withstand the placement and compaction of the crushed aggregate base layer. Material options that were considered were use of catalytically blown asphalt and a high strength geomembrane. The catalytically blown asphalt had been used in a project by Colorado DOT on US-40 near Elk Springs. **(Reference 6)** The membrane was placed at a thickness of 3/16 inch and covered with 2 inches of asphalt emulsion treated sand base. A wearing course of 2.5 in. of asphalt concrete was placed throughout. Numerous conversations with local asphalt contractors and equipment distributors revealed a general lack of knowledge regarding material properties and application of a catalytically blown asphalt material. Thus a search began for a geomembrane which would have the required durability. Inquiries to the local material distributor yielded no such material.

Continued searches also ended with little success in locating the required material. The prevailing concern was whether such a geomembrane material even existed.

A visit with the Mirafi representative at a Highway Geology Symposium finally yielded some promising information. He introduced us to a geomembrane product called Nicotarp. This material is a coated reinforced geomembrane, made from a HDPE (High Density Polyethylene) reinforcement geotextile that is coated on both sides with a LDPE (Low Density Polyethylene). It is typically used as a water storage liner. After explaining the intended use of this product and the need to for it to have a high tear and puncture resistance, the representative assured us of his confidence in this material's performance capabilities. He then volunteered to donate a roll of the Nicotarp to use in a field test to simulate the conditions which it would be subjected to during construction.

This field test was conducted at an ODOT maintenance yard near the upcoming Interstate 35 project. (Figures 4 – 8) A test section in the maintenance yard was graded smooth, the Nicotarp rolled out and the aggregate base was dumped on top of it. The aggregate was bladed to a uniform thickness and then compacted with a rubber tired roller. A section of the Nicotarp was then uncovered and inspected for damage. With the exception of a few minor pinholes, the Nicotarp performed very well. All present at the demonstration were in agreement that the operations during the field test were probably more severe than would be expected during the actual project construction. Based on its performance at the field test, the Nicotarp was chosen for use as the horizontal moisture barrier.



Figure 4 – Field Test of Proposed Moisture Barrier, dumping the crushed aggregate onto the membrane



Figure 5 – Field Test of Proposed Moisture Barrier, spreading the crushed aggregate



Figure 6 – Blading the aggregate across the membrane



Figure 7 – Compacting the crushed aggregate



Figure 8 – Exposing the membrane to check for punctures

Since the layout of the moisture barrier was modified from a vertical orientation to horizontal due to the utility and drainage structure obstructions, the decision was made to extend the membrane across the entire grading section plus an additional 20 feet beyond each side. This would make for a total width of 110 feet. For the project station extents requiring pipe underdrain which would intercept any groundwater seepage, the membrane was extended to the bottom of the pipe underdrain trench. By placing the membrane an additional 20 feet beyond each side of the grading section, the belief was that it would achieve the same effectiveness of the deep vertical moisture barrier placed along the pavement shoulder (Figure 9).

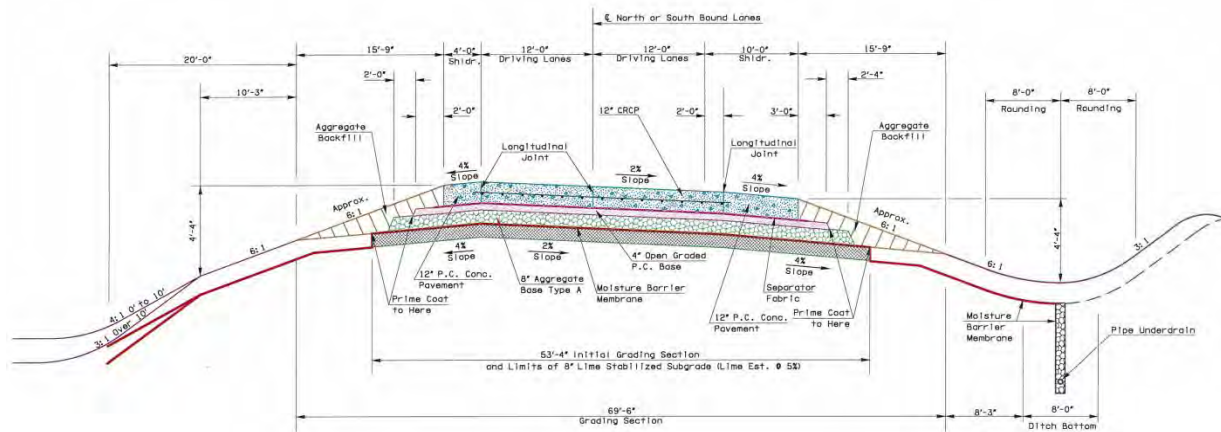


Figure 9 – Typical Section of Reconstructed Pavement

The design was finalized and the project was let out for bid. The bids received, in the first bid letting, exceeded the amount budgeted so the decision was made to divide the originally proposed 7 mile project in to 2 separate projects. The first project would begin at the Carter-Love county line and extend north approximately 4.1 miles. A second project would begin after completion of the first project and complete the 7 mile extent. The first of the 2 projects was awarded in August 2006 and completed in 2008. The second project was awarded in October 2009 and is currently under construction. Figures 10 through 23 show the sequence of removing the old pavement and reconstruction.



Figure 10 - Removal of the old pavement; note the thickness of the overlay and the condition of the old concrete pavement



Figure 11 – Lime Stabilization operations



Figure 12 – Trenching for pipe underdrain



Figure 13 – Moisture barrier placed across the grading section



Figure 14 – End dumping the crushed aggregate. Construction equipment was prohibited from driving on the membrane



Figure 15 – Spreading the crushed aggregate



Figure 16 - The aggregate base layer is completed. Twelve inches of top soil and slab sodding will be placed on the shoulders



Figure 17 – Placing the open graded base on top of the crushed aggregate base. A non-woven geotextile separates the two layers



Figure 18 – Compacting the open graded base layer



Figure 19 – Placing the steel reinforcement for the CRCP, another layer of non-woven geotextile was placed upon the open graded base



Figure 20 – Tying the steel reinforcement



Figure 21 – Sawing control joints in the new pavement



Figure 22 – The completed project.



Figure 23 - Open to traffic

References

1. Hayes, Curtis J., Geologic Assessment Report for the I-35 Carter County Project, 2003
2. Engineering Classification of Geological Materials for Division 7, Oklahoma Highway Department Research and Development Division, 1969
3. –Field Conference Guide Book Pennsylvanian of the Ardmore Basin, Southern Oklahoma,” Ardmore Geological Society, 1966
4. –Soil Survey of Carter County, Oklahoma,” USDA, Soil Conservation Service, Soil Survey Staff,, 1979.
5. Nelson, John D. and Miller, Debora J. –Expansive Soils, Problems and Practice in Foundation and Pavement Engineering” , John Wiley & Sons
6. Brakey, B. A. Moisture stabilization by membranes, encapsulation, and full depth paving. Proc. Workshop on Expansive Clays and Shales in Highway Design and Construction, University of Wyoming, Laramie, 1973

88.1	4.7	TURN RIGHT at EXIT 24
88.4	0.3	TURN LEFT at STOP SIGN; State Highway 77S to Lake Murray State Park.
88.8	0.4	STOP SIGN, junction with U.S. Highway 77, go straight.
91.3	2.5	STOP SIGN, TURN LEFT (north).
92.5	1.2	TURN RIGHT onto Cisco Road to Tipp’s Point.
93.0	0.5	Cisco Picnic Pavilion, STOP 3.

STOP 3. LUNCH

LAKE MURRAY STATE PARK AND REGIONAL GEOLOGY

Leaders: Kenneth V. Luza and Stanley T. Krukowski, Oklahoma Geological Survey

History of the Lake Murray

Lake Murray is located 2 mi east of US Highway 77 and 4 mi south of Ardmore in southern Carter and northern Love Counties, Oklahoma. The major arms of the lake occupy the deep valleys of the West and East Anadarche creeks as well as the eastern tributary of Fourche Maline Creek (Fig. 1). It sits among hills forested by blackjack and post oak.

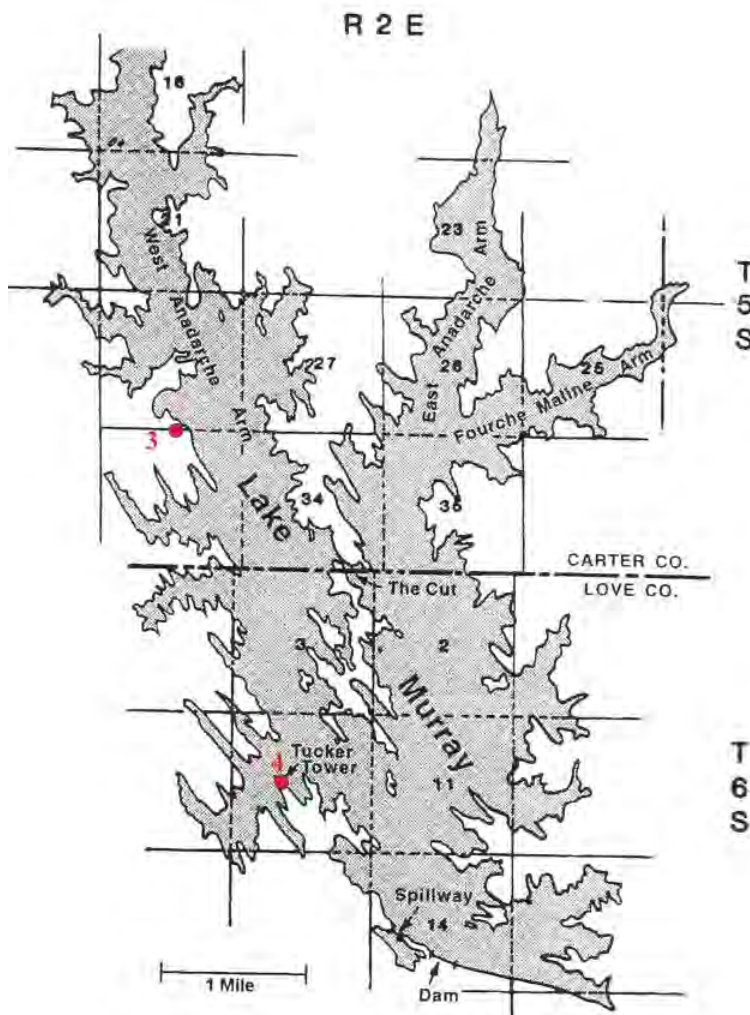


Fig. 1. Map of Lake Murray in Carter and Love Counties (Allen, 1996) and Stops 3 and 4.

In 1928, the Gypsy Oil Company (later Gulf Oil) initiated a research program to map the surface geology in Ardmore Basin. Charles A. Milner, Jr., W. Morris Guthrey, and later, Charles W. Tomlinson mapped these beds by plane table and meticulously searched each bed for fusulinids for correlation purposes. They mapped a unit in the lower Deese called the Devil's Kitchen Member. It contained a massive bed of sand and chert that stands as an almost vertical wall where Anadarche Creek cuts a 600-ft wide and 130-ft deep channel through it. They recognized that this feature could be adapted for use as a dam to form a lake.

They lobbied their local senators and representatives for the dam. Senate bill 382 was passed in 1933, giving the State Board of Affairs authority to condemn and buy the land for Oklahoma's first state park. The land (with minerals) was purchased for \$90,000.

The federal government formed the CCC (Civilian Conservation Corps) and the WPA (Work Projects Administration) by 1933. The Lake Murray project was submitted for federal evaluation. Approval was granted, and work on the project began in July 1933. CCC workers cleared the area of vegetation; WPA workers built the dam. Most work was done with mule teams, wagons, and hand tools.

More than 10,000 men, who had been on relief, shared the jobs. Each man worked a five-day week, for \$1.80 per day. Wages for one day provided food for a work week. The balance was enough to feed a man's family for about one month. A group of approximately 1,000 men would work for one week then another group would relieve them. The dam, 600 ft long and 150 ft high, was completed in 1937. The park was open to the public in 1938.

Self-liquidating bonds were proposed to finance the construction of a lodge after World War II. The bonds would be sold, and then later they would be paid back with money earned from rental property. The Supreme Court of Oklahoma approved the idea. It was a first for the State of Oklahoma and a second for the entire nation. (Self-liquidating bonds were first sold to build a toll road in Pennsylvania.) The lodge was dedicated in 1949.

Lake Murray is a 5,728-acre body of water; it took seven years to fill. It became the largest body of water in the State at that time. At the dam, the water is 130 ft deep; 8 mi from the dam the water depth averages 25 ft (Fig. 2). The park covers 21,000 acres of land.

Geology of the Park

The park is located in the Ardmore Basin and on the east flank of the Criner Hills Uplift (Fig. 3). Middle Pennsylvanian to lower Cretaceous units are exposed in the park. Rock units of Deese and Hoxbar Groups crop out along the Lake Murray shoreline. The strata dip at angles up to 90° and form long, linear, forested ridges. Many of the beds produce oil just to the west of the Lake Murray area.

The Dornick Hills Group (Atokan-Morrowan) contains the oldest strata that crop out in the southwest part of the Park. Only the upper part of the Dornick Hills is exposed in the park.



Fig. 2. Marina and beach area at Lake Murray State Park.

It consists predominantly of light brown-gray, platy shale with minor amounts of coarse conglomerate, limestone, and sandstone. Two major limestone units occur in the park. The top of the group is defined by the Pumpkin Creek Limestone, a 92-ft thick limestone that has a chert pebble conglomerate near its base. The Frenshley Limestone occurs below the Pumpkin Creek. It consists of six variable limestone beds interstratified with gray shale.

The Deese Group (Desmoinesian) contains strata from the base of the Confederate Limestone down to the top of the Pumpkin Creek Limestone. The group consists dominantly of gray, gray-brown, and red platy shale. About 15% of the strata are sandstone beds, which are most abundant in the lower and middle portions of the group. They attain thicknesses up to 50 ft. At the Lake Murray spillway, sandstones thicken to 150 ft. The limestone beds are generally less than 10 ft thick, hard, thin-bedded, impure, and locally conglomeratic. Locally one limestone member, the Arnold Limestone, attains a thickness of 25 ft.

The Hoxbar Group (Missourian) contains strata from the top of the Zuckerman Sandstone to the base of the Confederate Limestone. This group consists dominantly of greenish-gray to gray platy shale beds. The Hoxbar has more limestone units and fewer sandstone units than the underlying Deese. There are four prominent 10- to 20-ft thick limestone beds within the Hoxbar. The limestone beds are spaced about 400–500 ft apart. The lowermost limestone, the Confederate Limestone, with a maximum thickness of 60 ft, forms the base of the Hoxbar. The limestone beds are generally thin-bedded and contain numerous shale seams. The Zuckerman Sandstone is the most prominent sandstone member in the Hoxbar. It consists of four to five light gray, fine-grained, hard, limy sandstone beds up to 10 ft thick.

The Oscar Group (Virgilian) overlies the Hoxbar in the northern part of the park. There is an angular unconformity between the lowermost Oscar beds and the uppermost Hoxbar beds. The Oscar consists predominantly of maroon to gray shale beds and minor amounts of soft, brown sandstone and arkosic sandstone beds. Several relatively soft conglomerate beds occur in

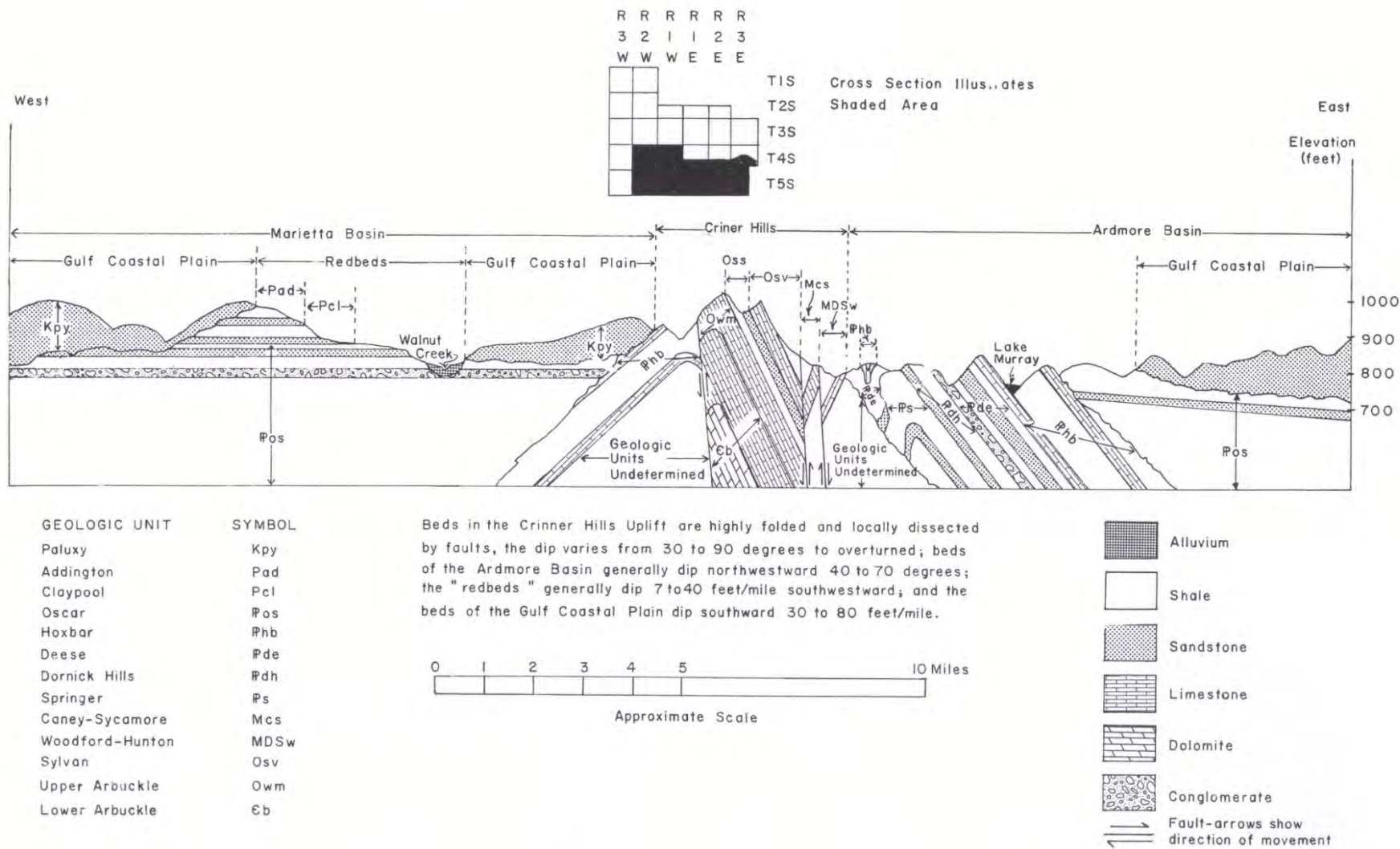


Fig. 3. Idealized cross section (shaded area) in Carter County (Hartronft and others, 1969).

the upper 100 ft of the Oscar. The unit generally forms gently rolling prairies with only slight tree-covered scarps formed by thicker sandstone and conglomerate beds.

The Antlers Formation (Paluxy in Fig. 3) overlies the Oscar Group on the east side of the park. This Lower Cretaceous unit is white to yellow, medium-grained, weakly-indurated sandstone. Varicolored shale beds occur throughout the Antlers. As an aquifer, it yields moderate to large amounts of water of good quality.

References

- Allen, R. W., 1996, A history of Lake Murray: Oklahoma Geology Notes, v. 56, no. 3, p. 106–115.
- Frederickson, E. A.; Redman, R. H.; and Westheimer, J. M., 1965, Geology and Petroleum [of] Love County: Oklahoma Geological Survey Circular 63, 91 p.
- Hart, D. L., Jr., 1974, Reconnaissance of the water resources of the Ardmore and Sherman quadrangles, southern Oklahoma: Oklahoma Geological Survey Hydrologic Atlas 3, scale 1:250,000, 4 sheets.
- Hartronft, B. C.; Smith, M. D.; Hayes, C. J.; and McCasland, Willard, 1969, Engineering classification of geologic materials and (related soils): Oklahoma Highway Department, Division 7, 302 p.



Devils Kitchen Conglomerate above Tucker Tower parking lot

93.5	0.5	STOP SIGN, TURN LEFT (south)
94.6	1.1	Lodge and Park entrance (left); GO STRAIGHT.
98.3	3.7	Road to Tucker Tower, TURN LEFT.
99.2	0.9	Tucker Tower parking lot, STOP 4.

STOP 4. TUCKER TOWER AND LOCAL GEOLOGY

Leaders: Kenneth V. Luza and Stanley T. Krukowski, Oklahoma Geological Survey

Picturesque Tucker Tower, 65 ft high and named after State Senator Fred Tucker, sits on steeply dipping outcrops of the Devil's Kitchen Conglomerate. Governor William H. "Alfalfa Bill" Murray originally planned the tower as a summer retreat (Fig. 1). At first he had opposed the state park project, but Alfalfa Bill changed his mind when the lake was named after him, citing his effort in locating the lake and state park in southern Oklahoma. Lake Murray was the first state park built in Oklahoma and remains the largest.



Fig. 1. View of Tucker Tower perched on the Devils Kitchen Conglomerate. Picture taken from Lake Murray marina.

In 1933 construction began on the castle-like building as part of the public works project as part of the Works Progress Administration (WPA) and Civilian Conservation Corps (CCC) depression-era programs. Although the lake was finished in 1937 and opened to the public in 1938, work on the tower stopped in 1935 when federal officials determined that it was too costly and took too long to complete. The tower remained unfinished without windows, doors, floors, or ceilings until the state park service completed its construction.

In 1954 Tucker Tower opened as a geology museum, featuring the granular hexahedrite meteorite found on state park property in the 1930s. Today the focus of the tower is that of a nature center featuring wildlife as well as geology. The 90 million-year-old meteorite, the largest of its kind, is also the fifth largest meteorite in the world. It was sawed in half by the Institute of Meteorites in New Mexico to observe its interior.

The Devil's Kitchen Member of the Deese Group, about 500 ft thick, begins 800 ft above the top of the Pumpkin Creek Limestone. It is divided into three intervals. Its base has a medium-grained buff sandstone 100–200 ft thick. A 160-ft thick argillaceous shale and fossiliferous thin bedded limestone occurs in the middle. At the top there is a 110-ft thick chert-pebble conglomerate sometimes called the Devil's Kitchen Conglomerate (Fig. 2).

The upper sandstone unit develops southeastward from Ardmore into a coarse conglomerate that contains angular to subangular chert pebbles (Fig 3). This phase grows thicker and more dominant southeastward from here for almost 6 mi. The angularity of pebble clasts suggests a relatively close source such as the Quachita Mountains (Tomlinson, 1929). The absence of limestone pebbles from the Devil's Kitchen Conglomerate may indicate that there was no great relief above sea level in the Criner Hills, the nearest source of limestone (Tomlinson, 1929).

References

- Frederickson, E. A., 1957, Geologic map of the Criner Hills area, Oklahoma: Oklahoma Geologic Survey Map GM-4, scale: 1:20,000 (approximate).
- Tomlinson, C. W., 1929, The Pennsylvanian System in the Ardmore Basin: Oklahoma Geological Survey Bulletin 46, 79 p.
- Tomlinson, C. W.; and McBee, Jr., William, 1959, Pennsylvanian sediments and orogenies of Ardmore district, Oklahoma, *in* Mayes, J. W.; Westheimer, Jerome; Tomlinson, C. W.; and Putman, D. M. (eds.), *Petroleum Geology of Southern Oklahoma: The American Association of Petroleum Geologists, Tulsa, Oklahoma, v. 2, p. 3-52.*



Fig. 2. Beds of the Devils Kitchen Conglomerate dip about 25° to the north at the east end of Lake Murray spillway.



Fig. 3. Angular and subangular chert clasts in the Devils Kitchen Conglomerate.

100.0	0.8	STOP SIGN, TURN RIGHT (north).
103.7	3.7	TURN LEFT (west), State Highway 77S.
106.1	2.4	STOP SIGN, junction with U.S. Highway 77, GO STRAIGHT.
106.5	0.4	RIGHT at entrance to I-35 northbound.
115.1	8.6	Ardmore, Exit 32.
126.8	11.7	Mile marker 44.
130.0	3.2	TURN RIGHT at EXIT 47 to Turner Falls.
130.4	0.4	STOP SIGN, TURN LEFT (west).
130.5	0.1	STOP 5.



Differential weathering and erosion of alternating hard and soft limestone layers produce a unique “tombstone topography” (best seen on U.S. Highway 77 near the West Spring Creek Formation sign)

STOP 5. BRIDGE CONSTRUCTION IN KARST TERRAIN

Leaders: Oklahoma Department of Transportation and Kenneth V. Luza and Stanley T. Krukowski, Oklahoma Geological Survey

At this stop, and in the adjacent roadway, jointed distorted limestone and dolomite beds of the Royer Dolomite are locally dissolved to produce systems of vertically oriented caves or chimneys partially or completely filled with clay. The Royer Dolomite is a cream to yellowish pinkish gray (stained yellowish orange), coarsely crystalline, slightly glauconitic, massive tectonic dolomite. The Royer contains numerous networks of honeycomb-shaped solution pits and vugs.

The dissolution of pipes and chimneys are remnants of a paleokarst profile developed in the Pennsylvanian Period after the Arbuckle Mountains were uplifted. “Recent” dissolution (karsting) of the former surface formed large vugs, small caves, and sinks filled in with red (terra rosa) fines, vegetation, and breccia clasts. Most infill is derived from terra rosa (red, clay-rich sediment) soils that developed on the Pennsylvanian paleokarst surfaces and subterranean cavities (Fig 1). The terra rosa subsequently was washed into the Royer paleokarst profile. Not all infill fines, however, are from the development of a terra rosa. Some infill is cream to gray in color, and may have originated at a different time (Chaplin and Gomez, 2006).



Fig. 1. Chaotic blocks of Royer Dolomite with small sinkholes, caves, and dissolution channels filled in with red clay-rich sediment (south side of U.S. Highway 77).

A low-angle thrust fault separates the younger Fort Sill Limestone from the Royer Dolomite on the north side of the road cut (Fig. 2). The Fort Sill consists of gray, shallow-water, interbedded, thin, light-gray carbonate mudstones, dolomitic limestones, and laminated brownish dolomites occurring in beds measuring 1–2 in. in thickness. Limestone rip-up clasts in a dolomitic matrix produce an edge-wise conglomeratic appearance. Mottled (bioturbated) textures occur throughout the carbonates. Rare greenish gray shale partings appear locally. Limestone beds increase toward the base of the exposure. The beds become more strongly folded near the fault plane. Veins and fractures of sparry calcite, 1–2 mm wide, crisscross the face of the outcrop.

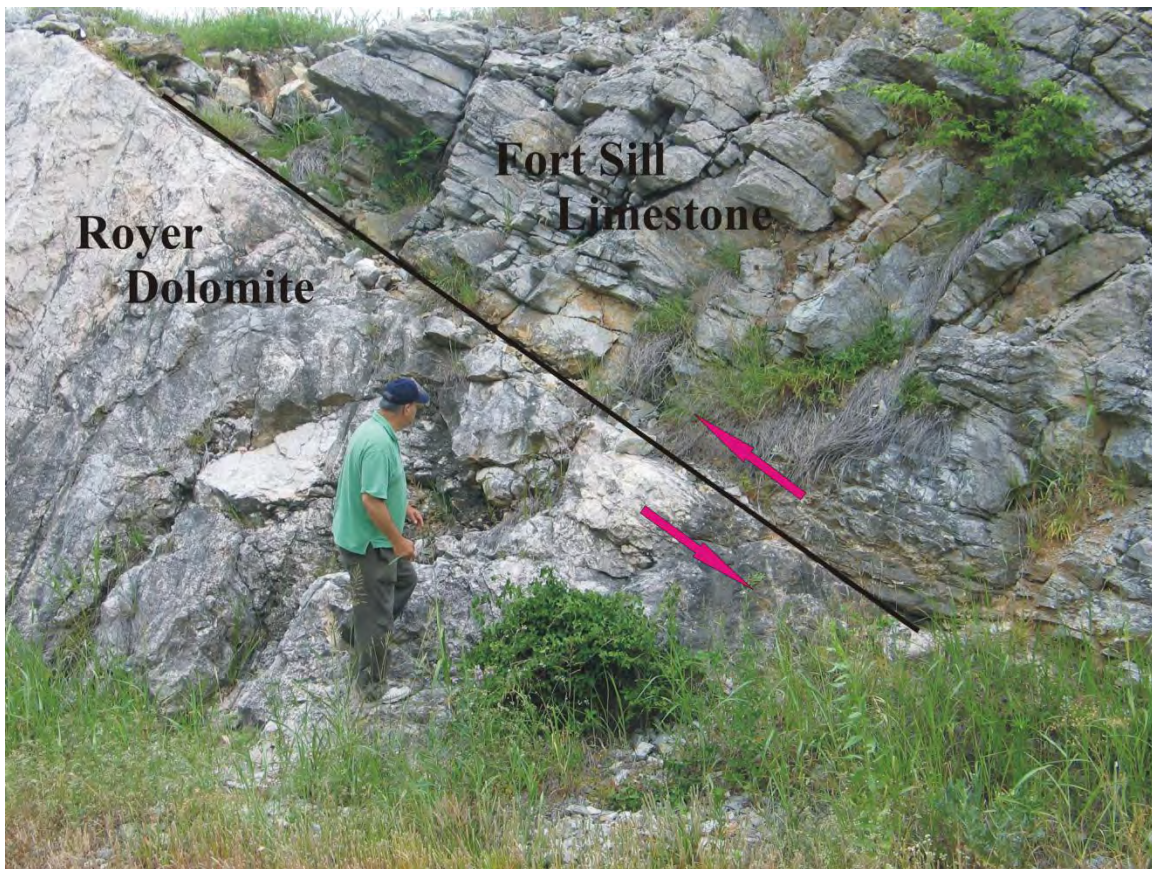


Fig. 2. Thrust fault on north side of U.S. Highway 77, west of I-35, southbound lane.

Numerous steeply dipping faults, joints, and bedding planes allow surface water to pass into and through the rock formations, eventually producing the chimneys. Routine drilling and exploration did not reveal the presence of any sizeable cavities within 20 ft of the subgrade elevation at this stop. During I-35 construction, the tops of several chimneys were exposed in the roadbed. Their diameters ranged from 4 ft to 12 ft, and depths varied greatly, from 1–2 ft to about 20 ft. A road grader broke through one weak cave roof and fell 14 ft into a small cavern in the Fort Sill Limestone on November 22, 1968 (Fay, 1989) about .65 mi north of this stop. Water was still actively moving through the cavern, which may have developed by carbonate dissolution along a fracture plane or by solution-widening of a pre-existing paleocavern. Similar caverns are present along the north flank of the Arbuckle Mountains.

At the juncture of I-35 and SH 77 stop on the US 77 roadway, the two 56-70-56-foot continuous plate girder overpass structures are at approximately ground level while the US 77 was constructed in a ½ : 1 cut section. Borings for the bridge indicated massive dolomite and limestone from the top of the ground to well below the grade line of the US 77 roadway elevation. The piers for the bridge were set on spread footings just below the elevation of the bottom of the roadway ditches.

The abutments were designed to set on top of the rock cut backslope in what the borings showed to be massive dolomite and limestone. But at the location of the south abutment of the west structure and the location of the north abutment of the east structure, clay filled solution channels were wide enough to cover a major portion of the abutment area (being originally planned to set on top of rock). This problem caused a change in plans.

To correct for the chimneys uncovered in the I-35 roadbed, the holes were filled with 3/8 inch gravel, and a concrete cap was poured over the top as a seal. The continuously reinforced concrete paving used across the entire Arbuckle Mountains area was deemed adequate to bridge the filled and capped cavities as well as any small chimneys that did not fail during construction.

The effects of the wide clay-filled cavities and chimneys encountered in two of the four abutments for the overpass were minimized by changing construction plans to set the abutments on stem footings seated into firm rock (Fig.3). Slope walls were required to retain the clay material at the these two abutments and still conform to the ½ : 1 backslope design (Figs. 4–5).



Fig. 3. South bridge abutment of northbound I-35 bridge over U.S. Highway 77, and blocks of Royer Dolomite filled in with red, clay-rich sediment.

References

Chaplin, J.R.; and Gomez, L.D., 2006, Field guide to some selected geological features in the western Arbuckle Mountains, southern Oklahoma: Oklahoma Geological Survey, Unpublished Open-File Report, 137 p.

Hayes, C. J.; Nevels, Jim; and Luza, Ken, 1988, Geotechnical problems in the Arbuckle Mountain area of southern Oklahoma: Oklahoma Department of Transportation unpublished 13th annual southwest geotechnical engineers conference field trip guidebook, 35 p.



Fig. 4. Slope wall used to retain the clay and loose rock at the northbound bridge abutment.

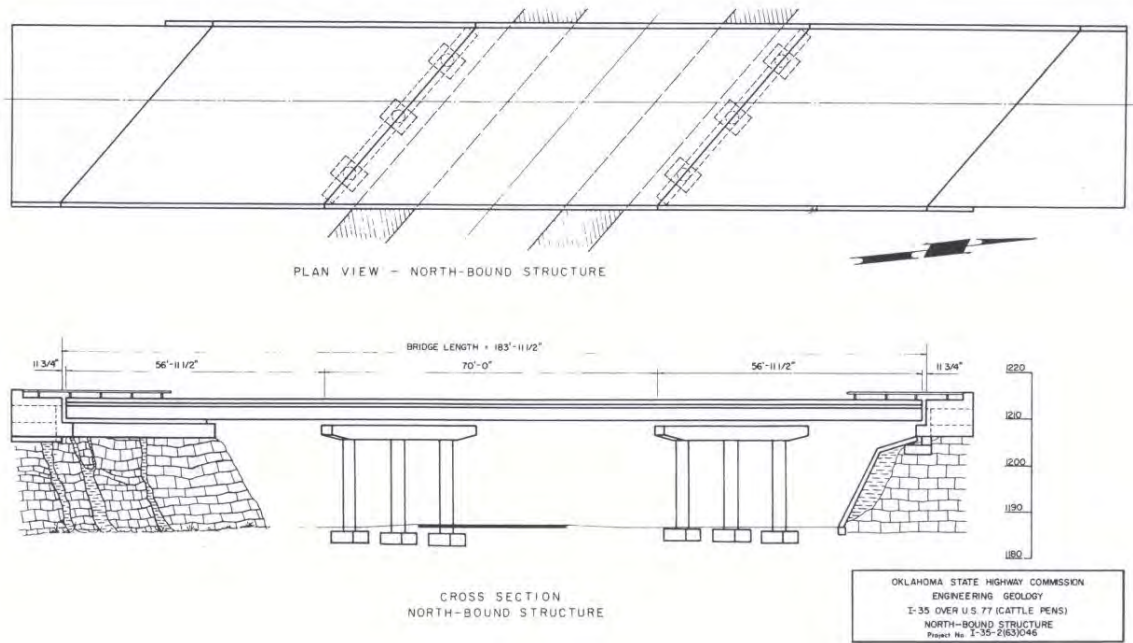


Fig. 5. Plan view and cross section of I-35 Bridge at interchange with U.S. 77, northbound lane (Hayes and others, 1988).

132.7 2.2 **STOP 6**

STOP 6. TURNER FALLS OVERLOOK
Leaders: Stan Krukowski and Kenneth V. Luza

Spring-fed Honey Creek is the water source for 77-foot high Turner Falls. The falls were named after Mazeppa Thomas Turner, who represented Murray County in the Oklahoma Legislature from 1907 until 1911. Turner a native Virginian, married Laura J. Johnson, a Chickasaw, and became a farmer. In 1878 the couple moved to the Honey Creek area where he discovered the waterfall that bears his name.

Turner Falls is one of Oklahoma's most popular tourist destinations. Today the 1,500-acre resort offers visitors recreational activities that include swimming, cave exploration, hiking trails, picnicking, and overnight camping. The city of Davis has owned the park since 1919 and operated it from 1919 to 1950. The city resumed management of the park in 1978 after the city had leased it previously to outside interests (Sanchez, 2007).

Off to the right (north) of the falls from the overlook one can spot Collings Castle. Inspired by Olde English Architecture the castle was constructed with Native materials in the early 1930's by Dr. Ellsworth C. Collings, a professor at Oklahoma University for many years (Fig 1.). The structure served as the BAR-C Ranch headquarters as well as Dr. Collings summer home." (Inscription found on monument at the site commemorating the castle.)

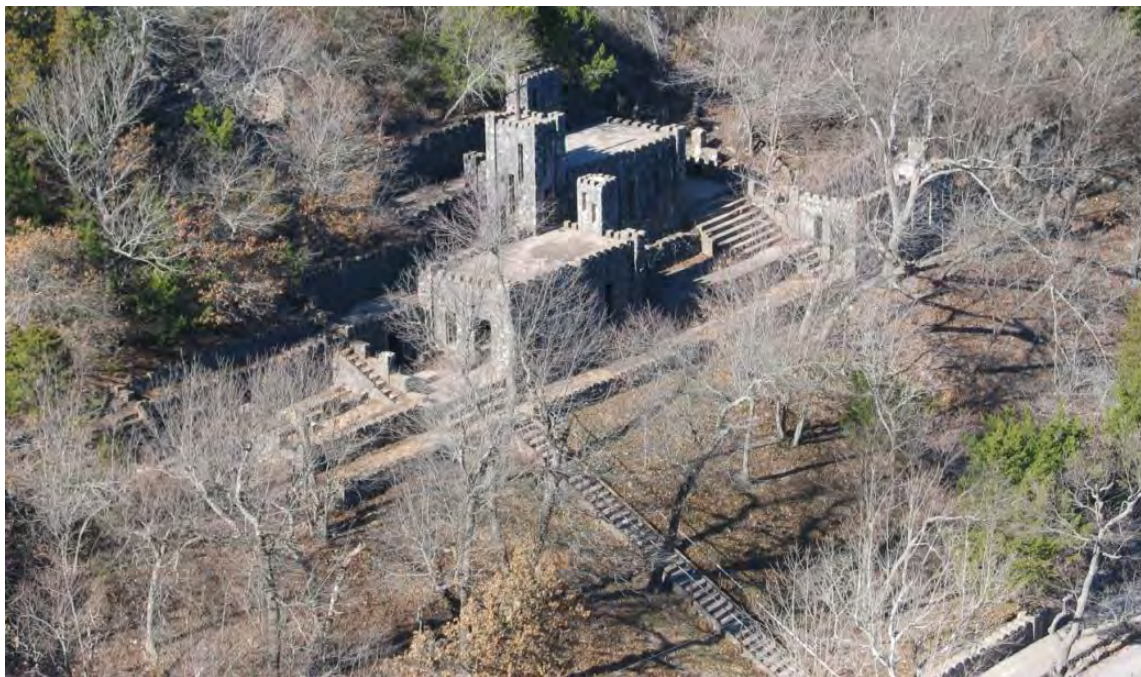


Fig. 1. Collings Castle as seen from the Turner Falls overlook.

The East Timbered Hills, composed of Carlton Rhyolite, provides the scenic background to Turner Falls. The microwave transmission towers on the hill to the southwest are located at one of the highest points in the Arbuckle Mountains. Between the Carlton Rhyolite and the Turner Falls overlook are the complexly deformed units of Late Cambrian and Early Ordovician rocks on the north limb of the Arbuckle Anticline.

At the overlook one can examine a section of the Ordovician McKenzie Hill and Cool Creek Formations (Arbuckle Group). The contact between them is fault related; the fault trace runs almost at the base of the falls. The cliffs on either side of the falls represent the footwall of the fault. Just north of the overlook is the trace of the Washita Valley Fault zone, which is crossed a number of times along US-77 north of the Turner Falls stop. The fault at the base of Turner Falls probably represents one of the many splays that extend from the Washita Valley Fault. Immediately to the north of the Washita Valley Fault is the Collings Ranch Conglomerate. Steep road cuts in the Collings Ranch along the hairpin curves of US-77 just north of Turner Falls overlook provide an excellent opportunity to observe the poorly sorted, limestone boulder conglomerate of Pennsylvanian age.

The water from Honey Creek, above the falls, deposits travertine and tufa (Fig. 2). The travertine appears as yellowish-tan material exposed in the streambed and falls. The amount of carbonate minerals deposited here is equal to, or slightly exceeds, the amount of carbonate dissolved and mechanically eroded along Honey Creek during times of flooding; consequently, Turner Falls is prograding rather than receding as do most waterfalls.

Tufa forms from supersaturated alkaline water. In limestone terranes or karst areas, stream water may tend to be supersaturated with calcite; however, tufa commonly forms only at waterfalls and cascades. Physical changes at waterfalls are largely responsible; these include aeration, jet-flow, and low-water-pressure effects. These in turn produce basic changes in the physical conditions of the water, namely the size of the air-water interface and stream flow velocity. An increase in either condition can lead to rapid CO₂ degassing with resultant calcite precipitation. When the air-water interface area and water velocity increase, the pH of the stream water is raised and calcite (or aragonite; CaCO₃) is precipitated.

The outcrops at the overlook belong to the Cool Creek Formation, which is about 1,300 ft thick. The Cool Creek is typical of much of the lithologies of the Arbuckle Group exposed in the Arbuckle Mountains. Two sections of the Cool Creek are exposed at this location. The lower boundary (contact with the McKenzie Formation) is recognized by the abundance of quartz sand in the sequence. The thick, stratigraphically lower section is exposed in the cliff face below; however, the stone stairway leading down to the base of the cliff (about 300 ft below) is closed to pedestrian traffic due to its deterioration. Another section is exposed along the road cut along US-77 across the road from the Turner Falls gift shop.



Fig. 2. Turner Falls looking down from the overlook toward the west. Brown tufa with its cascading waters contrast with the dark gray of the limestone water gap.

The Cool Creek represents peritidal deposition along a broad, carbonate ramp (Chaplin and Gomez, 2006). Fifth-order, cyclic sedimentation is evident in many exposures. Major lithologies in the Cool Creek include the following: stromatolitic boundstones; intraformational conglomerates; quartz-rich, oolitic packstones and grainstones; peloidal wackestones, packstones, and grainstones; thin, small-scale, trough-cross-bedded quartz sandstones; lime mudstones; and heterolithic units (e.g. flaser deposits).

Stromatolitic boundstones and intraformational conglomerates are readily recognizable and constitute a substantial portion of the outcrops. The fairly large, hemi-spherical stromatolite mounds characterize the subtidal components of the cycle. The mounds are exposed near the steps behind the gift shop (Fig. 3). Various forms of stromatolitic and thrombolitic boundstones are the result of algal growth patterns responding to varying depths of water and their associated energy regimes. Chert nodules are common within the thrombolite units.



Fig. 3. Large, hemi-spherical stromatolite mounds characterize the subtidal environment of deposition in the Cool Creek Formation.

The intertidal facies have smaller, digitate stromatolite (or algal buildup) intervals, interbedded between flat-pebble conglomerates (algal, rip-up clasts that were immediately re-deposited; Fig. 4) and centimeter- to millimeter-scale (rhythmic, algal mat accumulations) carbonate mudstones with mud cracks. The intraformational conglomerates are composed of lime-mud clasts, but they also include fragments of stromatolites, algal mats, and other lithologies. Most conglomerates are mud-supported.

Allochems found in the grainstones are primarily intraclasts and ooliths. Invertebrate skeletal debris is uncommon, but fragments of trilobites, brachiopods, and gastropods can be found. Peloids are the dominant allochems observed in packstones and wackestones; some have well-developed laminations, while others show evidence of bioturbation.



Fig. 4. Flat-pebble conglomerates with algal, rip-up clasts that were re-deposited immediately during and after a storm event.

Examples of the intertidal facies can be seen on the other side of the road. The increased frequency of thin sandstone beds, and planar laminated carbonate mudstones with abundant desiccation cracks characterize the shoaling, supratidal facies.

The Cool Creek lithofacies and sedimentary structures suggest a hypersaline, peritidal, semi-arid or arid environment. Lithofacies suggest depositional environments ranging from subtidal to supratidal. Evaporite relicts within supratidal units may provide evidence for a sabkha environment.

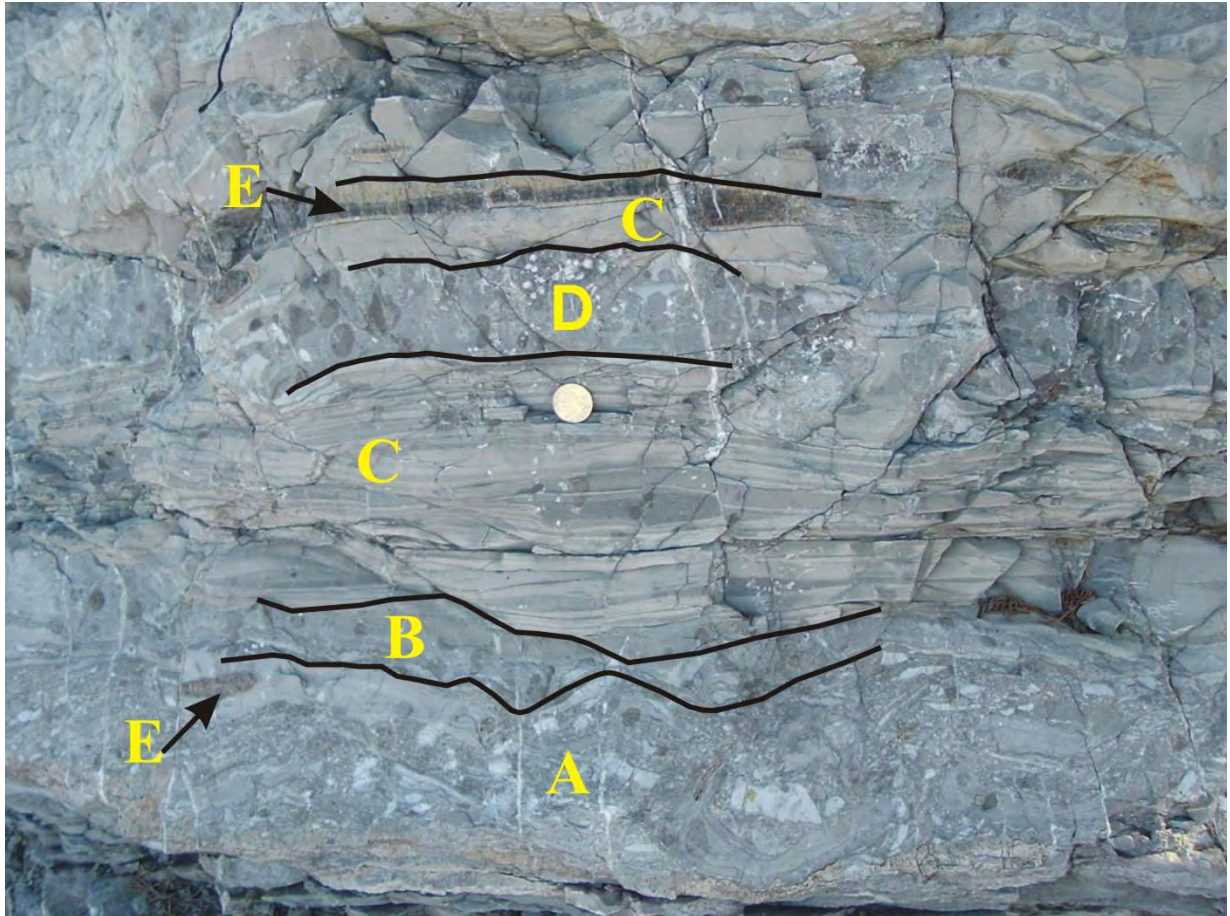
The Cool Creek carbonates show evidence of an upward shoaling sequence. About half the cycles recorded from the Cool Creek are complete, shoaling-upward sequences. Each cycle is about 14 ft thick. In many instances each cycle is asymmetrical or incomplete, where one facies dominates a particular cycle.

References

Much of the text came from many sources dealing with the Arbuckle Mountains region including the following:

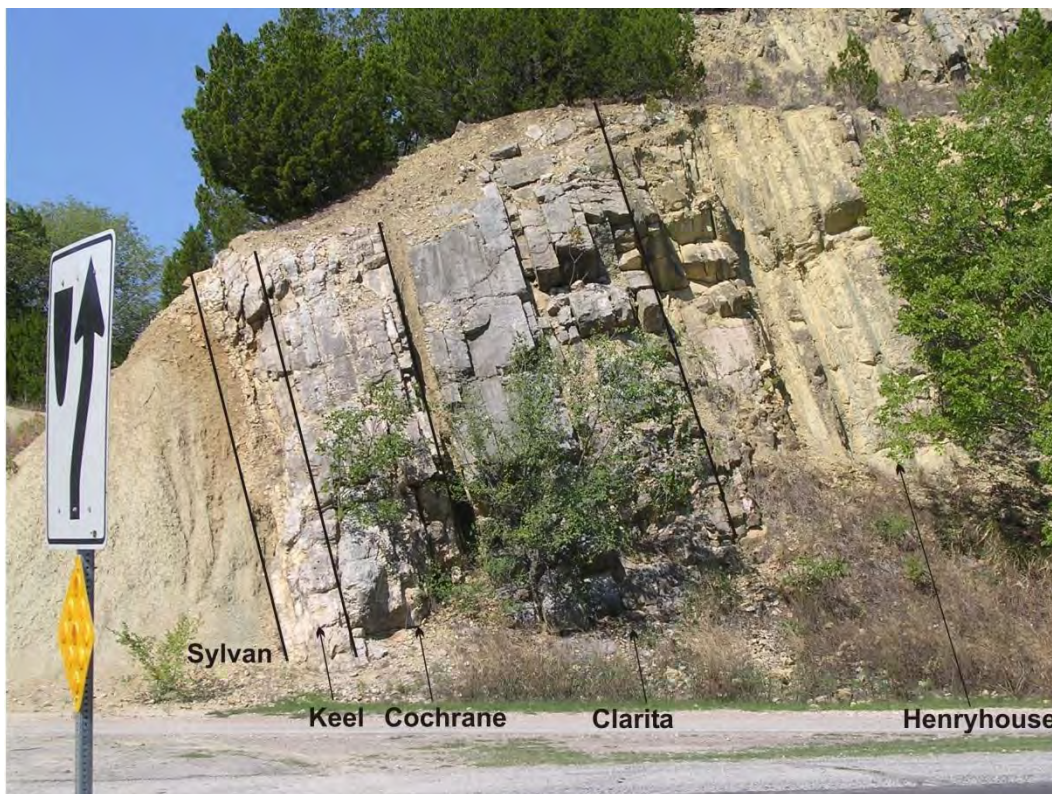
- Brown, W.G.; and Grayson, R.C., 1985, Tectonism and sedimentation in the Arbuckle Mountain region, southern Oklahoma aulacogen: Baylor University, 43 p.
- Chaplin, J.R.; and Gomez, L.D., 2006, Field guide to some selected geological features in the western Arbuckle Mountains, southern Oklahoma: Oklahoma Geological Survey, Unpublished Open-File Report, 137 p.
- Fay, R.O., 1989, Geology of the Arbuckle Mountains along Interstate 35, Carter and Murray Counties, Oklahoma: Oklahoma Geological Survey Guidebook 26, 50 p.

- Ham, W.E., 1969, Regional geology of the Arbuckle Mountains, Oklahoma: Oklahoma Geological Survey Guidebook 17, 52 p.
- Sanchez, Joe, 2007, Turner Falls, Oklahoma Encyclopedia of History and Culture, <http://digital.library.okstate.edu/encyclopedia>, accessed May 13, 2010).
- Stanley, T.M., 2001, Stratigraphy and facies relationships of the Hunton Group, northern Arbuckle Mountains and Lawrence Uplift, Oklahoma: Oklahoma Geological Survey Guidebook 33, 72 p.



Photograph of Cool Creek Fm. Limestone taken along US Highway 77 east of the curio store at Turner Falls overlook: A. intraformational conglomerate; B. algal encrustation along the top of unit A; C. flaser bedding with alternating lime mudstone and quartz packstone; D. algal boundstone with characteristic cross section of early thrombolite development; E. chert beds and/or nodules

Across from the fried pie store, good exposures of the Sylvan Shale, Hunton Group, Sycamore Limestone, and base of the Caney Shale can be seen at this location. The Woodford Shale is poorly exposed and only its very base can be seen. The outcrop here is in the south limb of the Washita Valley Syncline. Structural orientation of the formations is steeply dipping to the east, and is well illustrated by the Sylvan Shale-Hunton Group contact on the west side of the outcrop.



Steeply dipping contact between the Sylvan Shale and Hunton Group

The Hunton is composed of a number of thin lithostratigraphic units that were deposited throughout the Late Ordovician then ending in the Early Devonian. The units of the Hunton represent shallow-water to moderately deepwater sedimentation along a carbonate ramp. Most units are very fossiliferous, and many world-renown Silurian and Devonian fossil localities occur within the Group.

The Woodford consists of an organic-rich, fissile black shale with abundant chert nodules and beds. Phosphate nodules are common throughout, and sandstone usually occurs at the base of the formation. Given the shale's high organic content, the Woodford has been interpreted as being deposited in deepwater, anaerobic conditions and so represents the most likely source for hydrocarbons in Oklahoma. Deepwater deposition and subsidence continued in this area as the Woodford grades into the overlying Sycamore Formation and Caney Shale. Here, the Sycamore is represented by a dense, slightly argillaceous, unfossiliferous, carbonate mudstone, with local shale partings and interbeds.



Overturned contact between Sycamore Limestone and Caney Shale

132.9	0.2	Collins Ranch Conglomerate
134.0	1.1	Honey Creek Bridge
135.6	1.6	TURN LEFT at entrance ramp to northbound I-35.
139.8	4.2	Davis/Duncan, Exit 55, State Highway 7.
161.2	21.4	Washita River Bridge

The Washita River begins its course in the eastern Texas panhandle and continues flowing through western and southern Oklahoma terminating in Lake Texoma. The river is 295 mi (475 km) long. As it encounters the Arbuckle Mountains, the Washita cuts through a granite gorge dropping 150 ft/mi (3%). The streambed is mostly mud and fine sand making its sediment load unusable for most sand and gravel applications; however, the fine sand can be mined for masonry and fill sand. Along most of its course the Washita's deeply incised banks consist of red shale and mudstone, making it one of the most silty/muddy streams in the U.S.

The river is also known for the Battle of the Washita River, which took place on November 27, 1868. Hostilities commenced when Lt. Col. George Armstrong Custer and his 7th U.S. Cavalry attacked Cheyenne Chief Black Kettle's village in the early morning hours near what is today the town of Cheyenne, Oklahoma.



NOAA Severe Storms Laboratory's Doppler radar unit (white ball) and producing oil well on North Campus, The University of Oklahoma

196.1	34.9	I-35/Main Street bridge in Norman
213.0	16.9	North Canadian Bridge.
213.3	0.3	TURN LEFT, EXIT 126, to I-40 west.
214.2	0.9	TURN LEFT, EXIT 150C, to Robinson Ave. and downtown Oklahoma City; take NORTH ROBINSON EXIT.
214.5	0.3	TURN RIGHT to Robinson Ave.
215.0	0.5	TURN RIGHT at Sheridan.
215.1	0.1	TURN LEFT at Broadway.
215.2	0.1	TURN RIGHT on Park to Skirvin Hotel entrance.

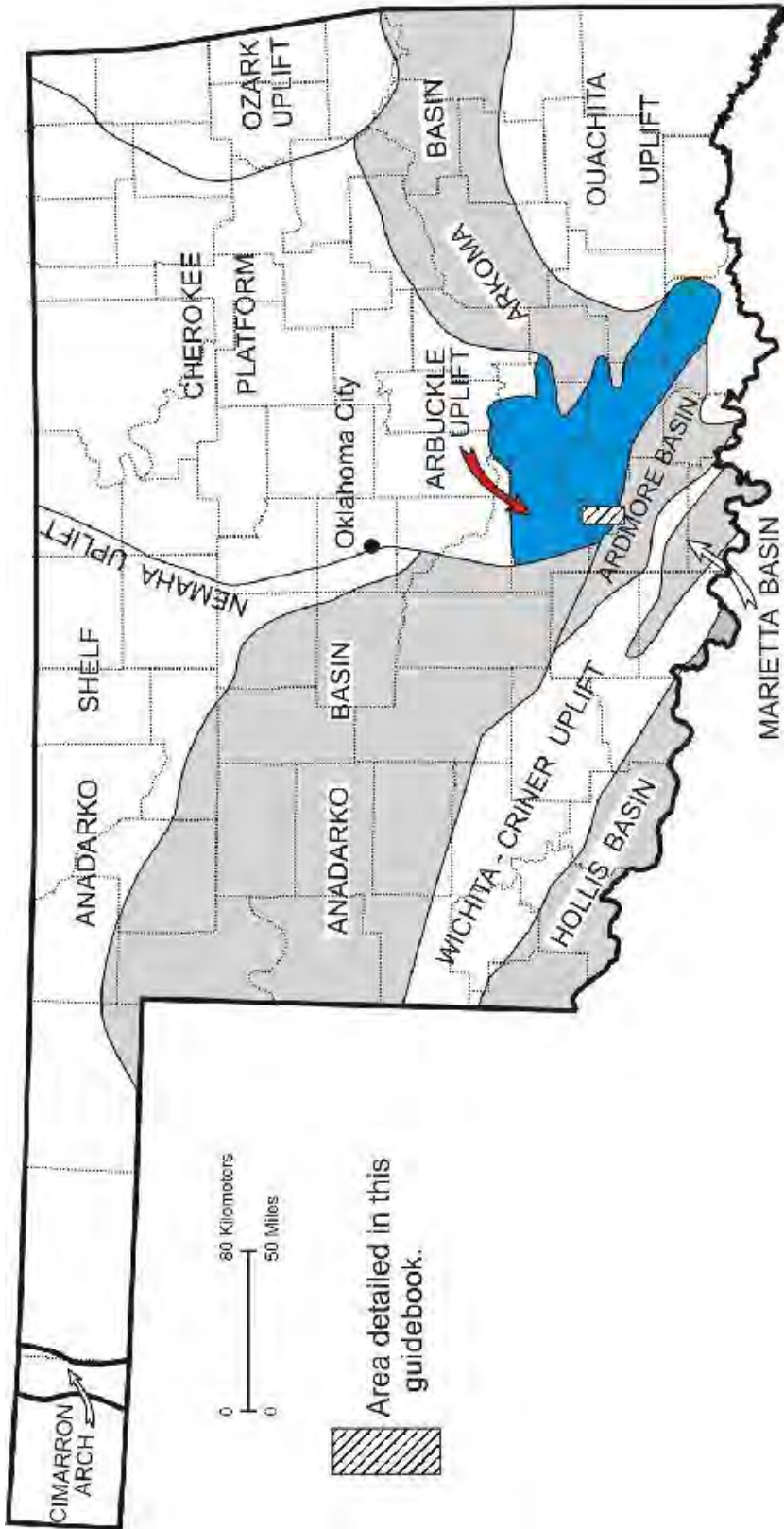
The Skirvin Hilton Hotel, in the middle of the downtown area, is within walking distance of many attractions such as the Cox Convention Center, Ford Center Arena, Bricktown Canal and Entertainment District, Bricktown Ballpark, Oklahoma City National Bombing Memorial, Oklahoma City Arts Museum, and Civic Center; it is only a five-minute drive from the State Capitol.

Known for its elegance for over 95 years, the historic Skirvin Hotel has hosted oil barons, dignitaries, political leaders, and Presidents. Having undergone a major renovation, the project restored the Skirvin to its original grandeur that was responsible for making it an Oklahoma City landmark. The restoration preserved historic elements whenever possible; guests may appreciate original moldings, tiles, and ceilings as well as all the conveniences of a modern luxury hotel.



Skirvin Hotel (photograph by David K. Luza)

Historical and statistical information comes from community web sites, Wikipedia, and Oklahoma Place Names by G. H. Shirk (1987)





Preliminary Agenda

GAM Symposium at HGS: “Asset Management in a World Of Dirt”

August 23 - Oklahoma City, OK

- 12:00 Opening/Introduction – Larry Pierson/Vanessa Bateman/Dave Stanley
- 12:15 Keynote Speaker: J. Erik Loehr (University of Missouri) – Overview of Geotechnical Asset Management
- 12:45 Blaise Hansen (WYDOT) – “Database Development for GAM”
- 1:15 Kirk Beach/Robert Liang (Ohio DOT/University of Akron) – “Enterprise Database for GAM”
- 1:45 Chris Power (Mott MacDonald) – “GAM for United Kingdom Highways”
- 2:15 Break
- 2:30 Matt DeMarco (FHWA) – “National Park Service Retaining Wall Inventory”
- 3:00 Darren Beckstrand (Landslide Technology) – “Alaska’s Unstable Slope Management Program – Field Data Collection and Management”
- 3:30 John Thornley (HDL Anchorage) – “Geotechnical Asset Management of Buried Structural Components”
- 4:00 Discussion
- 5:00 Closing

WYDOT GEOLOGY PROGRAM'S DATABASE DEVELOPMENT FOR GEOTECHNICAL ASSET MANAGEMENT

By Blaise Hansen and Mike Schulte

*Abstract...*The Wyoming Department of Transportation (WYDOT) recognizes that the implementation of Transportation Asset Management (TAM) programs is an essential component to improve cost effectiveness and project scheduling. The Geology program contributes to this process by managing over 15,000 records of data pertaining to geotechnical engineering. Working with the Information Technology (IT) program, the Oracle Application Express 3.2.1.00.10 software was utilized to develop and design databases for Library/Maps, Aggregate Sources, Water Wells, Rockslopes, Geosynthetics, Bedrock Properties, Geophysics, Pile Driving, Landslides and Projects. Establishing a central storage location and is indispensable to accessing, searching, and the sharing of information. This has resulted in the ability to establish trends to enhance design recommendations and to organize the increasing amount of geotechnical information obtained with every investigation that is undertaken. The status of integration is almost 100% complete with future applications to include the ability to display information geographically and combining data with other agencies for project development.

Enterprise Database System for Effective Geotechnical Asset Management at Ohio DOT

Kirk Beach
Geology Program Manager
Office of Geotechnical Engineering
Ohio Department of Transportation
Columbus, Ohio 43223

Robert Y. Liang
Professor
Department of Civil Engineering
University of Akron
Akron, Ohio 44325-3905

Asset management has been recognized as an important agency function in performing strategic and systematic evaluation of cost-benefits of various built infrastructures so that maintenance, repair, or rehabilitation decisions can be made with well-defined objectives, known conditions, constraints, and desired outcomes. Priority setting and resource allocation, based on various scenario investigations, would ultimately help preserve values of the built infrastructure, and extend their service life with optimum repair and maintenance strategies. In short, asset management is about agency's operating, maintaining, and preserving the built infrastructure system in the most cost-effective manner to achieve desired service objectives. To facilitate effective asset management, there is a need for developing an enterprise level tool that is built on GIS based database platform with internet connectivity. Ohio DOT has spent a considerable amount of effort in developing a general tool for building their enterprise level geological hazard management system. The developed tool can be easily adapted for their geotechnical asset management as well. In this presentation, the makeup of the system in a GIS based database platform will be briefly described with emphasis on analogies between the database for geotechnical asset management and geological hazard management. The four components of the system include: (a) an inventory module containing relevant information such as traffic count, physical attributes of the inventory site, and maintenance record, (b) heuristic condition rating matrices for each physical site, (c) a repair and maintenance cost estimation module, and (c) a project tracking module. The functionalities of each component will also be described in detail, again with particular attention to its applications in asset management. More interestingly, the special tools (Tablet PC with blue tooth connections with various site reconnaissance devices) for field work in collecting physical conditions of the site, such as spatial coordinates, images of features, wireless connections with different physical measurement devices and internet connections, etc. As an illustrative example, ODOT current practice on collecting mechanically stabilized wall (MSEW) performance data will be used to demonstrate the usefulness of such an enterprise level Asset Management System. The challenges and benefits in developing such an enterprise based geotechnical asset management system will be discussed at the end of this presentation.

Geotechnical Asset Management Symposium
Highway Geology Symposium – August 23-26, 2010 – Oklahoma City

Title: Making Informed Decisions: Geotechnical Asset Management for the UK Highways Agency

Authors: David Patterson (UK Highways Agency), Christopher Power (Mott MacDonald), Mark Rudrum (Arup), David Wright (Atkins)

Abstract

The UK Highways Agency has responsibility for the maintenance and upkeep of a network of over 7,000 km (4350 miles) of Motorway and major trunk roads in England. As with any major road authority, this stewardship role includes management of a diverse range of assets (pavements, structures, drainage, technology etc.) all of which are supported by the crucially important Geotechnical Asset. The UK Highways Agency is no different from any US federal, state or local transportation agency in that key budgetary decisions have to be made across all assets that are balanced to provide a selected level of service provision for a minimum optimum Whole Life Cost.

The Highways Agency has an established Geotechnical Asset Management (GAM) process in place that is now underpinning the development of increasingly sophisticated Decision Support Tools (DSTs). These DSTs are not yet fully integrated into the HA business, but are now beginning to be recognised as a major part of the wider Agency Integrated Asset Management (IAM) strategy.

This paper will describe the GAM processes of the UK HA. It will describe the collection of Geotechnical Asset inventory and condition information (that underpins the entire process), the storage of core data in a Geotechnical Data Management System (HA GDMS), the importance of data quality and currency and the development of Decision Support Tools to assist in long-term asset investment planning. It will describe current research and development projects that are being undertaken to support the developing strategy of the HA and will outline the vision of the Agency for a future integrated asset management strategy.

The paper will hopefully enable UK and US geotechnical practitioners to recognise that despite major differences in scale and geographical location, we are all seeking to overcome the same challenges, and that an exchange of experience can be extremely beneficial to future developments.

The National Park Service Retaining Wall Inventory and Assessment Program (WIP): 3,500 Walls Later

Matthew J. DeMarco, Geotechnical Group Lead
FHWA, Central Federal Lands Highway Division
Lakewood, CO Matthew.DeMarco@fhwa.dot.gov

Abstract

Beginning in 2004, the FHWA Federal Lands Highway Division (FLH) teamed with the National Park Service (NPS) to develop and implement a retaining wall inventory and condition assessment program supporting roadway asset management efforts underway throughout U.S. Parks. The vast majority of Park earth retaining structures were built prior to 1960, with many built circa 1935, making the assessment of this aging asset a high priority within the NPS.

The NPS Retaining Wall Inventory and Assessment Program (WIP) assesses wall performance and develops preliminary repair/replace work orders by measuring, describing, and/or evaluating nearly 60 wall parameters within five main categories: Location, Function, Geometrics, Condition, and Required Action. Beyond the basic inventory aspects of the WIP, the condition assessment considers 25 numerically rated wall elements along with apparent design criteria, failure consequence, and cultural concerns to determine recommended actions and costs to monitor, maintain, repair or replace a given wall. To date, approximately 3,500 walls have been assessed in 33 National Parks, including 20+ wall types within a wide range of geographic settings. Findings indicate the overall health of the 4 million square feet of inspected retaining wall assets within the NPS is good, with approximately a third of the walls requiring minor maintenance or repair and less than 3% of the total asset requiring substantial element repair or complete wall replacement despite the relative old age of the inventory.

This presentation describes key development and implementation aspects of the WIP and overviews the condition assessment and wall performance findings for the various wall types encountered. In addition, remedial actions by wall type are discussed, identifying common wall element distresses and deficiencies and recommended repair strategies. The soon-to-be-published comprehensive WIP Procedures Manual will be made available to meeting participants at the time of the presentation.

Alaska's Unstable Slope Management Program – Field Data Collection and Management

Darren Beckstrand, C.E.G., Landslide Technology, 10250 SW Greenburg Road, Suite 111, Portland, Oregon

Thomas Westover, Landslide Technology, 10250 SW Greenburg Road, Suite 111, Portland, Oregon

Lawrence Pierson, C.E.G., Landslide Technology, 10250 SW Greenburg Road, Suite 111, Portland, Oregon

David Stanley, C.P.G., Alaska Department of Transportation and Public Facilities, 5750 E. Tudor Road, Anchorage, Alaska

Landslide Technology in partnership with the Alaska Department of Transportation and Public Facilities (AKDOT&PF) have begun a multi-year project to implement an unstable slope asset management program (USMP). Unstable embankments, and soil and rock slopes will be inventoried and rated according to hazard and risk criteria initially developed by University of Alaska Fairbanks and subsequently finalized by Landslide Technology and AKDOT&PF geotechnical and maintenance personnel.

For such efforts in the past, it had been common practice to collect field data on paper forms and then to transcribe the information into an electronic database. In order to automate this process and avoid common data entry and transcription errors, an electronic database was prepared with data entry forms that matched the rating system that accepted all field rating information, digital photographs, and GPS positions. This concept is not new. Electronic field data has been used to collect similar field information with a number of methods that require various hardware and software packages that range from handheld GPS computers with custom database software to laptop computers with spreadsheets.

For the USMP, a ruggedized convertible tablet Windows-based computer with built-in GPS was selected as the primary piece of hardware. This provided the benefits of a laptop computer, such as familiar operations, large screen size, and ease of use with the added capabilities of a built-in GPS and pen-based data entry. The tablet PC also allows the annotation of photographs in the field with notes and conceptual mitigation measures. Other supporting hardware includes digital cameras with built-in GPS and geotagging capabilities, and laser rangefinders.

The field data collection database was built using Microsoft Access as the database software. The database was coded with the interoperability with Google Earth, enabling simplified visualization and accessibility of rating data and site photographs. For more detailed geographic analysis and mapping, the database functions well with ArcGIS software. Using this common software package will enable the Department to easily augment the database in the future to add standard of service and life-cycle information as the asset management efforts are completed and the ultimate goal of completing a Geotechnical Asset Management system for unstable slopes is realized. This database will serve as the basis for the gathering system wide information and managing data for this asset management program.

ASSET MANAGEMENT OF BURIED GEOTECHNICAL STRUCTURAL COMPONENTS – A CASE STUDY

By: John D. Thornley and David Stanley

ABSTRACT

Geotechnical components such as retaining structures used in transportation systems are assets that are often difficult to quantify and manage until a premature failure occurs. One area of concern for geotechnical structures includes the potential for corrosion of buried components such as soil nails used in slope stability applications and buried reinforcements used in mechanically stabilized earth (MSE) walls. The Nevada Department of Transportation has over 150 MSE walls at 39 locations. Recently, high levels of corrosion were observed due to accidental discovery at two of these locations. The resulting investigations of these walls produced direct measurements of metal losses and electrochemical properties of the MSE reinforced fill. One MSE wall was replaced with a cast-in-place concrete tie-back wall at great expense.

It is shown that the original MSE reinforced fill approval electrochemical test results are significantly different from those measured in post-construction investigations. The internal stability analyses (using AASHTO 2007 LRFD) of two remaining MSE walls at an intersection were also performed and estimated remaining service lives are significantly less than the design life of 75 years. A geotechnical asset management evaluation contrasts the cost framework of wall failure, wall replacement due to accidental discovery as seen in this case study, and the proactive method of corrosion monitoring and management. Very few owners of MSE walls use monitoring as a management technique. However, this case study offers evidence that corrosion monitoring of buried geotechnical components should be a tool in the toolbox of Departments of Transportation across the United States.

The Geology Program's contribution to the Wyoming Department of Transportation Asset Management program.

By Blaise Hansen, GIT, EIT, and Mike Schulte, PG

*Abstract...*The Wyoming Department of Transportation (WYDOT) recognizes that implementing Transportation Asset Management (TAM) programs is an essential component to improve cost effectiveness and project scheduling. The Geology Program contributes to this process by managing over 15,000 records of data pertaining to geotechnical engineering. Working with the Information Technology (IT) program, the Oracle Application Express 3.2.1.00.10 software was utilized to develop and design databases for Library, Geologic Maps, Aggregate Sources, and Projects. Establishing a central storage location is indispensable to accessing, searching, and the sharing of information. This has resulted in the ability to establish trends to enhance design recommendations and to organize the increasing amount of geotechnical information obtained with further investigations. The status of integration is almost 100% complete, with future applications to include the ability to display information geographically and combining data with other agencies for project development.

INTRODUCTION

The Wyoming Department of Transportation (WYDOT) recognizes that implementing Transportation Asset Management (TAM) programs is an essential component to improve cost effectiveness and project scheduling. The Geology Program contributes over 15,000 records to decision making in WYDOT. Establishing a central storage location allows for the efficient administration of this volume of data and eases accessing, searching, and the sharing of this information. It will also preserve this body of knowledge for future generations when group members retire or move to different jobs. The Geology TAM program provides the ability to establish trends to enhance design recommendations, display information geographically, and to manage the increasing amount of geotechnical information obtained with future investigations. Prior to this undertaking, records were kept in an Access database or a Quattro Pro spreadsheet. The Information Technology (IT) program took preexisting data and imported it into Oracle Application Express 3.2.1.00.10 software. After highlighting several of the software features utilized to operate the database, the content and some initial applications of the Library, Geologic Maps, Aggregate Sources, and Projects sections of the Geology database will be summarized in this paper.

Access to the database is established through a secure log-on process. The default screen displayed is the Projects section (Figure 1) as indicated by the highlighted word on the top row. This row contains the links to the sections which comprise the Geology database. The Administration link allocates rights to utilize and access the database. Geology and Information Technology are the only WYDOT programs that have the capacity to manipulate information, but other state agencies will be permitted to view the database in the future. Access by a Federal agency could be obtained if required but, it will not be offered to the public. The middle row displays the headings that compose a selected portion of the database. The bottom row contains links to tables that serve two functions. The majority of these are entries to drop down menus utilized to create or edit entries within the database. Others perform as links to additional sources of information.

Project	Description	Project Geologist	LRS	Reference Marker	Primary Location	County	Improvement Type	Number of Combined Jobs	Active	De Loc
00000	-	All Geologists	-	-	-	-	-	-	N	-
0007068	CHEY STS/SUMMIT/RIDGE-COLLEGE	Mike Schulte	NA	0-.335	Y	Laramie	Reconstruction	1	Y	-
003-6(10)	-	All Geologists	-	-	-	-	-	-	N	-
010-3(21)	-	All Geologists	-	-	-	-	-	-	N	-
010-3(38)	-	All Geologists	-	-	-	-	-	-	N	-
0103(3)	-	All Geologists	-	-	-	-	-	-	N	-

Figure 1. Screen shot of the default display for the WYDOT Geology database. The highlighted word on the top row indicates which portion (Projects) of the database the user is viewing. This screen is referred to as the Parent Page of the database. The Child Page is accessed through the paper and pencil icon located to the left of each row entry.

Records in the database are stored and managed in what are referred to as Parent and Child Pages. The Parent Page is the first screen users see when they log into the database. It contains rows of single entries which allow users to navigate the columns of information within the database. This is an important step to establish trends in data because users can gather different projects under similar topics and compare the results of the investigations. If a record requires multiple entries, for example several projects have utilized the same aggregate source for construction materials, the Child Page will accommodate this information in a table form. The Child Page is accessed through an icon placed to the left of each individual entry. It is in the Child Page that information is added, or changed, to each column on the Parent Page. An important feature of the Child Page is the entries coded by the red font color (Figure 2). These inputs are required to establish a new record in the database and are incorporated so that essential information will not be inadvertently left out of a record. Drop down menus are utilized for these, wherever possible, to organize information under standardized topics and reduce the number of misspellings or other human errors that occur with data entry. As mentioned earlier, entries in the drop down menus are specified via the links on the bottom row of the Parent Page.

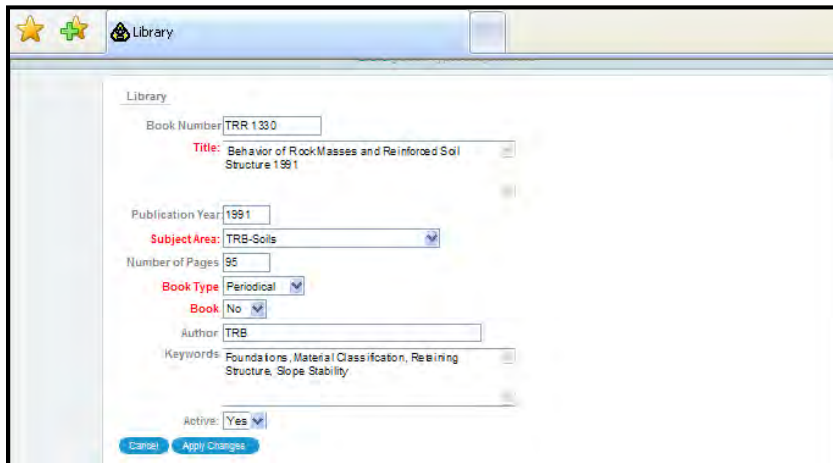


Figure 2. Screen shot of the Child Page for the library portion of the database. The entries with the red font are required inputs to establish a new record in the database.

Navigating data stored in the database is efficient due to a multifaceted action menu affectionately referred to as the “little green wheel” (Figure 3). Searches will return all entries that contain letters within the search criteria. This feature is helpful in the case of misspellings or if the entire title is not known by the user. The most useful applications are the select columns, filter, sort, control break, save report, and the download features. The select columns, filter, sort, and control

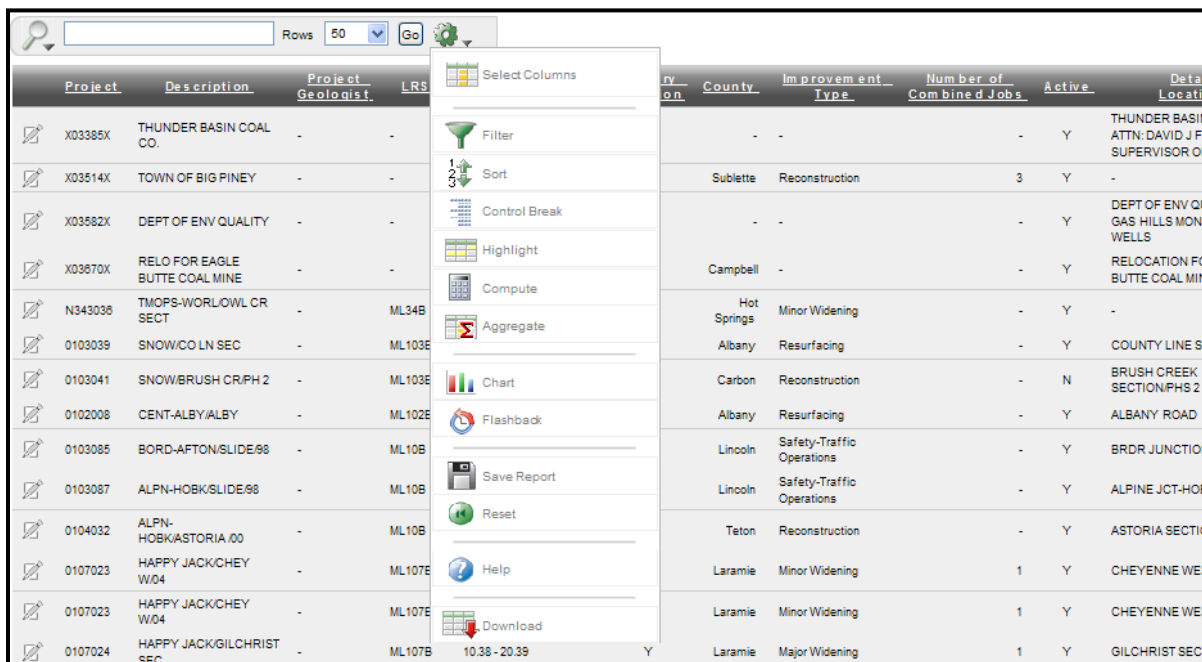


Figure 3. Screen shot of the navigation tool for the database. This menu appears once the down arrow to the lower right of the “little green wheel” is selected.

break commands allow the user to customize the column arrangement and/or column entries that display on the screen. The use of the save report command will store any specified arrangement to be presented every time the user logs into the database. If additional tasks are required, the information can be exported into an Excel spreadsheet with the download command. This command is especially useful for calculating and graphing because Excel is a superior application when compared to the compute and chart commands accessible from the navigation menu. The compute command requires a unique program language (similar to FORTRAN) to initiate calculations, and the chart command is limited in design options for graphing.

SECTIONS OF THE DATABASE

The design of the database was developed from existing program duties and from new areas identified as future applications for geology work. The existing records have been divided into sections for management by an individual or a team within our program. This volume of data only reflects what has been digitally saved in the last 25 years, essentially since computers have influenced storage procedures. There are also numerous boxes containing paper copies of project data from when the program began in the late 1950's. This information is also stored on microfilm and managed by the Records Program of WYDOT. The version of the Geology database, as presented in this paper, is divided into four sections - Library, Geologic Maps, Aggregate Sources, and Projects.

The Library and Geologic Maps sections are intended to be an inventory of the resources available for planning geologic investigations and substantiating geotechnical recommendations for design. These two sections combine for a total of 5,588 records. The Library database (Figure 4) contains 4,666 records for manuals, textbooks, periodicals, etc., that the Geology Program possesses for design and training purposes. The default display is an alphabetized listing, accomplished with a Title, Control Break operation, of the current material available in the library. Once again, numerous search methods are available to the user. The most applicable of these is by author or subject area. The Child Page contains a list of the sub-reports that compose the contents of the resource.

The screenshot shows the 'Geology' database interface with the 'Library' section selected. It features a search bar, a 'Rows' dropdown set to 50, and a 'Go' button. Below the search area, there are checkboxes for 'Active = Y' and 'Title'. The main content area displays three groups of records, each with a title and a table of details.

Title : 23rd Highway Geology Symposium Guidebook for Field Trip Norfolk, Virginia						
Book Number	Subreport Title	Publication Year	Number of Pages	Author	Subject Area	Book Type
-	[Main Entry]	1971	28	Meadors, George S.	Hwy. Geo. Symposium Proceedings	Spiral
Title : A Field Guide to the Rocks and Minerals of Wyoming						
Book Number	Subreport Title	Publication Year	Number of Pages	Author	Subject Area	Book Type
GB 51	[Main Entry]	1965	72	Wilson, William H.	USGS-Structure	Periodical
Title : Aerial Photographs in Geologic Interpretation and Mapping						
Book Number	Subreport Title	Publication Year	Number of Pages	Author	Subject Area	Book Type
Paper 373	[Main Entry]	1920	230	Ray, Richard Godfrey	Photogeology	Periodical

Figure 4. Screen shot of the Parent Page of the library portion of the database. The Control Break command has been utilized to alphabetize the material available for the Geology Program. An Active Filter has also been applied to indicate that the source actually exists as a hard copy within the library.

The Geologic Maps portion (Figure 5) is a list of maps available for use in planning or during the course of a field investigation. Several search methods are available, but the most useful are by Township and Ranges (T Min/Max and R Min/Max) or by Locations. The latter is accomplished by selecting a county or a combination of counties in which the region resides. The digital maps and a

The screenshot shows the 'Geology' website header with the Wyoming Department of Transportation logo. The navigation menu includes 'Aggregate Sources', 'Projects', 'Library', 'Geologic Maps', and 'Administration'. Below the menu, there are tabs for 'Geologic Maps' and 'Google Map'. A search bar is present with a magnifying glass icon, a 'Rows' dropdown set to '50', a 'Go' button, and a gear icon. A 'Digital Map' link is visible in the top right. The main content is a table of geologic maps.

Description	File Reference	T Min	T Max	R Min	R Max	Author	Map Year	Locations	Media Copy
Preliminary Geologic Map of the Crooks Peak Quadrangle, Fremont and Sweetwater Counties, Wyoming	OF-77-322	26	28	91	93	Schmitt, L.J.	1977	FR, SW	-
Geologic Map of the Squaw Rock Quadrangle Platte County, Wyoming	GQ-626	22	23	69	70	McGrew, Laura W.	1967	PL	-
Prelim. Geol. Map, Rawhide School Quad	OF-73D	51	52	72	73	Mapel, W.J.	-	CL	-
Geologic Map and Cross Sections of Mt. Thompson and Adjacent Areas, Sublette and Lincoln Counties, Wyoming	TH-FRUCHEY	29	-	115	116	Fruchey, Richard A.	1962	LN, SB	-
Geologic Map and Structure Sections of Red Canyon Creek Area, Fremont County, Wyoming	TH-MCKAY	30	31	98	100	McKay, E.	1947	FR	-

Figure 5. Screen shot of the Geologic Maps portion of the database.

Google Map are accessible from this screen. The digital map link simply allows the user to view a map from their computer terminal. The Google Map (Figure 6) is intended to allow WYDOT agencies, throughout the state, the ability to view information. The Geology Program contributes information from their Aggregate Sources, Landslides, Rock Slopes, and Water Wells databases. A specific location is accessible by selecting either the green arrow or purple bubble icon. The information about that site is presented, in a read-only format, in the callout pointing to the chosen area.

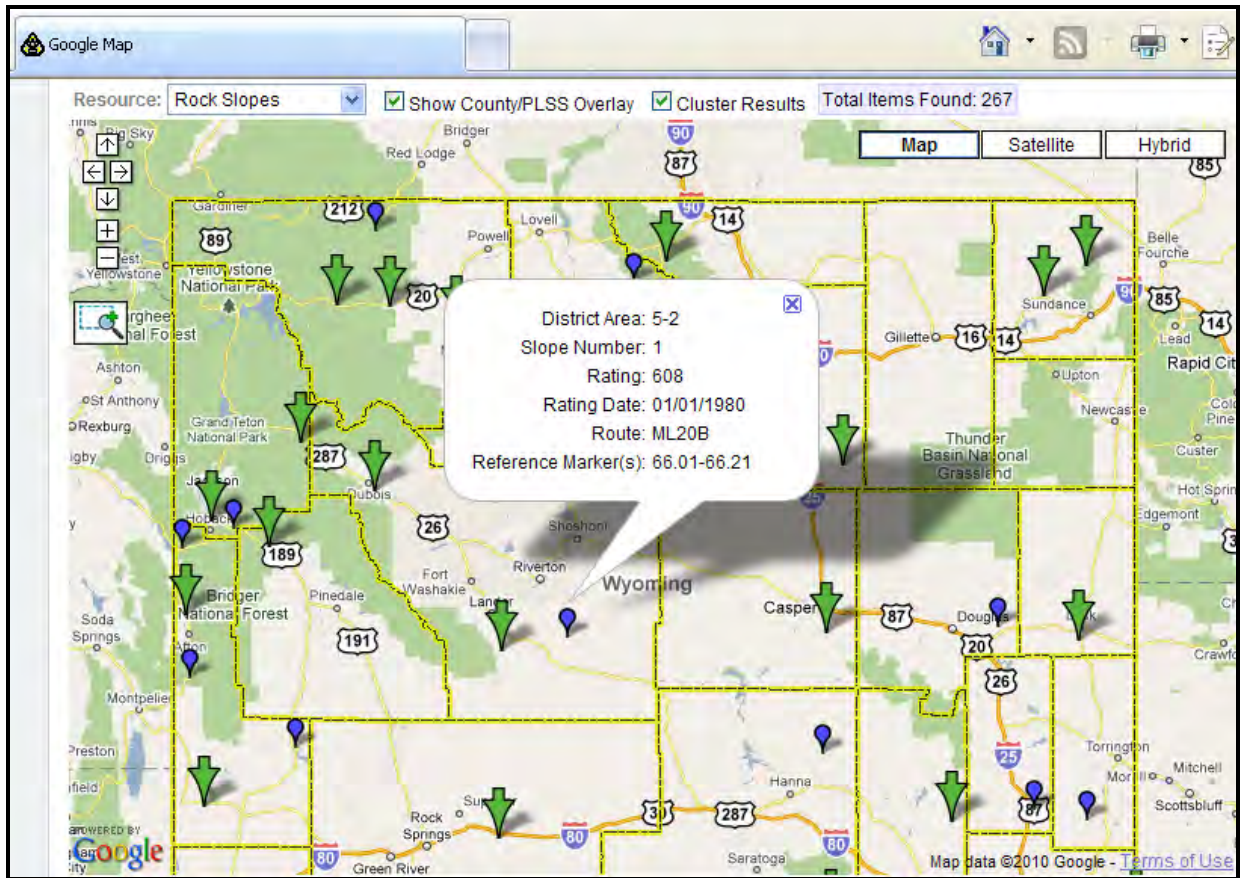


Figure 6. Screen shot of the Rock Slope information as available through the Google Map link. The green arrow indicates multiple entries and the purple bubble indicates a single entry. The green arrow is necessary because of the scale of the map. As the user zooms into a location, the green arrow divides into individual purple bubbles.

The Aggregate Sources database houses 3,852 records regarding sites that supply the majority of material for road construction in Wyoming. This is a multi-departmental database (Figure 7) with input provided by Geology, the Materials Laboratory, Contracts and Estimates, and Resident Engineers. Geology conducts the field investigation of the pit location and provides the report describing the material quality and quantity, cross-sections of the pits, and other information relevant to project planning. The Materials Laboratory provides material descriptions of the aggregate available at these locations. The Contracts and Estimates Program manages the Blue Folder number. This refers to the color and reference number of an actual hard copy file that functions as a depository for legal documents associated with the project. Examples of this are royalty payments, landowner agreements, Department of Environmental Quality (DEQ) permits and the National Pollutant Discharge Elimination System (NPDES) permits. Once again, numerous search methods are available for the user. Quick

Project	Pit ID	Pit Name	Location	Owner	Pit Status	Pit Type	T146 Format	Blue Folder Number	NPDES Permit Number
034-5(29)	BH-149B	Little Dry Creek	Gov't Agreement #2176	U.S. GOV'T	Active	Sand	Hardcopy	2176	WYR320052
7175	BH-149	Little Dry Creek	Gov't Agreement #2176	U.S. GOV'T	Active	Sand	Hardcopy	2176	WYR320052
034-5(41)	BH-202	Little Dry Creek	U.S. Government	U.S. GOVERNMENT	Active	Sand	Hardcopy	2176	WYR320052
034-5(60)	BH-218	Little Dry Creek	U.S. Government	U.S. GOVERNMENT	Depleted	Sand	Hardcopy and Digital	2176	WYR320052
-	CB-161	Pass Creek Road	U.S. Government	U.S. GOV'T	Active	Sand	Hardcopy	3397	-
022-1(27)	CB-176	Pass Creek Pit	U.S. Government	U.S. GOV'T	Active	Sand	Hardcopy	3397	-
022-1(27)	CB-213	Pass Creek Pit	Walcott Jct.-Saratoga	U.S. GOV'T	Active	Sand	Hardcopy and Digital	3397	-
F-012-2(1)	SW-32	Underpass Pit	US 30 N-Granger Jct.	UNION PACIFIC RAILROAD	Active	Unknown NA	Hardcopy	5846	-

Figure 7. Screen Shot of the Aggregate Sources portion of the database. Note the multiple entries under the Owner column. This indicates that there is a different owner of the landowner rights and the mineral rights for the aggregate source.

searches can be conducted with a county and material type. This yields a location and available product immediately and can be refined with additional filters as more specific needs require. This will be especially useful for Resident Engineers who can access this map to find the most efficient site, in terms of issues such as material quantity, quality, and haul distance, for construction projects in their vicinity. Pit units can be in either English or Metric, Pit Types indicates if it is sand, gravel, borrow, or is a quarry. Pit status indicates if the pit is active, depleted or if the exact status is unknown. T146 Format indicates if the material deposition sheets exist as hard copies, digital or if the reproduction of the data is unknown. The project shown on the Parent Page is the most current project that has utilized the aggregate source, and the Child Page contains the history of projects that have been involved with each pit.

The Projects database (Figure 8) is the default display once the user logs into the program. It is divided into the ten sections that comprise the primary activities of the Geology Program. Due to the extensive nature of these subdivisions, each section is managed by an individual at the Project Geologist level in our program. These act not only as a central storage location for information, but can contribute to project planning and design requirements. A brief outline of these divisions will be addressed in the following.

Projects	Landslides	Pile Driving	Stored Plans	Water Wells	Rock Slopes	Geosynthetics	Bedrock Properties	Geophysics	Drill Logs
Projects	ERP Projects	Work Types							

Figure 8. Screen shot of the headings that comprise the Projects database.

Landslides is one of the more involved sections because it is linked to several locations that store data. The Parent Page (Figure 9) contains the general location data of the slide in several columns. Two other important items on this page are the Inclinometers and Slide Photos links on the bottom row. Inclinometers is a table of information about the instruments utilized to measure movement in slide

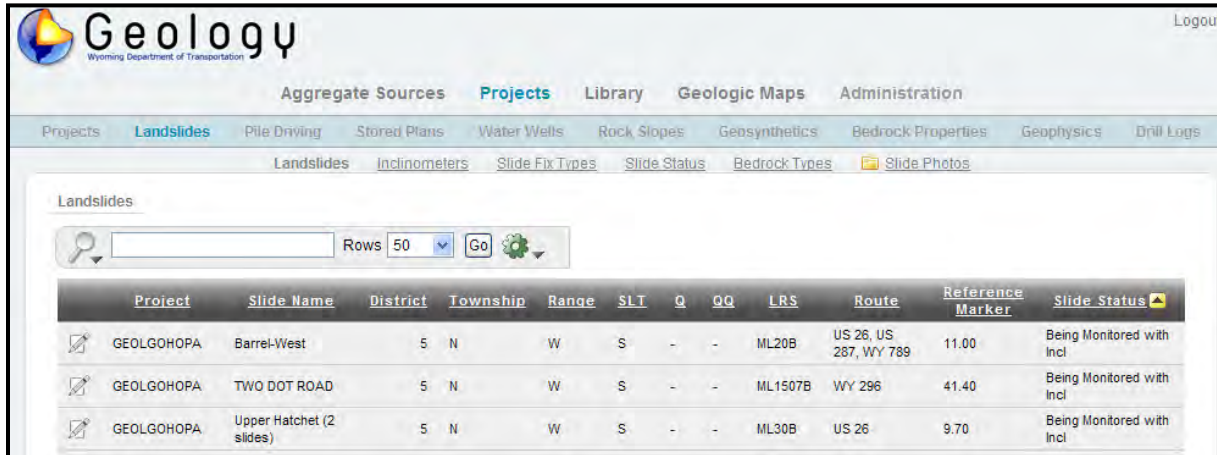


Figure 9. Screen shot of the Landslides Parent Page. This database has been filtered to show the GEOLGOHOPA projects.

masses. The Slide Photos link takes the user to directories and subdirectories that contain reports, pictures, CADD drawings and other information related to the project. Additional photos can be found on the Child Page (Figure 10) under the headings of Slide Photos and Slide Photo Terrashare. The former is an inventory of the location for hard copies of pictures and the latter is a viewer which allows the user to look at photos digitally. The digital pictures are managed by the WYDOT Photogrammetry and Surveys Program. Another interesting entry on the Child Page is the Slide Fixes. This is a catalog

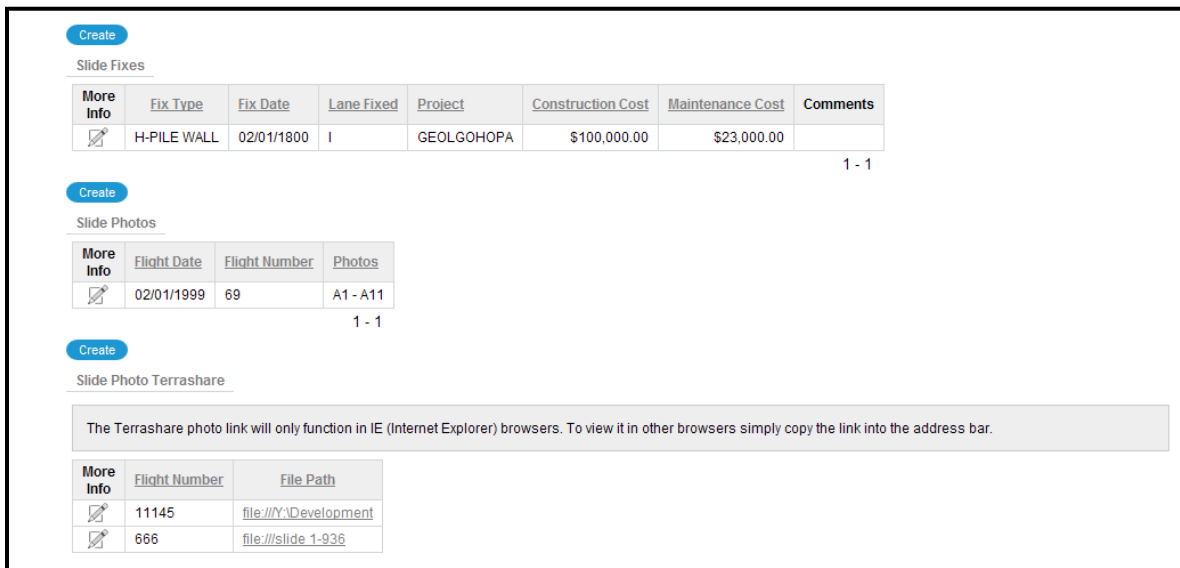


Figure 10. Partial screen shot of the Landslides Child Page. There is also a table for geologists who have worked on the project and a location of inclinometers placed within the landslide.

of efforts taken to remediate the landslide. Most landslides have a single entry. However, some of the older slides have failed numerous times and different techniques have been employed to stabilize the movement.

Pile Driving is a new addition to the database. The thirty five columns on the default display are the most columns in any portion of the database. Once completed, it will be utilized to refine design recommendations for pile driving at bridge sites. The intention will be to compile field measurements for qualities such as, end bearing, skin friction, and hammer efficiency, and compare it to theoretical specifications. A long term goal will be to establish typical values for various material types that are encountered at bridge locations throughout the state.

Stored Plans and Drill Logs are directories containing over 10,000 records and serve an administration purpose for the Geology Program. Stored Plans indicates the storage location for boxes containing historical files of reports and project information. Drill Logs is a record of drill logs taken throughout the history of the Geology Program. It does not contain the drill hole information, but rather, it is an inventory of who drilled the hole, what type of investigation was conducted, how many holes were drilled at the location, and the date of the investigation.

The Water Wells database (Figure 11) provides two services to the Geology Program. The first service is an internet link that connects to the State Engineers Office (SEO). This feature, titled State Wells, allows a view of separate well information that different agencies have been associated with in the state. Secondly, it is a collection of 406 records of wells that the Geology Program has either drilled or contracted to drill. The Parent and Child Pages both have searchable information. The Parent Page contains the general information about the project such as the location, depth of the well, and a completion diagram. The completion diagram is a cross-section of the geologic units, water level, perforation zone, and other pertinent data relating to the completion of the well. It is viewed through a link established on the Child Page. It will be applicable for all future well images that can be stored in a portable document format. Pump test yields, chemical tests, and geophysical log information are also contained on the Child Page. This information can be explored with the navigation tool in the cases where multiple testing has been conducted. This database will be useful for future planning needs, as the legal description provides the capacity to anticipate the depth of the water bearing formation and how much water the well will yield for new wells installed near existing well locations.

Geology
Wyoming Department of Transportation

Logout

Aggregate Sources **Projects** Library Geologic Maps Administration

Projects Landslides Pile Driving Stored Plans **Water Wells** Rock Slopes Geosynthetics Bedrock Properties Geophysics Drill Logs

Water Wells Monitoring Wells Well Casings Well Uses State Wells

Water Wells

Search [] Rows 50 Go []

County : LA

District	Location	Well Casing	Casing Size	Depth	SEO Permit	Completed	Township	Range	SLT	Q	QQ	Completion Diagram
1	CHEYENNE EAST	Plastic	5	520	79217	05/23/1990	14N	05W	32S	SW	NE	-
1	JUBILEE WELL #2	Steel	7	200	34851	03/10/1977	14N	04W	1S	SE	SW	-
1	BURNS REPLACEMENT WELL	Plastic	6	363	175359	07/24/2008	17N	02W	17S	SW	SW	-
1	College Drive North	Plastic	6	435	128554	01/11/2001	13N	07W	34S	NW	SW	-

Well Tests

Search [] Rows 15 Go []

Test Date	Yield Min	Yield Max	Ground Water Surface	GWS Date	Pump Depth	Chemical Test	Pump Rate Min	Pump Rate Max	Geophysical Log
-	25	-	-	05/21/1990	450	Y	25	-	N

Figure 11. Screen shot of the Parent (top image) and Child Page (bottom image) for the Water Wells section of the database. The County, Control Break function has been employed on the Parent Page to organize the wells into the county in which they reside. This is an occasion where information on the Child Page can be manipulated with the navigation tool. In this example, only one test has been conducted on this well. However, there are several well locations that have experienced multiple testing.

Rock Slopes is another multi-departmental section of the Geology database (Figure 12). There are 353 records identifying rock slope areas in the state. They are individually designated by a specific slope number located in an area/district according to the reference markers (a range of mile posts)

District	Area	Slope #	LRS	Route	Reference Marker	Slope Report	Field Data	Rating	Rating Date	Rock Slope Mesh	Comments
1	1	1	ML80B	I-80	333.8	-	-	112	01/01/1980	No	Road Section: I-80 Summit
1	1	2	ML80B	I-80	324.9	-	-	57	01/01/1980	No	Road Section: I-80 Summit
1	1	3	ML80B	I-80	324.5	-	-	-	-	No	Road Section: I-80 Summit
1	1	4	ML80B	I-80	322.1 - 322.4	-	-	106	01/01/1980	No	Road Section: I-80 Summit
1	1	8	ML80B	I-80	320.3	-	-	73	01/01/1980	No	Road Section: I-80 Summit
1	1	10	ML80B	I-80	319.05	-	-	63	01/01/1980	No	Road Section: I-80 Summit
1	1	12	ML80B	I-80	318.65	-	-	112	01/01/1980	No	Road Section: I-80 Summit

Figure 12. Screen shot of the Parent Page for the Rock Slopes database. Note the column titled Rock Slope Mesh. This infers that Mesh is the only measure undertaken by WYDOT to mitigate rock slopes. While this is true for approximately 90% of rock slopes in Wyoming, other measures, such as shotcrete and rock bolts, have been utilized as mitigation measures. Renaming this column is currently in committee.

that designates where on the road section that the slope is located. The Rockfall Files link is connected to a directory which contains information specific to individual slopes. This includes rating information, rockfall analysis and photos of individual slide locations. This database is also designed to track rockfall incidents on Wyoming Highways. The Child Page contains a 23 column table to store accident reports from Highway Patrol (Figure 13). The Highway Safety Program enters these reports into Agile Assets which then populates this section of the Geology database. Accidents are not linked to a specific rock slope number because, in the Geology Program, this information is primarily utilized to determine areas in the state that may be prone to rockfall incidents. This, in turn, aids in establishing the necessity and priority of remediation efforts regarding rockfall along Wyoming highways.

Accidents

Notice: The below data should only be used for internal engineering/analysis purposes. For questions contact Highway Safety.

Search: Rows: 15 Go

Crash ID	LRS	Highway Route Sign	Highway District	County	Hwy Section Number	Milepost	Crash Date	Military Crash Time	State Report Number	Number Injured	Number Killed	Lighti
175143	ML2000B	WY22	3	TETON	04	10	05/12/2000	2330	0007582	1	0	Darknes Unlighte
169468	ML2000B	WY22	3	TETON	04	10.75	05/31/2000	1830	0007887	0	0	Daylight
169468	ML2000B	WY22	3	TETON	04	10.75	05/31/2000	1830	0007887	0	0	Daylight
249782	ML2000B	WY22	3	TETON	04	11.5	07/13/2000	2155	0010527	3	0	Darknes Unlighte

Figure 13. Screen shot of the Accidents table located on the Child Page of the Rock Slopes database. This table contains 23 columns and is in a read-only format.

Geosynthetics contains the results that the Geology Laboratory has obtained from numerous geogrid and fabric tests. Records have been kept for 25 years in various spreadsheet versions until the implementation of this database. Hundreds of tests, from 38 different manufacturers, have been conducted to determine material parameters, such as strength, elongation, and permittivity. A useful application (using the Download command) is the ability to compile our test data and compare it to specifications published by the manufacturer. Figure 14 is an example of the Machine Direction Grab Tensile Test conducted on the PROPEX 601 brand, nonwoven separation fabric. It is apparent that the majority of our test results are above the Minimum Average Roll Value (MARV) as specified by the manufacturer. The MARV is the minimum strength value a fabric must demonstrate in order to be regarded as usable for construction purposes. It should be noted that test numbers 8 and 10 would most likely be given a passing rating. This is due to a 10% allowance for testing conditions. The testing machine can actually tear or separate the fabric at the area where the machine teeth hold the fabric while it is being tested. To resolve this occurrence, the practice of taping the section of fabric held in the teeth was implemented for a period of time. This practice had the propensity to attain higher strength values than the standard deviation values. This may explain the values determined in test numbers 1, 12 and 13.

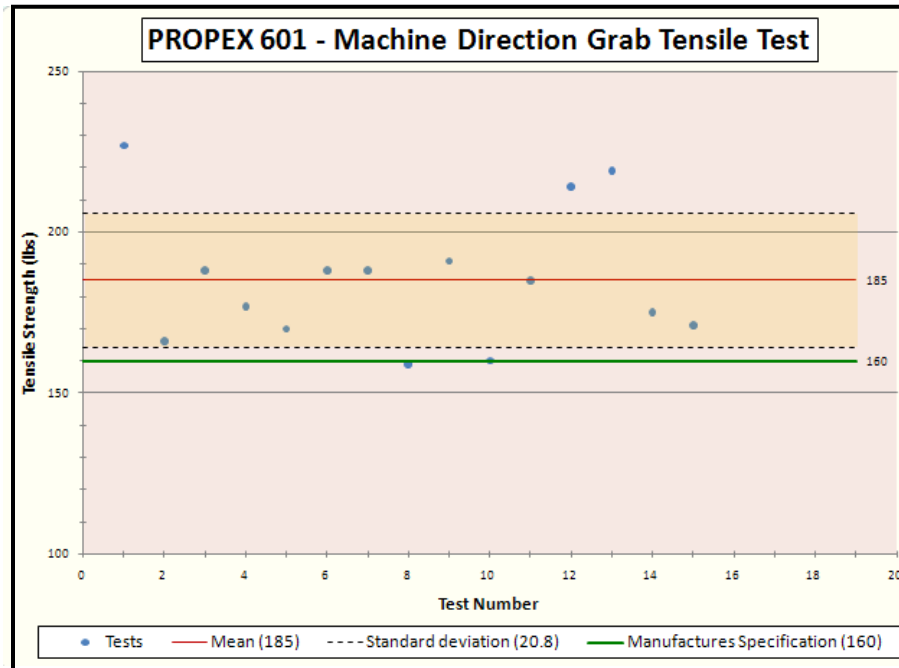


Figure 14. Screen shot of the Machine Direction Grab Tensile Test results as conducted on the PROPEX 601 brand nonwoven separation fabric. (This image was produced with an application of the download command on the navigation tool).

Bedrock Properties was established as a location to house information regarding rock types unique to the state of Wyoming. It contains 22 columns, with 14 of these dedicated to the engineering properties utilized in our geotechnical recommendation for structure design. These properties are obtained from a variety of sources. Characteristics such as Geologic Strength Index (GSI) and Rock Quality Designation (RQD) are measured during field observations. Values for Poisson’s Ratio and phi angle are attained from empirical literature. The Geology Laboratory determines the values of compressive strengths, density, and the intact rock modulus through testing. This database was expanded from its original configuration and therefore, the majority of the columns are not populated with data. Even though it is in the beginning stages of development, as additional information is added, this section will be a valuable component for estimating the engineering properties of bedrock.

The Geophysics database is a record of rippability for rock types encountered at project locations throughout the state. The Parent Page contains project and location information, as well as an entry for total lines ran for the project. Lines ran refers to the number of traverses conducted during the seismic refraction survey (SRS). The Child Page contains the seismic velocity table (Figure 15). This table is a record of the SRS data and the conclusion determined from the rippability analysis. For the example below, it is apparent that an arbitrary datum was utilized to reference the layer positions. The table shows the surveys that were conducted and the rock velocity measurements obtained for several layers encountered at the bridge site. This was then utilized as an input to determine the ease of rippability for the material at this location. Rippability conclusions are submitted as an aid in equipment planning for contractors.

Geophysics

Location: Salt Creek Bridge

Project: P471001

Total Lines Ran: 3

Comments: Lines run to determine the depth to bedrock for new bridge

Cancel Apply Changes

Seismic Velocity Table

More Info	Line Number	Station Offset Begin	Station Offset End	Layer Number	Rock Velocity	Top Layer Elevation @ Beginning	Top Layer Elevation @ End	Rippability	Rippability Rating	Rock Formation
✕	SC-1	438+23, 66' LT	439+12 70' Rt	1	1000	102	96	Easy	-	Frontier
✕	SC-1	-	-	2	1878	99	99	Medium	70	Frontier
✕	SC-4	436+50, 100' LT	437+22, 0	1	755	100	100	Easy	42	Frontier
✕	SC-4	-	-	2	3190	95	97	Medium	75	Frontier
✕	SC-5	437+00, 10' LT	437+57, 85' RT	1	947	100	100	Easy	12	Frontier
✕	SC-5	-	-	2	2332	96	94	Easy	72	Frontier

Figure 15. Screen shot of the Seismic Velocity table located on the Child Page of the Geophysics database.

CONCLUSION

The status of integration for the database is almost 100% complete. The framework, i.e., column and row headings, for all the database sections is complete and accurate. The only remaining issues are data entry. With the addition of drop down menus, the efficiency and accuracy of this task will be improved. The Bedrock Properties database will require the most work. The number of entries from its initial configuration was doubled when it was designed for this database. As a result, most of the columns are not populated. Information also needs to be added to the Pile Driving database. Fortunately, this section only contains 28 records so it should not take too long before it is operational. The Geology Program realizes that thorough recordkeeping is essential for locating information and enhancing project planning. Therefore, the completion of this database is a priority. Some changes have already been discussed the TAM committee. The addition of an Earth Retaining Systems database is being discussed by several programs at WYDOT. The primary issues are which programs would participate and the economic validity of actually developing this section of the database. The Aggregate Sources database is going to add individual columns for Environmental Services and Archeological Clearance rather than store this information in the Blue Folder. A Geographical Information System (GIS) map is being developed to allow users the ability to create maps based on their individual needs.

The implementation of this database has completely changed the means by which the Geology Program maintains and utilizes the information it possesses. Establishing a central storage location has eliminated individual copies of data and multiple areas that could house information. The ease at which information can be accessed and utilized has improved dramatically because the navigation tool allows virtually any search to be performed to find information. The ability to download the information to an Excel spreadsheet is indispensable in terms of calculation and presenting information in chart form. While only in the initial stages of operating this database, initial applications have shown that cost effectiveness and project scheduling can be improved for projects involving the Geology Program.

Resources

Geosynthetics, December 2007 January 2008, Volume 25 Number 6, 2008 Specifier's Guide
<http://www.propexinc.com/>

MSE WALL CORROSION IN NEVADA – A CASE STUDY IN GEOTECHNICAL ASSET MANAGEMENT

John D. Thornley, A.M. ASCE, P.E.¹, Raj V. Siddharthan, M. ASCE, Ph.D., P.E.²,
David A. Stanley, J.D., C.P.G., L.G., L.E.G.³

¹ Geotechnical Engineer, Hattenburg Dilley & Linnell, LLC, 3335 Arctic Boulevard, Suite 100, Anchorage, AK 99503; PH (907) 564-2139; FAX (907) 564-2122; email: jthornley@hdlalaska.com

² Professor, Department of Civil and Environmental Engineering, University of Nevada, Reno, Mailstop 258, Reno, NV 89557-0258; PH (775) 784- 1411; FAX (775) 784-1390; email: siddhart@unr.edu

³ Chief Engineering Geologist, Alaska Department of Transportation and Public Facilities, 5800 E. Tudor Rd. Anchorage, Alaska 99507; PH (907) 269-6236; Fax (907) 269-6231; email: dave.stanley@alaska.gov

ABSTRACT

Transportation system geotechnical assets such as earth retaining structures may be difficult to manage due in part to a shortfall in knowledge about their performance, service lives and life cycle costs. One area of concern for geotechnical structures is the lack of understanding about the potential for corrosion-related failure of buried reinforcements used in mechanically stabilized earth (MSE) walls. Recently, the Nevada Department of Transportation discovered high levels of corrosion at two wall locations in Las Vegas. The resulting investigations of these walls produced direct measurements of metal losses and electrochemical properties of the MSE reinforced fill. One MSE wall was replaced with a cast-in-place concrete tie-back wall at great expense.

It is shown in this paper that the original MSE reinforced fill approval electrochemical test results at the two wall locations are significantly different from those measured in post-construction investigations. The internal stability analyses (using AASHTO 2007 LRFD) of two un-repaired MSE walls were also performed and determined that the estimated remaining service lives are significantly less than the design life of 75 years.

Asset management alternatives evaluation contrasts the cost framework of wall failure, wall replacement, and proactive initiatives such as corrosion monitoring and management. Although monitoring programs for MSE walls are recommended (FHWA, March 2001), few owners of MSE walls use monitoring as a routine management technique. This case study offers evidence that corrosion monitoring of buried geotechnical components can be an effective tool in the toolbox of transportation agencies across the United States.

By following asset management principles, transportation agencies can understand what assets they have through inventorying processes, can understand the

condition of the assets through condition surveys, can set service lives and performance standards and use life-cycle cost tools to compare alternatives for mitigation, rehabilitation or repair of the assets in order to meet the agency minimum performance standards. Case studies such as this demonstrate that the essential link between technical analysis and management principles can yield a more efficient and fiscally responsible transportation system that can focus on preservation of assets while maintaining the agency required level of service.

INTRODUCTION

Geotechnical assets, as with other assets such as guardrail, pavements, bridges, signs, culverts, light standards, etc., can be managed following the principles of transportation asset management (TAM or asset management). (Sanford Bernhardt, Loehr and Huaco, 2003; Loehr, Sanford Bernhardt and Huaco, 2004) TAM is a strategic approach encompassing multiple business processes and in reliance on good information and analytical capabilities. The goals of asset management are to build, preserve and operate transportation facilities and assets cost-effectively and with improved performance to provide best value for public funds and enhance the credibility and accountability of the responsible agency (AASHTO, 2002). TAM addresses five core questions about assets (FHWA, 2009):

1. What is the current state of my assets?
2. What are my required levels of service and performance delivery?
3. Which assets are critical to sustained performance delivery?
4. What are my best investment strategies for operations, maintenance, replacement and improvement?
5. What is my long-term funding strategy?

The principles of asset management offer a systematic way of identifying and executing the optimum allocation of resources for transportation assets (Brutus and Tauber, October 2009). As the U.S. changes focus from expanding new transportation infrastructure to preserving existing infrastructure, asset management offers the tools to manage that change (Virginia DOT, 2009).

Geotechnical assets such as earth retaining structures may be difficult to manage throughout their service lives when we lack the understanding of how the condition of these assets changes over time. Numerous factors can contribute to deterioration and failure of a wall before the end of its service life is reached. Among them:

- Use of techniques too new to verify design service life based on actual field performance,
- Errors during construction such as improper application of shotcrete or use of materials that degrade in exposure to UV,
- Unpredictability of corrosion effects on wall components due to chemical or electrical activity in the retained soil,

- Post-construction site changes due to utility installation, runoff, damage to membranes or unforeseen circumstances.

The majority of these problems are hidden behind the wall face and only become evident when the wall begins to fail or show signs of distress such as bulging, deflection, cracking, etc. (Brutus and Tauber, 2009).

AASHTO requires retaining structure designs be based on potentially deleterious factors such as material deterioration, seepage and stray currents. AASHTO recommends a minimum service life of 75 years for most applications of MSE walls. For those MSE walls supporting bridges, buildings or other critical structures, a service life of 100 years is recommended. AASHTO also notes that designing walls to be essentially maintenance free does not preclude the need for periodic inspections to assess conditions throughout the life of the wall (AASHTO, 2010).

A greater understanding of the life cycle of geotechnical assets such as earth retaining structures is needed. Assigning a design life of 75 or 100 years to a critical structure or element can create serious issues if its actual service life is only a fraction of that due to unanticipated conditions during design. When a premature failure occurs, life and safety issues are implicated along with the ability of our transportation systems to deliver the required functionality and the ability of transportation agencies to budget for design, maintain and repair critical assets.

Asset management is based in part on performance standards for the assets. These standards provide the basis against which the asset condition is judged. A condition survey may be able to fully describe the status of a retaining wall, but unless there is an understanding of how much life is left in the wall (where is it on the condition curve?) and of the standards the wall is supposed to meet, the survey will be of little use in managing the wall. An essential feature of asset management is the ability to compare alternatives to support decision-making about when, whether and how the asset should be repaired, rehabilitated, or replaced. TAM allows optimization of allocation of resources and funding and allows moving away from a “worst first” inefficient spending model.

RETAINING WALLS IN THE U.S. AND NEVADA

Modern mechanically stabilized earth wall systems have only been in use in the U.S. since the 1960s (FHWA, 2001). Thousands of these cost effective earth retaining structures have been built for transportation applications around the United States. However, despite the apparent success of these walls, the actual service life of MSE walls is essentially unknown and failures have occurred without warning (FHWA, 2008). As noted above, current design practice anticipates 75 to 100 year design lives for these wall structures, but the oldest steel strip-reinforced MSE wall in the US was not built until 1972 (FHWA, 2001). Although rare, failures and loss of

life caused by failures of earth retaining structures is a significant issue because the walls support critical transportation features such as bridges and embankments (FHWA, 2008).

In Nevada, the state Department of Transportation (NDOT) has constructed over 150 MSE walls, exclusively using metal reinforcements. These MSE walls are primarily located in the urban areas of Las Vegas and Reno. At two locations in Las Vegas, MSE wall soil reinforcements were found to have high amounts of corrosion. These two locations include the three MSE walls at the I-515/ Flamingo intersection, constructed in 1985 using welded wire fabric (WWF) that was not galvanized; the other MSE wall is at the I-15/Cheyenne intersection, constructed in 1998 using galvanized ribbed metal strips. The former wall reinforcement corrosion was found by accident during construction of a soundwall at the top of one wall. The later was also found by accident during demolition of a portion of an MSE wall for an expansion project. The Flamingo walls will be the focus of this case study. However, it should be noted that the Cheyenne MSE wall experienced a similar level of corrosion even though it was galvanized and the wall was approximately only nine years old at the time of discovery.

The Flamingo intersection is of significant interest because the case study is well documented. In 2004, the reinforcements in the largest of the three walls were found to be highly corroded and the Federal Highway Administration recommended the wall be mitigated. A cast-in-place concrete tie-back wall was constructed in front of the existing MSE wall to provide adequate support. Also during that time, McMahon & Mann Consulting Engineers (MMCE) were hired to investigate the corrosion of all three MSE walls at this intersection (Fishman, 2005). Their investigation evaluated the corrosive nature of the reinforced fill and collected direct measurements of the soil reinforcements at all the MSE walls at this intersection. From their analysis, an estimate of uniform average metal loss rates was estimated. Stability analyses were also performed for the remaining two MSE walls at the intersection based on remaining reinforcement capacity from the average uniform loss estimates.

The results from the Flamingo MSE wall investigation led NDOT to assess how many other MSE walls may experience stability issues due to high rates of corrosion. From a geotechnical asset management perspective this case study is of particular interest. These findings suggest a re-evaluation of design concepts and an assessment of whether these walls will perform adequately through their anticipated service lives. One proactive method that should be considered by state departments of transportation and other MSE wall owners is monitoring.

Below are discussions of some of the anticipated service life predictions for the remaining I-515/Flamingo walls. In-depth examination of the data used, analysis methods, and other findings are presented in previously published papers (Thornley et. al., 2010). Methods for owners to be more proactive in internal performance

monitoring are also discussed. This paper highlights the importance of geotechnical asset management for critical structures such as MSE walls where corrosion inside the walls can reduce internal stability without showing outward signs of distress.

CORROSION AND ITS EFFECTS ON WALL STABILITY

It is well documented that when metals are buried they can experience corrosion due to the electrochemical interaction with the soil. This also holds true for metal soil reinforcements used in MSE walls. One part of the MSE wall design process involves adding extra cross sectional area or protective coating, also referred to as sacrificial thickness, to account for metal loss due to corrosion over the planned lifetime of the structure. Only MSE reinforced fill soils that are mild to non-corrosive are allowed by specifying a series of pass/fail controls (specifications) in order to limit the amount of corrosion. Metal loss models developed from corrosion studies are used to arrive at the sacrificial thickness estimates. When the combination of sacrificial thickness and mildly corrosive soils are used together, MSE walls are expected to perform as desired. However, if adequate sacrificial thickness is not used or an aggressive environment exists in the reinforced fill, there will be higher than anticipated rates of corrosion. This can directly affect the internal stability of a MSE wall.

As discussed in the introduction, only Wall #1 at the Flamingo intersection was mitigated by constructing a concrete tie-back wall in front of it. However, there are two remaining walls that have not been mitigated. These two remaining unmitigated walls at I-515/Flamingo are the focus of the stability analysis as failure or rehabilitation/repair/replacement of the walls would cause disruption to the Las Vegas transportation corridor and potential loss of life if they fail. The results from the loss measurement statistical analyses performed also provide a framework to identify other walls that may be experiencing similar rates of corrosion (Thornley, 2009). With the development of predictive loss rates outlined in a recent paper (Thornley, et. al., 2010), it is possible to address the stability concern at other Flamingo wall locations.

The approach for the analysis of the two remaining MSE walls is based on the current practice for MSE wall design and analysis, as presented AASHTO LRFD Bridge Design Specifications 4th Edition (AASHTO 2007). Using this approach, an analysis of the existing wall internal stability, based on tensile strength of the soil reinforcements, has been conducted for both of the remaining MSE walls at the Flamingo intersection. Both static and seismic evaluations were conducted. Two seismic cases were evaluated where the design motions at the surface have maximum accelerations of (1) $a_{\max} = 0.15g$, a value traditionally used by NDOT Bridge Division in the Las Vegas region, and (2) $a_{\max} = 0.21g$, estimated from United States Geological Survey (USGS) maps.

In LRFD static and seismic analyses, a capacity to demand ratio is calculated (C/D ratio), replacing the technique (Allowable Stress Design – ASD) of calculating the Factor of Safety. The load and resistance factors are included in each calculation instead of using a factor of safety, resulting in the need to have a C/D ratio greater than unity for adequate design and stability analysis. The remaining unmitigated sections of Walls #2 and #3 have effective heights of 32 and 15.5 feet, respectively. Using the predictive loss estimates, the wall behavior can be evaluated over time (Siddharthan, 2009).

When using the LRFD method, a factor is placed on the yield stress of the steel. This effectively keeps the yield stress of the soil reinforcements within the linear-elastic region of the stress-strain behavior of the steel. When evaluating the life expectancy of these MSE walls, the full yield strength of 70ksi is used for both static and seismic cases. It should be noted that the difference between static and seismic response may be smaller than one might expect. This is due to the fact that during design the yield strength is multiplied by a resistance factor for the seismic case of 0.85, while the static case uses a resistance factor of 0.65. This allows for higher stresses to develop during a seismic event while still staying at an acceptable level below the yield stress.

Two estimated loss models were used in the analyses (Thornley, et. al, 2010). The first estimated loss model evaluates the results of corrosion if the soil reinforcements experience losses approximate to the average power loss model calculated from the diameter loss measurements. The second loss model uses the wall behavior expectations at the 84th percentile loss. When evaluating important structures it is common to evaluate the 84th percentile (average value plus one standard deviation) case when there is a level of uncertainty and a conservative design is needed. For highway structures that have more importance and stringent safety requirements, such as these retaining walls, a more conservative estimate of the expected behavior is warranted. The results from these internal stability analyses for the remaining walls at I-515/Flamingo have been summarized in Table 1. It can be seen that these walls are not likely to remain internally stable for a 75-year design life, either under static or seismic loading conditions. These stability calculations assume that the reinforcements will fail along the edge of the reinforced fill failure wedge at the interface of the active and resistant zones.

Table 1. Expected Failure Lifetimes for Wall #2 and #3 at I-515/Flamingo (C/D ratio < 1).

Load Case	Expected Failure Lifetimes of Remaining I-515/Flamingo Walls			
	Wall #2		Wall #3	
	Average Power Loss Model (yrs)	84 th Percentile Power Loss Model (yrs)	Average Power Loss Model (yrs)	84 th Percentile Power Loss Model (yrs)
Static	42	35	39	27
$a_{\max} = 0.15g$	39	32	35	24
$a_{\max} = 0.21g$	38	31	33	23

To predict wall failure the tensile capacity of the steel reinforcements should be compared to the tensile load introduced by the reinforced fill soil. As a baseline case, the original steel cross sections are used to calculate initial internal stability of Wall #2 (Figure 1). This baseline analysis has also been used to evaluate the internal stability of Wall #3. It was decided to focus on Wall #2 in this paper because it is significantly taller than Wall #3 and therefore of greater potential consequence upon failure. With the baseline case established, further analysis accounting for corrosion using the power loss models has been conducted. The results of stability calculations estimating the corrosion of the I-515/Flamingo Wall #2 have been presented for three time periods in a snapshot fashion. These snapshots are in twenty-five year increments starting from the date of completion. As the time progresses, calculated capacity becomes smaller, due entirely to metal losses. The 84th percentile metal loss rate tensile values have been used in the results presented in Figure 1. After fifty years there is very little to no structural capacity remaining in the reinforcements.

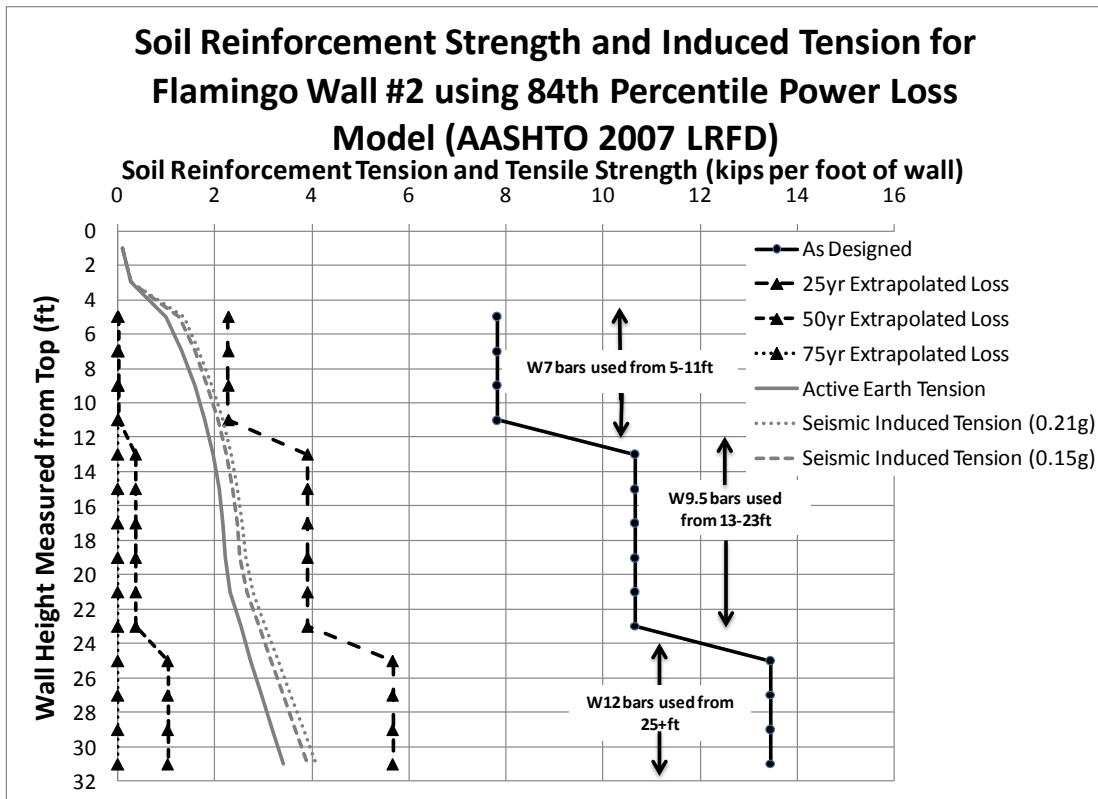


Figure 1. Soil Reinforcement Strength and Induced Tension for I-515/Flamingo Wall #2 – 84th Percentile Power Loss Model.

Wall #2 is constructed using three different WWF sizes, including W7, W9.5, and W12 with diameters of 0.298, 0.348, and 0.391 inches, respectively. Near the top of the wall, there is no remaining steel cross sectional area after about forty-five years of service life. However, it is more likely that Wall #2 would fail prior to complete loss of cross sectional area. Using the 84th percentile analysis with the larger longitudinal bars it is apparent that the remaining cross sections of the W9.5 and W12 bars will experience complete metal loss at approximately 55 years and 60 years of service life, respectively.

Further evaluation of the results detailed in Figure 1 are presented in Figure 2 detailing the possible seismic demand based on an input motion of 0.21g in the same snapshot method using the LRFD C/D values. In the case of Wall #2 with the 84th percentile metal power loss model we estimate that a 25 year service life would bring the wall to near failure. It should be reiterated that the walls at the Flamingo intersection have been in service approximately 24 years.

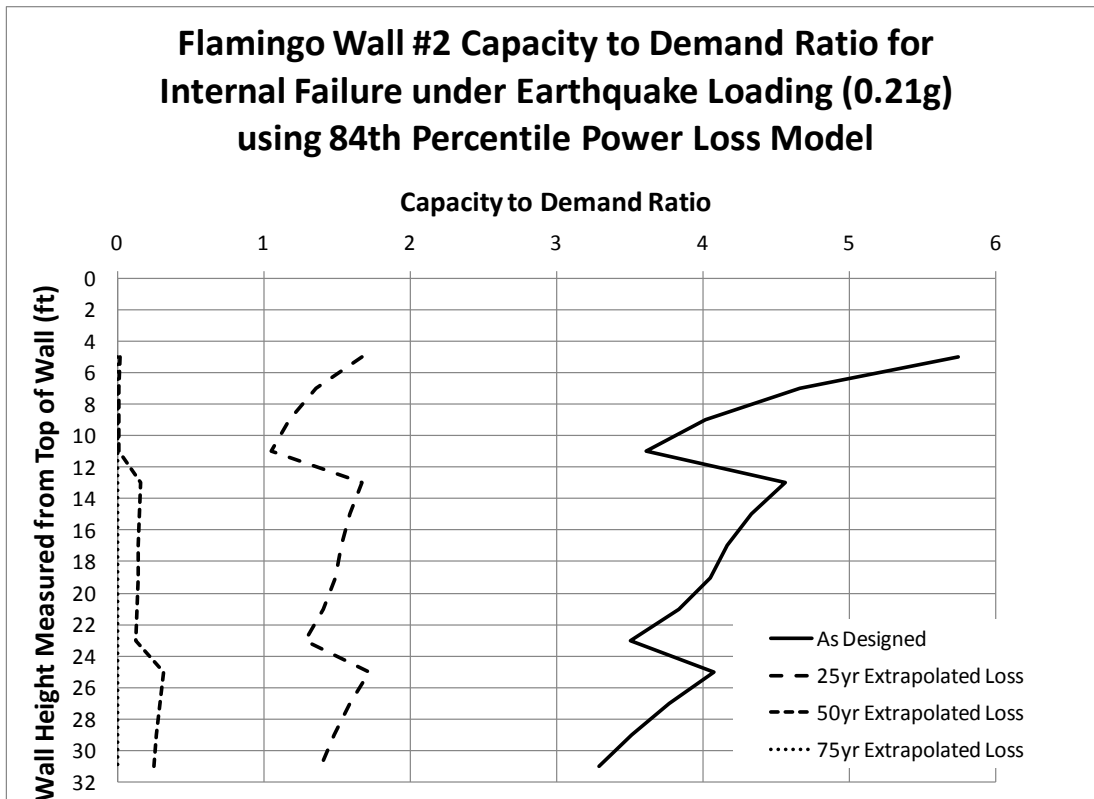


Figure 2. I-515/Flamingo Wall #2 C/D Ratio for Seismic Loading ($a_{max} = 0.21g$) – 84th Percentile Power Loss Model.

ANALYSIS OF OTHER NEVADA WALLS

Asset management programs have as a first principle that one cannot manage what one does not know. Inventory of geotechnical assets such as earth retaining structures is a critical first step. Recent survey data indicates that most highway agencies have only fragmentary data about their retaining walls (Brutus and Tauber). In order to be proactive, the authors and Nevada Department of Transportation developed a database of MSE walls and the relevant information that would be needed to evaluate other potentially degrading walls. This database assisted in identifying the potential MSE walls that may be in danger. Of the walls at the 39 locations, 12 locations were identified as potentially needing future evaluation in the next phase of the project.

Based on the findings from these evaluations, asset management decisions can be made relative to mitigation alternatives. However, some attention needs to be focused on how the evaluation should be conducted. The initial research and recommendations provided several steps that should be followed in order to properly evaluate existing walls, or geotechnical assets, as well as how to develop evaluation

techniques for existing and future MSE walls. These recommendations, while developed for Nevada can be used by any MSE wall owner.

1. Representative backfill soil testing – all walls should be evaluated to ensure proper characterization of the backfill used during construction (this is especially useful for older walls where corrosion testing was not as stringent);
2. Installation of non-stressed soil reinforcements – reinforcement coupons should be installed so that baseline loss measurements can be estimated through direct observation;
3. Nondestructive monitoring methods – monitoring of corrosion loss should be conducted in a periodic manner;
4. Destructive direct observational methods – walls that are found to have aggressive backfills should be investigated further for direct observation of soil reinforcements.

Combining these four approaches could have a significant positive impact on the safety of MSE walls. The ability to monitor corrosion rates throughout the service life of an MSE wall is strongly recommended given the history and findings of MSE wall corrosion studies and the aggressive nature of the soils in Nevada and the southwest. This proactive approach will give MSE wall owners the ability to prevent failures in its MSE walls caused by internal stability due to high rates of corrosion. Other considerations may be incorporated including the assessment of wall drains or drainage and other potential changes that may affect the long-term behavior of these structures. It is only through these proactive tools that wall owners can make informed decisions regarding management of their existing geotechnical assets. The significant costs of these structures and the implications of potential failure highlight the need for monitoring.

CONCLUDING REMARKS

Mechanically stabilized earth walls are very economical and have been incorporated in a large number of NDOT projects resulting in over 150 walls in Nevada. However, as is commonly practiced with other structures, these retaining walls require periodic monitoring and performance evaluations. Corrosion monitoring is an important component in the successful performance of MSE walls. Corrosion monitoring can only be conducted by evaluation of the soil and reinforcement conditions behind the wall facing. This case study shows that accidental discoveries at two Nevada MSE wall locations (I-515/Flamingo and I-15/Cheyenne intersections) indicated high rates of corrosion with no visible evidence of abnormal wall movement or distress. One of the three MSE walls at the I-515/Flamingo intersection in Las Vegas has been retrofitted with a cast-in-place concrete tie-back wall, at a great expense.

Internal stability analyses of the two remaining I-515/Flamingo walls show that they are not likely to provide 75 years of service. After approximately 25 years of service a seismic event could impose enough stress on the corroded metal reinforcements to initiate failure. The results from such analyses and the past practice of using aggressive reinforced fill in other MSE walls point to a need for the immediate evaluation of other Nevada walls.

There is significant potential for other walls to have high rates of corrosion because of the unintentional use of aggressive MSE reinforced fill in Nevada. In order to evaluate these walls as assets they need to be assessed. In particular, the assessment process must include methods that evaluate the internal stability and its potential to change over time due to metal loss through corrosion.

[Geotechnical asset management offers a framework of inventorying and conducting condition surveys for monitoring the performance of earth retaining structures during their service life to assure the owner's minimum performance standards are met. Asset management principles also offer the analysis methodology to compare alternative courses of action when it is apparent that an asset such as a retaining wall is not meeting or will fail to meet standards. Adherence to asset management principles can provide agencies with the ability to make life-cycle cost-based decisions to preserve aging infrastructure or mitigate problems appropriately and defensibly.](#)

REFERENCES

- American Association of State Highway & Transportation Officials (AASHTO), Transportation Asset Management Guide, NCHRP Project 20-24(11), November 2002.
- American Association of State Highway & Transportation Officials (AASHTO), AASHTO LRFD Bridge Design Specifications 4th Ed., 2007.
- American Association of State Highway & Transportation Officials (AASHTO), AASHTO LRFD Bridge Design Specifications 5th Ed., 2010
- Federal Highway Administration (FHWA), Multi-sector Asset Management, FHWA-HIF-09-022, 2009
- Federal Highway Administration (FHWA), Earth Retaining Structures and Asset Management, FHWA-IF-08-014, 2008
- Federal Highway Administration (FHWA), Mechanically Stabilized Earth Walls and Reinforced Soil Slopes – Design and Construction Guidelines, FHWA NHI-00-043 (NHI Course No. 132042), 2001.

- Fishman, K. L., Consultant's Report: Corrosion Evaluation of MSE Walls I-515/Flamingo Road Las Vegas, Nevada. McMahon & Mann Consulting Engineers, P.C. May 2005.
- Brutus, Olivier and Tauber, Gil, Guide to Asset Management of Earth Retaining Structures, October 2009. (Prepared for NCHRP Project 20-07, Task 259, but is not an official publication of National Cooperative Highway Research Program or Transportation Research Board)
- Loehr, J. Erik, Sanford Bernhardt, Kristen L., and Huaco, Daniel R., Decision Support for Slope Construction and Repair Activities: An Asset Management Building Block, Midwest Transportation Consortium and University of Missouri – Columbia, February 2004 (MoDOT RDT 04-006/RI00-014).
- Sanford Bernhardt, Kristen L., Loehr, J. Erik, Huaco, Daniel R., Asset Management Framework for Geotechnical Infrastructure, ASCE Journal of Infrastructure Systems, September 2003;
- Siddharthan, Raj V., J.D. Thornley, B. Luke, Investigation of Corrosion of MSE Walls in Nevada, Nevada Department of Transportation Research Report 2009-03.
- Thornley, J. D., Use of Statistical Methods to Study Corrosion Aggressiveness at Nevada Mechanically Stabilized Earth Wall Sites, Master's Thesis, University of Nevada, Reno, May 2009.
- Thornley, J. D., R.V. Siddharthan, J.M. Salazar, and B. Luke, Investigation and Implications of MSE Wall Corrosion in Nevada, Accepted for publication in Transportation Research Record in March 2010.
- Virginia DOT – Office of Intermodal Planning and Investment and Cambridge Systematics, Virginia's Long-Range Multimodal Transportation Plan 2007-2035 – System Preservation and Maintenance, (2009).